

EPRI. *Proceedings: Fourth International Conference on Cold Fusion Volume 4: Theory and Special Topics Papers*, TR-104188-V4. 1994. Lahaina, Maui, Hawaii: Electric Power Research Institute.  
This book is available here:

[http://my.epri.com/portal/server.pt?Abstract\\_id=TR-104188-V4](http://my.epri.com/portal/server.pt?Abstract_id=TR-104188-V4)

**Product ID:** TR-104188-V4

**Sector Name:** Nuclear

**Date Published:** 8/9/1994

**Document Type:** Technical Report

**File size:** 48.03 MB

**File Type:** Adobe PDF (.pdf)

**Full list price:** No Charge

*This Product is publicly available*

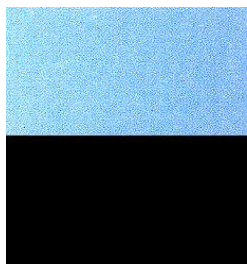
The LENR-CANR version of the book (this file) is 27 MB, and it is in “text under image” or “searchable” Acrobat format.



Electric Power  
Research Institute

Keywords:  
Deuterium  
Palladium  
Cold fusion  
Electrolysis  
Heat  
Heavy water

EPRI TR-104188-V1  
Project 3170  
Proceedings  
July 1994



**Proceedings: Fourth International  
Conference on Cold Fusion  
Volume 4: Theory and Special Topics  
Papers**

Prepared by  
Electric Power Research Institute  
Palo Alto, California

---

# **Proceedings: Fourth International Conference on Cold Fusion**

**Volume 4: Theory and Special Topics Papers**

**TR-104188-V4**

**Proceedings, July 1994**

**December 6-9, 1993  
Lahaina, Maui, Hawaii**

**Conference Co-chairmen**

**T.O. Passell  
Electric Power Research Institute**

**M.C.H. McKubre  
SRI International**

**Prepared by  
ELECTRIC POWER RESEARCH INSTITUTE  
3412 Hillview Avenue  
Palo Alto, California 94304**

**Sponsored by  
Electric Power Research Institute  
Palo Alto, California**

**T.O. Passell  
Nuclear Power Group**

**and**

**Office of Naval Research  
Arlington, Virginia**

**R. Nowak**

## **DISCLAIMER OF WARRANTIES AND LIMITATION OF LIABILITIES**

THIS REPORT WAS PREPARED BY THE ORGANIZATION(S) NAMED BELOW AS AN ACCOUNT OF WORK SPONSORED OR COSPONSORED BY THE ELECTRIC POWER RESEARCH INSTITUTE, INC. (EPRI). NEITHER EPRI, ANY MEMBER OF EPRI, ANY COSPONSOR, THE ORGANIZATION(S) NAMED BELOW, NOR ANY PERSON ACTING ON BEHALF OF ANY OF THEM:

(A) MAKES ANY WARRANTY OR REPRESENTATION WHATSOEVER, EXPRESS OR IMPLIED, (I) WITH RESPECT TO THE USE OF ANY INFORMATION, APPARATUS, METHOD, PROCESS, OR SIMILAR ITEM DISCLOSED IN THIS REPORT, INCLUDING MERCHANTABILITY AND FITNESS FOR A PARTICULAR PURPOSE, OR (II) THAT SUCH USE DOES NOT INFRINGE ON OR INTERFERE WITH PRIVATELY OWNED RIGHTS, INCLUDING ANY PARTY'S INTELLECTUAL PROPERTY, OR (III) THAT THIS REPORT IS SUITABLE TO ANY PARTICULAR USER'S CIRCUMSTANCE; OR

(B) ASSUMES RESPONSIBILITY FOR ANY DAMAGES OR OTHER LIABILITY WHATSOEVER (INCLUDING ANY CONSEQUENTIAL DAMAGES, EVEN IF EPRI OR ANY EPRI REPRESENTATIVE HAS BEEN ADVISED OF THE POSSIBILITY OF SUCH DAMAGES) RESULTING FROM YOUR SELECTION OR USE OF THIS REPORT OR ANY INFORMATION, APPARATUS, METHOD, PROCESS, OR SIMILAR ITEM DISCLOSED IN THIS REPORT.

ORGANIZATION(S) THAT PREPARED THIS REPORT:  
**ELECTRIC POWER RESEARCH INSTITUTE**  
**PALO ALTO, CALIFORNIA**

Electric Power Research Institute and EPRI are registered service marks of Electric Power Research Institute, Inc.

Copyright © 1994 Electric Power Research Institute, Inc. All rights reserved.

### **ORDERING INFORMATION**

Requests for copies of this report should be directed to the EPRI Distribution Center, 207 Coggins Drive, P.O. Box 23205, Pleasant Hill, CA 94523, (510) 934-4212. There is no charge for reports requested by EPRI member utilities.

## FOREWORD

These four volumes include the full text or, in five cases, just the visual materials of papers presented at the Fourth International Conference on Cold Fusion. This meeting was the latest in a series of conferences devoted to a new area of scientific endeavor, variously called, "Deuterated Metals Research", "Anomalous Nuclear Phenomena in Solids", and "Research on New Hydrogen Energy". The first three conferences were held in Salt Lake City, Utah, (U.S.A.), Como, (Italy), and Nagoya, (Japan), in March, 1990, June, 1991, and October 1992, respectively. The authors and participants in this fourth conference should be thanked for four days of stimulating presentations and discussions. A conscious effort was made to maintain a high standard of scientific content and avoid exaggerated claims propagated by various public media. It is gratifying that this effort was largely successful without the need for extraordinary measures.

A number of new experimental approaches were evident compared with the Nagoya meeting. Use of ceramic proton conductors at high temperature was one such. Another was the use of ultrasonic cavitation in heavy water to load palladium and titanium foils with deuterium. Many theoretical papers were given, with some progress evident toward explaining some of these puzzling experimental observations. However, the wide range of theoretical models and speculations shows that the field remains in an exploratory phase, at least for the majority of theorists.

The use of concurrent sessions for the first time caused some attendees to miss hearing significant papers. It is hoped that this compendium of papers will serve to redress that shortcoming. Proceedings, including only those papers passing a rigorous peer review, will appear later as a publication of the American Nuclear Society's Fusion Technology Journal, thanks to the initiative of Editor George Miley.

242 persons from 12 countries registered and attended the conference. The hotel facility and the weather were such as to allow concentration on the technical meetings without serious distraction. Attendees included 124 from the United States, 62 from Japan, 19 from Italy, 11 from Russia, 10 from France, 5 from Canada, 4 from China, 2 from Switzerland, 2 from Germany, and 1 each from Spain, India, and England. A large number of interested persons from the former Soviet Union and eastern Europe were unable to attend but sent several papers that are included in these volumes.

Some 156 abstracts were originally submitted of which 125 papers appear in these proceedings. Since some of the enclosed material is in an unfinished state, the authors would appreciate being contacted by those who desire to reference the work reported here. The papers are divided so that Volume 1 contains all the papers received from authors who participated in the four plenary sessions, Volume 2 includes contributed papers on calorimetry and materials, Volume 3 has contributions on nuclear particle detection and measurement, and Volume 4 contains the papers contributed on theory and special topics. The papers are ordered in the same order of abstracts in the two volumes distributed at the meeting, with a few minor exceptions.

Thanks are due to the International Advisory and the Organizing Committees for their supportive efforts in arranging a successful meeting on such a controversial, yet potentially significant and hence absorbing, topic. Persons particularly active in arranging the agenda were M.C.H. McKubre, S. Crouch-Baker, D. Rolison, T. Claytor, H. Ikegami, and P. Hagelstein. I also wish to thank the following persons who ably served as session chairmen or co-chairmen during the meeting: M. Srinivasan, S. Smedley, P. Hagelstein, F. Tanzella, A. Miller, D. Rolison, S. Crouch-Baker, M. McKubre, K. Kunimatsu, E. Storms, F. Will, T. Claytor, F. Scaramuzzi, H. Ikegami, J. Bockris, G. Miley, B. Liaw, A. Takahashi, J. Cobble and M. Rabinowitz.

Supporting the logistical and physical arrangements were EPRI and the Office of Naval Research (ONR), represented by L. Nelson and R. Nowak respectively. Cosponsoring the meeting in addition to EPRI and ONR, was Comitato Nationale per la Ricerca e per lo Sviluppo dell'Energia Nucleare e delle Energie Alternative (ENEA), represented by Franco Scaramuzzi. My sincere gratitude goes out to these persons and organizations. Many other organizations implicitly supported the meeting by funding the travel of a number of attendees. Notable among these were ENECO with 21, NEDO with 26, and IMRA with 10 attendees respectively.

The search for a definitive signature of some nuclear reaction correlated with the production of excess heat in the palladium-deuterium system was advanced by the presentations of D. Gozzi, G. Gigli, and M. Miles and their respective coworkers who reported measuring He<sup>4</sup> in the vapor phase of both closed and open electrochemical cells. However, the concentrations observed were at levels well below the atmospheric concentration of He<sup>4</sup> (5.2 ppmv) and hence are not robustly above criticism as possible atmospheric air contamination. On the other hand, the tritium results of F. Will and coworkers appear robust, with great care taken to establish reliable backgrounds and checking for contamination. I also found the tritium results of T. Claytor and coworkers convincing.

M. Fleischmann, S. Pons, and coworkers provided two papers elaborating the excess heat phenomena: one of the more intriguing results was the excess heat observed well after complete cessation of current flow due to evaporative loss of electrolyte in "boil-off" experiments of the kind first described at the Nagoya meeting.

Several papers using gas loading of palladium claimed evidence of nuclear reaction products. Y. Iwamura and coworkers appear to have replicated the experiment reported by E. Yamaguchi and his NTT coworkers at Nagoya, but emphasizing neutrons and a mass 5 peak in the mass spectrum tentatively assigned to the TD molecule.

The paper chosen by M. Fleischmann in the final panel session as the most outstanding of the conference was by D. Cravens, who on a very modest budget, had discovered many of the better methods for loading palladium with deuterium to high levels and getting the excess heat phenomenon.

Insight into the loading of hydrogen and deuterium into metals was provided by four excellent papers by R. Huggins, R. Oriani, K. Kunimatsu and coworkers, and F. Cellani and coworkers, respectively.

Particularly insightful papers on the theoretical side were presented by R. Bush, S. Chubb, P. Hagelstein, G. Hale, S. Ichimaru, Y. Kim, X. Li, G. Preparata, M. Rabinowitz, A. Takahashi, and J. Vigier .

A thoughtful paper by J. Schwinger was read by E. Mallove at a special evening session. Also, E. Storms gave an excellent summation of the meeting in the final panel session.

I apologize in advance for failing to mention here results from many other equally excellent and significant papers given at the conference.

I agree with and echo H. Ikegami's remarks in the preface of the Nagoya meeting proceedings, "It is my belief that cold fusion will become one of the most important subjects in science, one for which we have been working so patiently, with dedication and with courage, for future generations, for those who will live in the twenty-first century. In order to achieve our goal, our ultimate goal, we must continue and extend our interdisciplinary and international collaboration".

The International Advisory and Organizing Committees met late in the sessions to set the location of the next two meetings. For the next meeting (April 9-13, 1995) Monaco (near Nice, France) was chosen, and in 1996, Beijing, China.

Besides Linda Nelson of EPRI who ably handled the logistics before and at the Conference, S. Creamer of SRI International and E. Lanum of EPRI deserve our thanks for dealing with on-site issues that arise at every large gathering such as this.

I acknowledge with thanks the support of my colleagues at EPRI in planning and organizing this meeting, namely N. Ferris, L. Fielder, K. Werfelman, S. Ennis, B. Klein, R. Claeys, T. Schneider, F. Will, J. Byron, A. Rubio, R. Shaw, R. Jones, J. Taylor, K. Yeager, and R. Balzhiser.

Thomas O. Passell, Editor  
Electric Power Research Institute  
June 1994

## International Advisory Committee

J.O'M. Bockris (USA)  
H. Ikegami (Japan)  
X.Z. Li (China)  
G. Preparata (Italy)  
F. Scaramuzzi (Italy)  
A. Takahashi (Japan)  
M. Fleischmann (U.K.)  
K. Kunimatsu (Japan)  
S. Pons (France)  
C. Sanchez (Spain)  
M. Srinivasan (India)  
D. Thompson (U.K.)



**VOLUME 4**  
**THEORETICAL PAPERS AND SPECIAL TOPICS**  
**TABLE OF CONTENTS**

<b>J. Schwinger, "Cold Fusion Theory - A Brief History of Mine".....</b>	<b>1-1</b>
<b>X. Li, " The 3-Dimensional Resonance Tunneling in Chemically Assisted Nuclear Fission and Fusion Reactions".....</b>	<b>2-1</b>
<b>Y. Kim, A. Zubarev, and M. Rabinowitz, " Reaction Barrier Transparency for Cold Fusion with Deuterium and Hydrogen".....</b>	<b>3-1</b>
<b>R. Rice, Y. Kim, Rabinowitz, and Zubarev, " Comments on Exotic Chemistry Models and Deep Dirac States for Cold Fusion".....</b>	<b>4-1</b>
<b>H. Kozima, " Trapped Neutron Catalyzed Fusion of Deuterons and Protons in Inhomogeneous Solids".....</b>	<b>5-1</b>
<b>V. Vysotskii and R. Kuz'min, "On Possibility of Non-Barrier DD-Fusion in Volume of Boiling D<sub>2</sub>O During Electrolysis" .....</b>	<b>6-1</b>
<b>J. Vigier, "New Hydrogen (Deuterium) Bohr Orbits in Quantum Chemistry and "Cold Fusion" Processes".....</b>	<b>7-1</b>
<b>Y. Bazhutov and G. Vereshkov, "A Model of Cold Nuclear Transmutation by the Erzion Catalysis (The Erzion Model of "Cold Fusion")".....</b>	<b>8-1</b>
<b>K. Johnson, "Jahn-Teller Symmetry Breaking and Hydrogen Energy in Gamma-PdD "Cold Fusion" as Storage of the Latent Heat of Water" .....</b>	<b>9-1</b>
<b>S. Chubb and T. Chubb, "The Role of Hydrogen Ion Band States in Cold Fusion".....</b>	<b>10-1</b>
<b>J. Waber and M. de Llano, "Cold Fusion as Boson Condensation in a Fermi Sea".....</b>	<b>11-1</b>
<b>A. Takahashi, "Some Considerations of Multibody Fusion in Metal Deuterides".....</b>	<b>12-1</b>
<b>J. Yang, X. Chen, and L. Tang, "Cold Fusion and New Physics".....</b>	<b>13-1</b>
<b>T. Prevenslik, "Sonoluminescence, Cold Fusion, and Blue Water Lasers".....</b>	<b>14-1</b>
<b>R. Bush, "A Unifying Model for Cold Fusion".....</b>	<b>15-1</b>
<b>N. Yabuuchi, "Deuteron Waves and Cold Fusion".....</b>	<b>16-1</b>
<b>L. Sapogin, "I. Deuteron Interaction in Unitary Quantum Theory".....</b>	<b>17-1</b>

<b>L. Sapogin</b> , "II. On the Mechanism of Cold Nuclear Fusion".....	18-1
<b>K. Tsuchiya, K. Ohashi, and M. Fukuchi</b> , "Mechanism of Cold Fusion II" .....	19-1
<b>V. Vysotskii</b> , "Conditions and Mechanism of Nonbarrier Double-Particle Fusion in Potential Pit in Crystal".....	20-1
<b>S. Vaidya</b> , "Coherent Nuclear Reactions in Crystalline Solids".....	21-1
<b>M. Swartz</b> , "Catastrophic Active Medium (CAM) Theory of Cold Fusion".....	22-1
<b>S. Vaidya</b> , "On Bose-Einstein Condensation of Deuterons in PdD".....	23-1
<b>M. Rambaut</b> , "Account of Cold Fusion by Screening and Harmonic Oscillator Resonance".....	24-1
<b>Y. Bazhutov</b> , "Possible Exhibition of the Erzion - Nuclear Transformation in Astrophysics".....	25-1
<b>Y. Bazhutov and A. Kuznetsov</b> , "Isotopic and Chemical Composition Changes in Cold Fusion Experiments in the Erzion Model" .....	26-1
<b>Y. Bazhutov, V. Koretsky, and A. Kuznetsov</b> , "Burning Away of Radioactive and Production of Some Stable Isotopes Within the Framework of the Erzion Model" .....	27-1
<b>V. Filimonov</b> , "Synergetic Activation Model: Key to Intense and Reproducible Cold Fusion".....	28-1
<b>R. Takahashi</b> , "Cold Fusion Explained by Negentropy Theory of Microdrop of Heavy Water".....	29-1
<b>G. Federovich</b> , "Ferroelectrics for Cold Fusion".....	30-1
<b>Y. Kim</b> , "Possible Evidence of Cold D(d,p)T Fusion From Dee's 1934 Experiment" .....	31-1
<b>X. Li</b> , "Searching for Truth with High Expectations - 5 Year Studies on Cold Fusion in China".....	32-1
<b>H. Fox</b> , "Cold Nuclear Fusion & Enhanced Energy Devices: A Progress Report".....	33-1
<b>D. Morrison</b> , "Review of Progress in Cold Fusion" .....	34-1
<b>E. Mallove</b> , "Cold Fusion: The High Frontier -- Implications for Space Technology" .....	35-1
<b>K. Chukanov</b> , "New Pulse Gas Loading Cold Fusion Technology".....	36-1

<b>R. Cornog</b> , "Cheap Electric Power from Fusion?".....	37-1
<b>R. Bass</b> , "Proposed Nuclear Physics Experiment to Conclusively Demonstrate & Explain Aneutronic Cold Fusion".....	38-1
<b>J. Guokas</b> , "Cold Fusion and Nuclear Proliferation".....	39-1
<b>V. Romodanov, V. Savin, S. Korneev, A. Glagolev, and Y. Skuratnik</b> , "Ecological Aspects of Thermal Systems Using Hydrogen Isotopes".....	40-1
<b>E. Kennel</b> , "Investigation of Deuterium Glow Discharges of the Kucherov Type".....	41-1
<b>W. Collis</b> , "Oklo Isotope Anomalies and Cold Fusion".....	42-1
<b>J. Griggs</b> , "A Brief Introduction to the Hydrosonic Pump and the Associated "Excess Energy" Phenomenon".....	43-1
<b>H. Komaki</b> , "An Approach to the Probable Mechanism of the Non-Radioactive Biological Cold Fusion or So-Called Kervran Effect (Part 2)".....	44-1



## Cold Fusion Theory

### A Brief History of Mine

As Polonious might have said: "Neither a true-believer nor a disbeliever be." From the very beginning in a radio broadcast on the evening of March 23, 1989, I have asked myself—not whether Pons and Fleischman are right—but whether a mechanism can be identified that will produce nuclear energy by manipulations at the atomic—the chemical—level. Of course, the acceptance of that interpretation of their data is needed as a working hypothesis, in order to have quantitative tests of proposed mechanisms.

As a long-time nuclear physicist, the knee jerk reaction to the idea of a D-D reaction without significant neutron production brought in words like  ${}^4He$  and Mössbauer effect. I tried, without success, to contact P(ons) and F(leischman), to the point of sending a letter to the Los Angeles Times, which was garbled in the editing process. Finally, with the help of a friend, contact was made in the early part of April and I went to Salt Lake City.

There, I was assured that they knew about  ${}^4He$ , and was shown a peak in a spectroscopic read-out which, I was told, was  ${}^4He$ . Soon after my return to Los Angeles, references to  ${}^4He$  disappeared, to resurface only relatively recently.

I do not have to—but shall—remind you of the two fundamental problems that the acceptance, of P & F's excess heat as nuclear in origin, entails.

1. What accounts for the absence of particles that are familiar in ordinary hot fusion, such as the neutrons of  $D + D \rightarrow n + {}^3He$  and the high energy  $\gamma$ -ray of  $D + D \rightarrow \gamma + {}^4He$ ? Very early in my thinking I added the conventional reaction  $p + D \rightarrow \gamma + {}^3He$ . Why? Mostly because it would also be there. One cannot produce heavy water without some contamination by light water.

2. Hot fusion relies on achieving enough kinetic energy to overcome the Coulomb repulsion between like charges. How then can cold fusion, operating far below those levels, ever achieve fusion? Incidentally, I have read, and heard, that my solution to the Coulomb barrier problem is to forget it! Not even an absent-minded professor (which I am not) would go that far. Critics should learn to operate within the bounds of sanity.

My first attempt at publication, for the record, was a total disaster. "Cold Fusion: A Hypothesis" was written to suggest several critical experiments, which is the function of hypothesis. The masked reviewers, to a person, ignored that, and complained that I had not proved the underlying assumptions. Has the knowledge that physics is an experimental science been totally lost?

The paper was submitted, in August 1989, to Physical Review Letters. I anticipated that PRL would have some difficulty with what had become a very controversial subject, but I felt an obligation to give them the first chance. What I had not expected—as I wrote in my subsequent letter of resignation from the American Physical Society—was contempt.

“Hypothesis” was eventually published, after protracted delays, in a 1990 issue of a German periodical. Does it have any significance in 1993? I cite the following excerpts:

“... this cold fusion process (of P & F) is not powered by a DD reaction. Rather it is an HD reaction, which feeds on the small contamination of  $D_2O$  by  $H_2O$ .”,

and:

“The HD reaction  $p + d \rightarrow {}^3He$  does not have an accompanying  $\gamma$ -ray; the excess energy is taken up by the metallic lattice of Pd alloyed with D.”

and finally:

“... concerning the oft repeated demand for a control experiment using  $H_2O$ , one should note the possibility of a converse effect of the HD reaction: Through the natural presence of  $D_2O$  in ordinary water, such control experiments might produce an otherwise puzzling amount of heat.”

A following paper, entitled: “Nuclear energy in an atomic lattice, 1,” was sent directly to another German periodical, in November of 1989. As of today, the only memorable part is a quotation from Joseph Priestly:

“In this business, more is owed to what we call chance—that is, to the observation of events arising from unknown causes—than to any preconceived theory.”

The editor thought it necessary to add a total disclaimer of responsibility, ending with: “We leave the final judgement to our readers.” In my naivety I had thought that was always so. When part 2 of NEAL was submitted, it was simply rejected. The fix was in.

I gave a talk with the same title—“Nuclear Energy in an Atomic Lattice”—at Salt Lake City in March of 1990. The HD hypothesis—of the dominance of the pd reaction—has the pragmatic advantage of suppressing neutron production at the level of excess heat generation.

But, to quote from that lecture: “... a well trained hot fusioneer will instantly object that there must also be a 5.5 MeV  $\gamma$ -ray. He will not fail to point out that no such radiation has been observed. Indeed.”

"But consider the circumstances of cold fusion. (The quotation continues.) At very low energies of relative motion, the proton and deuteron of the HD reaction are in an s-state, one of zero orbital angular momentum, and therefore of positive orbital parity. The intrinsic parities of proton, deuteron, and  $^3He$  are also positive. Then, the usually dominant electric dipole radiation—which requires a parity change—is forbidden."

I turn from 'missing' radiation to Coulomb repulsion, and quote:

"... treatments of nuclear fusion between positively charged particles (usually) represent the reaction rate as the product of two factors. The first factor is a barrier penetration probability. It refers entirely to the electric forces of repulsion. The second factor is an intrinsic nuclear reaction rate. It refers entirely to nuclear forces. This representation ... may be true enough under the circumstances of hot fusion. But, in very low energy cold fusion one deals essentially with a single state, or wave function, all parts of which are coherent. It is not possible to totally isolate the effect of the electric forces from that of the nuclear forces: The correct treatment of cold fusion will be free of the collision dominated mentality of the hot fusioners."

To speak of transferring energy to the lattice is to invoke lattice excitations, or phonons. At about the time of the Salt Lake City meeting, or shortly after, I became dissatisfied with my treatment, and began to reconstruct phonon theory. A note entitled "Phonon representations" was submitted to the Proceedings of the National Academy of Sciences in June of 1990. The abstract reads:

"The gap between the nonlocalized lattice phonon description and the localized Einstein oscillator treatment is filled by transforming the phonon Hamiltonian back to particle variables. The particle-coordinate, normalized wave function for the phonon vacuum state is exhibited."

A month later, I submitted a second note with the title "Phonon dynamics." The abstract reads:

"An atomic lattice in its ground state is excited by the rapid displacement and release of an atomic constituent. The time dependence of the energy transfer to other constituents is studied ... ."

The third and last note is called "Phonon Green's function." Its abstract is:

"The concepts of source and quantum action principle are used to produce the phonon Green's function appropriate for an initial phonon vacuum state. An application to the Mössbauer effect is presented."

I remind you that the Mössbauer effect refers to "an excited nucleus of an atom, imbedded in a lattice, (that) decays with the emission of a  $\gamma$ -ray," thereby transferring momentum to the lattice." There is a certain probability ... that the phonon spectrum of the lattice will remain unexcited, as evidenced by the absence, in the  $\gamma$ -ray energy, of the red-shift associated with recoil energy."

A casual explanation of the Mössbauer effect has it that the recoil momentum is transferred to the lattice as a whole so that the recoil energy, varying inversely with the mass of the entire lattice, is extravagantly small. As Pauli would say, even to God, "Das ist falsch!" The spontaneous decay of a single excited atom in the lattice is a localized event, the consequences of which flow at finite speed, out into three dimensional space, weakening as they travel. This is a microscopic event, with no dependence on macroscopic parameters such as the total mass of the lattice.

Unmentioned in the abstract, but of far greater importance, is another situation. To quote: "What happens if the momentum impulse ... is applied, not to one, but all lattice sites?" The reader is invited to "recall that the lattice geometry is not absolute, but relative to the position of the center of mass for the entire system. Thus (the injected energy) can be read as the kinetic energy transferred to the lattice as a whole." More of this shortly.

In the last month of 1990, I went to Tokyo. The occasion was the 100th anniversary of the birth of a famous Japanese physicist, perhaps most familiar for his part in the Klein-Nishima formula for Compton scattering. On a day that, to my surprise, I found uncomfortably close to another-infamous-day, I delivered a lecture on: "Cold Fusion—Does It Have a Future?" The abstract reads:

"The case against the reality of cold fusion is outlined. It is based on preconceptions inherited from experience with hot fusion. That cold fusion refers to a different regime is emphasized. The new regime is characterized by intermittency in the production of excess heat, tritium, and neutrons. A scenario is sketched, based on the hypothesis that small segments of the lattice can absorb released nuclear energy."

I pick up the last sentence of the abstract with this quotation from the text:

"If the  $\gamma$ -rays demanded by the hot fusionists are greatly suppressed, what agency does carry off the excess energy in the various reactions? One must look for something that is characteristic of cold fusion, something that does not exist in the plasma regime of hot fusion. The obvious answer is: the lattice in which the deuterium is confined.

Imagine then, that a small, but macroscopic piece of the lattice absorbs the excess energy of the HD or DD reaction. ... I advance the idea of the lattice playing a vital role as a hypothesis. ... Intermittency is the hallmark of cold fusion. ... Does the lattice hypothesis have a natural explanation for intermittency? ... a close approach to saturation loading is

required for effective fusion to take place. But, surely, the loading of deuterium into the palladium lattice does not occur with perfect spatial uniformity. There are fluctuations. It may happen that a microscopically large—if macroscopically small—region attains a state of such lattice uniformity that it can function collectively in absorbing the excess nuclear energy that is released in an act of fusion. And that energy can initiate a chain reaction as the vibrations of the excited ions bring them into closer proximity. So begins a burst. In the course of time, the increasing number of vacancies in the lattice will bring about a shut-down of the burst. The start-up of the next burst is an independent affair. (This picture is not inconsistent with the observation of extensive cracking after long runs.)

What answer did I give, just three years ago to "Does cold fusion have a future"? I said: "I have little hope for it in Europe and the United States—the West. It is to the East, and, specifically, to Japan that I turn."

Inspired by good soba and sushi, I dashed off a short addendum that Progress of Theoretical Physics received in January and published in April of 1991. The abstract of "Nuclear Energy in an Atomic Lattice—Causal Order" is:

"The extremely small penetrability of the Coulomb barrier is generally adduced to dismiss the possibility of low energy (cold) fusion. The existence of other mechanisms that could invalidate this logic is pointed out."

Here are excerpts. "... Implicit in this line of thought (of negligible penetrability) is the apparently self-evident causality assignment that has the release into the surrounding environment, of energy at the nuclear level, occur after the penetration of the Coulomb barrier. One would hardly question that time sequence when the environment is the vacuum. But does it necessarily apply to the surrounding ionic lattice? ... another reading is possible, one in which the causal order is reversed. Why? Because, in contrast with the vacuum, the lattice is a dynamical system, capable of storing and exchanging energy.

The initial stage of the new mechanism can be described as an energy fluctuation, within the uniform lattice segment, that takes energy at the nuclear level from a pd or dd pair and transfers it to the rest of the lattice, leaving the pair in a virtual state of negative energy. ...

For the final stage ... consider the pd example where there is a stable bound state:  ${}^3He$ . If the energy of the virtual state nearly coincides with that of  ${}^3He$ , a resonant situation exists, leading to amplification, rather than Coulomb barrier suppression.

It would seem that two mechanisms are available ... . But are they not extreme examples of mechanisms that in general possess no particular causal order?"

The last lecture on cold fusion was delivered—twice—in the Fall of 1991, to celebrate the birthdays of former students, one of whom is at MIT, a hotbed of hot fusioneers. The cover title: “A Progress Report,” injects a bit of my own nostalgia. Not long after the simultaneous arrival of myself at Berkeley and World War II, Robert Oppenheimer gave a lecture with that title. As he explained, it meant only that time had elapsed. That also applied to the first part of my birthday lectures—“Energy Transfer in Cold Fusion”—with one exception:

“I note here the interesting possibility that the  $^3He$  produced in the pd fusion reaction may undergo a secondary reaction with another deuteron of the lattice, yielding  $^5Li$  (an excited state of  $^5Li$  lies close by). The latter is unstable against disintegration into a proton and  $^4He$ . Thus, protons are not consumed in the overall reaction, which generates  $^4He$ .”

To this I add, as of some time in 1992, that observations of  $^4He$ , with insufficient numbers to account for total heat generated, are consistent with the preceding suggestion. The initial pd reaction produces heat, but no  $^4He$ . The secondary reaction generates heat and  $^4He$ . There may be more total heat than can be accounted for by  $^4He$  production. The smaller the ratio of secondary to primary rates, the more the  $^4He$  production will be incapable of accounting for the heat generation.

The second part of “A Progress Report” is entitled: “Energy Transport in Sonoluminescence.” What is that?

The text begins with:

“The suggestion that nuclear energy could be transferred to an atomic lattice is usually dismissed ... because of the great disparity between atomic and nuclear energy scales; of the order  $10^7$ , say. It is, therefore, of great psychological importance that one can point to a phenomenon in which the transfer of energy between different scales involves (an) amplification of about eleven orders of magnitude.”

“It all began with the sea trials, in 1894, of the destroyer HMS Daring. The onset, at high speeds, of severe propeller vibrations led to the suggestion that bubbles were forming and collapsing—the phenomenon of cavitation. Some 23 years later, during World War I, Lord Rayleigh, no less, was brought in to study the problem. He agreed that cavitation, with its accompanying production of pressure, turbulence, and heat, was the culprit. And, of course, he devised a theory of cavitation. But, there, he seems to have fallen into the same error as did Isaac Newton, who, in his theory of sound assumed isothermal conditions. As Laplace pointed out in 1816, under circumstances of rapid change, adiabatic conditions are more appropriate.

During World War I, the growing need to detect enemy submarines led to the devel-

opment of what was then called (by the British, anyway) subaqueous sound-ranging. The consequent improvement in strong acoustic sources found no scientific applications until 1927. It was then discovered that, when a high intensity sound field produced cavitation in water, hydrogen peroxide was formed. Some five years later came a conjecture that, if cavitation could produce such large chemical energies, it might also generate visible light. This was confirmed in 1934, thereby initiating the subject of sonoluminescence; SL. I should, however, qualify the initial discovery as that of incoherent SL, for, as cavitation noise attests, bubbles are randomly and uncontrollably created and destroyed.

The first hint of coherent SL occurred in 1970 when SL was observed without accompanying cavitation noise. This indicates that circumstances exist in which bubbles are stable. But not until 1990 was it demonstrated that an SL stream of light could be produced by a single stable cavity.

Ordinarily, a cavity in liquid is unstable. But it can be stabilized by the alternating cycles of compression and expansion that an acoustic field produces, provided the sonic amplitudes and frequencies are properly chosen. The study of coherent SL, now under way at UCLA under the direction of Professor Seth Putterman, has yielded some remarkable results.

What, to the naked eye, appears as a steady, dim blue light, a photomultiplier reveals to be a clock-like sequence of pulses in step with the sonic period, which is of the order of  $10^{-4}$  seconds. Each pulse contains about  $10^5$  photons, which are emitted in less than 50 pico seconds, that is, in about  $10^{-11}$  seconds.

When I first heard about coherent SL (my term), some months ago (June 1991), my immediate reaction was: This is the dynamical Casimir effect. The static Casimir effect, as usually presented, is a short range non-classical attractive force between parallel conducting plates situated in a vacuum. Related effects appear for other geometries, and for dielectric bodies instead of conductors.

A bubble in water is a hole in a dielectric medium. Under the influence of an oscillating acoustical field, the bubble expands and contracts, with an intrinsic time scale that may be considerably shorter than that of the acoustical field. The accelerated motions of the dielectrical material creates a time dependent-dynamical-electromagnetic field, which is a source of radiation. Owing to the large fractional change in bubble dimensions that may occur, the relation between field and source could be highly nonlinear, resulting in substantial frequency amplification.

The mechanisms that have been suggested for cold fusion and sonoluminescence are quite different. (So I wrote in 1991.) But they both depend significantly on nonlinear effects. Put in that light, the failures of naive intuition are understandable. So ends my Progress Report."

In the more than two years that have elapsed since the birthday lectures, I have concentrated on the theory of coherent sonoluminescence. Why? Because, of the two physical processes that naive intuition rejects, it is coherent SL that exists beyond doubt. (No, Mr. Taubes, not even you could cry fraud. Too many people have seen the light.) With the advantage of reproducible data, under variable circumstances, constructing a convincing theory for coherent SL should be, by far, the simpler. That, in turn, should supply analogies for theory construction in a domain that is characterized experimentally by "irreproducibility and uncontrollable emission in bursts."

My gut feeling about the Casimir effect, in a dynamical role, first needed some brushing up in the static domain, which I had not thought about for 15 years. My progress in doing that, along with needed simplifications, is recorded in four notes, published in 1992. Two of them share the title "Casimir energy for dielectrics." Each note acknowledges the stimulation provided by the phenomenon of coherent SL. I give only this brief excerpt concerning the action quantity  $W_o$ :

"What the static and dynamic Casimir effects share is the reference to the quantum probability amplitude for the preservation of the photon vacuum state: (exponential of  $iW_o$ ). That the vacuum persistence probability is less than one, in a dynamical situation where photons can be emitted, is expressed by a nonzero imaginary part of  $W_o$ : ... . In a static situation where  $W_o$  is real, the shift in phase associated with a time lapse, ... identifies E, the energy of the system, ... ."

In the latter part of 1992, and in 1993, five papers were submitted under the cover title "Casimir light." The individual ones are called, successively: A glimpse; The source; Photon pairs; Pieces of the action; and, Field pressure. The first three notes adopted the over-simplification that the bubble collapse—the source of radiant energy—is instantaneous. "Pieces of the action" begins "to remove the more egregious aspects of that treatment." The Abstract reads:

"More realistic dynamics for the collapsing dielectric fluid are introduced in stages by adding contributions to the Lagrangian that forms the action. The elements are kinetic energy, Casimir potential energy, air pressure potential energy, and electromagnetic coupling to the moving dielectric. There are successful tests of partial collapse time and of minimum radius." This paper ends with a veiled question:

"If, as it would seem, a mechanism exists that transfers kinetic energy of a macroscopic body into energy of microscopic entities, could there not be—in a different circumstances—a mechanism that transfers energy of microscopic entities into kinetic energy of a macroscopic body?" What, in 1991, seemed to be only a pairing of two intuitively improbable phenomena ("The mechanisms that have been suggested for cold fusion and sonoluminescence are quite different."), now emerges as related ways of transferring energy between macroscopic and microscopic objects.

"Casimir light: Field pressure" begins with a question:

"How does a macroscopic, classical, hydromechanical system, driven by a macroscopic acoustical force, generate an astonishingly short time scale and an accompanying high electromagnetic frequency, one that is at the atomic level?"

In response, "I offer the hypothesis that light plays a fundamental role in the mechanism. Provocatively put:

The collapse of the cavity is slowed abruptly by the pressure of the light that is created by the abrupt slowing of the collapse."

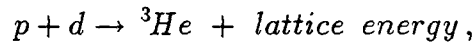
The hypothesis becomes more quantitative with this supplement:

"The conditions for light emission are at hand when the fluid kinetic energy becomes independent of  $t$  (time) for a short time interval, and that similar remarks apply immediately after the emission act. In effect, one is picking out the circumstances for spontaneous radiation, from a coherent state of definite energy, to another such state of definite, lower energy."

The equation of motion—along with the conservation laws—that is supplied by the action principle, leads to a picture of what happens during abrupt slowing." Just before that begins, there is no significant field, .... Then the field strength rises rapidly in the vacuum region, giving a positive value to the (outward pressure). ... the slowing has begun. That process will cease when the field, flowing at the speed of *light* toward the outer dielectric region, has produced the countering pressure."

"The somewhat mysterious initial hypothesis has emerged clarified, as an unusual example of a familiar fact—spontaneous emission of radiation by an electric system is a single indivisible act that obeys the laws of energy and momentum conservation."

Now, finally, returning to the 1991 "Causal order" note, for the example of the reaction



one also recognizes this as a single, indivisible act.

So ends this Progress Report.

JULIAN SCHWINGER



# THE 3-DIMENSIONAL RESONANCE TUNNELING IN CHEMICALLY ASSISTED NUCLEAR FISSION AND FUSION REACTIONS

Xing Zhong Li  
Department of Physics  
Tsinghua University  
Beijing 100084, CHINA

## Abstract

Resonance tunneling model has been extended to 3-dimensional case, and the centrifugal barrier is proposed to be the second barrier to form a well between the Coulomb barrier and centrifugal barrier. The cross-section for fusion reaction is calculated and compared with that of Jones' and Koonin's calculation. The experimental results for double barrier fission and meta-stable excited state of hydrogen molecule are cited to support this concept of double barrier penetration. In order to explain the nuclear products, a model of "split Coulomb barrier" is speculated. Some experiments are suggested to test this speculation.

## Introduction

A combined resonance model was proposed in ICCF3<sup>1</sup> to show that: (1) even if there is no resonance level at the low energy in d+d system, the resonance penetration is still possible; (2) the manipulation in atomic scale can effect on the reaction in nuclear scale. However, how to apply this combined resonance model in the three dimensional case was an open question. At that time the centrifugal barrier was proposed to be combined with the Coulomb barrier, and we believed that the combined resonance tunneling would facilitate the penetration of Coulomb barrier. In the present paper, the enhancement of penetration due to the resonance level between the Coulomb barrier and the centrifugal barrier is estimated and compared with the experiment. The experiment results in the double barrier nuclear fission and the meta-stable excited state of hydrogen molecule support the concept of resonance tunneling. The mismatching of "excess heat" and the "nuclear products" suggests the necessity to refine this resonance tunneling model. Two step process (molecular shrinkage followed by a nuclear process) is assumed to explain this mismatching. Never-the-less, the nuclear fragments imply the penetration of palladium nucleus with higher charge number ( $Z=46$ ). A speculation of "split Coulomb barrier" model is discussed. The high electron density region and the enhanced spontaneous fission of fissionable elements would be the corollaries of this model, and some possible experiments are proposed.

### 3-Dimensional Resonance Tunneling

In the 3-dimensional case, the combined resonance tunneling model should be modified, and the centrifugal potential barrier is the second barrier to be combined with the Coulomb barrier (Fig.1). Between these two barriers there is a potential well due to the interchange energy of the electrons of deuterium atoms. The virtual resonance level in this potential enhances the penetration of Coulomb barrier. A new simplified formalism of WKB method<sup>1,2</sup> was proposed to facilitate this calculation.

The radial part of the wave function  $\chi_l(r)/r$  is defined in different regions in Fig.1, which can be connected by W.K.B. connection formula. If in region I ( $0 < r < a$ ) and region V ( $d < r$ ),  $\chi_l(r)$  is defined as

$$\chi_{II}(r) = \frac{1}{\sqrt{k}} \left\{ A_a \cos \left[ \int_r^a k dr - \frac{\pi}{4} \right] + B_a \sin \left[ \int_r^a k dr - \frac{\pi}{4} \right] \right\}$$

$$\chi_{IV}(r) = \frac{1}{\sqrt{k}} \left\{ A_d \cos \left[ \int_d^r k dr - \frac{\pi}{4} \right] + B_d \sin \left[ \int_d^r k dr - \frac{\pi}{4} \right] \right\}$$

here  $k = \sqrt{\frac{2\mu}{\hbar^2}[E - U(r)]}$ , and  $\hbar$  is the Planck constant divided by  $(2\pi)$ .  $\mu$  and  $E$  are the reduced mass and the total energy of the relative motion of deuteron-deuteron system, respectively.  $U(r)$  is the potential energy. Then, the coefficients  $A_a$  and  $B_a$  are connected to coefficients  $A_d$  and  $B_d$  by the connection matrixes as follows

$$\begin{bmatrix} A_a \\ B_a \end{bmatrix} = C_{WB} B_{ab} C_{BW} W_{bc} C_{WB} B_{cd} C_{BW} \begin{bmatrix} A_d \\ B_d \end{bmatrix}$$

Here,  $C_{BW}$  is the connection matrix from well to barrier region and  $C_{BW}$  is that from barrier to well region;

$$C_{WB} = \begin{bmatrix} 2, & 0 \\ 0, & -1 \end{bmatrix}, \quad C_{BW} = \begin{bmatrix} 1/2, & 0 \\ 0, & -1 \end{bmatrix}$$

$B_{ab}$  is the propagation matrix in barrier region from  $a$  to  $b$ , and  $B_{cd}$  is that from  $c$  to  $d$ :

$$B_{ab} = \begin{bmatrix} 0, & \theta_N \\ \theta_N^{-1}, & 0 \end{bmatrix}, \quad B_{cd} = \begin{bmatrix} 0, & \theta_a \\ \theta_a^{-1}, & 0 \end{bmatrix}$$

Here,  $\theta_N \equiv \exp \left[ \int_a^b \beta dr \right]$ ,  $\theta_a \equiv \exp \left[ \int_c^d \beta dr \right]$ , and  $\beta = \sqrt{\frac{2\mu}{\hbar^2}[U(r) - E]}$ .  $\theta_N$  and  $\theta_a$  are very large number usually.  $W_{ba}$  is the propagation matrix in well region from  $b$  to  $c$ .

$$W_{bc} = \begin{bmatrix} \sin \gamma_{bc}, & -\cos \gamma_{bc} \\ -\cos \gamma_{bc}, & -\sin \gamma_{bc} \end{bmatrix}.$$

Here,  $\gamma_{bc} \equiv \int_b^c k dr$ . Hence

$$\begin{bmatrix} A_a \\ B_a \end{bmatrix} = \begin{bmatrix} -\frac{\theta_N}{\theta_a} \sin \gamma_{bc}, & -4\theta_N \theta_a \cos \gamma_{bc} \\ -(4\theta_N \theta_a)^{-1} \cos \gamma_{bc}, & \frac{\theta_a}{\theta_N} \sin \gamma_{bc} \end{bmatrix} \begin{bmatrix} A_d \\ B_d \end{bmatrix}$$

In addition,  $\chi_{ll}(r)$  has to satisfy the boundary condition:

$$\chi_{ll}(0) = 0$$

therefore,

$$\frac{A_a}{B_a} \equiv \bar{K} = -\tan \left[ \int_0^a k dr - \frac{\pi}{4} \right]$$

Here,  $\bar{K}$  is a complex number,  $\bar{K} = K_r + i K_i$ , because the nuclear potential,  $U(r)$ , is a complex number, i.e.  $\text{Im } U(r) \neq 0$  in the region  $0 < r < a$  due to the absorption of deuteron ( $d+d$  reaction).

$$K_r = -\frac{1}{2} \frac{\sin 2I_r}{\cos^2 I_r + sh^2 I_i}$$

$$K_i = -\frac{1}{2} \frac{sh 2I_i}{\cos^2 I_r + sh^2 I_i}$$

Here,  $I_r \equiv \int_0^a k_r dr - \frac{\pi}{4}$ ,  $I_i \equiv \int_0^a k_i dr - \frac{\pi}{4}$ .  $k_r$  and  $k_i$  are the real and imaginary part of  $k$ , respectively. Having defined these quantities  $I_r$  and  $I_i$  by nuclear potential, we have the amplitudes of outgoing and ingoing spherical wave function,  $A_d$  and  $B_d$ .

Consequently, we have the cross-section,  $\sigma_r^{(l)}$ , for the partial wave of angular momentum  $l$ .

$$\sigma_r^{(l)} = \frac{\pi}{k^2} (2l+1)(1 - |S_l|^2)$$

and

$$|S_l|^2 = \left| \frac{A_d - iB_d}{A_d + iB_d} \right|^2$$

or

$$\sigma_r^{(I)} = \frac{4\pi}{k^2} (2l+1) K_i / \{ 2K_i - \cos^2 \gamma_{bc} [(4\theta_a \theta_N)^2 + \frac{|\bar{K}|^2}{(4\theta_a \theta_N)^2}]$$

$$- \sin^2 \gamma_{bc} [ \left( \frac{\theta_N}{\theta_a} \right)^2 + \left( \frac{\theta_a}{\theta_N} \right)^2 |\bar{K}|^2 ] - K_r \sin 2\gamma_{bc} [ 4\theta_a^2 - \frac{1}{4\theta_a^2} ] \}$$

When the energy of the relative motion of the deuterons coincides with the virtual energy level of the potential well, i.e.,  $\cos \gamma_{bc} = 0$ , the cross-section is

$$\sigma_r^{(I)} = \frac{4\pi}{k^2} (2l+1) \frac{\left( \frac{-K_i}{\theta_N^2} \right) \left( \frac{1}{\theta_a^2} \right)}{\left[ \left( \frac{-K_i}{\theta_N^2} \right) + \left( \frac{1}{\theta_a^2} \right) \right]^2 + \left( \frac{K_r}{\theta_N^2} \right)^2},$$

For the low energy d-d reaction, the semi-resonance condition<sup>1</sup> in the nuclear well makes  $K_r \approx 0$ .

$$\sigma_r^{(I)} = \frac{\pi}{k^2} (2l+1) \frac{4T_N T_a}{(T_N + T_a)^2}$$

here,  $T_N = \left( \frac{-K_i}{\theta_N^2} \right)$  is the penetration rate for the single Coulomb barrier, and

$T_a = \left( \frac{1}{\theta_a^2} \right)$  is the penetration rate for the centrifugal potential well only.

Usually,  $T_a \gg T_N$ , then

$$\begin{aligned} \sigma_r^{(I)} &= \frac{\pi}{k^2} (2l+1) \frac{4T_N}{T_a} \\ &= \frac{4\pi}{k^2} (2l+1) (-K_i) \frac{\theta_a^2}{\theta_N^2} \end{aligned}$$

( $-K_i$ ) is a positive number in corresponding to the absorption in the nuclear well. This expression can be put into the conventional form:

$$\sigma_r^{(I)} = \frac{S(E)}{E} \theta_N^{-2} \frac{1}{T_a}$$

When there is no centrifugal barrier,  $T_a = 1$ , then

$$\sigma_r^{(I)} = \frac{S(E)}{E} \exp \left[ -2 \int_a^b \beta dr \right]$$

This is just the conventional fusion cross-section. (Some time the  $(\theta_N)^{-2}$  is called as penetration factor. In fact, the penetration rate should be  $-K_1(\theta_N)^{-2}$ ). Using the experimental data for low energy d+d reaction,  $S(E)$  is found to be independent of energy, and equals to 0.11 MeV-barn<sup>3</sup>.

Using the Morse potential, S.E. Jones<sup>4</sup> calculated the penetration factor:  
 $(\theta_N)^{-2} \approx \exp(-190)$

Koonin improved the calculation by considering the fact that the potential energy between two deuterium,  $U(r)$ , should approach to the energy of the helium atom, i.e.

$$U(r \rightarrow 0) \Rightarrow \frac{e^2}{r} + U_0$$

here  $U_0 = -1.9037$  Hartrees  $\approx -51.8$  eV. Then

$$(\theta_N)^{-2} \approx \exp(-177)$$

When the centrifugal barrier appears, and the energy coincides with the virtual resonance level, a big factor  $(1/T_a) = (\theta_a)$  would greatly increase the penetration.

### Estimation of Barrier Penetration Factors

A rough estimation of  $\theta_a$  can be done by a step-wise centrifugal barrier as Fig.2.

$$\begin{aligned} \theta_a &= \exp \left[ \int_{r_2}^{r_3} \sqrt{\frac{2\mu}{\hbar^2} (U(r) - E)} dr \right] \\ &\approx \exp \left[ \int_{r_2}^{r_3} \sqrt{\frac{2\mu}{\hbar^2} \frac{l(l+1)\hbar^2}{2\mu r^2}} dr \right] \\ &= \left( \frac{r_3}{r_2} \right)^{\sqrt{l(l+1)}} \end{aligned}$$

$r_2$  is about at the order of  $10^{-8}$  cm, and  $r_3$  may be limited by the lattice constant ( $\sim 4 \times 10^{-8}$  cm in the palladium). In some cases  $r_3$  may be quite large on the surface of the crystal. The maximum possible value for  $l$  is limited by the requirement that the bottom of the potential well should be lower than zero to ensure that the low energy incident deuteron would see a well between two barriers. For d+d reaction  $l_{\max} \approx 45$ . Hence, it is possible to enhance the penetration factor,  $(\theta_N)^{-2}/T_a$ , by a factor of  $10^{54}$  which is necessary to bring the cross-section value to the detected value in nuclear measurement. However, the centrifugal potential, which is added to Coulomb barrier will increase inner barrier height and its thickness as well; therefore, it is hard to make the cross-section greater further.

### Double Barrier Fission and Meta-Stable Excited State of Molecular Hydrogen

Three questions are always raised to the resonance tunneling model, i.e. the limited value of wave function inside the nuclear potential well ( $r < a$  in Fig.1) is too small;

the width of resonance energy level is too narrow; and the time needed for formation of resonance state is too long to be effective.

Usually, resonance tunneling is treated as a steady state in quantum mechanics. When the module of wave function in the potential well ( $b < r < c$ . in Fig.1) is assumed to be the deuterium density in the solid ( $\approx 10^{22} \text{ cm}^{-3}$ ), the square of the module of wave function inside the nuclear potential well would be very small<sup>5</sup> ( $\approx (\theta_N)^{-2} \times 10^{22} \text{ cm}^{-3}$ ). Since the fusion reaction rate is assumed to be proportional to the square of the module of wave function, then it must be extremely small.

In fact, the resonance tunneling should be treated as a non-steady state problem<sup>6</sup>, it should be normalized to the incident flux of particle, instead of the absolute value of wave function (The normalization for continuous spectrum is different from that for discrete spectrum<sup>7</sup>).

The sharpness of the resonance is due to the large value of  $(\theta_N)^2$  which makes the width of resonance energy level very narrow. Hence, only a few incident particles would be in resonance, if they are distributed in energy as a Maxwellian distribution. However, the deuterons in solid is somehow confined; therefore, we may expect that deuterons are condensed at one single energy level. Since deuteron is a boson, and local density of deuterons may be very high due to the phase transition inside the palladium, such condensation may happen in a small region.

In the treatment of steady state, the concept of wave packet is always used to imagine the formation time of this resonance state. Since the width of energy level is extremely narrow, the length of the wave packet becomes extremely long due to the uncertainty principle. Then, the necessary time for the formation of resonance state is too long to be valid. In reality, the penetration is a time-dependent problem. Roy<sup>6</sup> has developed a time-dependent procedure to describe the tunneling, and has found the differences between the time-dependent and time-independent treatments.

The best answer to those three questions is the experiment. The double barrier fission<sup>8</sup> has been confirmed by the experimental results. Fig.3 shows the excitation curve for nuclear fission induced by neutron, and the total neutron cross-section of  $^{240}\text{Pu}$  as a function of neutron energy. The large number of fine-structure resonance in Fig.3a, and the very few fine-structure resonance of appreciable strength, which are clustered into a few groups, in Fig.3b are the most striking example for the double barrier fission. When the energy level inside the inner barrier coincides with the energy level in the outer well, the penetration rate increases dramatically, and the fission cross-section increases (see the insert in Fig.3).

Fig.4 shows the potential energy of molecular hydrogen as a function of the separation between two protons. When the centrifugal potential is added to the Morse potential, the double barrier shape appears. The maximum value of angular momentum,  $l$ , for the double barrier shape is 38 for hydrogen. This has been confirmed by the experiment for meta-stable excited state of hydrogen<sup>9</sup>. The corresponding value for deuterium is about 56, and the critical  $l$  to have a potential bottom lower than zero is about 45. This is the number cited for the calculation of Ta

## Split Coulomb Barrier Model

The progressive "excess heat" experiments show that: (1) the "excess heat" power is confirmed already to be no less than 1 W/c.c. in a closed system<sup>10,11</sup>, which corresponds to  $10^{12}$  reactions/c.c. if 1 MeV energy is released in each reaction. This reaction rate require another factor of  $10^9$  enhancement further in the factor  $T_a$ ; (2) no quantitative nuclear products have been detected up to now.

These two facts mean that the main energy source for the "excess heat" may not be nuclear origin. If we look at the SRI data<sup>10</sup>, the total energy released in a closed system is about 1 MJ, and the total investment of D<sub>2</sub>O, D<sub>2</sub>, Pd, Li, and O<sub>2</sub> is about 0.5 mol. So the average energy released by each atom is still less than keV. Although it is greater than the energy released by any chemical or mechanical process with which we are aware, it is still not necessary to be nuclear origin.

On the other hand, the nuclear fragments in the discharge experiment<sup>12</sup> are showing that the high Z palladium nuclei might be penetrated also. Although the amount of nuclear fragments is so small to be account for the "excess heat" production, it gives some hints about the necessary process happened before the penetration.

The high Z Coulomb barrier is hard for the centrifugal barrier to be in balance with it, because the high Z Coulomb barrier would reduce the  $(\theta_a)^2$  by reduce the maximum value of angular momentum,  $l_{max}$ , and increase the  $(\theta_N)^2$  by enhancing the height and width of the Coulomb barrier. The possible solution is to speculate a "split Coulomb barrier" (Fig.5). Assuming a step-wise Coulomb barrier, we may calculate the corresponding penetration factor  $\theta_{N0}$  and  $\theta_{N4}$ .

$$\theta_{N0} = \exp\left[\int_{r_0}^{r_1} \sqrt{\frac{2\mu}{\hbar^2}(U(r) - E)} dr\right]$$

$$\theta_{N4} = \exp\left[\int_{r_4}^{r_5} \sqrt{\frac{2\mu}{\hbar^2}(U(r) - E)} dr\right]$$

For the rough estimation, we assume a triangular potential shape with a height of Coulomb barrier, i.e.

$$U(r) = \frac{Ze^2}{r_o} \frac{r_1 - r}{r_1 - r_o} \quad \text{for } r_o < r < r_1$$

$$U(r) = \frac{Ze^2}{r_4} \frac{r_5 - r}{r_5 - r_4} \quad \text{for } r_4 < r < r_5$$

Then ,

$$\theta_{N0} = \exp\left[\frac{2}{3}\sqrt{\frac{2\mu Z}{m_e a_0 r_0}} (r_1 - r_0)\right]$$

$$\theta_{N4} = \exp\left[\frac{2}{3}\sqrt{\frac{2\mu Z}{m_e a_0 r_4}} (r_5 - r_4)\right]$$

In order to have right penetration rate, we need

$$\left(\frac{\theta_{N4}}{\theta_{N0}}\right)^2 \sim 2.3 \times 10^{-32}$$

to obtain the neutron emission rate observed in experiments ( $\approx 10 \text{ sec}^{-1} \text{ cm}^{-3}$ , which corresponds to a reaction cross section of  $10^{-25} \text{ barns}$ ). This turns out to be a set of parameters as  $r_0=10^{-12} \text{ cm}$ ,  $r_1=2 \times 10^{-10} \text{ cm}$ ,  $r_4=5.5 \times 10^{-10} \text{ cm}$ ,  $r_5=5 \times 10^{-9} \text{ cm}$ . It is just a speculation of this split Coulomb barrier.

### A Proposed Experiment

This speculation can be tested in two ways. The first is to find a kind of penetration of Coulomb barrier caused by the surrounding electrons in a hydrogen-loaded metal. The second is to search the high electron density region which is necessary for the split of Coulomb barrier.

The uranium-238 is proposed to be a test material for its two features. It can absorb a huge amount of hydrogen as palladium and it has an unexpectedly high spontaneous fission rate. The fission barrier for uranium-238 is higher than that of uranium-235; however, the spontaneous fission rate of U-238 is much greater than of U-235 by several orders of magnitude. This implies that the spontaneous fission of U-238 may be enhanced by some resonance penetration. If we can change the electron density by loading the hydrogen, and detect the change of the spontaneous fission rate, this would be a direct proof that the nuclear process could be affected by the manipulation in the molecular scale.

We may imagine also that the high electron density region must be formed somewhere in the metal to split the Coulomb barrier; therefore, the positron annihilation technique might be useful to find this anomaly.

### Acknowledgments

This work is supported by the State Commission of Science and Technology, and the Natural Science Foundation of China. The author is grateful to Dr. Bor Y. Liaw for his hospitality during the sabbatical at University of Hawaii at Manoa, and to the EPRI for their support in travel.

## References

1. X. Z. Li, D. Z. Jin, and L. Chang. "The Combined Resonance Tunneling and Semi-Resonance Level in Low Energy D-D Reaction." in *Frontiers of Cold Fusion*, Edited by H. Ikegami, Universal Academy Press, Tokyo ,1993, pp.597-600.
2. X. Z. Li. "The Anomalous Nuclear Phenomena and the Plasma Discharge." Chinese Physics Letters. Vol.10, Supplement, p.362 (1993).
3. S. E. Koonin ,and M. Nauenberg, "Calculated Fusion Rates in Isotopic Hydrogen Molecules." Nature ,Vol. 339, p.690 (1989).
4. C.D.V. Siclen, and S. E. Jones. "Piezonuclear Fusion in Isotope Hydrogen Molecules." J. Physics G: Nucl. Physics. Vol.12, p.213 (1986).
5. M. Jandel. "The Fusion Rate in the Transmission Resonance Model." Fusion Technology. Vol.21, p.176 (1992).
6. D. K. Roy, *Quantum Mechanical Tunnelling and Its Applications*. Singapore, World Scientific, 1986, pp.1-79.
7. L. D. Landau, and E. M. Lifshitz. *Quantum Mechanics*. 2-nd editions, Pergamon, Oxford, Addison-Wesley, 1965, pp.15-17.
8. S. Bjørnholm, et al., "The Double-Humped Fission Barrier." Rev. Mod. Phys. Vol.52, p.725 (1980).
9. J. Simsons. "Roles Played by Metastable States in Chemistry." in *Resonances in Electron-Molecule Scattering, Van der Waals Complexes, and Reactive Chemical Dynamics*. Ed. D.G.Truhlar, ACS, Washington, D.C. 1984, pp.1-16.
10. M.C.H. McKubre, et al. "Excess Power Observations in Electrochemical Studies of the D/Pd System; the Influence of Loading." in *Frontiers of Cold Fusion*, Edited by H. Ikegami, Universal Academy Press, Tokyo ,1993, pp.5-19.
11. M. Fleischmann and S. Pons. "Calorimetry of the Pd-D<sub>2</sub>O System: from Simplicity via Complications to Simplicity." Physics Letters, A, Vol. 176, p.118 (1993).
12. A.B. Karabut, Ya. R. Kucherov and I.B. Savvatimova. "Nuclear Product Ratio for Glow Discharge in Deuterium." Physics Letters. A. Vol.170, p.265 (1992).

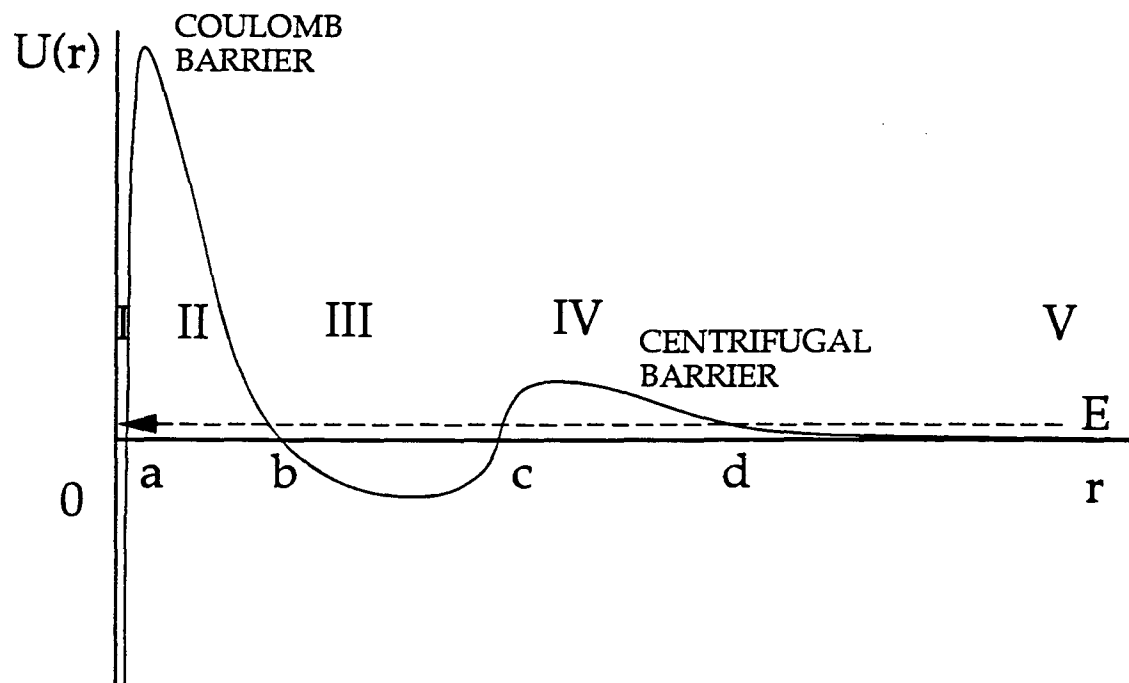


Fig.1. Combined Resonance Tunneling in 3-Dimensional Case

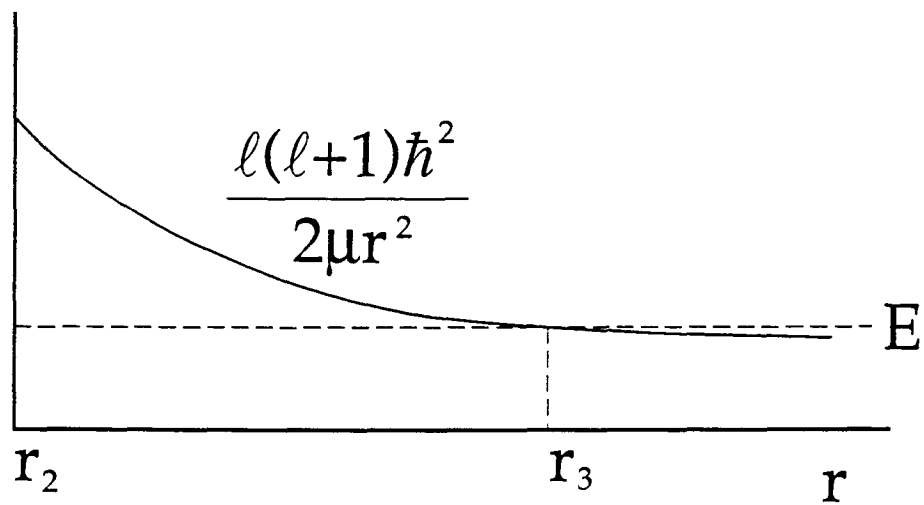


Fig.2 Centrifugal Potential Barrier

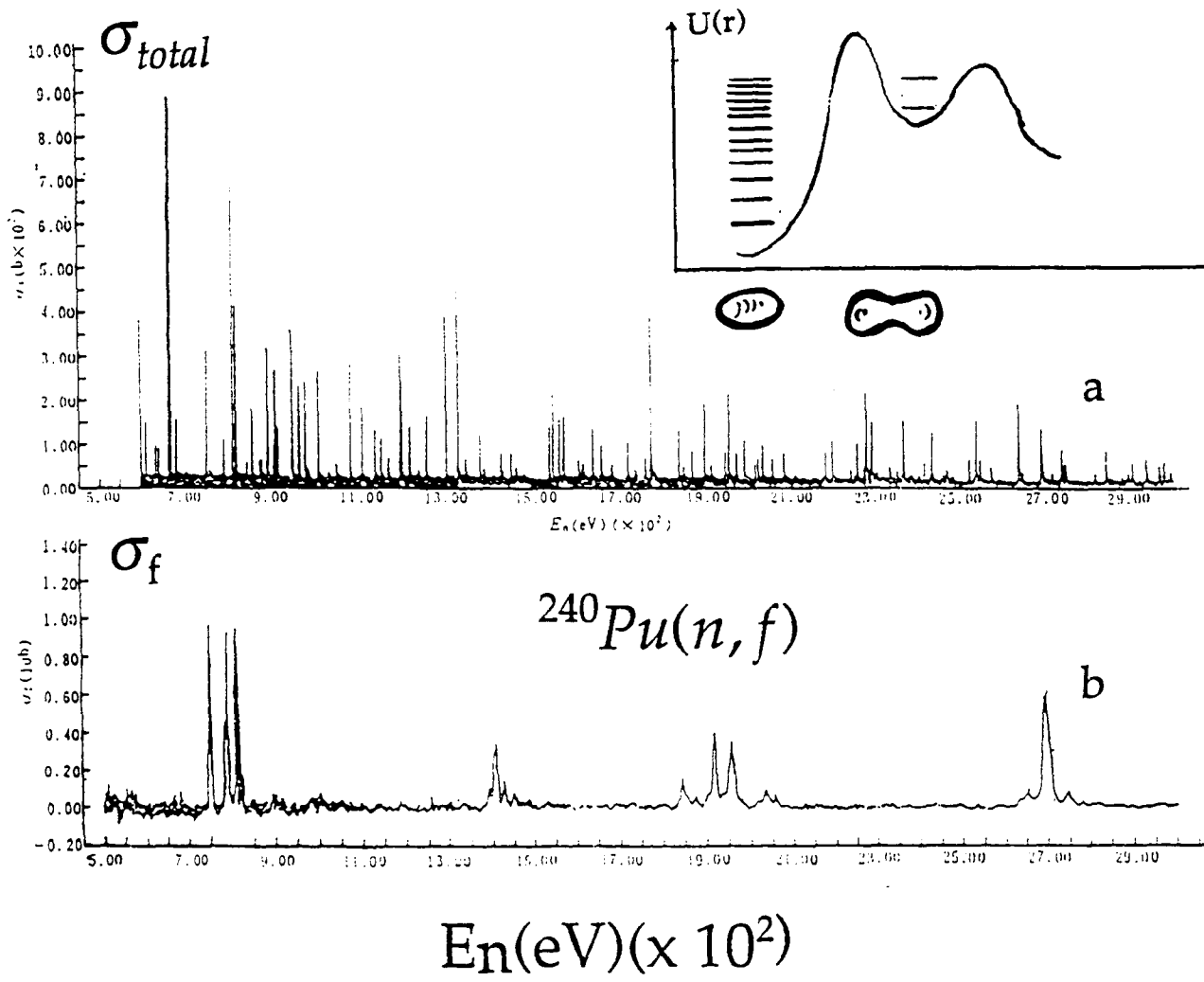


Fig.3. Above: The total neutron cross section of  $^{240}\text{Pu}$ , showing the large number of fine-structure resonances.  
 Below: The neutron fission cross section of  $^{240}\text{Pu}$ , showing a very few fine-structure resonances of appreciable strength and those clustered into a few groups that constitute intermediate resonances in the fission channel.

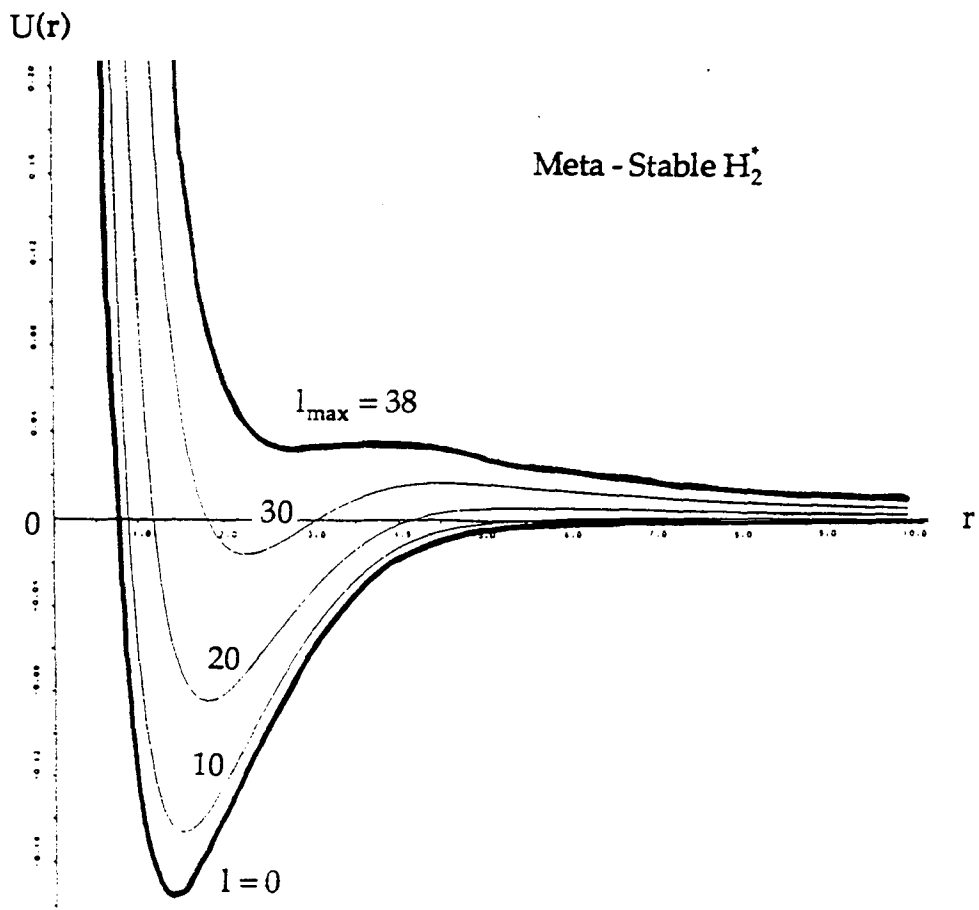


Fig.4. The Potential Energy Curves for Different Angular Momentum Cases  
 $l=0$ : the pure Morse potential for  $H_2$  molecule;  
 $l=38$ : the maximum possible centrifugal potential which may still allow a meta-stable state of  $H_2^*$ .

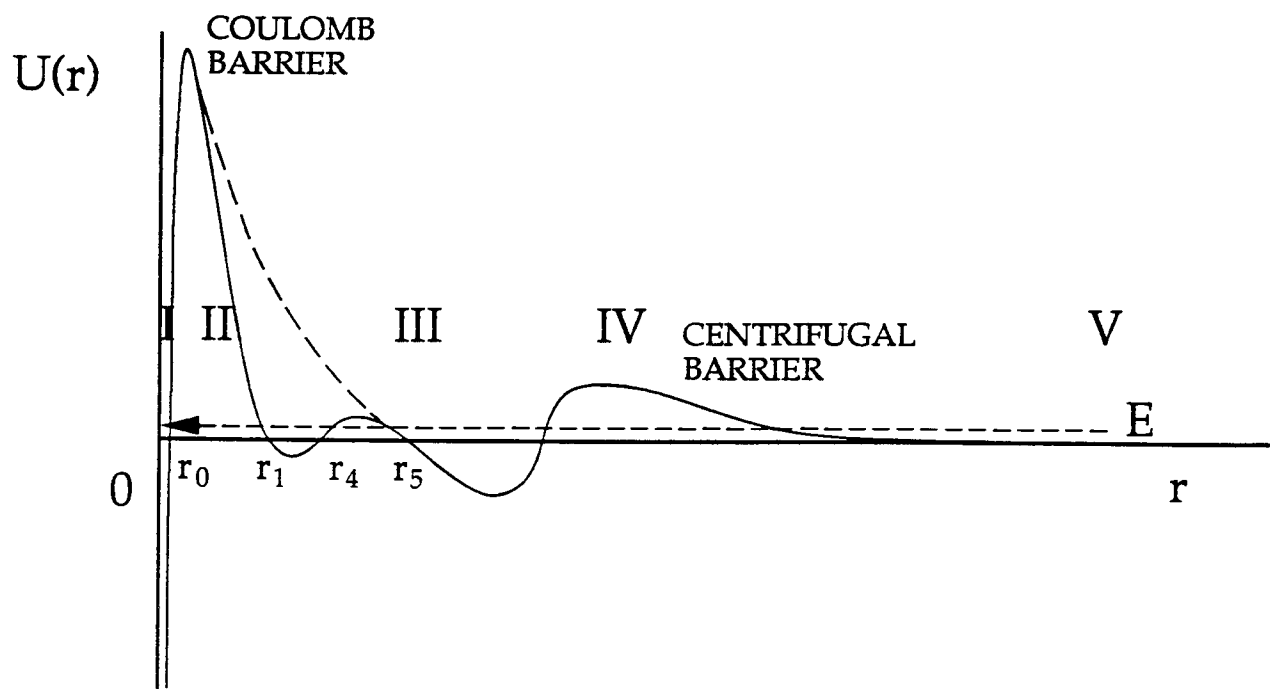


Fig.5. Split Coulomb Barrier Model



# REACTION BARRIER TRANSPARENCY FOR COLD FUSION WITH DEUTERIUM AND HYDROGEN

Yeong E. Kim,  
Jin-Hee Yoon

Department of Physics, Purdue University  
West Lafayette, IN 47907

Alexander L. Zubarev

Racah Institute of Physics, Hebrew University  
Jerusalem 91904, Israel

Mario Rabinowitz  
Electric Power Research Institute  
Palo Alto, CA 94303

## Abstract

An improved parametric representation of Coulomb barrier penetration is presented. These detailed calculations are improvements upon the conventionally used Gamow tunneling coefficient. This analysis yields a reaction barrier transparency (RBT) which may have singular ramifications for cold fusion, as well as significant consequences in a wide variety of fusion settings.

## 1. Introduction

Recently, Kim and Zubarev<sup>1</sup> developed a general and realistic barrier transmission model which can accommodate simultaneously both non-resonance and Coulomb barrier transmission resonance contributions. The derivations for both cases will be presented. The resonance analysis culminates in a reaction barrier transparency (RBT) which is due to the interaction of the transmitted and reflected waves yielding constructive interference in a narrow energy regime. Although RBT may have significant consequences for a wide variety of fusion problems, we will explore cold fusion applications here.

## 2. Conventional Parameterization

The conventional protocol for determining low-energy (< 20 keV) fusion cross-sections  $\sigma(E)$  is to extrapolate experimental values of  $\sigma(E)$  measured at high energies using the parameterization<sup>2</sup>

$$\sigma(E) = \frac{S(E)}{E} T_G(E) \quad (1)$$

where  $T_G(E) = \exp[-(E_G/E)^{1/2}]$ ,  $E_G = (2\pi\alpha Z_1 Z_2)^2 \mu c^2 / 2$  with the reduced mass  $\mu = m_1 m_2 / (m_1 + m_2)$  and  $E$  is the center-of-mass (CM) kinetic energy. The transmission coefficient (“Gamow” factor)  $T_G(E)$  results from the approximation  $E \ll B$  (Coulomb barrier height). This technique is used for nuclei in non-resonance reactions such as in standard solar model, and magnetic and inertial confinement calculations.

In order to generalize the conventional Gamow transmission coefficient, we introduce for the fusing system the following potential which consists of an interior square-well nuclear potential and an exterior Coulomb repulsive potential,

$$V(r) = \begin{cases} -V_0, & r < R \\ Z_1 Z_2 e^2 / r, & r \geq R \end{cases}. \quad (2)$$

For the potential barrier given by eq. (2), an approximate  $S$ -wave ( $\ell = 0$ ) solution for  $T(E)$  can be calculated in the Wentzel–Kramers–Brillouin (WKB) approximation as<sup>3</sup>

$$\begin{aligned} T_R^{\text{WKB}}(E) &= \exp \left\{ -2 \left( \frac{2\mu}{\hbar^2} \right)^{1/2} \int_R^{r_a} \left( \frac{Z_1 Z_2 e^2}{r} - E \right)^{1/2} dr \right\} \\ &= \exp \left( - \left( \frac{E_G}{E} \right)^{1/2} \left( \frac{2}{\pi} \right) \left\{ \cos^{-1} \left[ \left( \frac{E}{B} \right)^{1/2} \right] - \left( \frac{E}{B} \right)^{1/2} \left( 1 - \frac{E}{B} \right)^{1/2} \right\} \right) \end{aligned} \quad (3)$$

where  $B$  is the Coulomb barrier height,  $B = Z_1 Z_2 e^2 / R$ , and  $r_a$  is the classical turning point,  $Z_1 Z_2 e^2 / r_a = E$ . Note that  $T_R^{\text{WKB}}(E)$  is defined only for  $E \leq B$  and that  $T_R^{\text{WKB}}(B) = 1$ . The traditional Gamow transmission coefficient used in eq. (1) can be obtained from eq. (3) with  $R = 0$  (or equivalently  $E \ll B$ ):

$$\begin{aligned} T_G(E) &= T_R^{\text{WKB}}(E) = \exp \left\{ -2 \left( \frac{2\mu}{\hbar^2} \right)^{1/2} \int_0^{r_a} \left( \frac{Z_1 Z_2 e^2}{r} - E \right)^{1/2} dr \right\} \\ &= \exp \left[ - \left( \frac{E_G}{E} \right)^{1/2} \right]. \end{aligned} \quad (4)$$

### 3. Kim–Zubarev Parameterization

$T_G(E)$ , eq. (4), represents the probability of bringing two particles to zero separation distance. This implies that the Coulomb barrier  $Z_1 Z_2 e^2 / r$  also exists inside the nuclear surface of radius  $R$ , which is unphysical and unrealistic. In order to accommodate more realistic transmission coefficients, Kim and Zubarev<sup>1,4</sup> have recently introduced a more general parameterization for  $\sigma(E)$  based on the  $P$ -matrix parameterization of the fusion reaction  $S$ -matrix.

To obtain improved and more general transmission coefficients, we use partial wave solutions of the Schrödinger equation. For the potential described by eq. (2), a general solution of the radial Schrödinger equation for the exterior wave function in the exterior region ( $r \geq R$ ) is given by<sup>5</sup>

$$u_\ell^{\text{ext}}(r) = u_\ell^{(-)}(r) - \eta u_\ell^{(+)}(r) \quad (5)$$

where

$$u_\ell^{(+)}(r) = e^{-i\delta_\ell^c} [G_\ell(r) + i F_\ell(r)] . \quad (6)$$

$\delta_\ell^c$  is the Coulomb phase shift and  $u_\ell^{(-)}$  is the complex conjugate of  $u_\ell^{(+)}$ .  $F_\ell$  and  $G_\ell$  are the regular and irregular Coulomb wave functions normalized asymptotically ( $r \rightarrow \infty$ ) as

$$\begin{aligned} F_\ell(r) &\approx \sin[kr - \ell\pi/2 - \gamma\ell n(2kr) + \delta_\ell^c] \\ G_\ell(r) &\approx \cos[kr - \ell\pi/2 - \gamma\ell n(2kr) + \delta_\ell^c] \end{aligned} \quad (7)$$

where  $\gamma$  is the Sommerfeld parameter,  $\gamma = Z_1 Z_2 e^2 / \hbar v$ , and  $k$  is related to  $E$  by  $E = \hbar^2 k^2 / 2\mu$ .

In terms of the partial wave  $S$ -matrix,  $\eta_l$ , in eq. (5), the fusion reaction total cross-section  $\sigma_r(E)$  is given by<sup>5</sup>

$$\sigma_r(E) = \frac{\pi}{k^2} \sum_l (2l+1)(1 - |\eta_l|^2) . \quad (8)$$

To accommodate the statistical factor and to compensate the two-body approximation involved in deriving eq. (8), we introduce the partial wave  $S$ -factor,  $S_l(E)$ , which is expected to be nearly energy-independent or weakly energy-dependent, and rewrite

$$\sigma_r(E) \approx \sigma(E) = \frac{1}{E} \sum_{l=0}^{\infty} S_l(E) T_l(E) = \sum_l \sigma_l(E) \quad (9)$$

where  $S_l(E)$  is the  $l$ -th partial wave  $S$ -factor and

$$\sigma_l(E) = \frac{S_l(E)}{E} T_l(E) \quad (10)$$

with

$$T_l(E) = 1 - |\eta_l|^2 . \quad (11)$$

In order to determine the partial wave  $S$ -matrix  $\eta_l$  in eq. (5), we introduce the  $P$ -matrix as the logarithmic derivative of the interior wave function  $u_l^{int}(r)$  at  $r = R$ :

$$P_l^{int} = R \left. \frac{du_l^{int}/dr}{u_l^{int}} \right|_{r=R} = \Re P_l^{int} + i \Im P_l^{int} \quad (12)$$

where  $\Re P_l^{int}$  and  $\Im P_l^{int} (< 0)$  are the real and imaginary parts of  $P_l^{int}$ , respectively. For the exterior wave function, the  $P$ -matrix at  $r = R$  is defined as

$$P_l^{ext} = R \left. \frac{du_l^{ext}/dr}{u_l^{ext}} \right|_{r=R} = R \left. \frac{du_l^{(-)}/dr - \eta_l du_l^{(+)}/dr}{u_l^{(-)} - \eta_l u_l^{(+)}} \right|_{r=R} \quad (13)$$

We introduce the  $P$ -matrix for  $u_l^{(+)}$  as

$$P_l^{(+)} = R \left. \frac{du_l^{(+)} / dr}{u_l^{(+)}} \right|_{r=R} = \Delta_l + i s_l \quad (14)$$

where  $\Delta_l$  and  $s_l$  are the real and imaginary parts of  $P_l^{(+)}$ , respectively. By matching the logarithmic derivatives at  $r = R$ , i.e.,  $P_l^{int} = P_l^{ext}$ , we obtain<sup>1,4</sup>

$$T_l(E) = 1 - |\eta_l|^2 = \frac{-4s_l \Im P_l^{int}}{(\Delta_l - \Re P_l^{int})^2 + (s_l - \Im P_l^{int})^2} \quad (15)$$

where

$$\Delta_l = \Re P_l^{(+)} = R \left. \frac{G_l G'_l + F_l F'_L}{G_l^2 + F_l^2} \right|_{r=R}, \quad (16)$$

and

$$s_l = \Im P_l^{(+)} = R \left. \frac{G_l F'_l - F_l G'_L}{G_l^2 + F_l^2} \right|_{r=R}. \quad (17)$$

In the Kim-Zubarev parameterization of  $T_l(E)$ ,  $\Im P_l^{int}$  and  $\Re P_l^{int}$  are to be parameterized directly or in terms of a potential model wave function for the interior region ( $r < R$ ).

#### 4. Reaction Barrier Transparency

We note that the reaction barrier transparency(RBT),  $T_l(E) \approx 1$ , can occur when  $\Delta_l = \Re P_l^{int}$  and  $s_l = -\Im P_l^{int}$ . For simplicity, our discussion in this paper will be limited to the  $S$ -wave case,  $l = 0$ , in the following. Generalization to the  $l \neq 0$  cases is straight forward.<sup>4</sup>

For the potential given by eq. (2), a general solution for the interior ( $r \leq R$ ) wave function is

$$u^{int}(r) = e^{-iKr} + c e^{+iKr} \quad (18)$$

where  $\hbar^2 K^2/2\mu = V_0 + E$  with  $E = \hbar^2 k^2/2\mu$ . We introduce two real parameters  $\tau_0$  and  $\phi_0$  and write  $c = \tau_0 e^{i\phi_0}$  ( $\tau_0 < 1$ ).

If the lowest partial wave ( $l = 0$ ) contribution is expected to be dominant for low energies ( $\lesssim 20$  keV), then the total cross-section  $\sigma(E)$  is given by

$$\sigma(E) \approx \sigma_0(E) = \frac{S_0^{KZ}(E)}{E} T_0^{KZ}(E) \quad (19)$$

and  $T_0^{KZ}(E) = 1 - |\eta_0|^2$  is given by

$$T_0^{KZ}(E) = \frac{-4s_0 \Im P_0^{int}}{(\Delta_0 - \Re P_0^{int})^2 + (s_0 - \Im P_0^{int})^2} = \frac{4s_0 \bar{K}_1 R}{(\Delta_0 - \bar{K}_2 R)^2 + (s_0 + \bar{K}_1 R)^2} \quad (20)$$

where

$$s_0 = R[(G_0 F'_0 - F_0 G'_0)/(G_0^2 + F_0^2)]_{r=R} = [kR/(G_0^2 + F_0^2)]_{r=R} \quad (21)$$

$$\Delta_0 = R[(G_0 G'_0 + F_0 F'_0)/(G_0^2 + F_0^2)]_{r=R} \quad (22)$$

$$\bar{K}_1(E, \tau_0, \phi_0) = -\Im P_0^{int} = \frac{K(1 - \tau_0^2)}{1 + 2\tau_0 \cos(2KR + \phi_0) + \tau_0^2} \quad (23)$$

and

$$\bar{K}_2(E, \tau_0, \phi_0) = \Re P_0^{int} = \frac{-2K\tau_0 \sin(2KR + \phi_0)}{1 + 2\tau_0 \cos(2KR + \phi_0) + \tau_0^2}. \quad (24)$$

$T_0^{KZ}(E)$ , eq. (20), is described by four parameters,  $V_0$ ,  $R$ ,  $\tau_0$ , and  $\phi_0$ .  $T_0^{KZ}(E)$  contains both non-resonance and resonance contributions, and also the interference term between them. The four parameters can be determined from the cross-section containing both a resonance part (resonance energy and width) and a non-resonance background.

We note that  $T_0^{KZ}(E) \approx 1$  when RBT condition,  $\Delta_0 = \bar{K}_2 R$  and  $s_0 \approx \bar{K}_1 R$ , is satisfied in eq. (20). The resonance energy  $E_r$  (for  $T_0^{KZ}(E_r) \approx 1$ ) and width  $\Gamma$  are determined by the parameters  $\tau_0$  and  $\phi_0$  for fixed values of  $V_0$  and  $R$ . The resonance behavior of  $T_0^{KZ}(E)$ , generated from fitting  $\sigma(E)$  with particular values of parameters, is a reaction barrier transparency(RBT) due to an interplay of Coulomb barrier and nuclear interaction, and is to be distinguished from conventional resonances such as narrow neutron( $\Delta_0 = 0$ ) capture resonances, which are primarily due to the nuclear interaction. The resonances present in  $\sigma(E)$ , which are shown by some related experiments to be of a non-RBT type, are to be treated by conventional methods. Very broad resonance behaviors for cross-sections observed in many nuclear reactions<sup>6</sup> such as for reactions  $^2\text{H}(D, p)^3\text{He}$ ,  $^2\text{H}(D, n)^3\text{He}$ ,  $^3\text{He}(D, p)^4\text{He}$ , and  $^3\text{H}(D, n)^4\text{He}$  may correspond to RBT resonances and may yield different low-energy extrapolations from those obtained by the use of the conventional transmission coefficient,  $T_G(E)$ , since the low-energy tail of the RBT resonance is expected to be different from that of the conventional case.

For the case of a non-resonance cross-section,  $\tau_0 = 0$ , and  $T_0^{KZ}(E)$ , eq. (20), reduces to the result given by Blatt and Weisskopf<sup>5</sup>,

$$T_{BW}(E) = \frac{4s_0KR}{\Delta_0^2 + (s_0 + KR)^2}. \quad (25)$$

It should be noted that  $T_{BW}(E)$ , eq. (25), does not have a resonance structure while  $T_0^{KZ}(E)$  does.

In the previous parameterizations of  $\sigma(E)$ , the resonance part of  $\sigma(E)$  is parameterized with the Breit-Wigner resonance formula to be subtracted from the experimental data<sup>2,3</sup> or included in  $S(E)$  in eq. (1).<sup>6</sup> The non-resonance formula, eq. (1), is then used to fit the resultant "data." Our more general formula for  $T_0^{KZ}(E)$ , eq. (20), with eq. (19), will allow us to parameterize the experimental data exhibiting the RBT resonance behavior by the same formula, eq. (19), thus avoiding separate use of the Breit-Wigner formula for subtracting the resonance contribution from  $\sigma(E)$ . Furthermore, the interference term between the resonance and non-resonance contributions is automatically included in eqs. (19) and (20). The formulation described by eqs. (9), (15), (19), and (20) is a generalization of eq. (1) and thus can provide a more realistic and general parameterization method for low-energy nuclear fusion cross-sections needed for the solar neutrino and astrophysical calculations, magnetic and inertial confinement fusion calculations, and low-energy (cold) fusion rate calculations.

## 5. Fusion Rate Estimates with Narrow RBT

Since  $\cos(2KR + \phi_0)$  (in eqs. (23) and (24)) and  $\sin(2KR + \phi_0)$  (in eq. (23)) satisfies  $\cos^2(2KR + \phi_0) + \sin^2(2KR + \phi_0) = 1$ ,  $\tau_0$  can be expressed in terms of  $K$ ,  $\bar{K}_1$ , and  $\bar{K}_2$  as

$$\tau_0^2 = \frac{(K - \bar{K}_1)^2 + \bar{K}_2^2}{(K + \bar{K}_1)^2 + \bar{K}_2^2} \quad (26)$$

For the case of  $\bar{K}_2 R = \Delta_0$  and  $\bar{K}_1 R = N s_0$  (RBT condition) where  $N > 0$  is a real constant, we obtain using eq. (26)

$$\tau_0^2 = \frac{(KR - N s_0)^2 + \Delta_0^2}{(KR + N s_0)^2 + \Delta_0^2} \quad (27)$$

and

$$1 - \tau_0^2 = \frac{4N s_0 K R}{(KR + N s_0)^2 + \Delta_0^2} \quad (28)$$

After determining  $\tau_0$  from eq. (27),  $\phi_0$  can be determined from

$$\sin(2KR + \phi_0) = \frac{1 - \tau_0^2}{2\tau_0} \left( \frac{-\Delta_0}{Ns_0} \right) \quad (29)$$

From eq. (20), the maximum value of  $T_0^{KZ}(E)$  is then given by

$$T_0^{max}(E) = \frac{4Ns_0^2}{(1+N)^2 s_0^2} = \frac{4N}{(1+N)^2} \quad (30)$$

which yields  $T_0^{max}(E) = 1$  for  $N = 1$  and  $T_0^{max}(E) < 1$  otherwise.

Assuming that  $T_0^{KZ}(E)$ , eq. (20), has a Breit-Wigner resonance form with a width  $\Gamma$  at a resonance energy  $E = E_r$ , the width  $\Gamma$  at low energies can be written as<sup>4</sup>  $\Gamma \approx (s_0(E_r) + \bar{K}_1 R) \times 10^7$  eV. Since  $s_0(E_r) \approx 0.3 T_G(E_r)$  and  $\bar{K}_1 R = N s_0(E_r)$ , we obtain for  $N \gg 1$

$$\Gamma \approx (0.3 \times 10^7 \text{ eV}) N T_G(E_r) \quad (31)$$

and

$$T_0^{KZ}(E_r) \Gamma = (1.2 \times 10^7 \text{ eV}) T_G(E_r) \quad (32)$$

using  $T_0^{KZ}(E_r) \approx 4/N$  from eq. (30). Since  $T_G(E_r)$  is very small near ambient temperature,  $kT = E_r = 0.025$  eV,  $\Gamma$  is also very narrow;  $\Gamma = 10^{-10}$  eV and  $\Gamma = 100^{-100}$  eV for  $T_0^{KZ}(E_r) \approx 10^{17} T_G(E_r)$  and  $T_0^{KZ}(E_r) \approx 10^{107} T_G(E_r)$ , respectively. Precise values of  $\Gamma$  for different fusion reactions can only be determined by experiments at present.

For the fusion cross-section  $\sigma(E) \approx S(0)T_0^{KZ}(E)/E$  ( $S(E) \approx S(0) = 53$  keV-barns for  $D(D, p)T$  and  $D(D, n)^3He$ ), the fusion rate can be estimated as

$$\begin{aligned} \langle \sigma v \rangle_{new} &= \int \sigma(v) v f(v) d^3v \\ &= \left( \frac{8}{\pi \mu} \right)^{\frac{1}{2}} \frac{1}{(kT)^{3/2}} \int_0^\infty \sigma(E) E e^{-E/kT} dE \\ &= \left( \frac{8}{\pi \mu} \right)^{\frac{1}{2}} \frac{S(0)}{(kT)^{3/2}} \int_0^\infty T_0^{KZ}(E) e^{-E/kT} dE \\ &\approx \left( \frac{8}{\pi \mu} \right)^{\frac{1}{2}} \frac{S(0)}{(kT)^{3/2}} T_0^{KZ}(E_r) e^{-E_r/kT} \int_{E_r - \frac{\Gamma}{2}}^{E_r + \frac{\Gamma}{2}} dE \end{aligned} \quad (33)$$

or

$$\begin{aligned} \langle \sigma v \rangle_{new} &\approx \left( \frac{8}{\pi \mu} \right)^{\frac{1}{2}} \frac{S(0)}{(kT)^{3/2}} T_0^{KZ}(E_r) e^{-E_r/kT} \Gamma \\ &= \left( \frac{8}{\pi \mu} \right)^{\frac{1}{2}} \frac{S(0)}{(kT)^{3/2}} e^{-E_r/kT} T_G(E_r) (1.2 \times 10^7 \text{ eV}) \end{aligned} \quad (34)$$

Since the conventional estimate is given by

$$\langle \sigma v \rangle_{conv} = \left( \frac{8}{\pi \mu} \right)^{\frac{1}{2}} \frac{S(0)}{(kT)^{3/2}} \int_0^\infty T_G(E) e^{-E/kT} dE , \quad (35)$$

we can conclude  $\langle \sigma v \rangle_{new} \approx \langle \sigma v \rangle_{conv}$  for the equilibrium Maxwell-Boltzmann distribution  $f(v)$  at ambient temperature of  $kT \approx 0.025$  eV. However, non-equilibrium energy sweeping through the narrow RBT may result in a greatly enhanced fusion rate<sup>7</sup> as in cold fusion experiments. Recent observations<sup>8-11</sup> of anomalous neutron bursts during thermal cycling with deuterated high  $T_C$  superconducting materials may be attributable to energy sweeping involving a non-equilibrium state during the superconducting phase transition.

## 6. RBT Mechanism for Other Fusion Reactions

In view of our new result  $T_0^{KZ}(E)$ , eq. (20) or  $T_l(E)$ , eq. (15), it is appropriate to ask whether some fusing systems can support an RBT at low energies near the fusion threshold. This can only be answered at present by experiments. It should be emphasized that RBT cold fusion is possible not only with deuterium but also with hydrogen since  $T_0^{KZ}(E)$ , eq. (20), is applicable to both cases as long as the RBT exist in fusing systems involving deuterium or hydrogen, such as in nuclear fusion reactions with the entrance channels,  $D + D$ ,  $D + Li$ ,  $D + Pd$ ,  $H + D$ ,  $H + K$ , etc.

Given the RBT mechanism for cold fusion the question remains why fusion products are observed in cold fusion experiments at a much lower level than commensurate with the observed excess heat. This question can only be addressed separately for each fusion reaction since the exit channels are different for each reaction. The anomalous excess heat and tritium production reported in many electrolysis or similar experiments may not be due to  $D - D$  fusion, but may include nuclear fusion with hydrogen and/or impurity nuclei which are always present. This scenario and others such as  $^6Li(d,p)^7Li$ ,  $^7Li(d,^4He)^5He$ , etc. may explain the results of excess heat, tritium and neutron production observed in heavy water (with  $Li$ ) electrolysis experiments. Scenarios for other cases involving both deuterium and hydrogen may be possible and need to be investigated.

## 7. Summary and Conclusion

Our progressively more generalized parametric representation of Coulomb barrier tunneling yields significant improvements upon the conventionally used Gamow tunneling coefficient. This analysis yields RBT which is due to the interaction of the transmitted and reflected quantum waves yielding constructive interference in a narrow energy regime. RBT appears to have important ramifications for cold fusion.

## References

1. Y. E. Kim and A. L. Zubarev, "Coulomb Barrier Transmission Resonance for Astrophysical Problems", Purdue Nuclear Theory Group Report PNTG-93-8 (August 1993), to be published in Modern Physics Letters B.
2. W. A. Fowler, G. R. Caughlan, and B. A. Zimmerman, "Thermonuclear Reaction Rates", Annual Review of Astronomy and Astrophysics, 5, 525 (1967).
3. Y. E. Kim, M. Rabinowitz, J.-H. Yoon, and R. A. Rice, International Journal of Theoretical Physics, 32, 301 (1993).
4. Y. E. Kim and A. L. Zubarev, "P-Matrix Parameterization of S-Matrix for Fusion

- Reaction Cross-Section", Purdue Nuclear Theory Group Report PNTG-94-8 (1994), to be published.
5. J. M. Blatt and V. F. Weisskopf, *Theoretical Nuclear Physics*, Wiley, New York (1952), Chapter VIII.
  6. G. S. Chulick, Y. E. Kim, R. A. Rice, and M. Rabinowitz, "Extended Parameterization of Nuclear-Reaction Cross Section for Few-Nucleon Nuclei", Nuclear Physics, **A551**, 255 (1993).
  7. Y. E. Kim, "Time-Delayed Apparent Excess Heat Generation in Electrolysis Fusion Experiments", Mod. Phys. Lett. **6**, 1053 (1991).
  8. F. Celani et al., "Search for Neutron Emission from Deuterated High Temperature Superconductors in a Very Low Background Environment", Proc. of the Second International Conference on Cold Fusion, Como, Italy, June 6-July 4, 1991 (Italian Physical Society Conference Proceedings, Vol. 33), p. 113.
  9. F. Celani et al., "Measurements in the Gran Sasso Laboratory : Evidence for Nuclear Effects in Electrolysis with  $Pd/Ti$  and in Different Tests with Deuterated High Temperature Superconductors", AIP Conf. Proc. No. 228 (1991), p. 62.
  10. A. G. Lipson et al., "Possible Cold Nuclear Fusion in Deuterated Ceramic  $YBa_2Cu_3O_{7-x}$ ", Sov. Phys. Dokl. **36**, 849 (1991).
  11. A. G. Lipson et al., "Neutron Generation in  $YBa_2Cu_3O_{7-\delta}D_y$ , High Temperature Superconductors Stimulated by a Superconducting Phase Transition", Sov. Phys. Dokl. **38**, 119 (1993).

# COMMENTS ON EXOTIC CHEMISTRY MODELS AND DEEP DIRAC STATES FOR COLD FUSION

R.A. Rice

Y.E. Kim

Department of Physics

Purdue University

West Lafayette, IN 47907

M. Rabinowitz

Electric Power Research Institute

Palo Alto, CA 94303

A.L. Zubarev

Racah Institute of Physics

Hebrew University

Jerusalem 91904, Israel

## Abstract

Several models are examined in which it is claimed that cold fusion is the result either of tight binding of the electrons in H isotope atoms or molecules, or of an electron-H isotope resonance which allows a higher probability of Coulomb barrier penetration. In the case of models in which the electron is tightly bound to the H isotope atom, we show that states below the most deeply bound ( $-16.39$  eV) are impossible in principle. We also present evidence against the possibility of the existence of electron-H isotope resonances. Finally, a lower bound is found for the binding energy of H isotope molecules which is above that calculated in the tightly bound electron-H isotope models.

## 1. Tightly Bound Hydrogen and Deuterium

A number of models assume the existence of an exotic chemical system whose occurrence either precedes nuclear synthesis or makes it quite unnecessary. The similarity of these postulated models is in their tight binding of electrons in atoms and/or molecules. In one of the simplest, the authors<sup>1</sup> claim that in addition to the normal energy levels for the H atom, a more tightly bound sub-ground state of  $-27.17$  eV is possible. For them, the excess Cold Fusion (CF) power, with no nuclear products, is simply the extra 13.68

eV/atom obtained as H isotopes go into the sub-ground state. If their tight H abounds in the universe, one may ask why this spectral line has not been seen long ago.

Mayer and Reitz<sup>2</sup> claim that resonances of ep, ed, and et are created which, if they survive long enough, allow a high probability of Coulomb barrier penetration and subsequent nuclear reaction. Their resonance model is based on that of Spence and Vary<sup>3</sup>, who used single photon exchange in the Coulomb gauge. Recently, McNeil<sup>4</sup> reformulated the ep problem in a qualitative yet gauge-invariant way and finds no evidence for a resonance in the ep system in the energy range of interest. Therefore, it is possible that the results of Spence and Vary<sup>3</sup> and hence Mayer and Reitz<sup>2</sup> are spurious.

## 2. Deep Dirac States

Recently, Maly and Va'vra<sup>5</sup> carried out a calculation for the hydrogen atom based upon irregular solutions of the relativistic Dirac equation and obtained an extremely tightly bound electron orbit. They get a binding energy of  $\sim 500$  keV, and a radius of  $\sim 5 \times 10^{-13}$  cm, a nuclear dimension. For them, CF is primarily chemical. The excess energy is 500 keV/atom as these tightly bound atoms are formed. They suggest that this chemical ash of tightly bound H or D atoms may account for the missing mass (dark matter) of the universe. Their electron orbit radius of  $\sim 5$  fm is 50 times smaller than muonic orbits of 250 fm. If such tight D atoms existed, they should produce fusion upon collision at a much higher rate than in muon-catalyzed fusion. Moreover, there are some serious errors in their analysis. At the nuclear surface,  $r = r_n \neq 0$ , both regular and irregular solutions are allowed simultaneously for  $r \geq r_n$ . Therefore, a general solution is a linear combination of them for  $r \geq r_n$ . When the boundary conditions are imposed at  $r = r_n$ , it can be shown that the irregular component becomes nearly negligible compared to the regular component<sup>6</sup>. The results of Maly and Va'vra<sup>5</sup> are incorrect, since they assumed erroneously that the irregular solution is a general solution independent of the regular solution, as shown below in detail.

The radial part of the relativistic Schrödinger equation is<sup>7</sup>

$$\frac{1}{\rho^2} \frac{d}{d\rho} \left( \rho^2 \frac{d\psi}{d\rho} \right) + \left[ \frac{\lambda}{\rho} - \frac{1}{4} - \frac{\ell(\ell+1) - \gamma^2}{\rho^2} \right] \psi = 0 \quad (1)$$

for a point Coulomb potential  $e\phi(r) = -Ze^2/r$ , where

$$\rho = ar, \gamma = \frac{Ze^2}{\hbar c}, \alpha^2 = \frac{4(m^2c^4 - E^2)}{\hbar^2c^2}, \lambda = \frac{2E\gamma}{\hbar c\alpha}, \quad (2)$$

and  $E$  and  $m$  are the total energy and mass of the electron, respectively. Because of the centrifugal barrier, we need consider solutions of this equation for  $\ell = 0$  only because the energies corresponding to  $\ell > 0$  must be higher than the lowest  $\ell = 0$  energy. As  $\rho \rightarrow 0$ , the wavefunction  $\psi$  has the behavior

$$\psi \sim \rho^{s\pm}, \quad (3)$$

where

$$s_{\pm} = -\frac{1}{2} \pm \sqrt{\frac{1}{4} - \gamma^2}. \quad (4)$$

Because the wavefunction has the boundary condition  $\psi(\rho \rightarrow \infty) = 0$ , from eq. (2),

$$E = mc^2(1 + \frac{\gamma^2}{\lambda^2})^{-1/2}, \quad (5)$$

and  $\lambda_{\pm} = n' + s_{\pm} + 1$ , where  $n'$  is a positive integer. Furthermore, because  $\gamma = \frac{Ze^2}{\hbar c} \approx \frac{Z}{137} \ll 1$ ,

$$s_{\pm} \approx -\frac{1}{2} \pm (\frac{1}{2} - \gamma^2), \quad (6)$$

and the energy levels  $E_+$  and  $E_-$  are

$$E_+ \approx mc^2(1 + \frac{\gamma^2}{(n' + 1 - \gamma^2)^2})^{-1/2} \quad (7)$$

$$E_- \approx mc^2(1 + \frac{\gamma^2}{(n' + \gamma^2)^2})^{-1/2}. \quad (8)$$

Note that eq. (8) gives a binding energy of  $E_- - mc^2 \approx mc^2(\gamma - 1) \approx -510$  keV, so that, if the solutions corresponding to  $s_-$  were acceptable, deeply bound electron states might exist. However, these solutions are incorrect. Furthermore, eq. (7) gives the correct observed binding energy of  $E_+ - mc^2 = -13.6$  eV for  $n' = 0$  and  $Z = 1$ .

The energy levels, eqs. (7) and (8), obtained from the relativistic Schrödinger equation, eq. (1), are similar to those of Maly and Va'vra<sup>5</sup> (their eq. (24)) for the Dirac equation<sup>7</sup>. The same shortcoming, detailed below, applies to their solution; however, it is less transparent than our example because the Dirac equation involves a set of coupled differential equations<sup>7</sup>.

We can assume that the potential  $e\phi(r)$  is given realistically by

$$e\phi(r) = \begin{cases} -\frac{Ze^2}{r_n}, & r < r_n \\ -\frac{Ze^2}{r}, & r \geq r_n \end{cases}. \quad (9)$$

The wavefunction  $\chi(r) = r\psi(r)$  then, as  $r_n \rightarrow 0$ , has the following form:

$$\chi(r) = \begin{cases} AKr, & r < r_n \\ B\rho^{s_++1} + C\rho^{s_-+1}, & r \gtrsim r_n \end{cases}, \quad (10)$$

where  $(\hbar c)^2 K^2 = (E + \frac{Ze^2}{r_n})^2 - m^2 c^4$ . Note that, in eq. (10), we have used the regular solution  $\chi = A \sin Kr$  for the interior wavefunction, which is zero at the origin, as it must

be for a finite potential, and the form of the exterior wavefunction comes from the analytic solution of eq. (1).

When we equate logarithmic derivatives

$$\frac{1}{\chi} \frac{d\chi}{dr} \Big|_{r=r_n^-} = \frac{1}{\chi} \frac{d\chi}{dr} \Big|_{r=r_n^+} \quad (11)$$

we obtain,

$$\frac{C}{B} = -\frac{s_+}{s_-} (\alpha r_n)^{s_+ - s_-} \approx -\frac{\gamma^2}{1 - \gamma^2} (\alpha r_n)^{1 - 2\gamma^2}, \quad (12)$$

so that, for a physical wavefunction, as  $r_n \rightarrow 0$ , the solution corresponding to  $s_-$  does not contribute. However, because of the finite size of the nucleus, the wavefunction consists of a large component corresponding to  $s_+$  and a small component corresponding to  $s_-$  with a binding energy which is thus very close to the original binding energy  $E_+ - mc^2$ . For instance, for the case of a proton, the proton radius  $r_n \approx 1$  fm,  $Z = 1$ , and  $E \approx E_+ = mc^2 - 13.6$  eV; therefore  $\alpha \approx 3.78 \times 10^{-5}$  fm $^{-1}$ , and hence  $C/B \approx -0.2 \times 10^{-8}$ .

### 3. Tightly Bound H<sub>2</sub><sup>+</sup> and D<sub>2</sub><sup>+</sup> Molecules

The next set of models involve tight H isotope molecules of radius  $\sim 0.25$  Å in which excess energy may result chemically, and/or from nuclear fusion as the tightly bound atoms more easily penetrate their common Coulomb barrier<sup>8</sup>. Actually, there seems to be no sound basis for assuming the existence of a superbound state of a D<sub>2</sub><sup>+</sup> ion. Some of the analysis is qualitative. The most critical region is barely at the boundary of applicability of the equations. An exact solution for the entire region under consideration will likely yield a potential with no local minimum. Thus the metastable state may not be present in a more rigorous analysis<sup>9</sup>. Hence, the superbound solution is at best unstable.

Gryzinsky<sup>10</sup> and Barut<sup>11</sup> present analyses to substantiate the existence of the metastable D<sub>2</sub><sup>+</sup> state based on three-body calculations for two d's and one electron. Gryzinsky treats the problem mainly classically, but invokes quantum mechanics to neglect radiation effects for his oscillating electron. Barut's analysis is based on the Bohr-Summerfeld quantization principle, and obtains a binding energy of 50 keV. Both authors, independently, conclude that a "superbound" (D<sub>2</sub><sup>+</sup>)\* molecular ion can exist in which an electron that is exactly half-way between the d's provides an attractive force and screens the d Coulomb repulsion. Vigier<sup>12</sup> presents an analysis almost identical to that of Barut<sup>11</sup>. For Barut, Gryzinsky, and Vigier, the analysis is predicated on very unlikely precise symmetry. The electron must be exactly the same distance on a line between the two d's. The tightness of the orbit violates the uncertainty principle for a Coulomb potential, but may not violate it with stronger potentials. Although a non-relativistic analysis may be warranted for the large mass H isotopes around the electron, a non-stationary electron will require a relativistic treatment because it will attain a velocity close to the velocity of light due to its small mass. Perhaps

a full relativistic calculation including spin-spin and spin-orbit coupling may save this model, but this has not been presented as yet.

#### 4. Rigorous Bound for the Binding Energies of $H_2^+$ and $D_2^+$

Recently, Kim and Zubarev<sup>13</sup> have shown a rigorous bound of  $-16.39$  eV for the binding energies of  $H_2^+$  and  $D_2^+$ , which poses a more serious difficulty for the tightly bound  $D_2^+$  models<sup>10,11,12</sup>.

The non-relativistic Hamiltonian for  $D_2^+$  (or  $H_2^+$ ) is

$$H = - \frac{\hbar^2}{2M_1} \nabla_{R_1}^2 - \frac{\hbar^2}{2M_2} \nabla_{R_2}^2 - \frac{\hbar^2}{2m_e} \nabla_{r_e}^2 - \frac{e^2}{|\vec{r}_e - \vec{R}_1|} - \frac{e^2}{|\vec{r}_e - \vec{R}_2|} + \frac{e^2}{|\vec{R}_1 - \vec{R}_2|} \quad (13)$$

where  $m_e$  and  $M_i$  ( $i = 1$  or  $2$ ) are the masses, and  $\vec{r}_e$  and  $\vec{R}_i$  are laboratory coordinates of the electron and deuteron, respectively. In terms of the center of mass coordinate  $\vec{R}_c = (m_e \vec{r}_e + M_1 \vec{R}_1 + M_2 \vec{R}_2) / (m_e + M_1 + M_2)$ , the internuclear coordinate  $\vec{R} = \vec{R}_1 - \vec{R}_2$ , and the relative electron coordinate  $\vec{r} = \vec{r}_e - (\vec{R}_1 + \vec{R}_2)/2$ , the Hamiltonian reads

$$H = - \frac{\hbar^2}{2M_t} \nabla_{R_c}^2 - \frac{\hbar^2}{2M} \left( \nabla_R + \frac{\gamma}{2} \nabla_r \right)^2 - \frac{\hbar^2}{2\mu} \nabla_r^2 - \frac{e^2}{|\vec{r}_e - \vec{R}_1|} - \frac{e^2}{|\vec{r}_e - \vec{R}_2|} + \frac{e^2}{R} \quad (14)$$

where  $M_t = m_e + M_1 + M_2$ ,  $M = (M_1 M_2) / (M_1 + M_2)$ ,  $\mu = m_e (M_1 + M_2) / (m_e + M_1 + M_2)$ , and  $\gamma = (M_1 - M_2) / (M_1 + M_2)$ . After separating the motion of the center of mass, one has the following Schrödinger equation

$$\mathcal{H}\psi(\vec{r}, \vec{R}) = E\psi(\vec{r}, \vec{R}) \quad (15)$$

where

$$\mathcal{H} = - \frac{\hbar^2}{2M} \left( \nabla_R + \frac{\gamma}{2} \nabla_r \right)^2 - \frac{\hbar^2}{2\mu} \nabla_r^2 - \frac{e^2}{|\vec{r}_e - \vec{R}_1|} - \frac{e^2}{|\vec{r}_e - \vec{R}_2|} + \frac{e^2}{R}. \quad (16)$$

The operator

$$-\frac{\hbar^2}{2M} \left( \nabla_R + \frac{\gamma}{2} \nabla_r \right)^2 = \frac{1}{2M} \left( \vec{P}_R + \frac{\gamma}{2} \vec{p}_r \right)^2 \quad (17)$$

where  $\vec{P}_R = \frac{\hbar}{i} \vec{\nabla}_R$  and  $\vec{p}_r = \frac{\hbar}{i} \vec{\nabla}_r$ , is positive. Note that  $\gamma = 0$  for  $M_1 = M_2$ . Therefore

$$\mathcal{H} \geq \tilde{H}. \quad (18)$$

or

$$\langle \psi | \mathcal{H} | \psi \rangle \geq \langle \psi | \tilde{H} | \psi \rangle , \quad \langle \psi | \psi \rangle = 1 \quad (19)$$

where

$$\tilde{H} = -\frac{\hbar^2}{2\mu} \nabla_r^2 - \frac{e^2}{|\vec{r}_e - \vec{R}_1|} - \frac{e^2}{|\vec{r}_e - \vec{R}_2|} + \frac{e^2}{R} . \quad (20)$$

But  $\tilde{H}$  is separable in confocal elliptic coordinates<sup>14</sup>, and hence the exact numerical solution of the Schrödinger equation,

$$\tilde{H} \zeta_R(\vec{r}) = E(R) \zeta_R(\vec{r}) \quad (21)$$

is well known to be<sup>14</sup>

$$\tilde{H} > E_{min}(R) = -16.39 \text{ eV} . \quad (22)$$

Since  $\mathcal{H} \geq \tilde{H}$ , we have

$$\langle \psi | \mathcal{H} | \psi \rangle > E_{min} = -16.39 \text{ eV} \quad (23)$$

for any  $|\psi\rangle$  with  $\langle \psi | \psi \rangle = 1$ .

The spin-orbit and spin-spin interactions are not expected to change the above bound of  $-16.39$  eV, eq. (23), dramatically.

## 5. Summary

We have examined several models which purportedly explain the results of Cold Fusion, and found each to be lacking in some respect. Models in which the electron is tightly bound to the hydrogen or deuterium nucleus were found to have serious qualitative or quantitative defects, and models in which it is claimed that an unusual electron resonance occurs are likely to be spurious. Finally, a lower bound for the binding energies of  $H_2^+$  and  $D_2^+$  was found which is considerably higher than the claimed binding energies in “superbound” models of the two H isotope molecules.

## References

1. R.L. Mills and S.P. Kneizys, “Excess Heat Production by the Electrolysis of an Aqueous Potassium Carbonate Electrolyte and the Implications for Cold Fusion”, *Fusion Technology* **20**, 65 (1991).
2. F.J. Mayer and J.R. Reitz, “Very Low Energy Hydrogenic Nuclear Reactions”, *Fusion Technology* **20**, 367 (1991).
3. J.R. Spence and J.P. Vary, “Electron-Proton Scattering Resonances at Low Energy from a Relativistic Two-Body Wave Equation”, *Phys. Lett. B* **271**, 27 (1991).
4. J.A. McNeil, “Relativistic Hyperfine Interaction and the Spence-Vary Resonance”, Proc. Second Cold Fusion Conf. (Como, Italy), 217 (1991).
5. J.A. Maly and J. Va’vra, “Electron Transitions on Deep Dirac Levels I”, *Fusion Technology* **24**, 307 (1993).

6. R.A. Rice, Y.E. Kim, and M. Rabinowitz, "Comment on 'Electron Transitions on Deep Dirac Levels I'", to be published in *Fusion Technology*.
7. L.I. Schiff, "Quantum Mechanics", Third Edition (McGraw-Hill Publishing Company, 1968).
8. G.F. Cerofolini and N. Re, "(D<sup>+</sup>D<sup>+</sup>)2e<sup>-</sup> Binuclear Atoms as Activated Precursors in Cold and Warm Fusion", *AIP Conf. Proc. (Provo, Utah)* **228**, 668 (1990).
9. W. Kolos *et al.*, "New Born-Oppenheimer Potential Energy Curve and Vibrational Energies for the Electronic Ground State of the Hydrogen Molecule", *J. Chem. Phys.* **84**, 3278 (1986).
10. M. Gryzinsky, "Theory of Electron Catalyzed Fusion in a Pd Lattice", *AIP Conf. Proc. (Provo, Utah)* **228**, 717 (1990).
11. A. O. Barut, "Prediction of New Tightly-Bound States of H<sub>2</sub><sup>+</sup> (D<sub>2</sub><sup>+</sup>) and Cold Fusion", *Int. J. Hydrogen Energy* **15**, 907 (1990).
12. J.-P. Vigier, "New Hydrogen Energies in Specially Structured Dense Media: Capillary Chemistry and Capillary Fusion", *Proc. Third Int. Conf. Cold Fusion (Nagoya, Japan)*, 325 (1991).
13. Y.E. Kim and A.L. Zubarev, "Rigorous Bound for Binding Energy of H<sub>2</sub><sup>+</sup> and D<sub>2</sub><sup>+</sup> Molecules", *Purdue Nuclear Theory Group Report PNTG 94-7* (1994), to be published.
14. H. Wind, "Electron Energy for H<sub>2</sub><sup>+</sup> in the Ground State", *J. Chem. Phys.* **42**, 2371 (1965).



# TRAPPED NEUTRON CATALYZED FUSION OF DEUTERONS AND PROTONS IN INHOMOGENEOUS SOLIDS

Hideo KOZIMA

Department of Physics, Faculty of Science, Shizuoka University  
836 Oya, Shizuoka 422, JAPAN

## Abstract

A proposal of a mechanism of the trapped neutron catalyzed fusion of deuterons and protons in inhomogeneous solids<sup>1,2)</sup> had been made to explain the Cold Fusion phenomena in materials occluding the deuterium (hydrogen). Some detailed analyses of the theoretical problems in the cold fusion are given in terms of the physics of thermal and cold neutrons in the inhomogeneous solids and the cascade shower induced by 6.25 MeV  $\gamma$ -ray in matrix solid. The Cold Fusion phenomena were explained semi-quantitatively and consistently by the trapped neutron catalyzed fusion model.

## The Trapped Neutron Catalyzed Fusion of Deuterons (Protons) occluded in Solids

The trial to realize the nuclear fusion on the earth has F. Paneth<sup>3)</sup> as a modern pioneer though its root could be traced to the medieval alchemists. In 1989, Fleischmann and Pons<sup>4)</sup> have opened a new passage to investigate the problem with a large possibility. Many positive results done until now show the reality of the fusion of deuterons (and protons) in transition metals. The complexity and the poor reproducibility of the experimental results obtained hitherto including the production of large excess heat, neutron bursts, much amounts of  $^4\text{He}$  and tritium etc. made the Cold Fusion phenomena<sup>1</sup> one of controversial problems in the history of science. A key to open the door to solve riddles of the Cold Fusion has been neglected by researchers until now is the thermal and cold neutrons existing everywhere abundantly. The neutron is able to fuse with another nucleus without Coulomb repulsion which is the stumbling block to realize d-d fusion by any existing methods. We will see that the difficulty to solve riddles in the Cold Fusion disappears if we take the catalytic role of the thermal and cold neutrons trapped in the sample into our consideration. A consistent explanation of almost all experimental results in the phenomena will be given along this line of consideration.

We will review the model first and then give theoretical verification of some key points assumed in it.

## Neutron as a Wave

Neutron behaves as a wave in a situation where the distribution of other object interacting with the neutron have a period  $a_0$  comparable with de Broglie wave length of the neutron.

<sup>1</sup>Perhaps it is necessary to discriminate two phenomena : the one is the excess heat generation accompanied with particle emission ( $n$ ,  $p$ ,  $t$ ,  $\gamma$ ,  $^4\text{He}$ ,  $^3\text{He}$ , etc.) and the other is without particle emission. We will call the former as the Cold Fusion phenomena. The latter may be explained as a mere chemical reaction or chemical reactions<sup>5)</sup>.

The de Broglie wave length  $\lambda$  is given as

$$\lambda = \frac{h}{p} = \frac{h}{\sqrt{2m\varepsilon}}. \quad (1)$$

where  $\varepsilon = p^2/2m$  is the energy of the neutron. If the energy of the neutron is measured in eV, the wave length in Å is given by the following relation:

$$\lambda = 2.86 \times 10^{-1} \varepsilon^{-1/2}. \quad (\text{Å}) \quad (\varepsilon \text{ in eV}) \quad (2)$$

Therefore, a thermal neutron with an energy of 1/40 eV ( $\sim 300$  K) has a wave length 1.80 Å comparable with lattice parameters of ordinary crystals. A neutron as a wave is reflected by a boundary of an ordered array of deuterons (and protons) in matrix lattices. The reflection occurs as results of the Bragg reflection and/or the total reflection. The Bragg reflection occurs when the Bragg condition

$$m\lambda = 2d \sin \theta \quad (3)$$

is satisfied, where  $m$  is an integer,  $\theta$  is the complementary angle of the incident one and  $d$  is the lattice spacing. On the other hand, the total reflection occurs when the  $\theta$  is smaller than or equal to an critical angle

$$\theta_c = \pi/2 - \sin^{-1} n_r \quad (n_r < 1), \quad (4)$$

where  $n_r = n_2/n_1$  is the relative refractive index of a medium 2 to a medium 1 and the neutron enters from 1 to 2 in the case of refraction. The refractive index  $n_i$  of the medium  $i$  is given according to the following relation :

$$n_i = 1 + \lambda^2 N_i \bar{a}_{coh}^{(i)} / 2\pi \quad (5)$$

where  $N_i$  is a number of nuclei per unit volume in the medium and  $\bar{a}_{coh}^{(i)}$  is a weighted mean of the thermal scattering lengths of the nuclei in it.

For neutrons with energy down to that of cold neutron,  $n_i$  differs not much from 1, and the critical angle of the total reflection  $\theta_c$  is given as follows:

$$\begin{aligned} \theta_c &= \lambda \left( \frac{\Delta}{\pi} \right)^{1/2}, \\ \Delta &= N_2 \bar{a}_{coh}^{(2)} - N_1 \bar{a}_{coh}^{(1)}. \end{aligned} \quad (6)$$

Therefore, the total reflection is feasible to occur at a boundary between two media with atomic nuclei whose neutron scattering lengths differ very much. The larger the difference in the scattering length, the larger the critical angle of the total reflection.

The neutron trapping time  $T$  is specified for a region surrounded by the neutron reflecting walls and depends on the geometry of the region. Because of a positive value of  $a_{coh}$  for deuteron, we can expect a total reflection by the occluded deuteron lattice in a matrix. However, because of a negative value of  $a_{coh}$  for proton, a neutron will be trapped in an occluded proton lattice surrounded by pure (low impurity) matrix.

If a region with linear dimension  $L$  larger than  $a_0$  ( $a_0 \leq L$ ) is bounded by walls of such a structure reflecting neutrons, a neutron might be trapped in the region for a time  $T$ . The time  $T$  will be determined by the state of the walls (atomic species in and widths of the walls, the geometry of the region, etc.).

On the other hand, the transit time  $\tau$  of a neutron with velocity  $v$  is given as follows for the region:

$$\tau = \frac{L}{v} = \frac{mL}{p}. \quad (7)$$

When a condition

$$\tau \ll T \quad (8)$$

is satisfied in the above mentioned situation, we may say the neutron is trapped in the region. If a neutron is trapped in a region containing nuclei which interact to fuse with the neutron, we can expect that fusion reaction is feasible to occur with high probability in the region. Fusion probability is, in the order of magnitude, becomes  $T/\tau$  times the value where there is no confinement. In an optimum situation, the neutron could be trapped with a large value of  $T/\tau$  in the sample making the fusion probability with one of deuterons very high.

### Scenario of the Cold Fusion

Thus, the scenario of the Cold Fusion in this model is summarized as follows:

(a) A particle of ambient (or artificial) thermal or cold neutrons incident on a sample (say inhomogeneous solids which occluded deuterons or protons) losing its energy in an effect of collision with nuclei in it propagates as a wave through the sample;

(b) the neutron is trapped as a standing wave in a region bounded by reflecting "walls" made of boundaries of ordered arrays of deuterons (protons). The trapping occurs as results of the Bragg and/or total reflections;

(c) the neutron as a standing wave interacts with one of deuterons (protons) in the region (and in the walls) to fuse into a triton (deuteron);

$$n + d = t(6.98\text{keV}) + \gamma(6.25\text{MeV}), \quad (9)$$

$$n + p = d(1.33\text{keV}) + \gamma(2.22\text{MeV}). \quad (10)$$

Smallness of the cross section of the reaction (9) (two orders of magnitude smaller than the cross section of d-d fusion in Eqs. (12) and (13) with appropriate energy) will be compensated with the large number and trapping of the relevant neutrons:

(d) the 6.98 keV triton produced in the reaction (9) may interact with deuterons in the sample to fuse into  ${}^4\text{He}$  and a neutron,

$$t + d = {}^4\text{He}(3.5\text{MeV}) + n(14.1\text{MeV}): \quad (11)$$

(e) the high energy neutron produced in this reaction may collide with many deuterons and accelerates them to induce d-d fusion reactions in the sample resulting in excess neutrons or tritons in an optimum situation:

$$d + d = {}^3\text{He}(0.82\text{MeV}) + n(2.45\text{MeV}), \quad (12)$$

$$= t(1.01\text{MeV}) + p(3.02\text{MeV}): \quad (13)$$

(f)  $\gamma$ -ray born in the reaction (9) (or (10)) may induce the pair creation of an electron and a positron when it passes by a nucleus  $A$ :

$$\gamma + A \rightarrow e^+ + e^- + A^*. \quad (14)$$

The probability of the pair creation is proportional to  $Z^2$  where  $Z$  is the proton number of the nucleus. The  $\gamma$ -ray also lose its energy by Compton scattering with electrons;

$$\gamma + e^- \rightarrow \gamma' + e'^-. \quad (15)$$

The probability of this reaction is proportional to  $Z$ .

(g) a lot of tritium may also be observed as an intermediate product of this process in the reaction (9) depending on the situation.

In the step (c), it is possible to occur absorption of the neutron by the matrix nuclei. The most probable result of this reaction will be a formation of a stable isotope or a reemission of a neutron in the case of Pd or Ti metal, though other reactions will be possible for other nuclei. Anyway, no remarkable events will occur between the neutron and the matrix nuclei in the case of our present interest.

### Explanation of Experimental Results

A qualitative explanation of the typical experimental results<sup>3~15)</sup> obtained hitherto in the Cold Fusion phenomena can be given using the trapped neutron catalyzed fusion model as follows.

First of all, it is recognized that the Cold Fusion phenomena have a stochastic character. Even in positive experiments, the phenomena occur accidentally<sup>3)</sup> as emphasized especially in a pioneering work<sup>4)</sup>. And it was also emphasized and observed that the non-equilibrium condition is necessary to realize the phenomena<sup>5,6)</sup>. These characters are understandable in terms of the stochastic nature of the formation of a trapping region for neutrons in Pd(Ti)-D system depending strongly on the quality of the sample and the condition of the experiments<sup>7,8)</sup>.

Secondly, the much number of tritium sometimes observed<sup>9,10,13)</sup> than expected in the reaction (13) is understandable, if neutrons are trapped effectively in Pd(Ti)-D system and the reaction (9) occurs frequently.

Thirdly, observation of unexpectedly much heat with a little reaction products<sup>4)</sup> should be related with the reaction (9) and a successive reactions (14) and (15) in optimum situations. The well-known fact that the large excess heat is more observed in Pd/D system than in Ti/D system may be explained by the higher probability of pair creation (14) and Compton scattering (15) near a nucleus with a larger atomic number  $Z$  where the probability is proportional to  $Z^2$  and  $Z$ , respectively. So, the reactions (14) and (15) are  $(46/22)^2 \approx 4.4$  times and twice easier respectively to occur in Pd/D than in Ti/D. If the process repeat to produce a cascade shower, this difference of the factor 4.4 and 2 in the single reaction becomes decisive factor for the excess heat generation.

Fourthly, the production of a large number of  ${}^4\text{He}$ <sup>8,10,11)</sup> should be related with the reaction (9) and a successive reaction (11) in an optimum situation. Because of the triton energy 6.98 keV produced in the reaction (9), the rate of the reaction (11) is fairly large in the system.

Fifthly, the neutron bursts observed sometimes<sup>3,8)</sup> may be explained as follows: the high energy neutron produced in the reaction (11) collide with many deuterons occluded in the matrix and accelerates them to high energy enough to induce d-d fusion reactions (12) and (13) effectively in the sample resulting in excess neutrons or tritons. This process is competitive with the heat producing process explained above with rapidity of the cascade shower process including the reactions (14) and (15). Perhaps, this is the reason that the simultaneous observation of neutron and excess heat did not occur frequently in Pd/D system.

In addition to the number of neutrons, there is another problem of neutron energy. The neutrons with the higher energy than 2.5 MeV were sometimes observed abundantly in Pd/D<sup>14)</sup> and in other metal deuterides<sup>15)</sup>. These data may be explained in terms of the neutron generated in the reaction (11).

Table 1: Thermal scattering length  $a_{coh}$  and number density of atoms

	$^1\text{H}$	$^2\text{D}$	$^7\text{Li}$	$^{22}\text{Ti}$	$^{26}\text{Mn}$	$^{28}\text{Ni}$	$^{46}\text{Pd}$
$a_{coh} (10^{-12}\text{cm})$	- 0.378	0.65	- 0.25	- 0.38	- 0.36	- 0.87	0.63
$N (10^{23} \text{ cm}^{-3})$			0.463	0.566	0.800	0.903	0.688

Table 2: The critical angle  $\theta_c$  (in degree and radian) of total reflection for neutrons with  $\lambda = 10\text{\AA}$  and specific number of totally reflected neutrons  $\Omega_c/2\pi$  (in percent)

	PdH	PdD	TiH <sub>2</sub>	TiD <sub>2</sub>
$\theta_c$ (degree)	0.52	0.68	0.67	0.88
$\theta_c$ (rad)	0.018	0.024	0.023	0.031
$\Omega_c/2\pi (\%)$	1.8	2.4	2.3	3.1

Though the experimental data on cross sections of neutron interactions with other nuclei are fairly well known, the problems on our hands are new ones - behavior of the light atoms (deuterium and hydrogen) in the more or less inhomogeneous matrix lattice, geometry of submacroscopic regions with homogeneous density of occluded light atoms, neutron reflection and refraction probability at boundaries (walls) of the regions , trapping probability of a neutron in the region with adequate walls, fusion probability of a trapped neutron with a deuteron or other nuclei in the region. fusion of energetic deuteron (or triton( with deuterons in an inhomogeneous solids and behavior of  $\gamma$ -ray induced cascade shower in Pd metal and etc.

### Theoretical Investigation of Problems involved in the Model

We will give a theoretical investigation of some problems in the model described above. The region is assumed to be surrounded with ordered deuteron lattices with spacing  $a_0$  parallel to the boundary and a number density of deuteron  $N$ .

### Model Calculation of Neutron Trapping

Neutrons with energies of the order of or less than the thermal one behave as waves in a solid and are then possible to be reflected by a boundary of an array of occluded deuterons (protons) with a characteristic spacing  $a_0$  when  $a_0$  is comparable with or smaller than the wave length  $\lambda$ . If a region with linear dimension  $L$  larger than  $a_0$  ( $a_0 \leq L$ ) is bounded by walls of such a structure reflecting neutrons. a neutron might be trapped in the region for a time  $T$ . The time  $T$  will be determined by the state of the walls i.e. atomic species in and widths of the walls, the geometry of the region, etc.

### Total reflection

Let us consider a plane boundary between media 1 and 2 through which a neutron passes from 1 to 2. The critical angle  $\theta_c$  of the total reflection is given by Eq. (6). The thermal scattering lengths  $a_{coh}$  are listed in Table 1 for several nuclei along with the number density of nuclei in typical solids.

Using these data, we can calculate the critical angle  $\theta_c$  of lattices of occluded deuterons in PdD and TiD<sub>2</sub> for a neutron with wave length 10 Å and the results are shown in Table 2. There are also included the specific number of totally reflected neutrons  $\Omega_c/2\pi$ , assuming

an isotropic distribution of neutron velocity where  $\Omega c$  is the solid angle corresponding to an angular range  $0 \leq \theta \leq \theta_c$ .

The critical angles for the total reflection in PdH and  $\text{TiH}_2$  lattices by a boundary between Pd and Ti lattices, respectively, are also listed in this table. An interesting feature occurs in relation with the difference of sign in the scattering length  $b$ .

This result shows that a neutron with wave length 20 Å ( $E = 2 \times 10^{-4} \text{ eV} = 2.5 \text{ K}$ ) has a critical angle  $1.32^\circ$  in the case of Pd/D system. For an optimum situation where the neutron is in a region surrounded by 270-sided piller and collides with each side with an angle  $\theta_c$ , the neutron in the plane perpendicular to the axis of the piller is completely trapped in this region.

The longer the wave length of the neutron is, the less the number of side of the piller is needed to satisfy this condition. This is, of course, an extreme example but shows a possibility making the time  $T$  very long compared with the transit time  $\tau$  of the neutron for the region defined by Eq. (7).

#### Bragg reflection

If a neutron is in a region surrounded by a lattice with spacing  $d$  satisfying the condition (3), the neutron with wave length  $\lambda$  can not pass through the lattice and reflected totally by the lattice.

Let us consider a simple example of a one dimensional lattice with spacing  $d$  where a neutron travels. From knowledge of the band calculation in solids, it is known that at the wave vector  $k = m\pi/d$ , there is an energy band gap  $\Delta E = 2|V_n|$ , where

$$V_n = \frac{1}{d} \int_0^d V(x) \exp(2\pi i n x/d) dx \quad (16)$$

and  $V(x)$  is the periodic potential for the neutron with a period  $d$ .

In three dimensional lattice with  $\theta = \pi/2$  and for a value  $d = 2 \text{ \AA}$  (3 Å), the energy at the center of the gap is given by

$$E\left(\frac{\pi}{d}\right) = \frac{\hbar^2}{2m_n} \left(\frac{\pi}{d}\right)^2 = 5.12 (2.28) \times 10^{-3} \text{ eV.}$$

This value corresponds to the energy of the cold neutron. So, some cold neutrons coming from outside with an energy in the range of  $E(\pi/d) \pm |V_n|$  are reflected totally by the lattice:

$$E(\pi/d) - |V_n| < E < E(\pi/d) + |V_n| \quad (17)$$

The value of  $|V_n|$  in a deuteron lattice was estimated to be  $0.211 (0.063) \times 10^{-6} \text{ eV}$  using the Fermi pseudopotential

$$\hat{V}_N = \frac{2\pi\hbar^2}{m_n} b \delta(\mathbf{r} - \mathbf{R}). \quad (18)$$

The bound scattering length  $b$  is taken as  $0.67 \times 10^{-12} \text{ cm}$  (for D) in the above calculation (S.W.Lovesey, Theory of Neutron Scattering from Condensed Matter, Vol.1, Oxford U.P.).

The value given above for  $\hat{V}_n$  means that 0.01% of the cold neutrons are trapped by a single gap at  $k = \pi/d$ . This number of neutrons seems sufficient to explain ordinarily observed amount of excess heat and emitted neutrons from inhomogeneous Pd/D and Ti/D systems if we consider the large number of background neutrons: For instance, in the data of Jones et al.<sup>5)</sup> the number of background neutrons above 100 keV is of the order of  $10^4$  compared with the 2.17 MeV neutrons ( $22.2 \pm 1.7$ ). Their data indicate that the number

of lower energy neutrons is more abundant. This fact supports strongly our hope to explain the Cold Fusion by the trapped neutron catalyzed fusion model.

In the case of the proton,  $b = -0.38 \times 10^{-12}$  cm (average value for singlet and triplet states), and  $|V_n|$  is 55 % of the deuteron case. If, however, it is possible to use polarized state of proton and neutron, the scattering lengths for triplet and singlet states can be used for effective trapping;

$$b^{(+)} = 1.04 \times 10^{-12} \text{ cm, triplet} \quad (19)$$

$$b^{(-)} = -4.70 \times 10^{-12} \text{ cm, singlet} \quad (20)$$

In the case of singlet scattering, the band gap  $\Delta E$  becomes wider by a factor of  $4.74/0.67 = 7.1$  than in deuteron lattice. In contrast, in the case of the deuteron, the difference of the scattering length is not so large ( $0.95$  and  $0.10 \times 10^{-12}$  cm), and the use of polarized state makes not so large effect as in the proton lattice.

Thus, the neutron is fully trapped in the region surrounded by such lattices in the optimum situations. In reality, however, the lattice has a finite width and there is a penetration probability for a neutron in the region even if the condition (3) and (17) be satisfied. But, for an optimum situation where the surrounding lattices have such an enough thickness as the neutron trapped in the region fuse certainly with one of deuterons in it, we can take the trapping time  $T$  as infinity.

From our knowledge of the band structure of electron spectrum in solids, it is possible to infer that the shorter the wave length satisfying the condition (3) for a fixed  $d$  is, the wider the energy range of neutrons reflected by the lattice is. So, the longest wave length reflected effectively by this mechanism is  $d$  when the neutron collide with  $\theta = \pi/2$ . Thus, the Bragg reflection is preferable for thermal neutrons with large  $\theta$  if the Bragg condition (3) is satisfied while the total reflection is for cold neutrons with small  $\theta$ .

We would like to emphasize here the stochastic nature of the formation of boundaries around a region favorable to trap the neutrons. This nature reflects in the lack of reproducibility of experimental data of the Cold Fusion phenomena, which is one of main reasons the phenomena could not get full confidence from some researchers.

### Fusion Probability of Low Energy Neutron and a Deuteron

Using an optical model with square well potential, we calculated the fusion cross section of thermal and cold neutrons with a deuteron<sup>2)</sup>. The result is shown in Fig. 1. In this figure, the fusion cross section in barns are plotted as a function of neutron energy in eV. This data is consistent with existing data at higher energy (e.g. T.Nakagawa, T.Asami and T.Yosida, JAERI-M 90-099, NEANDC(J)-153/U INOC(JPN)-140/L) and shows  $E^{-1/2}$  increase of the capture cross section with decrease of neutron energy. So, the multiplication factor for the fusion probability due to the neutron trapping is more larger than assumed before<sup>1)</sup> where only trapping time was taken care of. In the process of deceleration in ambience or in matrix, the neutron loses its kinetic energy and becomes thermal or cold neutron having a large probability of trapping and also a large fusion cross section with a deuteron when it is trapped.

This result verifies the assumption of the effective occurrence of fusion reaction (9) made in the model<sup>1)</sup>. The effect of the neutron trapping (the existence of a standing wave) will work further positive for our model at least by a factor  $T/\tau$ .

We did not consider a possibility of neutron fusion with matrix nuclei in this report. In reality, the fusion reaction may occur and the difference of the matrix will influence some features of the cold fusion phenomena.

### Fusion of 6.98 keV Triton with Deuterons occluded in Solids

The triton generated by the reaction (9) in-a matrix occluding deuterons has an energy of 6.98 keV. The triton passes through the matrix suffering deceleration and collides with deuterons occluded there. The  $t + d$  fusion cross section of the reaction (11) as a function of triton energy  $E$  is given by the following formula:

$$\sigma(E) = \frac{A_5 + [(A_4 - A_3 E)^2 + 1]^{-1} A_2}{E[\exp(A_1/\sqrt{E}) - 1]} \quad (21)$$

Here,  $\sigma$  is in barns,  $E$  in keV, and the coefficients have following values:

$$\begin{aligned} A_1 &= 56.27, & A_2 &= 7.53 \times 10^4, & A_3 &= 0.912 \times 10^{-2} \\ A_4 &= 1.076, & A_5 &= 614. \end{aligned} \quad (22)$$

For the triton energy 6.98 keV, this formula gives the fusion cross section of  $3.05 \times 10^{-6}$  barns.

This result means that in a Pd metal sample (density 12.16 g/cm<sup>3</sup>) of 1 mol occluding the same number of deuterium as palladium atoms, the triton suffers about  $10^{-6}$  fusion reactions before it comes out from the sample if we ignore deceleration in the matrix. Slowing down of the triton in the matrix will result in the decrease of  $t-d$  fusion probability in the sample.

### Chain Reaction Process of Fusions Breeding Neutrons

The neutron generated in the reaction (11) may make elastic collision with deuterons in the sample and give them kinetic energy. When the collision is head-on, the neutron loses its 8/9 of the initial energy and on the average its 16/27. A deuteron accelerated by  $n-d$  elastic collision makes elastic collisions with other deuterons losing its total initial energy by head-on collision and about its 5/6 in average in a strong screening case. The cross section of  $d-d$  elastic collision  $\sigma_{d-d}^{(el)}$  is about  $10^{-2}$  barns in this energy range.

Therefore, one 14.1 MeV neutron accelerates  $n_d \sim 250 \sigma_{d-d}^{(el)} N_d \bar{v}_d$  deuterons to energy higher than 100 keV where  $\bar{v}_d$  is an average deuteron velocity between  $E = 14.1 \times 16/27$  MeV and 100 keV (neglecting here slowing down of the deuteron by interactions with matrix though this effect is usually very important and should be treated carefully and quantitatively).

If we take the fusion cross section  $\sigma_{d-d}$  as  $10^{-2}$  barns, the number of  $d-d$  fusion reaction is

$$n_d N_d \sigma_{d-d} \bar{v}_d \simeq 250 \sigma_{d-d}^{(el)} N_d^2 \bar{v}_d^2.$$

Each fusion reaction generates 0.5 neutrons of energy 2.45 MeV. The 2.45 MeV neutron makes 6 elastic collisions with deuterons to accelerate them more energy than 100 keV. Considering  $d-d$  elastic collision, one 2.45 MeV neutron causes 70 candidates to realize  $d-d$  fusion. The number of  $d-d$  fusion thus induced is

$$70 \sigma_{d-d}^{(el)} N_d^2 \bar{v}_d^2.$$

This process succeeds endlessly to produce neutrons one by one but with limitations by sample size, change of the situation by generated heat, etc. in an optimum situation where the neglect of the slowing down induced by the interaction with the matrix is justified and the number given above is larger than 1. So, in such an situation, the collision of the neutron and deuterons occluded in the sample occurs frequently, and a neutron accelerates about 9

deuterons to higher energies than 100 keV necessary to accomplish  $d + d$  fusions (12) and (13) effectively. This process may explain the neutron bursts observed in experiments<sup>6,8)</sup>.

Recent experiment<sup>16)</sup> shows explicitly effective trapping of the background neutrons by HH, DH and DD molecules. This fact indicates there is another mechanism to trap thermal and cold neutrons in materials occluding protons and deuterons and supports indirectly our assumption of the neutron trapping in inhomogeneous media.

Another  $d - d$  fusion reaction

$$d + d = {}^4\text{He} (76.0\text{keV}) + \gamma (23.8\text{MeV}) \quad (23)$$

is possible. However, branching ratios of these reactions (12), (13) and (23) are known as 1 : 1 :  $10^{-7}$  in the Nuclear Physics and the last reaction may be ineffective. Thus, the neutrons with an energy 2.45 MeV observed sometimes<sup>2)</sup> should be explained by the successive reactions (9), (11) and (12). As in the case of  $n - d$  fusion, we did not consider interactions of the triton with matrix nuclei which certainly occur with finite probability. We will leave this problem for future .

If we don't accept the neutron catalyzed fusion mechanism, it is neccesary to solve riddles of much  ${}^4\text{He}$ , tritium and large excess heat (see next part) without remarkable neutron counts with other mechanisms. There have been trials to take up following rather difficult reactions to occur in solids as done in some works;

$$p + d = {}^3\text{He} (5.35\text{keV}) + \gamma (5.49\text{MeV}), \quad (24)$$

$$d + d + d = {}^4\text{He} (7.95\text{MeV}) + d (15.9\text{MeV}), \quad (25)$$

$$= {}^3\text{He} (4.76\text{MeV}) + t (4.76\text{MeV}), \quad (26)$$

$$p + d + d = {}^4\text{He} (4.77\text{MeV}) + p (19.08\text{MeV}). \quad (27)$$

These reactions may have some connections with the Cold Fusion phenomena but would not play main roles in them.

### Cascade Shower in Pd and Ti Metal induced by 6.25 MeV $\gamma$ -ray and Excess Heat

For photons passing through a homogeneous medium of density  $\rho$  ( $\text{g}/\text{cm}^3$ ) and thickness  $t$  ( $\text{cm}$ ), the intensity  $I$  remaining is given by the expression

$$I = I_0 e^{-\mu t} \equiv I_0 e^{-\rho t/\lambda_m}. \quad (28)$$

Here  $\mu$  is the mass attenuation coefficient ( $\text{cm}^{-1}$ ).  $\lambda_m = \rho/\mu$  is the mass attenuation length ( $\text{g}/\text{cm}^2$ ). and  $I_0$  is the initial intensity (number of photons). The data for elements Pb, Fe, Ar, C and H in the energy range from  $10^{-2}$  to  $10^2$  MeV are given in TRIUMF Kinematics Handbook (Table VII-16). Interpolation to other atomic number  $Z$  are done by scaling the cross section ( $\text{cm}^2$ )

$$\sigma = \frac{A}{\lambda_m N_A}, \quad (29)$$

where  $A$  is the atomic weight of the absorber material ( $\text{g}/\text{mol}$ ) and  $N_A$  is the Avogadro number ( $\text{mol}^{-1}$ ). For a mixture, the formula

$$\lambda_{eff}^{-1} = \sum_i f_i \lambda_{m,i}^{-1} \quad (30)$$

is used, where  $f_i$  is the proportion by weight of the  $i$ -th component.

Table 3: The e-folding length  $\ell$  of 6.25 MeV photons in Ti and Pd

	Z	A (g/mol)	$\sigma$ (barns)	$\lambda_m$ (g/cm <sup>2</sup> )	$\rho$ (g/cm <sup>3</sup> )	$\ell$ (cm)
H	1	1.00	0.07	23.7		
D	1	2.01	0.14	23.7		
Ti	22	47.9	2.2	36.2	4.5	8.0
Pd	46	106.4	6.6	26.8	12.16	2.2

Table 4: Effective e-folding length  $\ell_{eff}$  of 6.25 MeV photons in hydrides

	$\lambda_{eff}$ (g/cm <sup>2</sup> )	$\rho$ (g/cm <sup>3</sup> )	$\ell_{eff}$ (cm)
TiH	35.8	4.6	7.8
TiH <sub>2</sub>	355.5	4.7	7.6
PdH	26.8	12.3	2.2
TiD	35.5	4.7	7.6
TiD <sub>2</sub>	34.8	4.9	7.1
PdD	26.7	12.4	2.2

The plot of the cross section  $\sigma$  as a function of  $Z$  is shown in Fig. 2 for a photon energy  $E = 6.25$  MeV. From this figure by interpolation, we can estimate  $\sigma$  for Ti and Pd metals as  $0.22$  and  $0.66 \times 10^{-23}$  cm<sup>2</sup>, respectively.

Using these values of  $\sigma$ , we calculated the e-folding length  $\ell = 1/\mu$  for the 6.25 MeV photon in Ti and Pd using a relation

$$\ell = \mu^{-1} = \frac{\lambda_m}{\rho}. \quad (31)$$

The result is shown in Table 3.

The effective e-folding length  $\ell_{eff}$  of photon attenuation for hydrides and deuterides of Ti and Pd are given in Table 4, where the volume of the sample is assumed to be the same as the metal without hydrogen isotopes.

This table shows the effect of the hydrogen isotope occlusion on the photon attenuation is not large if the volume change is neglected. The volume change of the order of 5 % observed in the experiments gives density change of the same order to the opposite direction. This change of the density will give the fractional decrease of  $\ell_{eff}$  by the same order of percentage.

The estimated e-folding lengths  $\ell$  of the 6.25 MeV photon in Ti and Pd metals are 8.0 and 2.2 cm, respectively, as shown in Table 3. This result confirms our speculation made above and shows clearly that in Pd the photon created in the fusion reaction (9) lose its energy rapidly and the energy is given mainly to electrons and dissipate to increase thermal energy of the matrix solid. While in Ti matrix, the sample size used usually in the Cold Fusion experiment is not enough to decay the photon in the sample even if the fusion reaction (9) occurs there. This may be the main reason that the large excess heat has not been observed in Ti/D system though fusion products has been observed frequently.

Let us consider an extreme example of the Cold Fusion events: melting of Pd sample with dimension  $1 \times 1 \times 1$  cm<sup>3</sup>. If all the sample is melted away, the thermal energy to heat it from 0 °C to its melting point (1554 °C) + 4.72 kJ and its heat of fusion 1.91 kJ must be

supplied by 6.25 MeV photons in our model. So, the number of the photons  $N_\gamma$  for the process is  $6.63 \times 10^{16}$ . On the other hand, the number of neutrons generated by  $t-d$  fusion  $N_n$  in the sample is  $1.4 \times 10^{10}$  neglecting triton deceleration by matrix (minus effect) and the competitive chain process of  $d-d$  fusion by deuteron acceleration (plus effect). In this case, we obtain a ratio

$$N_\gamma/N_d \sim 10^7$$

which is a value very close to the experimental result obtained by Fleischmann and Pons<sup>4)</sup>.

### Conclusion

The discussion given above is not fully quantitative in points that it is not derived only from the first principle and that the absolute value of the numbers of the fusion products and the excess heat generated in Pd/D system is not determined. Not considering the former claim, it is necessary to know the exact situation of the sample and environments in the experiments to solve the latter problem and it is not possible to realize it now. Even so, the Cold Fusion phenomena observed in Pd/D and Ti/D solids are explained consistently in terms of the trapped neutron catalyzed mechanism of deuteron fusion. Especially, successfully explained were several hitherto unsolved problems in the phenomena, such as 1) the stochastic nature of the occurrence of phenomena, 2) the large excess heat with a little neutron production<sup>4)</sup>, 3) the large amount of tritium with no neutron emission<sup>13)</sup>, 4) the large amount of  ${}^4\text{He}$  observed with some amount of heat and tritium<sup>8)</sup>, 5) the fact that the large excess heat is observed mainly in Pd/D but not in Ti/D system, and 6) the higher energy neutrons than 2.5 MeV observed in several experiments in Pd/D<sup>14)</sup> and in other metal deuterides<sup>15)</sup>.

In addition, 7) the mass number 3 peak in Pd/H system<sup>8)</sup> accompanied with excess heat generation might be explained by deuteron formation by neutron - proton fusion (Eq.(10)) and the formation of HD molecules in the system.

Thus, it is possible to say that the Cold Fusion phenomena are the trapped neutron catalyzed fusion of deuterons (protons) occluded in Pd, Ti and other materials in its essential parts. To realize the Cold Fusion, it is desirable to have a submacroscopic structure where deuteron occluding and not occluding regions exist alternatively. A stratified alternative layers of Pd and Oxide is a candidate. Another candidate may be sintered structures of ceramics having characteristics of the proton conductor.

To make the resulting energy of the photons thermal, it is desirable to use elements as large  $Z$  as possible in those hydrogen occluding or proton conducting materials.

The author would like to express his sincere thanks to Dr. J.Guokas of J & J Manufacturing, USA for his information about the recent paper<sup>16)</sup> showing trapping of background neutrons by molecules. He would also like to express his thanks to Dr. K.Sasaki of NEDAC for his encouragements and helps obtaining some data during this work. He is also indebted to Messrs. S.Watanabe, Y.Okumura and H.Miyagi of his laboratory for their assistance in correcting errors in the manuscript.

### References

- (1) H.Kozima, "Trapping of Neutrons in Inhomogeneous Solids and the Cold Fusion" Fusion Technology (submitted).

- (2) H.Kozima, K.Kaki, T.Yoneyama, S.Watanabe and M.Koike, "Theoretical Verification of the Trapped Neutron Catalyzed Model of Deuteron Fusion in Pd/D and Ti/D Systems" Fusion Technology (submitted).
- (3) F.Paneth and K.Peters, "Ueber die Verwandlung von Wasserstoff in Helium", Naturwissenschaften 14 (1926) 956; "The reported Conversion of Hydrogen into Helium", Nature 118 (1926) 526; F.Paneth, "The Transmutation of Hydrogen into Helium", Nature 119 (1927) 706.
- (4) M.Fleischmann and S.Pons, "Electrochemically induced Nuclear Fusion of Deuterium", J. Electroanal. Chem. 261 (1989) 301.
- (5) S.E.Jones, E.P.Palmer, J.B.Czirr, D.L.Decker, G.L.Jensen, J.M.Thorne and S.E.Tayler, "Observation of Cold Nuclear Fusion in Condensed Matter", Nature 338 (1989) 737.
- (6) A.De Ninno, A.Frattelillo, G.Lollobattista, G.Martinio, M.Martone, M.Mori, S.Podda and F.Scaramuzzi, "Evidence of Emission of Neutrons from a Titanium- Deuterium System", Europhys. Lett. 9 (1989) 221.
- (7) A.Takahashi, T.Iida, F.Maekawa, H.Sugimoto and S.Yoshida,"Windows of Cold Nuclear Fusion and Pulsed Electrolysis Experiments", Fusion Technol. 19 (1991) 380.
- (8) E.Yamaguchi and T.Nishioka, "Cold Nuclear Fusion Induced by Controlled Out-Diffusion of Deuterons in Palladium", Jpn. J. Appl. Phys. 29 (1992) L666; "Direct Evidence for Nuclear Fusion Reactions in Deuterated Palladium", *Frontiers of Cold Fusion* p.179, ed. H.Ikegami, Universal Academy Press (Tokyo), 1993.
- (9) K.-H.Lee and Y.-M.Kim, "The Change of Tritium Concentration during the Electrolysis of D<sub>2</sub>O in Various Electrolytic Cells", *Frontiers of Cold Fusion* p.511, ed. H.Ikegami, Universal Academy Press (Tokyo), 1993.
- (10) J.O'M.Bockris, C.Chien, D.Hodko and Z.Minevski, "Tritium and Helium Production in Palladium Electrodes and the Fugacity of Deuterium Therein", *Frontiers of Cold Fusion* p.231, ed. H.Ikegami, Universal Academy Press (Tokyo), 1993.
- (11) M.H.Miles and B.F.Bush, "Search for Anomalous Effects Involving Excess Power and Helium during D<sub>2</sub>O Electrolysis using Palladium Cathodes", *Frontiers of Cold Fusion* p.189, ed. H.Ikegami, Universal Academy Press (Tokyo), 1993.
- (12) G.Shani, C.Cohen, A.Grayevsky and A.Brokman, "Evidence for a Background Neutron enhanced Fusion in Deuterium absorbed Palladium", Solid State Comm. 72 (1989) 53.
- (13) O.Matsumoto, K.Kimura, Y.Saito, H.Uyama, T.Yaita, A.Yamaguchi and O.Suenaga, "Detection of Neutron and Tritium during Electrolysis of D<sub>2</sub>SO<sub>4</sub>-D<sub>2</sub>O Solution", *Frontiers of Cold Fusion* p.495, ed. H.Ikegami, Universal Academy Press (Tokyo), 1993.
- (14) H.Q.Long, R.S.Xie, S.H.Sun, H.Q.Liu, J.B.Gan, B.R.Chen, X.W.Zhang and W.S.Zhang, "The Anomalous Nuclear Effects Inducing by the Dynamic Low Pressure Gas Discharge in a Deuterium/Palladium System", *Frontiers of Cold Fusion* p.455, ed. H.Ikegami, Universal Academy Press (Tokyo), 1993.
- (15) H.Q.Long, S.H.Sun, H.Q.Liu, R.S.Xie, X.W.Zhang and W.S.Zhang, "Anomalous Effects in Deuterium/Metal Systems", *Frontiers of Cold Fusion* p.447, ed. H.Ikegami, Universal Academy Press (Tokyo), 1993.
- (16) G.F.Cerofolini, G.Boara, S.Agosteo and A.F.Para, "Giant Neutron Trapping by a Molecular-species Produced during the Reaction of D<sup>+</sup> with H<sup>-</sup> in a Condensed-phase", Fusion Technol. 23 (1993)465.
- (17) For instance, A.G.Lipson, B.F.Lyakhov and B.V.Berjaguin, "Reproducible Anomalous Heat Production and 'Cold Fusion' in Au/Pd/PdO Heterostructure Electrochemically Saturated by Hydrogen (or Deuterium)", ICCF : Notebook Vol.1, C'2,S (1993).

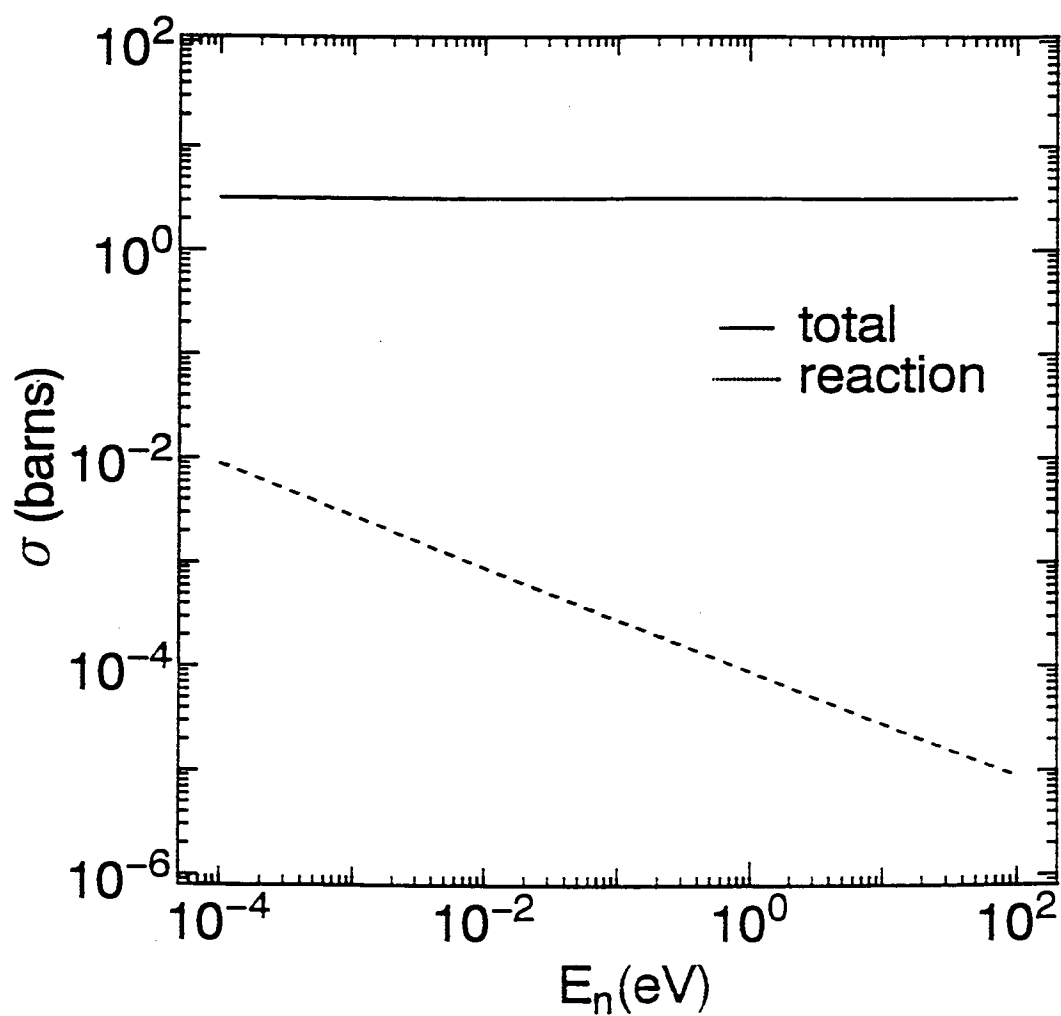


Fig. 1 Fusion and total cross section (barns) of neutron (energy  $E_n$  in eV) with a deuteron extrapolated to lower energy using the optical model.

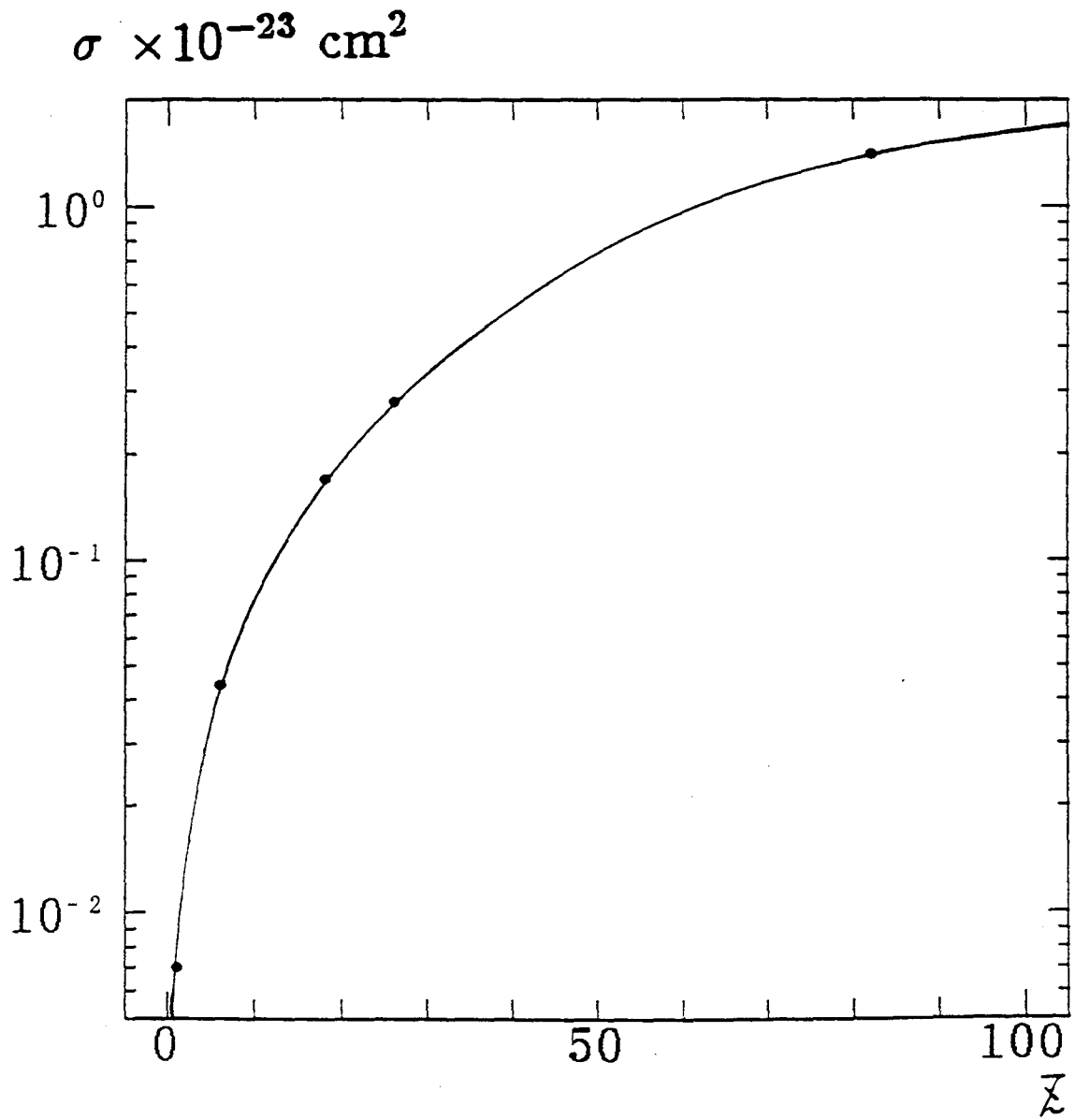


Fig. 2 Cross section of photon absorption by Eq. (29) to interpolate the photon mass attenuation coefficient for Ti and Pd.

## **On possibility of non-barrier dd-fusion in volume of boiling D<sub>2</sub>O during electrolysis.**

Vysotskii V.I.  
Radiophysical Dept.,  
Shevchenko Kiev University,  
Vladimirskaya st., 64,  
Kiev, Ukraine, 252017

Kuz'min R.N.  
Physical Dept.,  
Moscow State University,  
Moscow, Russia.

### **Abstract**

For the first time we regard the conditions (optimal temperature and pressure) of realization of non-barrier cold fusion on the basis of short-time (fluctuational) Fermi-condensate of deuterium atoms in quasi-equilibrium vapor micro-bubbles in volume of boiling D<sub>2</sub>O during electrolysis.

### **Theory and models.**

Previously we have shown [1-3] that non-barrier dd-fusion reaction (with eliminated Coulomb barrier) can be achieved during the forming of short-lived (fluctuational) Fermi-condensate of N<sub>1</sub> = 10...20 deuterium atoms in microholes of optimal size R<sub>0</sub> ≈ 4...7 Å in crystals. The strict requirement posed upon the size of microholes ( $\Delta R_0/R_0 \leq 0.1$ ) produces difficulties on the fusion observation and optimization because:

- there is not enough microholes of required size R<sub>0</sub> in the crystal;
- the exact value of R<sub>0</sub> is hardly calculable;
- there is no possibility of controlled creation of required size microholes and of self-adjustment R → R<sub>0</sub>.

On our opinion the problem of controlled non-barrier fusion can be solved using electrolysis in volume of boiling D<sub>2</sub>O in closed space at defined temperature T, electric current and external pressure p<sub>0</sub>. Let's explain the idea.

The process of boiling is accompanied by multiple formation of micro-bubbles in D<sub>2</sub>O, that bubbles containing both D<sub>2</sub>O-molecules and appeared due to electrolysis and later neutralized deuterons. In accordance with Laplace law the micro-bubbles with critical radius of  $R_{cr} = 2\sigma/(p_1 - p_0 + \rho g z)$  are equilibrium and stable. Here  $\sigma$  is surface tension quotient,  $p_1 = p_0 \exp(2\sigma/R_{cr} n_0 k_B T)$  - pressure inside the bubble,  $p_0$  - average liquid pressure,  $\rho g z$  - hydrostatic pressure.

At certain externally controlled pressure  $p_0$  it is possible to provide the condition  $R_{cr} \approx R_0$ . Thus the same condition requirements can be satisfied in the micro-bubble as were stated before for the crystal provided the required quantity  $N$  of deuterium atoms gets into the bubble.

The frequency of bubble birth  $I = 10^{31} \exp(-W/k_B T) \text{ cm}^{-3} \text{s}^{-1}$  is described by

Folmer - Zeldovich - Kagan theory, where  $W = \frac{4}{3}\pi R_{cr}^2 \sigma$  is bubble formation threshold. After the bubble appeared the deuterium atoms diffuse into it. The lifetime of equilibrium bubble with  $R_{cr} \approx R_0$  can reach  $\Delta t \approx 10^{-3} \text{ s}$ . During this time  $N \approx j_0 4\pi R_0^2 \Delta t$  atoms of deuterium get into the bubble. With current density  $j_0 \approx 0.5 \text{ A/cm}^2$  we have  $N \approx 50 \dots 100$ , which according to [1,2] is enough for the forming of short-lived Fermi-condensate of  $N_1 \approx 10 \dots 20$  atoms with probability  $f$  [1,2] and for realization of fusion.

In case of small difference between  $R_{cr}$  and  $R_0$  a self-adjustment  $R \rightarrow R_0$  takes place due to unavoidable (after  $\Delta t$ ) changing (either increasing or decreasing) of bubble radius.

The general expression for concentration of optimal micro-bubbles with fluctuational Fermi-condensate of D formed in them is  $n \approx I f \Delta t$ . The quantities  $I \sim \exp(-W/k_B T)$ ,  $\sigma \sim \ln(T/T_{cr})$  and  $f \sim T^{-3N_1/2} \exp(-A/k_B T)$  [1,2], that define  $n$ , have different temperature dependencies. The maximum of fusion

velocity in the unit volume of boiling D<sub>2</sub>O  $\Lambda = C n(N_1 - 1)/(4\pi R_0^3/3)$ , where C = 2 · 10<sup>-16</sup> cm<sup>3</sup>s<sup>-1</sup> is a constant of dd-fusion, is achieved at optimal temperature

$$T_{opt} \approx \frac{\pi \sigma R^2}{k_B N_1} + \frac{2\hbar^2}{k_B M R^2} (N_1 \pi)^{2/3} (3/2)^{1/3}, \text{ which at } R_0 \approx 4 \dots 7 \text{ Å equals}$$

T<sub>opt</sub> ≈ 500...700 °K. It corresponds to overheated liquid under high pressure p<sub>o</sub>. No experiments at such temperature were performed yet.

According to estimates, optimization of T and p<sub>o</sub> could raise the velocity of dd-fusion in the volume of electrolyte D<sub>2</sub>O up to  $\Lambda \approx 10^3 \dots 10^6$  cm<sup>-3</sup>s<sup>-1</sup>, which in case of big quantities of D<sub>2</sub>O can become an alternative to hot fusion.

1. Vysotskii V.I., Kuz'min R.N. *Proceedings of the Third International Conference on Cold Fusion*, 1992, Nagoya, Japan.
2. Vysotskii V.I., Kuz'min R.N. *Temperature-Time Dynamics of Cold Fusion in Crystals Based Upon Quantum Non-barrier and Microcumulative Mechanisms*. Cold Fusion, Moscow, 1992 (Ed. by Kuz'min R.N.), pp.6-13 (In Russian).
3. Vysotskii V.I., Kuz'min R.N. *Theory, Mechanism and Dynamics of Non-barrier Nuclear Catalysis in Solids*. Preprint of the Institute of Theoretical Physics, ITP-90-82p, 1992, Kiev.



# New Hydrogen (Deuterium) Bohr Orbits in Quantum Chemistry and "Cold Fusion" Processes

Jean-Pierre VIGIER  
Gravitation et Cosmologie Relativistes  
Université Paris VI - CNRS/URA 769  
Tour 22 - 4ème étage, Boîte 142  
4, place Jussieu, 75005 Paris

## Abstract

It is suggested that recent confirmation of the existence in dense matter of very small quantities of fusion "ashes" both in electrolysis and glow-discharge experiments<sup>(1)</sup>, can be heuristically interpreted (within the frame of conventional Quantum Mechanics and Nuclear theory) if one combines screening (i.e. tunneling) and the introduction of spin-spin and spin orbit couplings with the usual effects of the Coulomb Potential in atoms and molecules.

The new Quantum Chemistry associated to the corresponding new tight Bohr orbits in dense matter explains<sup>(2)</sup> the observed excess heat<sup>(3)</sup> (above break even) and predicts the existence of fusion processes which become dominant at high energy current input<sup>(4)</sup>.

## INTRODUCTION

After two recent important Japanese contributions<sup>(5)(6)</sup> the aim of this letter is to present a semi-empirical discussion of a possible answer (within the frame of presently known quantum mechanics and nuclear phenomena) to the problem of the origin of the excess (enthalpy/heat) (above break-even) now established (at low input) both in electrolysis and glow discharge experiments in dense matter.

It can be presented as follows.

A) If one accepts the facts

- 1) that there is excess heat produced, both in hydrogen and H<sub>2</sub>O based "cold fusion" experiments... which thus does not result from true fusion processes
- 2) that the excess enthalpy (observed) for the first time by Pons and Fleischmann<sup>(7)</sup> with D<sub>2</sub>O is indeed accompanied by a small amount of nuclear

fusion reactions but contain (by many orders of magnitude) not enough protons, neutrons, tritium  $^3\text{He}$  or  $\gamma$  rays (i.e. real fusion "ashes") to explain this excess... which nevertheless exceeds by far all possible energy coming from presently known chemical and conventional nuclear reactions such as



the only remaining possibility (with the most observed "ash") i.e.



being out due

- a) to its negligible probability i.e.= 50% for 1) and 2) and  $10^{-5}$  for 3).\* The suppression 1) and 2) and enhancements 3) i.e. an enhancement of a dominant D-wave state is a process never observed (until now) in experimental nuclear physics().
- b) to the remarkable absence in observations<sup>(6)</sup> of the  $\gamma$  predicted by 3).

3) The question of "fusion ashes" also raises problems: As recently summarized by Takahashi et al.(5)

- a) "Neutron emission with very weak level has now been observed by many laboratories in  $\text{D}_2\text{O}/\text{Pd}$  electrolyses and deuterium gas loading type experiments. Several laboratories have reported neutron spectra with 2.45 MeV peak which should be the evidence of D+D fusion. However, together with abroad component in 3 to 10 MeV region which cannot be explained with fusion reactions (D+D, D+t, D+Li, etc.)
- b) Beyond the 3 MeV proton peak of D+D reaction high energy charged particles ( $\alpha$ , p, t; etc.) have been observed in the 3-15 MeV region by deuteron beam implantation and gas loading experiments<sup>(3)</sup>.

---

\* As remarked by Takabashi et al.(5)  $\text{D} + \text{D} \rightarrow 4 \text{He} \rightarrow \text{n} + 3 \text{He}$  or  $\text{p} + \text{T}$  cannot either explain the observed excess heat (-kev/metal atom level) since observed neutron level are  $10^{-10}$  to  $10^{-12}$  smaller then the corresponding "virtual" reaction rates generating excess heat.

c) Tritium generation with significant level (but much weaker than excess heat level) has been observed in many laboratories<sup>(8)</sup> to result in anomalous N/T yield ratio. i.e. to  $10^{-4}$  to  $10^{-7}$ , referring to n/t ~1.0 for the known D+D fusion.

d)  $^4\text{He}$  generation with large level, which might correspond to observed excess heat level, has been reported<sup>(9)</sup> but meaningful-level generation of  $^4\text{He}$  by the known D+D fusion is very hard to be imagined. In all cases  $^4\text{He}$  is accompanied by a larger quantity of what appears as  $\text{D}_2$  molecules.

e) Large level excess heat (10-4000 w/cc or keV/atom) has been reported<sup>(10)</sup> from many laboratories in  $\text{D}_2\text{O}/\text{Pd}$  electrolyses, associating sometimes very weak neutron emission. No clear evidence that these excess heats are due to nuclear reactions have been shown yet<sup>(5)</sup>.

Finally the problem is further complicated by the confirmation by various authors<sup>(3)</sup> (also in very small quantities) of heavier "fusion ashes" (such as calcium<sup>(1)</sup> or palladium isotopes)<sup>(1)</sup> and of transmutation and fission products<sup>(1)</sup> which were not there, when the experiments started, and can be interpreted as resulting directly from  $\text{D}_2 + \text{Pd}$  or Potassium + Hydrogen fusion processes forbidden by apparently unsurpassable repulsive high Coulomb barriers.

B) If one assumes that the observed excess heat are (at least for H or  $\text{H}_2\text{O}$  based set-ups) not explainable in terms of fusion process and one looks for a common explanation of points 1) and 2) in A) this implies to quote again Takahashi<sup>(5)</sup>.

i) "that there exists a dynamical exothermic mechanism for forming close clusters of more than two deuterons within 0.02nm (comparable to the de Broglie wavelength of lev deuteron space in solids... an existence which suggests the existence of new "tight" Bohr orbits in H,  $\text{H}_2\text{O}$ ,  $\text{D}_2\text{O}$  etc and the corresponding apparition of new tight multibody quantum states (i.e. of a new exotic quantum chemistry) in special physical surroundings. This is supported by the high density ( $\geq$  liquid  $\text{D}_2$  density) of loaded  $\text{H}_2$  in  $\text{Pd}$ .

ii) that quantum mechanical tunneling through the Coulomb barrier i.e. barrier penetration probability should be enhanced very much to be more than  $10^{-6}$ : namely we need "super screening" to depress the Coulomb repulsive potential very much i.e. to produce fusion screening of quasi-free electrons in metal deuterides during the transient dynamics (which creates the new tight

Bohr orbit) which should happen near local points where new states of deuteron clustering is taking place.

All this suggests that some new mechanism (such as resonance phenomena) in high electron concentrations) favoring Coulomb screening<sup>(1)</sup> and quantum tunneling<sup>(2)</sup> is thus at work in cathodes (Pd, Ni, steel etc) which favors fusion of the new tightly bound molecules. The new chemical energy states observed<sup>(2)</sup> thus favor real fusion mechanisms: so that corresponding associated new quantum mechanical accumulators can/might transform into true fusion reactors.

The answer proposed in this letter rests on three points.

## § 1 SPIN-SPIN AND SPIN-ORBIT COUPLING

1) As first basis for the new phenomena one can add (following a suggestion of Barut<sup>(12)</sup>) to the Coulomb Potential (utilized in Hydrogen and Deuterium) spin-spin and spin orbit interactions. Usually neglected<sup>(14)</sup> they manifest themselves when  $\vec{L}$ ,  $\vec{M}_1$ ,  $\vec{M}_2$  are oriented (parallel) by internal electromagnetic interactions when H and D are in various types of electrodes. Indeed for two charged particles  $e_1$ ,  $e_2$  with magnetic moments  $\vec{M}_1$  and  $\vec{M}_2$  the usual quantum Schrödinger Hamiltonian is given by

$$H = \frac{1}{2m_1} \left( \vec{p}_1 - e_1 \vec{M}_2 \times \frac{(\vec{r}_1 - \vec{r}_2)}{|\vec{r}_1 - \vec{r}_2|^3} \right)^2 + \frac{1}{2m_2} \left( \vec{p}_2 - e_2 \vec{M}_1 \times \frac{(\vec{r}_2 - \vec{r}_1)}{|\vec{r}_2 - \vec{r}_1|^3} \right)^2 + \frac{e_1 e_2}{|\vec{r}_1 - \vec{r}_2|} - M_1 \cdot M_2 S_{12}(\vec{r}_1 - \vec{r}_2) \quad (4)$$

where  $S_{12}$  is the usual dipole-dipole interaction tensor\* and  $r$  their distance, i.e.

$$S_{12}(\vec{r}) = \frac{3\sigma_1 \cdot \vec{r} \times \sigma_2 \cdot \vec{r} - \sigma_1 \cdot \sigma_2}{r^3} + \frac{8\pi}{3} \sigma_1 \cdot \sigma_2 \delta(\vec{r}) \quad (5)$$

This 2-body problem with magnetic forces is separable, like the 2-body Coulomb problem. With\*\*

$$\begin{aligned} \vec{r} &= \vec{r}_1 - \vec{r}_2 & R &= \frac{m_1 \vec{r}_1 + m_2 \vec{r}_2}{M_0} & \vec{P} &= \vec{p}_1 + \vec{p}_2 \\ \frac{1}{M} &= \frac{1}{m_1} + \frac{1}{m_2} & P &= \frac{m_2 \vec{p}_1 - m_1 \vec{p}_2}{M_0} & M_0 &= m_1 + m_2 \end{aligned} \quad (6)$$

\* The following calculation, well known in the literature is an evident consequence of Quantum Mechanics. We reproduce it here in a simple relativistic form given by Barut<sup>(12)</sup>.

\*\* It has been shown both theoretically and experimentally that the quantized states of Hydrogen should be calculated w.r.t. relative motions of the system of both particles.

still utilizing Barut's rotations<sup>(13)</sup> we obtain after some calculation

$$H = \frac{1}{2M_0} \vec{P}^2 + \frac{1}{2\mu} \vec{p}^2 - \vec{p} \cdot \frac{\vec{a} \times \vec{r}}{r^3} - \frac{\vec{P} \cdot \vec{b} \times \vec{r}}{r^3} + \frac{A}{r^4} + \frac{e_1 e_2}{r} - \mu_1 \mu_2 S_{12}(\vec{r}) \quad (7)$$

where

$$\left\{ \begin{array}{l} \vec{a} = \frac{e_1}{m_1} \vec{M}_2 + \frac{e_2}{m_2} \vec{M}_1, \\ \vec{b} = \frac{e_1}{m_1 + m_2} \vec{M}_2 - \frac{e_2}{m_1 + m_2} \vec{M}_1, \\ A = \frac{e_1^2}{m_2} \mu_2^2 + \frac{e_2^2}{m_1} \mu_1^2. \end{array} \right.$$

Note that in addition to the center of mass kinetic energy we have another

magnetic term  $-\vec{P} \cdot \frac{\vec{b} \times \vec{r}}{r^3}$  for a moving atom, which vanishes both for identical particles and identical particle-antiparticle systems.

In the center of mass frame ( $\vec{P} = 0$ ) we have

$$H_{\text{relative}} = \frac{1}{2\mu} \vec{p}^2 - \vec{p} \cdot \frac{\vec{a} \times \vec{r}}{r^3} + \frac{A}{r^4} + \frac{e_1 e_2}{r} - \mu_1 \mu_2 S_{12}(\vec{r}) \quad (8)$$

Using  $-\vec{p} \cdot (\vec{a} \times \vec{r}) = \vec{p} \cdot (\vec{r} \times \vec{a}) = (\vec{p} \times \vec{r}) \cdot \vec{a} = -\vec{a} \cdot (\vec{r} \times \vec{p}) = -\vec{a} \cdot \vec{p}$

we see that the second term corresponds to a charge-dipole potential, and the last term to a dipole-dipole potential.

In the special case  $m_2 \gg m_1$ , hence  $\vec{a} = \frac{e_1}{m_1} \vec{M}_2$ ,  $\vec{b} = 0$   
 $A = \frac{e_1^2}{m_1} \mu_2^2$ , we have the simpler Hamiltonian

$$H_{\text{relative}} = \frac{1}{2\mu} \vec{p}^2 + \frac{e_1 e_2}{r} - \frac{e_1 \mu_2 \vec{r} \cdot \vec{L}}{m_1 r^3} + \frac{e_1^2 \mu_2^2}{m_1} \frac{1}{r^4} \quad (9)$$

We now try to solve exactly the eigenvalue problem  $H\Psi = E\Psi$  with  $H$  given in eq.

(6). For simplicity we take the spin of the particle 2 to be 1/2.

choosing for  $\psi$  the eigenstates of  $\vec{S}$ ,  $L$  with eigenvalues

$$\begin{aligned} \vec{S} - (e + \frac{1}{2}) &= -(\vec{j} + \frac{3}{2}) & \text{for } (\vec{j} = \ell - 1/2) \\ \zeta_\ell \swarrow & & \\ \ell = j - \frac{1}{2} & & \text{for } (\vec{j} = e + 1/2) \end{aligned}$$

we have the radial equation

$$\left( \frac{1}{2\mu} p^2 + \frac{e_1 e_2}{r} - \frac{e_1 M_2}{m_1} \cdot \frac{C_e}{r^3} + \frac{e_1^2 M_2^2}{m_1 r^4} \right) \psi = E \psi \quad (10)$$

The effective radial potential is then given by

$$\left\{ \begin{array}{l} V = \frac{\ell(\ell+1)}{2\mu r^2} + \frac{e_1 e_2}{r} - \frac{e_1 M_2 \cdot C_e}{m_1 r^3} + \frac{e_1^2 M_2^2}{m_1 r^4} \\ = \frac{\ell(\ell+1)}{2\mu r^2} + \frac{e \alpha}{r} - g \frac{e \alpha}{2m_1 m_2} \cdot \frac{C_e}{r^3} + g \frac{e^2 \alpha^2}{4m_1 m_2 r^4} \end{array} \right. \quad (11)$$

where  $\alpha = e^2 / \hbar c$ ;  $e = \text{sign}(e_1 e_2)$  and  $g$  is the g-factor of particle 2 (positive or negative). As also shown by Barut<sup>(13)</sup> if we write the typical form of  $V$  is shown in Fig. 4 when the sign of the third term is negative.

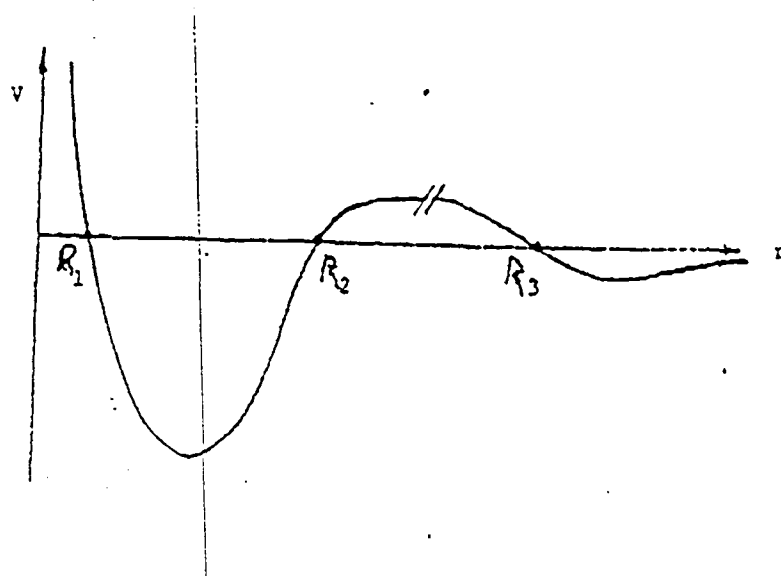


Fig. 1

The attractive spin-orbit case, hence the possibility of magnetic resonances in the deep potential well occurs in the following cases  $\ell \neq 0$ .

$j = \ell - \frac{1}{2}$ ( $C_e$ neg.)		$j = \ell + \frac{1}{2}$ ( $C_e$ pos.)		
$g/c$	-1	+1	-1	
+	yes	no	+	no
-	no	yes	-	yes

Thus for electron-proton-like systems ( $c = -1$ ,  $g$  pos.) we can have resonances (called superpositronium) in the states  $j = \ell - \frac{1}{2}$  only, i.e.  $P_{1/2}$ ,  $D_{3/2}$ , etc.

C) One can now calculate explicitly the new subground states (w.r.t. the Coulomb potential) associated to  $V(r)$  (i.e. derive new molecular interactions) which result from this analysis.

As we shall see, following de Broglie<sup>(14)</sup>, they are given by the relation

$$\frac{M^2 \hbar^2}{m_e r^3} + \frac{\partial V(r)}{\partial r} = 0 \quad (12)$$

where  $r$  denotes their radius and  $M$  an integer quantum number.

Two suggestions of possible existence of "subground states" (w.r.t. Coulomb) of  $H_2$  or  $D_2$  molecular states have already been presented in the literature

1) by Mills et al.<sup>(15)</sup> on the basis of a new model of orbital electrons described a charged spherical shells enclosing the nuclei. This leads to quantum fractional energy. Energy prediction (resonance induced) predictions ~27 ev.

This model contradicts the quantum mechanical predictions of point-like electron-electron scattering verified by experiments.

2) by Cerofolini et al.<sup>(16)</sup> which have proposed a model of binuclear molecular states surrounded by the same orbital electrons. This model also has not been justified theoretically and explains all excess heat in terms of unobserved real fusion mediated by (also unobserved) real neutron trapping.

To justify expression<sup>(12)</sup> we recall that stationary solutions of the Schrödinger equation for a central potential  $V(r)$  with

$$[-(\hbar^2/2m)\nabla^2 + V(r)]\psi = E\psi \quad (13)$$

have the form

$$\psi(r, \theta, \phi) = R(r)\Theta(\theta)\Omega(\phi) \quad (14)$$

where functions

To simplify this derivation we shall utilize the causal mathematical formalism associated by de Broglie<sup>(14)</sup> and Bohm<sup>(17)</sup> to quantum mechanics: a formalism which has been shown<sup>(15)</sup> to recover the usual Bohr-Sommerfeld quantization rules.

To simplify the presentation of this calculation we have used the formalism of de Broglie and Bohm shown to be equivalent in its prediction to the usual quantum formalism. In their model microobjects are waves  $\psi = Re^{iS/\hbar}$  with  $S = Et + \alpha(\vec{r})$  (which satisfy  $\nabla \cdot \vec{S} = 0$ ) and particles (with  $p_i = -i\hbar \vec{\nabla}_i S$ ) which follow the quantum Bohrian orbits in a central potential.

$$\begin{aligned}
 R(r) &= A F_n^l(r) \\
 \Theta(\theta) &= P_l^M(\cos \theta) \\
 \Omega_M(\phi) &= \exp(i M \phi)
 \end{aligned} \tag{15}$$

are the solutions of three separate differential equations

$$\begin{aligned}
 (1/R)[d(r^2 dR/dr)/dr + (2m/\hbar^2)r^2(E - V)]R &= -C \\
 (1/\Theta)[(1/\sin \theta)d(\sin \theta d\Theta/d\theta)/d\theta - C \sin^2 \theta] &= M^2 \\
 (1/\Omega)d^2\Omega/d\phi^2 &= -M^2
 \end{aligned} \tag{16}$$

By de Broglie's and Bohm's definition the quantum action is proportional to the phase of the wave function. Since the functions  $R(r)$  and  $\Theta(\theta)$  are real we conclude that

$$s(\vec{r}) = \hbar M \phi \tag{17}$$

Using (14) and (16) one easily determines the quantum potential

$$U_Q(\vec{r}) = -(\hbar^2/2m)\nabla^2(R(r)\Theta(\theta))/R(r)\Theta(\theta) = E - V - \hbar^2 M^2 / 2mr^2 \sin^2 \theta \tag{18}$$

Taking into account that  $\overrightarrow{\text{grad}} s = \overrightarrow{\text{grad}} \hbar M \phi = (\hbar M/r \sin \theta) \vec{e}_\phi$  (19)

we see that  $s$  satisfies the (quantum) Hamilton-Jacobi equation it yields

$$E = (\overrightarrow{\text{grad}} s)^2 / 2m - \underline{V(\vec{r})} - \underline{(\hbar^2/2m)\nabla^2(R(r)\Theta(\theta))/R(r)\Theta(\theta)} \tag{20}$$

In spherical coordinates  $m\vec{r}$  reads

$$m\vec{r} = m\vec{r}\dot{\phi} \sin \theta \cdot \vec{e}_\phi \tag{21}$$

Hence equating (4) to (16) on the basis of the definition of "momentum" we obtain

$$\dot{\phi} = \hbar M / mr^2 \sin^2 \theta , \quad r = r_0 , \quad \theta = \theta_0 \quad (22)$$

and finally

$$\phi = (\hbar M / mr_0^2 \sin^2 \theta) \cdot t + \phi_0 , \quad \theta = \theta_0 , \quad r = r_0 \quad (23)$$

Therefore, according to the causal interpretation in the stationary states the electron moves along circles lying in the planes parallel to the x-y plane for any central potential. For the same magnetic quantum number M these trajectories do not distinguish between different potentials. They have to be distinguished by their probability distribution.

For kinetic energy we find

$$T = \vec{p}^2 / 2m = p_\phi^2 / 2m = m^2 r^2 \dot{\phi}^2 \cdot \sin^2 \theta / 2m \quad (24)$$

By substituting this equality into (2) we obtain

$$E = V(r) + T + U_Q(r) \quad (25)$$

i.e. quantum energy is a sum of kinetic energy, Coulomb potential energy and quantum potential energy.  $U_Q(r)$  or  $V(r)$

The trajectories derived from  $\vec{p} = \nabla \phi$  for the hydrogen atom in particular are quite different from Bohr's (semiclassical) trajectories. Bohr's trajectories form a subset in the set of Kepler's orbits (this particular set satisfies the conditions of quantization). The nucleus lies in the plane of the orbit. This is not the case with these "causal" orbits whose planes in general do not contain the nucleus.

Bohr trajectories satisfy the relation  $\vec{p} = \overline{\text{grad}} \omega$  and the conditions of quantization, whereas the de Broglie-Bohm trajectories satisfy  $\vec{p} = \overline{\text{grad}} s = \overline{\text{grad}} \hbar M \phi$ .

To analyze these Bohr orbits and following a presentation given by Holland<sup>(2)</sup> we shall now examine the rotational analogue of the linear translation of the wavefronts corresponding to a momentum eigenfunctions. To do this we consider the eigenfunctions of a component of orbital angular momentum which for convenience we take to be  $\hat{L}_z$ . Since  $[\hat{L}_z, \hat{L}^2] = 0$  we seek

simultaneous eigenfunctions of  $\hat{L}_z$  and  $\hat{L}^2$ . In spherical polar coordinates  $(r, \theta, \phi)$  where

$$x = r \sin \theta \cos \phi, \quad y = r \sin \theta \sin \phi, \quad z = r \cos \theta, \quad (26)$$

we have following Schiff's notations <sup>(19)</sup>

$$\left. \begin{aligned} \hat{L}_x &= i\hbar \left( \sin \phi \frac{\partial}{\partial \theta} + \cot \theta \cos \phi \frac{\partial}{\partial \phi} \right) \\ \hat{L}_y &= i\hbar \left( -\cos \phi \frac{\partial}{\partial \theta} + \cot \theta \sin \phi \frac{\partial}{\partial \phi} \right) \\ \hat{L}_z &= -i\hbar \hat{e}/\partial \phi \\ \hat{L}^2 &= -\hbar^2 \left[ \frac{1}{\sin \theta} \frac{\partial}{\partial \theta} \left( \sin \theta \frac{\partial}{\partial \theta} \right) + \frac{1}{\sin^2 \theta} \frac{\partial^2}{\partial \phi^2} \right] \end{aligned} \right\} \quad (27)$$

and

$$\left. \begin{aligned} \hat{L}_z Y_{lm}(\theta, \phi) &= m\hbar Y_{lm}(\theta, \phi), \\ \hat{L}^2 Y_{lm}(\theta, \phi) &= l(l+1)\hbar^2 Y_{lm}(\theta, \phi), \end{aligned} \right\} \quad (28)$$

where  $Y_{lm}(\theta, \phi)$  are the spherical harmonics,  $l$  is the orbital angular momentum number,  $l = 0, 1, 2, \dots$ , and  $m$  is the azimuthal quantum number,  $-l \leq m \leq l$  (in this section we denote mass by  $m_0$ ). We have

$$Y_{lm}(\theta, \phi) = f_{lm}(\theta) e^{im\phi}, \quad (29)$$

where  $f_{lm}(\theta)$  are a set of real functions (proportional to the Legendre polynomials).

A stationary state corresponding to energy  $E$  is given by

$$Y_{lm}(\theta, \phi) = f_{lm}(\theta) e^{im\phi}, \quad (30)$$

where the function  $g_{Elm}(r)$  is real. The phase function is therefore

$$S(r, \theta, \phi, t) = m\hbar\phi - Et \quad (31)$$

apart from a constant.

For each  $t$  and  $m \neq 0$ , the wavefronts  $S = \text{constant}$  are planes parallel to, and ending on, the  $z$ -axis (which is a nodal line of  $\psi$  when  $m \neq 0$ ) since the spherical harmonics are proportional to  $\sin \theta$ . As  $t$  increases the planes rotate

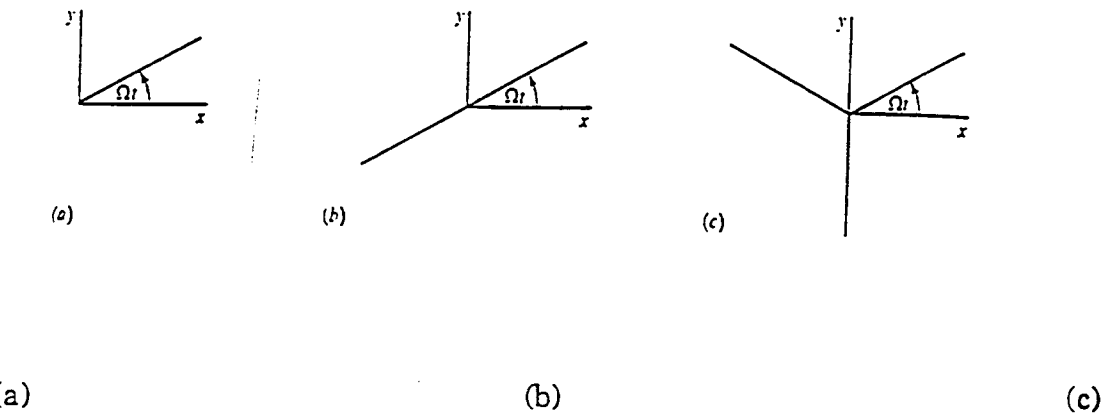


Fig. 2. The wavecrests  $S = nh$ ,  $n \in \mathbb{Z}$ , for the state (25) when (a)  $m = 1$ , (b)  $m = 2$ , (c)  $m = 3$ . The crests rotate anticlockwise with frequency  $\Omega = E/mh$  about the  $z$ -axis (a nodal line). The wavefronts of states for which  $m < 0$  rotate clockwise. The wavelength is  $\lambda_\phi = |2\pi r \sin \theta / m|$  where  $r$  and  $\theta$  specify a point on a wavefront.

about the  $z$ -axis with angular velocity  $\Omega = E/mh$  (see Fig. 2). The number of wavecrests, defined by  $S = nh$ ,  $n \in \mathbb{Z}$ , that come to an end on the  $z$ -axis is equal to  $|m|$ . This illustrates the interpretation of the single-valuedness requirement,

$$\oint dS = mh, \quad m \text{ integer} \quad (32)$$

It is evident from the orthogonality of the paths to the surfaces of constant  $S$  that the trajectories will be circles lying in planes parallel to the  $xy$ -plane. This is easily confirmed by solving the guidance equation (de Broglie,<sup>14</sup> 1956, p. 119; Belinfante, 1973, p. 190). In spherical polar coordinates

$$v_r = m_0^{-1} \partial S / \partial r, \quad v_\theta = (m_0 r)^{-1} \partial S / \partial \theta, \quad v_\phi = (m_0 r \sin \theta)^{-1} \partial S / \partial \phi \quad (33)$$

with  $v_r = \dot{r}, \quad v_\theta = r\dot{\theta}, \quad v_\phi = r \sin \theta \dot{\phi}$ . (34)

Substituting (31) into (33) yields

$$v_r = v_\theta = 0, \quad v_\phi = m\hbar/m_0 r \sin \theta \quad (35)$$

and hence from (34)

$$r = r_0, \quad \theta = \theta_0, \quad \phi = \phi_0 + m\hbar t/m_0 r_0^2 \sin^2 \theta_0, \quad (36)$$

where  $(r_0, \theta_0, \phi_0)$  are the initial coordinates. The result (36) is valid for all  $m$ . The particle orbits the  $z$ -axis along a circle of constant radius  $(r_0 \sin \theta_0)$  and with constant angular speed, which is a multiple of  $\hbar/m_0 r_0^2 \sin^2 \theta_0$  (Fig. ).

The initial coordinates are as usual arbitrary except that they

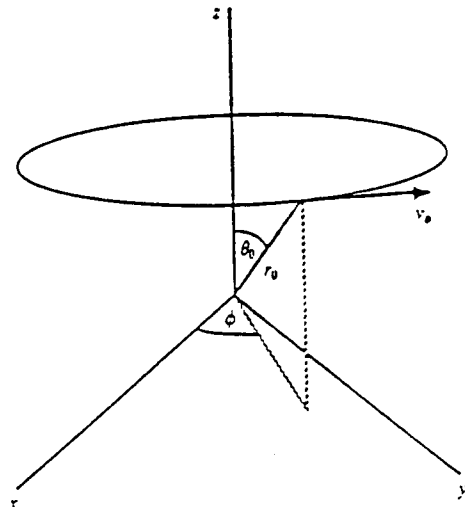


Fig. 3. The particle trajectory for a spherically symmetric external potential when the wave is a stationary state and an eigenfunction of  $\hat{L}$ , corresponding to the eigenvalue  $mh$ . When  $m = 0$  the particle is at rest [ $m$ ] wavelengths fit into one orbit.

cannot be chosen to lie in nodal regions<sup>6</sup>. In these coordinates the probability of a particle being between the points  $x$  and  $x + dx$  is given by

$$P = |\psi|^2 r^2 \sin \theta dr d\theta d\phi. \quad (37)$$

From the generalized de Broglie relation (12)  $\lambda_Q = h/m_0 |v_\phi|$  and we see that along the orbit the wavelength is given by  $\lambda_Q = 2\pi r_0 \sin \theta_0 / m$ . Since the circumference is  $2\pi r_0 \sin \theta_0$ , it follows that we can fit exactly  $|m|$  wavelengths into one quantum orbit. This should be compared with the usual de Broglie wavelength connected with Bohr-Sommerfeld quantization (Bohm, 1951,<sup>19</sup>) which is defined in terms of the momentum of a classical particle in the potential  $V$ . There, an integral number of wavelengths fit into a classical orbit.

The angular speed of the wavefronts and the particle are related by

$$\Omega \dot{\phi} = E/m_0 r_0^2 \sin^2 \theta_0. \quad (38)$$

The higher the quantum number  $m$  the faster the particle moves, and the slower the wavefronts rotate.

The fact that the radius of the circle is freely specifiable means in particular that it is independent of  $E$  or  $m$ . The picture is therefore somewhat different from the primitive Bohr model in which an electron moves in a circle in the equatorial plane ( $\theta_0 = \pi/2$ ) and the radius is a function of  $m$  (see below). The quantization here appears rather in the magnitude of the particle velocity.

Let us consider now the angular momentum of the particle,  $L = \mathbf{x} \times \nabla S$ . Since  $y$  is an eigenfunction of  $\hat{L}$  we know from the results of §3 that the  $-z$ -component of angular momentum will coincide with the eigenvalue of  $\hat{L}^2$ . Conventionally one would say that the  $x$ - and  $y$ -components of angular momentum are "undefined". Here though they are well defined and we have

$$L_x = -m\hbar \cot \theta \cos \phi, \quad L_y = m\hbar \cot \theta \sin \phi, \quad L_z = m\hbar \quad (4.5.14)$$

and hence

$$L^2 = m^2 \hbar^2 / \sin^2 \theta. \quad (39)$$

---

<sup>6</sup>In (31) we have assumed that the real coefficient in (25) is positive. In domains where the coefficient is negative we should add  $\pi$  to (31).

The total orbital angular momentum is given by

$$L^2 - \hbar^2(\mathbf{x} \times \nabla R)^2/R = l(l+1)\hbar^2. \quad (40)$$

Evaluated along a trajectory  $\vec{r} = \nabla S$  we see that  $L_z$  and the total angular momentum are conserved, but that  $L_x$  and  $L_y$  are not unless  $\theta_0 = \pi/2$ . Thus, although the classical force is central the motion is asymmetrical, which reflects the fact that a particular direction in space has been singled out as the quantization axis.

This suggests that the effective potential acting on the particle is not symmetric. To find its form we write down the quantum Hamilton-Jacobi equation, which reduces to

$$E = m^2\hbar^2/2m_0r^2 \sin^2 \theta + Q + V(r). \quad (41)$$

This enables us to find the effective force without knowing the explicit expression for  $R$ . We have

$$-\nabla(Q + V) = -(m^2\hbar^2/2m_0)\nabla(-1/r^2 \sin^2 \theta), \quad (42)$$

which shows that the effective potential is indeed not central. Notice that this potential does not depend on any feature of  $V$  other than that it is symmetric. The component of the total force (in direction  $\theta$ ) orthogonal to the line of action of the classical force (in direction  $r$ ) is therefore independent of the latter.

So far we have worked with an arbitrary  $V$  and unrestricted  $E$ . In the case of the hydrogen-like atom, with the nucleus placed at the origin of coordinates,  $V = -Ze^2/r$ , and  $m_0$  the reduced mass which may be approximately identified with the electron mass, we have

$$E_n = -m_0Z^2e^4/2\hbar^2n^2, \quad (43)$$

where  $n \geq l + 1$  and the stationary states will be denoted  $\psi_{nlm}$ . The most general stationary state corresponding to the quantum number  $m$  may be written

$$\begin{aligned}\psi_n(r, \theta, \phi, t) &= \sum_{l=0}^{n-1} \sum_{m=-l}^l c_{lm} \psi_{nlm}(r, \theta, \phi, t) \\ &= \left( \sum_{l=0}^{n-1} \sum_{m=-l}^l c_{lm} F_{nl}(r, \theta) e^{im\phi} \right) e^{-iE_nt/\hbar},\end{aligned}\quad (44)$$

where  $c_{lm}$  are arbitrary complex constants and  $F_{nl}(r, \theta)$  are real functions. The phase of  $\psi_n$  will be a complicated function of  $r, \theta$  and  $\phi$  and the trajectory will have a correspondingly complex structure (although of constant energy  $E_n$ ). In fact, we may generate an infinite set of possible motions by choosing different values of the constants  $c_{lm}$ . If the atom is in a stationary state it will remain there unless it interacts with another system. If this happens and the atom is left in another stationary state, i.e. a transition occurs, then in general the electron motion initially and finally will be determined by waves of the general form (44) rather than the simple eigenstates of angular momentum we have discussed above (during the transition the motion is guided by a superposition of stationary states).

In states for which the azimuthal quantum number  $m$  is zero the particle is at rest

$$v = 0 \Rightarrow r = r_0, \quad \theta = \theta_0, \quad \phi = \phi_0. \quad (45)$$

We have

$$V + Q = E_n \quad (46)$$

so that the quantum force exactly balances the classical force. For the hydrogen-like atom this will be so in particular for the ground state  $\psi_{100}$ . This result provides the explanation according to the quantum theory of motion for the stability of matter. For if the particle is at rest relative to the nucleus it is evidently not accelerating, and hence does not radiate. Therefore it does not lose energy and it will not spiral into the nucleus, the famous outcome predicted by classical electrodynamics.

This account of why matter does not collapse is different from that advanced by Bohr in the old quantum theory. It was assumed by Bohr that the electron moves along circles in the equatorial plane under the influence of the central Coulomb force, the allowed orbits being determined by a quantization condition imposed on solutions to the classical Hamilton-Jacobi equation. This was essentially a postulate and no explanation of its physical significance was offered. The ground state corresponds to a minimum radius. For us on the

other hand the electron is not confined to the equatorial plane and there is no minimum "radius" - the initial coordinates ( 45 ) are arbitrary.

Is there a relation between the trajectories of Fig. 3 and the Bohr orbits when  $m \neq 0$ ? Since the latter are associated with the classical Hamilton-Jacobi equation, we might expect to recover them when the effective force acting in the equatorial plane is just that due to  $-\nabla V$ . From ( 41 ) we have, when  $\theta = \pi/2$ , and  $V(r) = Ze^2/r$

$$Q = E_n - m^2\hbar^2/2m_0r^2 + Ze^2/r, \quad (47)$$

so that

$$-\hat{c}Q/\hat{c}r = -m^2\hbar^2/m_0r^3 + Ze^2/r^2. \quad (48)$$

The requirement that the quantum force ( 48 ) vanishes implies that

$$r = m^2\hbar^2/m_0Ze^2 \quad (49)$$

for  $r \neq 0$ . This indeed yields the set of Bohr orbits for  $|m| = 1, 2, \dots$  but they do not have quite the same meaning as in Bohr's theory. As we have seen, for us the ground state is characterized by  $m = 0$  and a state of rest, whereas for Bohr it is characterized by a circular orbit at a radius given by putting  $|M| = 1$  in (49). shows that the particle has finite quantum potential energy. And, of course, in the causal theory this is just a subclass of the permissible orbits and the particle may pass through regions where the quantum potential is not stationary, independently of the quantum numbers characterizing the state.

We can now explicitly calculate the new Bohr orbit with  $V(r)$  given by (10) in the case where  $m_2 \gg m_1, M_1 = 0$  i.e.  $\vec{a} = (e_1/m_1)\vec{M}_1, \vec{b} = 0$  and  $A = (e_1^2/m_1)M_2^2$  i.e.

$$V(r) = \frac{e_1 e}{r} - \frac{e_1 M_2 \vec{\sigma} \cdot \vec{\sigma} \cdot \vec{L}}{m_1} + \frac{e_1 M_2^2}{m_1} \cdot \frac{1}{r^4} \quad (50)$$

The relation (48) i.e.

$$\frac{m^2 \cdot \hbar^2}{m_1 r^3} + \frac{\partial V(r)}{\partial r} = 0 \quad |m|=1, 2, \dots$$

multiplied by  $r^5$  yields the relation :

$$\left( \frac{m^2 \hbar^2}{m_1} + B \right) r^2 = A r^3 + C r + D. \quad (51)$$

which can be written in the form

$$r^3 + a_2 r^2 + a_1 r + a_0 = 0 \quad (52)$$

Introducing  $Q = (1/3)\alpha_1 + (1/9)\alpha_2^2$  and  $R = (1/6)(\alpha_1\alpha_2 - 3\alpha_0) - (1/27)\alpha_2^3$   
 we see that  
 with  $Q^2 + R^2 > 0$  there is one real root and a pair of complex conjugate roots  
 if  $Q^2 + R^2 = 0$  all roots are real and at least two are equal

if  $Q^2 + R^2 < 0$  all roots are real.

Of course each real root denotes an infinite set  
 (with  $m = 1, 2, \dots$ ) of Bohr orbits. Introducing the two auxiliary quantities  
 $S_1 = [R + (Q^2 + R^2)^{1/2}]^{1/3}$  and  $S_2 = [R - (Q^2 + R^2)^{1/2}]^{1/3}$   
 one gets for these roots (which define three sets of Bohr orbits) the expressions

$$\left\{ \begin{array}{l} r_1 = (S_1 + S_2) - \frac{\alpha_2}{3} = f_1(m) \\ r_2 = -\frac{1}{2}(S_1 + S_2) - \frac{\alpha_2}{3} + i\frac{\sqrt{3}}{2}(S_1 - S_2) = f_2(m) \\ r_3 = -\frac{1}{2}(S_1 + S_2) - \frac{\alpha_2}{3} - i\frac{\sqrt{3}}{2}(S_1 - S_2) = f_3(m) \end{array} \right. \quad (53)$$

which satisfy three constraints, i.e.:

$$\left\{ \begin{array}{l} r_1 + r_2 + r_3 = -\alpha_2 \\ r_1 r_2 + r_1 r_3 + r_2 r_3 = \alpha_1 \\ r_1 r_2 r_3 = -\alpha_0 \end{array} \right. \quad (54)$$

According to the distance  $r$  one sees immediately

- that when  $A/r > (1/2)B/r^2 + (1/3)C/r^3 + (1/4)D/r^4$  i.e.  $Ar^3 > Br^2 + Cr + D$   
 one has a set of radii which varies like  $m^2$  i.e. which corresponds to Bohr's initial orbits when  $\Theta = \pi/2$ .

- that when  $C/3r^3 > A/r + (1/2)B/r^2$  i.e.  $Cr > Ar^3 + D$   
 then  $r \approx Cm_1/m^2\hbar^2$

This set varies like  $1/m^2$  and corresponds to a set of "tight" orbits never discussed by Bohr.

- that when  $(1/4)D/r^4 > (1/3)C/r^3 + (1/2)B/r^2 + A/r$   
 then  $r \approx (Dm_1/m^2\hbar^2)^{1/2} = (Dm_1)^{1/2}/m\hbar$

a <sup>which</sup> set also yields a new set of "tight" Bohr orbits unknown in the literature.

Since a detailed analysis of the corresponding new Bohr energy levels is in preparation (and will be shortly published) we will now limit ourselves to the following remarks. The existence of these new "deep" Bohr levels depend of course on the relative spin (and spin-orbit) orientations i.e. they can only be excited in spacial physical situations where they are determined by their surrounding. This appears now to be the case when Hydrogen-Deuterium etc are imbedded in dense media.

### §3 STABILITY AND SCREENING IN THE NEW 'TIGHT' MOLECULES

D/ The possibility of enhanced screening which induces real fusion starting from the states  $\bar{H}_2$ ,  $\bar{D}_2$ , etc has already been discussed in the literature<sup>(2)(20)</sup> and various experimental tests are under way.

The proposed mechanism can be summarized as follows:

- 1) Within a structured dense media one can find capillary like structures which when loaded with conductors containing  $H_2$  or  $D_2$  can carry electromagnetic microcurrents. In such structures one can/has observed the longitudinal force between current elements predicted by Ampère<sup>(2)</sup>

This longitudinal force in gaseous liquid and solid conductors has been shown (as illustrated in the two following figures (1) and (2) to distort the usual current i.e.



Fig. 4

Fig. 1 showing how a tungsten conductor is cut into pieces called usually ("beads"). The tungsten wire is photographed during the current pause (Uppsala experiments).

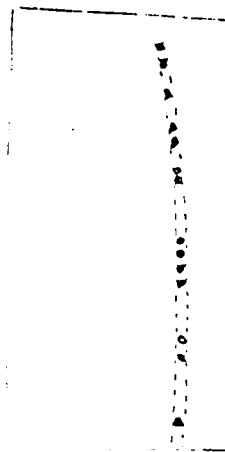


Fig. 5

Sketch of an X-ray photograph of deuterium fibre fragmentation

has the evident consequences of creating standing longitudinal current concentrations in conductors i.e. to split them into string of beads which interrupt the current at high intensities. This creation of strings of ((beads))

current concentrations correspond to the nodes of the longitudinal standing waves of wavelength  $\ell/n$  (with  $n$  integer) which appears between the extremities of a limited current with fixed end points separated by a distance  $\ell$ . If an electrode contains rows of capillaries the ionization or injected currents thus induces (as a quasi-static wave system is created) the possibility of screening effects (which facilitate fusion) and, as we shall see, new ion-electron-ion systems which might explain excess heat.<sup>(2)</sup>

In this model the apparition of strong electron concentrations (~1000 electrons around each ion) has two consequences

- They facilitate screening through the Coulomb barrier between pairs of H or D ions, i.e. the superscreening required by Takahashi<sup>(5)</sup>
- They allow the existence, in their midst, of new stable (possibly metastable in special situations) "light" combined  $p^+ + p^+ + e^-$  or  $D^+ + D^{++} - e^-$  combinations which have been suggested by Gryzinski<sup>(21)</sup> and Barut<sup>(22)</sup> as being a possible new chemical source of the essential part of excess heat at low current input both for Hydrogen and Deuterium \*. Such combinations are evidently unstable in free space, (see fig. 6) but stabilize within a surrounding electron cloud.

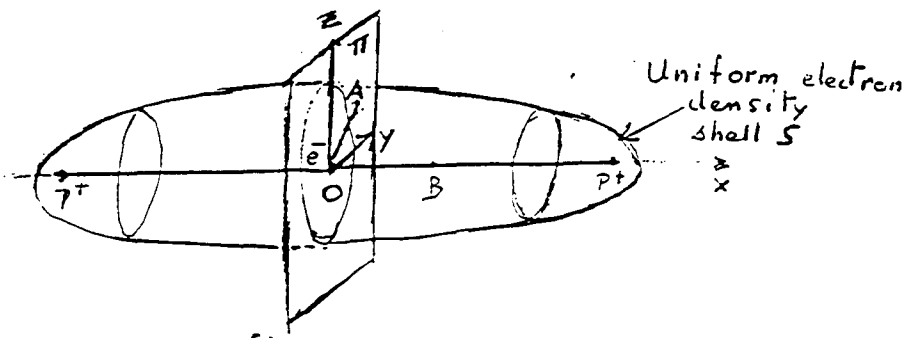


fig. 6

Indeed if one considers the situation described in Fig. 6 where two protons on an axis  $Ox$  are separated by an electron at point  $O$  at mid-distance (i.e. at the center of mass of the system) we see that any displacement of the middle electron located in the orthogonal  $P$  plane to a distance  $A$  in  $P$  is submitted to a recall force towards  $O$ : while a displacement towards  $B$  on  $Ox$  is amplified. This unstable situation in free space is canceled when the system is imbedded in a external electron cloud described by a superposition of uniform electron density shells  $S$ . A quantitative analysis will be shortly published.

\*The idea that the excess heat observed in glow discharge in Hydrogen originates in some presently unknown phenomena in nuclear physics (such as virtual neutron exchange etc) in phenomena of the type  $p^+ + p^+ + e^- \rightarrow D_2^+$  + neutrino evidently conflicts with quantum mechanics since the calculated corresponding probabilities are  $\sim 10^{-40}$ . Moreover the neutrino's energy could not be detected as "excess heat".

As we shall now see the formation of a new stable tight phase

$\bar{H}_2^+$  and  $\bar{D}_2^+$  of  $H_2^+$  and  $D_2^+$  can be justified, within the frame of present quantum theory (i.e. quantum chemistry), as a consequence of the introduction of spin-spin and spin-orbit forces (which always exist but cancel out in free-space due to random spin orientations) when they resonate with the surrounding electron plasma oscillations.

3) The existence of such new "tight" states is now supported by two facts:

(a) -The exothermic formation of the corresponding states which could correspond to resonance phenomena within the cathode (such as resonances within the electron clouds in internal regions suggested by Preparata). Their desexcitation (also corresponding to quantum jumps from one new Bohr orbit to another) leads to soft X ray spectra... and X rays have been observed in such experiments.<sup>(1)</sup>

-The formation of the new "tight" states  $\bar{H}_2^+$  and  $\bar{D}_2^+$  is not necessarily tied to the existence of the input current. Even when it can be supported by internal (ionization) currents or internal voltage differences carried by the Pd or Nickel... so that one could explain in this way the existence of the "heat after death" phenomena discovered by Fleischmann and Pons. The excess heat depends on the number of  $\bar{H}_2^+$  and  $\bar{D}_2^+$  (in light and heavy water) i.e. on the loading of the capillaries contained in the electrode. It is created only when they are formed i.e. not necessarily immediately since individual capillary situations change. The corresponding binding energies have been shown<sup>(2)</sup> to be of the order of ~50 kev instead of the usual ~5 ev of quantum chemistry. The corresponding heat is ~4 times as big for  $\bar{D}_2^+$  as for  $\bar{H}_2^+$ .

(b) When one utilizes D<sub>2</sub> or other types of fusing material the creation of excess heat by the tight  $\bar{D}_2^+$  states is generally accompanied by some real fusion processes: since a electron... (when located between ions) behaves (within the deeper potential due to spin-spin and spin orbit forces) as if it had acquired a heavier "effective" mass<sup>(4)</sup>. Indeed smaller Bohr orbits facilitate tunneling through the Coulomb barrier. Moreover, "Heavier" electrons<sup>also</sup> explain some types of observed regular collective motions (i.e. cluster formations) which can contain triangular, tetrahedral cubic... configurations which move collectively and have been observed to have strongly enhanced (by many orders of magnitude) with individual particles.<sup>(22)</sup> This configuration naturally arises when the Ampère force cuts the

current into beads in a capillary since the situation of the ions then resembles what happens to fast going cars which crash successively into each other during a slowdown (accident) on a modern highway<sup>(2)</sup>

This situation is very different from the usual quantum mechanical interpretation of chemical phenomena i.e. of the normal states of  $H_2^+$  and  $D_2^+$  which are assumed (according to the Born-Oppenheimer approximation) to correspond to the rapid motion of the electron in the field of two almost fixed nuclei. If one first neglects the spin and considers two masses  $M$  (with charges  $z$ ) rotating at a distance  $r$  from a mass (charge  $z$ ) i.e.

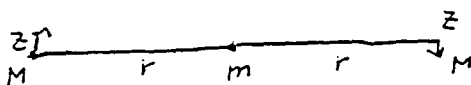


fig 7

this gives the Hamiltonian

$$H = \frac{P^2}{2M} + \alpha \left( \frac{2z^2}{r} + \frac{z^2}{2r} \right)$$

which yield when quantized by the usual Bohr-Sommerfeld method ( $\int p dq = n\hbar$ ) with ( $\hbar = c = 1$ ). Energy levels  $E_n = -(1/4)(M\alpha^2/n^2) Z^2 (2z + Z/2)^2$  i.e

- For the  $H_e$  atom this yields  $E_0 = 6,12$  Ryd close to the observed value  $\sim 5,69$  Ryd.

- For  $\bar{H}_2^+$  and  $D_2^+$  the Bohr energy levels are approached by  $E_n = -(9/16)(M\alpha^2/n^2)$

which correspond to ground states of 28,1 kev and 56,2 kev for  $\bar{H}_2^+$  and  $\bar{D}_2^+$ .

Some evidence in favor of this model is also given by two facts i.e.

- The fact that neutrons are produced when the beads are formed i.e. when there appears strong electron concentrations which contribute to the screening of the Coulomb barrier. See figure

<sup>1</sup>like in muon catalyzed fusion. If one denotes this effective mass by  $\overline{m}_e$  one forms exotic molecules  $H^+ e^- D^+$  which can fuse via a resonance mechanism with an enhanced fusion probability.

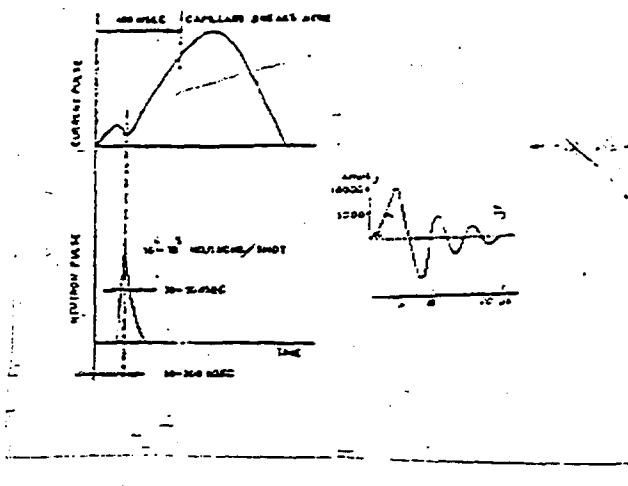


Fig. 8. Drawings reproduced from the refs. (2) and (14) showing the principal elements which describe the capillary fusion experiments performed by Lochte-Holtgreven et al. [14] F.C. Young et al. N.R.L. 20 (1983) 439. [16] J.D. Sethian et al. P.R.L. 59 (1987) 585.

—There exists the possibility to start chain formation of  $\bar{H}_2^+$  and  $\bar{D}_2^+$  which would explain heat bursts i.e. fusion waves of the Winterberg type. After some time the reaction stops and the new compound molecules ( $\bar{H}_2^+$ ,  $\bar{D}_2^+$ ) leave the system for good.

- The existence of tight  $\bar{D}_2^+$  enhance the neutron -  $\bar{D}_2^+$  cross section so that one should add to the observed yield of neutrons a number of unobservable thermalized neutrons.

In this model both theoretically and experimentally spin-spin and spin-orbital orbit forces are predicted to favor clustering and to induce differential propagation (i.e. separation) of isotopes, starting with uranium and heavy elements down to  $H_2$  and  $D_2$ .

Following Takahashi et al. one can thus assume that ionization currents (enhanced or not by bursts of input currents) generate at first real "tight" molecular states  $\bar{H}_2$ ,  $\bar{D}_2$  etc (denoted by the symbol \*, by Takahashi) which, when they split into beads generate real fusion procedures.

The second stage i.e. the existence of new tight Bohr orbits can be tested through the observation of the soft X-rays corresponding to the deexcitation of the new levels in  $\bar{H}$  or  $\bar{D}$  atoms. This can be done through a verification of their predicted values (which will be shortly published) through the use of soft X-ray germanium based detectors. Another test would be the confirmation of the new narrow resonances recently observed in electron-proton and electron-positron "scattering" (23).

## CONCLUSION

The first stage i.e. the existence of excess heat in H or H<sub>2</sub>O experiments: (in the author's opinion) be considered as already proven by a growing set of experiments<sup>(1)(3)</sup>. This shows the existence of  $\alpha$ , non-fusion origin for presently observed excess heat and seems to exclude its interpretation in terms of virtual neutron exchange.

The second stage i.e. the existence of new "tight" molecules such as  $\bar{H}_2$  or  $\bar{D}_2$  is in fact already suggested by the experiments of Mills et al. which have detected by cryometry and mass spectrometry the existence of new tight states of H<sub>2</sub>.

To quote the authors "an exothermic reaction is reported wherein the electrons of hydrogen atoms and deuterium atoms are stimulated to relax to quantized potential energy levels below that of the "ground state" via

electrochemical reactants K<sup>+</sup> and K<sup>+</sup>; Pd<sup>2+</sup> and Li<sup>+</sup>, or Pd and O<sub>2</sub> of redox energy resonant with the energy hole which stimulates this transition. Calorimetry of pulsed current and continuous electrolysis of aqueous potassium carbonate (K<sup>+</sup>/K<sup>+</sup> electrocatalytic couple) at a nickel cathode was performed. The excess power out of 41 watts exceeded the total input power given by the product of the electrolysis voltage and current by a factor greater than 8. The "ash" of the exothermic reaction is atoms having electrons of energy below the "ground state" which are predicted to form molecules. The predicted molecules were identified by lack of reactivity with oxygen by separation from molecular deuterium by centrifugation, and by mass spectroscopic analysis.<sup>j)</sup>

The third stage i.e. the prediction of  $\bar{H}_2$  or  $\bar{D}_2$  to explain excess heat at low energy input can also be considered as supported by the experiments of Miles, Bush et al. which report <sup>4</sup>H<sub>e</sub> (which they did not attempt to distinguish from  $\bar{D}_2$ )<sup>64</sup> and by the experiment of Yamaguchi and Nishiaka who have detected by mass spectroscopy (along with fusion "ashes" <sup>3</sup>H<sub>e</sub> with an energy of 4-5-6 Mev and protons with an energy of 3Mev) <sup>4</sup>H<sub>e</sub> accompanied (as it should in our model) by a heavier  $\bar{D}_2$  peak. Their input being dominant at low input. Further search for soft X-rays and also for the existence of  $\bar{H}_2^+$  in H or H<sub>2</sub>O experiments would help to prove (or disprove) the proposed model.

Proof of the last stage i.e. the possibility to add to the excess heat (generated by the new Bohr orbits) fusion energy generated by high energy input pulses is still in infancy<sup>64</sup> due to reluctance to accept the existence of the new phenomena.

Acknowledgements. The author wants to thank Akademician Baraboshkin, Professors A. Takahashi, Z. Maric, N. Samsonenko, M.C. Combourieu and M. Rabinowicz for helpful suggestions.

## References

- 1 Y.R. Kucherov et al. PLA 170 (1992) 265 and J. Dufour, Fusion Technology 24 (1993) 205.
- 2 J.P. Vigier, Frontiers of Cold Fusion. Proc. of the Third International Conference on Cold Fusion. Nagoya Japan Universal Acad. Press. H. Ikegami Ed. (1992).
- 3 For example see the contributions of Drs. Mac Kubre, Takahashi, Kumimatsu and Storms in Frontiers of Cold Fusion. Universal Academy Press Inc. Tokyo (1993) Ed. H. Ikegami.
- 4 R. Antanasijevic, I. Lakicevic, Z. Maric, D. Zivic, A. Zaric and J.P. Vigier, PLA 180 (1993) 25.
- 5 A. Takahashi, H. Miyamaru, M. Fukurara. Multibody Fusion Model to explain experimental results PLA (1994) to be published.
- 6 E. Yamaguchi and T. Nishioka. Helium 4. Production from deuterated Pdadium at low energies. Submitted to PLA.
- 7 M. Fleischmann and S. Pons, PLA 176 (1993) 118.
- 8 See A. Takahashi et al. Proc. 2d Como Conference on Cold Fusion "The Science of Cold Fusion. Italian Physical Society Publ. (1992).
- 9 E. Yamaguchi and T. Nishioka in "Frontiers of Cold Fusion". See Reference 3) and M. Miles, B. Busch et al. in "The Science of Cold Fusion" (see reference 8).
- 10 A. Takahashi et al. J.Appl.Electrom.Math 3 (1992) 221 and Mac Kubre et al. (see ref. 3).
- 11 R. Notoya. Fusion Technology 24 (1993) 202.
- 12 A. Barut. Prediction of new tightly bound states of  $H_2^+(D_2^+)$  and "cold fusion experiments" (private communication) (1992).
- 13 A. Barut, "Lectures on magnetic interactions of stable particles and magnetic resonances, American Institute of Physics (1991) Private communication.
- 14 L. de Broglie. Non-linear wave mechanics. Elsevier, Amsterdam (1960). See also A.O. Barut and M. Basic, Ann.Found. L. de Broglie 15 (1990) 67.
- 15 R.L. Mills, W.R. Good and R. Shanbach, Dihydrino molecule identification. Fusion Technology (in press).
- 16 G.F. Cerofolini, R. Dierich, A.F. Para and G.O. Haviani, Il Nuovo Cimento 13 (1991) 1347.
- 17 D. Bohm, Phys.Rev. 85 (1952) 166 and 180.

- 18 P. Holland, *The Quantum Theory of Motion*, Cambridge University Press (1993).
- 19 L.I. Schiff, *Quantum Mechanics*, Tokyo 1968.
- 20 See the summary given by M. Rambaut, *PLA* **163** (1992) 335.
- 21 M. Gryzinski. *Problems in Quantum Mechanics*. Gdansk 89 Ed. World Scientific Singapore (1990) 302.
- 22 C.F. Cerofolini, F. Corni, G. Ottaviani and R. Tonini, *Il Nuovo Cimento* **105** (1992) 741.
- 23 M. Fleischmann and S. Pons. See *Proceedings ICF4* in Hawaii (6-9 December 1993).



A MODEL OF COLD NUCLEAR TRANSMUTATION BY THE ERZION  
CATALYSIS (THE ERZION MODEL OF "COLD FUZION")

Yu.N.Bazhutov, G.M.Vereshkov.  
Scientific Research Center of  
Physical Technical Problems "Erzion"  
P.O.Box 134, 119633 Moscow, Russia  
Fax: (095) 292-6511 Box 6935 Erzion

**Abstract**

Cold nuclear transmutation model by erzion catalysis is proposed for explaining experimental data on so called cold fusion phenomenon. The erzions are the hypotetic massive stable hadrons which existence and fundamental characteristics were predicted in cosmic rays experiments. According this model the erzions are presented in the matter in extremely little quantity ( $10^2 - 10^7$ )sm<sup>-3</sup> and they are in bounded state. At definite conditions the erzions became released and provide multicycle nuclear transmutation at room temperature. With the help of the Erzion Model one can explain anomalous effects of cold fusion.

The process of so called Cold Nuclear Fusion (CNF) possesses a number of specific properties some of which are most important ones: 1) suppression of the neutron to tritium yield ( $10^3 - 10^{11}$  times) and reducing of tritium to energy yield ( $10^3$  times) /1-3/; 2) CNF reactions go in deliberately unstationary conditions: electrolysis /4-6/, mechanical stroke /7/, temperature and pressure changes /8/; 3) there are great yield fluctuations ( $10^5$  times) /4,5/; 4) attenuation and cessation of CNF process; 5) new isotops and elements production /2,9,10/.

First of the above mentioned properties reveals that the CNF process can not be interpreted in the standard framework, consisting of two reactions:



whose probability is approximately equal. On the basis of the existing data one may conclude that a channel (1a) for unknown reasons is practically closed. The problem of suppressing this channel still is not solved and in the

framework of alternatives of the CNF catalysis, by their schemes analogous with  $\mu$ -catalysis. By this reason a search for solid-state mechanisms of screening deuton charges may not be considered perspective.

Correlation between the CNF phenomenon and processes of destructing solid states is of principal nature. It is known that when solid states are cracking, charges are being localized in the crack walls during 1mks which create electric field in the crack. This field may accelerate particles including deutons up to 100 keV /11/. A hypothesis of so called "accelerated" CNF mechanism has been formulated in the framework of this conception /12/. Without denying the accelerating effect of deutons in cracks (more than that, paying special attention to it) nevertheless we believe that the accelerating mechanism can not solve a problem of interpreting CNF by two reasons: firstly, in each separate crack deuton acceleration stop after relaxation of charges on its walls; secondly, this mechanism does not close a channel (1a).

While trying to interpret CNF we based our assumptions of the following: 1) radical changes in the fusion scheme - supressing a channel with the neutrons outcome-demand a catalyst with totally new features. Unlike the  $\mu$ -catalysis schemes a new catalyst must be electrically neutral and participate in strong interactions; 2) a catalyst appearance in a working matter of the CNF reactor is connected with the matter destruction.

These suppositions out of their linking with concrete models of new hadrons-catalysts seem to be fantastic. However, in our case the situation was facilitated by the fact that at the moment of appearing news of CNF registering we were dealing with search for interpretation of new hadrons whose appearances had been noticed in Cosmic rays. Naturally, a hypothesis comes into existance that we had encountered the same hadron in the Cosmic rays and CNF. The paradox is that constructing a model of cold nuclear fusion by the catalysis of new hadrons helped to understand a number of abnormal developments in Cosmic rays physics.

Indirect indications of existing heavy ( $M_c > 100$  GeV) long-living hadrons in the Cosmic rays during various experiment have been noticed for 20 years /13/. Considering received data one may assume that these hadrons ( let us call them ERZIONS) possess a negative electric charge and present hadrons with somewhat higher ( comparing to common hadrons) penetrating ability.

Theoretical model of new hadrons corresponding with Cosmochemical limitations /14,15/, given by Cosmic rays and

CNF, is presented in detail in /16,17/. The model is based on  $U(1) \times SU_L(2) \times SU_R(2) \times SU(3)$  of the Calibrating theory. Erzions are being interpreted as bonded states  $J^P=0^-$  of the mirror antiquarks  $\bar{U}$  and common quarks u, d:

$$\Theta = (\Theta^0, \Theta^-), \quad \Theta^0 = \bar{U}u, \quad \Theta^- = \bar{U}d \quad (2)$$

The most important property of the isotopic duplet (2) is concluded in absence of one-pion bond with the nucleon doublet ( $N$ ). This circumstance brings to a fact that asymptotics of a strong  $\Theta-N$  interaction has a repulsive nature. Due to this reason erzions are not being captured by the nuclei and this fact lets to correspond the model with Cosmochemical limitations. Out of two hadrons (2)  $\Theta^0$  is absolutely stable, a charged erzion disintegrates along the weak channel with an approximate life-time of a neutron. Bonded erzion-nucleon states should be studied as colorless five-quark configurations. The latter make a neutral stable isotopic singlet which we called "enion":

$$\Theta_N = \bar{U}udud \quad (3)$$

Calculations by the meson theory of nuclear forces demonstrate that potential pits of all known nuclei are too small for creation of a bonded state of an enion within nucleus. That is why enions as well as erzions are not captured by nuclei.

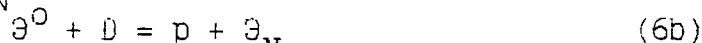
The problem of existence of new hadrons bonded states in common matter received a rather unexpected solution. A five-quark bag as colorless state with minimal number of quarks possesses a low but fixed polarization by electric field. That is the reason why this enion acquiring dipole moment in a nucleus field, may create a bonded state near its surface. Bonding energy of this state considering low enion polarization turns out to be relatively moderate for heavy nuclei:

$$E_{ads} = 20 Z^2 A^{-4/3} \text{eV} \quad (5)$$

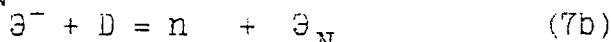
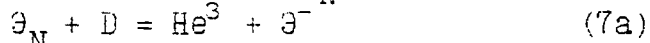
We call the effect of establishing such states an adsorption of enions on the surface of nuclei. For light nuclei whose mass is much less than enion's  $M_\Theta c^2 \approx 100 \text{ GeV}$ , adsorption level tends to reach the border of an continuous spectrum; there are tends to suggest that it does not exist in reality.

Spontaneous disintegration of the adsorption state may come as a result of a tunnelling nucleon from enion into nucleus. Absolute stability of this state suggests that difference of bonding energies of the neighboring nuclei is less than bonding energy of nucleon in the enion. We

shall demonstrate that this condition is being fulfilled particularly for some of the palladium isotopes. It is possible to release the absorbed enions for instance by irradiating a matter with ions with a mass  $M_i$  and energy  $E > M_i E_{ads} / M_i$  when the nucleus ionization goes along with the coulomb co-impacts. Under certain conditions on the bonding energy of the erzion with nucleon, enions and erzions are capable to perform catalysis of (1) reactions:



at  $2.2 \text{ MeV} < E_1 = [M(\Theta^0)c^2 + M(n)c^2 - M(\Theta_N)c^2] < 6.3 \text{ MeV}$ , or



at  $2.2 \text{ MeV} < E_2 = [M(\Theta^-)c^2 + M(p)c^2 - M(\Theta_N)c^2] < 5.5 \text{ MeV}$ .

The chain (6a), (6b) is being realized to all appearance, in the CNF reactions. It is known that emerging tritium possesses a low energy (no more than 100 keV), that is why we have to suppose that the bonding energy  $E_1$  is approaching 6.3 MeV, thus we have  $E_2 = 6.2 \text{ MeV}$ . It is not difficult to notice that with unstable  $\Theta^-$  and  $M(\Theta^-)c^2 - M(\Theta^0)c^2 > 0.6 \text{ MeV}$  cycle (7a), (7b) seems to be closed. Thus, the major property of CNF-suppression of the neutrons outcome - receives in the suggested model a simple and natural interpretation.

Now let us come to a short discription of the CNF process in general. Erzions in the Earth matter may have both relict (Cosmologic) and Cosmic radiation nature. According to preliminary experimental data, integral intensity of the erzion component in the Cosmic rays at the energy threshold  $\gtrsim 100 \text{ GeV}$  makes up  $I_s \approx 10^{-6} \text{ cm}^{-2} \text{ s}^{-1} \text{ ster}^{-1} / 20\%$ . According to the same data, absorption length for the erzions makes up  $\lambda = 10^4 \text{ g/cm}^2$ , i.e. the erzions are localized on the presurface Earth stratum  $L \approx 10^4 \text{ cm}$  thick. The erzion density by the Cosmic rays flux in this stratum is calculated by clearly empiric data

$$n_\Theta = I_s T / L \approx 10^7 \text{ cm}^{-3} \quad (8)$$

whereas  $T \approx 3 \text{ billion years} (10^{17} \text{ s})$  is geological time.

Erzions in the presurface stratum are being captured by nucleons and turn into enions. The latter, in their turn, find nuclei, energetically more profitable for adsorption. At

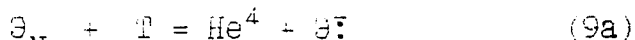
$E_1=6.2$  MeV,  $E_2=7.7$  MeV the Palladium isotop Pd-110 belong to such nuciei. According to (5) the enion adsorption energy on Palladium makes up 100 eV. It is necessary to pay attention here to two circumstances: 1) Erzions depth of  $L \approx 100m$  is comparable to the scape of geological developments of minerals. That is why various technological materials, depending on conditions of developing initical ores, may have a various erzion concentration; 2) enion adsorption energy on palladium guarantees preserving adsorbtion state in quasiequilibrium technological processes ,for instance ore refinément and metal smelting. Consequently,we may suppose that the Palladium electrodes keep an admixture of enions with density lower then or  $n \approx 10^7 \text{ cm}^{-3}$ .

So CNF process starts at cracking of the electrodes matter, i.e. after reaching critical hydrogenization in the course of electrolysis in a heavy water. Electric fields emerging in the cracks /3/ accelerate deutons up to character energies 10keV an even higher, which exceed the threshold of the enionization of Palladium nuclei  $E_0=E_{\text{ads}} M(\Theta_N)/M(D) \approx 5 \text{ keV}$ . Released enions participate in the (6a) - (6b) cycles, thus generating tritium. Channel (7a) with the  $\text{He}^4$  generation, and consequently connected with it channel (7b) with neutron generation, as already was mentioned, are fully closed by a condition for  $E$  bonding energy.

Presence of interstitial states means that (6a) and (6b) reactions at resonance energies may have very large cross-sections. Particularly at large erzion concentrations in  $n \approx 10^7 \text{ cm}^{-3}$  in palladium for explaining CNF effect at the Fleischmann-Pons level it is necessary to have cross-sections of the (6a) and (6b) reactions

$$\sigma v \approx 10^{-15} \text{ cm}^3 \text{ s}^{-1}.$$

Small neutrons outcome. which may be observed at the CNF experiments is being explained by catalyzed reactions on tritium



Comparing (6) and (9) cycles demonstrates that approximate evaluation of concentrations takes place:  $n/T \approx T/D$ . Thus observed  $n/T \approx 10^{-3} - 10^{-11}$  relations are being evaluated as connected with initial concentration of tritium in heavy water and with some increase during CNF process.

In the conclusion we should note that other CNF properties also are being explained in the qualitative way in the suggested model. Large fluctuations in intensity of the

CNF products outcome at various experiments may be linked with fluctuation of erzion density on various electrodes (depending on erzion concentration in initial ores). Effect of samples "aging" may be explained with ultimate cracking of samples and partial lossing of erzions at the previous series of experiments.

Thus, the presented model lets to explain in principle all seemingly abnormal properties of so called CNF, received during the experiment which it is impossible to explain everything in complex in the framework of the traditional conceptions.

### References

1. BARC Studies in Cold Fusion, BARC - 1500, 1989, Bombay
2. Bockris J.O., Lin G.N., Packman N.J., Fusion Technology, 1990, 18, 11-31
3. Tzarev V.A., UFN, 1990, 160, 11, 1-53; UFN, 1991, 161, 4, 152; UFN, 1992, 162, 10, 63-91
4. Fleischmann M., Pons S., Journal of Electroan.Chem., 1989, 261, 301-308
5. Jones S.E., Palmer E.P., Criss J.B., et al., Nature 1989, 338, 737
6. Iyengar P.K. 5-th ICENES, FRG, Karlsruhe, 1989, 3-6
7. Kluyev V.A. et al. Theses Reports at H-YVSMMTT, 1986
8. Menlove H.O. et al, LANL Report LA-VR-89-1570, 1989
9. Rolison D.R., O'Grady W.E., Proc. NSE/EPRI Workshap Anomaios Effects in Deuterated Materials.Washington, 1989
10. Bush R. Fusion Technology, 1991, 19, 313
11. Derjagin B.V. et al. Theses Reports at H-YVSMMTT, 1986
12. Golubnitchiy P.I., Kurakin V.A., Filonenko A.D. et al. Preprint - 113, PIAS, 1989
13. Bazhutov Y.N., Khrenov B.A., Kristiansen G.B. "Izv. USSR Academy of Science, Physical series, 1982, 46, 2425-2427
14. Smith P.F. et al. Nuclear Phys, 1982, B 206, 333
15. Norman E., et al Phys. Rev. Lett., 1987, 58
16. Bazhutov Y.N., Vereshkov G.N., Preprint-1, CSRI Mash, 1990
17. Bazhutov Y.N., Vereshkov G.M., Proc."Cold Nuclear Fusion" CSRI Mash, 1992, 22-28

# JAHN-TELLER SYMMETRY BREAKING AND HYDROGEN ENERGY IN $\gamma$ -PdD "COLD FUSION" AS STORAGE OF THE LATENT HEAT OF WATER

K.H. Johnson  
Massachusetts Institute of Technology  
Cambridge, MA 02138

## Abstract

In 1989, we proposed a common quantum-chemical basis for superconductivity and anomalous electrochemical properties of palladium loaded with hydrogen and deuterium, derived from H-H/D-D bonding molecular orbitals at the Fermi energy between tetrahedral interstices (" $\gamma$ -phase" PdD). Symmetry-breaking anharmonic vibrations of the protons/deuterons, induced by the dynamic Jahn-Teller effect, promote superconductivity in PdH/PdD at  $T_c = 9/10^{\circ}\text{K}$ , while the large vibronic anharmonicity explains the inverse H/D isotope shift of  $T_c$ . The calculated deuteron vibronic amplitude of  $0.46\text{\AA}$  implies a closest D-D approach of  $0.76\text{\AA}$  between neighboring tetrahedral sites and fusion rate of only  $\sim 10^{-24}$  per deuteron pair per second in  $\gamma$ -PdD at ambient temperature, much too small to explain reported excess heats. *Ab initio* quantum-chemical computations for  $\gamma$ -PdD further indicate that the "channels" connecting tetrahedral sites provide, via the Jahn-Teller effect, an "orbital pathway" for bulk catalytic recombination of atomic deuterium to rapidly diffusing dideuterium,  $4\text{D} \rightarrow 2\text{D}_2$ , the recombination heat equaling  $9.4\text{eV}$  per Pd atom per unit diffusion cycle time, equivalent to the storage and release of latent vaporization heat of 2.5 moles of  $\text{D}_2\text{O}$ . While the diffusion cycle time depends on cell conditions, for cycles between 1 and 100 minutes, this process could generate 17 to 1700 watts/cm<sup>3</sup> of stored latent heat in  $\gamma$ -PdD. The inverse isotope effect implies a slower hydrogen reaction,  $4\text{H} \rightarrow 2\text{H}_2$ , and diffusion in  $\gamma$ -PdH, leading to negligible latent heat power from Pd-based light-water cells. However, this mechanism could explain reported heat generation in light-water cells using nickel cathodes, where  $2\text{H} \rightarrow \text{H}_2$  catalysis is a rapid (110) surface or near-surface phenomenon.

## The Dynamic Jahn-Teller Effect, Superconductivity, and D-D Fusion

An abstract theorem proposed in 1936 by Jahn and Teller<sup>1</sup> laid the foundation for a theory of the static and dynamic coupling of nuclear motions to electronic structure. In a 1983 paper<sup>2</sup> on a "real-space" molecular-orbital basis for superconductivity, we first suggested that Cooper pairing and the inverse isotope shift,  $T_c = 9/10^{\circ}\text{K}$ , in PdH/PdD are associated with dynamic Jahn-Teller-induced *anharmonic* vibrations of the protons/deuterons inside Pd. The amplitudes of these vibrations are determined from the formula:<sup>2</sup>

$$\delta = (m/M)^{\beta} d \quad (1)$$

where  $M$  is the atomic mass,  $m$  is the conduction electron mass,  $d$  is the interatomic distance, and  $0 < \beta \leq 1/2$  is the anharmonicity. In the "harmonic limit,"  $\beta = 1/2$ , the dynamic Jahn-Teller-induced vibrations reduce to the "virtual phonons" of the BCS theory of superconductivity. In Ref. 2 it was shown how  $\beta$  follows directly from the bond overlap of degenerate molecular orbitals at the Fermi energy ( $E_F$ ). This theory has since been successfully applied to high- $T_c$  oxide and fullerene superconductors.<sup>3,4</sup>

In more recent work,<sup>5</sup> we have confirmed, from density-functional molecular-orbital and *ab-initio* Hartree-Fock calculations, that for high H/D loading in palladium, the sole occupation of octahedral interstices is Jahn-Teller unstable toward migration of H/D's to the tetrahedral interstices, forming the so-called "γ-phase" of PdH/PdD. Spatially extended, degenerate H-H/D-D bonding molecular orbitals at  $E_F$  between the tetrahedral sites in γ-PdH/PdD are found to be a precursor to Cooper pairing, superconductivity at  $T_c = 9/10^{\circ}\text{K}$ , and the inverse isotope effect on  $T_c$ . The hydrogen molecular orbitals at and just above  $E_F$  are  $s\sigma$ -bonding along and  $s\sigma$ -antibonding in "channels" of opposite phase  $\psi_+$ ,  $\psi_-$  connecting tetrahedral interstices, as shown schematically for γ-PdD in Fig. 1 and computationally in Fig. 2 as a contour map through a (110) plane. D-D  $s\sigma$ -bond overlap is enhanced by the "compression" effect of significant Pd(4d)-D(1s) antibonding at  $E_F$  (Fig. 2). Indeed Pd(4d)-D(1s) antibonding at  $E_F$  substantially weakens the effect of Pd(4d)-D(1s) bonding states below the Pd *d*-band, explaining the small heats of formation of PdD, while promoting delocalized D-D  $s\sigma$ -bonding molecular orbitals at  $E_F$ . Evidence for hydrogen atoms "banding" together on nickel (110) surfaces, with electron density similar to that shown in Fig. 1, has recently been reported.<sup>6</sup>

In the dynamic Jahn-Teller coupling between interstitial D-D  $s\sigma$ -bonding electrons at  $E_F$  and anharmonically vibrating deuterons required for Cooper pairing and superconductivity in PdD for  $T_c \leq 10^{\circ}\text{K}$ , there is continual symmetry-breaking dynamical interconversion between alternate D-D  $s\sigma$ -bond deformations,  $\delta$ , along the three crystallographically equivalent directions of the "bonding channels"  $\psi_+$  and  $\psi_-$  shown in Figs. 1 and 2. These rapid oscillations of the deuterons are equivalent to "anharmonic local optical phonons" of amplitude  $\delta$  given in Equation (1). For the calculated D-D bond overlap between tetrahedral sites in γ-PdD (Fig. 2),  $\delta = 0.46\text{\AA}$ .

Under the influence of the Jahn-Teller effect, the D-D nuclear fusion rate can be calculated from the formula:<sup>5</sup>

$$R = (\hbar\sigma/M\delta^3 d^4) \exp\left[-(2/\hbar)(d-2\delta)\sqrt{2M(V-\hbar^2/2M\delta^2)}\right] \quad (2)$$

where  $\sigma$  is the fusion cross-section extrapolated to ambient temperature and  $V$  is the Coulomb potential barrier between the γ-PdD tetrahedral sites ("T-sites") and the "S-sites" half way between neighboring T-sites along the D-D bond direction (Fig. 2). Combining formulae (1) and (2) and using the relationship between anharmonicity  $\beta$  and bond overlap,<sup>2,5</sup>  $R$  can be plotted as a function of D-D bond overlap, leading to the graph of Fig. 3. For the 20% D-D overlap characteristic of γ-PdD (Fig. 2), this graph gives a value of  $R = R_0 \cong 10^{-24}$  fusion per deuteron pair per second, resulting from the Jahn-Teller effect. This value is of the same order of magnitude as that determined from neutron counts in electrochemical experiments on deuterated electrodes by Jones *et al.*<sup>7</sup> Clearly, this very low level of fusion, while fifty orders of magnitude larger than that expected for an isolated D<sub>2</sub> molecule, is not large enough to produce significant amounts of heat under electrochemical conditions in PdD.

It is theoretically possible to enhance the effective D-D bond overlap in γ-PdD to almost 33% via alloying (see below), increasing the D-D fusion rate to a maximum of  $R \cong 10^{-21}$  according to Fig. 3, but still too small for significant heat production.

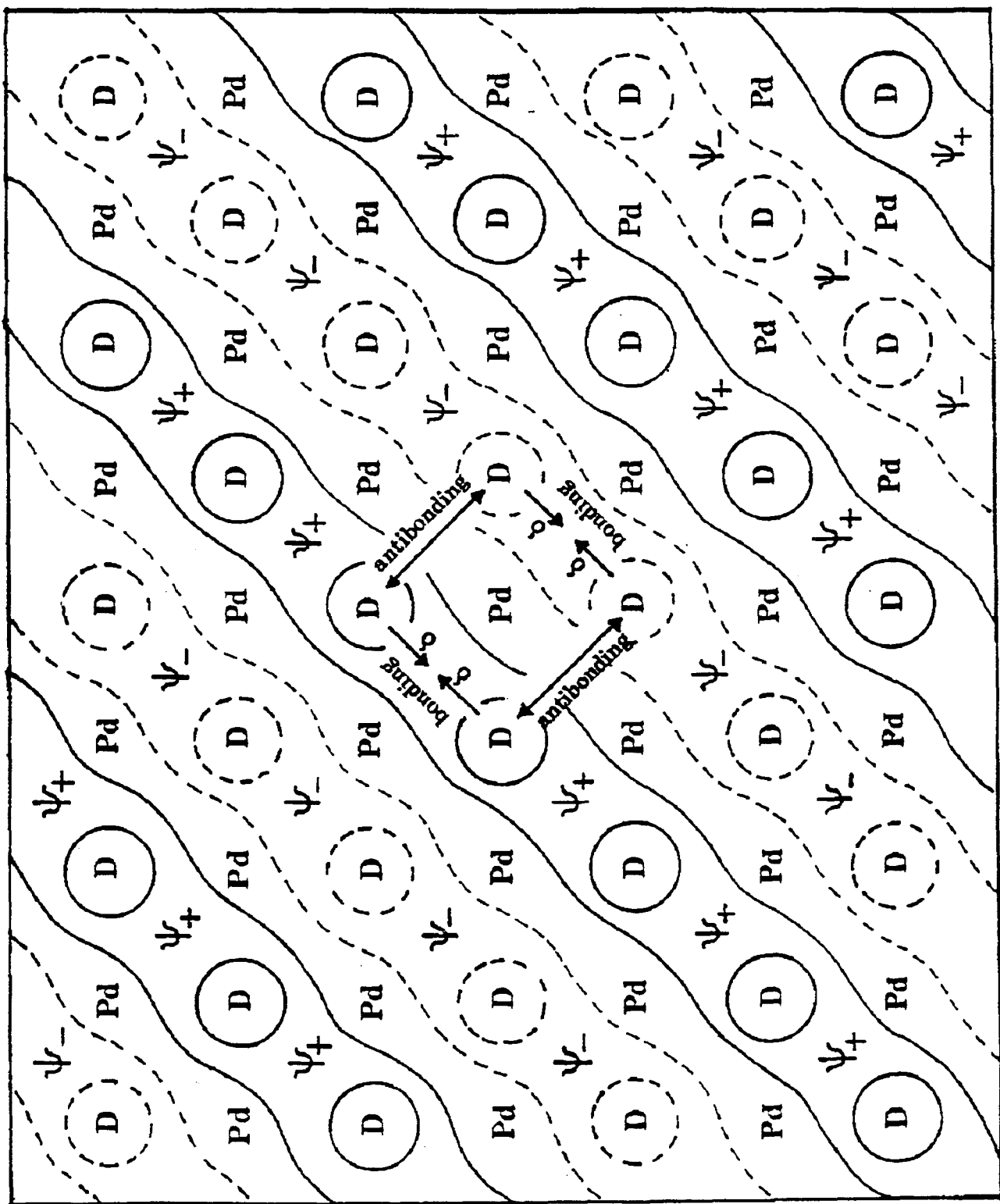


Fig. 1. Schematic representation of D-D bonding "channels" at the Fermi energy ( $E_F$ ) in  $\gamma$ -PdD. Solid and dashed contours represent positive and negative amplitudes of the wavefunction. The amplitude,  $\delta$ , of Jahn-Teller-induced D-D vibrations, calculated from Eq. (I), is indicated.

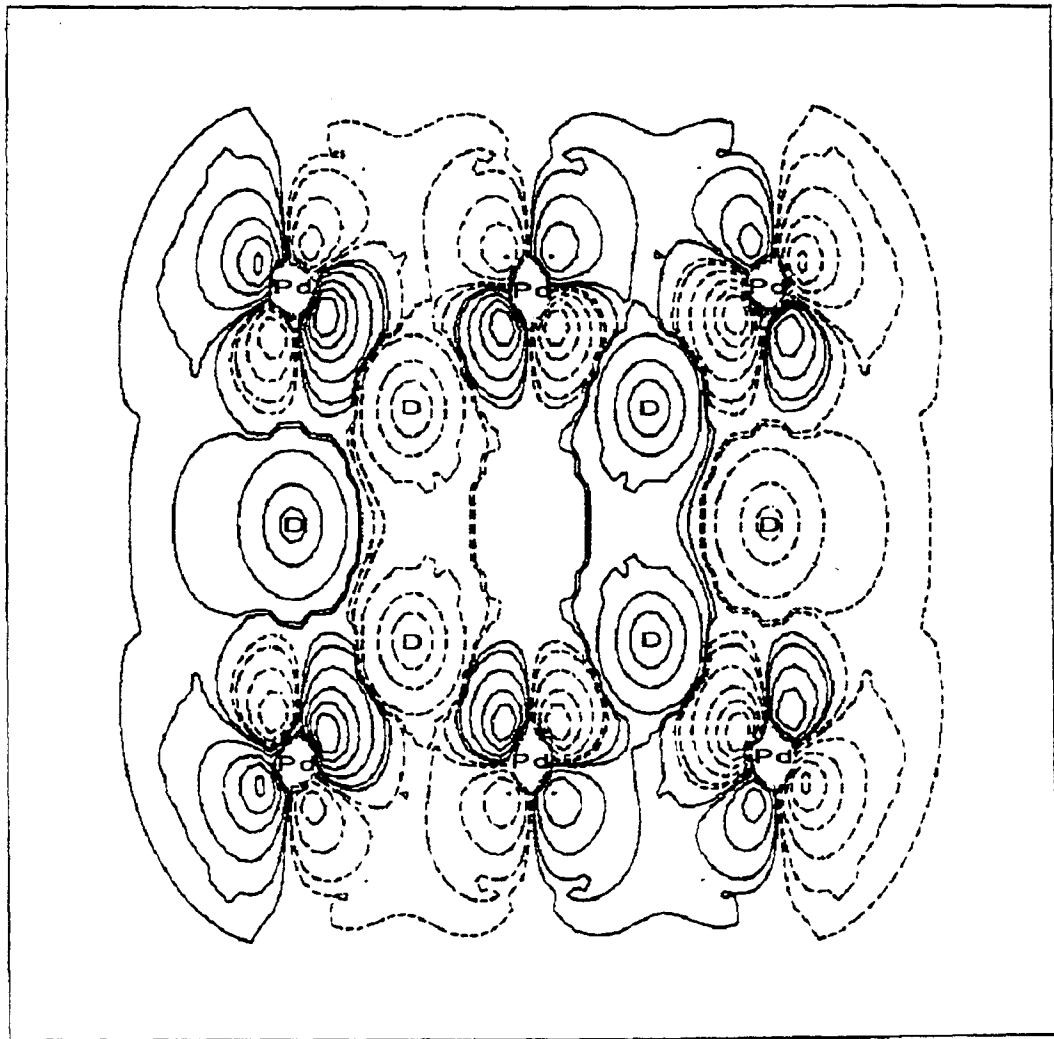


Fig. 2. Density-functional molecular-orbital wavefunction at  $E_F$  for  $\gamma$ -PdD plotted in a (110) plane.

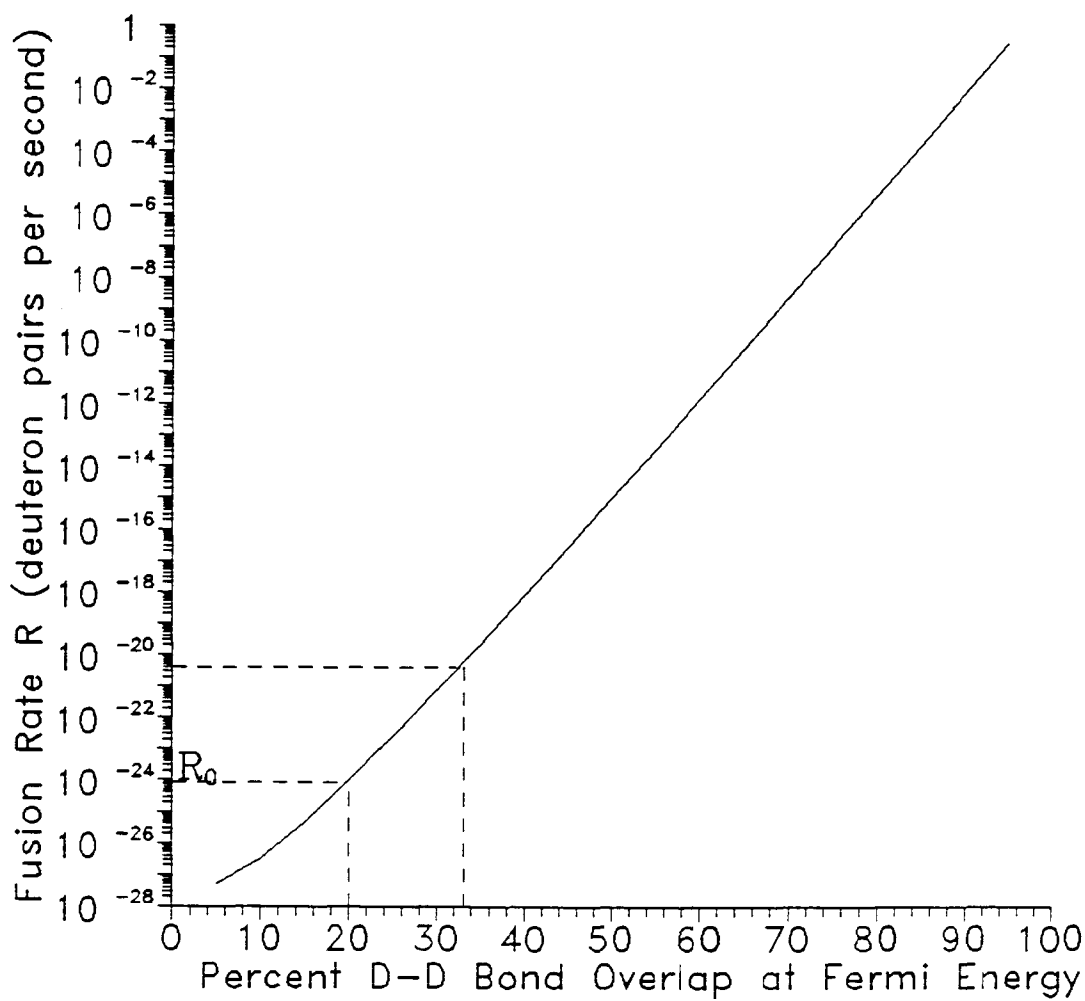


Fig. 3. D-D nuclear fusion rate in  $\gamma$ -PdD induced by the Jahn-Teller effect according to Eq. (2), plotted against D-D bond overlap between tetrahedral sites. The dashed lines bracket the practical limits of fusion.

**Symmetry Breaking, D-D Recombination, and Hydrogen Energy in PdD**  
The D-D potential energy surface in  $\gamma$ -PdD, calculated from *ab initio* Hartree-Fock theory, resembles the "Mexican hat" shown in Fig. 4. The high-symmetry ( $T_d$ ) coordination of a Pd atom by four D atoms in four of the eight surrounding face-centered-cubic Pd tetrahedral interstitial sites is Jahn-Teller unstable, leading to a central energy minimum of distorted tetrahedral ( $C_{3v}$ ) symmetry at the "crown of the hat" and a square coplanar ( $D_{2h}$ ) "broken-symmetry" energy minimum at the "brim of the hat," 9.4eV below  $T_d$  symmetry, for an equilibrium D-D distance of 0.76Å. The latter is practically equal to the equilibrium bond distance of a free D<sub>2</sub> molecule. The 9.4eV energy per Pd atom released in the Jahn-Teller distortion of each PdD<sub>4</sub> molecular unit in  $\gamma$ -PdD from  $T_d$  to  $D_{2h}$  symmetry is likewise remarkably close to the sum of the chemical bond energies of two free D<sub>2</sub> molecules.

Thus, the D-D "bonding channels" connecting tetrahedral sites in  $\gamma$ -PdD provide, via the symmetry-breaking Jahn-Teller effect, an "orbital pathway" for the bulk catalytic recombination, 4D  $\rightarrow$  2D<sub>2</sub>, of rapidly diffusing atomic deuterium to rapidly diffusing dideuterium, the large exothermic chemical heat of recombination equaling 9.4eV per Pd atom. Once a steady state of high electrochemical loading is achieved, this process is likely to be rapid and continuous, facilitated by the Jahn-Teller displacement of diffusing atomic deuterium from octahedral to tetrahedral interstices, forming the " $\gamma$ -phase", then rapidly diffusing as dideuterium through the  $\gamma$ -PdD "bonding channels" connecting the tetrahedral sites to the cathode surface, where the dideuterium escapes as D<sub>2</sub> gas.

It is impractical to calculate a precise cycle time for this process, because the diffusion depends on the input electrical current, the ambient temperature and pressure, the structural integrity of the Pd lattice, and the surface condition of the Pd cathode. However, if the cycle time for recombination, 4D  $\rightarrow$  2D<sub>2</sub>, is somewhere between 1 and 100 minutes, at 9.4eV per Pd atom per unit time, this process could generate heat at a rate of 17 to 1700 watts/cm<sup>3</sup> palladium. For this power range, the total heat released over ten minutes would be between 10KJ and 1MJ. This is consistent with the wide range of "excess" powers reported in laboratories around the world.

#### "Cold Fusion" Heat as Chemical "Latent Heat"; "Heat after Death"

This dynamical Jahn-Teller-induced catalytic mechanism is, of course, a chemical process, although an unusual one in that it corresponds to an internal phase change of the deuterium within  $\gamma$ -PdD. Since the energy release is effectively due an internal cyclic  $\gamma$ -phase change of atomic deuterium to dideuterium, the heat produced may be viewed as "latent heat" produced by repeated formation of the "interstitial sublattice" of D-D bonds between the tetrahedral interstices in  $\gamma$ -PdD, as atomic deuterium diffuses into palladium and dideuterium diffuses out. "Latent heat" of 9.4eV per Pd atom for  $6.8 \times 10^{22}$  Pd atoms/cm<sup>3</sup> adds up to 102KJ/cm<sup>3</sup> palladium. Since the latent heat of vaporization of D<sub>2</sub>O is 41.5KJ/mole at 100°C, the "latent heat" of 102KJ produced in one cm<sup>3</sup> of  $\gamma$ -PdD per unit diffusion cycle time is equal to the latent vaporization heat of 2.5 moles of D<sub>2</sub>O. In other words, the heat of "cold fusion" appears to be the storage and release of the latent vaporization heat of heavy water. Indeed, if the electric power input is turned off a fully loaded cell, this stored latent heat is sufficient to boil away 2.5 moles of D<sub>2</sub>O, the so-called "heat after death" of Pons and Fleischmann.

D-D POTENTIAL SURFACE  
IN PALLADIUM

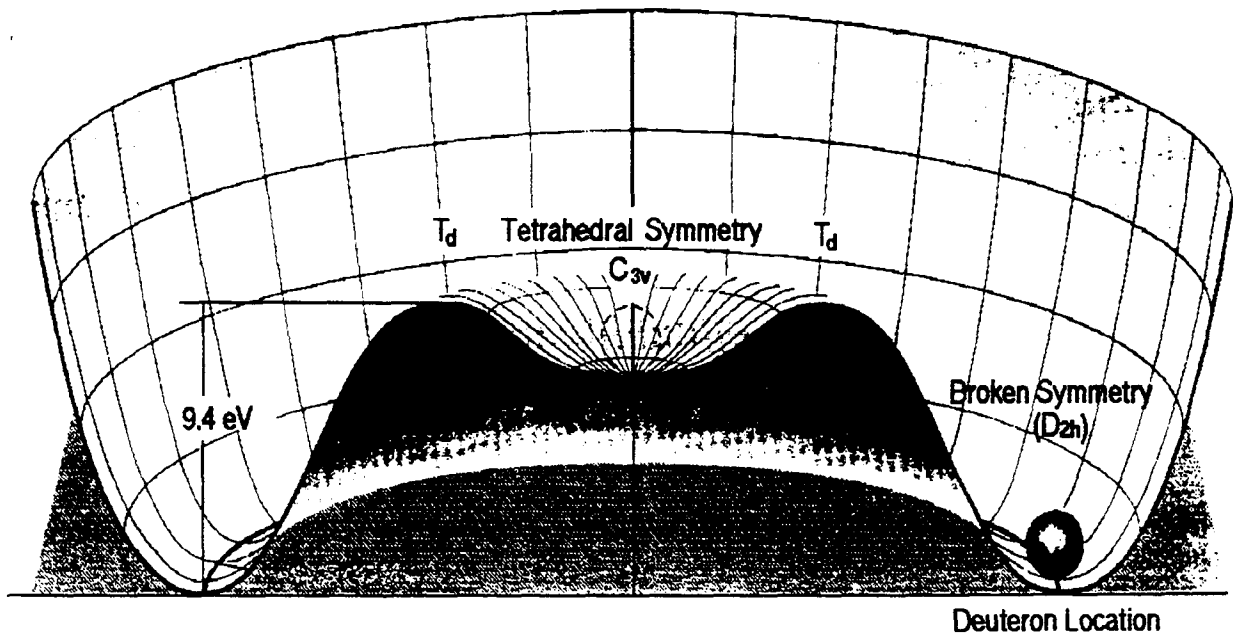


Fig. 4. Schematic "Mexican hat" representation of the D-D potential surface in  $\gamma$ -PdD.

**Equivalence of "Excess" Heat to the Latent Vaporization Heat of Water**  
Why then is this heat interpreted as "excess heat"? To answer this question, one must first understand the nature of the bonding between H<sub>2</sub>O/D<sub>2</sub>O molecules in water. It is commonly thought that the breaking of electrostatic or weakly covalent O-H or O-D "hydrogen bonds" between neighboring water molecules accounts for all the latent heat required to take water from the liquid to vapor phase. However, a recent experimental study of the interatomic structure of water at supercritical temperatures, reported in *Nature*,<sup>9</sup> has revealed that breaking of nearest-neighbor O-H and O-D bond correlations in the liquid accounts for only a fraction of the latent vaporization heat. Fig. 1 of Ref. 9 reveals that second-, third-, and even fourth-neighbor hydrogen-hydrogen (or D-D) bond correlations persist after the nearest-neighbor O-H/O-D and H-H/D-D bonds are broken at supercritical temperatures. These longer range H-H/D-D bond correlations account for the major part of the latent vaporization heat of water.

In the electrolysis of water, only the O-H/O-D bond correlations are broken as H/D penetrates the Pd cathode and O<sub>2</sub> is evolved at the anode. For high loading and the formation of  $\gamma$ -PdD, the D-D bond correlations accounting for a major part of the latent heat of the electrolyte are effectively "stored" cooperatively between the tetrahedral sites of the  $\gamma$ -PdD lattice, as described above and in Fig. 2. The release of the latent heat by the Jahn-Teller-induced bulk catalytic process, 4D  $\rightarrow$  2D<sub>2</sub>, per Pd atom, effectively a cooperative  $\gamma$ -phase transition between interstitial atomic deuterium and dideuterium, thus is interpreted as "excess" heat. Therefore, this mechanism of storage and release of the latent heat of heavy water by palladium is more appropriately viewed as a "new hydrogen energy," the terminology commonly used in Japan instead of "cold fusion."

#### Light Water Versus Heavy Water

Significant amounts of "excess" heat from Pd-based light-water cells are not observed, most likely because of substantially more sluggish hydrogen diffusion in  $\gamma$ -PdH, compared to deuterium in  $\gamma$ -PdD. Although the mass of D is twice that of H, this inverse isotope effect, comparable to the one discussed above for the superconducting  $T_c$ 's of PdH and PdD, is probably due to the effectively larger diffusion cross sections of H and H<sub>2</sub> versus those of D and D<sub>2</sub>, resulting from the larger amplitude,  $\delta$ , of dynamic Jahn-Teller-induced anharmonic vibrations for hydrogen versus deuterium, according to Eq. (1). The larger effective radii of H and H<sub>2</sub> in  $\gamma$ -PdH markedly impede hydrogen diffusion and thus lengthen the full 4H  $\rightarrow$  2H<sub>2</sub> cycle time, as compared to the rapid D and D<sub>2</sub> diffusion, leading to the much faster 4D  $\rightarrow$  2D<sub>2</sub> catalytic process in  $\gamma$ -PdD.

Nevertheless, this mechanism may explain reported heat production from nickel cathodes in light water cells, where catalytic hydrogen recombination, 2H  $\rightarrow$  H<sub>2</sub>, is mainly a rapid (110) surface or near-surface phenomenon. Nickel (110) surfaces harbor the tetrahedral interstices of the bulk crystal. While the solubility of hydrogen in nickel is much lower than in palladium, the latent heat of H-H bond formation between tetrahedral sites close to the (110) surface (the "surface  $\gamma$ -phase" of NiH) could yield substantial heat for high-surface-area nickel, since the diffusion path to the surface is much shorter.

#### Supporting Experimental Evidence for 4H $\rightarrow$ 2H<sub>2</sub> Conversion

Experimental evidence for H<sub>2</sub> molecular "excited states" in other transition-metal hydrides has recently been reported by Baker *et al.*<sup>10</sup> from proton spin-lattice relaxation data.

A molecular analogue of the  $4\text{H} \rightarrow 2\text{H}_2$  process has recently been reported by Wisniewski *et al.*<sup>11</sup> in the form of an  $\text{Ir}(\text{PR}_3)_2\text{ClH}_4$  complex, in which the H ligands undergo a rapid dynamical dimerization to the dihydrogen dihydride  $\text{Ir}(\text{PR}_3)_2\text{ClH}_2\text{H}_2$ , as shown in Fig. 5.

### The Importance of Lattice Structural Integrity in Palladium

For the  $\gamma$ -PdD lattice to maintain an "interstitial network" of D-D bonds (Figs 1 and 2), formed and reformed between rapidly diffusing deuterium at high loading, the structural integrity of the material is crucial. Crack tips and grain boundaries in transition metals can be sites of rapid catalytic hydrogen recombination, which tend to cause metallic decohesion, intergranular embrittlement, and crack propagation.

### Enhanced "Cold Fusion" and Superconductivity in $\gamma$ - $\text{Pd}_{0.75}\text{Ag}_{0.25}\text{D}$

Density-functional molecular-orbital calculations have been performed for a  $\gamma$ - $\text{Pd}_{0.75}\text{Ag}_{0.25}\text{D}$  alloy. Maximum hydrogen solubility near this composition has been reported by Lewis.<sup>12</sup> The pertinent wavefunction contour map for this alloy, showing D-D bonding between the tetrahedral sites at  $E_F$ , is displayed in Fig. 6 and may be compared with Fig. 2 for pure  $\gamma$ -PdD. As a result of the increased "compression" effect of  $\text{Ag}(4d)\text{-D}(1s)$  antibonding in  $\gamma$ - $\text{Pd}_{0.75}\text{Ag}_{0.25}\text{D}$  at  $E_F$ , the tetrahedral D-D bond overlap in Fig. 6 is enhanced to practically 33%, as compared with 20% in Fig. 2 for  $\gamma$ -PdD. From Fig. 3, this would suggest a possible increase of the D-D nuclear fusion rate from  $R \cong 10^{-24}$  in  $\gamma$ -PdD to  $R \cong 10^{-21}$  in  $\gamma$ - $\text{Pd}_{0.75}\text{Ag}_{0.25}\text{D}$ , which should be detectable by increased neutron emission, provided the  $\text{Pd}_{0.75}\text{Ag}_{0.25}$  alloy can be loaded with deuterium. However, this predicted increase in fusion rate is still too small to generate significant heat on its own.

Tracking this predicted increase in D-D fusion in the Pd-Ag alloy, is the experimental fact uncovered by Stritzker<sup>13</sup> that the superconducting transition temperature is raised from  $T_c = 9^\circ\text{K}$ ( $10^\circ\text{K}$ ) in  $\text{PdH(D)}$  to  $T_c = 15^\circ\text{K}$  in  $\text{Pd}_{0.75}\text{Ag}_{0.25}\text{H}$ . This is consistent with the dynamic Jahn-Teller anharmonic vibronic mechanism for high- $T_c$  superconductivity discussed above and in Refs. 2-5.

### "Cold Fusion" in High- $T_c$ Superconductors

In accord with the above thesis that a dynamic Jahn-Teller anharmonic vibronic mechanism is responsible for both high- $T_c$  superconductivity and "cold-fusion" manifestations is a recent report of low-level neutron production from deuterated high- $T_c$  ceramic superconductor,  $\text{YBa}_2\text{Cu}_3\text{O}_7$ , below the superconducting transition temperature.<sup>14</sup>

**Conclusion: Latent-Heat-of-Water Storage as Practical "New Hydrogen Energy"**  
Given the latent heat of vaporization content of a gallon of water, approximately 8MJ or 7,600BTU, its electrochemical storage and release by the process described above could be a viable method of hydrogen energy conversion. Ten gallons of water contain approximately 80 MJ or 76,000BTU of latent heat which, if stored and released electrochemically over one hour, approaches the heating capacity of a modest commercial household furnace. To convert this amount of latent heat from 10 gallons of water would require an electrochemical cell power output of 22KW. Since one cm<sup>3</sup> of Pd (or the equivalent surface area of Ni) is capable, under ideal conditions, of yielding upwards of 1.7KW of stored latent heat, this would require approximately 13cm<sup>3</sup> or 156g Pd, or the equivalent amount of much cheaper Ni. A power of 22KW corresponds to 30HP, suggesting the possibility of a "water engine" electrochemically generating both heat and hydrogen for a fuel cell, which could be used to power or partially power an automobile.

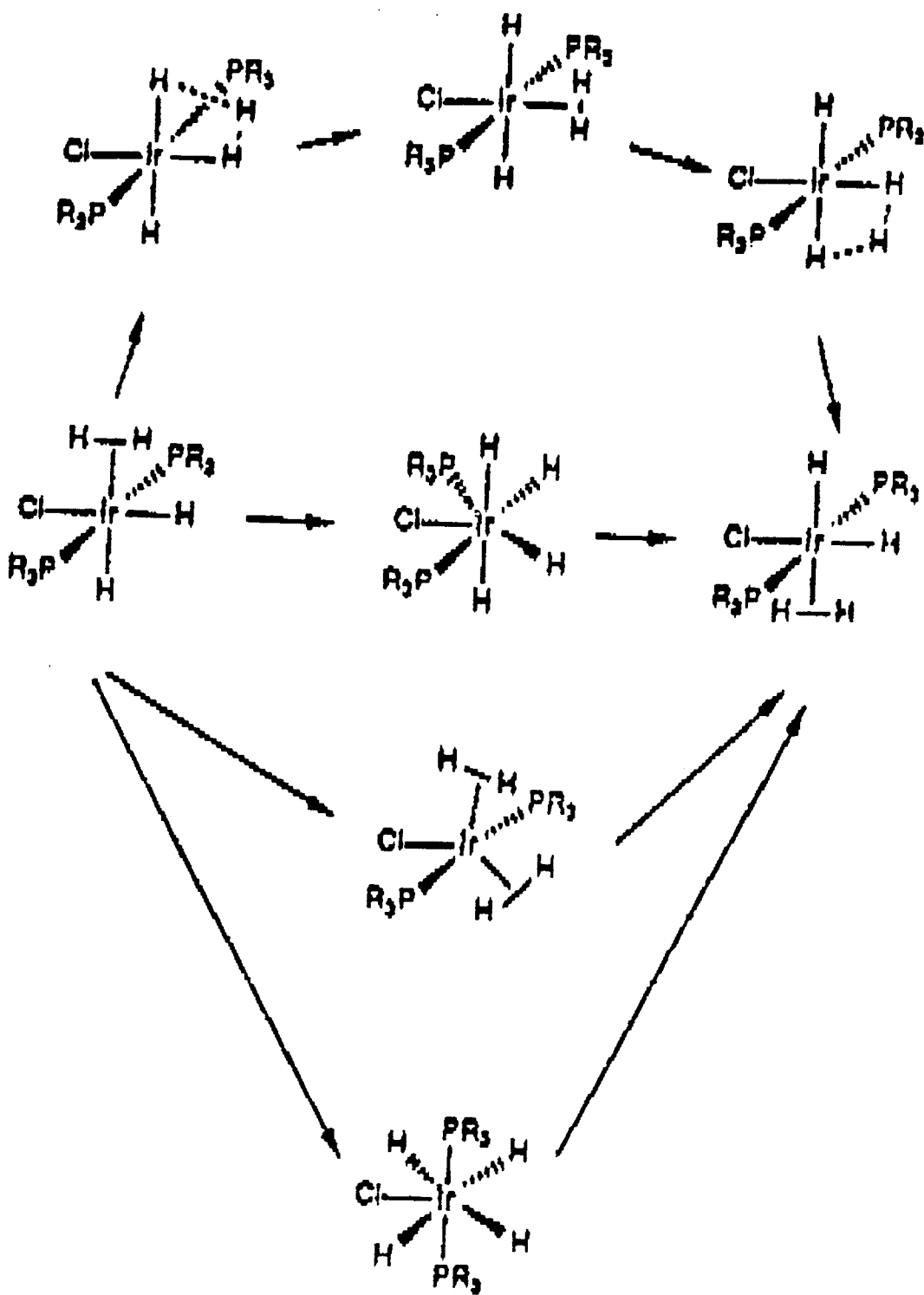


Fig. 5. A molecular analogue of the  $4D \rightarrow 2D_2$  process in  $\gamma$ -PdD: the molecular complex  $\text{Ir}(\text{PR}_3)_2\text{ClH}_4$ , in which the 4H ligands undergo a rapid dynamical dimerization to the dihydrogen dihydride  $\text{Ir}(\text{PR}_3)_2\text{ClH}_2\text{H}_2$  (see Ref. 11).

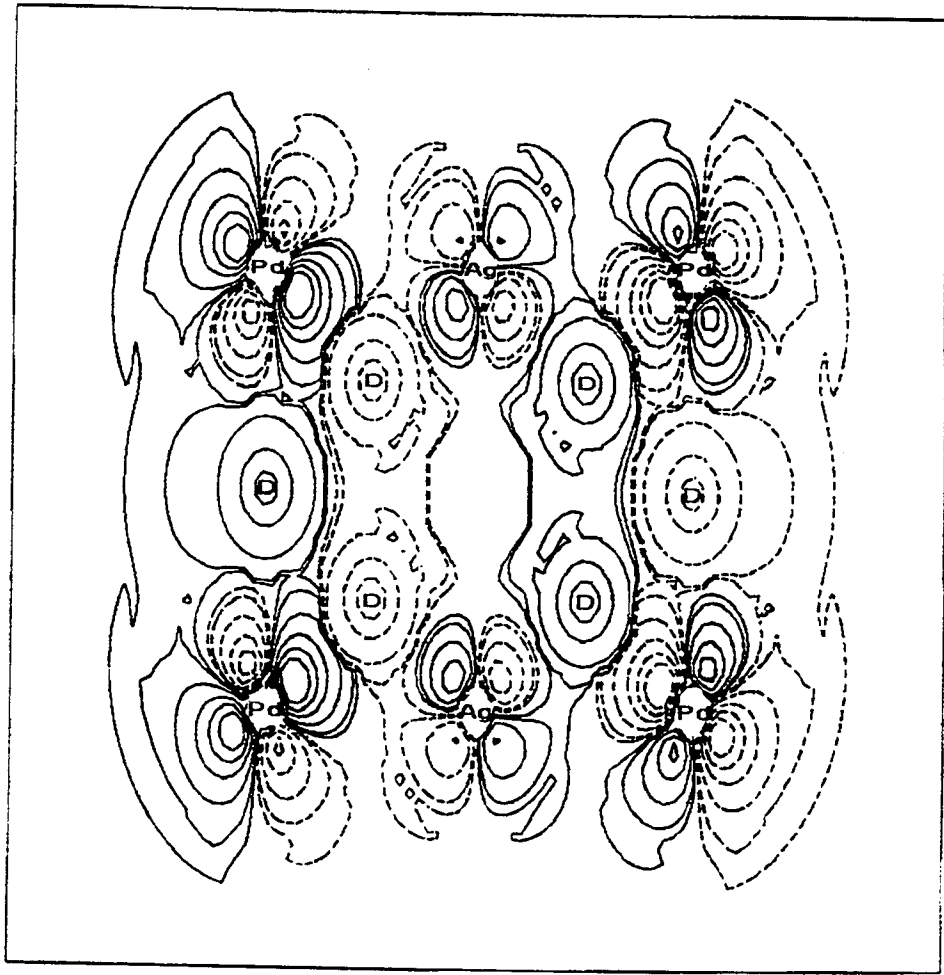


Fig. 6. Density-functional cluster molecular-orbital wavefunction at  $E_F$  for  $\gamma$ -Pdo.75Ag0.25D plotted in a (110) plane.

### Acknowledgements

I am very grateful to Dr. Kailash Mishra for performing the *ab initio* quantum chemistry calculations for the D-D potential surfaces in PdD, and for his helpful discussions.

### References

1. H. Jahn and E. Teller, "Stability of Degenerate Electronic States in Polyatomic Molecules," *Phys. Rev.* **49**, 874 (1936); See also I.B. Bersuker and V.Z. Polinger, *Vibronic Interactions in Molecules and Crystals*, Springer-Verlag, New York, (1989); M.C.M. O'Brien and C.C. Chancey, "The Jahn-Teller Effect: An Introduction and Current Overview," *Am. J. Phys.* **61**, 688 (1993).
2. K.H. Johnson, "Molecular Orbital Basis for Superconductivity in High and Low Dimensional Metals," *Synth. Metals* **5**, 151 (1983).
3. K.H. Johnson, D.P. Clougherty, and M.E. McHenry, "Dynamic Jahn-Teller Coupling, Anharmonic Oxygen Vibrations, and High- $T_c$  Superconductivity in Oxides," *Mod. Phys. Lett. B* **3**, 367 (1989).
4. K.H. Johnson, M.E. McHenry, and D.P. Clougherty, "High- $T_c$  Superconductivity in Potassium-Doped  $K_xC_{60}$  via coupled  $C_{60}(p\pi)$  Cluster Molecular Orbitals and Dynamic Jahn-Teller Coupling," *Physica C* **183**, 319 (1991).
5. K.H. Johnson and D.P. Clougherty, "Hydrogen-Hydrogen/Deuterium-Deuterium Bonding in Palladium and the Superconducting/Electrochemical Properties of PdH/PdD," *Mod. Phys. Lett. B* **3**, 795 (1989).
6. R. Nieminen, "Hydrogen Atoms Band Together," *Nature* **356**, 289 (1992).
7. S.E. Jones *et al.*, "Observation of Cold Nuclear Fusion in Condensed Matter," *Nature* **338**, 737 (1989).
8. S. Pons and M. Fleischmann, "Heat after Death," Paper presented at the *Fourth International Conference on Cold Fusion*, Maui, December 6, 1993.
9. P. Posterino *et al.*, "The Interatomic Structure of Water at Supercritical Temperatures," *Nature* **366**, 668 (1993).
10. D.B. Baker *et al.*, "Evidence for the High-Temperature Spin-Relaxation Anomaly in Metal Hydrides," *Phys. Rev.* **46**, 184 (1992).
11. L.L. Wisniewski *et al.*, "Mechanism of Hydride Scrambling in a Transition-Metal Dihydrogen Dihydride as Studied by Solid-State Proton NMR," *J. Am. Chem. Soc.* **115**, 7533 (1993).
12. F.A. Lewis, *The Palladium Hydrogen System*, p. 74, Academic Press, New York (1967).
13. B. Stritzker, "High Superconducting Transition Temperatures in the Palladium-Noble Metal-Hydrogen System," *Z. Physik* **268**, 261 (1974).
14. A.G. Lipson *et al.*, "Possible Cold Nuclear Fusion in the Deuterated Ceramic  $YBa_2Cu_3O_7$  in the Superconducting State," *Sov. Phys. Dokl.* **38**, 849 (1991).

# THE ROLE OF HYDROGEN ION BAND STATES IN COLD FUSION

Scott R. Chubb and Talbot A. Chubb  
Research Systems, Inc.  
5023 N. 38th St.  
Arlington, VA 22207

## Abstract

Quantum diffusion studies of hydrogen (H) and deuterium (D) inside and on the surfaces of transition metals indicate that both H and D may occupy wave-like band states (H and D ion band states) analogous to the electron band states that are responsible for making metals conductors. When these wave-like ion band states become occupied, fusion involving  $D+D \rightarrow {}^4He$  without emission of gamma rays or other high energy by-products can occur, provided a number of conditions are met. We have previously identified and used these conditions to predict a number of important experimental results that were subsequently observed. In part 1 we examine the underlying justification for believing that ion band state occupation can lead to nuclear reaction. We show that under suitable conditions associated with the underlying electronic structure, ion band state occupation may lead to wave function overlap between a small number of indistinguishable  $D^+$ . These conditions appear to be met as  $x \rightarrow 1$  in  $PdD_x$ . Then, ion-ion correlation effects that result from coulomb repulsion, which normally inhibit overlap, are not present in the ground state wave function, provided the number of indistinguishable ion band state deuterons is very much less than the total number ( $N_{cell}$ ) of unit cells in the crystal, and the crystal is sufficiently large :  $N_{cell} > 10^8$ . In part 2, we examine the implications of the ion band state fusion scenario, including a summary of important selection rules and reactions which follow as a result of the restrictions that are implied by the physical limit in which the theory applies.

## Introduction

Acceptance of cold fusion as a real phenomenon by the mainstream physics community has been delayed mainly for two reasons: 1) a refusal of physicists to believe that the coulomb barrier that normally prevents nuclear reactions at room temperature can be overcome in the solid state environment, and 2) a belief that  $\gamma$ -ray and high energy particle emission must inevitably accompany the release of nuclear energy. The cold fusion community for the most part bases its belief in cold fusion on the evidence for the reality of the cold fusion heat effect. Nonetheless, it shares with the larger physics community a belief that mainstream physics cannot overcome the coulomb barrier problem and cannot provide radiationless emission. This paper presents an alternate view, based on ordinary quantum mechanics, that

explains not only how the coulomb barrier can be overcome in a radiationless manner and why this can be done using the procedure developed by Fleischmann and Pons<sup>1</sup>, but also why this procedure leads to unexpected products, modes of energy release, and other effects that have been observed. The underlying ideas behind this alternative view are closely tied to the known electronic properties and structure of palladium deuteride PdD, and the governing rules of bound (as opposed to unbound) systems, and known effects associated with periodic order and the exchange of identical particles.

In the resulting picture, cold fusion is the result of a relatively small number of D<sup>+</sup> occupying wave-like (Bloch function) band states. Once this happens, as a result of the behavior of indistinguishable particles, these wave-like D<sup>+</sup> ions are free to overlap each other and fusion can occur. An important point is that the D<sup>+</sup> become delocalized as a result of occupying these states. The associated nuclear reactions also become distributed. This leads to different, distributed modes of interaction, in which the effects of periodic order and particle indistinguishability alter the relevant forms of reaction. From the underlying physics, it follows that in these distributed, transistor-like (as opposed to vacuum tube-like) modes of interaction, high energy particle and  $\gamma$ -ray emissions are not to be expected. Also, the underlying assumption that D<sup>+</sup> ion band state occupation should occur becomes valid in the limit that  $x \rightarrow 1$  in PdD<sub>x</sub>.

In the paper, we first examine what we believe to be the most compelling experimental evidence in support of excess heat. Then, using a concrete example, we explain the underlying logic, based on system energy minimization, behind our conclusion that the quantum mechanics of bound systems can potentially alter particle-particle overlap in a manner that may significantly affect the possibilities for nuclear reaction. We also explain why energy minimization precludes the possibility of nuclear fusion between chemically bound D or in D<sub>2</sub> molecules, but that the same principle can be used to demonstrate that under suitable circumstances nuclear reaction can occur between D<sup>+</sup> ions within a sufficiently large, periodically ordered solid as a result of ion band state occupation. In the remainder of the paper we examine the underlying implications and conditions associated with ion band state occupation and interaction, including a summary of the important restrictions and selection rules associated with potential ion band state mediated nuclear reactions.

## **I Underpinnings of Excess Heat Cold Fusion Theory**

### ***Evidence for Excess Heat***

Before exploring the theoretical aspects of cold fusion, we briefly consider the evidence for the reality of cold fusion heat. There have been many observations of excess heat in electrochemical system experiments. Among the hardest to refute are the observations of Fleischmann and Pons during temperature excursion events in which water in their electrolytic cell boils away.<sup>1</sup> The energy balance observed in their temperature-increase event published in *Phys. Lett. A* is:

- Heat of vaporization of 47 cc D<sub>2</sub>O: 102500 J in 10-minute boil-dry period
- Concurrent electrolysis power input: 22500 J
- Missing heat (cold fusion): 80000 J

The missing heat corresponds to 197 eV per Pd atom, which exceeds by a factor of 20 the value possible from stored chemical energy. The only mainstream physics possibility is that the heat was derived from the nuclear potential.

#### ***Why Ion Band State Matter Avoids the Coulomb Barrier: Guiding Principle***

There is considerable common ground among physicists concerning the principles of physics, and the requirements of a successful theory of the cold fusion heat effect. A successful theory must explain how the coulomb barrier is overcome and why fusion is radiationless. For nuclear reaction to occur there must be wave function overlap of the feedstock components and also wave function overlap with the product. There is also agreement that in free space this overlap can be explained by scattering theory, which provides transient overlap calculable from Gamow theory. On the other hand there does not seem to be an equal acceptance as to how one properly proceeds in applying the principles of physics to bound systems. It is worthwhile emphasizing that we believe that the governing principles of bound systems (as opposed to those of unbound systems) provide the appropriate framework for understanding cold fusion and that this fact has been largely ignored.

The applicable rules of physics for ground state bound systems are that 1) the overlap and other system properties are fully contained in the system wave function that minimizes total system energy, 2) the wave function is constrained by the natural boundary conditions of the environment, and 3) the rules of boson or fermion exchange symmetry (or anti-symmetry) that have been found to apply differently to sets of distinguishable and non-distinguishable particles must be included in an appropriate manner. These principles underlie the physics of atoms and molecules. They are the basis of atomic physics and quantum chemistry. The energy-minimizing wave functions have particle-particle avoidance terms, called correlation terms, which can be, but need not be required to restrict a specific particle A from being present at a point in space when particle B is present. In bound systems near room temperatures the amplitude of these particle-particle avoidance terms is determined by the energy minimization process. An important point is that in bound systems, system energy is constrained to be finite. For this reason, energy minimization principles always apply (often with unexpected results), and can be used to determine the ground state and lowest excited states. In unbound systems, such as plasma, the energy is not constrained to be finite. In this case the use of scattering theory and the associated quantum mechanics is the more appropriate approach for determining system dynamics.

#### ***The Helium Atom as an Example of a Bound Physical System***

A good example of the physics of bound systems is provided by the calculation of the 2-body wave function that describes the 2 electrons of the ground state helium

atom.<sup>2</sup> The Schrödinger equation for the helium atom (simplified by taking the nuclear mass as infinite) is

$$-\hbar^2/2m_e[\nabla_1^2 + \nabla_2^2]\Phi_s(\mathbf{r}_1, \mathbf{r}_2) + [e^2/r_{12} - 2e^2/r_1 - 2e^2/r_2]\Phi_s(\mathbf{r}_1, \mathbf{r}_2) = E\Phi_s(\mathbf{r}_1, \mathbf{r}_2)$$

where  $E$  is the band state energy of the 2-electron spatial wave function  $\Phi_s(\mathbf{r}_1, \mathbf{r}_2)$  for the zero-spin state, and  $r_{12} = |\mathbf{r}_1 - \mathbf{r}_2|$ .  $\Phi_s(\mathbf{r}_1, \mathbf{r}_2) = \Phi(\mathbf{r}_1)\Phi(\mathbf{r}_2)$  is symmetric with respect to interchange of  $\mathbf{r}_1$  and  $\mathbf{r}_2$ . In this equation the  $-\hbar^2/2m_e[\nabla_1^2 + \nabla_2^2]\Phi_s$  term represents the kinetic energy of the electrons, and the  $[e^2/r_{12} - 2e^2/r_1 - 2e^2/r_2]\Phi_s$  term represents the potential energy. The  $e^2/r_{12}\Phi_s$  term is the 2-electron coulomb repulsion term which results in correlated avoidance behavior by the two electrons.

The variational method was used by Hylleraas<sup>3</sup> to determine a sequence of 2-electron wave functions of increasingly better accuracy. Making use of the elliptical symmetry of the problem he reduced the six independent configurational coordinates of the 2 electrons that appear in the Schrödinger equation, namely  $\mathbf{r}_1$  and  $\mathbf{r}_2$ , to three independent elliptic coordinate variables  $s, t, u$  derived therefrom. He also made use of the symmetric spatial exchange symmetry of indistinguishable fermions with anti-parallel spins, which requires that candidate solutions be even functions of variable  $t$ . His third approximation is

$$\Phi_s = e^{-1.82 s/b} [1 + 0.29 u/b + 0.13 t^2/b^2]$$

where

$$s = |\mathbf{r}_1| + |\mathbf{r}_2|$$

$$t = |\mathbf{r}_1| - |\mathbf{r}_2|$$

$$u = r_{12} = |\mathbf{r}_1 - \mathbf{r}_2| = (\|\mathbf{r}_1\|^2 + \|\mathbf{r}_2\|^2 - 2|\mathbf{r}_1||\mathbf{r}_2|\cos\theta)^{1/2}, \text{ and}$$

$$b = \text{Bohr radius of hydrogen} = 0.53 \text{ \AA}$$

Consider what the Hylleraas solution tells us about particle-particle overlap in bound particle systems. The Hylleraas solution is dominated by the exponential decrease in  $|\Phi_s|$  with the mean distance of the 2 electrons from the nucleus, i.e., with  $s/2$ . To explore the electron-electron avoidance behavior we study the Hylleraas 6<sup>th</sup> approximation solution<sup>3</sup> on the surface of a sphere of fixed radius, i.e.  $s$  is fixed and  $t=0$ . A plot of the variation of the amplitude of  $\Phi_s$  with respect to the central angle  $\theta$  between the 2 electrons as viewed from the nucleus is given in Fig. 1. The wave function amplitude goes through a minimum at  $\theta=0$ , which corresponds to the point  $r_{12}=0$ . The wave function amplitude has been normalized to its value at  $\theta=180^\circ$ , which corresponds to the 2 electrons being on opposite sides of the nucleus.

Since the wave function amplitude at these two points is not much different, the figure shows that the 2 electrons of the helium atom have substantial overlap; in other words, if the electrons had the fusion capability of deuterons, they would fuse.

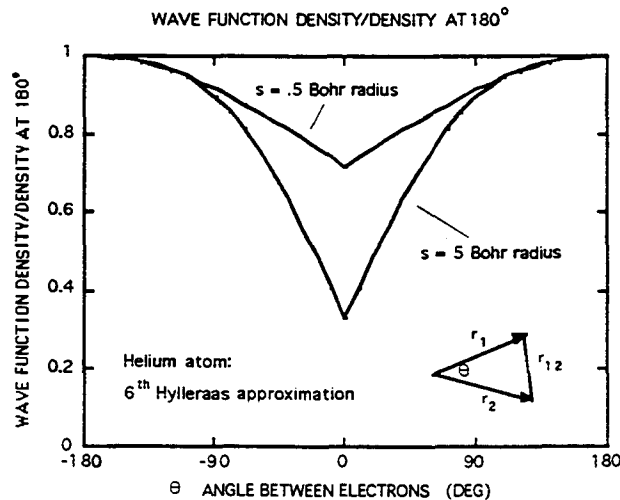


Fig. 1 Amplitude of helium ground state 2-electron wave function on the surfaces of 2 spheres for which  $s = \text{constant}$ . Values have been normalized with respect to the peak values, which occur when the 2 electrons are on opposite sides of the nucleus. Nature uses a cusp at  $r_{12} = 0$  to compensate for the infinite electrostatic potential existing at this condition. The values at  $\theta=0$  measure the degree of electron-electron overlap. If the electrons had the nuclear properties of deuterons, they would fuse.

### Wave Equation Singular Points

The behavior of the 2 electrons of the helium atom is an illustration of the more general behavior of particles in bound systems. The more general Schrödinger equation for electrostatically interacting particles in an external potential  $V_{\text{ext}}$  is

$$[-\hbar^2/2m \sum_i \nabla_i^2 + \sum_{i,j} e^2/r_{ij} + V_{\text{ext}}] \Phi_s(\mathbf{r}_1, \mathbf{r}_2, \dots, \mathbf{r}_N) = E \Phi_s(\mathbf{r}_1, \mathbf{r}_2, \dots, \mathbf{r}_N)$$

where  $r_{ij} = |\mathbf{r}_i - \mathbf{r}_j|$ .

The  $e^2/r_{ij}$  terms in the wave equation go to  $\infty$  at  $r_{ij}=0$ . However, because the system is bound, the eigenvalue  $E$  is always finite (and less than zero). This means that both the right and left sides of the equation must remain finite. (For unbound systems,  $E$  need not remain finite.) This means that at  $r_{ij}=0$ , because  $e^2/r_{ij} \rightarrow \infty$  either  $\Phi_s(\mathbf{r}_1, \mathbf{r}_2, \dots, \mathbf{r}_N) = 0$  or  $\sum_i \nabla_i^2 \Phi_s = \infty$ . In the latter case  $\Phi_s(\mathbf{r}_1, \mathbf{r}_2, \dots, \mathbf{r}_N)$  has a discontinuous derivative at  $r_{ij} = 0$ , i.e. the wave function has a cusp at  $r_{ij} = 0$ . In

practice Nature (i.e. energy minimization) makes use of both possibilities. If the kinetic energy terms  $-\hbar^2/2m \sum \nabla_i^2 \Phi_s(r_{ij})$  dominate the energy balance, Nature uses cusp solutions; if the potential energy terms dominate, Nature zeroes the wave function at  $r_{ij}=0$ . However, the situation for nuclei in molecules is different than for electrons in the helium atom. For nuclei in deuterated molecules  $m$  is the deuteron mass  $m_D$ , instead of the electron mass  $m_e$  used in the He solution. This reduces the importance of the kinetic energy terms by a factor of 3600. This reduction makes the potential energy term dominant. Nature then zeroes the wave function and no fusion is possible. (This condition also applies to any possible interstitial  $D_2$  configuration.)

Since interstitial occupations of a metal lattice by  $D_2$  are unable to fuse, the cold fusion heat observations require that the D be in some other configuration. We now show that when  $D^+$  is in a delocalized configuration, such as a Bloch state, then overlap can occur and fusion becomes possible.<sup>4</sup>

### ***Bound State Systems Containing Band State Ions***

The physics of bound solid state systems depends on the same laws as the physics of molecules. If one considers a Bloch state  $D^+$  population in a microscopic crystal resembling an atom cluster, no  $D^+ - D^+$  overlap can occur because the potential energy coulomb repulsion term in the wave equation dominates the kinetic energy term in determining the magnitude of the correlation terms in the wave function, just as it does in normal  $D_2$  molecules. On the other hand, Bloch states have the important property that their amplitudes are periodic functions of the underlying lattice. This means that in a periodically ordered lattice, if the band state  $D^+$  ions are spread out over successively larger crystal sizes, i.e. if  $N_{\text{cell}}$  is increased, the amplitude of each single particle wave function decreases, and the importance of the wave equation coulomb repulsion potential terms decreases relative to the importance of the kinetic energy terms. As shown below, this behavior means that wave function overlap occurs and fusion becomes possible.

To pursue our argument let us first look at the potential energy reduction that occurs as a result of introducing nodes or cusps into the wave function in order to reduce the amplitude of the wave function when  $r_{ij}=0$ . The particle-particle avoidance interaction reduces system potential energy by  $\Delta E_{\text{pot}}$

$$\begin{aligned} \Delta E_{\text{pot}} = & 1/2 \iint e^2 |\Phi_{\text{corr}}(\mathbf{r})|^2 |\Phi_{\text{corr}}(\mathbf{r}')|^2 / |\mathbf{r}-\mathbf{r}'| d\mathbf{r} d\mathbf{r}' \\ & - 1/2 \iint e^2 |\Phi(\mathbf{r})|^2 |\Phi(\mathbf{r}')|^2 / |\mathbf{r}-\mathbf{r}'| d\mathbf{r} d\mathbf{r}' \end{aligned}$$

where within the many-body wave function

$\Phi$  is a single particle Bloch function without correlation terms, and  
 $\Phi_{\text{corr}}$  is a correlated single particle function that also possesses Bloch function symmetry but is derived with  $r_{ij}$  avoidance terms (which results in dimples: nodes or cusps).

The particle-particle avoidance increases system kinetic energy by  $\Delta E_{ke}$

$$\Delta E_{ke} = \hbar^2/2m_D \int \nabla \Phi^*_{corr} \nabla \Phi_{corr} dr - \hbar^2/2m_D \int \nabla \Phi^* \nabla \Phi dr ,$$

where

$\nabla \Phi$  is the gradient of the wave function without correlation terms, and

$\nabla \Phi_{corr}$  is the gradient of the correlated wave function with  $r_{ij}$  avoidance terms (nodes or cusps).

With increasing  $N_{cell}$  both  $|\Phi|^2$  and  $|\nabla \Phi|^2$  decrease as  $1/N_{cell}$ . Since on a per unit cell basis  $\Delta E_{pot} \propto |\Phi|^4$ ,  $\Delta E_{pot}$  decreases as  $1/N_{cell}^2$ . In contrast,  $\Delta E_{ke} \propto |\Phi|^2$ . Then, at large  $N_{cell}$  it follows that  $\Delta E_{ke}$  dominates  $\Delta E_{pot}$ . This resulting dominance of kinetic energy over potential energy in the part of the wave equation controlling particle-particle avoidance means that total energy is minimized in a similar manner to the way kinetic energy dominance leads to energy minimization and overlap of the electrons of the ground state helium atom. As a result the many-particle energy-minimizing wave function has only a small amount of correlation wave function curvature, and has a shallow cusp at  $r_{ij}=0$ , i.e. particle-particle overlap is almost complete.

As discussed in the next paragraph D<sup>+</sup> ion band state fusion energy is released in a distributed fashion. The comparison between the D<sup>+</sup> ion band state picture including nuclear energy release and the situation involving the balance between kinetic energy and coulomb repulsion between electrons in the helium atom is especially meaningful provided the distributed nuclear energy release per unit cell is of the order of the characteristic D<sup>+</sup> vibration energies, which are in the 0.01 to 0.1 eV range. Since the distributed nuclear energy release = 23.8 MeV/ $N_{cell}$ , this requirement is that  $N_{cell} > \sim 10^8$ . Since the kinetic energy term in the wave equation relative to the potential energy term is reduced by the order of 10<sup>4</sup> in going from the electrons in the helium atom to D in the D<sub>2</sub> molecule, the value  $N_{cell} = 10^8$  is much greater than that needed to meet the requirement for D<sup>+</sup>-D<sup>+</sup> overlap. Thus with  $N_{cell} = 10^8$ , the essential overlap requirement for D<sup>+</sup>-D<sup>+</sup> fusion is satisfied.

### ***Why Ion Band State Fusion Is Radiationless***

We now consider why D<sup>+</sup> ion band state fusion produces no  $\gamma$ -rays or energetic particles. Interaction between band state occupations makes only a small amount of nuclear energy available in each unit cell. This is because, when both the reactants and products of the potential nuclear reaction occupy band states, only a small fraction of each reactant and product is located in each unit cell, meaning that only a small amount of each reaction occurs in each unit cell. In contrast, high energy particle and  $\gamma$ -ray emission requires concentration of the available energy into a small volume. At the near room temperature conditions used in cold fusion studies concentration of the available energy into a single unit cell by incoherent or

coherent processes is statistically impossible because of the large entropy cost associated with accomplishing this process.

### ***Where the Energy Goes***

The small amounts of energy made available in each unit cell by the  $2\text{-D}^+\text{band} \rightarrow {}^4\text{He}^{++}\text{band}$  reaction should be able to excite phonons, either thermally (through residual electron-ion interaction), or at the boundaries of the lattice where periodic order is lost. The large density of states that is provided by these processes is responsible for making the nuclear reactions irreversible. At low temperature, phonon generation occurs primarily at the boundaries of the crystal lattice, where periodic order is lost. In these regions, the electron-ion interaction is dominated by the requirement that the "spill-out" dipole layer associated with electrons near the surface and the surface ion band states adjust themselves in a manner that is consistent with Gauss's law and the applied electric field. (In the surface region, as opposed to the bulk, it is possible for a net distribution of charge to be present because there exists a net electric field flux into and out of this region.)

Although this readjustment process is dominated by the behavior of the electrons and the associated electron-ion interaction, it is possible to identify a prospective ground state ion configuration in the surface region that is consistent with the arrangement of electrons. In particular, at the surface, although three dimensional periodic order is lost, at low temperature, it is plausible (depending on loading conditions) that two dimensional order (defined by the lattice structure in planes parallel to the surface) will be present. Then, the same kinds of ion band state (as well as electron band state) considerations apply except that Bloch symmetry in this case applies only in directions parallel to the surface. In directions normal to the surface, each wave function is smoothly matched onto the appropriate solutions of the Schroedinger equation. The result of this construction is that each bulk-like (electron or ion) band state smoothly matches onto a surface state which possesses two-dimensional Bloch symmetry in the surface region (where the net electric field flux is non-vanishing), and exponentially decays in directions normal to the surface, in a manner similar to the exponential decays that occur in all negative kinetic energy region solutions associated with the bound state Schroedinger equation.

In the extreme low temperature limit it is plausible that the dominant phonons will result from extreme long wavelength acoustical phonons in which large portions of the bulk lattice effectively resonate with respect to each other. This is because these phonons, which can be generated through small fluctuations in the electrostatic zero (by the average value of the chemical potential), 1) are the most sensitive to the smallest variations in charge in the surface region, and 2) can also result from the large density of states associated with intermediate "horizontal" (or UmKlapp) processes, in which the lattice (or a large portion of the lattice) effectively recoils as a whole. An additional possibility is that long wavelength optical phonons will be generated through the volumetric stress associated with each fusion. Although it might appear that the possible modes of energy release associated with these optical phonon processes would occur with higher energies (and temperatures) than the

ones associated with long wavelength acoustical phonons, each fusion includes an effective softening of the ion band state in the zero-point motion of the ion band state material (owing to the larger mass of the  ${}^4\text{He}^{++}$  product).

### ***Ion Band State Matter as a Matter Field within a Host Lattice***

Limitations on cold fusion possibilities are determined in major part by limitations on allowed final state wave functions. To the extent that the coulomb barrier terms in the many-body wave function have vanishing amplitude, the ion band state approximates a non-relativistic quantized matter field<sup>5</sup> restricted to a finite volume  $V_{\text{xtal}}$ . For a D<sup>+</sup> band state population the quantum of mass is 2 AMU, i.e. the matter content of the field can only increase or decrease in discrete steps of 2 AMU. Within the matter field there is concurrent action at a distance, as required to resolve the Einstein, Podolsky, and Rosen<sup>6</sup> argument against the completeness of quantum mechanics. An important point is that the ion band state picture only makes sense if the ion bands remain occupied for a sufficiently long period of time relative to the required time necessary for nuclear reaction to proceed. For this to occur, each nucleus that occupies such a state must effectively dissociate from its own electron (as well as the remaining electrons) over a time scale that is short with respect to times associated with electrostatic processes, but long relative to nuclear process time scales. This requirement places important constraints associated with the underlying electronic structure on the kinds of environments where ion band state matter will form in a manner that will allow for appreciable nuclear reaction to occur.

The physical system includes the crystal interior lattice, the crystal surface boundary region where periodic order is lost, the interior D<sup>+</sup> ion band state matter field, and the matter field's surface stress region within which the band state matter wave function transitions into a decaying exponential, associated with the negative kinetic energy region outside the solid. The final state consists of bulk-like ion band state  ${}^4\text{He}^{++}$ , which depending on the temperature and degree of crystalline order in the surface region, may match onto any of a variety of functional forms in the surface region. In the extreme low temperature limit, as mentioned above, the ion band states can match onto localized surface states provided adequate crystalline order is present in planes parallel to the surface. An interesting point about this case is that these ion band surface states in principle can couple coherently to electron surface states (occupied by the host electrons as well as by the injected electrons that accompany the ion band state D<sup>+</sup>) in a manner that could preserve Bloch symmetry in planes parallel to the surface. The significance of this form of coupling is that neutral or ionized  ${}^4\text{He}$  could be ejected from the solid in a coherent manner, leading to a Bragg-like diffraction pattern, reminiscent of the diffraction patterns that are observed in low-energy  ${}^4\text{He}$  scattering experiments. In all cases, the large strain energies (and propensity for cracking, etc.) associated with multiple occupation of a unit cell by either D or He in a non-ion-band-like form, inhibit the final state  ${}^4\text{He}^{++}$  from occupying or coupling to non-ion-band-state  ${}^4\text{He}$  in bulk regions. This is the justification for the prediction that we made<sup>4,7</sup> prior to the

experimental measurements<sup>8,9</sup> that the  ${}^4\text{He}$  product should be found primarily at low energy and in regions outside heat-producing electrodes.

### ***The Reaction Process***

In the above picture there is no intermediate observable state between ejection of a normal  ${}^4\text{He}^{++}$  product and annihilation of 2 deuterons in the matter field. The normal astrophysical factors affecting fusion rate apply. The  $\text{D}^+ - \text{D}^+ \rightarrow {}^4\text{He}^{++}$  reaction would be restricted only by the requirement for anti-parallel spins, which, in most cases, reduces the reaction rate by a factor of 3. This last reduction factor would be reduced in a situation in which band state  $\text{D}^+$  is preferentially prepared so that spin populations of opposite spin are equally occupied. An interesting point is that by introducing a constant magnetic field  $\mathbf{H}$  (or a constant magnetic field  $\mathbf{H}$  accompanied by a perpendicular oscillating magnetic field, as in standard NMR measurements), it is possible to enhance both 1) spin alignment in directions parallel to  $\mathbf{H}$  and 2) anti-alignment of spins in directions perpendicular to the field. It is also interesting to note that the creation of  ${}^4\text{He}^{++}$  in ion band state form provides a source for reducing magnetism (since  ${}^4\text{He}^{++}$  is non-magnetic while the feedstock ion band state  $\text{D}^+$  is magnetic) in a delocalized manner that preserves periodic order. We have also shown<sup>4,10</sup> that for low  ${}^4\text{He}^{++}$  concentrations, the fusion rate is proportional to the concentration of final state  ${}^4\text{He}^{++}$ . As discussed below, it also is true that reductions in periodic order inhibit fusion. Together these observations suggest that the process of creating  ${}^4\text{He}^{++}$ , which is enhanced by preferentially preparing the feedstock  $\text{D}^+$  in a form in which equal populations of anti-parallel states are occupied, may help to preserve both crystalline and magnetic order in a manner that may further enhance the fusion process.

As discussed in part 2, the above picture conforms to the requirement of Born-Oppenheimer separability of the fast nuclear reactions with respect to the slower electrostatic interactions that affect only the center-of-mass coordinates. The nuclear/zero-point-motion volume ratio  $V_{\text{nuc}}/V_{\text{zp}}$  enters in as described in our 1991 *Fusion Technology* paper<sup>4</sup>. In contrast, reactions of the type  $\text{H}^+ - \text{H}^+$  going to a deuteron by electron capture or positron emission with emission of a neutrino would probably be excessively slow due to the required weak force interaction.

## **2 D<sup>+</sup> Ion Band State Fusion**

### ***Exotic Situation, Not Exotic Physics***

The arguments presented above show that cold fusion is not the result of exotic physics; instead it is mainstream physics applied to an exotic situation that can only occur inside condensed matter. It is the result of the formation of exotic types of compounds, wave-like occupations of energy bands, which become allowable when chemical thermodynamic conditions support their formation. We have suggested several types of compounds that could include such ion band state occupations, namely,  $\text{PdD}_{1+\delta}$ ,  $\text{AgD}_\delta$  or  $\text{NiD}_\delta$ . However, the designation  $\text{PdD}_{1+\delta}$  should not be taken too literally. Although it describes conditions that might allow ion band state

formation at low temperature, some  $D^+$  ion band state occupation will occur in  $PdD_x$  with  $x < 1$  even at low temperature. The cause of such occupations is the entropy term in the chemical potential associated with occupation of a fixed number of interstitial sites.<sup>11</sup> This term forces the chemical potential for D absorption to become infinitely positive before the value  $x=1$  is reached. Equally important, at finite temperature, some occupation of the band state would occur at  $x < 1$  even if the entropy term were not included. (Band state occupations are only required to occur over some finite lifetime that is considerably shorter than the typical time-scales associated with the dominant thermodynamic processes. Band state occupations occur only over a finite volume  $V_{xtal}$ , where  $V_{xtal}$  can be a sub-volume of the entire crystal.) The temperature dependence of excess heat production reported by Storms<sup>12</sup> suggests an energy of activation of ~15 kcal/mol for populating the heat release state, which we assume to be the band state. The proper designation for the palladium deuteride that supports fusion is  $PdD_{1-\eta+\delta}$ , where  $\eta(T) \ll 1$ .

The exotic character of the  $D^+$  band state matter state is shown in part by the very small concentration of ions required for the production of measurable heat. Calculations indicate that an occupation density of  $\sim 10^{-7}$  band state  $D^+$ /unit cell is sufficient to explain observed heating rates. Moreover, there are limitations on the top end values of  $x$  that are compatible with heat production. A population of  $\delta > 10^{-3}$  may be sufficient to force occupation of the Pd tetrahedral interstitial sites in  $PdD_x$ , which may destroy the periodic order needed for power production. The range in values of  $x$  that correspond to these  $\delta$  limits may be quite restricted. The drop in resistivity observed by McKubre<sup>13</sup> in  $PdD_x$  once  $x$  exceeds  $\sim 0.73$  is a qualitative measure of lattice order. Only the portion of D absorbed into Pd that increases ordering is important to the band state fusion process. Hydrogen uptake measurement of  $x$  can sometimes be misleading since other non-productive means of containment of D exist, e.g. filling of interstices, occupations of tetrahedral sites in octahedrally loaded metal, and possibly some kind of LiD/Pd alloying. Another important factor affecting ion band state formation in the different metals is host electronic structure.

### ***Experimental Evidence for the Existence of Band State Hydrogen***

Although  $D^+$  ion band state matter may be considered exotic, 2-dimensional ion band state matter is known to be present in H and D adsorptions on the surfaces of transition metals. This idea has been used to explain the vibrational spectra dependence on H- and D- coverage in the adsorptions of H and D on Cu(110) and Ni(100).<sup>14,15</sup> Ion Band State occupation potentially can be used to explain the huge diffusion lengths of D and H in many metals.

### ***Role of Electronic Structure***

An important aspect of ion band state occupation and the implications of ion band state occupation to cold fusion, that we have not emphasized in the past, is the role of electronic structure. Normal chemistry at room temperature inherently favors neutrality (or approximate neutrality). It is well known that this is true in the solid

state and this fact has been the cornerstone for understanding a large number of the cohesive, chemical, and electronic properties of solids. For this reason D<sup>+</sup> ion band states can become occupied and ion band state mediated fusion can occur only if specific conditions associated with the underlying electronic structure are fulfilled.

- 1) Sufficient periodic order must be present for a sufficiently long period of time.
- 2) Deuterium and host electrons must dissociate from D<sup>+</sup> band-state matter on time-scales that are long compared with those required for fusion through nuclear self-interaction.
- 3) D<sup>+</sup> band-state matter must distribute itself in a sufficiently diffuse manner as a result of interactions with the host lattice.

In the case of Pd and PdD, we know from neutron diffraction experiments<sup>16</sup> the structure of PdD, the presence of crystalline order, the location of the D, and its characteristic zero-point motion radius, which is relatively large (~0.2 Å). We know from the excellent agreement between a number of first-principles ab initio electronic structure calculations<sup>17</sup> and photoemission experiments<sup>18</sup> even some of the more delicate aspects of the associated electronic structure of both Pd and PdD, to a fair level of precision. Thermodynamic modeling<sup>11</sup>, and electronic structure calculations in particular, show that in PdD<sub>x</sub> as x is increased from values below 0.7 to unity, chemical bonding involves important hybridization between bonding 4d states and anti-bonding 5s states provided by the Pd.

In the case of the PdD<sub>1+δ</sub> that we have suggested is relevant to cold fusion, within the bulk, in each unit cell the concentration (=δ) of ion band state D<sup>+</sup> is balanced by an equal concentration of electrons (which also occupy band states). The assumptions that both the D<sup>+</sup> and the electrons may fractionally occupy band states in this manner is not only consistent with the known laws of solid state physics, it is consistent both with thermodynamics<sup>11</sup> and with the electronic structure calculations<sup>17</sup>. In particular, Wicke and Brodowsky<sup>11</sup> have summarized the behavior of the chemical potential with respect to changes in D-loading. Their figure 3.11 shows that large lattice strain energy costs are associated with D-occupation of a Pd unit cell when x is small, from which one concludes that huge lattice strain energy costs would be associated with D-occupation of a unit cell by more than one D in the limit that x→1+δ in PdD<sub>x</sub>. This result essentially is tied to the dominant Pd-to-H bonding-anti-bonding features associated with the 4d-5s hybridization identified by Papconstantopoulos et al.<sup>17</sup>.

An important point is that it follows from a minor generalization of local density theory<sup>19</sup> (which provides the basis of these calculations) that, when δ is sufficiently small, as D is loaded into PdD to form PdD<sub>1+δ</sub>, the energy associated with the accompanying additional concentration (δ) of electrons is minimized provided 1) these electrons fractionally occupy the lowest unoccupied states (immediately above the PdD Fermi level), and 2) variations in electronic structure associated with these fractional occupations does not alter the density of ion band state deuterons. Although it is not rigorously necessary to impose these last two constraints, it does follow rigorously that they provide a means of constructing a self-consistent local

density approximation method for determining the ion band states in the limit in which  $\delta$  becomes infinitesimally small. This minimization of electronic energy requires that the added D<sup>+</sup> be in a band state.

Additional results of Papaconstantopoulos et al.<sup>17</sup> suggest that variations in electronic structure associated with fractionally occupying new states immediately above the Fermi energy E<sub>F</sub> of PdD probably would not appreciably affect the ion band state densities that we have used previously<sup>20</sup>, nor would the densities differ importantly from those that would result from self-consistent local density approximation calculations carried out in this fashion. These earlier ion band state calculations were carried out using minimum uncertainty wave packets of a characteristic size defined by the known<sup>16</sup> zero-point motion volume of D in PdD. Papaconstantopoulos et al.<sup>17</sup> have shown that, as a result of the 4s-5d hybridization discussed above, near E<sub>F</sub> electron occupation involves anti-bonding 5s-like states primarily in regions in the vicinity of Pd ion cores, and only a very small (~0.1 e), predominantly s-like electronic charge is found in the vicinity of the octahedral site zero-point-motion volume in which deuteron cores are known to bind to the solid.

Both results indicate that effectively D<sup>+</sup> ions do dissociate from host electrons on time-scales that are large enough to allow for fusion to occur. In particular, in ref. 21, we have used the minimum uncertainty packets mentioned above to determine meaningful bounds on the electrostatic ion-ion self-interaction, which we find to be ~ 10<sup>-17</sup> second. This value, which is the rate-limiting effect associated with the coulomb repulsion between potentially interacting D<sup>+</sup>, is much smaller than the time-scales (~10<sup>-14</sup> s) associated with the 10's of meV bandwidths characteristic of the coupling between D<sup>+</sup> and electrons in PdD. This value is also considerably larger than the typical time-scales (~10<sup>-22</sup> s) associated with nuclear self-interaction.

It is worthwhile noting in passing that it is possible to consider generalizations of the above picture associated with relaxing the restriction (implied by local density theory) requiring that variations in ion band state density become independent of variations in electron band state density. This restriction applies rigorously for the ground state wave functions provided electron-ion-band-state correlation effects are not present that could lower system energy. Although in the extreme low ion concentration limit, these correlation effects must become unimportant, it is possible that, at finite ion band state concentrations, electron-ion pairing mechanisms could lower system energy in a manner similar to the way pairing between electrons through phonon coupling to the lattice lowers system energy in the formation of Cooper pairs. Waber<sup>21</sup> has identified this possibility and suggested potential nesting features in the Fermi surface associated with the fractionally occupied electronic states that could trigger these forms of correlation.

### ***Transistor vs Vacuum Tube Thinking***

To visualize the cold fusion process one must adopt a different mode of thinking relative to that employed in hot fusion and conventional nuclear physics. In hot fusion one thinks in terms of collisions between randomly moving ions. These

collisions are analogous to the electron-electron collisions that electrons undergo in the electron cloud surrounding the hot filament of a vacuum tube. To visualize the cold fusion process one must switch from thinking about the localized discrete particles encountered in "vacuum tube thinking" to thinking in terms of the collective action of the delocalized wave-like "particles" existing in semiconductors, i.e. to "transistor thinking". Once an individual D occupies an ion band state, it no longer is located in any specific unit cell. It is located everywhere. This is analogous to the behavior of electrons in metals. Potential interactions and modes of interaction are altered dramatically. More importantly, the coulomb barrier idea of particle-particle Gamow theory is replaced by the correlation properties of the many-body wave function.

### ***How Ion Band State Nuclear Reactions Occur***

The physics of collectively interacting wave-like ions has substantial implications with respect to potential nuclear interactions. Under the rules of solid state physics, cold fusion can occur as a transformation of wavelike deuterium into wavelike  ${}^4\text{He}$ . As previously discussed<sup>4,7,10</sup>, the energy release from the transformation involves no high energy concentration, and no high energy particles are emitted. The nuclear interactions are governed by a self-consistent, non-relativistic quantum field theory that we have named Lattice Induced Nuclear Chemistry (LINC)<sup>7</sup>. LINC is based on ordinary non-relativistic quantum field theory as it should apply to an indistinguishable collection of ion band state D (also called a Bose Bloch condensate) corresponding to the small band state concentrations  $\delta$  of  $\text{D}^+$  associated with the  $\text{PdD}_{1+\delta}$ ,  $\text{AgD}_\delta$ , and  $\text{NiD}_\delta$  compounds. Energy is minimized through elimination of lattice stress and by the occupation of uncorrelated many-body wave functions that are constructed from single particle ion band states. The resulting potential nuclear reactions preserve the requirement that the locations of both the potentially reactive D and the reaction products cannot be determined on the time-scales associated with maintaining periodic order.

### ***Born-Oppenheimer Separability and Selection Rules of LINC***

Through LINC, transistor-like (i.e., distributed solid-state-like) as opposed to vacuum tube-like (collision dominated) rules about particle overlap and transport become valid. The mathematical basis for this is provided by the underlying assumption of LINC and its reactions: reactions and overlap can occur provided the dominant electrostatic interactions are between the lattice and the center of mass of potentially nuclear reactive nucleons, and not between the individual nucleons. This limit can occur when amplitudes of the ion-ion correlation terms in the many-body wave function become small, and provided the time-scales for nuclear reaction are very much shorter than those associated with electrostatic interaction.

When the time-scales for particular nuclear processes are very different than those associated with the motion of the nucleus within an applied electrostatic field, it then becomes appropriate to write the wave function of the nucleus as the product of a rapidly varying function that describes the motions of the individual nucleons

within the nucleus relative to the center of mass  $\mathbf{r}_{\text{cm}}$  multiplied by a more slowly varying function that describes the center of mass motion of the nucleus with respect to the applied electrostatic potential. This factorizing of the wave function is referred to as Born-Oppenheimer separability. This assumption holds rigorously provided the time-scales associated with the center of mass motion and the motions of the individual nuclei always remain very different. This representation applies to the initial state provided the center of mass motion of each  $D^+$  is well-described by a band state. Expressed in terms of the separation coordinates of the protons and neutrons in p-n pairs ( $\mathbf{r}_n - \mathbf{r}_p$ ), the wave function of each deuteron is given by

$$\Phi(\mathbf{r}_n, \mathbf{r}_p) = \Psi_{\text{nuc}}(\mathbf{r}_n - \mathbf{r}_p) \Psi_{\text{band}}(\mathbf{r}_{\text{cm}}) ,$$

where  $\Psi_{\text{nuc}}$  is the rapidly varying nuclear wave function that describes the probability amplitude of finding a proton or neutron within a small volume centered about the center of mass, and  $\mathbf{r}_n$  and  $\mathbf{r}_p$  respectively are the locations of the proton and neutron.

The assumption of LINC is that this form of Born Oppenheimer separability applies rigorously as a function of time in all multi-particle fluctuations (governed by the underlying field theory) that are consistent with the requirements that the nuclear and electrostatic time scales associated with these fluctuations remain very different. This means that at any time during the reaction the final state must be representatable in a Born-Oppenheimer separable form:

$$\Phi(\mathbf{r}_1, \dots, \mathbf{r}_m) = \Psi_{\text{nuc}}(\mathbf{r}_1 - \mathbf{r}_{\text{cm}}, \dots, \mathbf{r}_m - \mathbf{r}_{\text{cm}}) \Psi_{\text{band}}(\mathbf{r}_{\text{cm}}) ,$$

where  $\Psi_{\text{nuc}}(\mathbf{r}_1 - \mathbf{r}_{\text{cm}}, \dots, \mathbf{r}_m - \mathbf{r}_{\text{cm}})$  now describes the nuclear (multiple-nucleon) wave function. In refs. 7 and 10, we have derived important selection rules associated with this constraint. In particular, the constraint automatically rules out a large number of potential reactions. This is because the constraint is only meaningful provided 1) zero-point motions of the center of mass of potentially reacting nuclei are sufficiently large both during and subsequent to the reactions, and 2) these center of mass motions must remain independent from the motions of the individual nucleons at all times during the reaction.

Because nuclear reactions between closely separated nucleons are always independent of the absolute location of the center-of-mass, there exists an important symmetry which insures that the final state representation is meaningful since it preserves this symmetry. Because of the requirement that the zero-point motions of the center of mass must be sufficiently large, the limitations of the representation are closely tied to the underlying electronic structure. Using reasonable wave functions, based on known values of zero-point motion for D in  $\text{PdD}_x$ , we have estimated in refs. 7 and 20 suitable bounds for the electrostatic self-interaction and

nuclear self-interaction, where we have shown that separability can be expected to apply for a  ${}^4\text{He}$  product.

Perhaps of greater significance is the following: The assumption that Born-Oppenheimer separability must be maintained in the final state and during all intermediate states involving multi-particle fluctuations associated with band state overlap leads to an important selection rule. Beginning from a state consisting entirely of  $\text{D}^+$  ion band states, the many-nucleon portion of the final state wave function  $\Psi_{\text{nuc}}(\mathbf{r}_1-\mathbf{r}_{\text{cm}}, \dots, \mathbf{r}_m-\mathbf{r}_{\text{cm}})$  must be formed exclusively from unbroken proton-neutron pairs.

As we have shown in ref. 10, this rule is based on rigorous requirements associated with constraining the governing field theory so that the nuclear and band state wave functions evolve independently from each other. We have demonstrated this using the defining constraints of canonical quantization (using Poisson Brackets) associated with the problem of constructing a field theory that maintains Born-Oppenheimer separability starting from an initial state consisting of ion band state  $\text{D}^+$ . We have previously used the terminology<sup>7,20</sup> "bosons in and bosons out" to refer to the resulting selection rule that proton-neutron pairs cannot be broken.<sup>20</sup>

The presence of unpaired proton-neutron pairs, or of unpaired protons or neutrons, in the initial state requires that this rule be modified. In ref. 10, we have discussed these modifications. The resulting selection rules and reactions associated with LINC, both when either unpaired protons and neutrons are and are not present, are summarized below.

### ***Many-body Wave Function***

The initial state many-body wave function is constructed from a summation of terms. Each term consists of a product of all of the single deuteron wave functions in which each deuteron is assigned a specific location. The summation imposes the required particle-exchange symmetry, ensuring that the many-body wave function describes indistinguishable bosons. Because of Born Oppenheimer separability, automatically, the summation of terms can be factored into a product consisting of a single factor derived from a subproduct of the localized wave functions ( $\Psi_{\text{nuc}}$ ) multiplied by a sum of terms associated with the slowly-varying band state  $\text{D}^+$  many-body function. (Because of Born Oppenheimer separability, the effects of particle exchange symmetry of the entire many-body function appear only through the many-body band state wave function.) Band state  $\text{D}^+$  matter has magical properties that are implicit because of the exchange symmetry that is embodied in the many-body band state wave function. Because each single particle band state wave function has Bloch function symmetry, when the many-body band state wave function becomes occupied, the lattice strain (associated with injection of non-band state  $\text{D}$  into the host) vanishes. For this reason, this function minimizes system energy in crystals that are sufficiently large, when the number of band-state  $\text{D}^+$  is

much less than the total number of unit cells, and the band state D<sup>+</sup> remain uncorrelated.

This many-body wave function can also be written in a "vacuum tube-like" form, based on a particle-like (Wannier state) representation<sup>4</sup>. The resulting description is characterized in a manner involving particle-like occupations (involving whole numbers of D<sup>+</sup>), in which each occupation is transient and possesses a finite life time Δt. Specifically, ΔE-Δt~h, Δt~10<sup>-16</sup> s. The particle-aspect of the matter field's behavior is shown in the Wannier form (analogous to an inverse Fourier transform) of the many-body bosonic wave function.<sup>4</sup>

$$\Psi(\epsilon_p, r) = (1/N_D!)^{1/2} \sum_{\{r_m\}} (1/N_{\text{cell}})^{N_B/2} \left\{ \prod_{m=1}^{N_D} \sum_{s=1}^{N_{\text{cell}}} \Phi_s(r_m) \exp(i\mathbf{k}_p \cdot \mathbf{R}_s) \right\}$$

Here  $\{r_m\}$  means the sum is over all products in which distinct pairs of particles are exchanged. All terms are of the form

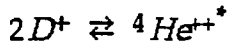
$$\Phi_{121}(r_{11}) \cdot \Phi_{61}(r_{77}) \cdot \Phi_{18214}(r_{480}) \cdot \Phi_{2107}(r_{396}) \cdots \cdots \Phi_{97}(r_{11}) \cdots$$

Each term contains N<sub>D</sub> factors, where N<sub>D</sub> is the number of deuterons in the many-body band state. There are  $N_D!(N_{\text{cell}})^{N_D}$  terms in the wave function. In the many-body wave function the deuteron index never repeats, but the unit cell index may repeat. The expansion contains terms that correspond to zero, single, double, triple, etc. occupations of specific unit cells. The existence of multiple occupation terms reveals that D<sup>+</sup>-D<sup>+</sup>, or D<sup>+</sup>-D<sup>+</sup>-D<sup>+</sup>, etc. overlap can occur. In other words, the algebraic properties of the many-body wave function imply that overlap occurs. The underlying reason that this becomes possible is that in the localized, Wannier representation, occupation of an individual site can become short-lived. Another way of understanding this point is that in the "usual" (or vacuum tube) way of looking at deuterons, they appear to be long-lived particles, while if a collection of them occupy ion band states, this particle (i.e., Wannier state) picture can breakdown because the lifetime of a "particle" at any individual location can become very short. Underlying the resulting overlap process is this question of lifetime. If the lifetime for electrostatic overlap (as a result of the band state occupation) is considerably longer at a lattice site in this "particle-like" representation than the comparable "particle-like" lifetime associated with nuclear decay, nuclear reaction can occur. As a result, a variety of reactions become possible.

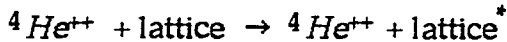
### ***The 2-body Reaction***

The number of double occupations of unit cells exceeds the number of triple occupation by the factor 1/δ, where δ is the number of band state ions per unit cell.

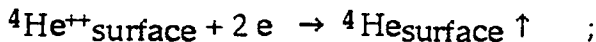
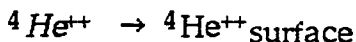
Since  $\delta$  may be of the order of  $10^{-6}$ , 2-body interactions are expected to dominate. All the reactions involve delocalized  $D^+$  ions and proceed as volume distributed interactions. The first reaction step is a reversible coalescence of p-n pairs



The reaction is made irreversible by excitation of the lattice



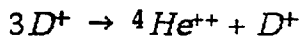
Helium is ejected from the lattice either as a neutralized surface species



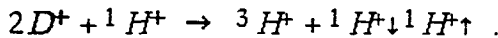
or (as discussed above), at low temperature, possibly as a Bragg scattered neutral atom or ion. The species in italics are delocalized configurations (Bloch states). The surface ejection of He was predicted<sup>4,7</sup> before being observed<sup>8</sup>. In the 2-body reaction overlap of p-n pairs allows nuclear fusion  $2D \rightarrow {}^4He$ : (As little as 0.3 ppm of wavelike  $D^+$  may be needed to produce 600 W/cc.<sup>4</sup>)

### ***Multiple- and Mixed-body Reactions***

Other interactions between band states include<sup>10</sup> the three body reactions



and



where the small arrows indicate the relative directions of nuclear spins. The latter reaction requires occupation of both deuteron and protium band states, and has been suggested as a possible tritium-creating band state side reaction. In all the reactions energy release is distributed over the lattice, only a small amount occurs in each unit cell. (As applied to a proposed "normal" water reaction, concentrations of  $10^{-7}$  D/Pd and  $10^{-3}$  H/Pd may be adequate to produce claimed heat.)

### ***Predictions***

Predictions made before experimental verification include the requirement for ~1:1 D/Pd ratio (McKubre et al., Kunimatsu et al.)<sup>22,23</sup>, no appreciable radiation or neutrons (many groups), and primary products being heat and low-energy  ${}^4He$  in the outgases (Miles et al., Yamaguchi and Nishioka)<sup>8,9</sup>. Cracking, overloading, and

other processes that cause loss of periodic order should impede cold fusion heat release.

Other predictions include: Reactions are fractional, involving infinitesimal energy release in each unit cell. Energy is transferred to the lattice through coupling to phonons, excitation of high frequency sound modes, inelastic scattering of products with host electrons, etc. Lattice disintegration terminates heat generation. High energy particle release may occur if periodic order is lost suddenly. Optimal heating occurs when lattice disintegration is minimized, with energy release occurring dominantly through extreme long-wave phonons caused by release of products in regions where periodic order is lost. Reaction products are distributed at surfaces, near cracks, at interfaces, and in the out-gases. At low temperature, lattice termination and motion may induce nuclearly mitigated near-surface stresses, leading to the potential for surface isotopic anomalies (Rolison effect). We interpret these anomalies to be the result of stress imbalance and not a direct nuclear isotope reaction. At sufficiently low temperature, if a single crystal is used, outgassing products (primarily  $^4\text{He}$ ) will distribute themselves in the form of a Bragg diffraction pattern. Also, we find<sup>4,10</sup> that fusion rate is proportional to the concentration of final state ion band state  $^4\text{He}^{++}$ , suggesting that the reaction possibly has a "self-triggering" mechanism, possibly consistent with a number of run-away heating episodes that seem to have been observed<sup>1</sup>. We also find<sup>10</sup> that steady-state power density should be proportional to current density.

### ***Conclusion***

There is experimental evidence for cold fusion which is difficult to explain away. The poor repeatability is understandable in view of the nonequilibrium chemistry required for creating  $\text{PdD}_{1+\delta}$  and the problem of cracking due to differential expansion during D loading. There exists a quantum mechanics rationale by which release of fusion energy in a solid can occur without production of energetic particles. This energy release requires the presence of delocalized wavelike  $\text{D}^+$  and involves a volume distributed reaction.

### ***References***

1. M. Fleischmann and S. Pons, Phys Lett. A. Vol. 176, p. 118 (1993); see p. 128.
2. F. Seitz, *The Modern Theory of Solids* (McGraw-Hill, New York, 1940), pp. 227-234.
3. E. A. Hylleraas, Zeit. f. Phys. Vol. 54, p. 347 (1929).
4. T. A. Chubb and S. R. Chubb, Fusion Technology. Vol. 20, p. 93 (1991)
5. P. Roman, *Advanced Quantum Theory*, (Addison-Wesley, Reading, MA 1965), pp.63-90.
6. A. Einstein, B. Podolsky, and N. Rosen, Phys. Rev., Vol. 47, p. 777 (1935).
7. S. R. Chubb And T. A. Chubb, "Lattice Induced Nuclear Chemistry", *AIP Conference Proc.*, Vol. 228, titled *Anomalous Nuclear Effects in Deuterium/Solid Systems*, Eds. S. E. Jones, S. Scaramuzzi, and D. Worledge, p. 691 (1991).

8. M. H. Miles and B. F. Bush in *Frontiers of Cold Fusion*. H. Ikegami, Editor, (Universal Academy Press, Tokyo, 1993), p. 189.
9. E. Yamaguchi and T. Nishioka, in *Frontiers of Cold Fusion*. H. Ikegami, Editor, (Universal Academy Press, Tokyo, 1993), p. 179.
10. S. R Chubb and T. A. Chubb, *Fusion Technology*. Vol. 24, p. 403 (1993).
11. E. Wicke and H. Brodowsky, in *Hydrogen in Metals II*, p. 73, G. Alefeld and J. Volkl, Eds., Springer , Berlin (1978).
12. E. Storms, "Some Characteristics of Heat Production Using the 'Cold Fusion' Effect", *ICCF4 Notebook*, p. C 2.6 (1993).
13. M.C.H. McKubre, Presentation at ICCF4 in Maui, December 1993.
14. M. J. Puska, J., R. M. Nieminen, M. Manninen, B. Chakraborty, S. Holloway, and J. K. Norskov, *Phys. Rev. Lett.*, Vol. 51, p. 1081 ( 1983).
15. C. Astaldi, A. Bianco, S. Modesti, and E. Tosatti, *Phys. Rev. Lett.*, Vol. 68, p. 90, (1992).
16. G. Nelin, "A Neutron Diffraction Study of Palladium Hydride", *Phys. Status Solidi*, Vol. 45, p. 527 (1971).
17. D. A. Papaconstantopoulos, B. M. Klein, J. S. Faulkner, And L. L. Boyer, "Coherent-potential-approximation calculations for  $PdH_x$ ", *Phys. Rev. B* , Vol.18, p. 2784 (1978). A. C. Switendick, "Electronic Energy Bands of Metal Hydrides - Palladium and Nickel Hydride", *Ber. Bunsenges. Phys. Chem.*, Vol. 76, p. 535 (1972).
18. T. Riesterer, J. Osterwalder, And L. Schlapbach, "Inverse photoemission from  $PdH_{0.65}$ ", *Phys. Rev. B*, Vol. 32, p. 8405 (1985). D. E. Eastman, J. K. Cashion, And A. C. Switendick, "Photoemission Studies of Energy Levels in the Palladium-Hydrogen System", *Phys. Rev. Lett.*, Vol. 27, p. 35 (1971).
19. P. C. Hohenberg and W. Kohn, *Phys. Rev. B*, Vol. 138, p.864 (1964). W. Kohn and L. J. Sham, *Phys. Rev. A*, Vol. 140, p. 1133 (1965).
20. S. R Chubb And T. A. Chubb, "Quantum Mechanics of 'Cold' and 'Not-So-Cold' Fusion," *Proc First Annual Cold Fusion Conf*, Salt Lake City, Utah, March 28-31, 1990, p. 119 (1990). S. R. Chubb and T. A. Chubb, "Fusion Within a Solid through Solid State Effects: 'The Grand Identity Crisis,'" *Proc. EPRI-NSF Workshop on Anomalous Effects in Deuterated Metals, Oct, 16, 1989*, (ed. Schneider, Electric Power Research Institute), p. 29-1 (1993).
21. J. T. Waber and M. de Llano, "Cold Fusion as Boson Condensation in a Fermi Sea", in this Proceedings.
22. M. C. H. McKubre, S. Crouch-Baker, A. M. Riley, S. I. Smedley, and F. L. Tanzella in *Frontiers of Cold Fusion* H. Ikegami, Editor, (Universal Academy Press, Tokyo, 1993), p. 5.
23. K. Kunitatsu, N. Hasegawa, A. Kubota, N. Imai, M. Ishikawa, H. Akita, and Y. Tsuchida, in *Frontiers of Cold Fusion..* H. Ikegami, Editor, (Universal Academy Press, Tokyo, 1993), p. 31.

## COLD FUSION AS BOSON CONDENSATION IN A FERMI SEA

James T. Waber  
Physics Department  
Michigan Technological University  
Houghton, MI 49931

Manuel de Llano  
Physics Department  
North Dakota State University  
Fargo, ND 58105

### **Abstract**

Boson condensation and the important selection rule "Bosons in, Bosons out" were presented earlier as a means of predicting the primary products of Cold Fusion and understanding how two deuterons in a crystalline medium might fuse. An important connection with superfluidity and superconductivity was stated, since all three phenomena involve bosons. The Born-Oppenheimer separability of the nucleonic and electronic functions was an essential ingredient of the theory; the reformulation of the wave functions in the Wannier representation is equally important here. The problem is recast as a further modification of a BCS-Bose formulation of superconductivity for high  $T_c$  materials as proposed by Fujita and coworkers.

### **Treatment of Condensed Matter**

There are two different approaches to treating condensed matter and molecular physics. In the first, the "Heitler-London" method of atomic eigenfunctions, one assumes widely separated atoms so that a specific electron belongs to a specific nucleus. The behavior of such an atom differs from that of an isolated atom only inasmuch as it is modified by the local dielectric constant. This is what Chubb and Chubb<sup>1</sup> refer to as the "Free Space Paradigm". Aside from certain inner core energy level problems that can adequately be treated in this manner, a more proper quantitative approach is based on the "Hund-Mulliken"

approximation, namely, of closely spaced nuclei plus a collective treatment of the electrons involved. An electron then is not assumed to be assigned to a single nucleus, since it is acted on by the force field of all the surrounding nuclei and electrons. The mutual interaction between different electrons is treated as a small perturbation. This is represented by the "band model". The transition to the many-electron band model lies not in using an inter-electron interaction but simply in filling the energy levels of the one-electron problem with all the electrons which must be accommodated in the crystal.

In order for the energy of a system of atoms assembled in condensed matter to minimize itself, the corpuscular aspect of the electrons is replaced by their wave aspect with the latter spread throughout the solid. Consequently, (1) the locations of a "particle" cannot be defined, (2) only a small fraction of any one particle can be found within a unit cell of the material, and (3) each nuclear reactions which may occur will do so at all of the periodically equivalent crystalline sites.

The prerequisite boundary condition of the solid state model is that the system is periodic and the energy in the low temperature limit minimizes itself with respect to changes in the electronic structure. Each atom eigenfunction is split into a quasi-continuous band and the splitting becomes greater as the atoms become closer together. From the Bloch theorem, one obtains a band spectrum of broadened states. Using Brillouin's treatment of an electron as a wave, it is understandable that for some special wavelengths and propagation directions, the wave will encounter Bragg reflections. Interference with the lattice leads to reflection of an electron wave of exactly the same energy. But the apparent degeneracy is lifted by the periodic lattice; Bloch demonstrated that the discrete atomic levels are split into allowed bands of energy which arise from the periodicity of the lattice potential. Brillouin's treatment shows that the continuous energy of free-electron waves is further split into groups of forbidden energy bands. The Bloch functions are time-independent.

When the energy of an electron approaches the upper band edge, the condition for Bragg reflection is more nearly fulfilled and the lattice potential reflects more of the incident wave in the form of a reflected wave. When they become equal in magnitude at the band edge, they form a standing wave and no propagation occurs; the velocity of the electron under an accelerating field falls to zero since the electron mass becomes negative (it comes from the Bragg reflection of the lattice.) This is at the heart of what Chubb and Chubb<sup>2</sup> call the "Solid State Paradigm."

In the Free Space Paradigm, particles collide with similar

particles (or collision partners) - i.e., hydrogens with other hydrogen molecules. In contrast, because of their wave nature, electrons move unhindered and uniformly throughout a perfect lattice. In practice, a lattice may not be perfect even at 0° K--- it may contain missing atoms, imperfections or impurities. The electrons are scattered off these disturbances. At non-zero temperatures, there is an additional type of "collision partner." Density changes occur in the lattice and these are treated as acoustic and optical vibrations, called phonons.

Local, inhomogeneous electrostatic fields bind the deuterium atoms into the palladium deuteride lattice and lattice-induced broadening occurs. So, in contrast to the free space situation, the nuclear charge is broadened. Further, many-body interactions give it an effective electrostatic volume which is comparable to the atomic volume since zero-point motion must be included.

The Coulomb interactions between electrons and the ion cores are equal and opposite in sign. To a large extent, they cancel each other out. If we take a specific electron, then it interacts with the system of N ions and N-1 electrons; the system as a whole has a net charge of +e. It is desirable to distinguish between two types of condensed matter (a) amorphous or disordered and (b) crystalline or ordered.

A rephrasing of the statement of Chubb and Chubb<sup>1</sup> is in order: "Just as electrons cease to be point particles when they are injected into a solid; so do particles such as deuterons." Chubb and Chubb also state that "...Just because a deuteron looks like [and acts like] a particle in one situation ..." it need not do so in other situations and ..." just because the energy from nuclear fusion is released entirely in one place ..." in one situation, the release need not be constrained or to be so highly localized in another situation. It can occur, for example, throughout the lattice as in the Mössbauer phenomenon.

Electrons, or similar particles, when treated by the Bloch theorem, are extended over the entire lattice and are in equilibrium. The important point is that the interaction strength of any specific electron or particle is greatly reduced by the screening of the N-1 electrons in the system.

#### Details of the Band Structure Model

In a crystal, there are energy levels  $E_n(\mathbf{k})$  and associated Bloch eigenstates. They are identified by a band index  $n$  and by a wave vector  $\mathbf{k}$  having three Cartesian components. Each such band state has both  $\uparrow$  and  $\downarrow$  spins associated with it, so that each state is at least two-fold degenerate. The Bloch electrons (or particles) obey Fermi-Dirac statistics independent of any interaction between

them.

A denumerable set of Fourier components  $\langle G_i \rangle$  can be determined from the lattice potential and each is labelled by a reciprocal lattice vector  $G_i$ . A further condition is that dot-product  $G_i \cdot R_n$  is equal to  $2\pi \times$  integer where  $R_n$  is a distance to the  $n^{\text{th}}$  atom in the unit cell, i.e., a basis vector of the structure. An arbitrary amount of momentum  $\hbar G_i$  can be given to any particle in the solid (where  $\hbar$  is Plank's constant) but the momentum of a specific particle is not conserved over a long time-scale. That is, the solid as a whole can coherently adsorb an arbitrary amount of momentum without altering the Fourier transforms of  $V_{\text{elect}}$ . The band energies of  $V_{\text{elect}}$  are defined by a continuous set of eigenvalues by the condition

$$E_n(\mathbf{k}) = E_n(\mathbf{k} + \mathbf{G}_n) \quad (1)$$

The energy band is infinitely degenerate at each value of  $\mathbf{k}$ . Bloch's theorem eliminates this huge degeneracy - that is, a single eigenfunction  $\Phi^n$  for the  $n^{\text{th}}$  energy band has the property that

$$\Phi_{\text{Bloch}}^n(\mathbf{k}, \mathbf{r} + \mathbf{R}_n) = \Phi_{\text{Bloch}}^n(\mathbf{k}, \mathbf{r}) \exp(i\mathbf{k} \cdot \mathbf{R}_n). \quad (2)$$

The particle density can then formally be written as

$$n(\mathbf{r}) = \sum_{n,k} |\Phi_{\text{Bloch}}^n(\mathbf{k}, \mathbf{r})|^2 F(E_n(\mathbf{k})) \quad (3)$$

where  $F$  is a statistical weight factor, namely

$$F[E_n(\mathbf{k})] = \left( \frac{[\exp(E_n(\mathbf{k}) - \mu(T)]}{(k_B T)} + A \right)^{-1} \quad (4)$$

Here  $A=+1$  for  $A$  corresponds to Fermi-Dirac statistics, (namely, to the occupation of  $N_F$  Fermions but only two per state - differing by their spin. When  $A=-1$ ,  $F$  corresponds to Bose-Einstein statistics, (occupation of  $N_B$  Bosons, i.e., to many bosons being in the same state).  $A=0$  corresponds to Boltzmann statistics. The chemical potential is  $\mu$  and  $k_B$  is the Boltzmann constant. The Bloch functions are time-independent.

### Born-Oppenheimer Separability

An important ingredient is the Born-Oppenheimer separability of the electronic and nuclear functions. For any deuterium ion located in the lattice at or near an  $s$  site, the nucleon wavefunction  $\psi$  can be written as

$$\psi_{\text{nucleon}}(\mathbf{r} - \mathbf{r}_{cm}) = \psi_{\text{nucleon}}(\mathbf{r} - \mathbf{r}_{cm,s}) \Theta_{\text{elect}}(\mathbf{r}_{cm,s}) \quad (5)$$

where  $\mathbf{r}_{cm,s} = (\mathbf{r}_p + \mathbf{r}_n)/2 - \mathbf{R}_s$  is the center-of-mass of a deuteron located to within a small radius of the center of the zero-point motion in cell  $s$ .

The nuclear behavior is governed by the highly localized, i.e., short ranged nuclear function  $\psi_{\text{nucleon}}$ , and vanishes when the range exceeds a few Fermis. Inasmuch as the internucleon force is charge independent, one could have included the isospin function  $\zeta(t)$  as a factor in  $\psi$ , which distinguishes between the two charge states of the nucleons.

On the other hand,  $\Theta_{\text{elect}}$  is a slowly varying function over a length-scale associated with the electrostatic force between deuterons in nearby cells. The electrostatic potential is periodic, hence each  $\psi$  can be approximated either by the single-particle Bloch state  $\Phi_{\text{Bloch}}(\mathbf{k}_m, \mathbf{r}_n)$  or by its Wannier representation  $\Psi_s(\mathbf{r}_m, T_R)$ . These two forms of wave-function appear to be rigorously valid in the limit in which the energy-scale of the nuclear interaction is very different from the scale associated with the single-particle electrostatic potential or its first order perturbations. Moreover, the nuclear forces associated with the possible interaction between two deuterons (in a boson condensate) within a common cell, are invariant under a rigid translation of all the deuterons.

Without belaboring the point, Chubb and Chubb<sup>3,4,5</sup> have shown that non-separable nuclear-electrostatic interactions are prohibited. Since  $\psi_{\text{nucleon}}$  is a Fermion field while  $\Theta_{\text{elect}}$  is a Boson field, it becomes impossible to construct non-vanishing forms, when these fields are quantized, in which both sets of functions (or their complex conjugates) evolve independently of each other. Consequently the short range nuclear wave-functions are constrained to be independent of the electrostatic wave-function only during an intermediate stage when the nuclear portions are constructed of paired neutron-proton bosonic wave-function  $\psi_{np}$ . Recently Chubb and Chubb<sup>6</sup> have investigated this question further using Poisson Brackets and the condition for separability is even stronger than initially supposed.

The calculation of Switendick<sup>7</sup> *inter alia*<sup>8</sup> of the band structure and of the charge on the hydrogen atom show that the protonic model of PdD with  $(D^+)$  is not more correct than the anionic mode 1 with  $(D^-)$ . That is, when the content of deuterium atoms in the compound approaches  $x = 1$ , principally anti-bonding states are occupied and the H atoms to the first approximation are neutral. The optical phonons bring about an ionization of atoms into deuterons and excited electrons.

### **Wannier Representation**

It is illuminating to cast the wave-function into the Wannier representation  $\Psi_n(\mathbf{r}, \mathbf{R}_n)$  where each state is specific to a given site and is normalized to the volume of the solid. Note that each  $\Psi$  is orthogonal to all the other Wannier functions centered on different sites. The applicable formula is

$$\Phi_{\text{Bloch}}(\mathbf{k}, \mathbf{r}) \exp(-E(\mathbf{k}) t/\hbar) = (1/N_L)^{1/2} \sum_n \Gamma_n(\mathbf{r}, \mathbf{T}_n) \exp(i\mathbf{k} \bullet \mathbf{R}_n) \quad (6)$$

The summation runs over all the  $N_L$  lattice sites. Because each deuteron which occupies a band state is indistinguishable from all others in like states, we can define a new cooperative state which Chubb and Chubb<sup>9</sup> calls a Bose Bloch Condensate or BBC. The periodic order in  $\text{PdD}_x$  leads to the BBC as a means of reducing the localized lattice strain by allowing a small number of deuterium atoms (injected into the solid by electrolytic charging) to occupy empty band states. The Coulomb repulsion between deuterons is uncorrelated (and overlap could occur at a specific site) on a time-scale compatible with a nuclear reaction but too short to be compatible with electrostatic processes. In terms of this particle-wave \*duality, a deuteron could appear particle-like on a short time-scale but wave-like with respect to electrostatic processes.

The present treatment is in terms of both the time-independent Bloch functions which spread throughout the solid and their time-dependent Wannier representations which are localized on individual lattice cells. The selection rule, "**boson in, bosons out!**", is developed and leads to the conclusion that  $^4\text{He}$  will be the primary reaction product, rather than tritium or  $^3\text{He}$  which are fermions.

### **Fermi Surface and Band Structure of Palladium and Its Deuteride**

The theoretical basis for interpreting experimental measurements of the Fermi surface of a material is the collection of  $E_n(\mathbf{k})$  curves. In Figure I, such a collection is plotted versus the wave vector  $\mathbf{k}$ . The Fermi level is determined by summing all of these energy states, taking into account the degeneracy  $p'$  of each  $\mathbf{k}$  states (which can hold  $2p'$  electrons) until the number of conduction electrons per atom is reached. In the present case, the number is 11. In addition, one must keep track of the band index  $n$ . Notice the shaded areas near points  $X$  and  $L$  in the Brillouin Zone. These are unoccupied states at  $0^\circ\text{K}$ . They correspond to pockets in the Fermi surface. The Fermi level corresponds to the chemical potential  $\mu$  of adding an electron to the solid.

COHERENT-POTENTIAL-APPROXIMATION CALCULATIONS

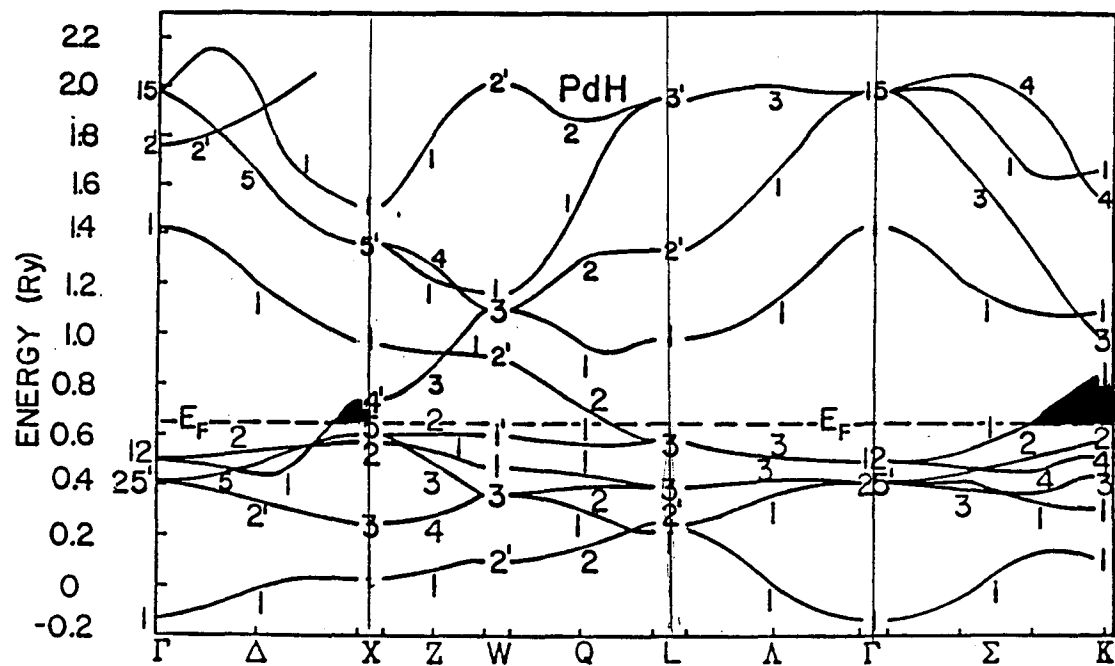


Figure I. A plot of the band structure of palladium hydride, where the individual  $E_n(\mathbf{k})$  values are plotted versus the wave vector  $\mathbf{k}$ . Note that two shaded regions lie above the Fermi Level. The labels on the horizontal axis of the graph refer to high symmetry points in the Brillouin Zone.

The Fermi surface determination of Bakker et al.<sup>10</sup> is based on de Haas-van Alfen measurements for the hydride, the deuteride and the tritide of palladium and one of these is shown as Figure II.

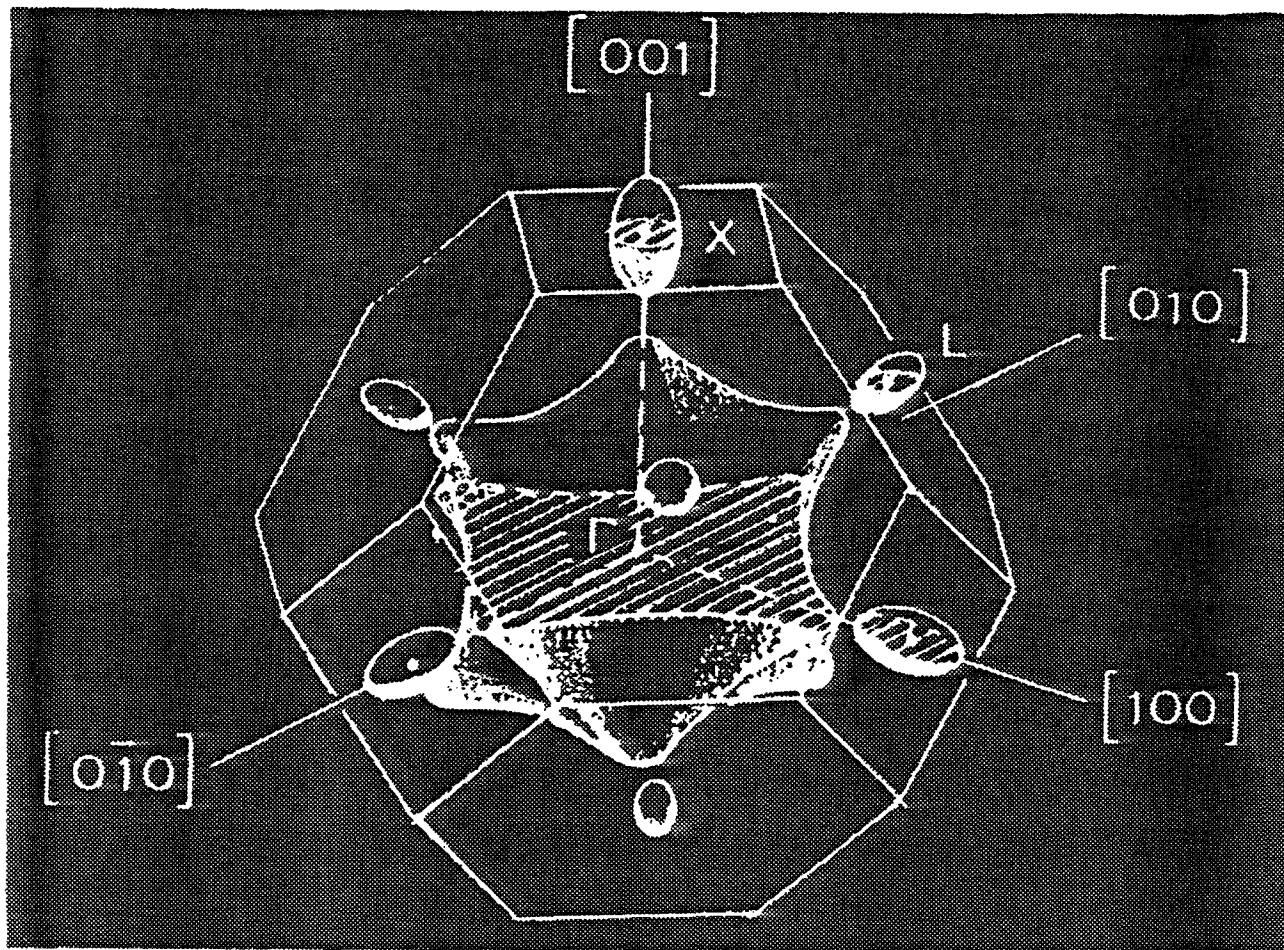


Figure II. Plot of the Fermi Surface of Palladium Hydride determined by Bakker et al. The cross section is on a (100) plane passing through the zero momentum state  $\Gamma_1$ . Note the pockets in the X and L directions. The band index indicates which sheet of the Fermi surface is involved, i.e., on which sheet the unoccupied pocket lies.

The external cross-section (which is what is actually measured) is indicated in this figure by cross hatching.

The effect of adding either of the hydrogen isotopes to palladium is to lower the d-bands associated with the palladium as well as to introduce additional states below  $\Gamma_1$  of the metallic element. The former effect lowers the position of both the  $\Gamma_{25^*}$  and

$\Gamma_{12}$  states relative to the Fermi level. The net effect is to lower  $N(E_F)$ , the density of states at the Fermi level, as seen in Figure III based on the calculation discussed in Reference 8.

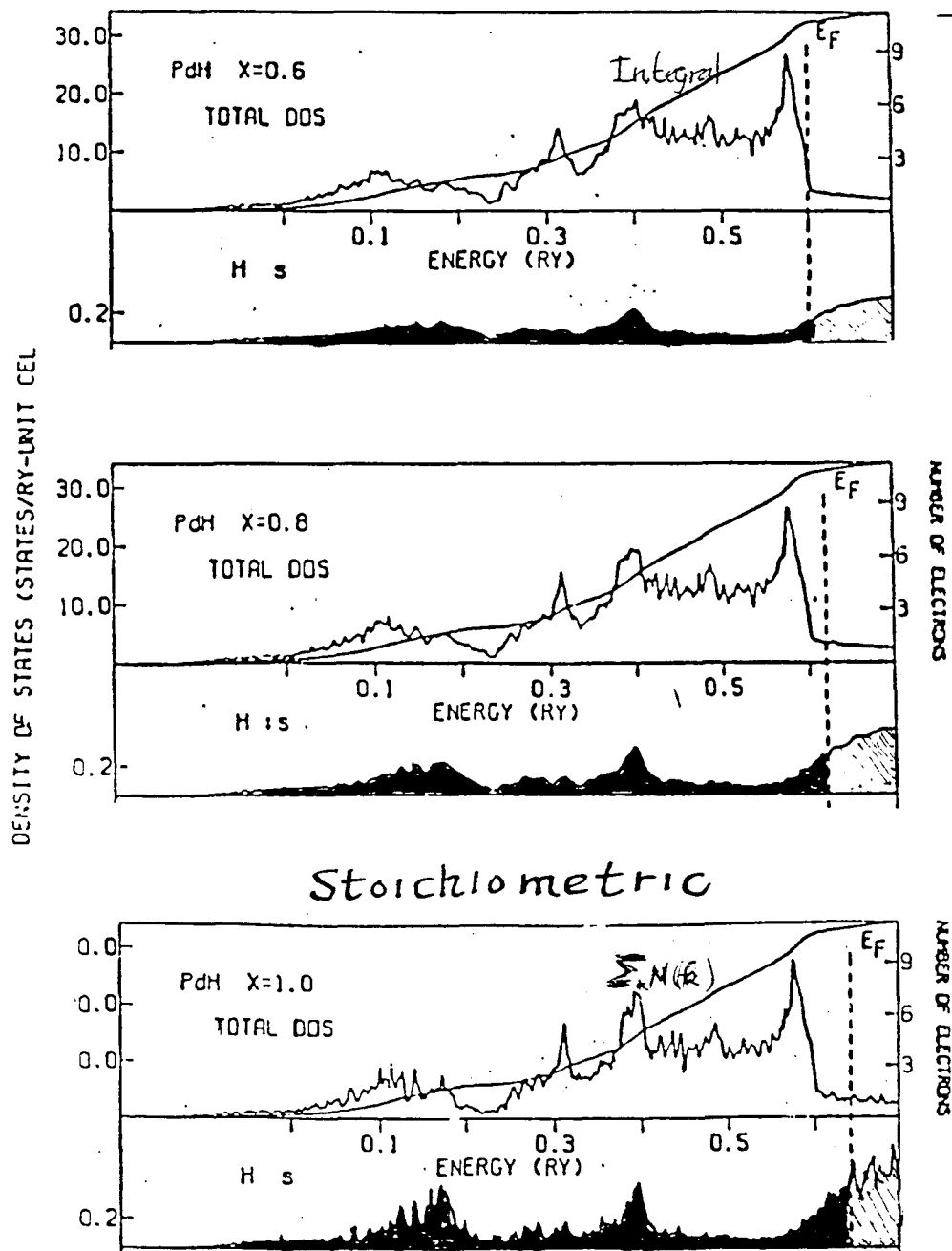


Figure III. Three Plots of the Densities of States of Palladium Hydride for Different Hydrogen Contents, i.e., different  $x$  values. The lower portion of each graph is the Partial Density of States of only the Hydrogen Atoms. Note the shift of the Fermi level  $E_F$  with  $x$ .

Note that on the right hand scale, the number of electron is given as a function of energy. The sum  $\sum_n N(\mathbf{k}_n)$  is shown in each upper panel of the figure as a continuous line.

When more deuterium atoms are introduced into the  $\beta$ -hydride  $PdD_x$ , where  $x$  is approximately 0.67, they occupy octahedral sites - for higher  $x$  values they may occupy tetrahedral sites as suggested by Johnson<sup>11</sup>. Each of these deuterons must have a wave function solution of the Schrödinger equation of a bound particle imbedded in a periodic electrostatic potential.

A further consequence of the lower density of states, is that introducing more deuterium atoms can be "expensive." Because any electrostatic energy must be overcome, only an infinitesimal number of electrons can be added and these go in above the Fermi level in the model of Chubb and Chubb. The "single particle" electrostatic potential is a periodic function of the Bravais lattice vectors  $\mathbf{R}_n$  which define the solid. That is

$$V_{\text{elect}}(\mathbf{r}) = V_{\text{elect}}(\mathbf{r} + \mathbf{R}_n) \quad (7)$$

The net charge of these pairs  $2e(Q_e + Q_d)$  is distributed throughout the crystal and the electrostatic repulsion greatly reduced by rearrangement of the electrons and ions in the bulk crystal. The strain which occurs when two correlated deuterons try to occupy the same site, i.e., compete for a common location, is minimized when the small number of injected deuterons is distributed uniformly over all the unit cells of the lattice. Clearly these solid state energy and physical charge distributions differ radically from the comparable free-space distributions of widely spaced nuclei. It is important to point out here that this wave-function differs from other many-boson eigenfunctions in which the bosons interact weakly with each other, because these deuteron bosons, in contrast, interact weakly with the periodic lattice potential.

The BBC many-body wave function for  $N_b$  deuterons in band states can be written as

$$\Psi[(E_p)] = (1/N_b!)^{1/2} \sum_{(r_m)} \prod_n \Phi_{\text{Bloch}}(\mathbf{k}_m, \mathbf{r}_n) \quad (8)$$

where the summation over  $(\mathbf{r}_m)$  includes the interchange of each coordinate with the remaining  $N_b-1$  coordinates and the product is symmetric as required for bosons. This, in turn, can be substituted back into the expression above for  $\Psi_{\text{Bloch}}(\mathbf{k}, \mathbf{r}) \exp(-E(\mathbf{k})t/\hbar)$ . The resulting sum of products in which the Wannier index  $s$  of a cell

in  $\Phi_s(\mathbf{r}_m, T_R)$  is almost never repeated since  $N_B \ll N_L$ . However, a small fraction of the terms contain products in which the cell designator  $s$  appears twice. These terms contain a product of *cospacial* eigenfunctions centered at the center of unit cell  $s$ . They also involve the zero-point motion of the excited  $D^+$  ions in the 3-D potential well. Those cells labelled with a common index have a double occupancy by deuteron bosons. The mere existence of the overlap in such cells does not, in itself, lead to nuclear interaction. The important point is that the BBC must evolve in a quantum-mechanically controlled manner.

Chubb and Chubb estimate the fractional occupancy of a unit cell by excited  $D^{++}$  to be  $10^{-7}$ . When the initial state is formed exclusively from excited deuterons, all intermediate states prior to energy release must involve an integer number of neutron-proton pairs. This leads to the selection rule<sup>1</sup>, "**bosons in, bosons out!**" which prohibits the formation as primary products<sup>12</sup> of tritons,  ${}^3\text{He}$ , neutrons or protons --- which are all Fermions --- these reaction products are known to occur in the Free Space Paradigm. Reaction paths with n-p pairs have a large overlap with the initial BBC. The normally large electrostatic repulsion between deuterons in free space is substantially reduced when these excited species occupy band states. The Chubb-Chubb theory<sup>13</sup> applies to 0° K.

#### The BCS Theory of Superconductivity

Bogoliubov<sup>14</sup>, working with the Fröhlich electron-phonon Hamiltonian, used his method developed for superfluidity, and independently derived the principal results and formulae of the BCS theory. He showed that the creation of a pair of "virtual" particles from vacuum, without phonons, had some unpleasant or "dangerous" effects. The transition energy of such paired electrons is small in comparison with the phonon energy  $\hbar\nu$ . In the second paper from Bogoliubov's group, there are small terms in the perturbation operator (see eq. 17) of Tolmachev and Tiablikov<sup>15</sup> which describe the creation of four particles from the vacuum. They discuss the dynamics of electrons near the Fermi surface induced by the electron-phonon interaction. The third paper by Bogoliubov<sup>16</sup> deals with diagrammatic methods to obtain the BCS equations.

Waber<sup>17</sup> discussed the connection between superconductivity, superfluidity and cold fusion. He treated deuterons as bosons and

---

<sup>1</sup> See Reference 6. 11-11

indicated the influence of phonons and rotons (which may be appropriate for higher temperatures).

#### ***The BCS-Bose Formulation of Superconductivity***

The connection is that superconductivity involves a sea of bosons which do not interact with the crystalline lattice. If the particle is in a field of phonons, a pair of Bloch particles can interact by exchanging massless phonons and lower their energy. Yukawa<sup>18</sup> pointed out that nucleons, either neutrons or protons, would experience attraction by exchanging pions which are massive bosons. It is a similar process here since band deuterons (spin 1 massive bosons) involve interactions with phonons (massless bosons).

It is postulated here that near the Fermi Level, there is an instability that is induced by the phonons which leads to the formation of two Cooper pairs (i) a Cooper pair of electrons and as well as (ii) the formation of Cooper-like pair<sup>19</sup> of deuterons (in place of the usual electron holes). Each of the D<sup>+</sup> ions has a spin-paired (neutron and proton) in their band states.

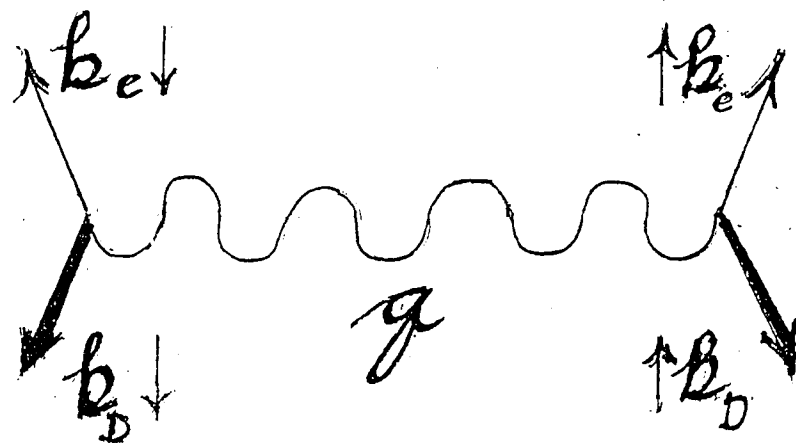


Figure IV. Feynman Diagram showing the Two Cooper and Cooper like Pairs. With momenta  $k_e$  of the paired spins of the electrons and  $k_D$  of the pair of bosonic deuterons. The optical phonon  $q$  is indicated.

If the distance between the centers of mass of either type of Cooper pair is large, the effective Coulomb interaction is modified

by the Debye-Hückel screened potential. The small Coulomb interaction between the deuteron states (reduced by the electrons and ions) further stabilizes the pairs.

One can infer good equations of motion diagonalized in a net momentum  $\mathbf{q}$ . The Cooper pairs, both above and below the condensation temperature  $T_c$ , move independently because the net momentum  $\mathbf{q}$  is a constant of motion. The wave functions  $A_j(\mathbf{k}, \mathbf{q})$  are coupled with respect to  $\mathbf{q}$  - this implies, according to Fujita and Watanabe that the true wave function is a superposition of "electron pair" and "hole (or deuteron, in our case) pair" plane-wave functions. The conditions for the separability of the "superimposed" wave function still applies (*vide supra*).

A compound semiconductor provides a medium in which optical phonons can easily be virtually excited. Further, it is likely to have more than one Fermi sheet so that the effective masses and local curvatures can be different. The hypothesis of supercondensation brought about by the exchange of massive bosons may be checked by the sign of the isotope effect( which is known to be anomalous in  $\text{PdD}_x$ ). The lowest frequency is  $\pi/a$  with a mass dependence of  $M_2^{-1/2}$ .

The Bose-Einstein Condensation temperature  $T_c^{BE}$  can be estimated in the following manner, given that the experimental value of  $T_c^{BE(4\text{He})}$  for helium is about 2.2°K

$$\frac{T_c^{BE(\text{PdD}_x)}}{T_c^{BE(4\text{He})}} = \left( \frac{\rho_{\text{PdD}}}{\rho_{4\text{He}}} \right)^{2/3} \frac{(M_{4\text{He}})}{(M_D)}$$

$$= (10^4 \text{ g/L}) / (0.2 \text{ g/L})^{2/3} \times (2)$$

$$\approx 2,700 \quad (9)$$

so  $T_c$  is approx. 6,000 K. Here  $\rho$  is the density.

Fujita's theory accounts for the coherence distance of the electronic Cooper pair in high  $T_c$  materials being about 10 Å instead of the familiar 10,000 Å for conventional materials. However, the coherence length  $\lambda$  is mass dependent; thus  $\lambda$  is further reduced because of the heavy deuteronic bosons. Since a deuteron weighs more than 3,000 electron masses, the value of  $\lambda$  becomes roughly 30 Fermis.

#### Requirements for Applicability of the FW Model

An important condition for "cold fusion" using this model is that the Fermi Level of occupied states must be in the immediate

vicinity of the Brillouin Zone boundary. That is, one possibility is that the lattice is fully loaded and essentially stoichiometric, i.e.,  $x = 1 \pm \delta$ . Recent experimental evidence by the IMRA group<sup>20</sup> suggests that  $x > 0.8$  is adequate for Cold Fusion. It is interesting that the Density of States at the Fermi level, namely  $N(E_F)$  or chemical potential  $\mu$  falls to a minimum as a function of  $x$  near  $x = 0.85$  as shown in Figure V.

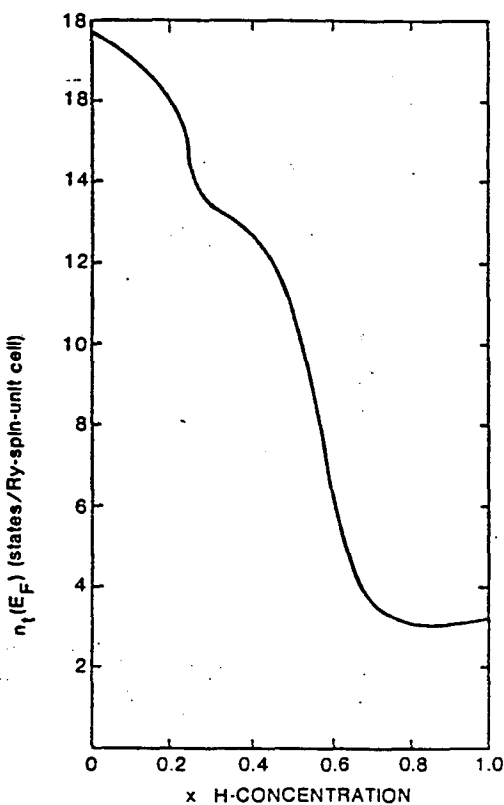


Figure V. Variation of the Chemical Potential  $\mu$  as a Function of the Hydrogen Content. (After Reference 8)

The chemical potential is the partial molar free energy of an electron at the highest occupied electronic level. The implication of this graph is that it costs progressively less energy to add an occupied electronic state at the Fermi level as  $x$ , the number of hydrogen atoms, is incorporated into the lattice until  $x$  becomes approximately 0.85.

Several *ab-initio* band calculations have shown that in such a case bonding occurs via anti-bonding states and these are associated with the hybridization between the s-electrons, provided by the additional deuteriums, and the 4d plus 5s states, provided by the metal.

Fujita<sup>21</sup> and Fujita and Watanabe<sup>22</sup> postulate that the Coulomb interaction generates a correlation among (but not between) the pairs of negative and positive charges. Because of the low density of states of the anti-bonding orbitals, the D atoms are only weakly bound and undergo large zero-point fluctuations.

Fujita and Watanabe<sup>23, 24</sup> point out that a requirement of their theory is that there be one or more pockets in the Fermi Surface where the density of states is high, and secondly that the phonons involved in creating the two pairs be optical, rather than acoustical.

The energies of the excited Cooper pairs form a continuous energy band. Chubb and Chubb call these ionic band states (IBS) and a Boson-Bloch-Condensate BBC can form in excited states above the Fermi Level. In contrast to their assumption, the deuteronic Cooper pair of the present theory has energies below the Fermi Level, but they are still band states.

Fujita and Watanabe (who assume electron holes as the positive charge carrier) postulate that the Coulomb interaction generates a correlation among (but not between) the pairs of negative and positive charge. They modified the BCS theory as stated elsewhere. We have further modified their theory while retaining most of their changes, by replacing the electron holes by deuterons. We will label the electronic pairs with a subscript e and the deuterons by d. The corresponding individual correlation strengths are called  $V_{dd}$ ,  $V_{ee}$ ,  $V_{ed}$  and  $V_{de}$  and in the same vein, we have assumed that

$$V_{dd} = V_{ee} < V_{de} = V_{ed} \quad (10).$$

It should be noted that these interactions which they assumed were between fermions whereas the inequalities just cited mix fermions and bosons. The energy gap constants ( $\Delta_1$ ,  $\Delta_2$ ) for electrons (and deuterons) may be on different Fermi sheets and have different densities of states  $N_d(0)$  and  $N_e(0)$

The presently modified BCS theory has been constructed with pairs of electrons (and deuterons) with opposite spins ( $k\uparrow$ ,  $-k\downarrow$ ), and the two different momenta have been restricted to energies in the narrow range of 0 to  $\hbar\omega_b$ , relative to  $E_F$  or  $\xi$  (the chemical potential) where  $\omega_b$  is the Debye frequency. Fujita and Watanabe lifted the BCS restriction of equal momenta. The two pair are restricted to lie in a thin shell either side of the Fermi level surface. While the energy difference is small, the effect of these pairs is quite large. Fujita and Watanabe point out that permitting unequal interactions and unequal momenta has some important consequences. It is interesting, for example, that Type I, Type II, organic superconductors as well as high  $T_c$  cuprates can be handled by the same theory.

One can infer good equations of motion diagonalized in a net momentum  $q$  involving  $B$  which will be defined in terms of creation and annihilation operators below. The Poisson brackets are

$$[H, B_{kq}^{(e)\dagger}] = (E^{(e)}_{k+q} + E^{(e)}_{-k+q}) B_{kq}^{(e)\dagger} - V_{ee} \sum' B_{k'q}^{(d)\dagger} - V_{ed} \sum' B_{k'q}^{(d)\dagger} \quad (11)$$

and the bracket  $[H, B_{kq}^{(d)}]$  terms are equivalent for the excited deuteron  $D^{++}$ . The creation operator for the excited, non-zero momentum Cooper pair is defined by

$$B_{kq}^{\dagger} \equiv B_{k_1\uparrow, k_2\downarrow}^{\dagger} = C_{k+q\uparrow}^{\dagger} C_{-k+q\downarrow}^{\dagger} \quad (12)$$

Equation (11) shows the Cooper pairs, both above and below the condensation temperature  $T_c$ , move independently because the net momentum  $q$  is a constant of motion. The conditions for the separability of the "superimposed" electron pair and deuteron (bosonic) pair wave functions still applies. It should be noted in passing that Chubb and Chubb are slightly vague about the electrons which are introduced by the ionization of the deuterium atoms and which accompany the formation of deuterons in their BBC. They say they go into the next unoccupied electronic state but do not discuss pairing.

### Phonons

Cho and Leisure<sup>25</sup> observed, in addition to the usual Zener-type of relaxation peak found in both compounds, a strong optical phonon in the "alpha-prime" deuteride ( $x > 0.64$ ) which was not present in the hydride. These frequency dependent peaks are shown in Figure VI.

They interpreted the larger peak, i.e., the lower frequency one as arising from a longitudinal optical phonon propagating in the [110] direction polarized along [001]. Also it was found to be very persistent. The relevant Einstein temperature was 590°K. Thus all the requirements of the FW theory are met.

### Effect of Pions and Other Bosons

The exchange forces between electrons, i.e., the spin information is conveyed by virtual photons. The exchange of acoustical phonons between particles is long range since they are massless bosons and the interaction is appropriate for Type I superconductors where the coherence distance lies in the range of 1000 to 10,000 Å. While acoustical phonons are probably extant for the high  $T_c$ , they cannot account for the smaller value of lambda, namely two unit cell dimensions. Optical phonons on the other hand have the lowest energy and their wavelengths are of the order of lattice spacings. The attraction generated by the exchange of massive bosons is short-range like the nuclear forces between two nucleons discussed by Yukawa<sup>26</sup>. More generally speaking all the possible causes for pair attraction should be examined. The presence and exchange of pions has been overlooked so far. Kenny<sup>27</sup> points out that the attraction caused by the exchange of these spin 0 bosons is seven times that of the nucleonic constituents. He has presented a table of several reaction paths.

The effect of the pion exchange is to stabilize the deuteronic bosons and despite any strong repulsive effect of the deuterons being 50 Fermis apart, the exchange will bring them close enough that they will fuse.

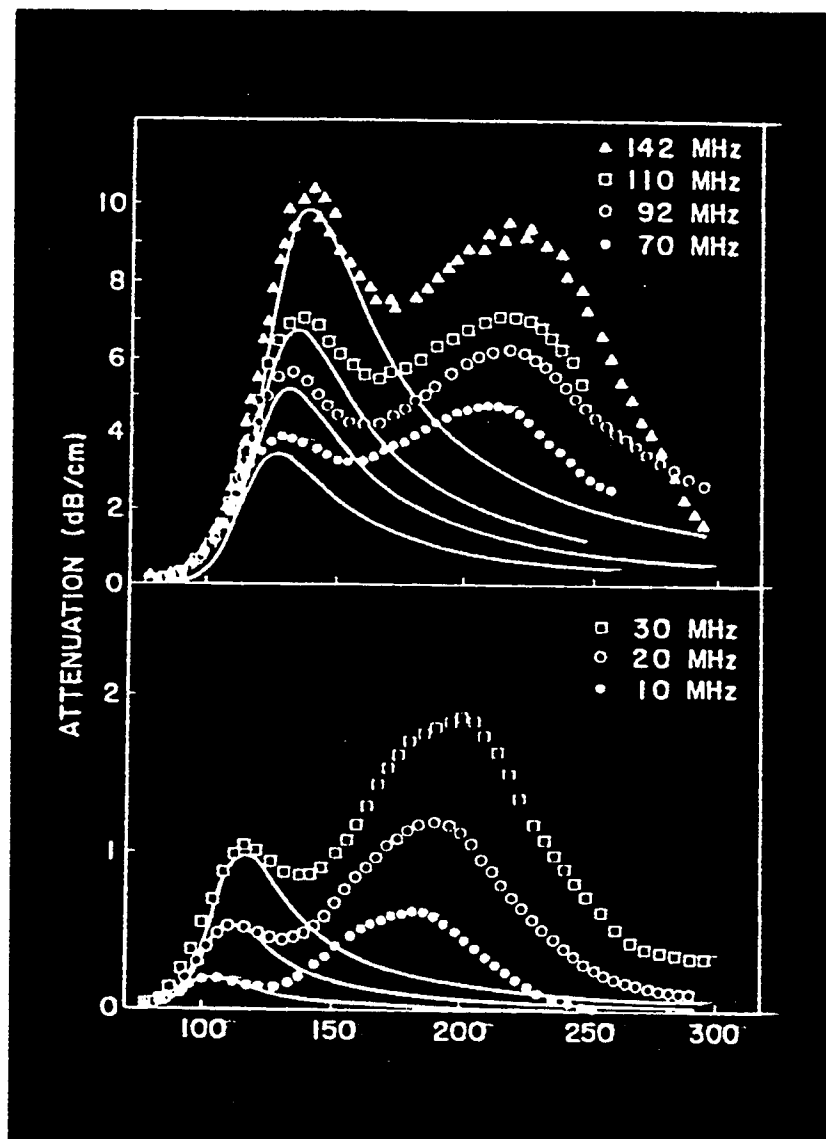


Figure VI. Plot of the Ultrasonic Attenuation as a Function of Frequency Observed in Palladium Deuteride but not in the Hydride. (After Reference 25)

Oppenheimer-Phillips<sup>28</sup> paper indicates that the range of the neutron portion of the deuteron wave-function extends to about 5 Fermis. Rarita and Schwinger<sup>29</sup> discuss the deuteronic wave-functions and the potential well they deduced from scattering

experiments.

## DISCUSSION

We propose that the closely spaced pair of  $D^+$  in ionic band states (with the modification of Chubb and Chubb that they lie below the Fermi Level) become the precursor of  ${}^4He$  ionic band states with the energy release spread over the crystal. So coalescence of the two  $D^+$  bosons becomes quite feasible.

Fujita and Watanabe together with the Chubb and Chubb provide a means of resolving three or more issues raised as objections by many others, namely that (1) the deuterons must behave as particles, (2) they must penetrate a strong Coulomb barrier of the Gamow type, and (3) the length scale associated with nuclear reactions must be of nuclear dimension and (4) the by-products of reaction must be released from the solid since there are no known electrostatic processes capable of "trapping" product particles with energies in the vicinity of tens of MeV, without violating momentum or energy conservation.

## SUMMARY

The solid state nature of cold fusion and the important fact electrons and similar particles are not localized has been largely overlooked in the literature. The connection with superfluidity and superconductivity is also not apparent as long as the deuterium atoms in palladium deuteride are treated as isolated particles in free space. Chubb and Chubb have repeatedly drawn attention to the extended wave nature of the electrons involved in the Bloch state and the Brillouin zone treatment of solids. This explains how the electrons move in virtually a zero potential field, since they are screened by the other N ion cores and N-1 electrons. Further, the correct prediction of  ${}^4He$  as the principal product stems from the selection rule they derived, on the basis of solid state theory, namely *boson in, bosons out*.

The role of bosons as Cooper pairs links cold fusion with superconductivity. Extension of the BCS theory by Fujita and Watanabe have indicated certain requirements for superconductivity. Their theory is further modified herein for cold fusion by allowing the optical phonons to create two kinds of Cooper pairs, namely (a) excited electrons and instead of electron holes, (b) Cooper-like pair of deuteron band states which lie below the Fermi level. Both deuterons in the pair are bosons and their spins ( $\pm 1$ ) are also paired. The coherence length is shown to be of the order of a few Fermis due to the mass dependence and the larger mass of the deuterons. The Bose-Einstein condensation temperature of the bosonic deuterons is estimated to be as high as  $6,000^\circ K$ , so that one is well within the estimated condensate regime. The FW requirement of strong optical phonons in the deuteride is also met as is the requirement of pockets in the Fermi surface. Given these facts, the exchange separation of the two  $D^+$  ions brings them

within the range of attractive nuclear forces, Exchange of virtual pions further increases the likelihood of two deuterons fusing to form  ${}^3\text{He}$  as the "ash."

#### Note added in Proof

Johnson<sup>30</sup> raised the question of whether the Meissner Effect could be observed at temperatures well above room temperature? If it were observed, the present proposal would have powerful support. However, there might not be sufficient of these Cooper-like bosonic pairs to exclude the magnetic field. Chubb and Chubb estimate the concentration of excited deuterons to be only  $10^{-7}$ , whereas there are roughly  $10^{-4}$  conventional Cooper pairs per electron in metallic superconductors. Because of the low concentration of the deuteronic pairs, the skin depth will be large and thus scattering of the electrons will be significant. Thus little evidence of superconductive current or Meissner effect would be anticipated. This does not argue against the pairing of the deuterons.

Two papers at this conference discuss aspects of deuterons being bosons, although they come to negative conclusions. Tsuchiya et al.<sup>31</sup> treat the interaction between two particles as though it occurred in free space. Vaidya<sup>32</sup> does consider screening of the deuterons by conduction electrons and proposes a method of producing additional optical phonons which he says would enhance the fusion rate. However, He bases his overall conclusion on penetration of a Gamow-like barrier. It is the present author's opinion that the enhanced mobility of deuterium can be attributed to a strong interaction with optical phonons not with barrier penetration.

#### Acknowledgements

Research supported in part by the U. S. Army Research Office

#### References

1. Scott R. Chubb and Talbot A. Chubb, *EPRI-NSF Workshop on Anomalous Effects in Deuterated Metals*, Eds. S. E. Jones, F. Scarmuzzi and D. Worledge, Washington D. C., Oct. 16-18, 1989. See also *Proc. Anomalous Nuclear Effects in Deuterium/Solid Systems*, *AIP Conf. Proc.* 228 (Amer. Inst. Phys., New York, 1991) p. 691-710 .
2. Talbot A. Chubb and Scott R. Chubb, "Interaction between Ion Band States," *Fusion Technology*, VOL. 20 p.93 (1991)
3. T. A. Chubb and S. R. Chubb, See Reference 2.
4. Scott Chubb and Talbot Chubb, "Ion Band States Fusion and Fusion Products, Power Density and the Quantum Reality Question," *Fusion Technology*, Vol. 24 p. 2403-2416. See also "Bloch Symmetric Fusion in  $\text{PdD}_x$ " *ibid.* Vol. 17 p. 710-712.

5. Scott Chubb and Talbot Chubb, "An Explanation of Cold Fusion and Cold Fusion By-Products Based on Lattice-Induced Nuclear Chemistry," *Proc. Second Annual Cold Fusion Conference, Sept. 27, 1991 Conference Proceedings Volume 33: Science of Cold Fusion* Eds. T. Bersanni et al. (Italian Phys. Soc., Bologna, 1993) p. 93-99.
6. Scott Chubb and Talbot Chubb, See Reference 4. See particularly "Bloch-Symmetric Fusion in PdD<sub>x</sub>," *Fusion Technology*, Vol. 17 p.710-712 (1990).
7. A. C. Switendick, "Electronic Energy Bands of Metal Hydrides: Palladium and Nickel Hydride," *Ber. Bunsengesellschaft Phys. Chemie*, Vol. 76 p. 535 (1972)
8. D. A. Papaconstantopoulos, B. M. Klein, J. S. Faulkner and L. L. Boyer, "Coherent-potential Approximation Calculations for PdH<sub>x</sub>" *Phys. Rev., B* Vol. 18 p. 2784 (1978)
9. S. R. Chubb and T. A. Chubb, Reference 5.
10. H. L. M. Bakker, R. Feenstra, R. Griessen, L. M. Huisman and W. J. Venema, "Isotope Effects on the Electronic Structure of Palladium Hydride" *Phys. Rev. B*, Vol. 26 p. 5321 (1982).
11. Keith Johnson, "Symmetry Breaking and Hydrogen Energy in PdD<sub>x</sub>" *This Conference Paper T 2.12.*
12. The possibility of tritium etc, as secondary products is not specifically covered at this point.
13. This restriction applies equally to References 1 through 6.
14. N. N. Bogoliubov, "A New Method in the Theory of Superconductivity, I" *Soviet Physics JETP*, Vol. 34 p. 41-46 (1957)
15. V. V. Tomachev and S. V. Tiablikov, "A New Method in the Theory of Superconductivity. II" *Soviet Physics JETP* Vol. 34 p. 46-50 (1958)
16. N. N. Bogoliubov, "A New Method in the Theory of Superconductivity. III" *Soviet Physics JETP* Vol. 34 p. 51-55, (1958)
17. James T. Waber, "Solid State Boson Condensation in Cold Fusion," *Frontiers in Cold Fusion*, Ed. H. Ikegami, Tokyo, World Scientific Press, Sept 1992, pp. 627-630.
18. H. Yukawa, *Proc. Phys. Math. Soc. Japan.* Vol. 17 p. 48 (1935)

19. The distinction is made here that the electron and electron holes in the original Cooper pairs involve fermions, where the deuterons are bosons.
20. See for example, Yumiko Tshuchida, Hidemi Akita, Toshihide Nakata, and Kenji Kunitatsu. "Adsorption of Hydrogen into Palladium Hydrogen Electrode - Effect of Thiourea," *This Conference, Paper M 2.10*.
21. S. Fujita, "Theory of Superconductivity I." *Jour. of Superconductivity, Vol. 4* p. 297 (1991)
22. S. Fujita and S Watanabe, "Theory of Superconductivity II - Excited Cooper Pairs - Why Sodium Remains Normal Down to 0°K" *Jour. of Superconductivity, Vol. 5* p. 83-94 (1992).
23. S. Fujita and S. Watanabe, "Theory of Superconductivity III. 2D Conduction Bands for High  $T_c$ . Bose-Einstein Condensation Transition of the Third Order." *Jour. of Superconductivity, Vol. 5* p.219-237 (1992).
24. S. Fujita and S. Watanabe, "Theory of Superconductivity IV. Relationship between Superconductivity and Band Structures of Electrons and Phonons," *Jour. of Superconductivity Vol. 6* p. 75-79 (1993)
25. Youngsin Cho and R. G. Leisure, "Novel Ultrasonic Attenuation Peak in  $\alpha'$ -  $PdD_x$ ," *Phys. Rev. B38* (8) 1988 pp. 5748-5751.
26. H. Yukawa, See Reference 17.
27. J. P. Kenny, *Fusion Technology, 19* (1991) 547-551
28. Frank Oppenheimer and M Phillips, *Phys. Rev., Vol. 48* p. 500 (1935).
29. Rarita and Schwinger, *Phys. Rev., Vol. 53* p. 436ff (1941).
30. Keith Johnson, *Private Comm.*, Dec. 1993
31. Ken-ichi Tsuchiya, Kazutoshi Ohashi and Mitsuru Fukuchi, "Mechanism of Cold Fusion II," *This Conference Paper T 3.12*
32. S. N. Vaidya, "On Bose-Einstein Condensation of Deuterons in  $PdD_x$ ," *This Conference Paper T 4.5*. A related paper by him is "Coherent Nuclear Reactions in Crystalline Solids," *Paper T 4.3*



# SOME CONSIDERATIONS OF MULTIBODY FUSION IN METAL-DEUTERIDES

Akito Takahashi

Department of Nuclear Engineering, Osaka University  
Yamadaoka 2-1, Suita, Osaka-565, Japan

## Abstract

Some supplementary considerations are given to follow up our previously proposed multibody fusion model in metal-deuterides, for deuteron clustering processes in non-equilibrium conditions and decay channels of virtual compound nuclei of 3D and 4D fusion reactions.

Consequences, namely nuclear products of 4D fusion are  $\alpha$ - particles ( $^4\text{He}$ ) with kinetic energies of 46 keV, 5.75 MeV, 9.95 MeV and 12.8 MeV, possibly associating the electromagnetic transitions of  $^8\text{Be}^*$  nuclear excited energy to lower  $4+$  states and  $0+$  ground state and transferring most of nuclear excited energy directly to lattice vibration. Products of 3D fusion are suggested to be 7.9 MeV  $\alpha$ -particle, 15.9 MeV deuteron, 4.75 MeV triton and 4.75 MeV  $^3\text{He}$ . However, the possibility of direct generation of  $^6\text{Li}$  by 3D fusion is also suggested by considering the electromagnetic transitions of  $^6\text{Li}^*$ .

## 1. Introduction

Anomalous effects observed in cold fusion experiments of metal-deuterides systems since 1989<sup>1,2)</sup> can be summarized as follows; 1) several keV/atom excess power without significant neutron emissions<sup>3,4)</sup>, 2) significant amount of  $^4\text{He}$  generation which might be corresponding to excess power(heat)<sup>5,6)</sup>, 3) very anomalous n/T ratios<sup>1,2)</sup>, namely  $10^{-3}$  to  $10^{-7}$ , 4) emission of high energy charged particles (p,  $\alpha$ , etc.)<sup>2)</sup>, 5) very low level emission of neutrons with high energy (3-10 MeV) component<sup>1,2)</sup>, and so on. Explanations based on the usual d+d fusion, which should result in almost equally branched two decay channels of (n +  $^3\text{He}$ ) and (p + T), can no longer fit to the anomalous results. Namely, experiments tell us that "cold fusion" is not the usual d+d fusion. We have to seek possibilities of "new" nuclear reactions in metal-deuterides. So many theoretical models on unusual reactions have been therefore proposed, without complete successes<sup>1,2)</sup>. The author et al. have also proposed a hypothetical multibody fusion model<sup>7)</sup> and elaborated it to study a competing process of 2D, 3D, 4D, H+2D and H+3D fusions in non-equilibrium deuteron motions<sup>4,8)</sup> and their nuclear products in detail<sup>8)</sup>. Many of anomalous experimental results look supportive to the consequences of the multibody fusion model<sup>4,8)</sup>, although the model itself is not complete and still fully speculative. Difficulties to overcome in modeling the multibody fusion process are<sup>8)</sup>; 1) existence of proper deuteron-clustering process in non-equilibrium conditions of metal deuterides, 2) conditions of transient electron clouds to screen strongly enough the repulsive Coulomb barrier, and 3) multibody strong interactions.

In this paper, the author gives a supplementary discussion to our previous model<sup>8)</sup> on deuteron clustering process and a further detail about the decay channels of virtual compound nuclei, <sup>6</sup>Li\* and <sup>8</sup>Be\*. Especially, somewhat detailed discussions are given on the possibilities of low energy  $\alpha$ -particle emissions via electro-magnetic transitions, by 4D fusion, and direct generation of <sup>6</sup>Li by 3D fusion, since the consequences are testable by cold fusion experiments measuring particle spectra, <sup>4</sup>He generation, n/T ratio, X-ray and  $\gamma$ -ray spectra, isotope shift etc..

## 2. Deuteron-Clustering Process

In our previous work<sup>4,8)</sup>, we proposed a model of transient deuteron clustering at an isolated domain around a tetrahedral deuteron surrounded by 4 octahedral deuterons in PdDx lattice, conceiving a triggering mechanism of non-equilibrium motion by vibrational excitations of deuterons in the lattice. Very rough estimations was made for cluster formation probabilities, using empirical fitting of squared wave function integrals. To estimate the screening effect on Coulomb barrier by transient electron clouds, we borrowed G. Preparata's idea<sup>9)</sup> of "deep hole" at tetrahedral site due to the QED plasma oscillation of 4d shell electrons of Pd. Since these non-equilibrium deuteron motions should be treated in coupled condition with the motions of 4d electrons, the separated treatment of our previous work<sup>8)</sup> might have given a wrong physical picture. We have also a difficulty for "squeezing of many free electrons" toward a tetrahedral position, because of the fermion nature of electrons with large wave length: Likely as super-conduction phenomenon, we may assume a Cooper pair of 1s electrons around a deuteron, but we need more electrons clustering so as to realize the required "super-screening" with anomalously large (more than  $10^{-10}$ ) barrier penetration probability<sup>8)</sup>. We meet a severe constraint of Pauli's exclusion rule to "many free electrons". The problem might be common to that of high temperature super-conductivity, for which a concrete theory is yet to be established. Therefore, the problem of transient deuteron clustering with strong electron screening effect remains yet to be solved. Chances of transient deuteron clustering might also happen around a lattice defect or an irregular lattice point of grain boundary. However, we meet there essentially the same difficulty with our t-site domain model, for expecting the "super-screening" condition.

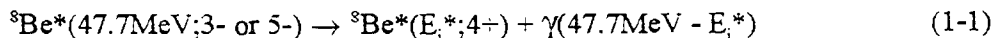
An approach from another angle might be helpful to investigate the transient deuteron (or hydrogen) clustering problem; it is known in the study of negative ion sources that  $D_2^-$  and  $D_3^-$  states can exist, which can realize inter-nuclear distances closer than 0.074 nm of  $D_2$  molecule. Fusion rate of  $D_2$  molecule is estimated to be about  $10^{-64}$  d+d fusion/molecule<sup>10)</sup>; namely the barrier penetration probability is about  $10^{-52}$ . We need a further gain of  $10^{42}$  to meet the super-screening condition. The first approach suggested is to investigate the total system energy, the inter-nuclear distance and the fusion rate for the  $D_2^-$  state which has coupling of three electrons outside two deuteron nuclei; then we proceed to clustering states like  $D_3^-$ ,  $D_3^{2-}$ ,  $D_4^-$ , and so on. If we will be able to find meaningfully large enhancements of barrier penetration probabilities for  $D_2^-$ ,  $D_3^-$  and so on with either stable or meta-stable states, compared with that of  $D_2$  molecule, we can still keep a hope to the multibody fusion model in metal-deuterides. To this respect, a recent experiment by Iwamura et al<sup>11)</sup> is interested since they have claimed to observe significant amount of  $D_2H$  (mass 5) cluster production by mass-spectroscopy analysis of their deuteron desorption experiment from a Pd plate with thin gold film on both surfaces. It can be speculated that the stimulation of deuteron sputtering by rapid desorption from PdDx lattice may generate meta-stable cluster molecules like  $D_2H$  and  $D_3$  to be ionized in the

mass-spectrometer. The deuteron-clustering under deuteron spouting from metal-deuteride, near metal-vacuum (or metal-liquid) boundary, may therefore be another interesting possibility to be investigated by experiments.

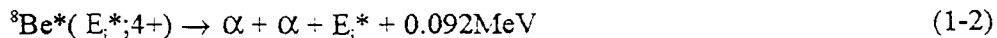
### 3. Nuclear Products

A detailed analysis on possible decay channels for 2D, 3D, H+2D, 4D and H+3D fusion processes is given in our previous study<sup>8)</sup>. Since the identifications of nuclear products with particle-types and their specific kinetic energies, as the consequences of multibody fusions, can be directly tested by beam implantation or gas loading-delocalization experiments, further analyses as detailed as possible are useful. To this end, some considerations are added in the following. As established in nuclear physics study, virtual compound nucleus  ${}^4\text{He}^*(23.8\text{MeV})$  by d+d fusion decays into two major channels of ( $n + {}^3\text{He} + 3.25\text{MeV}$ ) and ( $p + T + 4.02\text{ MeV}$ ) with about 50 % and 50 % weights due to the charge-independence (charge-symmetry) of final state strong interaction. The life time of  ${}^4\text{He}^*(23.8\text{MeV})$  is very short ( $10^{-21}$  to  $10^{-22}$  sec) because of large energy widths ( $\Gamma n \simeq \Gamma p \simeq 0.5\text{MeV}$ ). The probability of electromagnetic transition of  ${}^4\text{He}^*(23.8\text{MeV})$  to  ${}^4\text{He(g.s.)}$  is very small (about  $10^{-5}$  %) because the gamma energy width ( $\Gamma\gamma$ ) is much smaller than  $\Gamma n$ ;  $\Gamma\gamma/\Gamma n = 10^{-7}$ . This property of strong interaction can not be changed, from the viewpoint of nuclear physics, from in-vacuum to in-solids conditions. However, dominant electromagnetic transitions may happen for  ${}^6\text{Li}^*(25.32\text{MeV})$  by 3D fusion and  ${}^8\text{Be}^*(47.7\text{MeV})$  by 4D fusion, as discussed in the following.

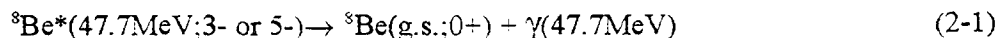
We first discuss the 4D fusion. As studied in our previous work<sup>8)</sup>, the excited state of  ${}^8\text{Be}^*(47.7\text{MeV})$  can be regarded as a P-wave state with higher spin (3- or 5-), although spin-parities of  ${}^8\text{Be}$  for higher levels than about 27 MeV have not been studied well until now in nuclear physics. Due to the spin-parity selection rules, decay channels with emissions of charged particles ( $\alpha$ , p, d, t and  ${}^3\text{He}$ ) and neutrons are forbidden for  ${}^8\text{Be}^*(3- \text{ or } 5-)$ ; while the decay channels by electromagnetic transitions (one phonon  $E_1$  and multi-phonon  $E_1$  transitions) are allowed quantum-mechanically to move to lower excited states with 4+ spin-parity or the 0+ ground state. This is illustrated in Fig.1. Typical decay channels are:



where lower excited energies  $E_i^*$  we know are 25.5MeV, 19.9MeV and 11.4MeV, and corresponding  $\gamma$ -ray energies are respectively 22.2MeV, 27.8MeV and 36.3MeV. Due to the spin-parity selection rules for decay channels of  ${}^8\text{Be}^*(E_i^* ; 4+)$ , bosonic symmetry is required and only  $\alpha$ -decay is allowed:



where kinetic energies of emitted  $\alpha$ -particles ( ${}^4\text{He}$ ) are 12.8MeV, 9.95MeV and 5.75 MeV, respectively corresponding to  $E_i^*$  values (25.5, 19.9 and 11.4 MeV). The multi-phonon  $E_1$  transition (or one phonon  $E_2$  transition) is also possible to transit to the ground state of  ${}^8\text{Be}$ :



It is well known that the  $^8\text{Be}$  ground state decays to two  $\alpha$ -particles with very low kinetic energies (46 keV) and life time of about  $10^{-16}$  sec:



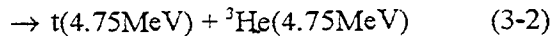
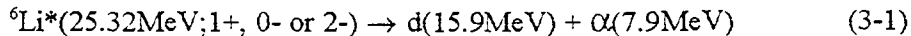
As consequences, nuclear products of 4D fusion are  $\alpha$ -particles ( $^4\text{He}$ ) with isolated peaks in spectrum at 46keV, 5.75MeV, 9.95MeV and 12.8MeV, and high energy  $\gamma$ -rays (22.2, 27.8, 36.3 and 47.7MeV).

However, the latter high energy  $\gamma$ -rays may not be produced due to the following reason. As proposed by Schwinger<sup>12)</sup> and Preparata<sup>9)</sup>, nuclear excited energy can be transferred to lattice vibration via QED photons. Assuming the size of domain for QED plasma oscillation to be 1 nm, QED photons need about  $3 \times 10^{-18}$  sec to carry electromagnetic energy of  $E_1$ , oscillation of  $^8\text{Be}^*(47.7\text{MeV};3\text{- or }5\text{-})$  to deposit to QED electrons in lattice plasma oscillation. Life time of electromagnetic  $E_1$  transition is usually in the order of  $10^{-14}$  to  $10^{-15}$  sec, according to the established nuclear physics. So, we can assume the life time of  $^8\text{Be}^*(47.7\text{MeV};3\text{- or }5\text{-})$  is about  $10^{-15}$  sec, which is much larger than  $3 \times 10^{-18}$  sec of QED photon propagation time. Assuming about 1000 (at least) QED photons carry 47.7MeV (47.7 keV/photon) to electrons in the domain, cross section of photo-electric effect at 47.7keV for PdDx is large enough to absorb all the energy to plasma oscillation. Thus, it is plausible that electromagnetic energies of  $E_1$  transitions (Eqs.(1-1) and (2-1)) are directly transferred to lattice vibration and no high energy  $\gamma$ -rays are emitted. To make this scenario definite, of course we have to investigate quantitatively the transfer rates.

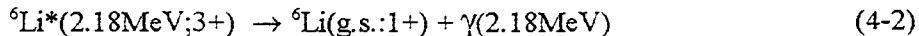
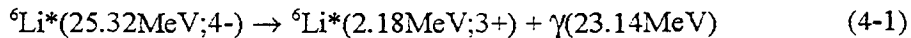
High energy  $\alpha$ -particles (5.75, 9.95 and 12.8 MeV) by 4D fusion should produce bremsstrahlung X-rays and characteristic X-rays (about 20keV for Pd) during their slowing down processes in PdDx and  $\text{D}_2\text{O}$ . As a consequence, we expect strong X-ray radiation from cold fusion cells if 4D fusion takes place. The high energy  $\alpha$ - particles also dissociate deuterons (threshold energy 2.23 MeV) in the system to produce neutrons with continuous spectrum in the 0 to 10 MeV region; the neutron yield of this process is estimated to be in the order of  $10^{-8}$  n/ $\alpha$ . If we suppose 1 watt excess power is generated by 4D fusion (about  $10^{11}$  4d-fusions/w), neutron emission with about  $10^3$  n/sec should be observed.

However, the most extreme scenario is the following. If the electromagnetic transition to the  $^8\text{Be}$  ground state (Eq.(2-1) then Eq.(2-2)) is the predominant decay channel and the QED photons work fully to transfer the nuclear excited energy to lattice vibration, we will have no neutron emission and have only low level X-rays, since 46 keV  $\alpha$ -particles can not induce any nuclear reactions and can produce only soft X-rays which are difficult to be detected because of strong attenuation in solids and electrolyte. This extreme scenario looks matching to the features of Fleischmann-Pons effect<sup>3)</sup> and observations of large level  $^4\text{He}$  generation without detectable neutrons<sup>5,6)</sup>. This scenario of 4D fusion is illustrated in Fig.2, using Feynman-like diagram.

Nuclear products of 3D fusion is speculated in our previous work<sup>8)</sup> as follows, for major decay channels of  $^6\text{Li}^*(25.32\text{MeV})$  with low spin states of either S-wave (1+) or P-wave(0- or 2-):



Somewhat differing from the case of  ${}^8\text{Be}^*(47.7\text{MeV})$ , we have no definite speculation that  ${}^6\text{Li}^*(25.32\text{MeV})$  may have higher spin states, e.g., 4- P-wave state. If we could simply assume that the 4- state is major population in  ${}^6\text{Li}^*(25.32\text{MeV})$ , the following electromagnetic transitions might happen:



This is a typical example and there are other intermediate excited states<sup>8)</sup> of  ${}^6\text{Li}^*$ . Thus, we can not deny the direct transition to  ${}^6\text{Li}(\text{g.s.})$  for 3D fusion and the nuclear excited energy (25.32MeV) transfer to lattice vibration, by the same reason with the case of 4D fusion.

#### 4. Conclusion

Some supplementary considerations are given for the deuteron clustering process in non-equilibrium PdDx lattice and for the plausible nuclear products of 3D and 4D fusions. The status of model for the clustering process is still fully speculative, and further studies for reasonable modeling are needed. Analyses of cluster molecule-states like  $D_2^-$ ,  $D_3^-$ ,  $D_3^{2-}$ ,  $D_4^-$  and so on may help the difficult questions be answered. Validity of multibody fusion model can be tested by cold fusion experiments for observing types and spectra of nuclear products (particles), since consequences of the model predict emissions of specified particles and their monochromatic kinetic energies. 4D fusion predicts the emission of  $\alpha$ -particles with 46 keV, 5.75MeV, 9.95MeV and 12.8MeV. At this stage, we do not know which  $\alpha$ -peak is strongest. The model however predicts the possibility that 46 keV  ${}^4\text{He}$  generation can be predominant, no neutrons are emitted and direct transfer of 47.7MeV nuclear excited energy of  ${}^8\text{Be}^*$  to lattice vibration may take place. 3D fusion predicts emission of 7.9 MeV  $\alpha$ -particles and possible generation of  ${}^6\text{Li}$ .

#### References

- 1) Proceedings of the 2nd Annual Conference on Cold Fusion, Como Italy (June 1991), Conf.33, "The Science of Cold Fusion", Italian Physical Soc., (1992)
- 2) Proceedings of the 3rd International Conference on Cold Fusion, Nagoya Japan (October 1992), "The Frontiers of Cold Fusion", Universal Academy Press (1993)
- 3) M. Fleischmann and S. Pons, "Electrically Induced Nuclear Fusion of Deuterium", J. Electroanal. Chem., 261, p.301 (1989)
- 4) A. Takahashi, T. Iida, T. Takeuchi and A. Mega, "Excess Heat and Nuclear Products by  $D_2\text{O}/\text{Pd}$  Electrolysis and Multibody Fusion", J. Appl. Electromag. Mat., 3, p.221 (1992)
- 5) M. Miles, B. Bush, G. Ostrom and J. Lagowski, "Heat and Helium Production in Cold Fusion Experiments", Ref.1, p.363 (1992)
- 6) E. Yamaguchi and T. Nishioka, "Direct Evidence for Nuclear Fusion Reactions in Deuterated Palladium", Ref.2, p.179 (1993)
- 7) A. Takahashi, T. Iida, F. Maekawa, H. Sugimoto and S. Yoshida, "Windows of Cold

- Nuclear Fusion and Pulsed Electrolysis Experiments", Fusion Tech., 19, p.380 (1991)
- 8) A. Takahashi, T. Iida, H. Miyamaru and M. Fukuhara, "Multibody Fusion Model to Explain Experimental Results", Proc. Russian Conf. Cold Fusion, Abrau-Durso Russia (September 1993), to be published; also submitted to Fusion Technology
  - 9) G. Preparata, "Cold Fusion: What Do the Laws of Nature Allow and Forbid", Ref.1, p.453 (1992)
  - 10) S. E. Koonin and M. Nauenberg, Nature, 339, p.690 (1989)
  - 11) Y. Iwamura, T. Itoh and I. Toyota, "Observation of Anomalous Nuclear Effects in D2-Pd System", Proc. 4th Int. Conf. Cold Fusion, Maui USA (December 1993), to be publ.
  - 12) J. Schwinger, Proceedings of the 1st Annual Conference on Cold Fusion, Salt Lake City USA (March 1990), p.130 (1990)

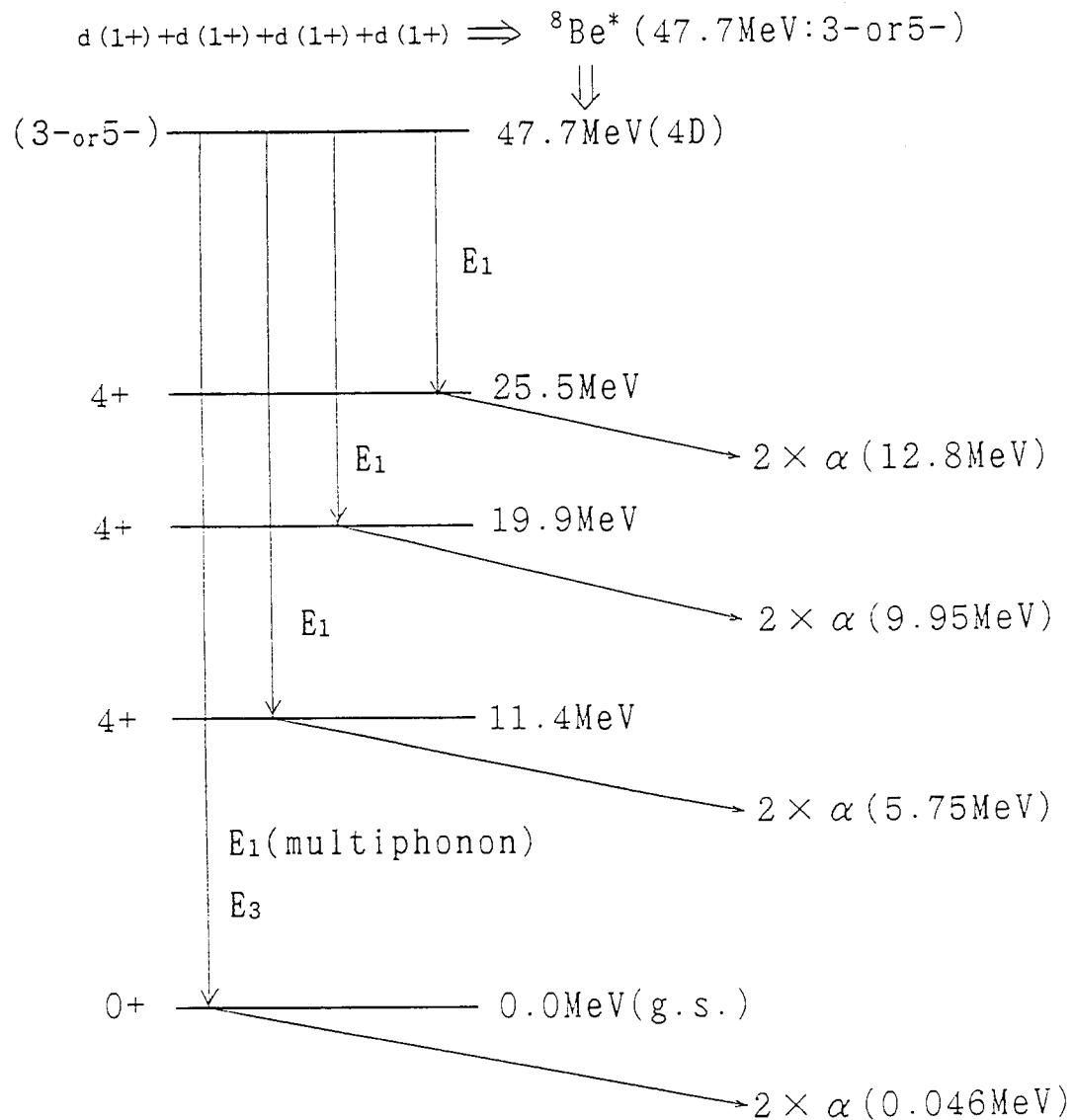


Fig.1: Typical decay channels of 4D fusion;  $E_1$  transition may be induced with electromagnetic energy transfer via QED photons to lattice plasma oscillation. Major nuclear products are  ${}^4He$  with specified kinetic energies.

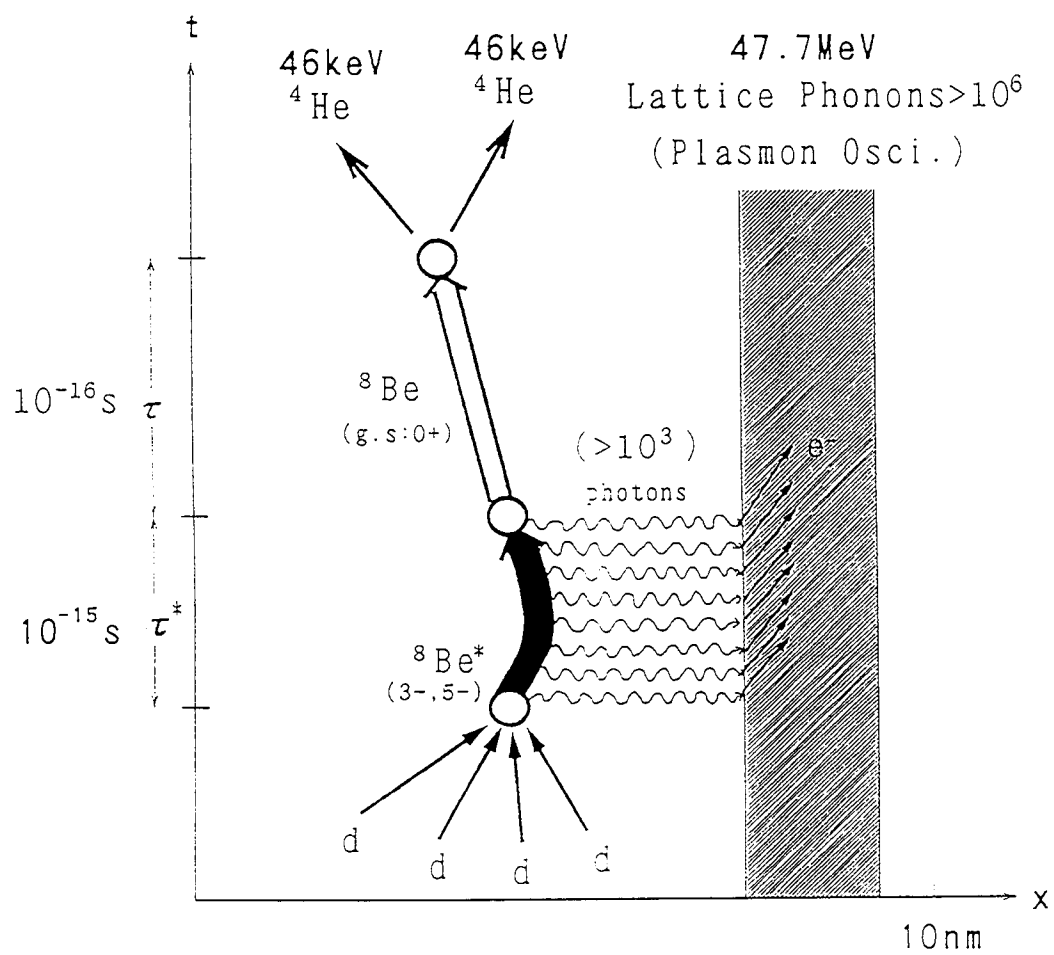


Fig.2: Illustration of extreme scenario of decay channel for 4D fusion;  
final nuclear products are 46 keV  $\alpha$ -particles and most energy  
( $47.7 \text{ MeV}$ ) is transferred to lattice vibration via QED photons.

# COLD FUSION AND NEW PHYSICS (1)

J. F. Yang  
X. M. Chen  
L. J. Tang  
Hunan Normal University  
Changsha, 410006  
Hunan Province, China

## Abstract

This paper point out the cold fusion has revealed new physics process and approach the condition of producible this process and exciting enexgy.

## Introduction

The experimental condition of the cold fusion includes external condition and internal condition. The internal condition has relation to the character of the electrode absorbs deuton and its absorptance. it is inevitable that the experimental failure if the internal condition has no repeat, we can not mistakenly look on it as a nagative result<sup>1</sup>.

Some problems be revealed by cold fusion, which are frontiers problems of science and revealed new physics. The cold fusion is a new fusion, its fusion mechanism is different from traditional deuter-deuteron fusion<sup>1</sup>. It is meaningless if we understand and appraise it by traditional idea.

Based on the fact that there is weak interaction in nuclear force<sup>2</sup>, a deuton can be excited by gathering energy effects in absorbing deuton process, and a dineutron can be produced by a excited deuton to capture an electron in including deuterium-solid. we discuss the mass of a dineutron and requisite energy for the exciting deuton in this paper.

## New Phenomena Revealed New Nuclear Process

The traditional fusion idea is the nucleus-nucleus fusion, for example, deuton-deuton fusion or deuton-triton nuclear fusion, this fusion has an obstacle of Coulomb potential hill.

Tradition fusion method requires high temperature (e. g.  $T \sim 10^8$  K heat nuclear fusion by name) or high voltage (e. g.  $V \geq 10^5$  V, under the name of accelerated nuclear fusion ) to increases nuclear kinetic energy. under ordinary temperature and low voltage conditions(e. g. cold fusion condition), the nuclear fusion of a biggish probability is impossible.

However, cold fusion has been occurring in many laboratory (what is called "abnormal" nuclear pheomena because it can not explained by traditional nuclear theory ), lately, the experimental results of several laboratories of China show: the reappearing ratio of the new nuclear phenomena can reach 100%, the neutron yield is above  $10^4$ /s, and produced X and  $\gamma$  raies, which can repeat at any once by the experimental method of full deuterium-glow discharge except the electrode loses efficency<sup>3</sup>. In addition, the "excess heat" experiment of Fleischmann and Pons obtained progress too<sup>4</sup>.

- There is a new fusion under ordinary temperature condition, it is possible if the fusion occurs between a neutral particle and a nucleus, which requires a new physics process to produces the new neutral particle, namely requires a nuclear process to remove the Coulomb potential hill before the fusion.

## Nuclear Process before Cold Fusion

After deeply analyse cold fusion experiment and 4 kinds interaction in natural world, we think that the way of producing neutral particle may be weak interaction process. For example, an excited deuton ( ${}^2_1H^*$ ) to capture an electron (e), which can produce a neutral particle  ${}^3_2N$  at the smae time. The process is



where  ${}^3_2N$  is dineutron,  ${}^3_2N^*$  is excited state of  ${}^3_2N$ ,  $\nu_e$  is e-neutrino and  $\gamma$  is light-quzntum. There is no obstacle of Coulomb potential hill when a dineutron reacts with a nucleus, this fusion reaction can produce at any temperature.

The process of producing dineutron is weak interaction process, and the basis is weak interaction force field. Jie Fu Yang finds 2050 samples that exist weak interaction process from he investigated 2319 nuclides<sup>1</sup>, these facts clearly show that weak interaction has universality in nucleis, and that, there is a part weak interaction force in nuclear force<sup>2</sup>.

There is nuclear force between the proton and neutron in a deuton, it contains weak interaction force too, a deuton has the force field to capture an electron and itself becomes a dineutron (Notice: there is non-nuclear force between a proton and an electron, they have no weak interaction force too, so that, a solitary proton can not capture an electron to become a neutron).

A stable nucleus can not become spontaneously a other nucleus, but various changes may occur when a nucleus be excited. For example, it can produce the change as equation (1) if a deuton be excited. An excited denton to capture an electron, which must satisfies condition as following:

$$\Delta E = [M(^2_1H^+) + m_e - M(^2_0N)]C^2 - E_v - Er + We \geq 0 \quad (2)$$

$$M(^2_1H^+) + m_e > M(^2_0N^+), \quad (3)$$

where  $M(^2_1H^+)$ ,  $m_e$ ,  $M(^2_0N^+)$  is respectively the mass of excited deuton, electron and dineutron.

### Estimation of Dineutron Mass and Deuton-exciting Energy

If we look on a triton as a constitution from a deuton and a neutron, the binding energy is

$$[M(^2_1H) + m_n - M(^3_1H)]C^2 = \Delta m_1 C^2 \quad (4).$$

We, too, can look on a triton as a constitution of a dineutron and a proton. Similarly,

$$[M(^2_0N) + m_p - M(^3_1H)]C^2 = \Delta m_2 C^2 \quad (5)$$

We replace  $M(^2_1H)$ ,  $m_n$ ,  $M(^3_1H)$  and  $m_p$  by their mass respectively in equations (4) and (5), then

$$M(^2_0N) = 2.0149u. \quad \text{when } \Delta m_1 = \Delta m_2 \quad (6)_1$$

$$M(^2_0N) \leq 2.0149u. \quad \text{when } \Delta m_1 \geq \Delta m_2 \quad (6)_2$$

There is reaction  $^2H + ^2N \rightarrow ^3H + n + Q$  in dineutron model<sup>5</sup>, the reaction energy

$$Q = (M(^2_1H) + M(^2_0N) - M(^3_1H) - m_n)C^2 > 0 \quad (7)$$

$$\therefore M(^2_0N) > M(^3_1H) + m_n - M(^2_1H) = 2.010613u. \quad (8)$$

The dineutron mass can be determined by measurement of fusion neutron spectrum. For example

$$\begin{aligned}
 M(^2_0N) &= 2.01348u. & \text{when } En = 2.0\text{MeV}, \\
 M(^2_0N) &= 2.01414u. & \text{when } En = 2.5\text{MeV}, \\
 M(^2_0N) &= 2.0149u. & \text{when } En = 3.0\text{MeV}, \\
 \therefore En < 3\text{ MeV}^3 & \quad \therefore M(^2_0N) < 2.0149u.
 \end{aligned} \tag{9}$$

From equations (8) and (10), we obtain the mass range of a dineutron as following

$$2.01063u. < M(^2_0N) < 2.049u. \tag{11}$$

The energy-change of a deuton from ground state to excited state, which can write out from mass-energy relation

$$\Delta E' = [M(^2_1H^+) - M(^2_1H)]C^2. \tag{12}$$

In equation (2), there is

$$\begin{aligned}
 M(^2_1H^+) &\simeq M(^2_0N) - m_e + m_\gamma + m_\nu, \text{ when } \Delta E = 0, \\
 \therefore \Delta E' &\simeq [M(^2_0N) - m_e - M(^2_1H)]C^2 + E_\gamma + E_\nu.
 \end{aligned} \tag{13}$$

Because the rest energy of an electron is  $m_e C^2 = 0.51\text{MeV}$ , and the energy of a neutrino is equal to kinetic energy of the recoiling  $^2_0N^+$ , if  $E_\nu = 0.0276\text{ MeV}^3$  and neglect  $E_\nu$ , we can estimate the energy range

$$\Delta E' \simeq M(^2_0N)C^2 - 2.01462u. \leqslant 0.26\text{ MeV} \tag{14}$$

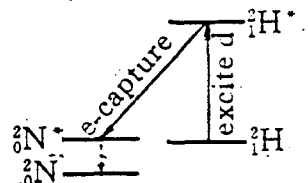
and the mass of excited state:

$$M(^2_0N^+) \leqslant 2.01493u. \tag{15}$$

$$M(^2_1H^+) \leqslant 2.01438u. \tag{16}$$

the excitative and capturing process as following figure.

if the neutrion energy  $E_\nu$   
or the neutron energy  $E_n$   
can be measured by  
experiment, the  $M(^2_0N)$   
can be determined.



## Reference

1. J. F. Yang et al. "Abnormal" Nuclear Phenomena and weak Interaction Process. ICCF3, (1992) «Frontiers of Cold Fusion», Universal Acadeny Press (1993) Japan: «Fusion Technology» March, (1994) (to be publication)
2. For example, V. M. Lobashov et al. Phys. Lett. 25B, Aug. 7, (1967). Yu. G. Abov et al. Phys. Lett. 27B May 27(1968).
3. «Ordinary Temperature Meeting »conference, june 1–3, (1993) Peking, China.
4. Fleischmann—Pons:phys. Lett. A 176(1993), 188–129.
5. J. F. Yang et al. Dineutron Model of the Cold Fusion. ICCF3(1992), «Frontiers of Cold Fusion», Japan Press(1993).

## **SONOLUMINESCENCE, COLD FUSION, AND BLUE WATER LASERS**

Thomas V. Prevenslik  
Consultant  
Tokyo, Japan

### **Abstract**

The blue light observed in sonoluminescence experiments with water is explained by Rayleigh scattered ambient UV light reflected in a blue Raman line of water. The ambient UV light incident on the spherical liquid geometry is concentrated to a high intensity and reflected in a Raman line that appears to the observer as blue light. Since Raman emission in water is highly polarized, tests to determine the polarization of the blue light are recommended. If the intensity of the blue light is significantly diminished by the use of a polarizer, then not only is the explanation of blue light given here correct, but also because the ambient UV light intensity is very low, the spherical liquid geometry may be a spherical UV lens of significant concentration. By modifying the sonoluminescence test to include an external spherical UV laser cavity driver congruent to the spherical liquid lens, the concept of a blue water laser is developed where the UV laser driver is pulsed with the acoustic field to fuse the hydrogen in water molecules in the presence of an oxygen catalyst. Potential applications of the blue water laser are industrial hydrogen and deuterium gas generators, and a low temperature, < 50 C, heavy water heater for residential heating.

### **Introduction**

Sonoluminescence (SL) is described [1] as a non-equilibrium phenomenon in which the energy in a sound wave becomes highly concentrated so as to generate synchronous repetitive flashes of blue light in liquid water at room temperature. Measurements of each flash indicate a power of 1 mW and a duration less than 100 ps. With regard to cold fusion, SL as a significant mechanism of energy focusing in combination with a heavy D-O-D water target [2] is important because it would offer the prospect of a mechanism of fusing deuterium at room temperature.

In the standard model [3] for SL, bubble collapse energy is delivered to a number of molecules and the molecules are excited to emit blue light upon recombination. However, it is possible that the blue light observed in SL is nothing more than Rayleigh scattered light reflected in the blue Raman line of water. The Raman effect is the phenomenon of light scattering from the material medium whereby the light undergoes a frequency change in contrast to Rayleigh scattering where a frequency change does not

occur. The reflected blue Raman line from incident mercury light is observed in spectrofluorimetry [4] of water, but only at low intensity, and an even lower blue line intensity might be expected if spectrofluorimetry is made on water with ambient UV light. Hence, the geometric concentration of ambient UV light by the spherical geometry may be significant in SL. The SL explanation given here is that the low intensity ambient UV light scattered inside the spherical water geometry is concentrated at the center and after reflection in a visible blue Raman line of water is of a sufficient intensity to be visible by the observer as blue light. This SL explanation is referred hereinafter as the Light Scattering (LS) model. In contrast, the standard SL model contends the blue light is generated in the water. Since the ambient UV light is not visible, the appearance of blue light alone may have led the observers [1] to conclude that the blue light was being emitted from the water consistent with the standard SL model when, in fact, the blue light is reflected ambient UV light.

Since the visual observation [1] of blue light does not quantify the wavelength, the blue wavelength is taken to be 470 nm for the purposes of this paper. In the standard SL model, light absorption for hydrogen takes place on the order of 10 ns. However, both Rayleigh and Raman scattering do not involve light absorption and for Raman scattered blue light at 470 nm, takes place in a much smaller time, or within the period of vibration, < 1 fs. The LS model is consistent with but much faster than the < 100 ps duration reported [1], and may explain why the blue flashes cannot be resolved by the fastest photomultiplier tubes available.

SL experimental data for Rayleigh scattered UV light reflected in the Raman lines of water is not available. However, data [4] for solvents at various frequencies of exciting mercury light shows wavenumber shifts of about 0.3 / micron for all solvents containing hydrogen atoms. The Raman lines are caused by totally symmetric molecular C-H and O-H vibrations of the solvent. The data for water shows that for blue light to be emitted in a Raman line at 470 nm, the Rayleigh scattered incident UV line is required to be about 405 nm. Hence, the observed blue light at 470 nm during SL in water in the LS model is actually a Raman line corresponding to UV light at 405 nm and a wave number shift of 0.34 / micron.

In addition to reflected blue light, the ambient UV light is also reflected in UV Raman lines to produce a spectrum of reflected Raman light. Since the energy of the UV photon is greater than blue photon, the average wavelength of the reflected light is less than the 470 nm wavelength of the blue photon. Photon energy measurements [1] give a frequency of 8.0e14 Hz that corresponds to an average wavelength of 375 nm which is less than the blue wavelength of 470 nm and consistent with the LS model. This wavelength decrease may be due to a prominent Raman line at 350 nm in water [4] that is excited by a 313 nm UV line.

In the LS model of SL, the ambient UV light is focused at the center of the spherical water geometry and reflected in the Raman line of water. However, the molecular structure or how it is formed and cooperates with or scatters the UV light during SL compression or expansion is not described in the LS model. During SL expansion, the molecular order is lost because the intermolecular spacing exceeds the range of electrostatic interaction, and therefore the cooperative liquid crystal structure can only be formed in the compression phase where the order of the molecular structure is constrained to the geometry of the spherical compression field. Since the direction of the incident UV light in the spherical geometry is radial, a molecular structure comprising strings of radially disposed water molecules is indicated as the Raman scattering centers.

Currently, the reflection of color from liquids is known to most commonly occur in the liquid crystal state and specifically the chiral liquid nematic phase where the order is a twisted helical rotation. In terms of molecular order, the liquid crystal as a state of matter between the solid and the liquid state together with the molecular order in the chiral nematic state are illustrated in Figure 1. With regard to water, this means for a cooperative structure to be formed in SL, the molecules are generally, in the manner of a helix, rotated sequentially along the radially disposed strings and periodically repeat at a pitch equal to the wavelength of blue light in water. However, the hypothesized chiral liquid nematic phase, or the hypothesized blue phase for water, formed in the compression wave during SL is not known to exist at present. A brief review is presented of known chiral nematic liquid crystalline blue phases of other liquids.

Chiral or twisted helical molecular structures are known to produce blue phases in cholesteric systems [5,6] when the pitch of the helix is less than about 500 nm. The first observation of a blue phase [7] was made over 100 years ago. Upon cooling the liquid phase of cholesteryl benzoate, an appearance of a violet and blue phenomenon was observed which quickly disappeared. Currently, the molecular models [5] of the cholesteric blue phase focus on factors that affect the pitch of the helix between the nematic or liquid crystal and the isotropic liquid phase. Density or pressure and temperature changes are the common parameters affecting the helical pitch. In any event, to assess whether a liquid crystal phase change has occurred, the order parameter,  $S$ , is used and is defined in terms of the average taken over all molecules in terms of the angle,  $\theta$ , between the molecular pointing axis and the director.

$$S = \langle 3\cos^2\theta - 1 \rangle / 2$$

In the isotropic or disordered state, the order parameter is zero while in the ordered state the order parameter is unity as illustrated in Figure 1.

In cholesterogens, C-H atoms are linked to each other by chemical bonds to form a carbon based chain-like helical configuration. However, water molecules are separately distinct, and although dimer and trimer water chains of H-O-H and D-O-D clusters are well known, it is not known whether an oxygen based chain-like helical configuration of water molecules can be formed.

Water is a polar molecule with a high dipole moment and responds to incident light as an oscillating dipole. If the incident light is visualized by a electric vector, E, oscillating at a frequency, f, in water of a polarizability,  $\alpha$ , the dipole moment, P, induced is,

$$P = \alpha E \sin(2\pi ft)$$

Without SL, in a isotropic and disordered water medium without a liquid crystal phase, the water molecules function as randomly distributed scattering centers. Excitation of the molecules by UV light with a transverse electric vector, E, and frequency, f, causes the molecular dipoles to emit Rayleigh scattered light at the same frequency, f. The relation of the incident UV light to the spherical SL water geometry is illustrated in Figure 2. If the water molecules and material medium are rigid, the only scattering produced would be Rayleigh scattering. However, because of the molecular O-H bond vibration of individual molecules at a frequency,  $f_0$ , the molecular dipole is modulated and a blue Raman line at frequency ( $f-f_0$ ) is also scattered.

With SL and during the compression wave, the water molecules as scattering centers are ordered into radially disposed strings, but water molecules along a string are disordered in rotation. For incident UV light with a transverse polarization of frequency, f, directed in the radial direction, the electric vector, E, is orthogonal to the direction of light. However, for incident UV light with a circularly polarized content, the electric vector, E, rotates in a right or left handed manner about the direction of the light. Depending on the local constraint of adjacent molecules, the molecules rotate under the action of the dipole moment, P, tending to align the molecular dipole moment vector with the direction of the incident UV light. If the incident UV light is transversely polarized, the molecules are aligned in a nematic crystal state. If the incident UV light is circularly polarized, the molecules are aligned in a chiral nematic crystal state, or helical structure. In any event, the UV light at frequency, f, is Rayleigh scattered at the same frequency, f, and for OH vibration at frequency,  $f_0$ , a Raman line at frequency ( $f-f_0$ ) is also scattered.

In a SL compression field, the radially disposed and rotational order of the water molecules may be increased by the alignment of the dipoles in the direction of the incident UV light electric vector, E. However, alignment can only occur if the dipole orientation response time is less than the period of UV light. In water at 20 C, the response time for dipole orientation is about

10 ps, but is greater than the < 1 fs period of UV light. Hence, an increased order of the molecules does not occur. Instead, the molecular dipoles respond to the UV light only by small oscillations at frequency,  $f$ , about the angular position acquired in the compression field. There is simply not enough time for any large reorientation of the molecules to occur. At 20 C, the dielectric constant for water is large only up to about 1.e10 Hz and falls rapidly to the value for a nonpolar liquid at about 1.e11 Hz. This means any significant dipole reorientation in water can only occur for electromagnetic frequencies less than about 1.e10 Hz. Possibly the electric field of the acoustic driver at 20 kHz, itself, may be the source of increased molecular order in water during SL. Further, the rapidly fluctuating electric field of the acoustic driver may also be the source of the UV radiation, referred herein as ambient UV light. The proposed research here is to determine the optimum SL excitation carrier wave < 1.e10 Hz for the UV light, instead of the 10-20 kHz acoustic sonic carrier wave commonly used in SL.

If the water medium in SL is in a chiral nematic crystal state, most of the incident UV light will be transmitted except for the one wavelength equal to the pitch. However, whether the helical structure in the chiral nematic is right or left handed is important. If the blue light reflected is either right or left circularly polarized, the same handedness may be deduced for the pitch of the liquid crystal. This means either right or left circularly polarized UV light will penetrate to the center while the light of the other chirality is reflected back to the observer as blue light. Since the velocity of light in water is reduced by the index of refraction, the pitch in the liquid crystal is smaller than the wavelength of blue light in a vacuum. If the observer sees blue light at 470 nm and if the index of refraction of water is 1.33, then the pitch in the liquid crystalline state is about 353 nm. Hence, the UV wavelength selectively reflected from the ambient is also about 353 nm, but is less than the 405 nm UV wavelength required to produce a prominent blue Raman line at 470 nm. This means that either the chiral nematic phase does not cooperate with the LS model in the production of blue light as hypothesized, or that the index of refraction is lowered in the liquid crystal state. A study of the lowering of the index of refraction of water in a chiral nematic liquid crystal state is indicated.

With regard to cold fusion, it is an open question whether pumping UV incident light in phase with the sonic pumping and in combination with stimulated Raman scattering in water is or is not a cooperative mechanism in the production of blue light as seen by the observer. However, for UV wavelengths in the liquid crystal near the blue line, the transmission of UV energy to the center may be significant. This cooperative lasing action, collectively termed here a blue water laser, may function as a cold fusion spherical focusing device to concentrate UV energy on the water molecules at the center of the compression field and possibly fuse hydrogen and deuterium.

### Molecular Water Model

Generally, the Molecular Dynamics (MD) simulation of simple monatomic liquids [9] without Coulomb charge interaction proceeds on the basis of Lennard-Jones (LJ) interatomic pair potentials to describe the internal energy. However, the MD simulation is more complex for water. The internal energy description by simple LJ pair potentials alone is not sufficient because the polarizability of water causes the long range Coulomb charge interactions to be dominant. In the liquid crystal interpretation of SL, the long range Coulomb interactions are important in developing the twisted helical structure. The first simulation of liquid water [10,11] in the early 1970's included both van der Waals and Coulombic interactions together in the manner of an effective pair potential. However, the simple point charge (SPC) developed [12] was selected here for the SL study.

The SPC model is of a tetrahedral geometry consisting of an O-H distance of 0.1 nm with point charges of -0.8476e on the oxygen position and +0.4238e on each of the hydrogen positions. The tetrahedral angle between the vector pairs connecting the oxygen and hydrogen atoms is 109.4 deg is illustrated in Figure 2. The Coulomb potential for o-o, o-h, and h-h charge separations is,

$$V_C = q_h q_o / 4\pi \epsilon_0 r_{ij}$$

where,  $e = 1.6 \times 10^{-19}$  coul, and  $\epsilon_0 = 8.854 \times 10^{-12}$  coul<sup>2</sup> / j-m

The LJ potential based only on oxygen-oxygen separations is,

$$V_{LJ} = 4\epsilon [(\sigma/r_{oo})^{12} - (\sigma/r_{oo})^6]$$

where,  $\epsilon = 78.38 * K_b$ ,  $K_b = 1.38 \times 10^{-23}$  j, and  $\sigma = 0.316$  nm.

### MD Simulation

The MD simulation is directed to the dynamic response of bulk water at 300 K under a uniform isotropic expansion and compression. Consistent with a spherical liquid crystal structure, the isotropic geometry should be spherical with a characteristic length at least about equal to the wavelength of blue light, 470 nm. However, typical MD calculations assume a bulk fluid and are carried out in a cubic computational box with periodic boundary conditions. Although a cubic box could be assumed to be in a state of isotropic expansion and compression, the number of molecules required is significant. At 300 K the density of water [0.998 gm/cc] with a 400 nm cubic box would contain about 2 billion molecules. Hence, the attendant MD simulation would require an exorbitant amount of computation.

In order to obtain a representative MD simulation of water in a chiral nematic phase with reasonable computation times and still maintain consistency with a spherical geometry undergoing isotropic expansion and compression, a 1D chain of water molecules was selected. An exact representation would consider a spherical sector geometry with proper boundary conditions such as frictionless rigid walls that permit motion only in the radial direction. This is usually achieved by simulating the rigid walls with dummy molecules and fictitious LJ potentials. However, the rigid simulation increases the number of molecules and attendant computer time significantly. In this arrangement, a 1D chain of water molecules aligned in the radial direction with lateral constraint in the transverse directions gives a reasonable approximation to a spherical geometry with acceptable computing time. This configuration points the 1D chain in the direction of the incident UV light as shown in Figure 2.

To achieve liquid density in a 1D chain of water molecules at 300K, the initial configuration consist of about 1400 water molecules in a  $0.3 \times 0.3 \times 400$  nm computational box in the x, y, and z directions respectively. The chain is free to move in the z-direction and periodic boundary conditions are imposed at the top and bottom. In the x and y directions, periodic boundary conditions are also imposed, but lateral motion is restrained by constraining the oxygen atom to the z-axis. The hydrogen atoms are placed in a vector pair laying in the x-y plane so that their respective vector cross product was pointing parallel to the positive z-axis. The initial spacing in the model z-direction is 0.3 nm. Here, the water molecules are free to rotate about the oxygen atom. Constraining the water molecule about the center of mass is correct, but the oxygen atom was chosen as the point of rotation for analytical convenience.

The SHAKE algorithm [13] was used to maintain constant bond lengths and tetrahedral angle as well as constraining the oxygen atom of each water molecule to the z-axis. In order to include a reasonable amount of long range effect in the computation of electrostatic forces, each molecule was assumed to interact with the neat 5 molecules above and 5 below it in the 1D chain. The time step in the solution was 1 fs.

### Results and Extensions

In the MD simulation, the bulk water temperature was held near 300 K. Density was changed by varying the initial spacing between the molecules in the z-direction. However, the number of molecules was adjusted to maintain the 400 nm wavelength. The crystal order parameter is computed based on the angular position of the H-O-H normal relative to the z-axis. It is found that the water molecules are ordered into a helical geometry for initial molecular spacings less than about 1 nm. The order parameter indicates a molecular rotation of about 80 degrees, but the H-O-H normal also rotates around the z-axis as shown in the simplified sketch of the blue phase of water in Figure 3.

Since the molecules are generally oriented in the manner of a twisted helical structure during SL compression, a structure that transmits ambient 400 nm UV light of a left or right chirality while reflecting the opposite chirality is predicted. The MD analysis to show that the 400 nm structure cooperates with the production of 470 nm blue light was not performed.

Because the full scope of analytical and experimental effort in the future development of the blue water laser concept is beyond the capability of the author, the following blue water laser experiments and applications are presented to the cold fusion community for review and comment.

#### Confirmation of SL Model

Polarization measurements of the reflected blue light in the SL experimental set-up [1] should be made. Since Raman emissions are highly polarized, the LS model predicts that the intensity of the blue light as viewed through the polarizer will be significantly diminished. If the blue light is found to be circularly polarized, that is, either right or left handed, it can be concluded that the water is a chiral nematic liquid crystal with the pitch equal to the wavelength of blue light in water. If the blue light is found to be linearly polarized, it can be concluded that the water is a nematic liquid crystal. In either case, the blue light in SL is caused by UV light reflected in a blue Raman line as predicted with the LS model.

#### Stimulated Raman Scattering

Stimulated Raman scattering experiments of the blue water laser directed to establishing the energy gain caused by resonance of UV ambient light with the helical structure of water in the liquid crystal state should be performed. The experimental set-up suggested is the same SL arrangement [1], except modified to include a surrounding spherical cavity coincident with the spherical compression field in the light or heavy water as shown in Figure 4. The surrounding cavity surface is lined with mercury lamps emitting UV radiation in the 300 to 400 nm range and flashed in sync with the SL acoustic frequency, or only with the SL acoustic pulsed in a steady UV radiation field. In effect, the mercury lamps function as a UV laser driver source, but other more appropriate UV exciting lines may also be used.

Of interest to cold fusion are stimulated Raman scattering experiments of the blue water laser to determine energy gain and heat produced as a function of UV wavelength. Experiments to determine the liquid crystal focusing with bulk water temperature are of importance. In carbon based molecules, hydrogen-deuterium asymmetry is known [8] to produce a twisted chiral nematic cholesterogen. However, in water molecules little is known about the effects of asymmetry in neutron mass. The effects of asymmetry of water molecules caused by neutron mass on liquid crystal structure is recommended for blue water laser research.

### Blue Water Laser Applications

Conceptually, the blue water laser is a UV transparent spherical container of light or heavy water surrounded by a spherical UV laser driver cavity with the spherical acoustic driver exterior to the UV laser driver. During operation the blue water laser is a cold fusion heat source, and therefore openings are required in the spherical arrangement to permit flowing water to transfer the fusion energy to a heat sink. Openings may be made in the spherical arrangement without significantly affecting the isotropic irradiation of the water molecules. In this arrangement, the blue water laser may find application as a hydrogen or deuterium gas generator or a D-O-D water heater as illustrated in Figure 5.

At low UV energy laser driving, O-H or O-D bonds of the water molecules at center are broken and the molecules dissociate into hydrogen or deuterium and oxygen ions and, if in addition, the water includes an oxygen catalyst, recombination to hydrogen or deuterium molecules may occur. Hence, the blue water laser may find application as an industrial hydrogen or deuterium gas generator.

For high UV energy drivers and depending on the spot size, a group of water molecules may be ionized to high temperatures causing fusion of hydrogen or deuterium atoms and a fusion energy release. By providing a through flow of heavy water, the blue water laser may find application as a residential home heater by increasing ambient temperature water to about 50 C without a loss of the spherical liquid crystal focusing structure. However, oxygen catalysts may be precluded here because of potential quenching of the hydrogen or deuterium fusion plasma. Further, the fusion plasma may also be quenched by the oxygen in the water molecule. Conversely, the quench in fusing of water molecules in the presence of oxygen catalysts may serve as a natural safety mechanism to prevent a runaway fusion process. The fusion of water molecules in the presence of oxygen and oxygen catalysts is recommended for future blue water laser research.

In both low and high UV energy driver applications, the UV radiation from the surrounding spherical cavity is concentrated at its center by the geometric focusing. Hence, contamination of the hydrogen and deuterium plasma by oxygen and oxygen catalysts may not be a problem because the very large concentration of UV energy may accommodate the contamination and still achieve fusion temperatures. Because of the significant concentration of UV driver energy, it is possible that ambient UV light alone is sufficient to cause hydrogen or deuterium fusion in water molecules, and therefore it is not whether cold fusion can occur during SL, but rather why has cold fusion not been detected to date. The answer given here is that for a small number of fusing water molecules, the low level energy release and helium nuclear products would be difficult to detect. However, with higher UV energy lasers, nuclear products may be detectable.

### Discussion and Summary

The blue water laser is similar to the Inertially Confined Fusion Reactor (ICFR) hot fusion concept [14] where fabricated D-T fuel pellets are ignited at fusion temperatures by imploding the fuel pellets through laser ablation of the exterior pellet surface. However, the blue water laser is a far simpler concept than the ICFR because fuel pellets do not need to be fabricated as the water molecules at the focal point of the liquid crystal structure function as the fuel pellet. Further, the mercury lamp arrangement is a simple laser driver. Since the spherical liquid crystal structure is perfectly reformed after each SL pulse, a continual and reliable flow of fuel is provided for repetitive ignition and a likewise channel is provided for the UV light to irradiate the water molecules at the center of the spherical liquid crystal structure.

The advantage of the blue water laser over conventional ICFR concepts is that a very small quantity of D-O-D fuel is repetitively ignited. This means that the UV energy required for D-D ignition is small and the external UV laser energy may also be small because of the geometric concentration by the spherical lens. Further, since the D-D energy release is small, only a small temperature rise and shock pulse in the bulk water occurs during each ignition. Still further, the blue water laser would make possible the neutron free D-D reaction at reasonable UV power instead of opting for the lower ignition energy D-T reaction with attendant neutron radioactivity problems common in ICFR concepts. Still further, miniature blue water lasers may be envisioned instead of the large size of ICFR laser drivers.

In contrast to ICFR concepts that fuse D-T fuel, the blue water laser concept attempts to fuse deuterium in heavy water by UV irradiation of D-O-D molecules. It should be noted that the blue water laser is a cold fusion device because the liquid crystalline structure required in the transmission of UV radiation to the fusing water molecules would only operate, say below 50 C, even though the local hot fusion D-D reaction is actually producing the heat. However, the quenching of the D-D plasma temperatures by the oxygen catalysts or the oxygen in the D-O-D water molecules or the helium reaction product itself may be a difficult obstacle for the blue water laser concept to overcome. If not, miniature blue water lasers can serve as a limitless energy source in providing residential home heating. Otherwise, the blue water laser is likely to find commercial application as a hydrogen or deuterium gas generator.

1. B.P. Barber and S.J. Puttermann, "Observations of Synchronous Picosecond Sonoluminescence." Letters to Nature, Vol. 352, pp. 318-320, (1991).
2. K. Fukushima, "Is Sono-Fusion to be a Possible Mechanism for Cold Fusion?" Frontiers of Cold Fusion, Universal Academy Press, pp. 609-612, 1993.
3. A. J. Walton and G. T. Reynolds, "Sonoluminescence", Advances in Physics, Vol 33, No. 6, pp. 595-660, (1984).
4. C. A. Parker, "Raman Spectra in Spectrofluorimetry." Analyst, Vol. 84, pp. 446-453,(1959).
5. S. Chandrasekhar, Liquid Crystals, Cambridge University Press, pp. 292-298, 1992.
6. T. Seideman, "The Liquid Crystalline Blue Phases." Rep. Prog. Phys., Vol. 53, pp. 659-705, (1990).
7. R. Reinitzer, Monatsh. Chem., 9, (1888).
8. D. Coates and G. W. Gray, "The Synthesis of a Cholesterogen with Hydrogen-Deuterium Asymmetry." Molecular Crystals and Liquid Crystals, Vol. 24, pp. 163-177 (1973).
9. M.P. Allen and D.J. Tildesly, Computer Simulation of Liquids, Oxford, 1990.
10. A. Rahman and F.H. Stillinger, "Molecular Dynamics Study of Liquid Water." J. Chem. Phys., Vol. 55, No. 7, pp. 3336-3400. (1977).
11. F.H. Stillinger and A. Rahman, "Improved Simulation of Liquid Water by Molecular Dynamics." J. Chem. Phys., Vol. 60, No. 4, pp. 1545-1557 (1974).
12. H.J.C. Berendsen, et al., "The Missing Term in Effective Pair Potentials." J. Chem. Phys., 91, pp. 6269-6271 (1987).
13. J.P. Ryckaert et al, "Numerical Integration of the Cartesian Equations of Motion of a System with Constraints: Molecular Dynamics of n-Alkanes." J. Comput. Phys., Vol. 23, pp. 327-341 (1977).
14. J.A. Maniscalco, W.A. Meir, and M.J. Monsler, "Design Studies of a Laser Fusion Plant", Proceedings of a Technical Committee Meeting and Workshop on Fusion Reactor Design Concepts, Madison, Wisconsin USA, pp 299-314, 1977.

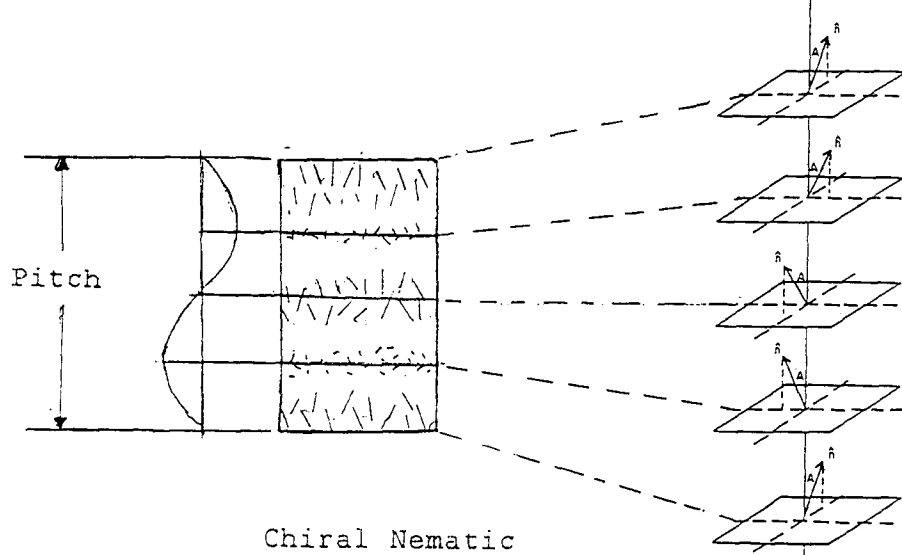
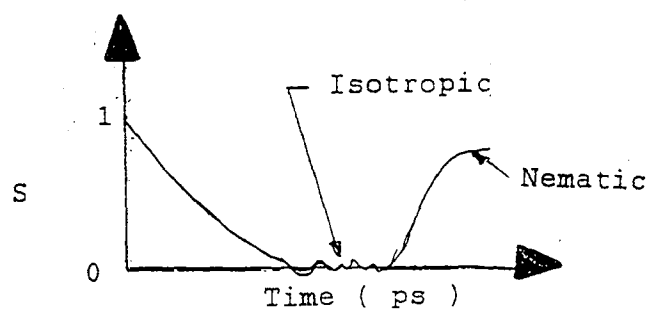
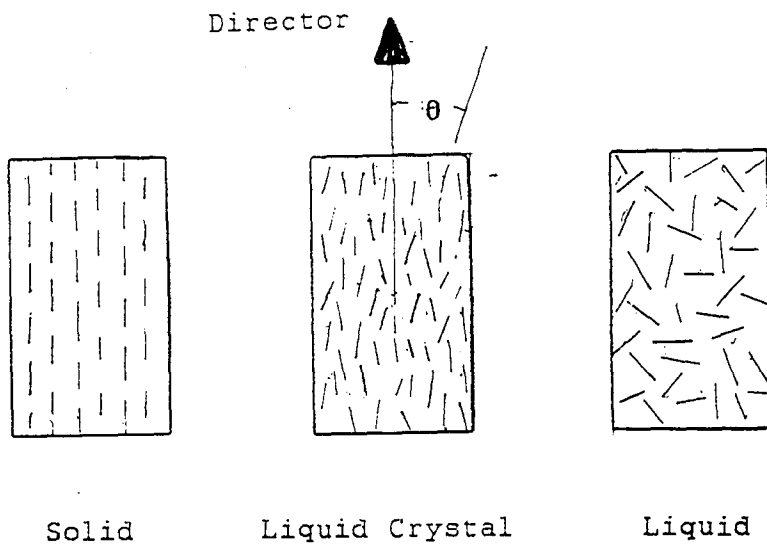


Figure 1    Liquid Crystal Notation

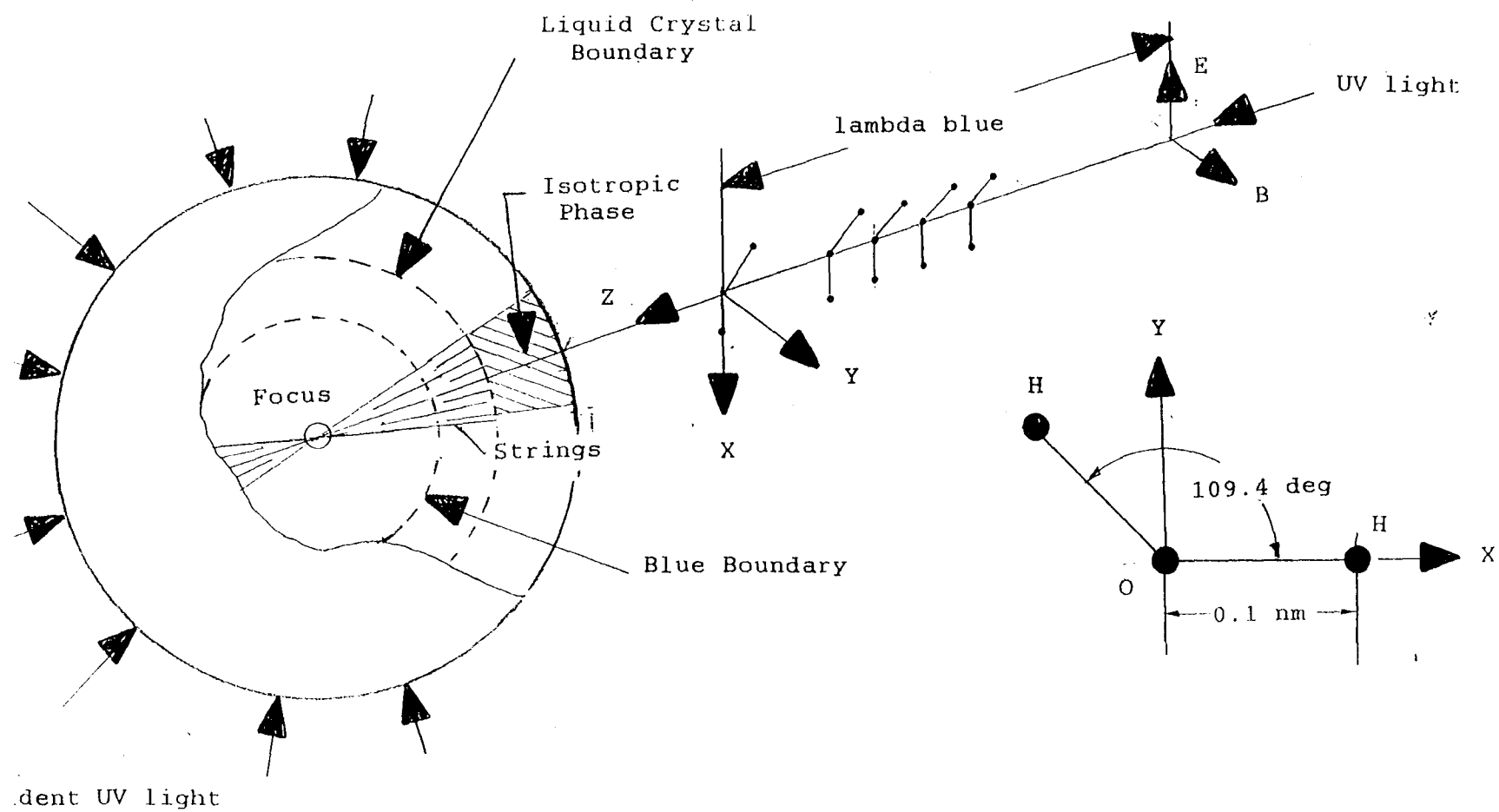


Figure 2 Spherical Water Liquid Crystal Geometry, Radially Disposed Strings of Molecules, and Water Molecule Model Geometry

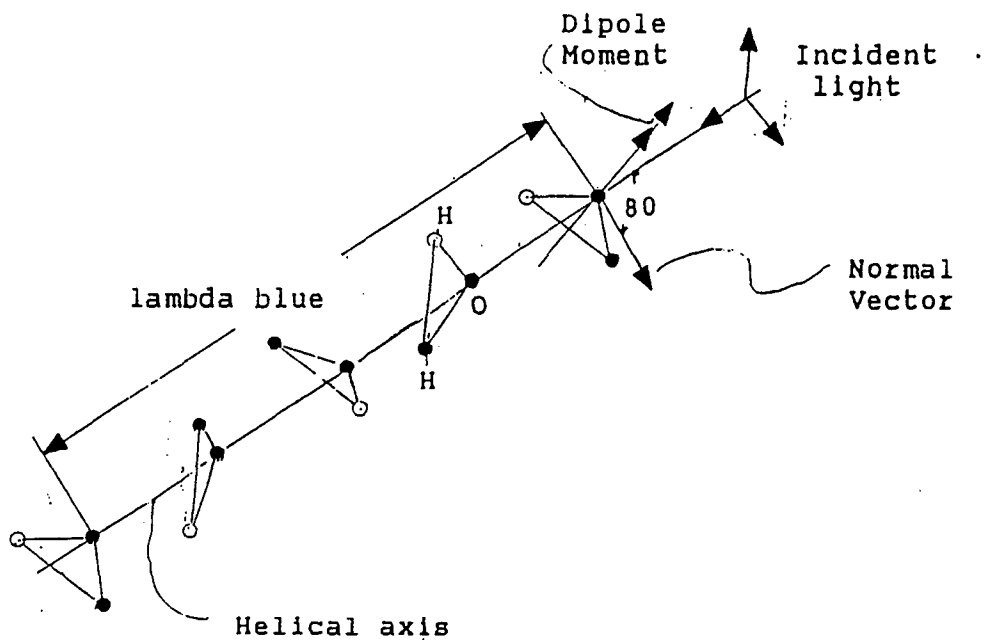


Figure 3 Simplified Sketch of the Blue Phase of Water

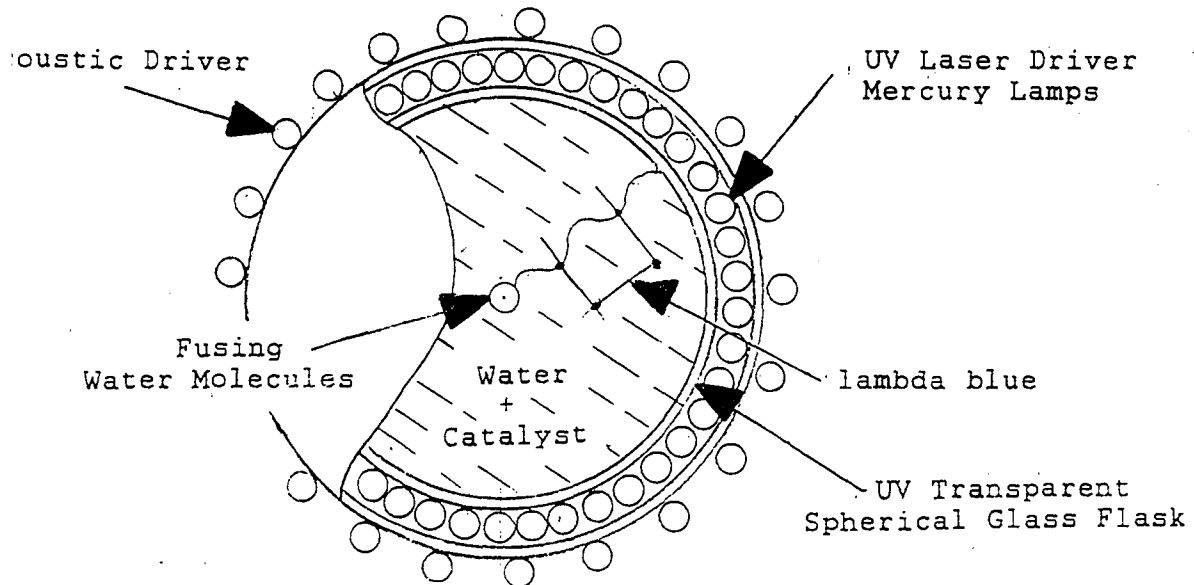


Figure 4 Blue Water Laser Concept

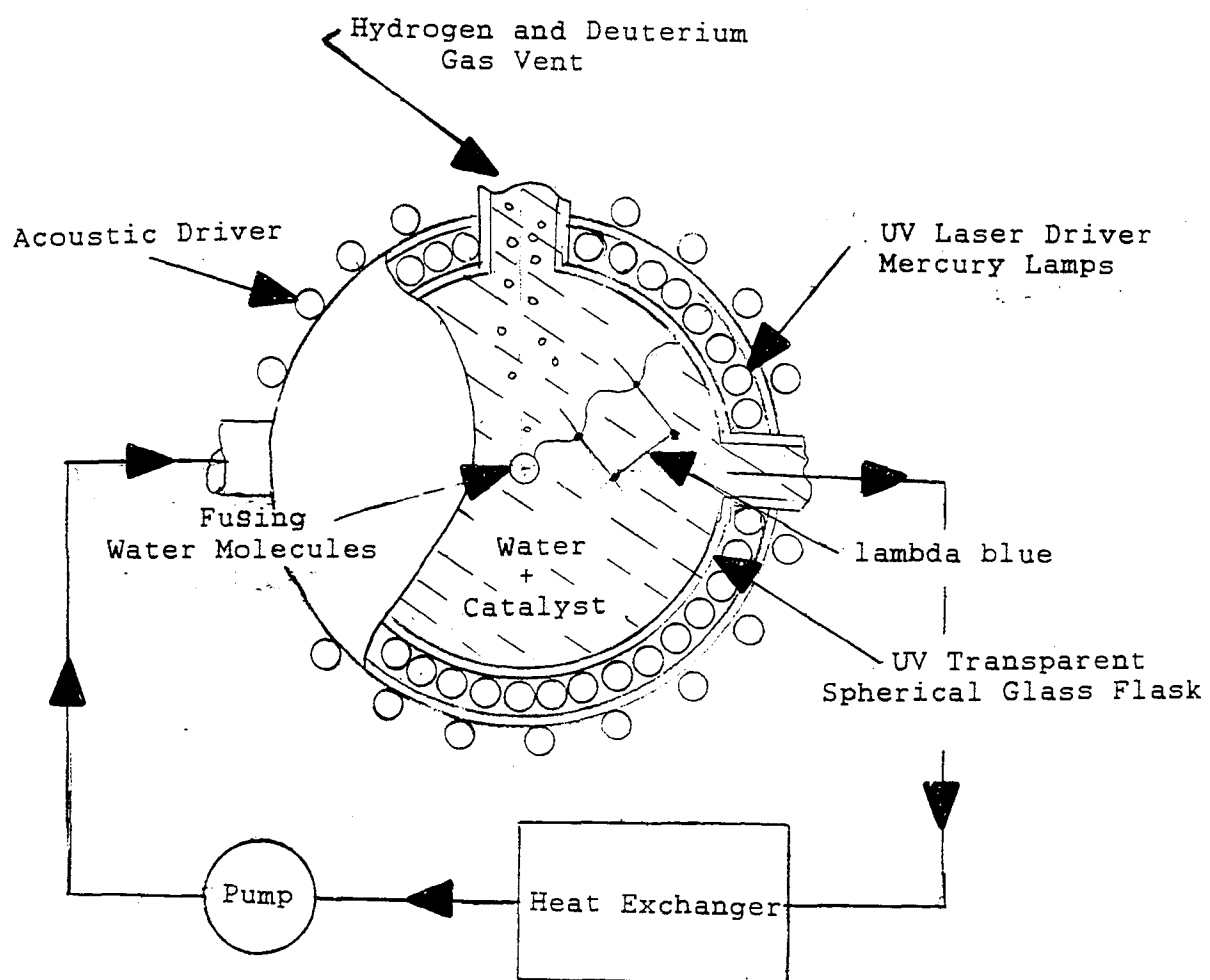


Figure 5 Blue Water Laser Applications



## A UNIFYING MODEL FOR COLD FUSION

Robert T. Bush

Physics Department, California State Polytechnic University\*

ENECO\*\*

Proteus Processes and Technology, Inc.\*\*\*

### Abstract

A theoretical model<sup>36</sup> has been devised that accounts for the heavy water excess heat effect (Fleischmann and Pons<sup>5</sup>) and light excess heat effect (Mills and Kneizys<sup>8</sup>, Noninski<sup>25</sup>, Bush<sup>10</sup>) as resulting from genuine cold fusion. Among the features of interest are the following: The model

1. provides a unique and highly novel mechanism to sufficiently enhance tunneling through the Coulomb barrier to account for empirically-observed cold fusion rates.
2. accounts for the role of lithium in electrolytic experiments.
3. accounts for the depletion of Li<sup>6</sup> relative to Li<sup>7</sup> observed by Thompson et al.<sup>20</sup> in post-run palladium cathodes and shows that it is associated with a difference in reduced masses rather than quantum symmetry.
4. predicts<sup>36</sup> excess power density (W/cm<sup>3</sup>) as a function of loading, S, and temperature, T, to be as follows for the D-D case for the heavy water-Pd system:

$$P(S,T) = 26.07 \cdot \{[(2 - S)/(1 - S)]^3 S\} \cdot (e^{\theta/T} - 1)^{-1} \cdot 10^{[23.6 - (24.774)S^{-1/12}]}$$

(W/cm<sup>3</sup>)

(θ is the Debye temperature for the deuterided Pd.)

5. excess power expression P(S,T) gives a good fit to the data of McKubre et al.<sup>7</sup> (SRI International/EPRI) and to the data of Kunimatsu<sup>13</sup> et al. (IMRA).
6. can account for the excess power density of about 4kW/cm<sup>3</sup> achieved by Fleischmann and Pons<sup>6</sup> in their "boil-off experiments" and by Bush and Eagleton<sup>12</sup> in their thin film experiments (cathode: 5 micron thin film of Pd on a silver substrate).
7. accounts for the Fleischmann and Pons<sup>14</sup> "heat after death" phenomenon.

8. yields a positive temperature coefficient reaching a limiting value of about  $1\text{W/cm}^3\cdot\text{C}$  at 600C.
9. predicts tritium and neutron production: For tritium<sup>36</sup>:  

$$N(S,T) = 6.789 \times 10^{12} \cdot \{S(1 - S)[1 - (1-S)S^2]^{-3}\} \cdot (e^{\theta/T} - 1)^{-1} \cdot 10^{[23.6 - (24.774)S^{-1/12}]}$$
(Tritons/cm<sup>3</sup>/s)  
In particular, it can account for the result of Bockris' curve<sup>15</sup> for which tritium production mirrors excess heat production, but only at about one-thousandth of the level to account for the latter; and shows that tritium production is ordinarily not observed when excess heat is being observed.
10. shows that tritium production peaks at around  $S = 0.83$  (loading fraction) for all temperatures.
11. suggests a relatively "radiationless" de-excitation mechanism.

## Introduction

A signal theoretical difficulty has led to a lack of acceptance of cold fusion by physicists; viz., the absence of a mechanism to cope with the Coulomb barrier. In what follows, results will be employed from a relatively new branch of physics, "stochastic electrodynamics" (SED), to suggest a solution to cold fusion. Stochastic electrodynamics (SED), based upon classical concepts, offers an alternative to quantum electrodynamics (QED) in treating the interactions between charged point-mass particles and the zero-point electromagnetic field. Extending the earlier work of Boyer<sup>1,2</sup> (1975), Puthoff<sup>3</sup> (1987) employed zero-point fluctuation (ZPF) modelling within the framework of stochastic electrodynamics (SED) to demonstrate that the ground state for hydrogen is a dynamic state of equilibrium. According to Boyer's<sup>1</sup> original hypothesis the power radiated by the accelerated electron in its circular orbit in the ground state is exactly compensated for by the power absorbed from the zero-point electromagnetic field. If this is correct, and no flaw has yet surfaced, the Boyer-Puthoff result constitutes the most satisfying derivation for the first Bohr radius. In what follows a heuristic treatment appealing strongly to physical argument is presented in support of the hypothesis that cold fusion, in both its heavy water- and light water aspects, is explained on the basis of shifts in this dynamic equilibrium

state to lower radius orbits ("collapsed orbits") produced by a modification of the zero-point field mode distribution. This mode distribution alteration is hypothesized to be imposed by the lattice environment for the heavy water-LiOD-palladium system (Fleischmann/Pons<sup>5</sup>) and for the light water-alkali atom-nickel system (Mills and Kneizys<sup>8</sup>, Noninski<sup>25</sup>, Bush<sup>10</sup>).

Such a modification of the zero-point field would not be new to physics since it is achieved, for example, in the case of the well-known "Casimir effect", or "Casimir force"<sup>4</sup>. Of this, Puthoff<sup>3</sup> writes; "A simple but elegant example of a ZPF-determined system is provided by the attractive quantum force (Casimir force) between conducting parallel plates, where the force results from the redistribution of viable normal modes (and hence in the associated vacuum electromagnetic ZPF energy) as the distance between the plates changes." In what follows it will be convenient to coin a phrase by referring to such conducting parallel "plates" (functioning to redistribute the zero-point field energy), or matter configurations such as a lattice planes acting as a radiation reflectors and, thus, capable of limiting the zero-point field, as "Casimir reflectors", or "Casimir diffractors". (The relation to the diminution of the zero point field at conducting boundaries such as internal metal boundaries and the conjectured "swimming electron layer" of Miley et al.<sup>31</sup> is treated in reference 36.)

The resulting collapsed electron orbits (Heavy water system: D atoms, Li<sup>6,7</sup> atoms; light water system: H-, Li-, Na-, K-, Rb-, Cs-atoms) result in an enhanced shielding effect, which promotes tunneling through the Coulomb barrier and, thus, genuine cold fusion. Therefore, this "electron-catalyzed fusion" (ECF) is analogous to the well-known "muon-catalyzed fusion"<sup>16,17</sup> or "muonization". In both cases, increased binding causes the classical turning point in the tunneling problem to

move inward. This decrease in the width of the Coulomb barrier boosts tunneling rates. For convenience, fusion rates are calculated for the ECFM ("Electron-Catalyzed Fusion Model") by employing known results for the equivalent electron "effective mass" problem. However, due to limitations of space in this presentation the following sketch of the ECFM applies essentially to the heavy water-palladium system. The light water-nickel system will be treated extensively in reference 36.

### Hydrogen Ground State: Dynamical Balance

Building upon the work of Boyer (1975)<sup>1,2</sup>, Puthoff<sup>3</sup> (1987) showed that the first Bohr orbit is associated with a state of dynamical balance:

Power lost via radiation (accelerating electron) = Power absorbed by the circling electron from the zero point electromagnetic field.

$$P_{\text{rad}} = e^2 r_0^2 \omega_0^4 / 6\pi\epsilon_0 c^3 \quad (1)$$

$$P_{\text{abs}} = e^2 \hbar \omega_0^3 / 6\pi\epsilon_0 m c^3 \quad (2)$$

where,  $e$  is the electronic charge,  $r_0$  is the usual hydrogen first Bohr orbit radius,  $\epsilon_0$  is the permittivity of free space,  $c$  the velocity of light,  $\hbar$  Planck's constant devided by  $2\pi$ , and  $\omega_0$  the electron angular velocity. Equating (1) and (2) yields the condition for the first Bohr radius,  $r_0$ :

$$m\omega_0 r_0^2 = \hbar \quad (3)$$

Puthoff<sup>3</sup> (1987) also shows,

$$P_{\text{abs}} = \frac{(e^2 \hbar \omega_0^3 / 6\pi\epsilon_0 m c^3) \int_0^\infty \Gamma \omega^7 d\omega}{(\omega_0^2 - \omega^2)^2 + \Gamma^2 \omega^6}, \quad (4)$$

where  $\Gamma = e^2 / 6\pi\epsilon_0 m c^3$  (5)

The form of (4) shows that absorption is essentially a resonance process:

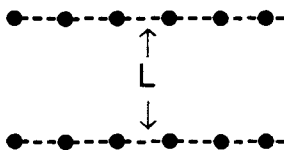
$$\begin{array}{ccc} \omega & = & \omega_0 \\ (\text{Frequency of} & & (\text{Electron angular velocity} \\ \text{absorbed radiation}) & & \text{in first Bohr orbit}) \end{array} \quad (6)$$

### **Collapsed Ground State: "Casimir Reflectors"**

Going beyond the Boyer-Puthoff results<sup>1,2,3</sup> we note that dynamic balance is upset if a minimum frequency  $\omega_{\min}$  is established for the zero point field which is greater than  $\omega_0$  by limiting the maximum wavelength  $\lambda_{\max}$ :

$$\omega_{\min} = 2\pi c / \lambda_{\max} \quad (7)$$

$\lambda_{\max}$  is established by "Casimir reflectors" hypothesized to be lattice planes with alkali metal atoms occupying a fraction of the lattice sites: e.g. Isotopic Hydrogen, Li, Na, K, Rb, Cs, Fr.



#### Casimir Reflector Condition:

$$\lambda_{\max}/2 = L(\text{Casimir reflector separation}) \quad (8)$$

An increase in  $\omega_{\min}$  of the zero point field associated with the establishment of  $\lambda_{\max}$  causes the electron to spiral inward to increase its angular velocity  $\omega_0$ , i.e.,

$$\omega'_0 = \omega_{\min} \quad (9)$$

The Bohr radius collapses to  $r'_0 < r_0$ :

$$m \omega_{\min} (r'_0)^2 = \hbar \quad (10)$$

From (7), (8), and (10) the collapsed Bohr radius becomes

$$r'_0 = (\hbar L / m \pi c)^{1/2} \quad (11)$$

### **Equivalent Electron "Effective Mass Problem":**

Recall for the nth Bohr radius  $r_n$  the proportionality

$$r_n \propto n^2 \hbar^2 / m e^2 \quad (12)$$

The inverse proportion of radius to mass in (12) means that we can adapt the formalism of the fictitious electron effective mass problem: From Walling and

Simons<sup>18</sup> the fusion rate, R (fusions/sec/D), can be expressed in terms of a fictitious electron effective mass  $m^*$  as

$$\log R = 13.6 - 76.92(m/m^*)^{1/2} \quad (13)$$

Mathematical equivalence to the ECFM is expressed by employing (12) and (11):

$$r_0/r_O = (m/m^*)^{-1} = (227.8/L)^{-1/2}, \quad (14)$$

where L is in Angstroms. Substituting into (13),

$$\log R = 13.6 - 76.92 (227.8/L)^{-1/4}. \quad (15)$$

#### Theoretical Excess Power (D-D Cold Fusion in Palladium):

Theoretical excess power:  $P_{exc}(W/cm^3) \propto R \cdot N \cdot E$  (16)

For Pd:  $N = (6.79 \times 10^{22}) \cdot S,$  (17)

where S("Stoichiometry") = fractional loading with D's.

$$E = 24 \text{ MeV} = 3.84 \times 10^{-12} \text{ J.} \quad (18)$$

(18) assumes that excess heat production is associated with  $\text{He}^4$  production, for which there is good initial evidence from Miles et al.<sup>9</sup>. From (15), (16), (17), and (18),

$$P_{exc} \propto (26.07) \cdot S \cdot 10^{(10+\log R)} = (26.07) \cdot S \cdot 10^{[23.6 - (76.92) \cdot (227.8/L)^{-1/4}]} \quad (19)$$

That (19) is incomplete can be seen from the following 1-d lattice configuration:

Key: • represents an interstitial D, o represents an empty interstitial site

○   •   ○   •   ○   •   ○   •   ○   •   ○   ... etc. (20)

(20) represents a hypothetical one dimensional lattice configuration for which no cold fusion occurs due to a lack of nearest- neighbor D's.

We hypothesize that the cold fusion reaction  $D + D \rightarrow \text{He}^4 + 24 \text{ MeV}$  occurs for lattice configurations with nearest-neighbors on either side to produce a "sideways

charge polarization" of the D's with protons directly opposite neutrons so that collisions are highly "guided" (lattice assisted anti-Tokamak regime):

$$\begin{array}{ccccccccccccc} \bullet & \bullet & \bullet & \bullet & \bullet & o & + & o & \bullet & \bullet & \bullet & o & + & o & \bullet & \bullet & \bullet & \bullet & o & + & \dots & \text{etc.} \end{array} \quad (21)$$

$$(S^3) \qquad \qquad (S^4) \qquad \qquad (S^5)$$

Thus, each D near the center of these configurations sees a nearest-neighbor D on either side. It is further hypothesized that tritium and neutrons result from the opposite situation; viz. the oscillatory collision of two nearest-neighbor D's isolated from their neighbors for which charge polarization favors neutronic components of the D's facing each other, thus heavily favoring tritium production via  $D + D \rightarrow T + p + 4.03 \text{ Mev}$  as an Oppenheimer-Phillips type nuclear reaction <sup>27-30</sup>:

$$\begin{array}{ccccccccccccc} \bullet & \bullet & \bullet & o & + & o & \bullet & \bullet & o & \bullet & \bullet & o & + & o & \bullet & \bullet & o & \bullet & \bullet & o & + & \dots & \text{etc.} \end{array} \quad (22)$$

$$(1 - S)^2 S^2 \qquad (1 - S)^3 S^4 \qquad (1 - S)^4 S^6$$

For  $\text{He}^4$  production the configurations in (21) yield a sum of probabilities (dependent upon fractional occupation, S):

$$p = S^3 + S^4 + S^5 + \dots \quad \text{etc.} \quad (23)$$

Treating this as essentially an infinite series allows us to write  $Sp = p - S^3$ , so that

$$p = (S^3 / 1 - S) \quad (24)$$

Now, the power production associated with the sum of the configurations (19) in terms of an energy release E and a mean time  $\tau$ , is proportional to :

$$S^3 E / (\tau/2) + S^4 E / (\tau/3) + S^5 E / (\tau/4) + \dots \quad \text{etc.} \quad (25)$$

Dividing by  $(E/\tau)$  to extract the statistical factor, P,

$$P = 2S^3 + 3S^4 + 4S^5 + \dots \quad \text{etc.} \quad (26)$$

Treating this as an effectively infinite series it is readily shown that

$$P = S^3 (2 - S) / (1 - S)^2 \quad (27)$$

For a 1-d lattice the normalized statistical factor is found from (24) and (27) to be

$$(P/p) = (2 - S) / (1 - S) \quad (28)$$

However, since each interstitial D is a member of three independent orthogonal chains in the actual 3-d Pd lattice, the total statistical factor, including the S factor already contained in (19), is given by

$$\text{Total Statistical Factor} = \{(2-S)/(1-S)\}^3 S \quad (29)$$

Vibration of the lattice is necessary for the oscillatory collisions of the nearest-neighbor D's to produce tunneling. Thus, a phonon probability factor as follows must be inserted into  $P_{\text{exc}}$ .

$$\text{Planck-Debye Factor} = (e^{\theta/T} - 1)^{-1}, \quad (30)$$

where  $\theta$  is the PdD Debye temperature and T is the Kelvin temperature. Combining (19), (29), and (30) yields for the theoretical excess power density:

$$P_{\text{exc}}(\text{W/cm}^3) = (26.07) \cdot \{(2-S)/(1-S)\}^3 S \cdot (e^{\theta/T} - 1)^{-1} \cdot 10^{[23.6 - (76.92) \cdot (227.8/L)^{-1/4}]} \quad (31)$$

Finally, L itself should be dependent upon S: So, in the sense of average values of L and S, we hypothesize:

$$(N \cdot S) \cdot L^3 = 1 \text{ cm}^3 = 10^{24} (\text{\AA})^3 \quad (32)$$

$$L = 2.451 \cdot S^{-1/3} (\text{\AA}) \quad (33)$$

Substituting (33) into (31) yields

$$P_{\text{exc}} = (26.07) \cdot \{(2-S)/(1-S)\}^3 S \cdot (e^{\theta/T} - 1)^{-1} \cdot 10^{[23.6 - (24.774)S^{-1/12}]} \quad (34)$$

A plot of  $\log P_{\text{exc}}(S,T)$  versus S for T = 60C in Fig. 1 reveals that the ECFM (Electron Catalyzed Fusion Model) readily encompasses approximately ten orders of magnitude of excess power in going from S = 0.1 to about S = 0.95. Table I displays  $P_{\text{exc}}$  for a range of S values extending from S = 0.5 to S = 0.985 for T = 60C and  $\theta$  = 1080K. For the specific excess power level of about 4 kW/cm<sup>3</sup> achieved by Fleischmann and Pons<sup>6</sup> in their "boil off" experiments, and by Bush and Eagleton<sup>12</sup> in their thin film experiments (5μm Pd electroplated on Ag substrate), Table I gives

a value for S of about 0.975. However, for higher temperatures, the S-value could be substantially lower. This is revealed by Fig. 2 containing a plot of  $P_{exc}$  versus S for three different temperatures, 26.8C, 60C, and 276.8C, exhibiting a positive temperature coefficient.

### **Comparing the ECFM with Data of McKubre et al.<sup>7</sup> (SRI/EPRI) and Kunimatsu et al.<sup>13</sup> (IMRA)**

$P_{exc}$  in (34) has been compared to the data of McKubre et. al.<sup>7</sup> by fitting to the averaged data point of (S=0.93,  $P_{exc} = 1.30W$ ) in Table II. McKubre<sup>19</sup> has indicated that the depth of penetration of Li in the SRI cathode was probably about 10 microns or more with an active length for the cathode of about 30 cm. This information taken together with the radius of 0.5 mm implies an active power producing region in the form of a thin annular cylinder of about  $0.00942 \text{ cm}^3$  volume. For a cathode temperature<sup>19</sup> of 60C it is found that the best fit to the averaged data of Table II is given by a Debye temperature for the PdD of approximately 1,140 K. Fig. 3 displays the fit of the ECF Model to the data of McKubre et. al.<sup>7</sup> with an average deviation of about 20% between the theoretical and averaged experimental powers of Table I.

Less information was available for the data of Kunimatsu et. al.<sup>13</sup> Nevertheless, a scaling factor was chosen by fitting to an averaged data point of (S = 0.88,  $P_{exc} = 19.0\%$ ) as shown in Table III. Fig. 4 exhibits this fit of the ECF Model overlying the Kunimatsu data. The average deviation between the theoretical powers and the averaged experimental powers of Table III was about 14%.

Fig. 5 shows a plot of the temperature coefficient,  $dP_{exc} / dT$ , versus temperature for two loading fractions (S), 0.85, and 0.90. Note that for S= 0.90 the temperature coefficient reaches nearly its maximum value of about  $1.0 \text{ W/cm}^3 \cdot \text{C}$  at 600 C,

whereas it reaches its maximum value of about  $0.2\text{W}/\text{cm}^3\cdot\text{C}$  for  $S = 0.85$  at around 400C.

### **Role of Lithium (ECF Model)**

The ECFM predicts that excess power can be achieved without lithium. However, that Li can play a key role as a catalyst in producing excess power emerges from the ECFM: As alkali atoms, the Li and D, or a mixture, are hypothesized to serve as crucial ingredients in the Casimir reflecting planes. However, since Li enters the lattice substitutionally, as opposed to interstitially as in the case of the D's, the Li-plane Casimir reflector separation is  $d$ , corresponding to the Pd lattice spacing. On the other hand, the Casimir separation for the D-planes is  $2d$ , or twice as great. This is shown in the lattice schematic of Fig. 6. Then because of the great sensitivity of  $P_{\text{exc}}$  to the Casimir separation  $L$ , as shown in (31), it is apparent that D-D fusion catalyzed by Casimir reflectors in the form of Li-planes is favored over D-D fusion catalyzed by the D-planes. According to the ECFM, then, the anomalously long loading time relative to that required for loading of the D's is explained as corresponding to the much longer time required for the inward diffusion of Li.

In between the Li-plane case and the D-plane case is that for the (D-Li) - plane case: With a Casimir separation of  $\sqrt{2} d$  lying in between the other two values, these may catalyze  $\text{Li} + \text{D} \rightarrow \text{Helium}$ . Because lower reduced mass favors tunneling for the Li-D cold fusion reaction, as shown in reference 36,  $\text{Li}^6\text{-D}$  fusion would be favored over  $\text{Li}^7\text{-D}$  fusion. This would lead to a depletion of  $\text{Li}^6$  relative to  $\text{Li}^7$  that might be observed in postrun cathodes. Just such an effect has been observed by Thompson et al.<sup>20</sup> in postrun cathodes of Fleischmann and Pons.

Finally the phenomenon of "heat after death" reported by Fleischmann and Pons<sup>14</sup> can be accounted for by the relatively vast deuterated interior of the cathode serving as a source of D's, once the current has been turned off, for the relatively thin outer active annular cylindrical region in which the cold fusion reactions are catalyzed by the Li.

### Tritium Production

(34) can be adapted to obtain the  $P_{exc}$  associated with tritium production<sup>36</sup> by multiplying it by the ratio of the energies released in the tritium and  $\text{He}^4$  producing reactions (4.03MeV/24MeV), respectively, and by substituting the appropriate statistical factor analogous to (29) for  $\text{He}^4$  production. From (22) the sum of the probabilities is

$$p = (1-S)^2 S^2 + (1-S)^3 S^4 + (1-S)^4 S^6 + \dots \quad \text{etc.} \quad (35)$$

Treating this as an essentially infinite series,

$$p = (1-S)^2 S^2 / [1 - (1-S)S^2] \quad (36)$$

Analogously to (25) the power associated with tritium production is proportional to

$$(1-S)^2 S^2 E/\tau + (1-S)^3 S^4 E/(\tau/2) + (1-S)^4 S^6 E/(\tau/3) + \dots \quad \text{etc.} \quad (37)$$

Dividing by  $(E/\tau)$  yields the statistical factor

$$P = (1-S)^2 S^2 + 2(1-S)^3 S^4 + 3(1-S)^4 S^6 + \dots \quad \text{etc.} \quad (38)$$

It is readily shown that

$$P = p / [1 - (1-S)S^2] \quad (39)$$

Therefore, the normalized 1-d statistical factor contains

$$P/p = 1/[1 - (1-S)S^2] \quad (40)$$

Also, since each interstitial D is a member of 3 independent orthogonal chains in the actual lattice, the total statistical factor contains this term in (40) cubed. And since no tritium is produced when either  $S = 0$  or  $(1 - S) = 0$ , the total statistical factor should

also contain the product S(S-1). Thus, analogously to (29), we have a total statistical factor, including the S from (19) given by

$$\text{Total Statistical Factor} = S(S-1)/[1 - (1-S)S^{2/3}] \quad (41)$$

Substituting into (34) we obtain

$$P_{\text{exc, trit.}}(S, T) = (4.38) \cdot S(1-S)[1 - (1-S)S^{2/3}] \cdot (e^{\theta/T} - 1)^{-1} \cdot 10^{[23.6 - (24.774)S^{-1/12}]} \quad (W/cm^3) \quad (42)$$

Modifying<sup>36</sup> this to give the triton production rate per cm<sup>3</sup>,

$$N(S, T) = (6.789 \times 10^{12}) \cdot S(1-S)[1 - (1-S)S^{2/3}] \cdot (e^{\theta/T} - 1)^{-1} \cdot 10^{[23.6 - (24.774)S^{-1/12}]} \quad (\text{Tritons}/cm^3/\text{sec}) \quad (43)$$

Fig. 7 portrays a graph of N(S, T) versus S for a temperature of 60C showing a peak value at about S = 0.83 of approximately  $1.6 \times 10^9$  tritons/cm<sup>3</sup> of Pd/sec. Fig. 8 displays a graph of excess power (W/cm<sup>3</sup>) associated with tritium production versus S for three different temperatures, 100C, 600C, and 1200C, illustrating the positive temperature coefficient. The latter is anticipated from the fact that the temperature dependence for tritium and neutron production is the same as that for excess heat production. A key feature is that the production peak at about S = 0.83 does not shift with temperature. Fig. 9 shows a plot of the relative ratio of excess power in tritium production to that in He<sup>4</sup> production versus S superimposed upon the graph of relative tritium production. Fig 7 and 9 illustrate why, according to the ECFM, observable excess power production is usually not accompanied by observable tritium production: Thus, Fig. 7 and Fig. 9 show that tritium production peaks around S = 0.83 and falls dramatically as one moves into the region of higher S above about S = 0.9 favoring increasingly higher excess power production as S approaches 1. Fig. 9 provides some support for Bockris' ratio<sup>15</sup> of about 0.001 for the ratio of excess power associated with tritium power production to that associated

with He<sup>4</sup> production assuming that a fractional loading (S) of about 0.7 would have been adequate in that particular experiment to observe excess heat.

### **Neutron Production**

Based upon the ECFM<sup>36</sup>, neutron production is given by N in (43) multiplied by an appropriate branching ratio highly favoring (T,p)-production over (He<sup>3</sup>,n)-production. Bush<sup>21</sup> has derived an extreme limiting branching ratio based upon charge polarization considerations given by

$$\text{BR} = [(r/R)^{12} / ([1 - (r/R)^3] \{ [1 - (r/R)^3]^3 + 4(r/R)^3 [1 - (r/R)^3]^2 + 6(r/R)^6 [1 - (r/R)^3] + 4(r/R)^9 \})], \quad (44)$$

where r is the protonic charge radius, and R is the deuteronic charge radius.

Substituting r = 0.8x10<sup>-13</sup> cm, and R = 4.31x10<sup>-13</sup> cm, from DeBenedetti<sup>23</sup>, yields

$$\text{BR} = 1.64 \times 10^{-9}, \quad (45)$$

which compares well with the best experimental value<sup>21</sup> for the smallest branching ratio given by about

$$(\text{BR})_{\text{exp}} = 2 \times 10^{-9}. \quad (46)$$

### **Relatively Radiationless De-excitation Mechanism**

A possible de-excitation mechanism is that of enhanced internal conversion in which de-excitation energy of the excited nucleus is transferred directly to the catalyzing electrons in highly collapsed orbits. Such a mechanism was also suggested by Walling and Simons<sup>18</sup>. Bremsstrahlung associated with the decelerating electrons would remain mostly in the lattice and electrolyte. Evidence of such electron fluxes has been found by Srinivasan et al.<sup>26</sup> and at Cal Poly<sup>33</sup>. In addition it seems impossible to rule out the possibility of direct phonon formation to absorb

some of the energy. Direct gamma ray formation is frustrated, as described by the author in reference 10.

### **"S > 1": Case for More Deuterons Than Palladium Atoms**

In what has been sketched thus far, it has been assumed that the loading fraction ( $S$ ) is less than one. Indeed, in this scheme  $P_{\text{exc}}$ (excess power) formally goes to infinity and  $P_{\text{exc}}$ (tritium) formally goes to zero in the limit as  $S$  goes to one. However the model can also treat cases where the number of deuterons within the sample is greater than the number of palladium atoms. Again, though, it is key to know what fraction of the interstitial sites are occupied, since this will determine behavior. It would even be possible to have a scenario in which increased loading reduces excess power: Thus, if increased loading induces a phase change in which the number of interstitial sites is increased, there would be an attendant decrease in the occupying fraction (i.e., fraction of interstitial sites occupied), which, in turn, reduces the excess power based upon the ECFM. However, there would also be a decrease in the average  $L$  value (Casimir separation) so that the power decrease would be moderated. Upon reattaining the occupying fraction  $S$  achieved prior to the phase transition, the excess power, according to the ECFM, should then be significantly higher than before the phase transition since the average Casimir separation,  $L$ , has now decreased. Clearly, then, for the ECFM it is important to distinguish between "occupying fraction",  $S$  (the fraction of interstitial lattice sites filled with D's) and the "loading fraction" (the ratio of D's in the sample to Pd atoms in the sample). (Previously we have not made that distinction.) Indeed, a case was recently reported in which an increase in loading actually reduced the excess power for a sample<sup>37</sup>.

### **Relation to other Models: Mills and Farrell, TRM**

The ECFM has a radically different physical basis than the "novel chemistry" of Mills and Farrell<sup>22</sup>. However, while this author has been able to find no theoretical corroboration of the latter, this in no way diminishes the achievement of Mills<sup>8</sup> as a pioneer in the discovery of the light water excess heat effect involving potassium. So, while both models are based upon collapsed electron orbits, the ECFM finds its inspiration in the zero point field work of Puthoff<sup>3</sup> building upon Boyer<sup>1,2</sup>. In addition, much of the agreement of the ECFM with the empirical observations of cold fusion is essentially independent of the particular mechanism inducing tunneling and arises, rather, from the statistical treatment of deuteron occupation (loading fraction) resulting in the total statistical factors in equations (29) and (41) for excess power production and the tritium production rates, respectively. This is a novel feature unique to the ECFM. Finally, the ECFM shows<sup>36</sup> that collapse is great enough to also account for the light water excess heat effect as a nuclear effect, whereas Mills<sup>8</sup> hypothesizes too small a collapse to lead to nuclear effects. In support of the ECFM there is now substantial evidence for nuclear effects in the case of the light water excess heat effect to which references 10, 11, 24, 26, 32, 33, 34, and 35 attest. Of course, both the ECFM and the novel chemistry of Mills<sup>8</sup> predict radiation given off in association with collapsing electron orbits. Mills<sup>8</sup>, in fact, claims to have detected such radiation.

Finally, it should be emphasized that the author has not repudiated his "Transmission Resonance Model" (TRM)<sup>21</sup>. Nevertheless, the author has reinterpreted the physics of the TRM in references 10, and 24. A possible connection with the ECFM arises from the fact that the collisions between incoming "resonant" deuterons and those in the interstitial lattice can produce changes in vibrational amplitude for these interstitial D's on the order of 0.1 Angstrom. Changes of this

size in L (Casimir separation) can produce a large increase in excess power density according to equation (31). Additional empirical evidence has recently been acquired by the author<sup>33,34</sup> for the "hill-and-valley curves" well known from the author's early theoretical work and explained on the basis of the TRM<sup>21</sup>.

### **Conclusions:**

The ECFM gives a good fit to the independent data of McKubre et al.<sup>7</sup> and of Kunimatsu et al.<sup>13</sup> on excess power versus loading fraction (S), and generally appears to explain much of cold fusion. The ECFM provides a unified approach (Ref. 36) to the heavy and light water excess heat effects as nuclear effects both arising from genuine cold fusion. The mechanism accelerating quantum tunneling through the Coulomb barrier is, however, very novel with the most questionable aspect being that of the validity of the Casimir reflection mechanism. Nevertheless, many of the model's predictions appear to depend more upon the statistical mechanical aspects of the fractional loading of the deuterons and the temperature, rather than upon the explicit tunneling mechanism. Thus, these latter aspects appear to be testable even in the absence of any consensus concerning the exact mechanism for enhancing tunneling. Finally, it will be ironic if, after much conceptualization over employing the vacuum as an alternate energy source, an energy source is revealed that depends crucially upon the existence of regions of diminished energy density in the vacuum.

### **Acknowledgments**

The author thanks G. Miley, Editor, *Fusion Technology*, P. Hagelstein (Electrical Engineering, M.I.T.) and T. Passell (EPRI) for their encouragement. M. McKubre is appreciated for discussions of the (SRI/EPRI) data and for his encouragement. ENECO (formerly FEAT) (Salt Lake City, UT) and Proteus Processes and Technology, Inc. (Denver, CO) are thanked for their encouragement and financial support. Bernice Gilbert of the Instructional Support Center of the College of Science of Cal Poly (Pomona) is appreciated for her assistance with manuscript preparation. My son, Roger, and R. Eagleton are appreciated for their help with number crunching of

a "black box" nature. Finally, my colleague, R. Eagleton is especially thanked for his encouragement, help with manuscript preparation, and for serving as a sounding board for my ideas.

**References:**

1. T. Boyer, Phys. Rev. D, **11**, 790 (1975).
2. T. Boyer, Phys. Rev. D, **11**, 809 (1975).
3. H. Puthoff, "Ground State of Hydrogen as a Zero-Point-Fluctuation Determined State", Phys. Rev. D, **35**, 3266 (1987).
4. T. Boyer, Ann. Phys. (N.Y.), **56**, 474 (1970).
5. M. Fleischmann and S. Pons, "Electrochemically Induced Nuclear Fusion of Deuterium", J. Electroanal. Chem., **261**, 301 (1989).
6. M. Fleischmann and S. Pons, "Calorimetry of the PD ED20 System: from Simplicity via Complications to Simplicity", Proc. 3-ICCF, 47 (1993).
7. M. McKubre, S. Crouch-Baker, A. Riley, S. Smedley and F. Tanzella, "Excess Power Observations in Electrochemical Studies of the D/Pd System; the Influence of Loading," Proc. Third Intl. Conf. on Cold Fusion (hereafter: Proc.3-ICCF), Universal Academy Press, Inc. (Tokyo), 5 (1993).
8. R. Mills and K. Kneizys, "Excess Heat Production by the Electrolysis of an Aqueous Potassium Carbonate Electrolyte and the Implications for Cold Fusion", Fusion Technol., **19**, 1991.
9. M. Miles, R. Bush, G. Ostrom, and J. Lagowski, "Heat and Helium Production in Cold Fusion Experiments", Proceedings of the Second Annual Conference On Cold Fusion, 363 (1991).
10. R. Bush, "A Light Water Excess Heat Reaction Suggests That 'Cold Fusion' May Be 'Alkali-Hydrogen Fusion'", Fusion Technol, **22**, 301 (1992).
11. R. Notoya and M. Enyo, "Excess Heat Production in Electrolysis of Potassium Carbonate Solution with Nickel Electrodes", Proc. 3-ICCF, 421 (1993)
12. R. Bush and R. Eagleton, "A Calorimetric Study of the Excess Heat Effect in Thin Films of Palladium," delivered by Bush at the Second Annual Conference on Cold Fusion, June 29-July 4, 1991, Como, Italy.
13. K. Kunimatsu, N. Hasegawa, A. Kubota, N. Imai, M. Ishikawa, H. Akita, and Y. Tsuchida (IMRA), "Deuterium Loading Ratio and Excess Heat Generation during Electrolysis of Heavy Water by a Palladium Cathode in a Closed Cell Using a Partially Immersed Fuel Cell Anode", Proc.3-ICCF, 31 (1993).
14. M. Fleischmann and S. Pons, "Heat After Death," Proc. 4- ICCF, 1994.
15. J. Bockris, Remarks at 2- ICCF, Como, Italy, June 29-July 4, 1991.
16. J. Jackson, Phys. Rev., **106**, 330 (1957).
17. C. van Sichlen and S. Jones, J. Phys., G **12**, 213 (1966).
18. C. Walling and J. Simons, "Two Innocent Chemists Look at Cold Fusion", J. Phys. Chem., **93**, 4693 (1989).
19. M. McKubre, S.R.I., International, Private communication, November 1993.
20. D. Coupland, M. Doyle, J. Jenkins, J. Notton, R. Potter, and D. Thompson, "Some Observations Related to the Presence of Hydrogen and Deuterium in Palladium", Proc. 3- ICCF, 275, 1993.

21. R. Bush, "Cold 'Fusion': The Transmission Resonance Model Fits Data on Excess Heat, Predicts Optimal Trigger Points, and Suggests Nuclear Reaction Scenarios", *Fusion Technol.*, **19**, 313.
22. R. Mills and J. Farrell, The Grand Unified Theory, Science Press, 1989.
23. S. DeBenedetti, Nuclear interactions.
24. R. Bush, "Towards a Nuclear Physics of Condensed Matter", accepted for *Fusion Technol.*, under revision, est. issue: March'94.
25. V. Noninski, "Observation of Excess Energy During the Electrolysis of a Light Water Solution of  $K_2CO_3$ ", *Fusion Technol.*,
26. M. Srinivasan, A. Shyam, T. Sankaranarayanan, M. Bajpai, H. Ramamurthy, U. Mukherjee, M. Krishnan, M. Nayar, and Y. Naik, "Tritium and Excess Heat Generation during Electrolysis of Aqueous Solutions of Alkali Salts with Nickel Cathode", Proc. 3- ICCE, 123, 1993.
27. M. Ragheb and G. Miley, "On the Possibility of Deuteron Disintegration in Electrochemically Compressed  $D^+$  in a Palladium Cathode," *Fusion Technol.*, **16**, 243 (1989).
28. P. Paolo, *Nature*, **338**, 711 (1989).
29. R. Bush, "A Transmission Resonance Model for Cold Fusion", Winter meeting, American Society of Mechanical Engineers, San Francisco, California, Dec. 12, 1989.
30. R. Bush and R. Eagleton, "'Cold Nuclear Fusion': A Hypothetical Model to Probe an Elusive Phenomenon," *J. Fusion Eng.*, **9**, 397 (1990).
31. G. Miley, J. Patel, J. Javedani, H. Hora, J. Kelly, and J. Tompkins, "Multilayer Thin Film Electrodes for Cold Fusion", Proc 3-ICCE, 659 (1993).
32. R. Bush and R. Eagleton, "The Transmission Resonance Model for Cold Fusion in Light Water: I. Correlation of Isotopic and Elemental Evidence with Excess Power", Proc. 3-ICCE, 409 (1993).
33. R. Bush and R. Eagleton, "Experimental Studies Supporting the Transmission Resonance Model for Cold Fusion in Light Water: II. Correlation of X-Ray Emission with Excess Power", Proc. 3-ICCE, 409 (1993).
34. R. Bush and R. Eagleton, "Calorimetric Studies for Several Light Water Electrolytic Cells with Potassium Carbonate and Sodium Carbonate Electrolytes and Nickel Cathodes", Contributed to Proc. 4-ICCF, 1994
35. R. Bush and R. Eagleton, "Strontium Production in Two Electrolytic Cells with Light Water Based Rubidium Carbonate Electrolytes and Nickel Mesh Cathodes", Contributed to Proc. 4-ICCF, 1994
36. R. Bush, "An Electron-Catalyzed Fusion Model (ECFM) Suggests a Unification of Heavy- and Light Water Cold Fusion Phenomena", Manuscript submitted for publication to *Fusion Technology*.
37. T. Passell, EPRI, Private Communication, Winter 1994.

\* 3801 West Temple Avenue, Pomona, CA 91768.

\*\* University of Utah Research Park, 391-B Chipeta Way, Salt Lake City, UT 84108

\*\*\* 1570 Emerson Street, Suite 100, Denver, CO 80218-1450

**FIGURE 1**

15-19

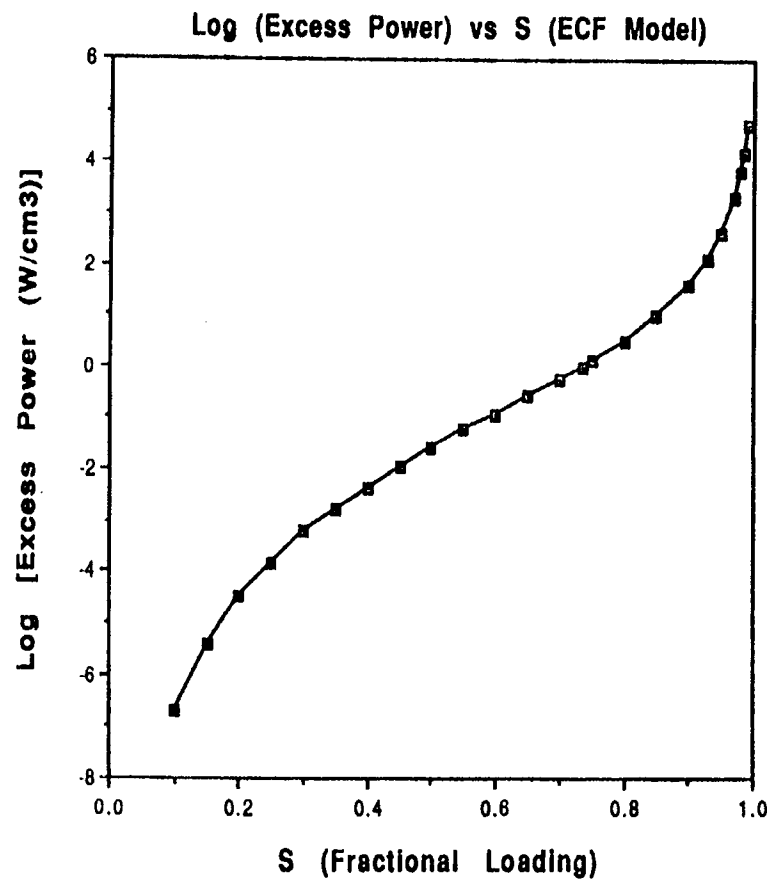


**TABLE I**

**Theoretical Excess Power Predictions  
versus Loading for ECFM  
 $T = 60^\circ\text{C}$ ,  $\theta = 1080\text{K}$**

<b>S (Loading Fraction)</b>	<b>P<sub>exc</sub> [ECFM: Based upon (34)]</b>
0.5	$3.2 \times 10^{-2} \text{ W/cm}^3$
0.55	$7.1 \times 10^{-2} \text{ W/cm}^3$
0.60	$1.5 \times 10^{-1} \text{ W/cm}^3$
0.65	$3.3 \times 10^{-1} \text{ W/cm}^3$
0.70	$7.2 \times 10^{-1} \text{ W/cm}^3$
0.75	$1.67 \text{ W/cm}^3$
0.80	$4.21 \text{ W/cm}^3$
0.85	$12.5 \text{ W/cm}^3$
0.90	$51.5 \text{ W/cm}^3$
0.92	$108.1 \text{ W/cm}^3$
0.94	$274.3 \text{ W/cm}^3$
0.96	$987.2 \text{ W/cm}^3$
0.97	$2,413.3 \text{ W/cm}^3$
0.975	$4,233.4 \text{ W/cm}^3$
0.98	$8,391.7 \text{ W/cm}^3$
0.985	$20,183.4 \text{ W/cm}^3$

**FIGURE 2**

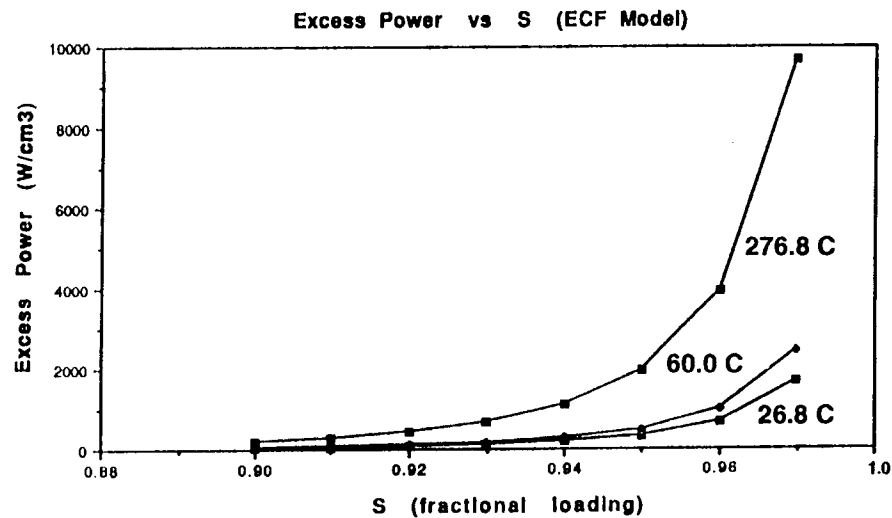


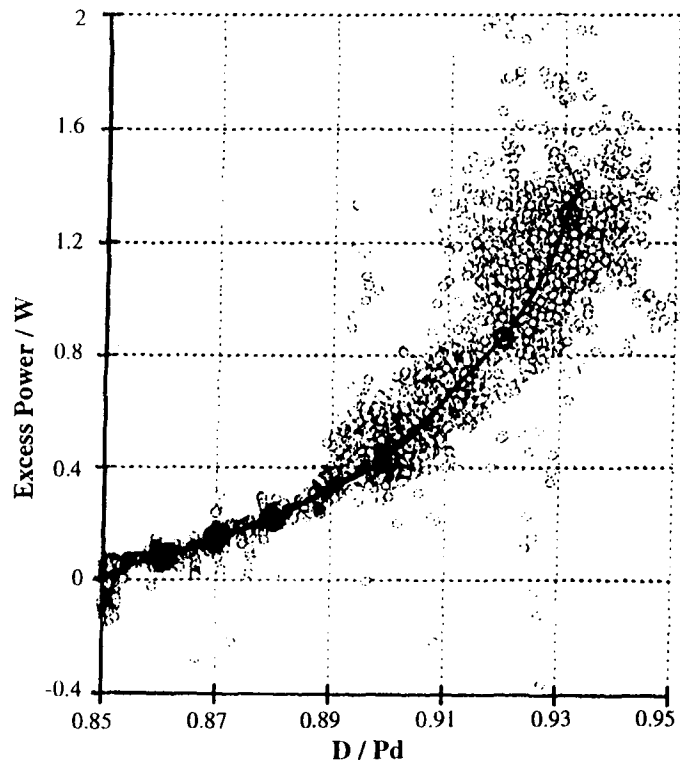
**TABLE 2**

Comparison of ECF Model with Data of McKubre et al.  
(SRI-EPRI)

Loading S	Excess Power (McKubre et al.)	Excess Power (ECFM)
0.86	0.08 W	0.12 W
0.87	0.15 W	0.16 W
0.88	0.26 W	0.22 W
0.90	0.50 W	0.40 W
0.92	0.98 W	0.84 W
0.93	1.30 W	1.30 W

**FIGURE 3**

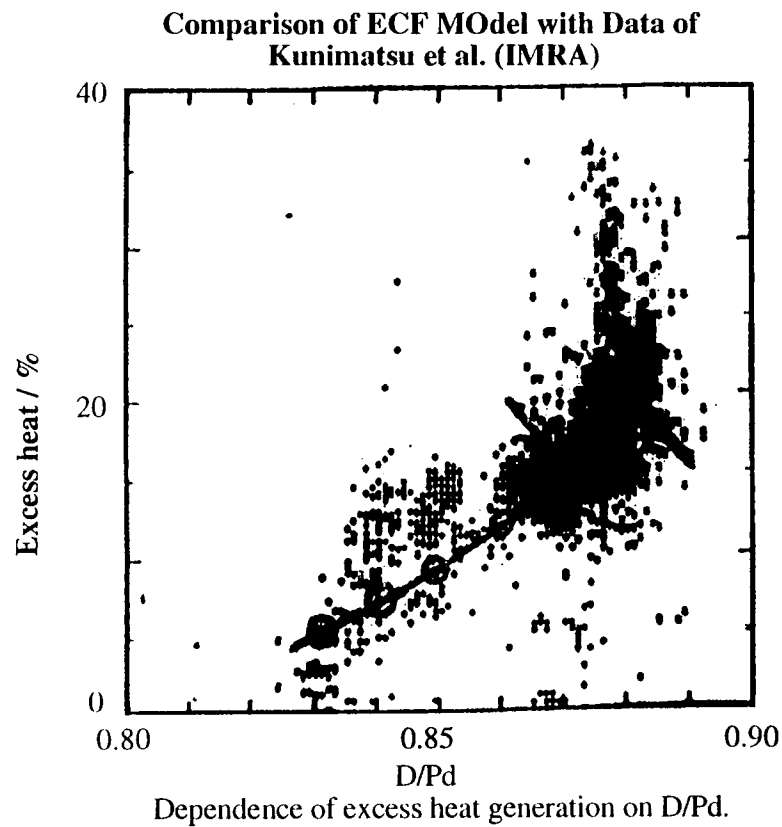
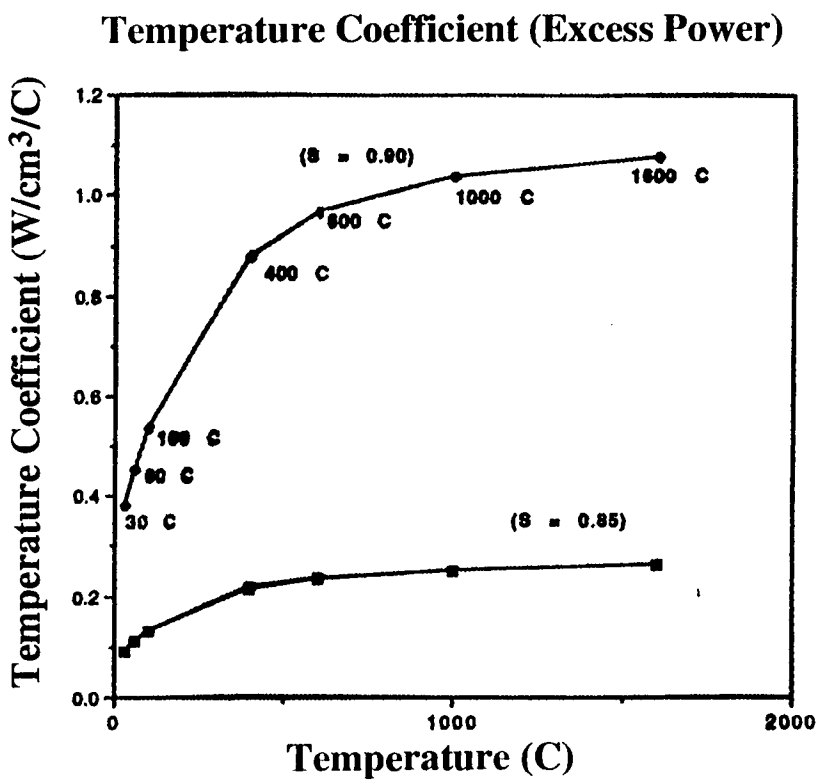
Comparison of ECF Model with Data of McKubre et al. (SRI-EPRI)

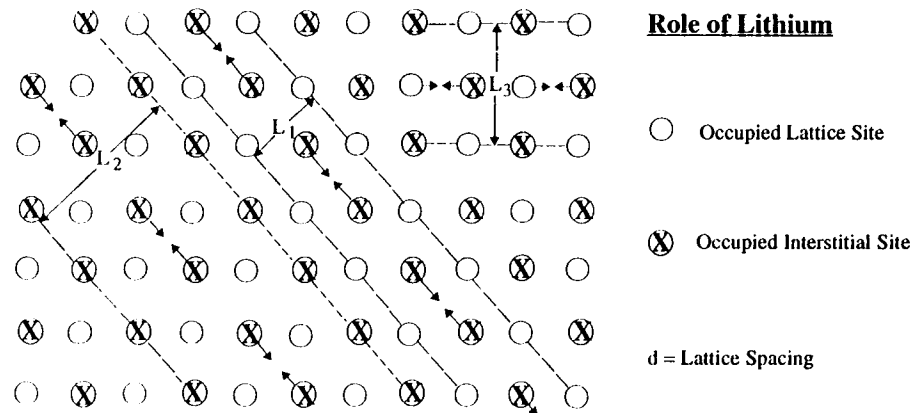


**TABLE 3**

Comparison of ECF Model with Data of Kunimatsu et al. (IMRA)

S	Excess Power/Input Power (Kunimatsu et al.)	Excess Power/Input Power (Theoretical: ECFM)
0.83	3.5%	5.4%
0.84	7.5%	6.8%
0.85	10.2%	8.6%
0.86	11.5%	11.0%
0.87	14.0%	14.3%
0.88	19.0%	19.0%

**FIGURE 4****FIGURE 5**

**FIGURE 6**

$L_1 = d$  [Li - plane Casimir Reflector Separation  
catalyzing:  $(D + D \rightarrow He^4)$ ]

$L_2 = 2d$  [Li = plane Casimir Reflector Separation  
catalyzing:  $(D + D \rightarrow He^4)$ ]

$L_3 = \sqrt{2}d$  [(D - Li) plane Casimir Reflector Separation  
catalyzing:  $(Li^6 + D \rightarrow 2He^4)$  ( $Li^7 + D \rightarrow 2He^4 + n$ )]

**FIGURE 7**

### Relative Tritium Production Rate vs Loading (ECFM)

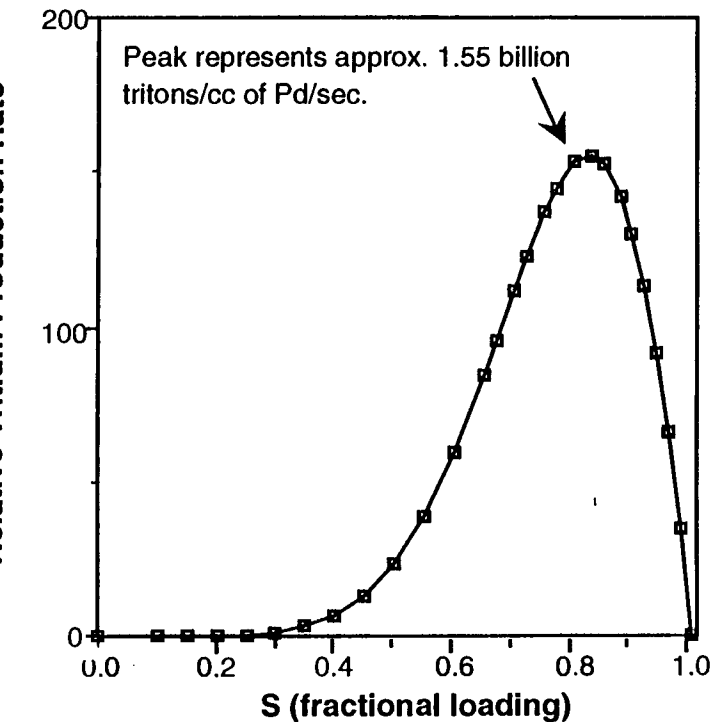


**FIGURE 8**

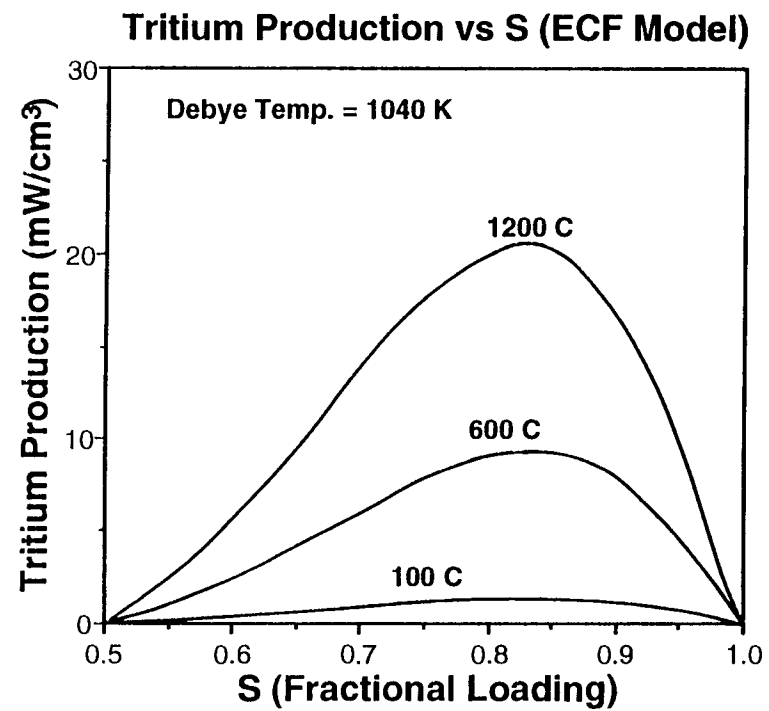
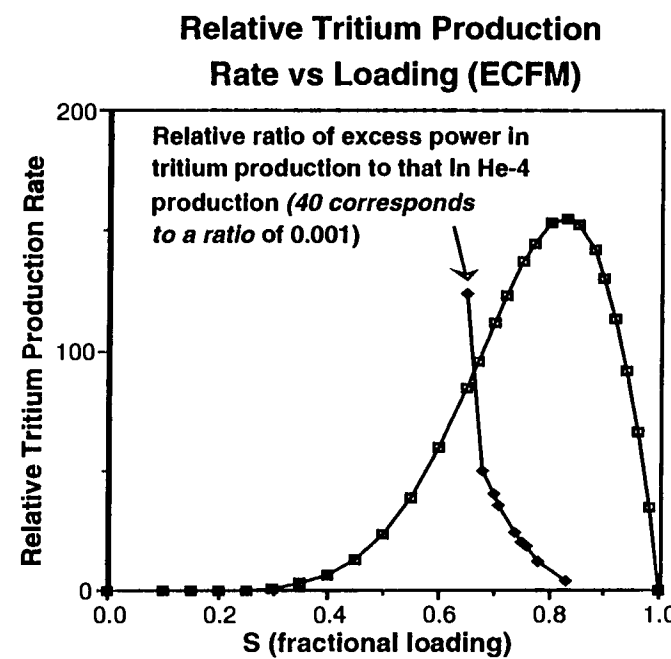


**FIGURE 9**



# DEUTERON WAVES AND COLD FUSION

Norio Yabuuchi  
High Scientific Research Laboratory  
204 Marusen Building  
Marunouchi, Tsu, Mie 514 Japan

## Abstract

Deuterons accumulate as Bose particles in minute vacuum cracks produced in metallic palladium and existing in compounds such as  $\text{SrCO}_3$  and  $\text{CeO}_2$ . The width of these cracks is believed to be approximately two or three times  $0.1 \mu\text{m}$ . When a large number of deuterons collect as Bose particles in these minute cracks, they become a fluid in terms of quantum mechanics, and the configuration of their wave motion is enhanced. When deuterons exist in large numbers in the minute spaces formed by these cracks, their range of movement is restricted considerably, and because Heisenberg's uncertainty principle holds that  $\Delta x \Delta p \geq h$ , the deuterons'  $\Delta x \rightarrow 0$ ,  $\Delta p \rightarrow \infty$ , and the linked movement energy increases. When this occurs, the deuteron waves in the minute cracks are excited and move at an increased frequency of oscillation. If the electrolysis switch is turned on and off while in this state to cause a soliton tsunami in the deuteron wave, the solitons in the deuterons collide with each other and resonate, and because of this low-temperature fusion with a strong tunnel effect takes place in the cracks within the solid.

## Introduction

Metallurgically, 150 hours is required for the deuterons to penetrate the crystalline lattice of the palladium metal as impurities and produce minute occluded vacuum cracks within the solid. Because the attraction between the metal atoms is extremely strong, it can be conjectured that cracks are produced if deuterium invades a particular area with a density of approximately 90%. Because the compounds such as  $\text{SrCO}_3$  and  $\text{CeO}_2$  -- FCC-type hydrogen-absorbing substances similar to palladium -- prepared by Mizuno and Enyo of Hokkaido University are in fact compounds, cracks between the foreign substances form spontaneously, and accordingly no time is required for crack formation.

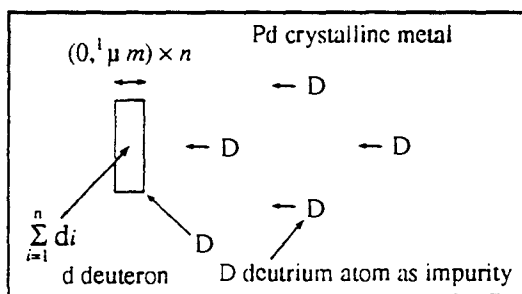


Fig. 1

Fig. 1 shows that when minute cracks exist or are produced in the metal, impurities congregate near the cracks in order to reinforce weak crack areas. This is the Suzuki effect, discovered previously by Suzuki of Tohoku University.

The deuterons as impurities are Bose particles, and therefore possess the following characteristics.

1. Because they do not follow Pauli's exclusion principle, they can exist in large numbers in a quantum state.
2. When they collect in large quantities, their wave motion is strengthened and they exhibit characteristics of phonons.
3. Because they are atomic nuclei, their mass at rest is much larger than that of electrons, and so their heat-motion energy is large and the vacuum cracks correspond to extremely low temperatures; consequently, Bose-Einstein condensation is involved.
4. They exhibit the phenomena of superconductivity and superfluidity.

For these reasons, the deuterons as Bose particles invading the cracks which correspond to a supercooled state first collect in the cracks in large numbers because of the Suzuki effect. At this time the temperature of the metal is lowered slightly.

Next, when the deuterons collecting in the cracks as Bose particles reach a saturated state, their range of movement becomes extremely constricted. That is to say,  $\Delta x$  approaches zero ( $\Delta x \rightarrow 0$ ). When this occurs, Heisenberg's uncertainty principle that  $\Delta x \Delta p \geq h$  holds  $h$  to be a constant, and so the deuteron momentum  $\Delta p$  approaches infinity ( $\Delta p \rightarrow \infty$ ). When the correspondence principle is used to employ classical methods and integrate momentum with velocity,

$$\int mv dv = \frac{1}{2} mv^2 + c \quad (T = \frac{1}{2} mv^2) \quad (1)$$

holds, and the movement energy  $T$  also approaches infinity ( $T \rightarrow \infty$ ), becoming extremely large. By analogy with energy as the same Bose particles, the frequency of oscillation as deuteron waves,  $hv = \frac{1}{2} mv^2$  rises to extremely high levels.

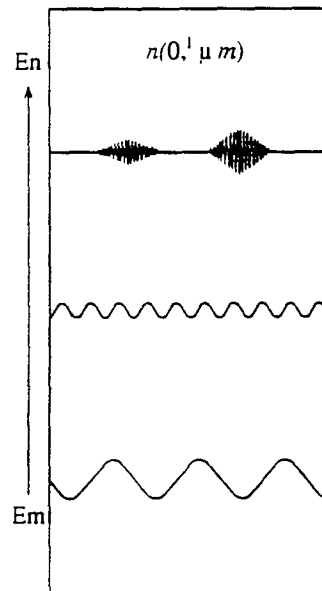


Fig. 2

The collection of deuterons in the cracks as a quantum fluid receives the energy of the lattice vibration, increasing the oscillation frequency of the deuteron wave. As the oscillation frequency grows larger, the velocity of wave motion also increases, and the temperature within the crack rises.

As shown in Fig. 2, enclosing the crack in aluminum in this case strengthens the quantum closure effect, thereby enhancing the reliability of the experiment.

$$\log T = A + B \log v \quad (2)$$

Equation 2 is the Geiger-Nuttall law. According to Max Born, the larger the velocity  $v$  of an alpha particle, the greater is the probability of piercing the nucleus barrier. One condition for the mutual fusion of the deuterons in the crack is therefore fulfilled.

At ICCF-3, the author announced the prediction that the Bose particle deuterons will interact and give rise to superconductivity because electrical current is flowing through the metal and the crack is within an electrical field, and that deuteron waves coalesce to form a compound nucleus (see Fig. 3).

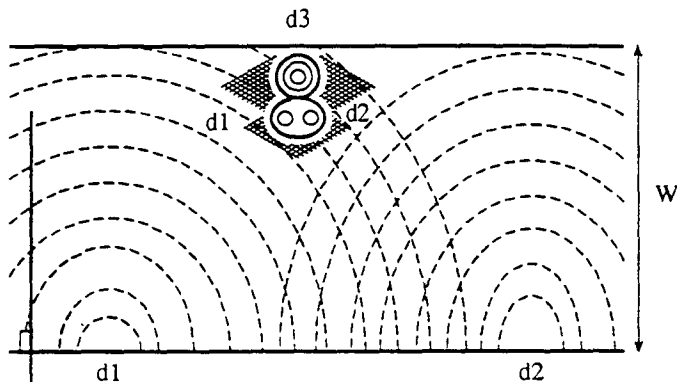


Fig. 3

The Schrödinger equations for two- and three-body reactions, taking the tunnel effect into consideration, are as shown in the following two equations.

As shown in Fig. 3,

$$\begin{aligned} & -\frac{\hbar^2}{2\mu_1} \nabla^2 \Psi_{2d} - \frac{\hbar^2}{2\mu_3} \nabla^2 \Psi_{d3} + U_1 \Psi_{2d} + U_3 \Psi_{d3} \\ & = -\frac{\hbar^2}{2m_n} \nabla^2 \Psi_n - \frac{\hbar^2}{2m_{^3He}} \Psi_{^3He} + U\Psi_n + U\Psi_{^3He} + 3.27 \text{ MeV} \\ & \nabla^2 = \frac{\partial^2}{\partial x^2} + \frac{\partial^2}{\partial y^2} + \frac{\partial^2}{\partial z^2} \end{aligned} \quad (3)$$

2-body reaction

This  $\Psi_{2d}$  is an included state.

$$\begin{aligned}
 & -\left(\frac{\hbar^2}{2\mu_1}\nabla^2 + \frac{\hbar^2}{2\mu_2}\nabla^2\right)\Psi_{2d} + (U_1 + U_2)\Psi_{2d} + w\Psi_{2d} - \left(\frac{\hbar^2}{2\mu_3}\nabla^2\right)\Psi_{d3} + (U_3)\Psi_{d3} \\
 & = -\frac{\hbar^2}{2m_T}\nabla^2\Psi_T + U\Psi_T - \frac{\hbar^2}{2m_{^3He}}\nabla^2\Psi_{^3He} + U\Psi_{^3He} + 9.5\text{MeV}
 \end{aligned} \tag{4}$$

This  $\Psi_{2d}$  is a kind of compound nucleus state.

3-body reaction

Switching the power to the device on and off is a required condition for the reactions. According to Drude's theory, turning the power on and off can cause a momentary over-current in the electrical field of the crack. When this takes place, as shown in the upper part of Fig. 2, solitons which do not decay simply are generated, and the collision of one soliton with another achieves nuclear fusion. If two- and three-body reactions occur within a narrow crack, four-body reactions can subsequently be caused. Although it has not yet been quantized, the anlinear Schrödinger equation is expressed as follows. In the future, it will be possible to express Equations 3 and 4 as Equation 5.

$$\begin{aligned}
 iA\tau + pA_{\xi\xi} + q - |A|^2 A &= 0 \\
 A = A_0 \operatorname{sech} \left( \sqrt{\frac{q}{2p}} A_0 \xi \right) \exp(iqA_0^2 \tau / 2)
 \end{aligned} \tag{5}$$

Fig. 4 shows the soliton in detail.

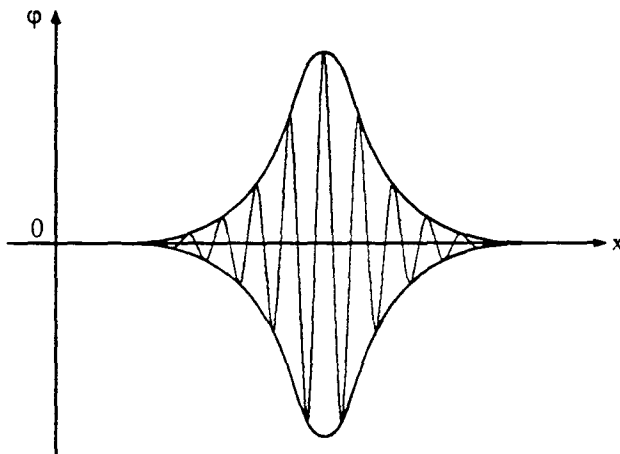


Fig. 4

## References

- Takahashi et al., A.E.S. of Japan, 1993 Spring Conference C33.
- Kamata et al., A.E.S. of Japan 1993, Spring Conference C32.
- Taniguchi, A.E.S. of Japan, 1993 Spring Conference C29.
- Yabuuchi A.E.S. of Japan, 1992 Spring Conference D31, 1992 Fall Conference A1, 1993 Spring Conference C28.
- M. Born, Atomic Physics, VII, §1.
- Yoshida, Plasma Science and Nuclear Fusion Research.
- Yabuuchi, Frontiers of Cold Fusion, No. 4 22PI-26.

## I. DEUTERON INTERACTION IN UNITARY QUANTUM THEORY

Lev G. Sapogin

Department of Physics, Technical University (MADI),  
Leningradsky prospect 64, A-319, 125829, Moscow, Russia

### **Abstract**

The Unitary Quantum theory regards charged particles interaction. It is shown that the distance to which the particles can approach each other is dependent upon the wave function phase not only upon the energy, which is not discussed in the conventional quantum theory.

### **Introduction**

A unitary quantum theory (UQT) with a new perspective on the problem of particle interaction was developed in the author's papers (1-8). According to this theory any elementary particle is a condensed bunch of some unitary field travelling in a packet of partial waves. Dispersion and nonlinear nature of the process spreads the wave packet periodically across space and assembles it; the envelope of the process happens to coincide with the de Broglie wave. The formalism of the theory amounts to the relativistically invariant system of 32 non-linear integral-differential equations from which relativistic quantum mechanics in the form of Dirac's equation follows. On the other hand Hamilton-Jacobi's relativistic mechanics follows strictly mathematically from the theory. We can solve this problem in a different way though for this purpose we must sacrifice part of the ideology of the UQT - refraining from dividing particles (wave packets). As a matter of fact we can do this if the energies are low when the interactions are elastic though there are exceptions. I will show you that despite the roughness of the approach the results may be

outstanding. The approximate solution of some of the UQT equations (7,8) gives the value of the electric charge alongside with that of a fine structure constant, the data being in a very good agreement with experimental results. This achievement allows to give a heuristic description of a moving particle as a charge oscillation with the de Broglie wave frequency. In other words in all macro experiments the effective value of a charge is measured, the oscillation being unnoticeable.

### Equation of Motion

Newton equation for a moving mass point with an electric charge  $q$  and a modified equation for the electric force acting on the electric charge oscillating at the de Broglie wave frequency in the field with intensity  $E$  are suggested as the model basic equations:

$$(1) \quad \mathbf{F} = m \ddot{\mathbf{r}} = qE 2\cos^2 \varphi, \quad \varphi = \frac{m \dot{\mathbf{r}}^2}{2 \hbar} t - \frac{m}{\hbar} \dot{\mathbf{r}} \cdot \mathbf{r} + \varphi_0,$$

where  $E = -\nabla V$ ,  $V(\mathbf{r})$  is a potential. Such approach is a natural outcome of (8). Further on only spherically symmetrical potentials will be considered.

To simplify the non-linear equation given let us introduce scale coefficients for coordinates, time and velocity:  $\mathbf{r}=S_r \mathbf{r}_s$ ,  $t=S_t t_s$  and  $S_v=S_r/S_t$ , respectively. Assuming  $mS_r^2/\hbar S_t=1$ ,  $k=qmS_v^3/\hbar^2$  we will obtain the following normalized equation (omitting "s" indices):

$$(2) \quad \ddot{\mathbf{r}} = kE 2\cos^2(\dot{\mathbf{r}}^2 t/2 - \dot{\mathbf{r}} \cdot \mathbf{r} + \varphi_0)$$

which despite the apparent simplicity of the initial premises can drive any mathematician to deep despair. As the first scale coefficients relation provided a simplified expression for the phase, the second relation unambiguously describing  $S_r$  and  $S_t$  will be chosen proceeding from the simplified expression for the potential examined. Let us

consider the main properties of equations (1) and (2). For simplicity's sake it will be assumed that the particle can move along the axis of  $\mathbf{r}=(x, 0, 0)$  in the field of  $\mathbf{E}(\mathbf{r})=(E(x), 0, 0)$ .

### Fixed charge

If  $x=0$ , then the electrostatic force is  $F = kE^2\cos^2\varphi_0$

and  $\int_{\text{c}}^{T\pi} F d\varphi_0 / \pi = F_{\text{clas}}$  is classical electrostatic force.

Averaging a great number of elementary charges results in a force equal to  $F_{\text{clas}}$ .

### Uniformly accelerated motion

If  $E(x)=E>0$  is a uniform constant field, then equation (2) has a particular solution  $x(t)=at^2/2$ , where  $a = kE^2\cos^2\varphi_0$

and  $\int_{\text{c}}^{T\pi} ad\varphi_0 / \pi = A$  is classical particle acceleration aligned

with the uniform constant field. If the uniform field acts in a  $D$ -size range, the accelerated particle kinetic

energy is equal to  $T=maD$  and  $\int_{\text{c}}^{T\pi} T d\varphi_0 / \pi = T_{\text{clas}}$  is classical kinetic energy. As  $v(\varphi_0) = 2aD = v(0) |\cos\varphi_0|$ , then at the

uniform phase distribution  $\varphi_0=0..T\pi$  probability density of velocity distribution after acceleration is equal to  $2/\pi [v(0)^2 - v(\varphi_0)^2]^{1/2}$ . Motion studies at the constant phase of

$= \text{const}$  show that  $\dot{x} = (x/t)^2 + [(x/t) - 2(\varphi - \varphi_0)/t]^{1/2}$  and the particular solutions will be  $x(t) \sim t^2$  (linearly accelerated) and  $x(t) \sim \sqrt{t}$  (diffusive). Within the force field the particle will move uniformly (due to inertia) at  $\varphi \approx \frac{\pi}{2}$  accelerating in all other cases. Such non-uniform motion in respect to average values gives rise to relations similar to uncertainty quantum relations.

### Tunneling

If we take up the problem of particle/bell-shaped potential interaction, all known qualitative quantum-mechanical implications will remain valid. This results from the fact that in a potential there is a repelling part similar to the potential step considered above and an accelerating part which does not hinder motion. But, unlike quantum mechanics, there is no above barrier reflection in the model at velocities  $v$  over certain threshold value. As an example, we will consider the way the particle passes a symmetrical potential barrier of the Gaussian type  $V(x)=\exp[-(x/\sigma^2)]$ . The particle motion should meet equation  $\ddot{x}=2(x/\sigma^2)\exp[-(x/\sigma)^2] 2\cos^2(\dot{x} t^2/2-\dot{x}x+\varphi_0)$ , with the initial conditions of  $x(0)=-4\sigma$ ,  $\dot{x}(0)=v$ ,  $\varphi_0=0.. \pi$ . Fig.1 shows probability  $P(v)$  of particles passing through the potential barrier vs velocity (energy)  $v$  and uniform initial phase distribution  $=0.. \pi$ . Fig.2 shows probabilities  $P(\sigma)$  of a particle passing through potential barrier vs tunneling distance. It can be seen that the curve has resonance peaks at small  $v_c$ . An increase in velocity  $v_c$  leads to threshold effect when all the particles pass through a sufficiently wide barrier without reflection. The regularities observed in passing through potential barrier are similar to quantum-mechanical predictions. But in quantum mechanics particle passage probability is proportional to its squared wave function modulus and is entirely independent of the phase. So it is apt to ask why some particles reflect from the barrier while some others pass through it. Our model answers the question: the probability of a particle passing through the barrier is dependent on the particle phase. If the phase is such that the charge is small, the particle will fly through the barrier without "noticing" it.

### Particle in the parabolic well

Let  $V(x)=fx^2$ ,  $E(x)=-2fx$ . We'll assume  $2kf=1$  and start examining particle behavior in such a potential well. The initial equation is  $\ddot{x}=-x^2\cos^2(\dot{x}^2 t^2/2-\dot{x}x+\varphi_0)$ , the initial

conditions are  $x(0)=0$ ,  $\dot{x}(0)=v_0$ ,  $\gamma=0..77$ . Numerical analysis of the equation leads to four solution types:

1. Unstable periodic solutions. When velocity  $v$  goes down, oscillation period approaches  $\sqrt{2\pi}$  asymptotically, as is to be expected.
2. Irregular dying particle oscillation in a potential well. For some initial values the particle oscillation amplitude first goes up and then down.
3. Irregular oscillations with an infinitely increasing amplitude. For some initial values the amplitude of particle oscillations first goes down and then infinitely up.
4. Diffusion at which the particle can be tunneling through the potential for an indefinitely long time is similar to the particle behavior in the potential step problem. With a limited depth parameter the particle will leave it by all means, though it might spend sufficiently long time doing it. Periodic and irregular oscillation states can be defined as discrete and continuous (blurred) zones, respectively.

#### **Above barrier reflection from a potential well**

In considering particles flying through the potential well the following phenomena are observed. Unlike quantum mechanics there is a threshold velocity for flying particles, above which all the particles fly over the potential well without reflection. If the initial velocity  $v_0$  is under the threshold value, the particle will get into a potential well and will either tunnel through the barrier or start oscillating in the well. It can "jump out" of the well and go on with its motion (reflection or flight through) or form a bound state similar to the one discussed in the parabolic well problem.

#### **Deuteron interaction**

Let's consider two charged particles (deuterons) moving towards each other along an  $X$  axis. Let's choose a starting point on the reference frame in the center of one of the

particles with a (charge  $Q$ ). Let the second particle with a charge  $q$  and velocity  $V_0$  moves from a coordinate point  $X_0$ . If opposite beams collide we can arrive at to the above-state situation having introduced the normalized mass. The particles are expected to approach each other at a distance of  $X_{clas}$  where their velocity will drop down to zero and then start to accelerate again. In accordance with the classic Coulomb's law this distance can be calculated by the expression:

$$(3) \quad X_{clas} = \frac{2QqX_0}{\frac{2}{m} + \frac{m}{2} X_0 V_0}$$

If the charge  $q$  oscillates by the de Broglie wave frequency, equation moving could be written in the Gauss's system as

$$(4) \quad m \ddot{X} = \frac{2Qq \cos^2(mXt/\hbar - m\dot{X}x/\hbar + \varphi_0)}{X^2}$$

The factor 2 approximately regards the effective value of the charge  $q$ . In a natural system of units  $m=1, c=1, \hbar=1$ . The value  $\varphi_0$  - is the initial phase. Then we obtain an equation of the type

$$(5) \quad \ddot{X} = \frac{k}{X} \cos^2(\frac{k}{2}t - \frac{2}{2} \dot{X}x + \varphi_0), \text{ where } k = 2Qq;$$

#### **The validity of equation**

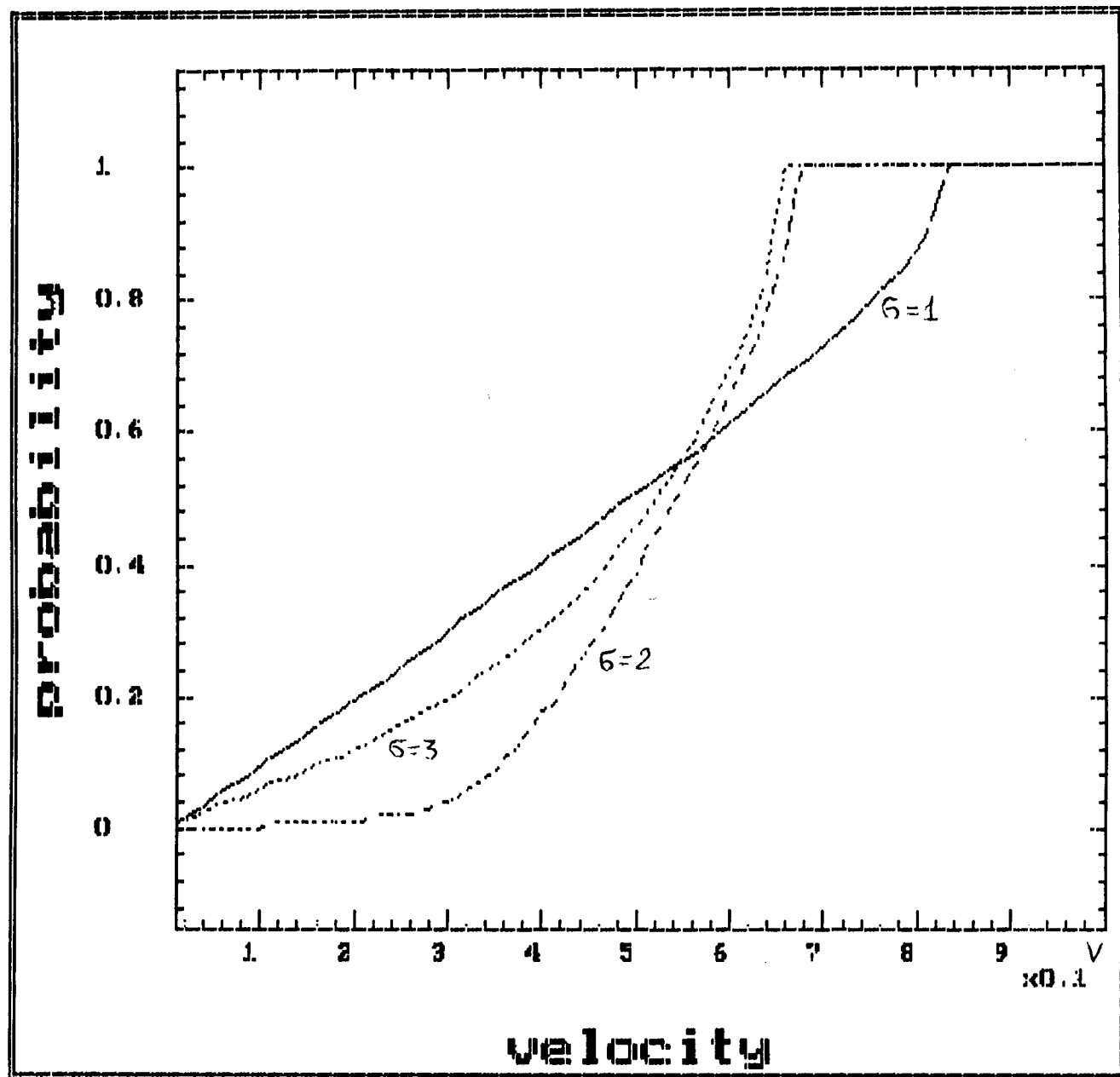
To clarify the physical situation the digital computation of equation 5 was done by a computer, the initial conditions being provided to make it quicker: with  $X_0=10$ , different

values for the initial velocity and phase variations from 0- $\pi$ . It was discovered that the laws of energy and momentum conservation was only partially observed. In case of particle reflection at a distance of  $X_0$  its velocity ranged about 20-30% higher or lower, respectively. But if we sum up the incident and reflected particles throughout all the phases, the entire energy value will be preserved. As was expected the effect of particle accelerating occurred at the largest value of the charge. On the other hand at the last stage of moderating (for a number value of velocity and phase values) we could observe a fantastic process: the velocity and charge being too small, the repulsive force is also small. This phenomenon can continue for quite a long period of time and the particle has an additional opportunity to penetrate the repulsive potential for an indefinite depth. All that reminds very much of a furtive clandestine penetration upon the enemy territory. This outstanding phenomenon occurs only within some phase range close to  $\frac{\pi}{2}$  and it can be conveniently called the "phase precipice" as is shown on fig.3. The relative depth of the "phase precipice" equals to  $X_{min}/X_{clas}=1E-6-1e-9$  and is independent on the energy. Under very small energies ( $0.01-1eV$ ) the precipice is exist but it is narrow ( $1E-10-1E-8$ ) and not easily traced in terms of digital computation. For instance, the phase change in  $1E-10$  may eliminate the precipice. As a matter of fact energy and momentum conservation laws are not observed for an individual particle but they are related by the relations of uncertainty type, though of a different origin. The regularities observed in passing through potential barrier are similar to quantum-mechanical predictions. But in quantum mechanics particle passage probability is proportional to its squared wave function modulus and is entirely independent of the phase. It would only be fair to ask why some particles reflect from the barrier while some others pass through it. My model answers the question: it is because the probability of a particle passing through the barrier depend on the particle phase. If the phase is such that the charge is small the particle will fly through the barrier without "noticing" it. Now the quantum mechanics may be slightly kicked notwithstanding its attractiveness. I've

never understood why God has not used the phase in any way in his quantum Universe though he hasn't ever been noticed making any surpluses before. At least now it is obvious that the phase might be used like that, but nobody has ever guessed it.

### **References**

1. L. G. Sapogin. "Unitary Field and Quantum Mechanics." Investigation of systems. (in Russian, Vladivostok), No. 2, p. 54(1973).
2. L. G. Sapogin. "On Unitary Quantum Mechanics." Nuovo Cimento. vol. 53A, No. 2, p. 251(1979)
3. L. G. Sapogin. "An Unitary Quantum Field Theory," Annales de la Fondation Louis de Broglie. vol. 5, No. 4, 285(1980)
4. L. G. Sapogin. "A Statistical Theory of Measurements in Unitary Quantum Mechanics." Nuovo Cimento. vol. 70B, No. 1, p. 80(1982).
5. L. G. Sapogin. "A Statistical Theory of the Detector in Unitary Quantum Mechanics." Nuovo Cimento. vol. 71B, No. 3, p. 246(1982).
6. V. A. Boichenko, L. G. Sapogin. "On the Equation of the Unitary Quantum Theory." Annales de la Fondation Louis de Broglie. vol. 9, No. 3, p. 221(1984).
7. L. G. Sapogin, V. A. Boichenko. "On the Solution of One Nonlinear Equation." Nuovo Cimento. vol. 102B, No. 4, p. 433(1988).
8. L. G. Sapogin, V. A. Boichenko. "On the Charge and Mass of Particles in Unitary Quantum Theory." Nuovo Cimento. vol. 104A, No. 10, p. 1483(1991).



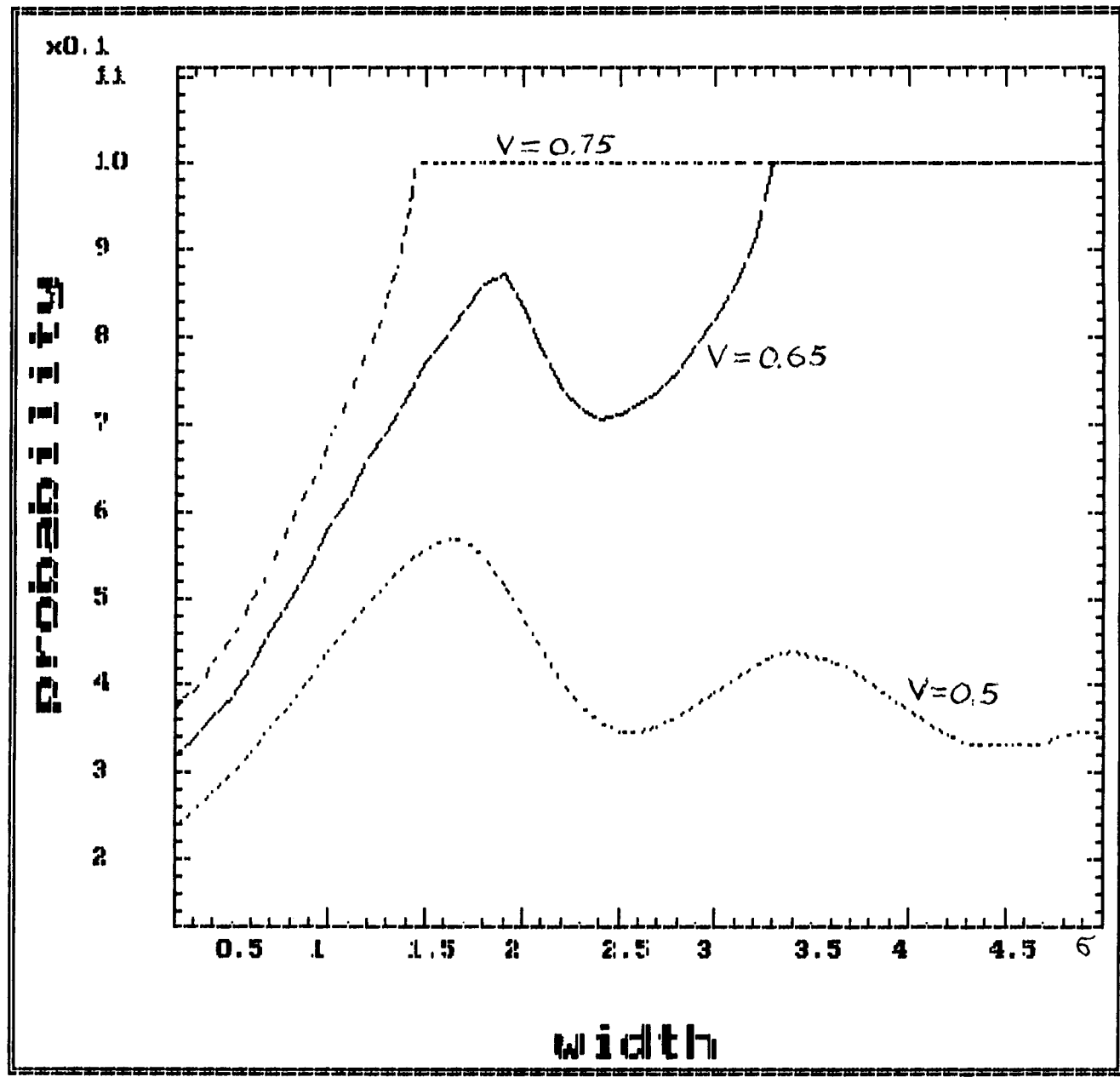
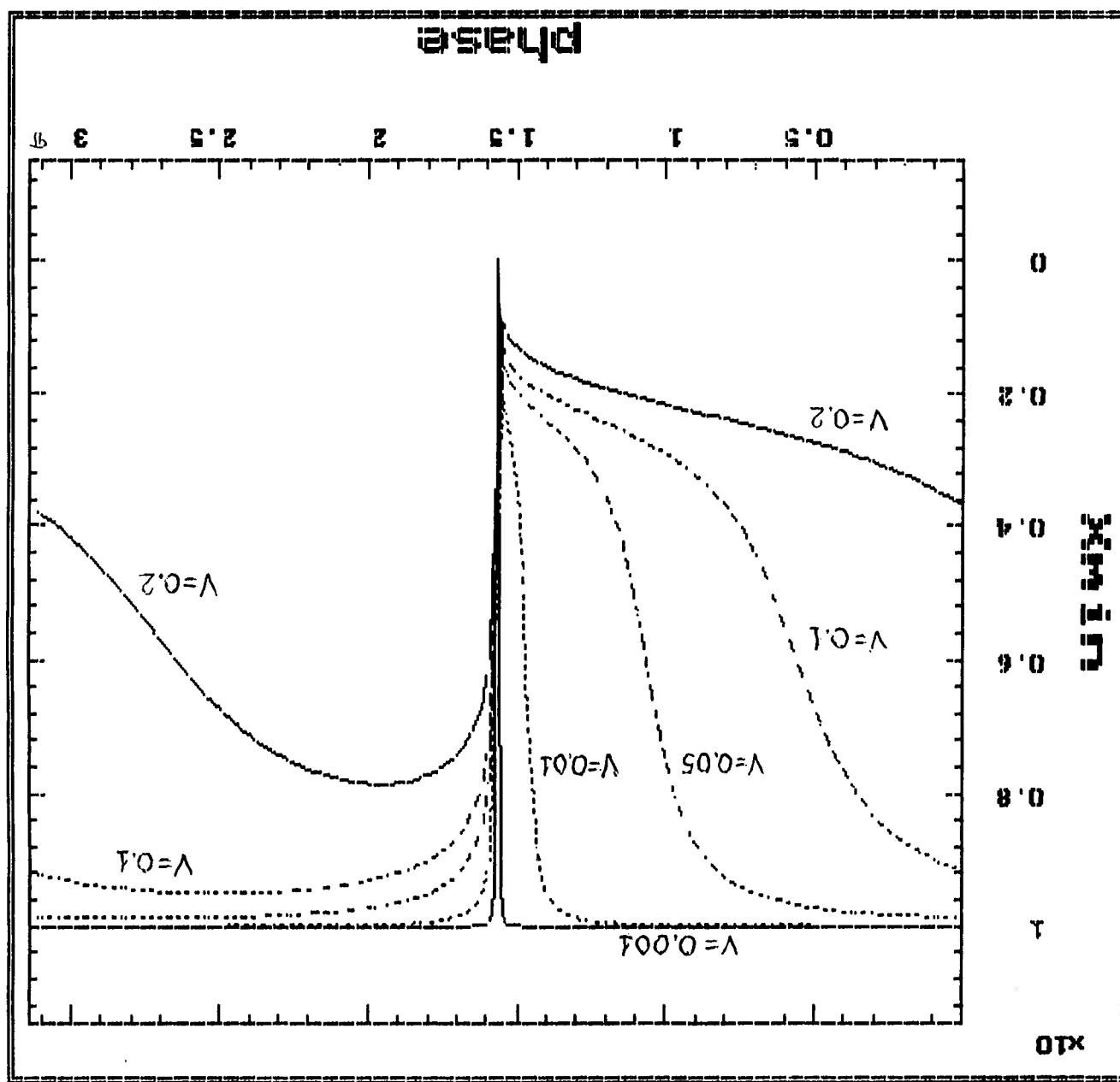


FIG. 3





## **II. ON THE MECHANISMS OF COLD NUCLEAR FUSION**

Lev. G. Sapogin

Dept. of Physics, Technical University (MADI)  
Leningradsky av. 64, A-319, 125829 Moscow, Russia

### **Abstracts**

On the basis of observing deuterons interaction the unitary quantum theory considers the problem of cold nuclear fusion. It is shown that, apparently, this approach has the advantage of being able to describe all the basic experimental facts in cold nuclear fusion.

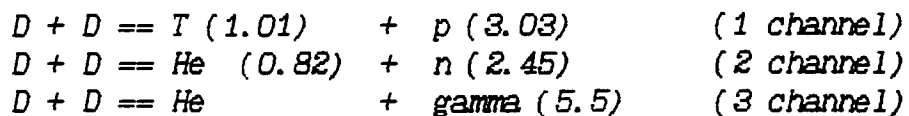
### **Introduction**

Let us try to consider from these viewpoint the epoch-making experiments of Fleischmann and Pons, the John's group and other. The results of this works can be briefly summarized as follows: the cold nuclear fusion (CNF) phenomenon exists but nobody knows how to explain it. In spite of the fact that the number of fantastic theories explaining CNF mechanisms increases, most of them seem unbelievable. Let us analyze some of the above-mentioned experiments: increases, but only few believe them.

### **Principle of CNF**

Let us give some estimation of these experiments. The minimum classical distance  $X_{\text{clas}}$ , at which deuteron nuclei may approach each other, equals  $X_{\text{clas}}=14(A)/E(\text{eV})$ . The deuteron nucleus size is about  $4E-12 \text{ cm}$ , the nuclear force range is  $4E-13 \text{ cm}$  (deuteron is very friable). The solution of equation 5 from (1) for that initial conditions  $X_0=34$  and  $\gamma_0=1.57079632$  is shown, that **nuclear reactions can occur with the energy more than 1 eV**. If the phase  $\gamma_0$  approximates  $\pi/2$  the energy value may decrease hundreds times. The fig.1 shows the dependence of  $X_{\min}$  on the energy in fixed phase.

One shouldn't think that the phase precipice phenomenon causes the nuclear reaction in the wide range of the precipice. The Coulomb's repulsion at this moment may happen be less than the attraction of small interaction, but nobody knows when it may happen, because the phase may similarly influence the nuclear forces value. Besides, sometimes the particle arrives at the turning point  $X_{min}$  having "thinned" sufficiently. Will it be able to take part in full-scale nuclear reaction or will it pass through rapidly as an electron usually does when in an s-atom state? But there exist the narrow ranges of the phase, where particle charge increases rapidly and the particle accelerates after stopping. The charge may amount to maximum value in the nuclear force action range. Apparently narrow phase range is responsible for the cold nuclear fusion. These data are essential for the development of new-generation nuclear reactors. Interaction D-D takes place in three channels (energy in MeV):

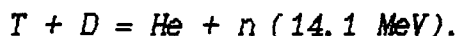


All of them are exothermic, have no threshold (now it is clear why) and may occur even at very small relative energies. For example in  $D_2$  molecule the balance distance between atoms 0.74A, in conventional theory the combination rate being very slow  $-1E-64 \text{ s}^{-1}$ . But at a distance 0.1A this value is sufficient for cold fusion explanation according to the classical theory.

The rate of reaction ratio for tritium and neutron channels is close to unit according to classical theory, but in numerous cold fusion experiments this ratio equals approximately  $1E9$  with a high experimental reproduction. Let us try explain the cause of the phenomenon. For a small velocity in a phase precipice the nuclear forces of attraction act on nucleons and the electrostatic forces of repulsion act on protons. Two deuterons are turned with the neutron parts facing each other on influence of these

forces. The nuclear forces saturation after the neutrons approach each other. So the proton connections grow weak and because of the electrostatic repulsion one of them leaves the nuclear system. It is like Oppenheimer-Philips effect. It is easy to calculate that for  $E > 10$  KeV deuterons have no time for turning, in this case the 2-nd and 3-rd channel reactions may occur.

The increase of the neutron channel may be due to the secondary neutrons birth in reaction



In case of rich deuterons environment the majority of the emerged tritons are transformed into neutrons by 5 barn cross-section reaction for  $E=70$  KeV. According to the estimations (3) the number of such secondary neutrons to the unit triton equals to  $7.9E-12$ ;  $1.7E-9$ ;  $2.7E-6$  for  $E = 10$ ;  $20$  and  $100$  KeV accordingly. So predominance  $T/n=1E6$  may be expected in those reactions, where triton emerges with the energy of  $E < 40$  KeV.

It should be noted that there is still a possibility to explain one of the nuclear physics anomaly, the existence of which they don't seem to notice. For nucleon energy 1 MeV,  $v=1E9$  cm/s,  $R_{nuclear}=1E-12$  cm  $t=R/v=1E-21$  s. the time range of nuclear disintegration is anomalic large -  $1E-14$  s. Apparently for the nuclear forces the phase precipice mechanism is working also, i.e. the nucleon is very slowly crawling into the nuclear system.

All the programs for controllable nuclear fusion are based on heating and squeezing of the reacting material. In spite of the progress achieved in this field Dr. Alan Gibson, the head of the research in England, said that it would take at least 50 years to build the first demonstrative model of the reactor. It should be noted that such a reactor would be extremely sophisticated, expensive and harmful to ecology.

No classic approach to this problem has hitherto given any positive results and this, in spite of the billions of dollars spend and the enormous number of research workers

and other personnel employed (physicists, engineers, managers, laboratory staff etc.). It is only natural that such a huge army of scientific workers should potentially antagonize any other alternative project of nuclear fusion. It has been noticed that the "creativity" of any scientific theory stands in direct proportion to the number of researchers employed and the money spent.

The reaction itself was experimentally confirmed in 1989 by M. Fleischmann and S. Pons in the US, where the two researchers were met with a strong opposition.

#### **Perspective**

All the programs for controlled thermonuclear fusion are defined by the adjective "controlled", though in reality there is no control as such. For this reason the provided quantity of reaction material is taken extremely small. For instance, a lithium deuteride ball is no more than 1-2 mm in diameter. The direct approach being used the fusion process is absolutely natural, because there are no means to influence this process in quantum mechanics. UQT provided us with such an opportunity. UQT equations show that the minimum distance to which the deuterons may approach each other depends greatly on the wave function phase. **The future of the really controllable nuclear fusion system is not in primitive squeezing and heating of the material, but in collision of small energy nuclei with fine adjustment of wave function phase.**

In principle, this can be achieved by applying the external controlling electromagnetic field upon the reacting system that contains quasi fixed ordered deuterium atoms and free (unbound) deuterons. The same properties may be also manifested by the special geometry of atomic frames. The diffractional scattering of deuteron flow on such frames will result in deuteron automatic selection in accordance with their energy and phasing. In this case the energy of colliding nuclei may be less than 1 eV.

Analysis of experiments so far made in CNF produces an impression that the reaction is effective only in cases of at least weak phasing, determined by either the inner structure of the environment or applied variable external fields.

Apparently, in the course of their electrochemical experimentation M.Fleischmann and S.Pons discovered this ordered system and observed occasional incomplete phasing that explained the experimental results.

In future reactor models, in contrast with the existing ones, only a very small portion of all deuterons will react simultaneously, their automatic selection being carried out by phase correlations. This will lead to discharging of small quantities of energy in a prolonged period of time until the reacting light nuclei source is exhausted. Doubtless, that such kind of nuclear fusion could be rightfully defined as "controllable".

### **Conclusion**

Is it possible that the considered Vendee and Austerlitz of the eq. 3 will collide with Waterloo in Bohr-Sommerfeld problem and other cases, moreover taking into consideration my reasonable ignoring the mass? What happened with the mass under the changing of the wave function phase? I can't give precise answer. It has been assumed implicitly, that the mass is either constant or a specific charge which depends on the phase.

An application of the eq. 3, which was done for D-D interaction ad hoc doesn't result in failure of Bohr-Sommerfeld and scattering models.

The states with  $l>0$  correspond to the electron trajectory similar to some beautiful flowers of buttercup sort. All results remind very much of the radial wave function, divided by spheric harmonics and can be used for good amusement at the computer for long nights.

If there is calculate the electric field intensity  $E(\mathbf{r})$  for the spatial charge in the describing of the equation resolution of the UQT (1) and is observed the problem about the electron, passing through such a field (s-state), so it is arisen the typical pendulum orbits, passing through the nucleus. That orbits had been excluded in the classic Bohr-Sommerfeld model as absurd. As all of that doesn't insert somewhat new knowledges in atom physics, but has only art interest, so we shall not stop on it.

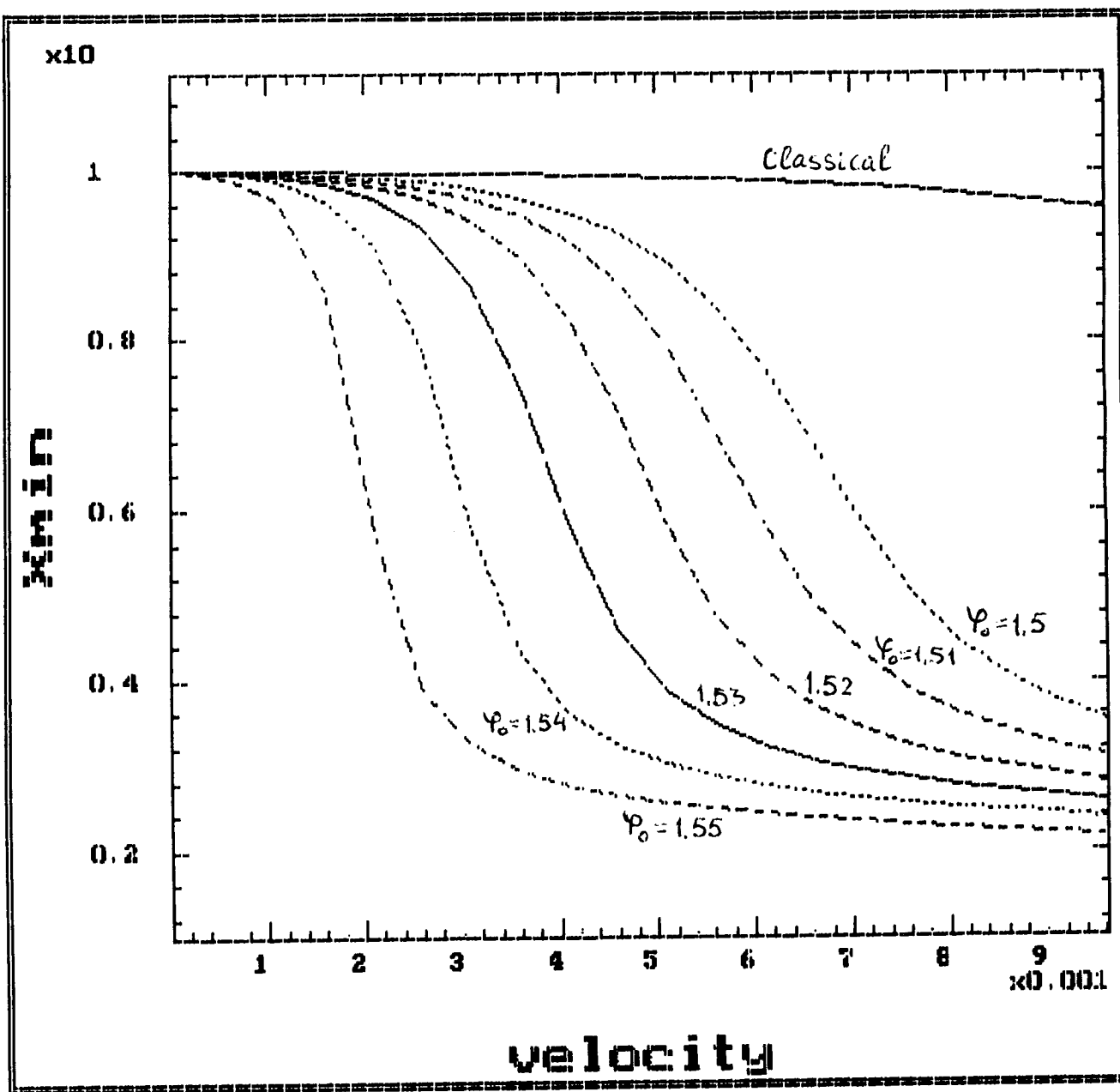
Apparently in atomic physics there are some situations when all the above said will not work. It doesn't mean the UQT failure, but means the eq. 3 roughness solely. Anyone can say: "if it is not the truth, it is a good invention". I would be very much surprised if God has ignored the beautiful chance of using the phase. If all that was said above is true it means that the resolving of the nuclear fusion problem is to be dealt with in a quite a different way. By the way, I theoretically predicted the cold nuclear fusion already in 1983 (2) and all that said above is the development of my old ideas. But the problem of nuclear fusion is the theme of further investigations.

#### **Acknowledgement**

My thanks to Prof. Vladlen S. Barashenkov (Dubna JINR, Russia) and Franz Mair (Innsbruck, MAITRON GmbH, Austria).

#### **References**

1. L. G. Sapogin (the preceding paper)
2. L. G. Sapogin. "Clear-cut picture of micro worlds". Technic for the young (in Russian) No. 1, p. 41(1983).
3. G. Shaw, P. Bland, L. Fonda et al. Nuovo Cimento. vol. 102B, No. 4, p. 1441(1989).





## Mechanism of Cold Nuclear Fusion II

*K. TSUCHIYA*

Department of Electronic Engineering,  
Tokyo National College of Technology,  
1220-2 Kunugida, Hachioji, Tokyo 193 (Japan)

*K. OHASHI*

Faculty of Engineering, Tamagawa University,  
Machida, Tokyo 193 (Japan)

*M. FUKUCHI*

Department of Instrumentation Engineering,  
Faculty of Science and Technology, Keio University,  
Hiyoshi, Yokohama, Kanagawa 223 (Japan)

### **Abstract**

If we regard a deuteron as a bound two-particle, which is slightly different from a bose particle,  $N$ -deuteron wave function and model Hamiltonian can be defined. In this paper, average force is derived as a function of the number of the deuterons by using Heisenberg's equation of motion. Numerical results show that this force is negative when  $N$  is smaller than 144, and reaches a minimum when  $N \sim 72$ . The cold fusion catalyzed by this force in a deuteron cluster is discussed.

### **Introduction**

Regarding deuterons as identical bosons, Bush et al calculated the power density generated from cold nuclear fusion by using the concept of symmetry force which describes the tendency of bosons to clump [1]. In our previous work, we also calculated the power density with assuming that two forces are effective to deuterons

[2]. One is attractive symmetry force, which increases tendency of deuteron to clump, and the other is d-d repulsive force, which decreases it.

In this work, we treat N-deuteron problem by using Lipkin's description in second quantization [3]. In this model, creation and annihilation operators  $a^\dagger$  and  $a$  for proton and neutron anticommute with one another, and bound two-particle system in a state with center of mass momentum  $2\hbar\mathbf{k}$  is considered. Then deuteron creation operator  $D^\dagger$  is given by

$$D_{2\mathbf{k}}^\dagger = \sum_{\mathbf{q}} g_{\mathbf{q}} a_{(\mathbf{k}+\mathbf{q})\uparrow}^\dagger a_{(\mathbf{k}-\mathbf{q})\downarrow}^\dagger , \quad (1)$$

where  $g_{\mathbf{q}}$  is the Fourier transform of the wave function for relative motion. The annihilation operator is then given by the Hermitian conjugate of eq.(1). The N-deuteron wave function  $\Psi_N$  is defined as

$$\Psi_N = \prod_i \frac{(D_{2\mathbf{k}_i}^\dagger)^{n_i}}{(n_i!)^{\frac{1}{2}}} |0\rangle , \quad (2)$$

where  $|0\rangle$  indicates the vacuum state and  $n_i$  indicates the occupied number of state  $i$ , which satisfies  $\sum_i n_i = N$ .

The commutation relation between deuteron creation and annihilation operators is given by

$$[D_{2\mathbf{k}'}, D_{2\mathbf{k}}^\dagger] = \delta_{\mathbf{k}', \mathbf{k}} - \Delta_{\mathbf{k}', \mathbf{k}} , \quad (3)$$

where extra term  $\Delta_{\mathbf{k}', \mathbf{k}}$  is written as

$$\Delta_{\mathbf{k}', \mathbf{k}} = \sum_{\mathbf{q}} g_{\mathbf{q}} (g_{\mathbf{k}'-\mathbf{k}+\mathbf{q}} a_{(2\mathbf{k}-\mathbf{k}'-\mathbf{q})\downarrow}^\dagger a_{(\mathbf{k}'-\mathbf{q})\downarrow} + g_{\mathbf{k}'-\mathbf{k}-\mathbf{q}} a_{(2\mathbf{k}-\mathbf{k}'+\mathbf{q})\uparrow}^\dagger a_{(\mathbf{k}'+\mathbf{q})\uparrow}) . \quad (4)$$

Since  $\Delta_{\mathbf{k}', \mathbf{k}}$  is proportional to the small quantity  $g_{\mathbf{q}}$ , we can neglect it for small N systems. However, it should not be neglected for large N systems. This means that we can not regard deuterons as bose particles when cluster size  $N$  is large. Therefore, extra term  $\Delta_{\mathbf{k}', \mathbf{k}}$  has a role to reduce the tendency of deuterons to clump.

In our previous work [2], we discussed cold fusion catalyzed by deuteron clusters in Pd. In this work, the method how to estimate the most probable cluster size  $N$  is given by using Lipkin's description in second quantization.

### Normalized N-Deuteron Wave Function

If we assume that all deuterons have same momentum, normalized N-deuteron state is given by

$$|N\rangle = \frac{(D_{2k}^\dagger)^N}{\sqrt{N!}} |0\rangle . \quad (5)$$

For  $\mathbf{k}'=\mathbf{k}$ , eqs.(3) and (4) are written as

$$[D_{2k}, D_{2k}^\dagger] = 1 - \Delta_{kk} \quad (6)$$

and

$$\Delta_{kk} = \sum_{\mathbf{q}} g_{\mathbf{q}} (g_{\mathbf{q}} a_{(\mathbf{k}-\mathbf{q})\downarrow}^\dagger a_{(\mathbf{k}-\mathbf{q})\downarrow} + g_{-\mathbf{q}} a_{(\mathbf{k}+\mathbf{q})\uparrow}^\dagger a_{(\mathbf{k}+\mathbf{q})\uparrow}) . \quad (7)$$

Using a simplified deuteron wave packet in eqs.(1),(4) and (7), which are built up of waves over some finite region of  $\mathbf{q}$  with equal amplitudes  $g_{\mathbf{q}}=1/\sqrt{\alpha}$  [3], the commutation relation between  $\Delta_{kk}$  and  $D_{2k}^\dagger$  is written as

$$[\Delta_{kk}, D_{2k}^\dagger] = \frac{2}{\alpha} D_{2k}^\dagger . \quad (8)$$

In this equation,  $\alpha$  is the number of states within the momentum range  $\Delta p$ , so it is written as

$$\alpha = (\Delta p)^3 L^3 / h^3 , \quad (9)$$

where  $L^3$  is the volume of the box and  $h$  is the Planck's constant. On the other hand,  $\Delta p$  satisfy uncertainty principle

$$\Delta p \Delta x \sim h , \quad (10)$$

where  $\Delta x$  is the uncertainty in real space and  $h$  is the Planck's constant. In this work, we assume that deuterons clump together in a vacancy. Therefore,  $L^3$  corresponds to volume of a vacancy and  $(\Delta x)^3$  corresponds to the volume of a deuteron, and  $\alpha$  is given by

$$\alpha = \left( \frac{L}{\Delta x} \right)^3 = \left( \frac{A^3}{4} \right) / \left( \frac{4}{3} \pi r_0^3 \right) , \quad (11)$$

where  $A$  is lattice constant of fcc Pd and  $r_0$  is degenerate radius of deuteron. The values of these constants, we used for eq.(11), are  $a=3.89\text{\AA}$  and  $r_0=0.23\text{\AA}$ , so  $\alpha \sim 289$ . Using eqs.(5) to (8), we can obtain

$$D_{2k}^\dagger |N\rangle = \sqrt{N+1} |N+1\rangle , \quad (12)$$

$$D_{2\mathbf{k}}|N\rangle = \sqrt{N} \left(1 - \frac{N-1}{\alpha}\right) |N-1\rangle \quad (13)$$

and

$$D_{2\mathbf{k}}^\dagger D_{2\mathbf{k}} |N\rangle = N \left(1 - \frac{N-1}{\alpha}\right) |N\rangle \quad (14)$$

Eqs.(13) and (14) are slightly different from usual equations for bose operators.

### Hamiltonian

We made model Hamiltonian for N-deuteron systems, which is defined as

$$H = \varepsilon_{2\mathbf{k}} D_{2\mathbf{k}}^\dagger D_{2\mathbf{k}} + \frac{1}{2} V_0 D_{2\mathbf{k}}^\dagger D_{2\mathbf{k}}^\dagger D_{2\mathbf{k}} D_{2\mathbf{k}} , \quad (15)$$

where first and second terms indicate kinetic and d-d interaction, respectively. In this equation,  $\varepsilon_{2\mathbf{k}}$  indicates

$$\varepsilon_{2\mathbf{k}} = \frac{4\hbar^2 k^2}{2m} , \quad (16)$$

and  $V_0$  indicates the zero component of the Fourier transform of d-d interaction, which is written as

$$V_0 = \frac{1}{V_c^2} \int d\mathbf{r}_1 \int d\mathbf{r}_2 V(|\mathbf{r}_1 - \mathbf{r}_2|) . \quad (17)$$

And then we define the operator for adding a state with momentum  $2\hbar\mathbf{k}$  as

$$P = p_{2\mathbf{k}} D_{2\mathbf{k}}^\dagger , \quad (18)$$

where  $p$  is the c-number with dimension of momentum. The commutation relation between  $H$  and  $P_H = \exp(iHt/\hbar)P\exp(-iHt/\hbar)$ , where  $P_H$  is the momentum in Heisenberg representation, gives

$$\frac{dP_H}{dt} = \exp(iHt/\hbar) \frac{1}{i\hbar} [P, H] \exp(-iHt/\hbar) , \quad (19)$$

which is called Heisenberg's equation of motion. Operating commutator  $[P, H]$  to the state  $|N\rangle$ , we obtain

$$[P, H] |N\rangle = -p_{2\mathbf{k}} \varepsilon_{2\mathbf{k}} \sqrt{N+1} \left[ \left(1 - \frac{2N}{\alpha}\right) - \frac{V_0}{\varepsilon_{2\mathbf{k}}} N \left(1 + \frac{2N}{\alpha} + \frac{1}{\alpha}\right) \left(1 - \frac{N}{\alpha} + \frac{1}{\alpha}\right) \right] |N+1\rangle . \quad (20)$$

### Average Force as a Function of the Number of Deuterons

Defining  $\psi_1$  and  $\psi_2$  as

$$\psi_1 = \exp(-iHt/\hbar) \frac{dP_H}{dt} \exp(iHt/\hbar) |N\rangle \quad (21)$$

and

$$\psi_2 = D_{2k}^\dagger |N\rangle , \quad (22)$$

we obtain average force  $f_N$  as a function of the number of deuterons by making an inner product of  $\psi_1$  and  $\psi_2$  as

$$\begin{aligned} f_N &= \langle \psi_2 | \psi_1 \rangle \\ &= -\frac{p_{2k}\varepsilon_{2k}}{i\hbar} (N+1)[(1-\frac{2N}{\alpha}) + \frac{V_0}{\varepsilon_{2k}} N(1-\frac{2N}{\alpha}+\frac{1}{\alpha})(1-\frac{N}{\alpha}+\frac{1}{\alpha})] . \end{aligned} \quad (23)$$

For  $N \gg 1$ , this is approximately written as

$$f_N = -\frac{p_{2k}\varepsilon_{2k}}{i\hbar} N(1-\frac{2N}{\alpha})[1+\frac{V_0}{\varepsilon_{2k}} N(1-\frac{N}{\alpha})] . \quad (24)$$

If  $\alpha$  is infinite and  $V_0$  is zero in eq.(24),  $f_N$  is proportional to  $N$ . This means that  $f_N$  is proportional to  $N$  when deuterons are regarded as free bosons. This is consistent with Bush's theory [1].

### Conclusions

In refs.[1] and [2], it is shown that cold fusion is catalyzed in deuteron clusters. In this work, most probable cluster size is given by constant  $\alpha$ , which is determined by eq.(11).

The numerical results of average force  $f_N$  normalized by  $k \equiv p_{2k}\varepsilon_{2k}/i\hbar$  are plotted as a function of the number of deuterons in Fig.1 for parameter  $a \equiv V_0/\varepsilon = 1, 2$  and  $4$ . In all cases,  $f_N/k$  reaches a minimum when  $N \sim 72$ , which means that  $f_N$  is most attractive at this point. And it becomes zero when  $N \sim 144$ . This point is given by the solution of  $1-2N/\alpha=0$ , as is shown in eq.(24). When  $N$  is larger than this point, the force becomes repulsive. And for very large  $N$ , eq.(24) shows that the force may become attractive again. However, it will never happen, because  $\alpha$  in eq.(11) corresponds to a maximum number of deuterons included in a vacancy.

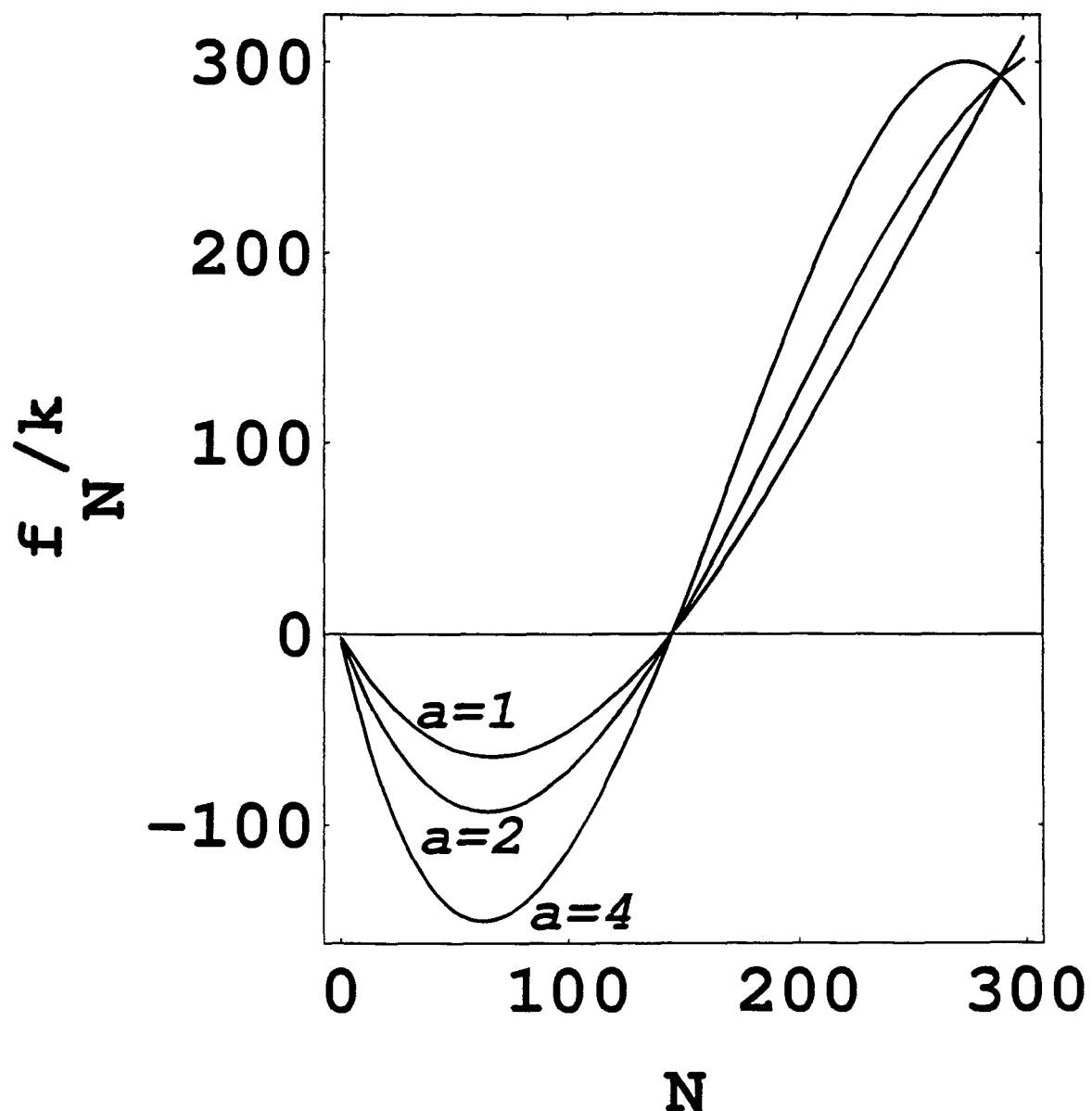


Fig.1 Average force  $f_N$  normalized by  $k \equiv p_{2k}\varepsilon_{2k}/\hbar$  as a function of the number of deuterons.  $a = V_0/\varepsilon$

### **Acknowledgements**

The authors wish to thank Professor S.Haruyama for his encouragement and financial support.

### **References**

1. R.T.Bush and R.D.Eagleton,  
    ""Cold Nuclear Fusion": A Hypothetical Model to Probe Elusive Phenomenon",  
    J.Fusion Energy, Vol.9, p.397(1990)
2. K.Tsuchiya, K.Ohashi and M.Fukuchi,  
    "Mechanism of Cold Nuclear Fusion in Palladium",  
    proceedings of ICCF3, Nagoya (Oct. 1992),  
    Frontiers of Cold Fusion, Universal Academy Press (1993), p.633
3. H.J.Lipkin, *Quantum Mechanics* , North-Holland Pub. Co. (1973), Chapter 6.



## **Conditions And Mechanism of Nonbarrier Double-Particle Fusion in Potential Pit in Crystal.**

Vysotskii V.I.,  
Radiophysical Dept.,  
Shevchenko Kiev University  
Vladimirskaya st. 64,  
Kiev, Ukraine 252017

### **Abstract**

It is shown for the first time, that short-time localization of two deuterons (d-e-d system) in optimal parabolic potential pit in crystal at certain temperature may lead to the complete "suppression" of Coulomb d-d interaction and forming of fast non-barrier cold fusion channel.

### **Theory, models and conditions.**

Previously we have shown [1-4], that when multi-particle Fermi-condensate of  $N \geq 10-20$  deuterons is formed in a microhole of optimal size  $R \approx 4-7\text{Å}$ , there takes place stationary ( $N \geq 100$ ) or short-term fluctuational ( $N \approx 10-20$ ) suppression of Coulomb interaction mechanism with simultaneous initiation of fusion mechanism.

In present paper for the first time we suggest the conditions and mechanism of Coulomb barrier  $V(r)$  suppression with presence of only two deuterons in the pit of small radius  $R \approx 1-2\text{Å}$ . This is achieved by following:

Average interaction energy  $V_{\text{av}}$  turns itself into zero.

Interlevel transition probability  $W_{\text{av}}$  inside optimal parabolic pit  $U(r) = \frac{m\omega^2 r^2}{2}$  in crystal at strictly defined temperature  $T$  is resonantly self-suppressed.

Suppose that we have a pit containing deuteron A with electron, and at the moment  $t=0$  another deuteron B with antiparallel spin goes into the pit due to diffusion. The problem of d-e-d interaction in free space has been regarded earlier [5] and is characterized by energy

$$V(r) = \frac{e^2 (1+\rho) \exp(-2\rho) + (1-2\rho^2/3) \exp(-\rho)}{r} ; \quad \rho = \frac{r}{a} ; \quad a = \frac{\hbar^2}{m_e e} ; \quad 0 \leq r < \infty. \quad (1)$$

Quantizing potential pit  $U(r)$  makes probable the situation, when the interaction  $V(r)$  is unimportant (small perturbation), and  $U(r)$  is main potential. Perturbation is nonstationary :  $V(r, t) = V(r)F(t)$ . The particle gets into the pit at  $t=0$  and leaves it at

$$t=\tau, \text{ where } \tau = (2\pi/\omega) \exp[(U_{\max} - E_n)/k_B T], \quad E_n = \left(n + \frac{3}{2}\right)\hbar\omega.$$

Effect of  $V(r)$  will be unimportant, if

$$W_{ns} = \frac{1}{\hbar^2} |V_{ns}|^2 |F(\omega_{ns})|^2 = 0, \quad W_m = 0, \quad (2)$$

where

$$V_{ns} = \iint \psi_{nA}^*(\vec{r}_A) \psi_{nB}^*(\vec{r}_B) V(|\vec{r}_A - \vec{r}_B|) \psi_{sA}(\vec{r}_A) \psi_{sB}(\vec{r}_B) d\vec{v}_A d\vec{v}_B,$$

$$F(\omega_{ns}) = \int_0^\tau F(t) \exp(-i\omega_{ns}t) dt$$

If (2) is satisfied for all  $(n,s)$ , the motion of deuterons in the pit becomes mutually independent, is characterized by eigen-functions  $\psi_{nc}(\vec{r}_c)$  and defines dd-fusion velocity

$$\lambda_{nA,nB} = c \int |\psi_{nA}(\vec{r})|^2 |\psi_{nB}(\vec{r})|^2 d\vec{v}, \quad c = 2 \cdot 10^{-16} \text{s}^{-1} \text{cm}^3. \quad (3)$$

In main state  $n=0$  in the pit  $|\psi_0(r)|^2 = \frac{1}{\sqrt{\pi^3 u^3}} \exp(-r^2/u^2)$ ,  $u = \sqrt{\hbar/m\omega}$  and

$$V_{00} = \sqrt{\frac{2}{\pi}} \frac{1}{u^3} \int_0^\infty r^2 V(r) \exp(-r^2/2u^2) dr. \quad \text{The appearance of function } r^2 V(r) \text{ (Fig.1)}$$

shows, that  $V_{00} = 0$  with  $u \approx 0.8a$ , which corresponds to optimal value of

$$\hbar\omega \approx m_e^2 e^4 / 0.6 \hbar^2 m \approx 0.013 \text{ eV}, \quad U_{\max}/R^2 \approx m_e^2 e^8 / 0.7 \hbar^6 m \approx 0.08 \text{ eV/A}^2. \quad (4)$$

For all  $s \neq 0$  spectral density of perturbation  $|F(\omega_{0k})|^2 = [\sin(\omega_{0k}\tau/2)/(\omega_{0k}/2)]^2$  satisfies the condition  $|F(\omega_{0k})|^2 = 0$  on the frequencies  $\omega_{0k} = 2k\pi/\tau = k\omega \exp(-(U_{\max} - E_0)/k_B T)$ ,  $k = 1, 2, 3, \dots$  For parabolic pit with  $E_s = \hbar\omega(s + 3/2)$  we have  $\omega_{0s} = s\omega$ . Required condition  $W_{0s} = 0$  is met (See Fig.2) only with

$$\exp[(U_{\max} - 3\hbar\omega/2)/k_B T] = n, \quad n = 1, 2, 3\dots \quad (5)$$

When (4),(5) are satisfied, deuteron interaction is excluded, their wave functions overlap, and reaction velocity (3)  $\lambda \approx c/\sqrt{8\pi^3 u^3} \approx 2 \cdot 10^8 \text{ s}^{-1}$  !

In non-parabolic pit or at non-optimal  $R, U_{\max}, T$  interaction isn't small and fusion velocity  $\lambda$  rapidly decreases (unto its final value defined by tunneling effect in isolated  $D_2^+$  in free space).

In other levels of the pit the conditions of cold fusion change. Regard the situation, when one deuteron is situated on the ground level or one of the lowest levels  $\Psi_n(r)$  and another one gets to the higher level  $E_n$  with quasi-classical wave-function

$$|\Psi_n(r)|^2 = 2(\pi^2 R_n^3 \sqrt{1-r^2/R_n^2})^{-1}, \quad E_n = m\omega^2 R_n^2/2, \quad r \leq R_n.$$

Resulting value of diagonal matrix element (under the condition  $u \ll a$ ) is

$$V_{nn,nn} \approx 4\pi \int_0^{R_n} r^2 V(r) |\Psi_n(r)|^2 dr.$$

Analysis of this expression considering (1) shows, that  $V_{nn,nn} = 0$  at  $R_n \approx 1.7a$ , which corresponds to the particle energy  $E_n = m\omega^2 R_n^2/2$ . This together with the condition  $\exp[(U_{\max} - E_n)/k_B T] = k; \quad k = 1, 2, 3\dots$  leads to the possibility of non-barrier cold fusion. (6)

Let's compare the parameters  $R, U_{\max}$  required for non-barrier fusion with those typical to usual crystals. For example, in quasi-parabolic pits in octahedral internodes in Pd ( $U_{\max} \approx 0.25 \text{ eV}, R \approx 0.25 \text{ \AA}$ ), where  $U_{\max}/R \approx 4 \text{ eV/\AA}^2$ . Velocity  $\lambda$  swiftly increases when two deuterons get inside the vacation with  $R \approx 1 \div 1.5 \text{ \AA}$ .

We have also shown that the same phenomenon of fusion will take place at interaction of heavy atom ( $Z \leq 30 \div 40$ ) with a deuteron or proton in the pit.

- Vysotskii V.I., Kuz'min R.N. *Proceedings of Anomalous Nuclear Effects in Deuterium/Solid Systems Workshop*, 1990. Provo, UT.
- Vysotskii V.I., Kuz'min R.N. *Proceedings of the Third International Conference on Cold Fusion*, 1992. Nagoya, Japan.

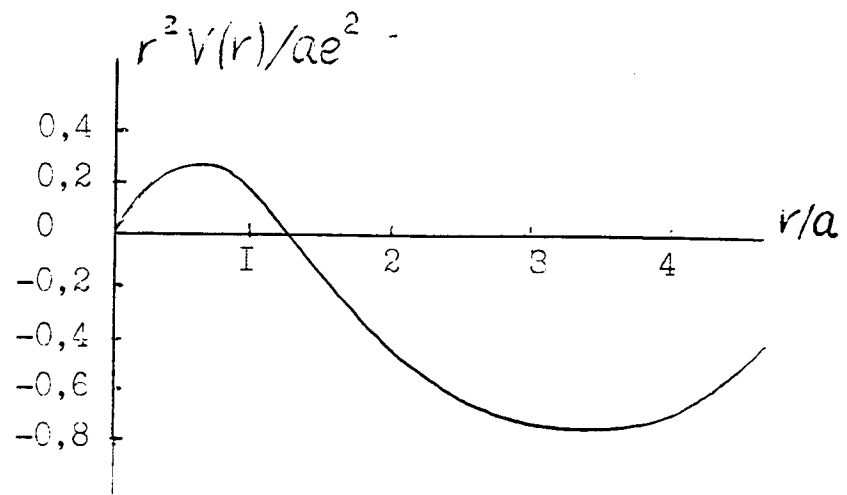


Fig. I

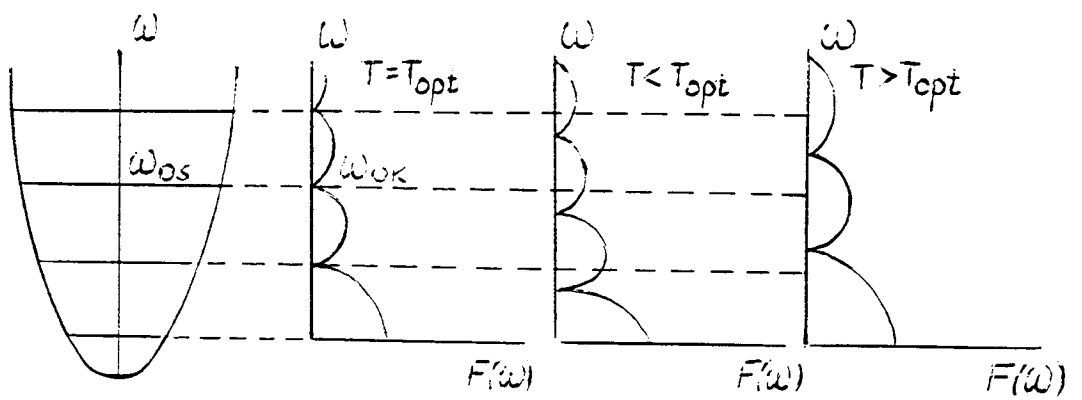


Fig. 2

3. Vysotskii V.I., Kuz'min R.N. *Theory, Mechanism and Dynamics of Non-barrier Nuclear Catalysis in Solids*. Preprint of Institute of Theoretical Physics ITP-90-82p, 1992, Kiev.
4. Vysotskii V.I., Kuz'min R.N. *Temperature-time Dynamics of Cold Fusion in Crystals Based upon Quantum Non-barrier and Microcumulative Mechanisms*. Cold Nuclear Fusion (ed. R.N.Kuz'min), 1992, Moscow, p.6 (in Russian).
5. Davidov A.S. *Quantum Mechanics*.



## COHERENT NUCLEAR REACTIONS IN CRYSTALLINE SOLIDS

S.N. Vaidya  
 Chemistry Division  
 Bhabha Atomic Research Centre  
 Bombay 400085, India

### **Abstract**

We derive a criterion for coherent  $(n,r)$  reaction between propagating neutrons and the nuclei at lattice sites in a crystal, and for coherent d-d reaction between itinerant deuterons and the lattice deuterons in a crystal of  $PdD_x$ . We show that the reaction rate increases by  $N$ , the number interacting nuclei (deuterons) in the coherence region. In the case of d-d fusion reactions, the effect of tunneling on the reaction rate is also considered. Some applications of coherent  $(n,r)$  reactions are discussed.

### **1. Introduction**

In-phase interactions between photons (or propagating quantum particles) and active centers in a medium can lead to coherence effects as a result of which total scattering amplitude (or interaction matrix) increases as  $N^{1/2}$ , where  $N$  is the number of active centres in the medium. Dicke superradiance and laser phenomenon are the established examples of such coherence phenomena. The state-of-art neutron interferometry experiments have not only reaffirmed the wave nature of neutrons but also established persistence of coherence over long distances. The present paper considers coherent  $(n,r)$  reactions between propagating monoenergetic neutrons and the nuclei in a crystalline solid. The coherent interactions between itinerant deuterons (deutrium ions) and lattice deuterons in crystalline  $PdD$  area also considered.

### **2. Coherent $(n,r)$ Reaction**

The wave nature of propagating neutrons allows them to interact simultaneously with all lattice nuclei in the crystal. Consider a neutron beam having De Broglie wavelength  $\lambda = \hbar/(2M_n E)^{1/2}$  propagating through a single crystal of rhodium along [100] direction (Fig.1). The neutrons will form compound nucleus state  $\Psi_i(0)$  at all lattice sites  $R_i = R_i + u_i$  in the overlap region  $0 < r < r_n$ , where  $r_n$  is the size of the nucleus. As in normal or anomalous scattering of neutrons, we associate a phase factor  $\exp(i\mathbf{k} \cdot \mathbf{R}_i)$  with the state  $\Psi_i(0)$ , where  $\mathbf{k}$  is propagation vector and  $|\mathbf{k}| = 2\pi/\lambda$ . Hence, the total overlap wave function<sup>1,2</sup>

$$\Psi(0) = \sum \Psi_i(0) = (1/v^{1/2}) \cdot \Psi_1(0) \cdot [\sum \exp(i\mathbf{k} \cdot \mathbf{R}_i)] \quad (1)$$

where  $\Sigma$  denotes sum over all the  $N$  sites and  $\Psi_i(0)$  is the wave function in the overlap region evaluated from the interaction

potential using the WKB method<sup>3</sup>. The rate of nuclear reaction  $^{103}\text{Rh} (n, r) ^{104}\text{Rh}$ ,  $R = |\Psi(0)|^2$  can thus be expressed as

$$R = (A/V) |\Psi(0)|^2 \cdot \exp - \langle k^2 u_{ik}^2 \rangle \cdot S^2 \quad (2)$$

$$S^2 = \sum \sum \exp [ik(R_{io} - R_{jo})]; |k| = 2\pi/\lambda \quad (3)$$

Here A is the nuclear rate constant and V is the volume of coherence region. It is seen that the reaction rate R depends on the Debye Waller factor and the structure term  $S^2$ . For neutrons propagating along [100] direction, phase coherence occurs when  $\underline{k} \cdot (\underline{R}_{io} - \underline{R}_{jo}) = 2\pi$  or

$$\lambda = (a/2m) \quad (4)$$

where a is the lattice parameter and m is an integer (Fig.1). From Eqs.(3) and (4),  $S^2 = N^2$  at coherence. For  $\lambda \neq (a/2m)$ , on the other hand,  $S^2 = N$ . Hence

$$R_{coh} = N \cdot R_{incoh}, \quad (5)$$

and the reaction rate increases by a factor N at coherence. Coherence conditions for simple lattices are given in Table 1. The number of participating nuclei N can range from  $10^3$  to  $10^9$  depending on the coherence of the incident neutron beam and the mosaic size of the crystal. The experiments for studying coherence enhancement using thermal neutrons from a research reactor have been mentioned elsewhere<sup>2</sup>.

## 2.1 Applications

Coherent (n,r) reactions can be used for production of isotopes at enhanced rates<sup>4</sup>. Pure isotopes or their suitable compounds must be used in form of single crystals.  $^{197}\text{Rh}$ ,  $^{181}\text{Ta}$ ,  $^{59}\text{Co}$ ,  $^{115}\text{In}$  and others which have nearly 100% natural abundance and belong to crystal structures of high symmetry can be used in such experiments.

Coherent (n,r) reaction can produce simultaneously a large number of nuclei  $^{n+1}\text{A}^*$  in excited state. This may be used for creating a large population of required nuclei  $^{n+1}\text{A}^*$  for graser action.

Coherent (n,r) reactions can produce intense gamma rays since, in analogy with Eq.(5),

$$I_{Coh} = N \cdot I_{incoh}. \quad (6)$$

The interference among the intense gamma rays produced by coherent interaction will give intensity maximums. The maximum for the gamma ray of wavelength  $\lambda$  will occur along the directions OP at an angle  $\phi$  to the direction of incidence OA when

$$d \cdot \sin \phi = n \cdot \lambda_g \quad (7)$$

**Table 1**

Coherence condition for simple lattices.

lattice; cell constant	example	direction of incidence	$n\lambda$ at coherence
face centered cubic; $a$	Au, NaCl	[100] [110] [111] [112]	$a/2$ $a/2\sqrt{2}$ $a/\sqrt{3}$ ( $a/2\sqrt{6}$ )
body centered cubic; $a$	Ta	[100] [110]	$a/2$ $a\sqrt{2}$
hexagonal close packed; $a, c$	Co/Tb	[0001] [1000]	$c/2$ $a/2$

where  $n$  is an integer and  $d$  is the lattice periodicity along OA (Fig.2). Large scale application of coherent  $(n,r)$  reactions will require technology for production of high flux, tunable, monoenergetic neutron beams from nuclear reactor or other sources.

### 3. Coherent d-d Reaction in $PdD_x$

In some theoretical studies, electron-deuteron screening, tunneling or coherent interactions have been suggested as possible mechanisms for enhancement of d-d reaction rate. According to the coherent interaction mechanism<sup>1</sup>, the of fusion reaction between the mobile deuterons and the lattice deuterons increases by  $N$  when the deuteron wavelength  $\lambda_d = \hbar/(2M_d E)^{1/2}$  meets the coherence condition. For deuterons propagating along [100] direction, in analogy with Eq.(4), coherence occurs when

$$\lambda_d = (a/2m) \quad ; m \text{ integer} . \quad (8)$$

In general, coherence criterarion can be expressed as

$$\lambda_d = x \cdot L \quad (9)$$

where  $L$  is the periodicity and  $x$  is a number which depends on the direction of propagation (Table 1). A propagating deuteron can tunnel through an array of one dimensional potentials having periodicity  $L$  (Fig.3) when the length of classically accessible region in each well is an odd multiple of  $\lambda_d/4$  :

$$(L - 2r_t) = (2m+1) \cdot \lambda_d/4 . \quad (10)$$

Here  $r_t$  is the turning distance which depends on the screening length. Following Turner<sup>5</sup> and Bush<sup>6</sup> we shall assume that the same condition is applicable for tunneling of deuterons through the crystal. Tunneling preserves the phase of propagating deuteron and hence, under ideal conditions, the coherence length  $l_c$  will be very large - equal to the length of the crystal. There is however considerable reduction in  $l_c$  on account of non-monochromaticity of deuterons and finite mosaic size of the crystal.

The coherence criterion Eq.(9), and tunneling criterion Eq.(10) are met simultaneously along a certain direction of propagation of deuterons if

$$(2r_t/L) = 1 - (2m+1)x/4; \lambda_d = x.L \quad (11)$$

Maximum d-d fusion rate will be attained when Eq.(11) is fulfilled.

We have here attempted to bring out the role of tunneling and coherence mechanisms which have hitherto been discussed separately. In case of (n,r) reactions, the tunneling criterion can be ignored since neutrons do not experience coulomb repulsions at lattice nuclei. Tunneling of deuterons can be increased by the application of longitudinal acoustic waves to the  $PdD_x$  crystal<sup>1</sup>. This will enhance the d-d reaction rate by increasing the screening parameter  $k_d$ . These aspects are discussed in the accompanying paper at this conference.

### References

1. S.N. Vaidya. "On Possibility of Coherent Deutron-Deutron Fusion in a Crystalline PdD Lattice". Fusion Technology. vol.20 No.4, p.481 (1991).
2. S.N. Vaidya. "Comments on Model for Coherent Deutron-Deutron Fusion in Crystalline PdD Lattice". Fusion Technology. Vol.24, No.1, p.112 (1993).
3. S.N. Vaidya and Y.S. Mayya. "Theory of Screening - Enhanced D-D Fusion in Metals", Japanese Journal of Applied Physics-Latters. Vol.28, No.12, P.L2258 (1989).
4. S.N. Vaidya. "Coherence of Nuclear Interactions in Crystalline Solids and its Applications". Bhabha Atomic Research Centre, Bombay. Nov. 1993, BARC-I/017.
5. L. Turner. "Thoughts Unbottled by Cold Fusion". Physics Today. Vol.42, No.9, p.140 (1989).
6. R.T. Bush. "Cold Fusion: The Transmission Resonance Model Fits Data on Excess Heat, Predicts Optimal Trigger Points, and Suggests Nuclear Fusion Scenarios". Fusion Technology. Vol.19, Nov 2, p.313 (1991).

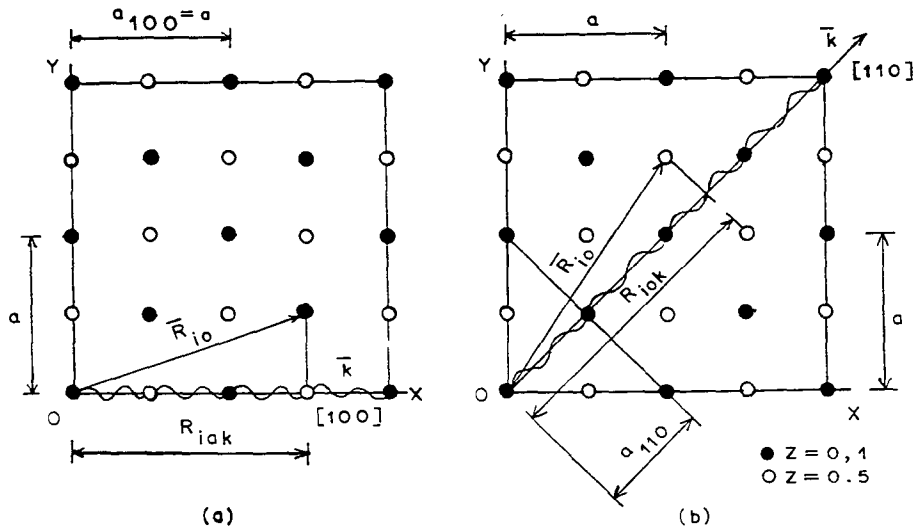


FIG. 1 PROJECTION OF FCC LATTICE ON C AXIS

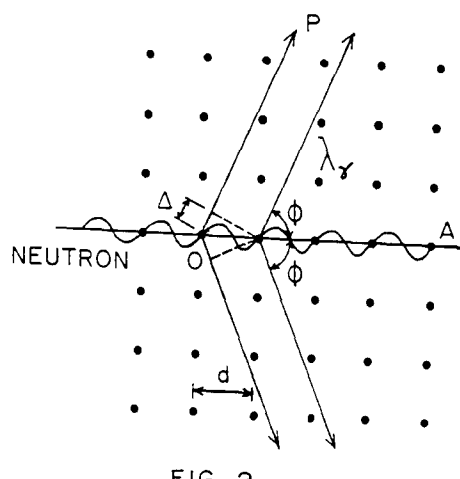
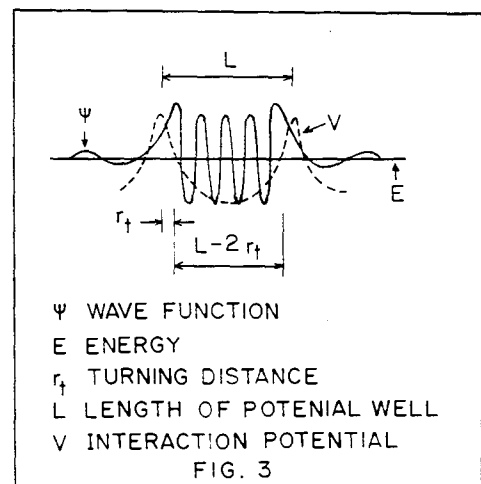


FIG. 2





# CATASTROPHIC ACTIVE MEDIUM (CAM) THEORY OF COLD FUSION

MITCHELL R. SWARTZ  
JET Technology Weston, MA USA 02193

Dr. Mitchell Swartz does not wish to have his papers uploaded to LENR-CANR.org. A copy of this paper can be found in the original EPRI proceedings, Vol. 4, p. 254

[http://my.epri.com/portal/server.pt?Abstract\\_id=TR-104188-V4](http://my.epri.com/portal/server.pt?Abstract_id=TR-104188-V4)

## ON BOSE-EINSTEIN CONDENSATION OF DEUTERONS IN PdD<sub>x</sub>

S.N. Vaidya  
Chemistry Division  
Bhabha Atomic Research Centre  
Bombay 400 085, India

### Abstract

In this paper we consider the aspects connected with the screening of coulomb interaction between deuterons in PdD<sub>x</sub>. We propose an experiment for increasing deuteron number density, their fluctuations and screening in a single crystal of PdD<sub>x</sub>, at low temperatures, to approach conditions for the Bose condensation of deuterons for achieving high d-d fusion rates.

### 1. Introduction

Following the work of Fleischmann and Pons<sup>1</sup>, several careful electrolytic and gas effusion experiments performed on palladium deuteride in the last four years have reported observation of excess heat, neutrons and charged particles. Measurements of excess heat which exceed several  $\sigma$ , observation of neutron emissions in PdD<sub>x</sub> and D<sub>x</sub>WO<sub>3</sub> systems, and of <sup>4</sup>He from in-situ mass-spectrometer experiments have steadily accumulated evidence in support of cold fusion<sup>2,3</sup>. Several theoretical models have been suggested to account for the enhancement of deuteron-deuteron (d-d) fusion rate from a low value of about  $10^{-74} \text{ s}^{-1} (\text{dd})^{-1}$  in an isolated D<sub>2</sub> molecule to about  $10^{-24} \text{ s}^{-1} (\text{dd})^{-1}$  deduced from some of the experiments. In this paper we shall consider the electron-deuteron screening<sup>4-6</sup>, tunneling<sup>7,8</sup> and coherent interaction<sup>9</sup> mechanisms which have been proposed for enhancement of d-d fusion rate. We propose an experiment for elucidating the role of deuteron screening and for increasing the fusion rate.

### 2. Electron-Deuteron Screening

Fusion cross-sections of <sup>2</sup>H(d,r)<sup>4</sup>He, <sup>3</sup>He(d,p)<sup>4</sup>He and <sup>3</sup>He(d,n)<sup>4</sup>He nuclear reactions<sup>10</sup> show an increase for centre-of-mass energies E<sub>CM</sub> < 15 Kev. This increase has been attributed to the screening of nuclear interaction by the electrons in target atoms<sup>11</sup>. The screening by conduction electrons in metals is well known, and it forms the basis of the free electron gas model. The d-d interactions in metal deuterides at E<sub>CM</sub> < 1 ev are likewise screened by the conduction electrons and as a result, the d-d fusion rate R increases<sup>4</sup> to about  $10^{-40} \text{ s}^{-1} (\text{dd})^{-1}$ . The formation of electron-deuteron (deuteron ions) plasma against the background of palladium lattice, under the experimental conditions, can increase the screening and R. At low energies, the electrons and ions in the plasma instantaneously rearrange themselves so that the polarization charge follows the

interacting ions. Carraro et al<sup>12</sup> have shown that both the electrons and ions make full contribution of screening at low  $E_{CM}$  but the screening falls off as the  $E_{CM}$  increases.

The effective interaction potential in an ideal plasma of electrons and deuterons<sup>4,5</sup> is  $(e^2/r) \exp(-Kr)$  with screening parameter

$$k^2 = k_e^2 + k_d^2 = [6\pi e^2 n_e / E_F] + [4\pi e^2 n_d / k_B T] [z g'_{3/2}(z) / g_{3/2}(z)] \quad (1)$$

Here  $n_e$  and  $n_d$  are the electron and deuteron number densities,  $E_F$  is the Fermi energy and  $g_{3/2}(z) = \sum_n (n^{-3/2} z^n)$ . The electron-deuteron screening model for PdD gives  $R \sim 10^{-16} \text{ s}^{-1}(\text{dd})^{-1}$  with  $n_e = 13.6 \times 10^{23} \text{ cm}^{-3}$  and  $n_d = 6.8 \times 10^{23} \text{ cm}^{-3}$ .

The deuteron screening parameter  $k_d$  decreases rapidly if the deuteron number density and mobility are small. This also follows from the expression<sup>13</sup>

$$k_d = 4\pi e^2 \langle y^2 \rangle / k_B T ; \langle y^2 \rangle = \langle \bar{n}^2 \rangle - \langle \bar{n} \rangle^2 \quad (2)$$

where  $\langle y^2 \rangle$  is the number density fluctuation and  $n$  is the average site occupancy number.

Bose condensation temperature of an ideal deuteron gas is

$$T_B = (2\pi \hbar^2 / M_d k_B) (n_d / 2.612)^{2/3}. \quad (3)$$

For PdD, Eq.(3) gives  $T_B = 6.65 \text{ K}$ . As the temperature  $T \rightarrow T_B$  and Bose condensation is approached, the screening parameter  $k_d$  in Eq.(1)  $\rightarrow \infty$  and the d-d fusion rate becomes very large. The superconducting transition temperature of  $\text{PdD}_x$  ( $T_C = 11 \text{ K}$ ) is higher than that of  $\text{PdH}_x$  ( $T_C = 8 \text{ K}$ ) for  $x = 0.6 - 0.7$ . The inverse isotope effect of  $T_C$  suggests that at low temperatures the screening of the interactions between electrons (which form Cooper pairs) is higher in  $\text{PdD}_x$  than in  $\text{PdH}_x$ .

Whaley's cluster model calculations<sup>13</sup> show that d-d fusion rate  $\sim 10^{-20} \text{ s}^{-1}(\text{dd})^{-1}$  requires large deuteron density fluctuation  $\langle y^2 \rangle \sim 0.1$ . Migration of deuterons in  $\text{PdD}_x$ , as in other transition metal hydrides and deuterides is at low temperatures governed by tunneling, and at high temperatures by over-the-jump mechanisms which are activated processes. The tunneling process, as opposed to other processes, preserves phase correlation among the migrating deuterons. Hence the increase in  $\langle y^2 \rangle$  by correlated tunneling of deuterons at low temperatures will increase the d-d fusion rate due to coherence as well.

### 3. Proposal for an Experiment

We propose, taking into consideration the aspects discussed in Sec.2, the following experiment for realizing high values of  $R$  in  $\text{PdD}_x$  crystal. We take a single crystal of palladium grown along

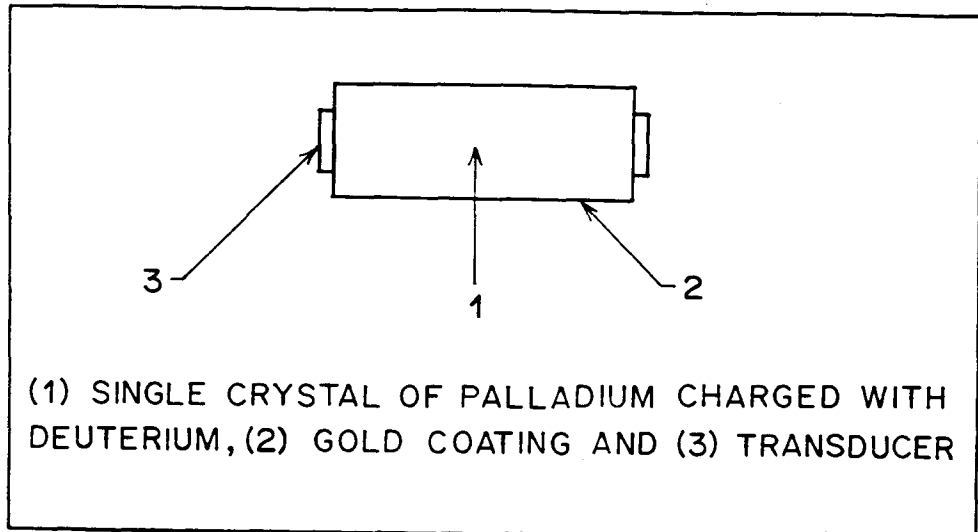


FIG.1

a principal crystallographic axis such as [100] or [111] with flat ends normal to the cylinder axis (Fig.1). The cylindrical surface is coated with gold as has been done by Yamaguchi and Nishiota<sup>14</sup>. The crystal is charged with deuterium by electrolysis or by gas loading to high D/Pd ratio. Flat ends of the crystal are capped by two similar transducers for propagating longitudinal acoustic waves of high frequency  $w > 10^9$  Hz. The transducers are aligned to direct the ultrasonic waves along the cylinder axis. The gold coating on the cylindrical surface helps ensure preferential migration of deuterons along the cylinder axis.

At low temperatures, deuterons occupy lowest energy levels in their potential wells in the face-centered-cubic lattice, have low mobility and deuteron transport is mainly due to tunneling between adjacent sites. The tunneling probability can be enhanced to yield high values of  $n_d$  and  $\langle y^2 \rangle$  by application of external perturbation in form of ultrasonic waves. The experiment consists in driving deuterons to the centre of the crystal by means of longitudinal acoustic (LA) waves from the two transducers which are operated at same amplitude and frequency. The phase difference between the transducers and the amplitude are varied to achieve maximum tunneling rate.

#### 4. Effect of Longitudinal Acoustic Waves on Tunneling

In order to understand the effect of LA waves, we shall review the results of typical analysis of the effect of periodic perturbation on tunneling in a double-well potential. The

Hamiltonian of a particle in a quartic double-well can be expressed in dimensionless variables, following Grossmann et al<sup>15</sup>, as

$$H(x) = -\frac{1}{2} \cdot \frac{d^2}{dx^2} - \frac{x^2}{4} + \frac{x^4}{64D} + x S \sin \omega t, \quad (4)$$

Here  $\omega_0$  is the frequency of small oscillation at the bottom of the well,  $E_B$  is the barrier height,  $S$  is the amplitude of perturbation in units of  $(\hbar/M_d \omega_0^3)^{1/2}$  frequency  $\omega$  and  $D = (E_B/\hbar \omega_0)$  (Fig.2). Using Floquet formalism it has been shown that the wave function

$$\Psi_k(x,t) = \exp(i\epsilon_{k1}t) \phi_{k,1}(x,t) \quad (5)$$

has periodicity  $T = (2\pi/\omega)$  and quasi-energies corresponding to the unperturbed state  $\epsilon_k$  are

$$\epsilon_{k1} \equiv \epsilon_k + l\omega; \quad l = 0, \pm 1, \pm 2, \dots \quad (6)$$

The values of  $E_B$  and  $\omega_0$  for  $D$  in Pd will be of same order of magnitude as those for  $H$  on W(100) surface<sup>16</sup>, namely,  $E_B = 240$  mev and  $\omega_0 = 2.4 \times 10^{13}$  Hz. Compared to this, the frequency of LA wave  $\omega \approx 10^9$  Hz is quite small. Tunneling probability for  $\omega < \omega_0$ , under adiabatic approximation, shows periodic variation with  $n$ , the number of cycles of  $\omega$ . The results of numerical calculations<sup>15</sup> for  $(E_B/\hbar \omega_0) = 1$ ,  $(\omega/\omega_0) = 0.06$  and  $s = 0.028$  reproduced in Fig.3 show variation of  $P$  between nearly 0 and 1 as a function of  $n$ . Under repeated application of perturbation  $\hbar \omega$ , the particle is progressively raised to states having higher  $l$ , and the  $P$  increases. As the tunneling progresses, the system returns to the original state and the cycle starts all over again.

The results of this analysis can be extended to an array of periodic potentials in the same way as Bohm's tunneling criterion is extended to a periodic array<sup>7,8</sup>.

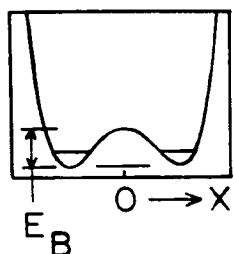
The application of ultrasonic waves, by changing the tunneling rate, will lead to periodic increases in  $n_d$  and to large fluctuations  $\langle y^2 \rangle$ . As increased number of mobile deuterons are driven to form a Bose condensate, there will be a substantial increase in the rate of production of heat and neutrons. The warming and cooling of the crystal will produce periodic bursts of heat and neutrons in such an experiment.

## 5. Conclusion

The above semi-classical analysis suggests that the application of LA ultrasonic waves to a crystal of  $\text{PdD}_x$  can increase the d-d fusion rate  $R$ . There might be further a) increase in  $R$  due to phase coherence among the tunneling deuterons.

The deuteron charge  $Z$  in  $\text{PdD}_x$  depends, among other things, on

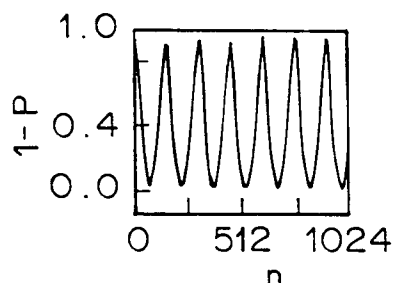
PARTICLE IN DOUBLE WELL POTENTIAL  
UNDER PERIODIC PERTURBATION  
(GROSSMAN et al. zeit. physik. B 84, 315, 1991)



$\omega_0$  = NAT. VIB. FREQVENCY  
 $E_B$  = BARRIER HEIGHT  
 $D = E_B / \hbar \omega_0$   
 $S$  = AMPLITUDE OF PERTURBATION  
 $W$  = FREQ. OF PERTURBATION

FIG. 2

$P$ , TUNNELING PROBABILITY FOR  $W < \omega_0$   
(APPLICABLE TO ULTRASOUND)



$D = (E_B / \hbar \omega_0) = 1$   
 $W / \omega_0 = 0.06$   
 $S = 0.028$   
 $n = \text{PERIODS OF } W$

$P$  SHOWS PERIODIC INCREASE WITH  $n$

FIG.3

their velocity. For  $Z < +1$ , the d-d fusion is hindered by the veil of electron around the deuteron as in a  $D_2$  molecule or  $D_2^+$  ion. It may not also be appropriate to apply Bose statistics to an assembly of partially ionized deuterons. It appears that  $Z$  approaches +1 (i) in the Fleischmann and Pons experiment at high current densities<sup>17</sup> and (ii) in the experiments with  $D_x WO_3$  crystals which give high fusion rates. Departure of  $Z$  from value +1 probably hinders the attainment of high fusion rates.

### References

1. M. Fleischmann and S. Pons. "Electrochemically Induced Nuclear Fusion of Deuterium". Journal of Electroanalytical Chemistry. vol. 261, No 2A, p.301 (1989).
2. K. Ikegami, Ed. Frontiers of cold Fusion. Proceedings of Third International Conference on Cold Fusion, Nagoya, Japan, Universal Pres Inc., 1993.
3. K.A. Kaliev, A.N. Baraboshkin, A.L. Simgin, E.G. Golikov, A.L. Shalyapin, V.S. Andreev and P.I. Golubnichiy. "Reproducible Nuclear Reactions During Interaction of Deuterium with Oxide Tungsten Bronze". Physics Letters A. Vol. 172 p.199 (1993).
4. S.N. Vaidya and Y.S. Mayya. "Role of Combined Electron-Deuteron Screening in d-d Fusion in Metals". Pramana - Journal of Physics. Vol.33, No.2 p.L343 (1989).
5. S.N. Vaidya and Y.S. Mayya. "Theory of Screening enhanced d-d Fusion in Metals". Japanese Journal of Applied Physics - Letters. Vol.28, No.12. p.L2258 (1989).
6. H. Takahashi. "Dynamical Screening of Potential by Mobile Deuteron". Emerging Nuclear Energy Systems. Ed. U. Von Mollendorff and B. Goel. World Scientific, 1989, pp.318.
7. L. Turner. "Thoughts Unbottled by Cold Fusion". Physics Today. Vol. 42, No.9, p.140 (1989).
8. R.T. Bush. "Cold Fusion: The Transmission Resonance Model Fits Data on Excess Heat, Predicts Fusion Scenarios". Fusion Technology. Vol.19, Nov p.313 (1991).
9. S.N. Vaidya. "On the Possibility of Coherent Deuteron-Deuteron Fusion in a Crystalline Pd-D Lattice". Fusion Technology Vol. 20, No.4, p.481 (1991).
10. A. Krauss, H.W. Becker, H.P. Trautvetter, C. Roffts and K. Brand. "Low-Energy Fusion Cross Sections of D+D and D+ $^3$ He Reactions". Nuclear Physics A. Vol.465, No.1, p.150 (1987).

11. K. Lananke and C. Rolfs. "On the  $t(d,n)\alpha$  Reactivity in Fusion Reactors". Modern Physics Letters A. Vol.4, No.22, p.2101 (1989).
12. C. Carraro, A. Schafer and S.E. Koonin, "Dynamic Screening of Thermonuclear Reactions". Astrophysical Journal Vol.331, p.556 (Aug. 1988).
13. K.B. Whaley. "Boson Enhancement of Finite-Temperature Coherent Dynamics for Deuterium in Metals". Physical Review B. Vol. 41, No.6, p.3473 (1990).
14. E. Yamaguchi and T. Nishioka. "Cold Nuclear Fusion Induced by Controlled Out-Diffusion of Deuteron in Palladium. Japanese Journal of Applied Physics Letters. Vol.29, No.4, p.L666 (1990).
15. F. Grossmann. P. Jung, T. Dittrich and P. Hanggi. "Tunneling in a Periodically Driven Bistable System". Zeit. Physik B. Vol. 84, p.315 (1991).
16. K.B. Whaley, A. Nitzan and R.B. Gerber. "Quantum Diffusion of Hydrogen on Metal Surfaces". Journal of Chemical Physics. Vol. 84, No.9, p.5181 (1986).
17. M. Fleischmann and S. Pons. "Calorimetry of the Pd-D<sub>2</sub>O System: From Simplicity via Complications to Simplicity". Physics Letters A. Vol. 176, No.1, p.1 (1993).



# Account of Cold Fusion by Screening and Harmonic oscillator resonance.

Michel RAMBAUT  
57H rue De La Hacquinière  
Bures-sur-Yvette, 91440, France.

## Abstract

A model of cold fusion process is proposed. It is based on earlier fusion reaction rate calculations, assuming electron accumulation around two colliding deuterons, and using a specific relationship between the parameters characterizing the non-thermonuclear process. In this paper this model is completed, making the hypothesis of harmonic oscillators on particle level. Those harmonic oscillators make deuterons quasi-free in some circumstances, for example when a high level fast transitory current is decreasing. This combined model reveals a good agreement with some unclaimed as being cold fusion experiments, of fast high voltage high transitory currents through deuterated media. It is particularly shown that this model accounts for a growth of fusion rate, varying like the tenth power of the peak current,  $I^{10}$ .

## 1. Introduction

The model which is presented in this paper is the consequence of the non-dependence on the medium which cold fusion seems to have. It has been shown two years ago that D-D fusion reactions could occur by crossing of the lowered Coulomb barrier between deuterons, the possibility of this lowering being due to what was called "Double screening" [1] [2]. This expression is not however very demonstrative of Coulomb barrier lowering process, which is essentially due to an electron accumulation around two deuterons, which are approaching at a distance of the order of the Bohr atom radius. So it seems more judicious to call this process "Nuclear Fusion by electron accumulation".

Being drastically different from the thermonuclear one, the correct description of this process on the macroscopic level, needs also a dimensional relationship between the physical variables, completely different from the one which is inferred from the Lawson criterion [2] [3].

In fact this model, using only the electron accumulation concept, does not describe completely the physical process. It does exist a necessary macroscopic cause for triggering the microscopic process of electrons accumulation and tunneling through the Coulomb barrier. It has been shown in the reference [2] that the possibility of the microscopic process was in agreement with a quasi-free status of ions, space distributed according the Poisson law. It seems, at first sight, to be contradictory with the existing Coulomb forces. Thus there is matter to answer the question, in what circumstances the medium could be considered as being reduced to an quasi free ions set. An hypothesis on the possible cause is in fact suggested by experiments consisting to let flowing high and fast transitory currents through

deuterated media. As it is shown it implies a plasma modeling by a set of harmonic oscillator.

According to this hypothesis, fusion reactions are the consequence of resonating harmonic oscillators, on the particle level, as much as of the electron accumulation phenomenon. A clue showing the underlying reality of such oscillators, comes from observations made by Lochte-Holtgreven at Kiel (Germany) during the seventies [4] [5], and Sethian et Al at NRL during the eighties [6]: neutrons are detected immediately when the current stops to grow (Figures 1&2).

In Kiel experiments, the neutrons production occurred only during the decrease of a relatively moderate peak current of the order of  $2 \times 10^4$  A, flowing in a capillary tube filled with  $\text{Li}(\text{ND}_3)_4$ . The nuclear reactions producing those neutrons were called pycknonuclear by Lochte-Holtgreven, who used a term useful in Astrophysics, build on a greek root ( $\pi\kappa\nu\omega$ =dense) [7]. It means that there would be collective effects in nuclear reactions occurring in dense media, which would modify the accustomed rate, known by ion collisions in accelerators. The proposed model of "Nuclear Fusion by electron accumulation", joined to the harmonic oscillator hypothesis, is a tentative modeling of the pycknonuclear process. Suggested by observing the neutron production only from the current peak, it is shown that such a model is in fact in agreement with the experimental rates of change of the neutron production, in function of the peak current, observed at NRL.

## 2. General delineation of the two process model: electron accumulation and harmonic oscillator resonance.

### 2.1. Harmonic oscillator resonances suggested by experiments.

One can assume that the ion and electron distributions are uniform during the growing current phase, as there are no produced neutrons during this phase. This no neutron production has been observed at Kiel University and at NRL, using effective short current pulse, that is whose duration was typically between 100 ns and 300 ns (figure 1). During the growing phase, the medium is more and more ionized, and above all, is ruled by Coulomb forces. One has also to mention that, although the medium is gaining much energy, in different amounts according to the experiment, the thermal turbulence of the ions is too low to qualify it as being "thermonuclear".

In Kiel experiments the ringing frequency of the capacitor bank was rather low, typically 200 KHz, but the current pattern was reshaped by a plasma instability, one can attribute to Ampère force: the effective peak current, it means the one which was correlated with the onset of neutron production was typically reached in some hundred of nanoseconde, according the diameter of the cylindrical deuterated medium, which was contained in a glass capillary pipe. The deuterated medium was almost completely ionized at the peak current, which was  $2 \times 10^4$  A, according to the [4] reference. The capacitor bank voltage was chosen to get an approximate voltage gradient of 30kV/cm. Given the relatively low peak current, the neutron rate was relatively moderate.

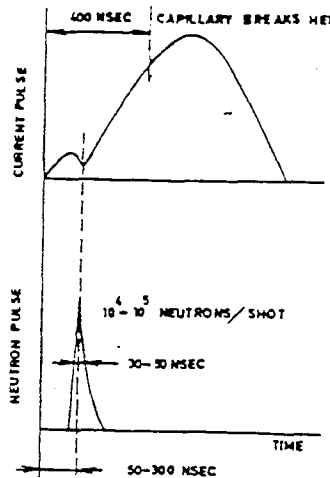


Figure 1: Figure from reference [5] showing that, in the Kiel experiments, the neutron burst occurred during the current decrease.

In NLR experiments, published in 1987 [6], a current pulse of typically 120 ns growing time, was flowing in a frozen deuterium fiber whose initial diameter was 125- $\mu\text{m}$ . The growth of the observed neutron burst in function of the peak current  $I$  (Maximum value: 640 kA), and beginning just at this peak (Figure 2), was claimed close to  $I^{10}$  (Figure 3). But the experimenters had some problem in detector calibration, so this mishap gave a rather great indetermination of the absolute rate of the neutron burst. After the first estimate of  $8.4 \times 10^{11}$  neutrons, this rate had to be divided approximately by a hundred factor [6]. But this is in fact unimportant given that the  $I^{10}$  growth has not been questioned. As it is shown further this result is in agreement with the model of Fusion by electron accumulation, and harmonic resonance, in the limits of experimental and calculations precision.

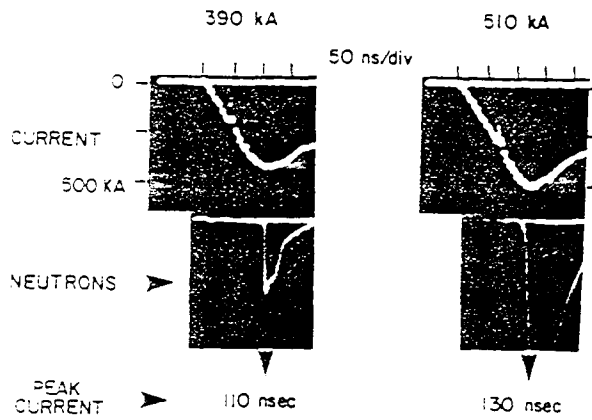
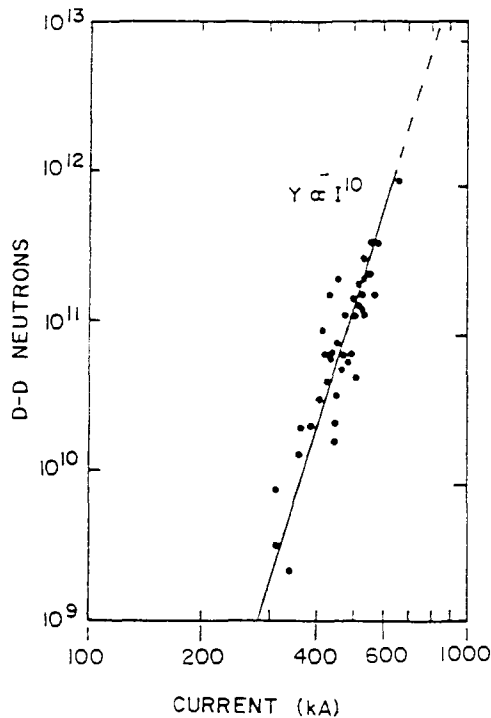


Figure 2: Figures from reference [6]. The fast onset of the neutron burst is clearly coincident with the current maximum. It appears on this second figure that this onset begins slowly just before the current maximum, but the rate becomes much faster at this maximum. The collective movement of the ions, taken into account in reference (1), is unimportant for the fusion reaction production, in comparison with the harmonic oscillations on deuteron level. This phenomenon plays a role of deuteron quasi-accelerator.



**Figure 3** From reference [6]. The neutron number per current burst, in function of peak current, for an 80  $\mu\text{m}$  initial diameter of the frozen deuterium fiber. The authors have given a fit to the power law  $Y=7.3 \times 10^9$  ( $I$  in Mega-Ampère).

But one has to take into account other results from NRL, obtained with different experimental conditions. In those experiments, the current was typically higher i.e. 800 kA, but the growing time was longer, i.e. 800 ns [8]. As well as a neutron production beginning at the current peak, other neutron bursts were observed, before and after the peak, for approximately 400 kA (Figure 4). The neutron production, in function of the peak current, was not varying approximately like  $I^{10}$ , but like  $I^5$ . (Figure 5).

There are essential differences between the Kiel and NRL experiments. Firstly there was a containment in Kiel experiments during the neutron production phase, but no containment in the NRL case. Secondly the amounts of energy introduced into the medium during the growing phase are very different. By the way one has to emphasize on the fact that just a few of experimental results are useful for the problem which is by now taken into account. The majority of high voltage capacitor discharges into deuterated media, performed since the fifties have been realized with the background idea to get "thermonuclear conditions". So the experimenters have too often realized experiments with too long ringing periods (at least some microseconds), and they missed the informative measurements: peak current and neutron burst in function of time. Experimenting in this way, it is easy to conclude falsely, for example like in reference [10], that the neutron burst vary like  $I^4$ .

One has also to mention other experiments, performed also at NRL, which consisted of using again a short current pulse, whose full width at mean current value was 80 ns, with a some hundred kilo-Ampere peak [9]. The structure of the medium was different, called X-pinch by the experimenters, who aimed at first to get X-rays. Nevertheless a supplementary information was given, comparatively to the other experiments: simultaneous the voltage and the current were measured

simultaneously in function of time, so the energy delivered to the medium is better known than in the other cases, where it can only be estimated (Table 1).

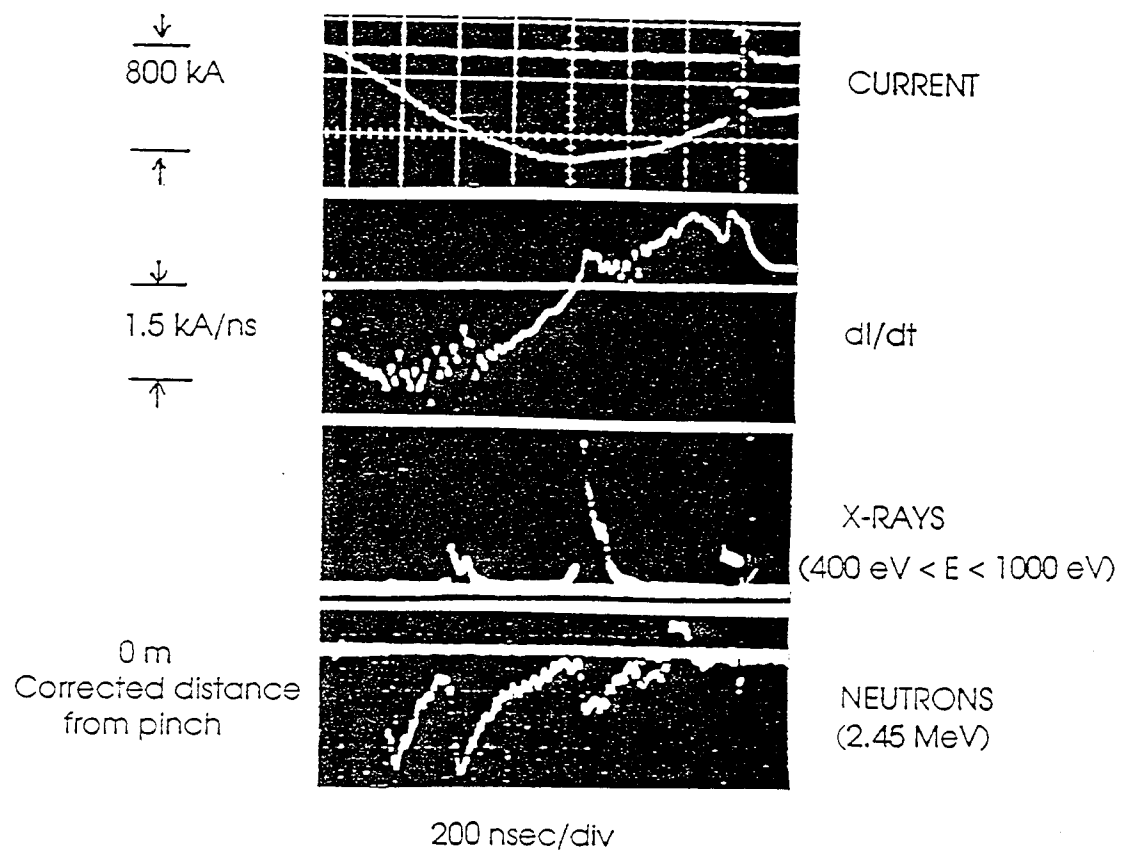


**Figure 4** From the reference [8], showing for a long current pattern, the most essential physical variables  $I$ ,  $dI/dt$ , X-rays, neutron burst.

Apparently the behaviour of the deuterated medium is the same for 10 kJ/cm<sup>3</sup>. and for 50 MJ/cm<sup>3</sup>: neutron production occurs only when the current begins to decrease (Table 1). The current decrease is the cause of the the instability formation. revealed by "beads" on X-pictures: this is the case in the Lochte-Holtgreven experiments performed in Kiel [4] [5], and in the J.D.Sethian experiments performed at NRL [6]. But in another experiments, the cause of instabilities is apparently the excess energy afforded to the medium, typically some hundreds of MJ/cm<sup>3</sup>: this is the case observed by K.C.Mittal et Al [9].

In both cases, a magnetohydrodynamic instability can occur, no matter which is its cause. (In the Kiel experiments the primary cause can be attributed to the "Ampère force"). But also in both cases, i.e. fast current decrease or magnetohydrodynamic instability the electron accumulation process can occur. consecutively to a cause making the deuterons quasi-free. The matter is now to examine in which extent the harmonic oscillator hypothesis is realistic.

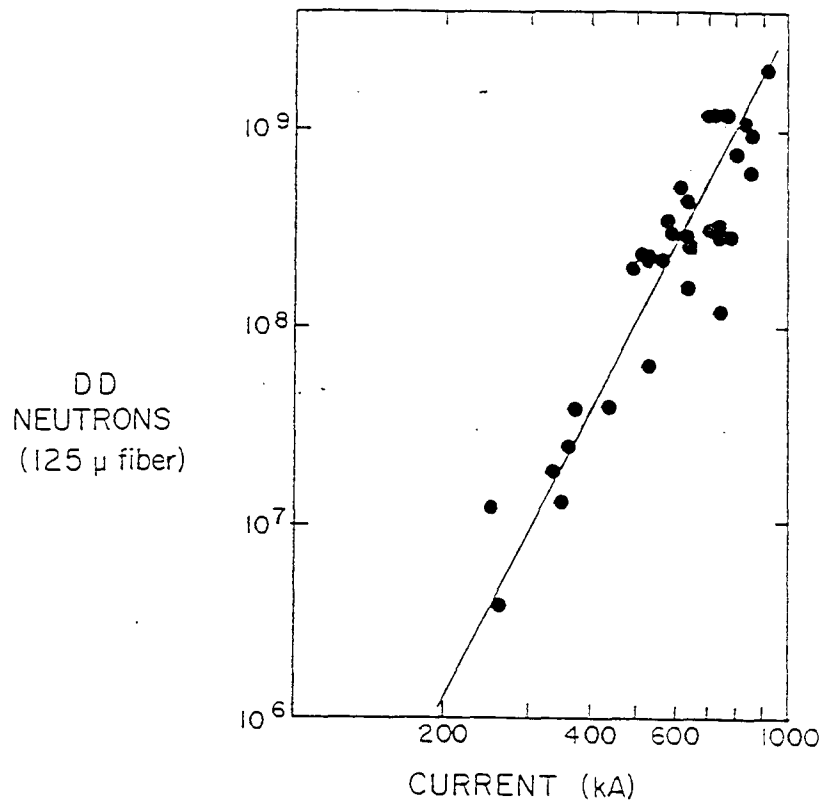


**Figure 5** From reference [8]. The current growth is slow, in comparison with the one of Kiel experiments, or with the one of NRL experiments performed in 1987. The medium is frozen deuterium, whereas Li(ND<sub>3</sub>)<sub>4</sub>, was used in Kiel experiments. Neutrons and X ray bursts come out not only from current maximum, but also before and after this maximum. A fit to a power law was given: Y=(3.9×10<sup>-6</sup>)I<sup>5</sup>, with I in kA.

## 2.2. Essential of the electron accumulation model.

It consisted to assume for the potential between two deuteron a semi-phenomenological expression U(r), containing the most important, that is the exponential. This exponential shape of screened potential is justified both by experimental results and theoretical calculations [16] [17]. The polynomial terms (r-a) and (r-b) were supposed to take into account the extra electron density approximately at a Bohr radius distance from the nucleus, and the term (e/r-V<sub>p</sub>) takes into account the change of reference level due to electron charge depopulation around the two colliding deuterons. The term V<sub>p</sub> is equal to the sum of the Coulomb positive potentials created by electron depopulation around the two colliding deuterons and its existence is grounded on more general considerations about the electromagnetic gauge [18].

$$U(r) = e(e/r - V_p)(r-a)(r-b) \exp(-kr) \quad (1)$$

The predominant terms were recognised as being the exponential one and the so called "Pedestal potential" V<sub>p</sub>. The a and b parameters are due to the electron

accumulation, and the results were robust relatively to any changes of the  $a, b, V_p$  parameters

Table 1

The most important parameters, characterizing the Kiel and NRL experiments.

	Leading edge duration second	Voltage Volt	Current at the onset of the neutron burst Amps	Current density at the current apex, for the initial 0 of the the medium (A/mm <sup>2</sup> )	Injected energy into the medium at the onset kJ	Injected energy density at the neutron burst onset MJ/cm <sup>3</sup>	Number of neutrons per current impulse
Kiel 1974	$1.5 \times 10^{-7}$	$2 \times 10^5$	$2 \times 10^4$	$2 \times 10^4$	0.6	$10^{-2}$	$10^4 - 10^5$
NRL87	$1.2 \times 10^{-7}$	$4 \times 10^5 - 6 \times 10^5$	$5 \times 10^5$	$4 \times 10^7$	30	50	$5 \times 10^9$
NRL90	$9 \times 10^{-7}$	$5 \times 10^5$	$4 \times 10^5$	$3 \times 10^7$	$10^2$	400	$10^8$
NRL91	$8 \times 10^{-3}$	$1.4 \times 10^6$	$3.5 \times 10^5$ $4 \times 10^8$	$2.5 \times 10^7$ $4 \times 10^8$	40	$1.3 \times 10^2$ $2 \times 10^3$	$4.5 \times 10^8$

The second item was the introduction of a new relationship between the nuclear reaction rate R, the Coulomb barrier crossing rate F, the barrier width L, the barrier crossing time  $\theta$ , n being the number of nuclei which could be involved in nuclear fusion reactions, and  $\sigma$  the nuclear cross section:

$$R = (1/4) n^2 \sigma F L/\theta \quad (2)$$

The introduction of this formula was estimated as necessary, given that the Schrödinger equation showed clearly that using only deuteron velocity, like in the accustomed formula deduced from the Lawson criterion, was inconsistent in the case of low velocities and electron accumulation process [2] [3].

The results of calculations using early results given by Feodorovich [16] have shown, for a constant couple ( $k, V_p$ ), that is for a constant number of accumulated electrons around the two colliding deuterons, the logarithm of the reaction rate R was a linear relation of logarithm of the incident deuteron energy [2]. Typical results are showed on figure 6. The slope p of the straight lines is bounded by two approximative limits: 1.4 and 2. Those values are typical of a fractal dimension. But one has to emphasize on the fact that the exact number of electrons around the two deuterons, corresponding to each straight lines, is not known, and would necessitate important specific calculations which have not been possible to perform at this time.

Approximate values were given for this number, assuming that all electron were confined in a sphere whose radius was the one of Bohr, but that is rather approximate, inspite there was concordance with the stochastic point of view. The stochastic theory gives in fact in a simple way the order of range of this electron number, which seems to be mostly in the range of  $10^3$  to  $2 \times 10^3$ . [2]. This electron number corresponds to a p-value in the medium range, that is around 1.6-1.7. The stochastic point of view consists of assuming that deuterons are not submitted to any force, that is they are quasi-free in space, and that their space distribution obeys a Poisson distribution. Nevertheless, as it is shown below, the most important result which is numerically in agreement with experiments, is the existence of the straight lines and of their p-slope values.

### 3. The two ways of putting the medium into condition.

#### 3.1 The medium is put into condition by energy excess.

In all cases where the way of getting the medium into condition consists of using an electric current, the final deuteron velocity, reached by electrodynamic interactions, is proportional to the square of r.m.s. current, obtained by integration between the onset and the peak. For similar current waves differing only by the peak, the deuteron energy is practically proportional to the fourth power of the peak current:

$$E'/E = (I'/I)^4 \quad (3)$$

The fusion reaction rate R is obtained by using the results of Coulomb barrier crossing by electron accumulation. For a specific number of accumulated electrons, and for a constant number n of deuterons which can be involved in the process, the logarithm of this rate R follows a linear relationship in function of the energy logarithm Log E [2], p being the slope of this linear relationship:

$$\frac{\log R' - \log R}{\log E' - \log E} = p \quad (4)$$

Using (1), one gets:

$$R'/R = (I'/I)^{4p} \quad (5)$$

The calculation of barrier crossing provides a p value which is bounded by two approximative limits:

$$1.4 < p < 2$$

Replacing p successively by the two limits one gets a  $R'/R$  variation between  $(I'/I)^{5.6}$  and  $(I'/I)^8$ . But one has to remark that the lower limit corresponds to a greater number of accumulated electrons than the higher limit. In a dense medium the accumulated electron number would be lower than in a more diluted one, simply because electrons have a greater mean free path in a diluted than in a more dense medium. As the experimental result  $I^5$  was obtained in a plasma which has been

heated during a relatively long time [9], its expansion was relatively important, and it is logical to consider the lowest limit of  $p$ . Given that apparently this 5 value was given for "typical", the corresponding  $p$ -slope could be as low as 1.25. Taking into account the uncertainty about the real number of accumulated electrons and consequently the  $p$ -value, there is an agreement between the experimental results and the electron accumulation model.

In this case the harmonic oscillator resonance hypothesis is not useful. To understand more completely the process it would be necessary to describe more completely the chaotic phenomenon generated by the excess energy, which contributes to make quasi-free deuterons.

### 3.2 The medium is put into condition by a fast current decrease.

In the case of fast current decrease, the modeling of quasi-free behaviour of the deuterons takes into account the resonance phenomenon at the particle level. One can describe simply the link between the pattern of electrodynamic force in function of time and the behaviour of the harmonic oscillator. What is an harmonic oscillator constituted of? We make the hypothesis that it is constituted of one ion and of the electrons which are in its near proximity. Those electrons having a relatively great velocity, there is no electron structurally associated with one deuteron to build one harmonic oscillator. It is sufficient to develop a non quantum picture. The return strength  $\Delta F$  acting on the deuteron is the difference between two Coulomb forces, each being multiplied by a coefficient  $k$ . Assuming also the isotropy of electron distribution, this coefficient  $k$  will be the same on both sides:

$$\Delta F = \frac{(kq)^2}{r^2} - \frac{(kq)^2}{r'^2} \# \frac{2(kq)^2 \Delta r}{r^3} \quad (6)$$

This model is very close to "One componant plasma model", which consists of assuming that the plasma is made of one species of charged particles, flooded in a uniform medium of neutralizing charges [14]. A mono-dimensional description of the deuteron movement is sufficient for accounting the resonance phenomenon.  $m$  being its masse,  $q$  the elementary charge,  $r$  the mean distance between the deuteron and its neighbouring electrons:

$$m \Delta r'' + 2(kq)^2/r^3 \Delta r = 0 \quad (7)$$

And the own pulsation of the oscillator:

$$\Omega = (2(kq)^2/mr^3)^{1/2} \quad (8)$$

One can give a more complete description, for taking into account the interaction between harmonic oscillators. Classically, remaining in unidimensionel case, the strength exerted on the oscillator  $n$  by the oscillators  $(n+1)$  and  $(n-1)$ , is function of the specific pulsation  $\Omega$  of the  $n$  oscillator, and also of a coupling term  $\Omega_1$ :

$$F_n = -m \Omega^2 x_n - m \Omega_1^2 (x_n - x_{n+1}) - m \Omega_1^2 (x_n - x_{n-1}) \quad (9)$$

The movement equation is thus:

$$\frac{d^2x}{dt^2} = -\Omega^2 x_n(t) - \Omega^2(2x_n(t) - x_{n+1}(t) - x_{n-1}(t)) \quad (10)$$

Changing the variable and using the mean distance  $l$  between harmonic oscillators:

$$u(k,t) = \sum_{n=-\infty}^{+\infty} x_n(t) e^{-inkl} \quad (11)$$

So the equation has the same shape than the initial one (7):

$$\frac{d^2}{dt^2} u(k,t) = -[\Omega^2 + \Omega_1^2 (2 - e^{ikl} - e^{-ikl})] u(k,l) \quad (12)$$

All oscillators have resonance pulsations between two limits, depending on the mean distance between two oscillators. This interval is analog to the one of the Brillouin zone, used in Solid state Physics [12].

It is interesting to mention the link that this model could have with a natural phenomenon which has been puzzling the scientific community for two centuries, i.e. the "Ball Lightning". Without discussing this phenomenon from an experimental point of view it is interesting to remark simply that the macroscopic balance of an harmonic oscillator set is possible, only in a spherical geometry. One can assume that the low amplitude oscillator movement is along the sphere radius. Given the spherical symmetry, the sum of the forces, acting perpendicularly to the sphere radius on a particular harmonic oscillator, and due to the other oscillators, is equal to zero. Such a phenomenon is observable as much during a thunderstorm, as well when a high voltage capacitor discharges into a dense medium. Many experiments have been performed during the last years, showing that brilliant long-living objects are formed at the time of a dense aqueous low temperature plasma collapses [15]. According the testimony of many observers, the ionized spherical structure is apparently soon destroyed by a light mechanical hurt, against a solid structure. The role of this mechanical hurt must be compared with the fast current decrease in an experiment like those of Kiel or NRL. It seems possible that there could be a link between the mechanical hurt which destroys a ball lightning and the premature current interruption in experiments of the Kiel type, the premature interruption being prompted partly by the hydrodynamic instability, caused by Ampère Force, and partly by the mechanical hurt: some specific experiments could let to conclude. It seems possible that this mechanical containment could favour the instability occurrence. The mechanical hurt or the fast current decrease produces a chaos status.

### 3.3. Numerical values.

During the current leading edge, and for a typical medium density of the order of  $10^{23}$  particles per  $\text{cm}^3$ , the mean distance between two deuterons is in the  $10^{-8}$  cm range. One can assume that, without electron accumulation phenomenon, those electrons are equally distributed in space. Without any electron excess in the medium, the number of electrons around one deuteron is typically equal to 6, from a purely topological point of view. If one choose this figure for the electron number

aking part to the non resonating harmonic oscillator's operation, so  $k=3$  and with  $n=34 \times 10^{-24}$  g, one gets:

$$\Omega = 1.44 \times 10^{14} \text{ rad/s}$$

In many high peak transitory currents experiments, performed in a deuterated medium, this medium is rich in electrons: this is exactly the case in Kiel experiments, where a compound of Lithium with heavy ammonium  $\text{Li}(\text{ND}_3)_4$  was used, or in some NRL experiments where deuterated fibers were used. Given the uncertainty about the electron number, which takes part to the harmonic oscillator operation, it is in fact possible to ascertain only that  $\Omega$  is typically of the order of  $10^{14}$  rad/s. In the case where one deuteron is so close to another for initiating the collision and electron accumulation process, leading to nuclear reaction, is the model pertinent? The pulsation is much higher in this case,  $r$  being typically in the range of  $10^{-9}$  cm, the electron number around the two deuterons being typically of the order of  $1 \times 10^3$  to  $2 \times 10^3$  [2]. With  $k=10^3$ , one gets:

$$\Omega = 2.6 \times 10^{17} \text{ rad/s}$$

The pulsation would be about at least  $10^3$  times higher when two deuterons are approaching together. However this model does not seem useful during the collision phase, the Coulomb barrier crossing being described by the Schrödinger equation, and the deuteron energy, supplied to the deuteron by the electrodynamic forces, being supposed constant during this crossing.

### 3.4. Forced movement of the harmonic oscillator, caused by a fast transitory current.

The description is purely classical. the equation of the harmonic oscillator forced movement is simply:

$$x'' + \Omega^2 x = (1/m) F(t) \quad (13)$$

One can get an estimate of the velocity which is given to the ions by harmonic oscillation, if one uses a realistic phenomenological current pattern. In first approximation, sufficient for getting a general delineation of the process, a "sawtooth" pattern is useful for describing the current wave, as well for Kiel experiments, as for the ones of NRL. The leading edge is thus a linear function:

$$F(t) = F_0 \frac{t}{\theta_0} \quad 0 < t < \theta_0 \quad (14)$$

Deuteron velocity, due to electrodynamic forces, is obtained by neglecting the electromagnetic waves propagation time in the inner part of the conduction canal:

$$x' = \frac{F_0}{\Omega^2 \theta_0} (1 - \cos \Omega t) \quad (15)$$

The first term corresponds to the collective deuteron velocity directed toward the conduction canal's axis. The second term describes the periodic movement of the harmonic oscillator.

The trailing edge is represented by the second part of the saw-tooth:

$$F(t) = F_0 \left( 1 - \frac{t - \theta_0}{\theta} \right) \quad \theta_0 < t < \theta_0 + \theta \quad (16)$$

Thus the deuteron velocity, during the current decrease, depends on the current growing time  $\theta_0$ , and also on the decreasing time  $\theta$ : this is a pure oscillatory process:

$$x' = \frac{F_0}{m\Omega^2} \left[ \left( \frac{1}{\theta_0} + \frac{1}{\theta} \right) \sin \Omega(t - \theta_0) - \frac{1}{\theta_0} \sin \Omega t \right] \quad (17)$$

The strength, acting on the deuteron, is practically the Lorentz force, particularly for the maximum  $F_0$ ,

$$F_0 = q v_0 B \quad (18)$$

$v_0$  being the medium collective velocity at the time of current maximum, corresponding to the maximum of the electrodynamic forces. At a specific point, located at the  $r$  distance from the axis,  $R$  being the radius of the conduction canal, one gets the induction  $B$  in function of the maximum current:

$$B = \frac{\mu_0 I r}{2\pi R^2} \quad (19)$$

Transferring the  $F_0$  expression in function of the velocity  $V_0$  and the induction  $B$ , brings to the fore the velocity amplification, the maximum velocity  $v$  being:

$$v = \frac{\mu_0 q v_0 I r}{m\Omega^2 2\pi R^2} \left( \frac{1}{\theta_0} + \frac{1}{\theta} \right) \quad (20)$$

For a numerical evaluation, one can consider the point just in the middle between the axis and the periphery of the cylindrical conducting canal, that is  $r=R/2$ . One can thus introduce the velocity amplification factor  $f$ , such as  $v = f v_0$ :

$$f = \frac{\mu_0 q v_0 I}{m\Omega^2 4\pi R} \left( \frac{1}{\theta_0} + \frac{1}{\theta} \right) \quad (21)$$

In comparison with the equation which rules the velocity during the current growth, the only difference is the change of the factor  $1/\theta_0$  into  $(\theta+\theta_0)/\theta\theta_0$ . If the trailing edge is much shorter than the leading edge, its duration only rules the process. For a trailing edge duration  $\theta_0$  equal to the leading edge duration  $\theta$ , the maximum deuteron velocity during the resonance is early multiplied by the 2 factor. But a shorter trailing edge would give the possibility to get a more effective quasi-

43/12

accelerating effect of the deuteron. One has also to notice that the formula (14) cannot be compared completely with the (16) one, because the medium is only in its growing ionization phase, during the leading edge. In another terms  $F_0$  has necessarily not the same value in (15) and (17) formulas. Nevertheless the deuteron velocity amplification does exist during the leading edge, but it becomes important to cause collisions leading to nuclear reactions by electron accumulation, only when the current stops to grow. The formula (20) suppose that the peak current is reached in a sufficiently long time, for getting a high ionization level: this is the case of the experiments related in references [4-6]

The maximum deuteron energy  $E$ , accelerated by resonance is thus proportional to  $(v_0 I)^2$ . Given that  $v_0$  is proportional to the square of peak current  $I$ , the deuteron energy is thus proportional to the sixth power of the peak current. In the case where this decreasing time  $\theta$  is sufficiently short in comparison with the growing time  $\theta_0$ , the maximum deuteron energy is also inversely proportional to the square of the current decreasing time.

$$E \approx I^6 \theta^{-2} \quad (22)$$

Like in the case where the medium is put into condition only by an excess of energy, one can get the nuclear reaction relative rate of variation, using the results of the nuclear reaction rate calculations [2], in function of energy, for a constant number of accumulated electrons, according to the (4) relation.

$$\log R'/R = p [6 \log (I'/I) + 2 \log (\theta/\theta')] \quad (23)$$

Calculations give for the  $p$ -parameter a value which is bounded by 1.4 et 2, according to the number of electrons accumulated around the two colliding deuterons. On the figure 3, reproduced from reference [6], the slope of the regression straight line, summarizing the experimental results, seems in fact closer to 8.5, instead of the 10 value claimed by the authors. The corresponding  $p$ -parameter is thus 1.41, and the accumulated electron number is rather high. But if one accept the value of 10 which is proposed by the authors, then the  $p$ -parameter is equal to 1.66, which corresponds, according to the calculations, to a lower number of accumulated electrons around the two colliding deuterons.

$$R'/R = (I'/I)^{10} \quad (24)$$

What it is important is that the  $p$ -value, deduced from experimental results, is in the range of the Coulomb barrier calculations. But one has also to emphasize on the fact that those crossing barrier calculations have not yet been performed with sufficient matrix dimensions [2]. Given this fact, the concordance can be estimated rather good between calculation and experiment. The same experiments, performed with lithium dissolved in heavy ammonia would have probably given a different result, but the  $p$ -value would be slightly different, given that the outcome of the experiments depends of many parameters, for example the density of the medium, which was different in the Kiel and NRL experiments.

The harmonic oscillator hypothesis putting the medium into condition on the particle scale, is thus validated by NRL experiments. One has also to remark that the

current density is relatively more important in the NRL experiments than in the Kiel experiments. This is an supplementary clue showing that the electron richness play a great role in the process.

#### 4. Experimental representative points, in the (Log T/T<sub>0</sub>, Log E/E<sub>0</sub>) diagram.

The current square integral can be supposed varying little, in first approximation, during the nuclear fusion reaction burst, as its duration is short in comparison with the current rising duration.

According the formula (20), the maximum deuteron velocity is achieved multiplying the velocity  $v_0$  by the f factor. If one chooses, for example, the parameters of Kiel experiment,  $I = 2 \times 10^4$  A,  $\theta = 10^{-7}$  s,  $R = 0.05$  cm, for a density of  $10^{23}$  particles per  $\text{cm}^3$ , and if one uses the pulsation of the elementary oscillator, according to (7), surrounded by a electron cloud, corresponding to an approach leading to a collision ( $\Omega = 1.44 \times 10^{14}$  rad/s), one gets a f-value in the  $10^6$  range. It could mean that the collective velocity at the apex should be multiplied by  $10^6$ . It would contradictory, that such a corresponding energy on the deuteron level would imply an energy quantity largely greater than the density of  $10 \text{ kJ/cm}^3$ , injected in Kiel experiments. The amplitude of the maximum deuteron displacement, gives more information. The deuteron maximum energy is then in the  $10^2$  eV range, corresponding to a maximum  $10^7$  cm/s velocity, and to an oscillation amplitude of the order of  $3 \times 10^{-8}$  cm/s. So oscillation amplitude is of the order of the distance between deuterons, for  $10^{23}$  particles per  $\text{cm}^3$ . The resonance of harmonic oscillator, constituting the medium, prompts collisions between deuterons, and a certain amount of thermalisation, by inelastic collisions. The quoted maximum amplitude velocity is difficult to reach, given the high density of the medium. The rate of deuterons participating to an electron accumulation, before thermalization is a growing function of density. So medium operation, leading to collisions and electron accumulations can be considered as being ruled by the thermal deuteron energy (of the 0.6 eV order in the Kiel case) (Figure 6).

The thermal energy is also the good parameter in the cas of case of NRL experiments performed in the eighties [6]. This energy is approximately  $2.5 \times 10^3$  times higher than in the Kiel experiments, that is approximately the ones obtained by cluster collisions in Brookhaven [19].

As for the Y-values, taking into account Helium 4 production rate which could be  $10^5$  to  $10^6$  times higher than the one of Hélium 3 [11], the new representative point of Kiel is well apart from the one drawn in the references [1] and [2], but it is nevertheless outside the thermonuclear range (Figure 6). For an neutron production rate, rectified approximately to  $10^{10}$ , the representative point of the NRL experiments performed during the eighties [6], is then a little above the Brookhaven point. With the parameter T proportional to R (such as  $T = \sigma F L/\theta$ ), the Kiel and NRL points are close to a straigth line in the diagram (Log T/T<sub>0</sub>, Log E/E<sub>0</sub>), which could correspond approximately to a number of accumulated electrons between  $1 \times 10^3$  and  $2 \times 10^3$ . However, as was shown before, it is not yet possible to put forward any more precise number.

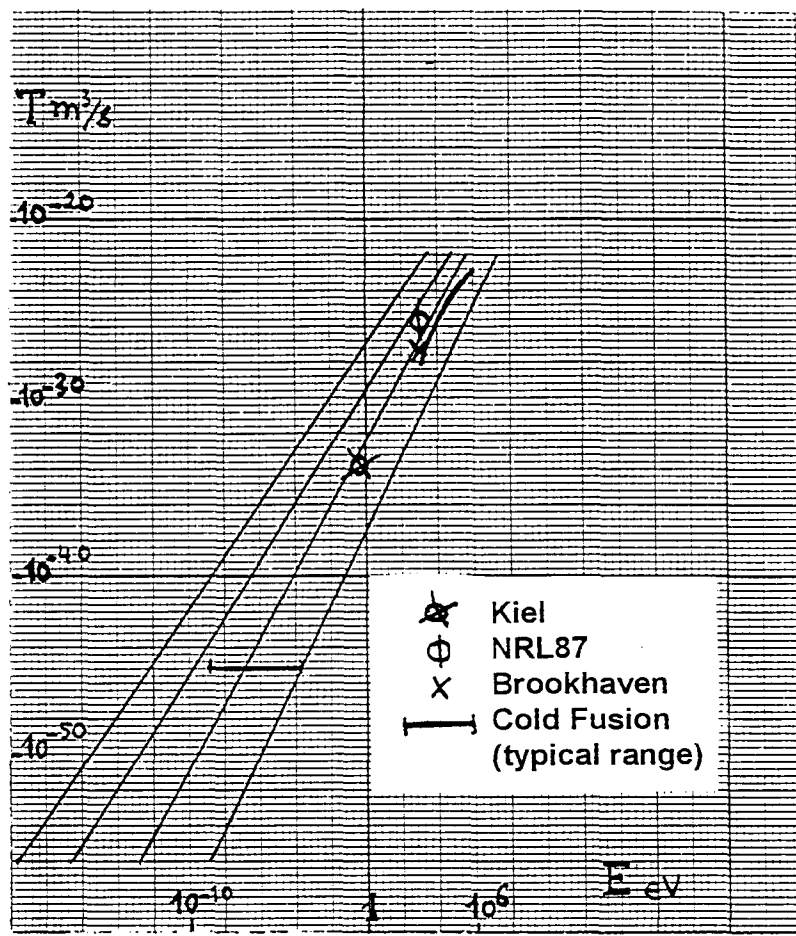


**Figure 6** Estimated position of the representative points for Kiel, NRL and also Brookhaven experiments, in the  $(\log E/E_0, \log T/T_0)$  diagram, taking into account the harmonic oscillator resonance. The results of barrier crossing calculations, after correction due to a limited matrix dimension number, give straight lines for a constant screening couple  $(K, V_p)$  (2).  $K$  is given in  $\text{cm}^{-1}$  and  $V_p$  in volts:  
 (  $3.22 \times 10^9 \text{ cm}^{-1}, 6.27 \times 10^2 \text{ volt}$  ) - ② (  $3.78 \times 10^9 \text{ cm}^{-1}, 2.01 \times 10^3 \text{ volt}$  ) - ③ (  $5.81 \times 10^9 \text{ cm}^{-1}, 4.59 \times 10^3 \text{ volt}$  ) - ④ (  $1.38 \times 10^{10} \text{ cm}^{-1}, 5.91 \times 10^4 \text{ volt}$  ).  
 Arc of curve D-D: thermonuclear process.

There is also another parameter which one would have to take into account, that is the possible dependance of the accumulated electron number on the medium density. Whatever would be the exact number of those accumulated electrons, their number is close to the one given by the stochastic model. The segment of straight line representing the specifically so called "cold fusion" experiments is obtained assuming the same high  ${}^4\text{He}$  number, as before. If one assumes also the electrodynamics forces effectiveness, which could be due to internal field transitory in the Palladium, and if one assume an  $f$  factor in the same range as before, one gets a segment of straight line, shifted toward higher energies and higher production rates, in comparison with [1] et [2] papers.

## 5. Conclusion

The correlations between theoretical calculations and experimental results give a greater consistency to the two points of view. Firstly it reinforces the NRL results which could have been looking as inexplicable. Secondly it reinforces the point of view of nuclear fusion by electron accumulation.

Given that all experiments have their place in the  $(\log R/R_0, \log E/E_0)T$  diagram, the experimental  $I^{15}$  and  $I^{10}$  laws give in fact a larger view on the cold fusion process. What is occurring while a fast current impulse is flowing in a deuterated medium, is really a cold fusion process. It is similar to the process which occurs during introduction of deuterium into Palladium, used as a substrat, whatever is the way of introducing this deuterium. In another terms, this phenomenon is possible as much in a plasma, formed by introduction of deuterons into Palladium, used as a substrat, than in a plasma formed by high voltage, high current discharges. Macroscopically and experimentally the processes seem very different, but they are the same on particle level.

## References

- [1] M.Rambaut, Physics Letters A 163 (1992) 335-342, 30 march 1992.
- [2] M.Rambaut, Physics Letters A 164 (1992), 155-163, 13 April 1992.
- [3] Lawson criterion made obsolete by cold fusion through the double screening process, M.Rambaut, ICCF3, Nagoya, October 21-25, 1993, 601-604.
- [4] - U.Fischer, H.Jäger and W.Lochte-Holtgreven, Physics Letters, Volume 44B, number 2, 16 April 1973.
  - W.Lochte-Holtgreven, Proceeding XIth International Conference on Phenomena in Ionized Gases, Prague 1973. Invited Lecture "Fusion Research at High Densities". (Edited by L.Pekarek and L.Laska).
  - W.Lochte-Holtgreven, Atomkernenergie (ATKE) Bd.28 (1976) Lfg.3, 150-154.
- [5] S.K.Händel and O.Jonsson, Atomkernenergie (ATKE) Bd.36 (1980) Lfg.3, 170-172.
- [6] J.D.Sethian, A.E.Robson, K.A.Gerber, and A.W.DeSilva, Physical Review Letters, Volume 59, Number 8, 24 August 1987. 892-895. See also the rectification for neutron detector calibration (Phys.Rev.Letters, March 1992).
- [7] Astrophysical Formulae, Springer-Verlag, 1986, page 385-389.
- [8] J.D.Sethian, A.E.Robson, K.A.Gerber and A.W.DeSilva. Evolution of a deuterium Fiber Z-Pinch driven by a long current pulse. Workshop on Alternative confinement scheme, Varenna, Italy, October 1990.
- [9] K.C.Mittal, D.H.Kalantar.N.Qi, and D.A.Hammer (Cornell University), K.A.Gerber and J.D.Sethian (NRL), J.Appl.Phys. 70 (11), 1 December 1991.
- [10] - Anurag Shyam and M.Srinivasan, Appl. Phys. 17, 425-426 (1978).
  - Anurag Shyam and M.Srinivasan, Atomkernenergie-Kerntechnik Bd.40 (1982) Lfg.4

- [11] Hikori SAKAGUCHI, Gin-ya ADACHI, ICCF3, Third International Conference on Cold Fusion, October 21-25, 1992, Nagoya, Japan, Universal Academy Press, Tokyo, 1993, pages 527-530.
- [12] Charles Kittel, Introduction to Solid State Physics, John Wiley, 1986.
- [13] Alpha-, Beta-, and Gamma-ray spectroscopy, edited by Kai Siegbahn, North-Holland Publishing Company, 1979.
- [14] Setsuo Ichimaru, Rev. Mod. Phys., Vol. 65, N°2, April 1993.
- [15] P.I. Goloubnitchi, V.M. Gromenko, V.M. Kroutov, Journal of Tech. Phys., Vol 60, Booklet 1, 183-186, 1990. (In Russian)
- [16] G.V.Fedorovich, Physics Letters A 164 (1992) 149-154, & Fusion Technology, Vol. 23, 442-464, July 1993.
- [17] M.Rabinowitz, Mod. Phys. Lett. B4 (1990) 665.
- [18] Costa De Beauregard, Statics of Filaments and Magnetostatics of currents: Ampère tension and the vector potential, Phys.Letters A, In press.
- [19] R.J.Behuler, G.Friedlander, and L.Friedman, Physical Review Letters, Volume 63, Number 12, 18 September 1989, PP 1292-1295.

\*\*\*\*\*



POSSIBLE EXHIBITION OF THE ERZION - NUCLEAR  
TRANSMUTATION IN ASTROPHYSICS

Yu.N.Bazhutov  
Scientific Research Center of  
Physical Technical Problems "Erzion"  
P.O.Box 134, 119633 Moscow, Russia  
Fax: (095) 292-6511 Box 6935 Erzion

**Abstract**

There are a lot of anomalous astrophysics phenomena, which can not be explained in the frameworks of traditional theoretical models. Erzion-nuclear transmutation, if it real exists, can explain some of them: 1.Davis effect; 2. Jupiter radiation; 3. Sygnus-X3 problem etc.

In modern astrophysics there are a lot of anomalous phenomena, which can not be explained in the framework of traditional theoretical models. Some of such phenomena are following: 1) Solar neutrino flux is 2,5 times smaller then one can suppose from Solar thermonuclear models (Davis effect) [1]; 2) correlation of Solar neutrino flux with Solar radioactivity (11-yars cycle) [2]; 3) Jupiter's radiation excess more then twice of its consuming Solar energy [3]; 4)catastrophic reducing of Li,Be,B contents in the chemical elements abundance curve of Solar and Earth matter [4]; 5) big flux of neutral high energy particles from local spacesources (Sygnus-X3 problem) [5].

The 1,2,3-th phenomena may be explained by hypothesis of Erzion nuclear transmutation which takes place in Solar and Jupiter matter. More detail investigation of these processes was done in paper [6].

The Erzion nuclear transmutation phenomenon is the nuclear transmutation process, which is going due to new elementary particles (Erzions and Enion) [7]. These particles are catalysts of this process. Their concentration in matter is very negligible ( $10^{-22}$  -  $10^{-17}$  per nucleon). But it is enough for nuclear reactions which are going in dense matter with high intensity ( $10^{10}$  -  $10^{15} \text{ cm}^{-3} \text{ sec}^{-1}$ ).

According to the Erzion Model the nature of processes in the Sun is so that not only thermonuclear fusion

reactions are running in the center of the Sun, but a mechanism of cold nuclear transmutation by erzion catalysis works too with energy balance about 70% or more. But in contrast to thermonuclear fusion it is running in the almost complete volume of the Sun.

So the Solar neutrino flux is three times smaller than it is believed in thermonuclear models. It correlates with Solar irradiation cycle, provided by processes in external strata of the Sun. As for Jupiter it is possible in the framework of Erzion Model that all its heat excess is provided by running of the cold nuclear transmutation reactions. In this case this process works only in small part ( $10^{-5}$ ) of Jupiter mass.

The 4-th anomalous phenomenon is described by the important feature of Erzion Model in which Li,Be,B - chemical elements with the deuterium are the best fuel among all existing chemical elements [6,8].

The last 5-th anomalous astrophysics phenomenon reflects the fact that in cosmic rays physics local space sources of high energy particles were found. The interactions of these particles shows that they must be neutral stable hadrons ( $t > 10^{12}$  sec). The same particles do not exist in standard elementary particles theoretical models. But erzions and enions are the same stable neutral hadrons as must be for explaining of this problem.

In conclusion I want to thank G.M.Vereshkov who gives strict theoretical basis for existence of erzions and enions in nature.

#### References

- 1.R.Davis et al. Proc.20-th International Cosmic Rays Conference, Moscow, 1987, 4, 328-355
- 2.R.Davis,B.T.Cleveland,J.K.Rowley.Proc.2-th International Symposium "Underground Physics, Moscow, 1988, 6-14
- 3.S.E.Jones,I.Rafelski et al.Preprint BYUPHYS, 1989,338-389. Phys.Values,Handbook,Moscow,Energoatomizdat,1991,1174
- 5.B.M.Vladimirsky, A.M.Galper, B.I.Luchkov et al. Uspekhi of Physical Science (UPS), 1985, 114, 255
- 6.Yu.N.Bazhutov, G.M.Vereshkov."Possible Role of Cold Nuclear Fusion by Erzion Catalysis in Solar and Planetary Physics" Proc."Cold Nuclear Fusion", CSRIMash, 1992, 29-32
- 7.Yu.N.Bazhutov, G.M.Vereshkov. "New Stable Hadrons in Cosmic Rays, their Theoretical Interpretation and Possible Role in Cold Nuclear Fusion Catalysis", Preprint N1, CSRIMash, 1990
- 8.Yu.N.Bazhutov, A.B.Kuznetsov. "Erzion-Nuclear Spectroscopy of Stable Isotopes", Preprint N4, CSRIMash, 1992

# ISOTOPIC AND CHEMICAL COMPOSITION CHANGES IN COLD FUSION EXPERIMENTS IN THE ERZION MODEL

Yu.N.Bazhutov, A.B.Kuznetsov  
Scientific Research Center of  
Physical Technical Problems "Erzion"  
P.O.Box 134,119633 Moscow, Russia  
Fax: (095) 292-65-11 Box 6935 Erzion

## Abstract

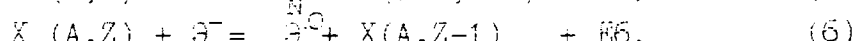
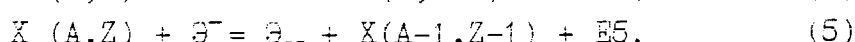
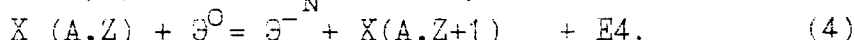
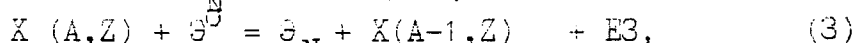
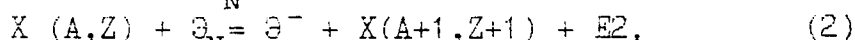
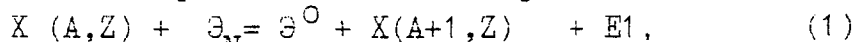
In framework of the Erzion Model it is given the explanation of isotopic and chemical compositions changes which took place in cold fusion experiments ( Rolison and O'Grady, Bush, Romodanov et al.). It is demonstrated that nuclear transmutation is important quality of Erzion Model. It is suggested some most sensitive methods of nuclear transmutation process analysis in traditional cold fusion experiments. The investigated phenomenon in the framework of Erzion Model becomes not fusion but transmutation.

### 1. Introduction

Cold fusion is considered in Erzion Model as cold nuclear transmutation by erzion catalysis. Nuclear reactions are running not by fusion process but by nucleon splitting and simultaneous nucleon adding to substantiating nuclei in accordance with energy advisability. A disguise of one phenomenon by another explains by identity of the fusion and the transmutation on deuterium nuclei. On heavy nuclei this process differs fundamentally.

### 2. Erzion Model and Nuclear Transmutation

In framework of Erzion Model /1/ the following six channels of reactions take place on each isotop :



where : X - element with atomic mass A and atomic number Z;

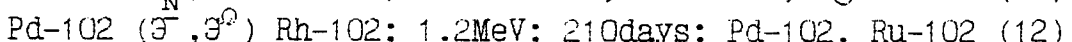
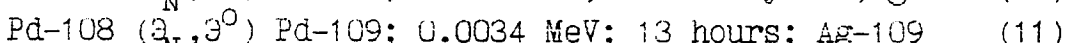
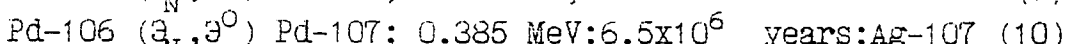
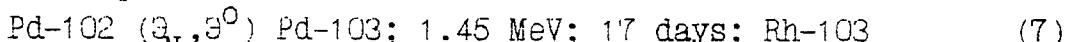
$\beta^-$ ,  $\beta^0$  - ion, negatively charged and uncharged erzions respectively; E1-E6 - reaction output energies.

Some of these reactions are exothermic and other-endothermic. Only exothermic reactions are running because of enions and erzions (reactions catalysts) have rather small energies. So if we know enion bond energies during dissociation to  $(\beta^-, p)$  pare and to  $(\beta^0, n)$  pare, we can find these exothermic reactions. Investigation of these reactions was done for all chemical elements in our work /2/.

### 3.Explanation of Transmutation Results.

In observing report /3/ J.Bockris told about Rolison and O'Grady /4/ experiment results on isotopic and chemical compositions changes (ruthenium, rhodium and silver elements appearance) of palladium cathode during electrolysis with heavy water. Interpretation of this experiment was done earlier /5/. Now we describe it shortly.

Palladium have six stable isotops. Therefore 36 reactions of (1) -(6) type take place. 29 reactions from them are prohibited as endothermal. Only seven reactions can take place by energy considerations /2/. These reactions are follows:

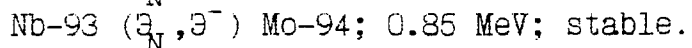
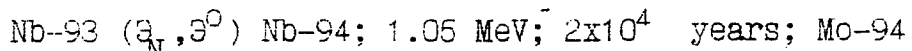


There are introduced the additional data: output energy, half-time and product of decay.

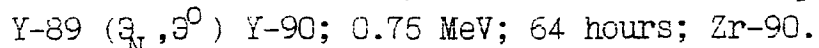
From (7)-(9),(11) it follows that quantity of Pd-102,104,105 must decrease considerably and Pd-108 -unconsiderably (Fig.1). Increase of Pd-106 quantity (9) is more speedily than its decrease (10). From (10) it follows, that practically stable isotop of Pd-107 appears. From comparison of (8) and (9) it follows, that quantity of Pd-105 must decrease also. Fast decay of Pd-109 gives Ag-109. From (7) and (12) it follows appearance of rhodium and ruthenium. Conversion of neutral erzion into enion originates due to deuterium in reaction (3). Reaction (!) for deuterium is uncompetitive analogous reaction for Pd isotops. Therefore appearing quantity of tritium must be considerably slower than appearing quantity of energy in reactions with Pd. It is coincided with experimental peculiarity of cold fusion: considerable predominance of heat

output over tritium output-noted Bockris/3/.

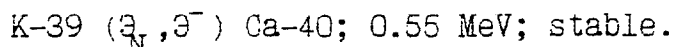
It is observed /6/ considerable increase of niobium-94 and absence of niobium-95. From Erzion Model it follows:



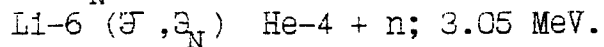
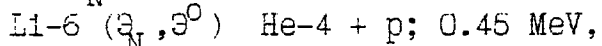
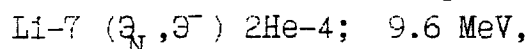
It is reported also /6/ the estimation of yttrium-90 generation from natural yttrium, that has a simple explanation:



In works /7,8/ it was registrated a generation of calcium-40 from kalium-39. The Erzion Model gives the following reaction:



M.Miles and B.Bush/9/ reported about generation helium from lithium. The Erzion Model gives the explanation of this fact:



So, the Erzion Model gives sufficient explanation of isotope and element changes in some experiments.

### References

- 1.Yu.N.Bazhutov,G.M.Vereshkov. "New Stable Hadrons in Cosmic Rays, their Theoretical Interpretation and Possible Role in Cold Nuclear Fusion Catalysis ",Preprint CSRIMash,1,1990.
- 2.Yu.N.Bazhutov, A.B.Kuznetsov. Erzion-nuclear Spectroscopy of stable Isotops. Preprint N4, CSRIMash, 1992
- 3.J.O'M.Bockris et al."A.Review of the Investigations of the Fleischman-Pons Phenomena".Fusion Technol.,v.18,N1,p.11,1990
- 4.D.R.Rolison,W.E.O'Grady. Proc. NCE/EPRI Workshop "Anomalous Effects in Deuterated Materials". Washington, 1989
- 5.Yu.N.Bazhutov, A.B.Kuznetsov,G.M.Vereshkov. Interpretation of CNF Experiments Results on Isotopic and Chemical Composition Change in Framework of Erzion Catalysis Model. "Cold Nuclear Fusion", USRIMash, 1991, p.33-36
- 6.V.A.Romodanov. "Nuclear Fusion in Condensed Matter". Proc.of the Third Intern.Conf.on Cold Fusion.Nagoja,Japan,1992,p.307
- 7.R.T.Bush "A Light Water Excess Heat Reaction Suggevts...", Fusion Technol. , v.22, p.301, 1992
- 8.R.Notoya,M.Enyo."Excess Heat Production in Electrolysis of Potassium Carbonate Solution with Nickel Electrodes" Proc.of the Third Intern.Conf.on Cold Fusion.Nagoja,Japan,1992,p.412
- 9.M.H.Miles and B.F.Bush."Search for Anomalous Effects Involving Excess Power and Helium during D<sub>2</sub>O Electrolysis Using Palladium Cathodes".Ibid, pp 189-198.

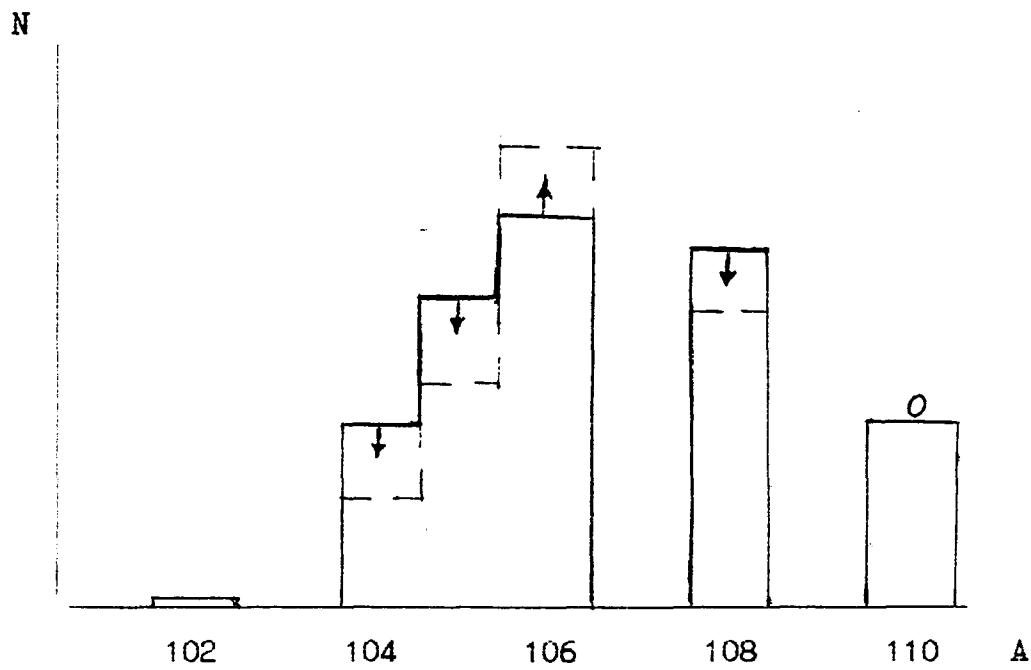


Fig.1 Palladium isotopic composition in experiment /3/

A - atomic mass, N - relative abundance,  
 solid line - before experiment,  
 dashed line - after experiment.

The Erzion Model predictions :

(↓) decrease, (↑) increase, (0) no change of N

BURNING AWAY OF RADIOACTIVE  
AND PRODUCTION OF SOME STABLE ELEMENTS  
WITHIN THE FRAMEWORK OF THE ERZION MODEL

Yu.N.Bazhutov, V.P.Koretsky, A.B.Kuznetsov.  
Scientific Research Center of  
Physical-Technical Problems "Erzion"  
P.O.Box 134, 119633 Moscow, Russia

**Abstract**

The possibility of elements transmutation in radioactive wastes of nuclear reactors was analized within the framework of the Erzion Model. The conditions for the majority of longlived isotopes Tc-99, I-129, Cs-137 et al. to be stable or short-lived (tens of hours) were defined. Furthemore some projects of the great practical significance can be implemented, for instance a doping of semiconductors by elements-donors (silicium - by phosphorus, germanium - by arsenium). Generation of gold Au-197 from mercury Hg-198 is one of the most attractive projects of the elements production.

**1. Burning away of Wastes**

The problem of the long-lived radioactive wastes transmutation or processing into the short-lived or stable ones occurred with the putting into operation the first nuclear reactors. This problem must be solved as quickly as possible. The wastes processing in fast reactors is one of radical way destruction. However a lot of money and time should be expended to demonstrate the technical possibility of this transmutation. For instance, it takes 4-7.5 billions US dollars and 15 years for realization such project [1].

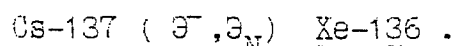
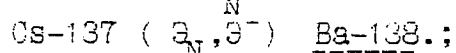
The wastes of nuclear reactors fuel after 10 years exposure maintain (by mass) 96% of uranium, 0.3% of longlived fission products (LFP), and about 1% of transuranium products (TP). The Table 1 shows the main isotopes of LFP and TP with maximum radiation hazard and their half-life. Possible reaction channels for the isotopes with the enion  $\Theta_N^+$  and the erzions  $\Theta^0$  and  $\Theta^-$  were analised with the help of erzion model [2-4]. These particles through the model may yield the most energy benefit exchanges of nucleons among nuclei. The enion is formed as the combination of neutral erzion with neutron (bonding energy  $E=6.15$  MeV) or negative erzion with proton ( $E=7.75$  MeV). There are six possible channels of nuclear reactions on each isotope with enion or erzions [3].

Table 1.  
The isotopic composition of wastes of nuclear reactor fuel.

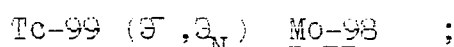
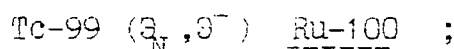
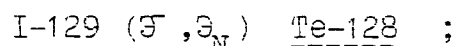
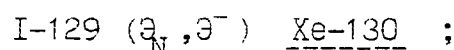
Wastes type	Longlived fusion - products	Transuranium products
Isotope Sr-90 Cs-137 I-129 Tc-99 Np-237 Am-241 Am-243 Cm-244		
Half-life,y 29 30	$1.6x \times 10^6$	$2 \times 10^5$ 432 7400 18

### 1.1.Long-lived fusion products

For Strontium - 90 all six channels are forbidden. On this reason the transmutation of this isotope can not be realized in the framework of the erzion model. Another isotopes of LFP may be effectively burned away under certain conditions. For Cesium - 137 two channels are allowed. It provides turning out the stable elements - Barium-138 and Xenon-136 in closed chain conversions  $\Theta_N \longleftrightarrow \Theta^-$ :



There are four allowed reaction channels for last two elements of LFP ( Iodine - 129 and Technetium - 99). Two channels provide turning out the stable elements with closed cycles of conversion  $\Theta_N \longleftrightarrow \Theta^-$ . The other two channels provide turning out the radioactive isotopes but with the relatively low half-life ( a maximum of 66 hours ):

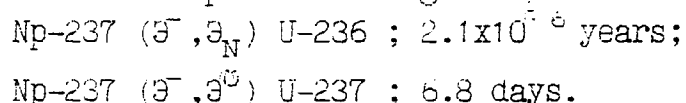


As the upper equations indicate, there are some channels with a loss of neutral erzions. To prevent these losses one may add some elements to initial LFP for converting the neutral erzions into the enions or negative erzions. There are about ten such elements in nature. The cheapest of them are

Deuterium, Lithium-6 (7.4%) and Beryllium - 9 (100%). It is desirable to prepare a homogeneous mixture of these elements with the initial radioactive isotope to ensure the effective reactions. It may be difficult problem to prepare Deuterium saturated isotopes. When Beryllium is used, the Beryllium-10 isotope will arise. It is beta-active isotope with more than one billion years of half-life. The Lithium-6 may be more preferable converter in which a stable Lithium-7 and Lithium-5 with Helium-5 will arise. Last two complexes decay instantly into proton, Helium-4 and alpha-particle, neutron respectively. Thus, the most part of LFP may be transmuted in the framework of the Erzion model.

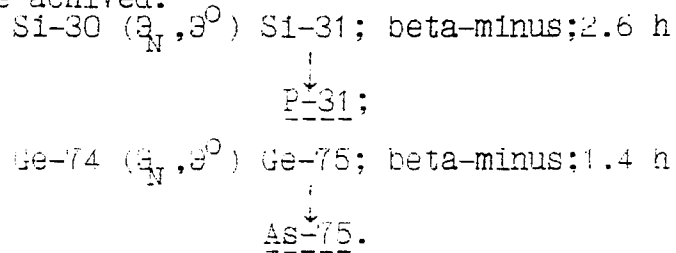
### 1.2. Transuranium products

The transmutation prediction for TP is not such optimistical. Two from six channels are allowed for each isotope of TP and reactions with negative erzions take place for both channels. This fact causes two negative consequences. Firstly, these two channels do not form the closed cycles with enion or erzions. Secondly, one of the turning out radionuclides has much more half-life than initial isotope of TP. As an illustration the possible reactions for Neptunium are given below:

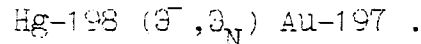


### 2. Production of Stable Isotopes

The Erzion Model makes possible to predict of turning out of stable elements for some practical implementations. For example, one may to initiate the reaction with enions in semiconductor material. It could result in generation of new stable elements which will be donors for the initial material. In this way a doping of Silicon by Phosphorus or Germanium by Arsenic may be achieved:



It may be of some interest to suggest a possible solution of the classic alchemical problem - to convert mercury into gold by the reaction:



It should be pointed out that the probability of such process is not sufficiently large. This is because the natural occurrence of this mercury isotope is equal to 10% and the closed cycles of reactions are absent.

### **3. Summary**

To summarize, we can say that the Erzion model of nuclear transmutation may be a useful tool for realization of some fundamentally new processes in such fields as burning away of radioactive wastes and semiconductors doping.

### **References.**

- 1.Y.V.Sivincev. "Transmutation of Radioactive Wastes with Accelerators". Atomnaya Tehnika za Rubezhom 1992, No 2,p.3.
- 2.Yu.N.Bazhutov, G.M.Vereshkov."New Stable Hadrons in Cosmic Rays, their Theoretical Interpretation and Possible Role in Cold Nuclear Catalysis". Preprint No 1, CSRIMash,1990.
- 3.Yu.N.Bazhutov, A.B.Kuznetsov. "Erzion-Nuclear Spectroscopy of Stable Isotopes". Preprint No 4, CSRIMash.1992.
- 4.Yu.N.Bazhutov,G.M.Vereshkov. "Model of Cold Nuclear Fusion through Erzion Catalysis". Cold Nuclear Fusion, Kaliningrad: CSRIMash.1992.pp.22-28.

**4th International Conference on Cold Fusion, 6-9 December 1993**  
**Lahaina, Maui, Hawaii, USA**

**SYNERGETIC ACTIVATION MODEL:  
KEY TO INTENSE AND REPRODUCIBLE COLD FUSION**

V.A.Filimonov  
Institute of Physicochemical Problems, Belarus State University  
14 Leningradskaya Str., Minsk 220080, Belarus

**Abstract**

It is stated that poor reproducibility of Cold Fusion (CF) is a sequel of non-execution of some important conditions of CF implementation been unknown. The Synergetic Activation (SA) model been created to resolve noted problem supposes that more gently sloped than exponential one distribution of atoms by energy fluctuations is implemented in highly non-equilibrium systems. SA model proposes certain mechanism of such redistribution concerned with CF and some other phenomena (chemical ones in particular). Noted mechanism is caused by the selforganization of matter in nonlinear wave front under shock (or detonation) wave action to solid or self-generation of the same within it. Conditions of noted self-generation (and self-focusing too) such as phase transition or phase separation region implementation in the system under experimental run and low extended defects content (dislocations,  $< 10^5 \text{ cm}^{-2}$ ) - are the key parameters execution of those is necessary for intense and reproducible CF implementation. Verification of the model using published experimental data is made successfully. A method of obtaining low-defect specimens for using as cathodes or targets in CF experiments and applications is claimed.

**Introduction**

The main controversy of any Cold Fusion model is: - to be consistent with the main principles of physics but to deal with phenomenon unpredictable from the main physics principles point of view. How is it possible?

Sergey Meyen (1933-1987, Russia) had proposed so-called principle of correspondence according to which: it is possible to set aside certain region of parameters (core) in phase space for any natural law to be executed in common inside that; the core to be surrounded by another region of parameters (periphery) noted law to be executed partly or sometimes within that; outside periphery noted law isn't executed at all. Noted parameters may be not evident and not elementary ones (unlike temperature, pressure, density, concentration etc.). Resolution of CF controversy is possible in framework of supposition that it is situated in the region of periphery of classical atomic and nuclear physics laws (1).

Possibility of CF implementation, from one hand, and CF experiments irreproducibility, from the other hand, may be caused therefore by unknown nature of key parameters. In the case it is impossible to control if their values correspond to the core region or no. The probability of eventual and coincidental situation of some non-common and non-controlled parameters in the core region is rather low.

### **Synergetic Activation Model: Speculations**

**What Are The Key Parameters for Cold Fusion?** The synergetic activation (SA) model (2) supposes that these parameters not considered by traditional nuclear physics are: the degree of non-equilibrium of a system and the degree of order of a substance.

Within the SA model approach intense CF implementation at "normal" temperatures and pressures is the sequel of self-organization processes in crystalline matter. Such situation differs significantly from "classical" approach in framework of which interaction between atoms to be stochastic one. Strongly non-equilibrium system, for our opinion, is such one which only unidirectional action takes place in.

#### ***The main points of SA model are as follows:***

1. The more gently sloped than exponential one distribution of atoms by energy (namely quasi-power one) that makes overcoming potential barriers by the system easier is possible in selforganizing systems.
2. Such distribution is realized in spatiotemporal limits of shock or detonation waves (SW and DW correspondingly) fronts that are therefore considered as dynamical dissipative structures.
3. A self-generation of SW (DW) and self-focusing of the same that promote gathering of energy in focal zones are possible under intense heat and mass transfer in perfect crystalline solids in vicinity of phase transition or phase separation region.

#### ***How does synergetic activation works?***

**Point 1** of the model shows that effective overcoming of potential barrier of nuclei repulsion may be caused not only by quantum phenomena but also by synergetic ones. Proposed power distribution of atoms by energy (see below) is seemed to be typical for strongly non-equilibrium systems in which energy dissipation and mass transfer are implemented by cooperative phenomena such as SW and/or DW.

**Point 2** of SA model states that noted waves in solids might be described as dynamical dissipative structures. The type of structuring is the spatial ordering of vibrational and/or electronic excitations in spatiotemporal limits of SW and/or DW front. It is the sequel of different drift velocities of noted excitations having different energies in noted fronts. Such dynamical structure is the staircase which the multistage excitations are implemented by. Resulting probability P of such multistage excitation of atom having average energy  $E_0$  up to the highest energy level  $E_n$  (e.g. effective activation energy of CF process with account of quantum tunnelling) is expressed (see above) by the power function:

$$P'_n = A \prod_{i=1}^n \{ \exp[-(\Delta E_i/E_{i-1})] \} \sim A (E_n/E_0)^{-\lambda}$$

$$\text{instead of } P^0_n = \exp[-(E_n/E_0)]$$

where  $\lambda = 1$ ,  $n$  is a number of intermediate steps;  $A$  is the factor that characterize a self-organization processes intensity;  $I$  is determined by the structure of excitation energy levels.

Predominance of non-linearity of medium over dispersion and dissipation of waves is necessary for SW (DW) self-generation (3,4) because noted multistage excitation takes prolonged SW runs. The necessary condition of noted predominance is (4):

$$\frac{[4/3\eta + \xi + \kappa(1/C_V - 1/C_P)]\omega}{r_0 v_0 c_0 (\gamma - 1)} < 1$$

where  $\eta$ ,  $\xi$  are shift and volume viscosities of the medium correspondingly,  $\kappa$  is heat conductivity,  $C_V$  and  $C_P$  are heat capacities under constant volume and pressure correspondingly,  $\omega$  is characteristic frequency,  $r_0$ ,  $v_0$ ,  $c_0$  are density of and SW and sound velocities in undisturbed medium,  $\gamma$  is the power factor in Poisson's adiabatic state equation.

**Point 3** states the necessary conditions of SW (DW) self-generation and propagation in solids: (i) vicinity of phase transition or phase separation region, i.e. maximal values of  $C_V$  and  $C_P$ ; (ii) perfectness of host crystal lattice and saving of the latter during the experimental run, i.e. minimal values of  $\eta$ ,  $\xi$ . Estimation of necessary perfectness gives a value of critical concentration of dislocations of about  $10^5$  per square centimeter, i.e. about  $3.10^2$  per linear centimeter: realization of noted excitation staircase takes about  $10^4 \tau \sim 10^4 \cdot 10^{-12} \sim 10^{-8}$  s, where  $\tau$  is the time period between atomic collisions. Taking into account SW velocity that is about  $3.10^5$  cm s<sup>-1</sup> one can obtain a value of necessary SW run:  $\sim 3.10^{-3}$  cm.

### Synergetic Activation Model: Verification

There are few published papers on CF concerning definite data on the real crystal structure of host lattice. Nevertheless, analyze of such data shows certain correlation between CF intensity and reproducibility, from one hand, and conditions mentioned in point 3, from other hand. We have made statistical analyze of sample of published experimental data from the point of view of SA model. The main parameter which choice of papers is made by is the (i) perfectness of structure.

Only about 30 papers contain certain or indirect evidence of the specimens real crystal structure (5-36). Analyze by (ii) degree of non-equilibrium of (or force of action to) the system and (iii) period of action to the system parameters is additionally made.

Parameters and effects values are estimated by 3 numbers scale: -1..+1: weak..strong appearing of parameter or effects correspondingly (see fig. 1).

Merit of such analyze isn't high due to non-uniqueness of methods and conditions of experiments and types of effects under analyze. Nevertheless, some correlations between chosen parameters and CF effects are observed (numbers in cells are Nos. of quoted papers).

(i) a distinct positive correlation of effects with structure perfectness may be seen;

- (ii) non-equilibrium of the system appears as necessary but not enough condition of CF implementation; supposed cause is possibility of structure distortion under strong actions.
  - (iii) correlation with period of action is absent; supposed causes are non-uniqueness of experiments and non-unidirectional changes of real structure of specimens under longitudinal actions;
- (Σ) overall diagram exhibits rather distinct positive correlation that we consider as nondirect confirm of synergetic activation model of cold fusion.

### **Synergetic Activation Model: Predictions**

*As for materials:* Requirements to object for CF implementation is caused by the type of the CF process selected. From the SA point of view, there are only three types:

First one - when CF is stimulated by the outer impact action, that introduces shock wave into solid (including fracto-fusion, cluster-impact fusion etc.). Such process requires perfect crystal specimen with high deuterium content.

Second one - when CF is concerned with self-generated shock waves induced by phase transition in solid. It takes perfect crystals too having high deuterium content and suitable relative position of deuterium nuclei in the crystal.

Third one - when CF is caused by self-generated shock waves from phase separation region, as it takes place in classical PonsFleischmann process. Requirements are following: it might be a system with weak-bonded deuterium and high mobility of the latter. High content of deuterium isn't required, so noted factor is extensive one. High gradient of deuterium content is necessary.

*As for process conditions:* It might be the mostly irreversible one and at the same time nondestructive one for ensuring stable and durable process. How to coincide such inconsistent requirements? It is almost impossible for two first types of CF process, but it may be executed easily for the third one. The point is to operate within a top of phase separation region (see fig.2).

*As for sample shape and dimension:* For first two types of cold fusion process - the more massive the better, but for the third type situation is more complicated. In the case we can state - the more intense mass and charge transport processes the better. So shape and dimension of specimen might provide intense and stable transport through the specimen and coexistence of two phases of deuteride in dynamics.

### **Conclusion**

SA model already succeeded in analyze of fast chemical processes in solids (37) such as reactions initiated by shock waves (SW) in solids, detonation of solids and cryogenic reaction in freezed gas mixtures under phase transitions (38). The difference between above mentioned reactions and CF is rather quantitative than qualitative: due to higher activation energy of CF and lower probability of elementary event CF implementation commonly don't lead to host crystal lattice destruction and therefore durable and stable process is possible in principle.

We possess the know-how on obtaining perfect metallic specimens providing intense and stable CF process when used as cathodes or targets (see fig.3) and propose collaboration for all interested colleagues.

### Acknowledgements

This work is carried out with financial support of Belarus Fundamental Researches Foundation, Grant No F54-144/1.

### References

1. M.Fleischmann, S.Pons, and M.Hawkins. Journ. Electroanal. Chem., Vol.261, No 5, p.301-308 (1989).
2. V.A.Filimonov. Journ. Radioanal. Nucl. Chem. (Articles), Vol.162, No 1,P.99-109 (1992); Russ. JTP. Vol.62, No6, p.221- 224 (1992); Russ. JTP Letters. Vol.16, No19, p.42-46 (1990); Ibid., Vol.16, No20, p.29-34 (1990).
3. I.A.Miklashevich, V.V.Selyavko. Journal of Applied Mechanics and Technical Physics (Russ.), No6, p.59-62 (1989).
4. L.K.Zaremba, V.I.Timoshenko. Non-linear Acoustics. Moscow, Moscow University Publ., 1984, p.104.
5. A.Takahashi, T.Iida, T.Takeuchi et al. Proc. 3rd Annual Conf. Cold Fusion, Nagoya (October 1992), p.93.
6. A.G.Lipson, D.M.Sakov, E.I.Saunin et al. Russ. JETP. Vol.76, No6, p.1070-1076 (1993).
7. K.A.Kaliev, A.N.Baraboshkin, A.L.Samgin et al. DAN (Repts. Russ.Acad.Sci), Vol.330, No2, p.214-216 (1993).
8. Y.Arata, Y.-C.Zhang. Fusion Technology, Vol.18, No8, p.95-102 (1990).
9. E.Palibroda, P.Gluck. Journ. Radioanal. Nucl. Chem. (Lett.) Vol.154, p.153-161 (1991).
10. B.Ya.Guzhovskii et al. Proc. All-Union Conf. "Cold Nuclear Fusion", Moscow-Dubna (March 1991), p.6.
11. A.A.Yukhimchuk et al. Ibid., p.7.
12. D.Lewis et al. Journ. Electroanal. Chem., Vol.316, p.353-360 (1991).
13. A.DeNinno et al. Europhysics Letters, Vol.9, p.221-224 (1989).
14. D.Gozzi et al. Il Nuovo Cimento, Vol.103A, p.143-154 (1990).
15. Y.Arata, Y.-C.Zhang. Proc. Jap. Academy, Vol.66B, No2, p.33-36 (1990).
16. E.Yamaguchi et al. Japan Journal Appl. Phys., Vol.29, p.L666- L669 (1990).
17. V.M.Golovkov et al. Proc. All-Union Conf. "Cold Nuclear Fusion", Moscow-Dubna (March 1991), p.8.
18. I.S.Yakimov et al. Ibid., p.15.
19. B.V.Deryagin et al. Ibid., p.17.
20. P.I.Golubnichy et al. Ibid., p.26.
21. N.P.Valuyev et al. Ibid., p.28.
22. R.N.Kuzmin et al. Ibid., p.31.
23. A.G.Lipson et al. Russ. JTP Letters, Vol.18, No16, p.90-95 (1992).
24. F.Botter et al. Physics Letters B, Vol.232, p.536-538 (1989).
25. M.Gai et al. Nature, Vol.340, p.29-34 (1989).

26. S.Blagus et al. Zeitschrift Phys. A - Atomic Nuclei, Vol.333, p.321-322 (1989).  
 27. F.Demanins et al. Solid State Commun., Vol.71, p.559-561 (1989).  
 28. P.Coelho et al. IPEN-Doc-3581, p.1-10 (1990).  
 29. M.Broer et al. Phys. Rev. C, Vol.40, p.1559-1562 (1989).  
 30. G.McCracken et al. Journ. Phys. D: Appl. Phys., Vol.23, p.469-475 (1989).  
 31. E.Kuzmann et al. Journ. Radioanal. Nucl. Chem. (Lett.) Vol. 137, p.243-250 (1989).  
 32. L.Lewis et al. Ibid., Vol.145, p.81-91 (1990).  
 33. J.Blasar et al. Chimia, Vol.43, No9, p.262-268 (1989).  
 34. X.-W.An et al. Thermochim. Acta, Vol.183, p.107-115 (1991).  
 35. N.Oyama et al. Bull. Chem. Soc. Japan, Vol.63, p.2659-2664 (1990).  
 36. M.I.Martynov et al. Proc. All-Union Conf. "Cold Nuclear Fusion", Moscow-Dubna (March 1991), p.16.  
 37. V.A.Filimonov, E.N.Naumovich. Proc. 2nd Int. Workshop "Self organization in Complex Systems": Polotsk, Belarus (February 1993), p.81-88.  
 38. V.A.Lishnevskii. J.Phys.Chem. (Russ.), Vol.52, No1, p.1-14 (1978).

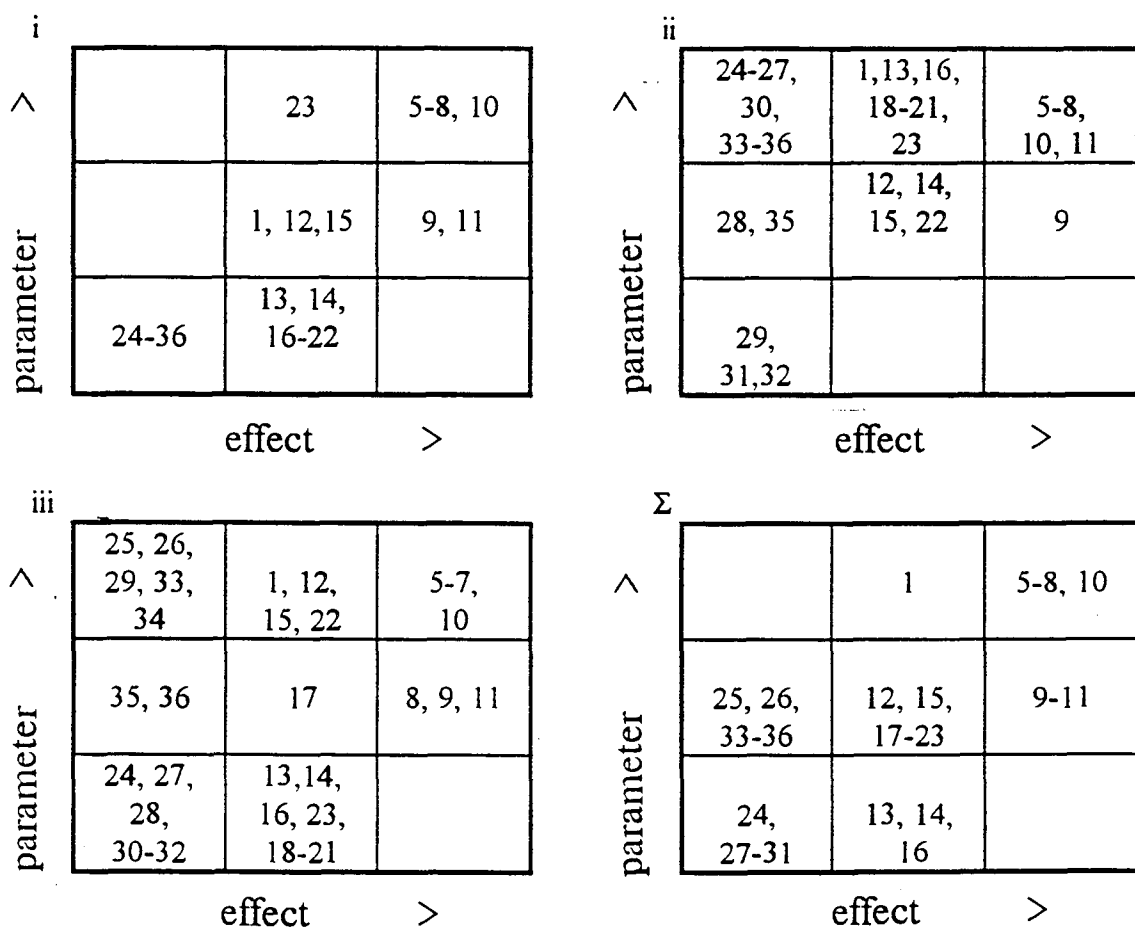
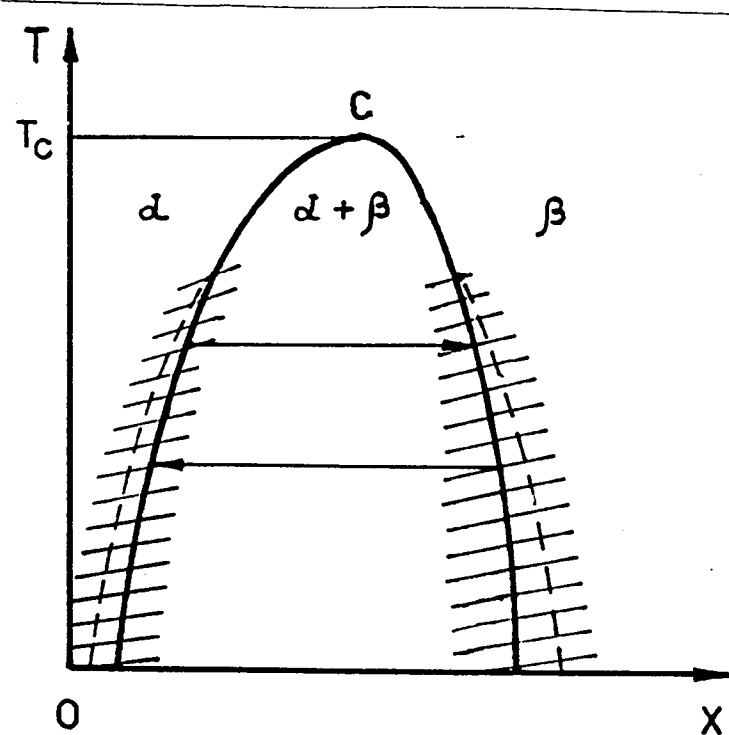
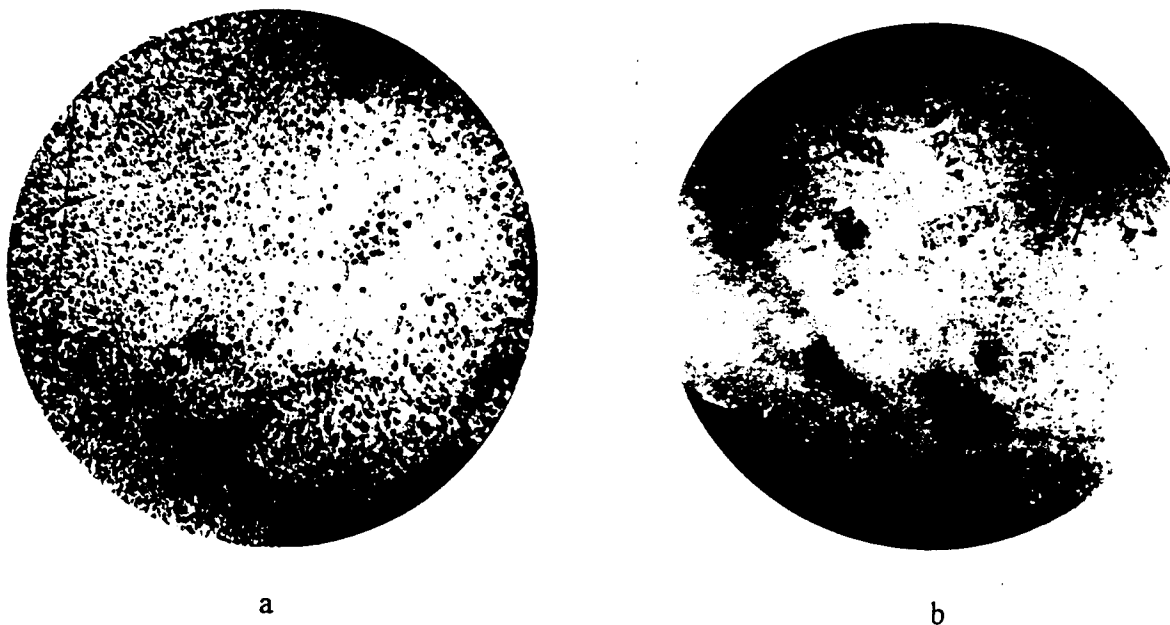


Fig.1. Correlation diagrams of cold fusion parameters and effects  
See notes in the text.



**Fig.2. A phase diagram of Pd-D and similar Me-D systems having phase separation regions**  
Here T is temperature, X is deuterium content,  $\alpha$ ,  $\beta$  are regions of deuteride  $\alpha$ ,  $\beta$  phases, C is the critical point of phase separation region.



**Fig.3. A view of control (a) and working (b) specimens surfaces by metallographic microscope (x200)**

Solid lines are the grain boundaries, small triangles are the etching holes of dislocations.

COLD FUSION EXPLAINED BY NEGENTROPY THEORY OF  
MICRODROP OF HEAVY WATER

Ryoji TAKAHASHI  
University of Tokyo (retired)  
Setagaya-ku Seta 2-26-21  
Tokyo, Japan 158

Abstract

The cold fusion which arises in the electrolysis of the Pd-D<sub>2</sub>O/salt system is well explained by the working of the microdrops of D<sub>2</sub>O created in the cathode. According to the negentropy theory of the microdrops of H<sub>2</sub>O and D<sub>2</sub>O, heat is evolved and the synthesis of substances including the nuclear fusion arises when it is actuated by receiving negative pressure. In this case the actuation is done by ionization. The principle of the microdrop engine, an examining of Miller's experiment and the explanation of the cold fusion are described.

1. Introduction

Since the work of Fleischmann and Pons[1] and Jones[2] published in 1989, so many experimental evidences for the cold fusion in the electrolysis of the Pd-D<sub>2</sub>O/salt system have been accumulated that the presence of the cold fusion is almost doubtless. However, the explanation of the generation of heat or the Fleischmann-Pons effect meets with more difficulty, since the effect is also observed for light water. So the problem is to find out the common mechanism of the effect to both D<sub>2</sub>O and H<sub>2</sub>O. A microdrop(MD) of water is a unique existence ruled by the negentropy (negative entropy) theory.[3] An examining of the engine work of the MD cleared out the synthesis action of the Miller's experiment.[4] Further it became clear that the cold fusion is also due to the MDs and the mechanism is explained by the working of the MDs. This paper shows first the introduction of the microdrop engine (MDE), including the explanation of the Miller's experiment, and second the application of the model to the cold fusion.

2. Outline of MDE

As there are only small differences in the properties of H<sub>2</sub>O and D<sub>2</sub>O, except for the nuclear property, the MDE is explained by H<sub>2</sub>O.

2.1. P-T-V curves for microdrops of water in moisture

The pressure P in a drop of water of radius r, in saturated moisture, is calculated as a function of temperature T by the Laplace's equation,

$$P = 2\gamma/r + Pv, \quad (1)$$

where  $\gamma$  and  $Pv$  represent the surface tension of water and the vapor pressure. The P-T curves for  $r=0.5\mu\text{m}$ ,  $1.5\mu\text{m}$  and  $3\mu\text{m}$ , and the P-r(V) curve at  $0^\circ\text{C}$  are shown in Fig 1. The P-T-V curves represent the corresponding phases of a microdrop shown in the top of Fig.1. The value of  $dP/dT$  is negative for small values of  $r$  at low temperatures. The microdrop which satisfies  $dP/dT < 0$  takes negentropy for the increase in the volume,  $V$ , by Maxwell's third thermodynamic relation.[3] This is the unique property of the MD.

## 2.2 Principle of MDE

When the MD receives a negative pressure,  $-\Delta P$ , the normal water changes into super water increasing the volume by  $\Delta V$  as shown in Fig.1 by taking negentropy from the surroundings and do work  $P\Delta V$ . So the energy balance in this action is given as,

$$E - T\Delta S = P\Delta V, \quad (2)$$

where  $E$ ,  $T$  and  $-\Delta S$  represent external energy which causes a negative pressure, absolute temperature and negentropy respectively. The balance of the entropy in this action is illustrated in Fig.2. Under an equilibrium condition the entropy is balanced between the microdrop and the surroundings as shown in Fig.2A, however, if the microdrop is actuated by receiving  $E$ , it takes in  $-\Delta S$ , so the surroundings acquires  $+\Delta S$  as shown in Fig.2B. If the negentropy is not fixed in the microdrop, the unbalanced entropy between the microdrop and the surroundings returns to the

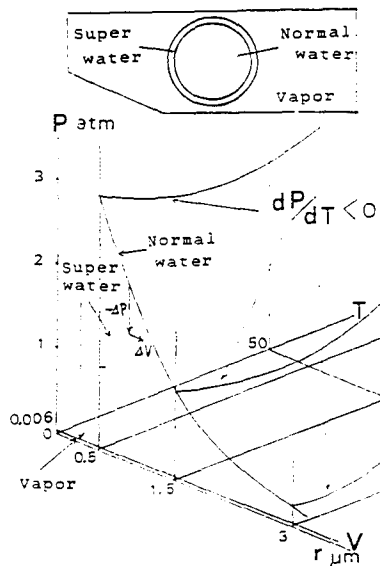


Fig.1 P-T-V( $r$ ) curves of MDs of water in moisture.

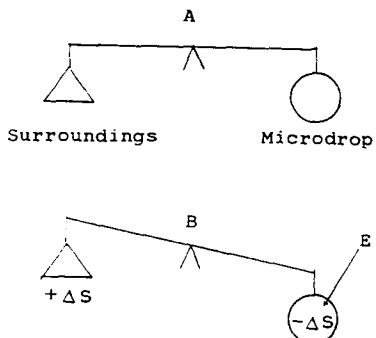


Fig.2 Balance of entropy between MD and surroundings: A, in equilibrium and B, when microdrop is actuated.

initial state after the actuation is finished, so there arises no continuous generation of heat by actuation. But if the MD contains substances, the negentropy is fixed by synthesizing any compounds, so the generation of heat is carried out smoothly by actuation. From Eq.(2) we get,

$$E = P\Delta V + T\Delta S. \quad (3)$$

Equation (3) shows that the generated heat  $T\Delta S$  is given by E. The work done by the microdrop is negligible here. It is clear that the microdrop works as a new type of engine and it is named here as microdrop engine. The negentropy range of the microdrop of water in moisture is limited, but if the microdrop is placed in relatively higher pressure of a gas than that of the vapor, the following Laplace's equation is held,

$$P = 2\gamma/r + P_0 \quad (4)$$

where  $P_0$  represents the outside pressure regarded as constant for a small change in temperature. In this case the negentropy is maintained in the wide ranges of T and r.

### 3. Explanation of Miller's experiment by MDE model

Miller's experiment is well known for the success in the synthesis of amino acids by circulating CH<sub>4</sub>, NH<sub>3</sub>, H<sub>2</sub>O and H<sub>2</sub> past an electric discharge, however, any satisfactory explanation has not yet been given. The reason why this problem is treated here is that this study just carried out an experiment pursuing the MDE, so the examining of Miller's experiment is unavoidable to understand the MDE.

An electric discharge through saturated moisture causes its condensation, so the microdrops are created in the Miller's apparatus. The surrounding pressure of the MDs is regarded as constant about 0.7 atm as initially provided. The MDs thus produced satisfy the Laplace's equation as following,

$$P = 2\gamma/r + 0.7 \text{ atm}. \quad (5)$$

From Eq.(5) it is seen that the created microdrops satisfy the negentropy condition as considered for Eq.(4). The actuation of the microdrop is done by the electric discharge. A microdrop situated between a pair of electrodes for the different polarity is shown in Fig.3. The presence of

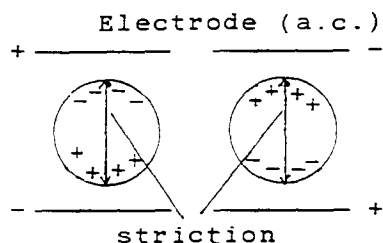


Fig.3

MD between a pair of electrodes for different polarity. Electrostriction gives negative pressure and actuation to MD in each change in polarity.

ammonia gives a weak alkaline property to the MD, so it polarizes and receives electrostriction for the change in the polarity of the electrode. The striction provides negative pressure and actuation to the MD for a moment until it is relaxed. The number of actuation  $N$  in the passing time  $t$  through the electric field is given as following,

$$N=2ft, \quad (6)$$

where  $f$  represents the frequency of the electric source. The balance of energy in one actuation of the microdrop is given as following,

$$E+T\Delta S_1-T\Delta S_2=E+T(\Delta S_1-\Delta S_2)=P\Delta V, \quad (7)$$

where  $\Delta S_1$  and  $-\Delta S_2$  represent an increase in entropy by Joule heating and the negentropy respectively. From Eq.(7) the condition for the MD to have negentropy is given by the following relation,

$$\Delta S_1-\Delta S_2<0. \quad (8)$$

Equation (8) shows that  $\Delta S_1$  should be as small as possible for the synthesis of substances to be done, and it is seen that a weak discharge is favorable as it decreases this value. These analysis of the Miller's experiment by MDE model well agrees with the description in the Miller's paper. Some other results obtained by MDE model are, 1)a high concentration of ion is unfavorable for this experiment, as it decreases the electrostriction and increases the positive entropy and 2)a slow circulation of the vapor is favorable because it provides fine droplets with long passing time.

#### 4. Explanation of cold fusion by MDE model

Alike the preceding description the cold fusion is explained by the MDE. However, the feature of the creation and actuation of the MDE in this case is different from that of the Miller's experiment. First we examine how the MDs are created in the cathode. Figure 4 shows a feature of the creation of a MD in a narrow channel in the cathode by the electrolysis. D<sub>2</sub> gas is formed at the wall of the cathode in small bubbles, so by the growing up of the bubbles the D<sub>2</sub>O in the middle of the channel is surrounded by the gas then a MD is created. Small MDs thus created are

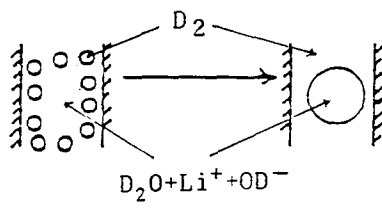


Fig.4.  
Creation of a MD in narrow channel in cathode by electrolysis: D<sub>2</sub> bubbles formed at the wall isolate the D<sub>2</sub>O and create a MD.

transported through the cathode and finally return to the initial D2O. So for the purpose to get great number of MDs there should be formed great number of narrow channels which allow the smooth circulation of the electrolyte in the cathode. The past data of the generation of heat obtained for Pd cathode show that the phenomenon arises when the cathode is heavily loaded with deuterium, which in general includes microcracks because of the nonuniform expansion of the lattice. This fact suggests that narrow channels leading electrolyte are fabricated in the cathode by a long time electrolysis, and if some material conditions are satisfied, many favorable channels are fabricated by the electrolysis. This tells why the generation of heat has poor reproducibility.

Second we examine how the microdrop in the cathode are actuated. In general the volume of an atom decreases when it is ionized, which noticeably arises for Deuterium and Hydrogen, whose volume almost disappears by ionization. It is clear that simple substances decrease the volume markedly by ionization. If a microdrop is ionized by the irradiation of a high energy particle, negative pressure arises for a moment until it is relaxed. This is the mechanism of the actuation of the MD by ionization. There are many sorts of high energy particles in our environment, so a MD among the many is easily ionized. The synthesis action in the MDE depends on the included substances: for the presence of alkali ions, alkali deuteride such as LiD, NaD and KD are formed and heat is generated, but if the concentration of D<sup>-</sup> is high, the D-D reaction and/or the reaction between the nuclei of D and alkali metal arise and high energy particles are produced. So the MDE has two types according to the synthesis action as shown in Table 1.

Table 1. Two types of MDE

Type	r	Alkali ion	Synthesized product
1st type	small	rich	Alkali deuteride and heat
2nd type	large	poor	High energy particles

The mechanism of the generation of excess heat in the cold fusion by the MDE model is shown in Fig.5. The 2nd type MDEs are created mainly in the rough surface and if one of them is actuated by an external particle, the others are actuated by mutual ignition. The 1st type MDEs created inside

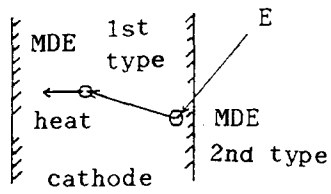


Fig.5  
Mechanism of generation of excess heat in cold fusion: if a 2nd type MDE is actuated by external particle the others are actuated by mutual ignition and the 1st type MDEs are actuated and generate excess heat.

the cathode are actuated by the high energy particles produced by the 2nd type MDEs. The excess heat per second is represented as,

$$\text{Excess Heat} = N_1 N_2 f T \Delta S \quad (9)$$

where  $N_1$  and  $N_2$  represent the number of the MDE of the first type and the second type and  $f$  is the frequency.  $T \Delta S$  shows the mean evolved heat by a MDE of the 1st type. A numerical estimation is performed as follows: if  $N_1$  and  $N_2$  are  $10^6$  and  $N=100$ , the excess heat/s=1cal by supposing  $T \Delta S=1 \times 10^{-14}$  cal.

### 5. Discussion

If the produced MDs are only of the second type, the actuation provides a low level of nuclear reaction and not heat. This type of working corresponds to the Jones' experiment. If numerous MDEs of both types are created the Fleischmann-Pons effect is observed. "The heat after death" talked by Pons in this meeting is explained by Fig.4, by replacing D<sub>2</sub> gas with the vapor of D<sub>2</sub>O, i.e. MDs are still alive and work after stopping the electrolysis in the burst state of the cold fusion. The probability of arising the nuclear reaction in the 2nd type MDE for light water is supposed to be very small as the burst of heat is not yet observed. The alkali deuteride formed in the MD is dissociated by the ionization in the massive heavy water, so this substance plays as an agent material for the cyclic work of the engine.

From the technical point of view, the design and the preparation of the cathode which creates large  $N_1$  and  $N_2$  are most significant. Probably the powder metallurgy is a useful way of obtaining fine channels in the cathode.

### 6. Conclusion

The MDE model well explained the mechanism of the cold fusion, from which the improvement of the cold fusion is expected. There are unknown relations of cause and effect in the synthesis action of the MD, which, however, attracts our interest to the study of the MDE.

### References

- [1] M. Fleischmann, S. Pons, M.W. Anderson, L.J. Li and M. Hawkins. "Calorimetry of the palladium-deuterium-heavy water system". J. Electroanal. Chem. 287 (1990)p. 293.
- [2] S.E. Jones, E.P. Palmer, J.B. Czirr, D.L. Decker, G.L. Jensen, J.M. Thorne, S.F. Taylor and J. Rafelski. "Observation of cold nuclear fusion in condensed matter". Nature 338(1989)p. 737.
- [3] R. Takahashi. "Negentropy in microdrops of water". Physics Letters A, 141 (1989)p. 15.
- [4] S.L. Miller. "A production of amino acids under possible primitive earth conditions". Science 117(1953)p. 528.

## FERROELECTRICS FOR COLD FUSION

G.V.FEDOROVICH

Theoretical Problem Department,  
Russian Academy of Sciences.  
Vesnina 12, Moscow, Russia, 121002.

### ABSTRACT

The purpose of the paper is the determination of parameters of crystals which are "optimal" for enhancement of the D+D fusion rate. The basis for recommendations is the model of a deuteron acceleration in ferroelectrical crystals. This phenomenon is the result of an interaction of deuterons with the field of the wave generated in the process of domain-polarization reversal. the correspondent model is considered. It is shown, that the maximal energy of deuterons can be >200 eV. It is sufficient for the reaction of D+D fusion to be detected. Some ferroelectrics with the perovskite-like structure, with the great spontaneous polarization (e.g.  $\text{LiNbO}_3$ ) and the small damping of oscillations in optical mode (e.g.  $\text{PbTiO}_3$ ), have turned out to be interesting from the viewpoint of "cold fusion".

### I.INTRODUCTION

There are strong grounds (both theoretical<sup>1,2</sup> and experimental<sup>3</sup>) to believe that the phenomenon of the enhancement of the D+D fusion rate during electrolytic infusion of deuterons into metallic Ti or Pd electrodes connects with the crack and break formation in the cathode material. To put this another way<sup>4,5</sup>, the physical mechanism of cold fusion in electrolytical cells is the same as the one in the case of a destruction of deuterated crystals<sup>6,7</sup>. A model of that mechanism (the stochastic acceleration of particles in the field of intensive oscillations, that are generated at the crack boundary) has been proposed in<sup>8,9</sup>. The analysis of the model allows to make some conclusions which are of interest for the following investigations. It has been found that, for deuterium-contained crystals, the emissions of high-energy electrons and an electromagnetic radiation (in the range from visual light to X-rays) are the indicator of creating conditions for enhancement of the nuclear fusion rate.

We consider a possibility of the D+D fusion catalysis in a solid by using methods which are not so destroying as the crystal crushing, the oversaturation of metals by deuterium etc. We call attention to the phenomenon of light<sup>10</sup> and high-energy electron<sup>11,12</sup> emissions that are involved in the process of polarization reversal of ferroelectrics. The direct evidences are found for the nuclear fusion in deuterated ferroelectrics during changes of

their crystalline structure in the processes of phase transition<sup>13</sup> and polarization reversal<sup>14</sup>.

The foregoing is a good reason to consider the phenomenon of the stochastic acceleration of D-ions in the field of the dominant mode oscillations, which are generated during the polarization reversal of ferroelectrics, more closely. This will allow an revealing the parameters of crystals that determine the D+D fusion rate. An understanding of the effect will guide the way to improvements in the design of experiments. This is the main purpose of the paper.

The space-time structure of the dominant mode oscillations is considered in Sec.II. The acceleration of D-ions, which are introduced into the crystalline lattice of ferroelectrics, is considered in Sec.III by the Poincare's mapping method<sup>15</sup>. The method enables one to describe uniformly both the stochastic heating of D-ions and the regular acceleration of those of D-ions that were captured by the dominant mode waves. In Sec.IV we discuss the problem of the energy losses of an accelerated deuteron. The theoretical approach to the energy losses used by Bohr, Bethe and Bloch (see e.g.<sup>16</sup>) are adequate, generally speaking, only for isolated atoms. For real crystals other approaches are required to account for the crystalline structure of the stopping media. Such an approach was first developed by Fermi<sup>17</sup>. Here we shall develop the theoretical energy loss model correspondingly to our purposes.

The summary result of the paper is the dependence of the maximal D-ion energy on the crystal parameters (see Sec.V). The result enables us to determine the crystals that are "optimal" for enhancement of the D+D fusion rate: they have a great value of the spontaneous polarization  $P_s$  and a small value of the damping constant  $\gamma$  of the dominant mode oscillations. These peculiarities are typical for ferroelectrics with the perovskite-like crystalline structure.

## II.MODEL OF A DOMAIN-WALL MOTION

Any strict description of phenomena in actual ferroelectrical crystals is very difficult because of a complex cell-geometry. It is not likely that it is possible today because of the lack of information about details of the atomic interactions in a lattice. In any case, this problem is beyond the scope of our present work. In this paper a simplified model, which has most of the features of the more physical problem and is easily capable of generalisation will be considered. At the same time the model allows to estimate the principal parameters of the processes.

Let us assume that for every polarization of the individual cell we can introduce certain quantitative characteristic - coordinate  $S$  - which is defined in such a manner that it is equal zero in a non-polarized cell and it has positive or negative value in variously polarized cells. It will be reasonable to assume that

temporal variations of  $S$  are described by the Hamiltonian

$$H = (1/2) \cdot M \cdot \dot{S}^2 + (1/2) \cdot \sum_n g \cdot (S_{n+1} - S_n)^2 + U(S) - e \cdot E \cdot S \quad (1)$$

where  $M$  and  $U(S)$  are effective mass and potential,  $g$  is the forced constant. In order to describe the possibility of the crystal polarization reversal, let us define the double-minimum potential energy function by the formula:  $U(S) = (a/2) \cdot S^2 + (b/4) \cdot S^4$ . This potential is minimal when  $S = S_{eq} = \pm(a/b)^{1/2}$ . One can see that if  $E=0$ , the system is in a symmetric potential well and it can oscillate e.g. at the left-hand side of the well. As the field  $E$  increases to the critical value  $E_c = (2a/3e) \cdot (a/3b)^{1/2}$ , the left-hand part of the well disappears. The summary potential transforms into the broad asymmetric well in which the system can oscillate near the right-hand equilibrium position.

In order to investigate the dominant mode oscillations, which are generated during the polarization reversal of ferroelectrics, it is convenient to use a continuum approximation. Let us determine  $k \equiv g \cdot d^2$  and introduce the coordinate  $X$  along the crystal. We obtain

$$M \cdot \partial^2 S / \partial t^2 - k \cdot \partial^2 S / \partial X^2 = e \cdot E + a \cdot S - b \cdot S^3 \quad (2)$$

The Eq.(2) is classed as a quasi-linear hyperbolic equation. All of the perturbations, described by this equation, extend with the velocity  $C = (k/M)^{1/2}$  in both directions of the  $X$ -axis. In order to determine the dependence  $S(X,t)$  it is necessary to add the corresponding initial and boundary conditions to the Eq.(2).

Let us suppose that the field  $E=E_0 > 0$  is applied to the crystal. The system of each cell was characterized by the  $S$ -value near the left equilibrium (unstable) position. In order to deduce the system out of this state, let us add the disturbing force  $f = f \cdot \delta(X) \cdot \delta(t)$  in the right-hand side of the Eq.(2). As a result, the breaks of the function  $S(X,t)$  will extend along both characteristics  $X = \pm C \cdot t$ . The magnitude of  $S(X,t)$  varies from  $S_0 = -(2/3b)^{1/2}$  (before a break) to  $S = S_0 + C \cdot f / 2$  (immediately behind a break). Let us consider variations of  $S$  in the area  $-Ct < X < Ct$ . The boundary conditions

$$S(X=\pm Ct) = S_1; \quad S'(X=\pm Ct) = 0 \quad (3)$$

is sufficient for the definition of  $S(X,t)$  over the whole area. It is obvious that the problem (2-3) has the solution  $S(X,t) = S(u)$ , where  $u = [(C \cdot t)^2 - X]^{1/2}$ . The function  $S(u)$  can be defined as the solution of the following boundary problem

$$S''_{uu} + S'_u/u - e \cdot E - a \cdot S + b \cdot S^3 = 0; \quad S(u=0) = S_1; \quad S'_u(u=0) = 0. \quad (4)$$

Let us insert new dimensionless variables:  $v = u \cdot \sqrt{a/k}$ ,  $S(v) = S(u) \cdot \sqrt{b/a}$ . For  $S(v)$  we have the boundary problem

$$S''_{vv} + S'_v/v - \varepsilon - S + S^3 = 0; \quad S(v=0) = S_1 > -1/\sqrt{3}; \quad S'_v(v=0) = 0. \quad (5)$$

where we determine  $\varepsilon \equiv (eE_0/a) \cdot \sqrt{b/a} = 2/3\sqrt{3} \approx 0.385$ .

The solution of the problem (5) was obtained numerically. The result is shown in Fig.1. The characteristical points of the diagram are  $S_m \approx 1.66$ ,  $S_{eq} \approx 1.155$ . The amplitude of the oscillations relative to the equilibrium value is  $\delta S = S_m - S_{eq} \approx 0.5$ , the frequency of oscillations is  $\omega_0 = (a/\mathfrak{M})^{1/2}$ . The obtained results bring us to the description of the domain polarization by the following function

$$P(x, t) = P_s \cdot S \left[ \sqrt{(a/k) \cdot [(Ct)^2 - x^2]} \right] \quad (6)$$

where the function  $S(v)$  (the solution of the problem (2.5)) is shown in Fig.1, and  $P_s$  is the value of the spontaneous polarization of ferroelectrics. One can see that the wave moves apart from the initial point in both directions of the X-axis. The velocity of this movement is  $C = (k/\mathfrak{M})^{1/2}$ . The relative amplitude of the oscillations is  $\approx 0.5$ . The space structure of the dominant mode oscillations is shown in Fig.2. The wave front is  $180^\circ$  domain-wall that moves in the direction transversal to the polarization axis.

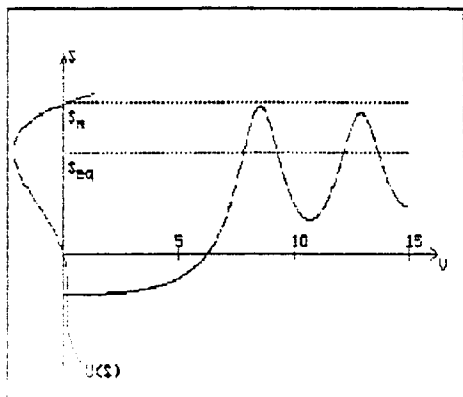


Fig.1. The result of the numerical solution of the problem (5). The characteristical points of the diagram are  $S_m \approx 1.66$ ,  $S_{eq} \approx 1.155$ .

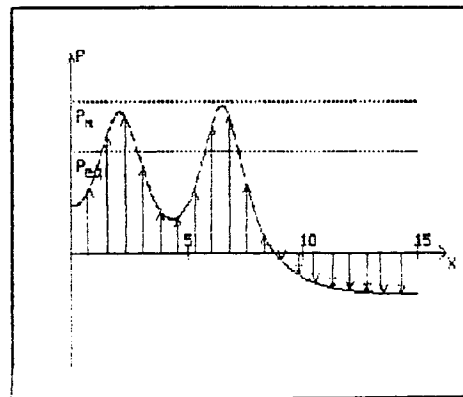


Fig.2. The space structure of the dominant mode wave. The domain wall is characterized by width  $\approx 3$  (in dimensionless variable).

### III. FERMI ACCELERATION OF DEUTERONS

Let us describe the model of a ferroelectric which is used below (see Fig.3a). Let us suppose that the ferroelectrical crystal consists of a sequence of layers of electrical dipoles  $\mathfrak{D}$  (arrows in Fig.3a) which are spaced  $d$  apart. The integral index  $j$  enumerates layers of dipoles. We suppose that a deuteron moves along the domain axis. The straight line represents the deuteron path. It crosses sequential layers of dipoles. If we assume that the crystal is found in closed electrodes then the depolarizing field  $E = 4\pi\mathfrak{D}/d$  exists in the crystal (here  $\mathfrak{D}$  is the average along

the crystal value of the cell dipole  $\mathfrak{D}_j$ ). The field compensates the summary potential difference on the bounds of the crystal.

The variations of the potential energy along the path of the movement of the D-ion is represented in Fig.3b ( $\Delta$  is the effective size of dipoles). The oscillations of atoms forming dipoles bring to the variations of the dipole moments with respect to the average value  $\mathfrak{D}$ . In general, the value of the difference  $p_j = \mathfrak{D}_j - \mathfrak{D}$  can be represented as the sum of the normal waves. However, we assume that the dominating oscillation exists in the crystal (see above Sec.2.1). It can be described by the function  $p(t) = p \cdot \cos(\omega \cdot t)$ . It is convenient to consider the limiting case where the size of dipoles is sufficiently small ( $\Delta \ll d$ ). In this case the D-ion trajectory  $Z(t)$  can be determined from the equation

$$M \cdot Z''_{tt} = e \cdot E - e \cdot \sum_j \mathfrak{D}_j(t) \cdot \delta(z - j \cdot d) \quad (7)$$

where  $M$  is the deuteron mass. This equation describes the uniformly accelerated movement of the D-ion on intervals  $j \cdot d < z < (j+1) \cdot d$  and the dampening shocks on the interval boundaries.

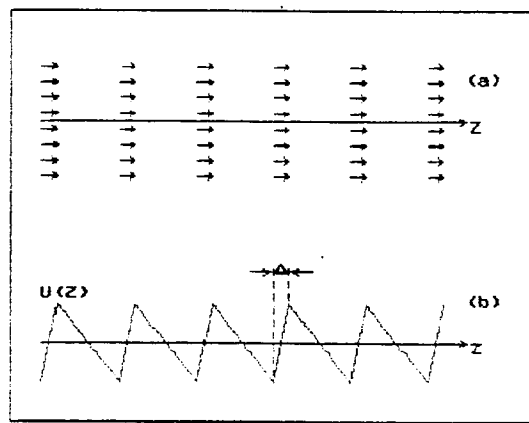


Fig.2. The scheme illustrating the area of the D-ion acceleration.

Let us assume that at  $t=t_n$  the D-ion is at the point  $Z=j \cdot d=0$ , it has the kinetic energy  $T_n > 4\pi e \mathfrak{D} / d^2$ , its velocity is directed in the positive direction of  $Z$ -axis! At  $t=t_{n+1}$  where  $t_{n+1}$  is determined by the relation

$$t_{n+1} = t_n + [d^3 \cdot (2M)^{1/2} / 4\pi e \mathfrak{D}] \cdot [T_{n+1}^{1/2} - (T_{n+1} - 4\pi e \mathfrak{D} / d^2)^{1/2}] \quad (8)$$

the D-ion will be at the point  $Z = d \cdot j_{n+1} = 0$ , where

$$j_{n+1} = j_n + 1 \quad (9)$$

it will have the kinetic energy  $T = T_{n+1}$ , determined by the relation

$$T_{n+1} = T_n - 4\pi e \mathfrak{D}_j(t_n) \quad (10)$$

The set of the relations (8-10) represents a mapping<sup>15</sup> which de-

fines the D-ion dynamics with a sufficiently large positive velocity. Similar relations can be defined for the case of a small positive velocity (if  $T < 4\pi eP/d^2$ ), and for the case of a negative velocity. For dimensionless variables  $W = T \cdot d^2 / 4\pi eP$  and  $y = \omega_0 t$  the set of mappings, which entirely defines the dynamics of the D-ion, has the form

$$\left. \begin{array}{l} W_{n+1} = W_n - q(y_n) \\ y_{n+1} = y_n + Q \cdot [W_n^{1/2} - (W_{n+1}-1)^{1/2}] \end{array} \right\} \text{if } W_n > 1 + q(y_n) \quad (11')$$

If  $W_n < 1 + q(y_n)$  then at  $t = t_n + 0$  the D-ion velocity becomes negative. Two possibilities exist in this case:

$$\left. \begin{array}{l} y_{n+1} = y_n + Q \cdot [W_n^{1/2} - (W_n - 1)^{1/2}] \\ W_{n+1} = W_n + q(y_{n+1}) \end{array} \right\} \text{if } W_n > 1, \quad (11'')$$

$$\left. \begin{array}{l} y_{n+1} = y_n + Q \cdot W_n^{1/2} \\ W_{n+1} = W_n \end{array} \right\} \text{if } W_n < 1. \quad (11''')$$

In these relations it is designated:

$$q(y) \equiv p(t)/P; Q \equiv \omega_0 \cdot d^2 \cdot (M/2\pi eP)^{1/2}$$

If the value  $p_i$  depends arbitrarily on  $t$ , the mapping (11) has the form of a radial twist mapping. For  $q \propto \cos(y)$  (11) becomes the standard mapping (also known as the Chirikov-Taylor mapping). This mapping has been well investigated lately in connection with the problem of the Fermi acceleration (see e.g. [15, 16]). It was shown, in particular, that a stochastic acceleration regime exists if  $P_i(t)$  is an oscillating function. In this case the particle energy  $W$  can noticeably exceed the value  $1 + \text{Amp}(q(y))$ .

For  $W \gg 1$  stochastic motion of the deuteron (at least, strong stochastic motion) disappears. Let us consider this case. It would appear reasonable that  $\text{Amp}(q(y)) < 1$ , so that variations of  $W$  are small ( $\Delta W \ll W$ ) for each steps of mapping. By assuming that  $Q$  is small too, we obtain that the phase  $y$  of a deuteron movement varies only slightly ( $\Delta y \ll 1$ ). The fulfillment of these conditions makes the transformation of difference equations (11) into differential ones possible. We can turn to the continuous variations of  $y$ . For definiteness we consider particles which move in the positive direction of  $Z$ -axis. The equations

$$dW/dn = -q \cdot \cos(y); dy/dn = Q \cdot [W^{1/2} - (W - 1)^{1/2}] \quad (12)$$

follow from (11') after this transformation. The system (12) has the first integral

$$(2/3) \cdot Q \cdot [W^{3/2} - (W - 1)^{3/2}] \cdot q \cdot \sin(y) = \text{const} \quad (13)$$

Let us suppose that the energy  $W$  exceeds 1 at some moment when the phase of its movement is  $y_0$ . Later the variations of  $W$  in

the course of moving are described by the implicit function

$$W^{3/2} - 1 - (W - 1)^{3/2} = \Gamma \cdot [\sin(y_0) - \sin(y)] \quad (14)$$

where we designate  $\Gamma \equiv 3 \cdot q/2 \cdot Q$ . Since the value of  $Q$  is small, the value of  $\Gamma$  is great. Under appropriate choice of the initial phase  $y_0$ , the value of  $W$  may be as much as  $\text{Max}\{W\} = (4 \cdot \Gamma/3)^{2/3} \gg 1$ .

It suggests that the effect of the deuteron acceleration in ferroelectrical crystals is quite actual. It is interesting to note that the considered mechanism of the deuteron acceleration is the combination of the two radically different mechanisms of acceleration: when the energy is small ( $W < 1$ ), the stochastic acceleration takes place, this mechanism is similar to the Fermi acceleration. In the region  $W > 1$  the D-ion energy increases (if particles enter into this region with the appropriate phase) at the expense of the resonance acceleration in the field of the dominate mode oscillations.

#### IV. DIELECTRIC FORMALISM IN THE THEORY OF ENERGY LOSS

The energy losses of an accelerated deuteron are determined by a combination of individual collision processes. At low energy the elastic atomic collisions dominate. In these collisions most of the energy loss is given as kinetic energy to the crystalline lattice. Here we shall develop the theoretical energy loss model that was first developed by Fermi.

We consider a deuteron, which moves (with the velocity  $V \ll c$ ) along the crystal polarization axis. Let us determine the electrical field generated by the moving deuteron. This field can be expressed in terms of the scalar potential  $\Phi$  only. The latter is determined by the Poisson's equation

$$\hat{\epsilon} \Delta \Phi = -4 \cdot \pi \cdot e \cdot \delta(r-Vt) \quad (15)$$

where "dielectric constant"  $\hat{\epsilon}$  is a tensor, its components are space- and time-dependent operators.

Let us assume, that atoms of the crystal can move along the crystal polarization axis only. In this case  $\hat{\epsilon}$  is the diagonal tensor:

$$\epsilon_{zz} = \hat{\epsilon}(r, t); \quad \epsilon_{xx} = \epsilon_{yy} = 1. \quad (16)$$

We introduce the Fourier transform  $\Phi_k$  of potential  $\Phi$ . It is determined by the equation

$$(\hat{\epsilon} k^2 + q^2) \Phi_k = (e/2\pi^2) \cdot \exp(-itVk) \quad (17)$$

where  $q^2 \equiv k_x^2 + k_y^2$ ;  $k \equiv k_z$ . We see that the function  $\Phi_k$  depends on  $t$  as  $\exp(-itVk)$ . The operator  $\hat{\epsilon}$  takes function  $\exp(-i\omega t)$  into function  $\epsilon(\omega) \cdot \exp(-i\omega t)$ . So that we have

$$\varphi_k = (e/2\pi^2) \cdot \exp(-itv_k)/[\epsilon(v_k, k) \cdot k^2 + q^2] \quad (18)$$

The energy loss is the work which the force  $F = e \cdot E$  does. Since  $E_k = -ik\varphi_k$ , the energy loss per unit path length of a deuteron moving in a crystal is

$$\begin{aligned} -dT/dZ &= F_d = - (ie^2/2\pi^2) \cdot \int_{-\infty}^{\infty} k \cdot dk / [\epsilon(v_k, k) \cdot k^2 + q^2] = \\ &= - (ie^2/\pi^2) \cdot \int_{-\infty}^{\infty} \omega \cdot d\omega \int_{-\infty}^{\infty} q \cdot dq / [\epsilon(\omega, k) \cdot \omega^2 + v^2 \cdot q^2] \end{aligned} \quad (19)$$

where  $k = \omega/v$ .

The dielectric function  $\epsilon(\omega, k)$ , depending on the wave vector  $k$  and frequency  $\omega$ , describes the crystalline lattice response to the longitudinal electric field initiated by a moving deuteron.

Let us write  $\epsilon = \epsilon' + i \cdot \epsilon''$ , where  $\epsilon'$  is even function of  $\omega$  and  $\epsilon''$  is odd function of  $\omega$ . We have

$$F_d = (e^2/\pi \cdot v^2) \cdot \int_0^{\infty} \omega \cdot d\omega \int_{-\xi}^{\infty} d\chi / (\chi^2 + 1) \quad (20)$$

where  $\xi$  denotes the ratio  $\epsilon'/\epsilon''$ .

For low-loss dielectrics,  $\xi \gg 1$ . So we have

$$F_d \approx (e^2/\pi \cdot v^2) \cdot \int_0^{\infty} \omega \cdot (\epsilon''/\epsilon') \cdot d\omega \quad (21)$$

The ratio  $\epsilon''/\epsilon'$  is the loss tangent of a dielectric, so that this expression has the clear physical meaning: the moderation of slow deuterons is accounted for by dielectric losses of the energy of the electric field initiated in a crystal by a moving particle. The further rearrangement of Eq.(21) can be made after the form of  $\epsilon(k, \omega)$  determination.

We consider the above introduced model of the individual cell polarization (see Sec.II). When employing the Eq.(12), it should be considered that: (i) when the system oscillates near the equilibrium position, the restorting force is  $F \approx M \cdot \omega^2 \cdot (S - S_{eq})$ ; (ii) there is the frictional force  $F_f = -M \cdot \gamma \cdot dS/dt$  (where  $\gamma$  is the frictional constant), which causes a damping of oscillations (iii) there is the strong coupling between all pairs of nearest-neighbor cells.

The resulting equation of motion is ( $S_j \equiv S_j - S_{eq}$ )

$$M \cdot (d^2 u_j / dt^2 - \gamma \cdot du_j / dt + \omega_0^2 \cdot u_j) = C \cdot (u_{j+1} + u_{j-1} - 2u_j) + e \cdot E(Z = jd, t) \quad (22)$$

Considering a response to the external field wave  $E(Z, t) = E \cdot \exp(ikZ - i\omega t)$  we look for solution of (22) having the form of traveling wave

$$u_j = u \cdot \exp(ikjd - i\omega t). \quad (23)$$

On substitution of (23) in (22), we have

$$u = (\epsilon E/M) / (\omega_k^2 + \omega_0^2 - \omega^2 - i\gamma\omega), \quad (24)$$

where  $\omega_k \equiv 2\sqrt{C/M} \cdot \sin(kd/2)$ . In the long-wave limit,  $\omega_k \approx k \cdot d \cdot \sqrt{C/M}$ . It should be mentioned that the value  $V = d \cdot (C/M)^{1/2}$  is the velocity of acoustics waves in the crystal.

The additional (to the spontaneous) dielectric polarization  $P$  is  $P = N e u$ , where  $N$  is the number of cells per unit volume. So we have

$$\epsilon = 1 + \Omega^2 / (\omega_k^2 + \omega_0^2 - \omega^2 - i\gamma\omega), \quad (25)$$

where  $\Omega^2 \equiv 4\pi e^2 N/M$ . The real and imaginary parts of permittivity have the forms

$$\begin{aligned} \epsilon' &= 1 + \Omega^2 / [(\omega_k^2 + \omega_0^2 - \omega^2)^2 + \gamma^2 \omega^2] \\ \epsilon'' &= \gamma \cdot \omega \cdot \Omega^2 / [(\omega_k^2 + \omega_0^2 - \omega^2)^2 + \gamma^2 \omega^2] \end{aligned} \quad (26)$$

If the frictional constant  $\gamma$  is small ( $\gamma \ll \{\Omega, \omega_0\}$ ), then

$$\epsilon''/\epsilon' \approx \gamma \cdot \omega \cdot \Omega^2 / (\omega_k^2 + \omega_0^2 - \omega^2) \cdot (\omega_k^2 + \omega_0^2 - \omega^2 + \Omega^2) \ll 1 \quad (27)$$

Let us now insert (27) in (21). On substitution  $\omega_0 = \lambda \cdot \omega$  ( $\lambda = V_a/V$ ) and integrating with respect to the frequency, we obtain

$$F_d = \gamma \cdot e^2 \cdot \Omega^2 \cdot V^{-2} \cdot (\lambda^2 - 1)^{-3/2} \cdot [\omega_0 + (\omega_0^2 + \Omega^2)^{1/2}]^{-1}. \quad (28)$$

If  $V \ll V_a$ , then

$$F_d \approx \Lambda \cdot V; \quad \Lambda = \gamma \cdot e^2 \cdot \Omega^2 \cdot V_a^{-3} \cdot [\omega_0 + (\omega_0^2 + \Omega^2)^{1/2}]^{-1}. \quad (29)$$

If  $V \geq V_a$ , the transition from (20) to (21) must be done more carefully.

## V.LIMITING ENERGY OF ACCELERATED DEUTERONS

Using the relations of Sec.IV, the value of the energy losses  $\Delta T$  at one collision can be estimated by the formula

$$\Delta T = F_d \cdot d = \Lambda \cdot d \cdot (2T/M)^{1/2} \quad (30)$$

For dimensionless variables (see Sec.III), we can write this formula in the form

$$\Delta W = \alpha \cdot W^{1/2}; \quad \alpha = \gamma \cdot e^2 \cdot \Omega^2 \cdot V_a^{-3} \cdot d^2 \cdot (2\pi e M D)^{-1/2} \cdot [\omega_0 + (\omega_0^2 + \Omega^2)^{1/2}]^{-1} \quad (31)$$

The accounting of the energy losses brings us to the variation of the form of the mapping (11). We have

$$W_{n+1} = W_n - q(y_n) - \alpha \cdot W_n^{1/2}$$

instead of the first relation of Eq.(11'). The other relations of

the mapping (11) must be changed similarly. The modified system (12) has the form (for  $W \gg 1$ )

$$dW/dn = -q \cdot \cos(y) - a \cdot W^{1/2}; \quad dy/dn = Q/2 \cdot W^{1/2} \quad (32)$$

The system (32) has the first integral

$$W = \text{Max}(W) \cdot \left[ \cos(y-y^*) + O(\exp[-\alpha(y-y_0)/Q]) \right]^2 \quad (33)$$

In this relation it is designated:

$$\text{Max}(W) = q^2/(Q^2+a^2), \quad \cos(y^*) = a/(Q^2+a^2)^{1/2}. \quad (34)$$

The second term in sum (33) is the exponentially damped contribution of the initial condition.

To make a qualitative estimate of the maximal energy, we consider<sup>13;14</sup> the deuteron acceleration in KDP ferroelectrical crystal. The estimates of the parameters  $a$  and  $b$  (see Sec.II) can be obtained, if we equate the value of  $e$  to the electron charge ( $\approx 4.8 \times 10^{-10}$  CGSE), the value of  $E_c$  to the coercive force  $E$  ( $\approx 7$  CGSE), and the value of  $\theta \cdot S_c/d^3$  to the spontaneous polarization  $P_s$  ( $\approx 1.5 \times 10^4$  CGSE). We have<sup>15</sup>  $S_c \approx 1.1 \times 10^{-8}$  cm,  $a \approx 0.79$  erg/cm<sup>2</sup>,  $b \approx 0.66 \times 10^{-16}$  erg/cm<sup>4</sup>. It should be noted that, though the value of  $S_c$  is nearly to the actual interatomic distances, it is some fictitious coordinate. Really, the process of the polarization reversal is connected with the displacements of many atoms, but for a significantly smaller distances. If we equate the effective mass  $M$  to the average atomic mass of the cell, then we have the estimation of the frequency of oscillations:  $\omega \approx 10^{11}$  rad/s. The correspondent value of  $Q$  is  $\omega (Md/2\pi eP_s) \approx 3 \times 10^{-2}$ . The scale of the energy is  $4\pi eD/d^2 = 4\pi eDP_s \approx 6.3 \times 10^{-12}$  erg  $\approx 3.7$  eV. The estimation of the value  $\alpha$  has the form

$$a = (\gamma e^2/V_a^3 d) \cdot (2e/M\pi P_s)^{1/2}$$

Let us assume  $V \approx 10^5$  cm/s, according to<sup>16</sup>  $\gamma = 10^{13}$  s<sup>-1</sup>, then  $\alpha \approx 10$ . According to the Eq.(34) (if  $Q \ll a$ ), the maximal energy of accelerated deuteron is

$$\text{Max}(T) \approx 2 \cdot \pi \cdot V_a^6 \cdot M \cdot \pi \cdot P_s^2 / \gamma^2 \cdot e^4 \cdot N \quad (35)$$

Given parameters as defined above, the value of  $\text{Max}(T)$  is  $\approx 1$  eV. This value is of no interest to "cold fusion", but we may choose the ferroelectrics with more suitable characteristics. According to<sup>20</sup>, the value of  $\gamma$  can be as small as  $\approx 10^{-10}$  s<sup>-1</sup> (e.g. in  $\text{PbTiO}_3$ ). Some ferroelectrics (e.g.  $\text{LiNbO}_3$ ) have<sup>21</sup> the spontaneous polarization  $P_s$  as much as 10 CGSE. For these ferroelectrics the value of  $\text{Max}(T)$  is  $\approx 40$  eV (in  $\text{PbTiO}_3$ ) or 1.4 keV (in  $\text{LiNbO}_3$ ). The ferroelectric properties of these compounds is not well established to date. In a few cases, however, compounds of this type have turned out to be interesting from the viewpoint of cold fusion, so that it may be worth devoting some space to them.

## VI.CONCLUSION

Let us summarize the obtained results. We can conclude that the mechanism of the Fermi acceleration in the field of the wave generated in the course of the polarization reversal of ferroelectrical crystals can bring to the D-nuclei acceleration up to the energy  $>200$  eV. It is sufficiently for the reaction of D+D fusion to be detected. We think this way of the realization of the cold nuclear fusion in solid to be the most perspective among all the realized in laboratory conditions at present.

The crystal, which is "optimal" for the cold nuclear fusion, must have at least two properties:

- (1) it must be ferroelectrics of great value of the spontaneous polarization,
- (2) the structure of the crystal must provide the great mobility of D-ions (may be it must be superionic crystal).

## ACKNOWLEDGMENTS

This work was supported by the Research Enterprise "Actual Technologies".

## REFERENCES

1. J.S.Cohen and J.D.Davies. "Is Cold Fusion Hot?" Nature. Vol. 342, p.487 (1989).
2. S.E.Segre, S.Atzeni, P.Briguglio, and F.Romanelli. "A Mechanism for Neutron Emission from Deuterium Trapped in Metals." Europhys.Lett. Vol.11, p.201 (1990).
3. P.I.Golubnichni, V.V.Kuzminov, G.T.Merson et al. "Correlative Acoustic and Neutron Emission from the Palladium Deuterated Target." Sov.Phys.: JETP Lett. Vol. 53, p.115 (1991).
4. S.E.Jones, E.P.Palmer, J.B.Czirr et al. "Observation of Cold Nuclear Fusion in Condensed Matter." Nature. Vol.338, p.737 (1989).
5. M.Fleischmann and S.Pons. "Electrochemically Induced Nuclear Fusion of Deuterium." J.Electroanal.Chem. Vol.261,p.301 (1989)
6. V.A.Kluev, A.G.Lipson, Yu.P.Toporkov et al. "High-energy processes during destruction of solids." Sov.Phys.:JTP Lett.Vol. 12, p.1333 (1986).
7. A.De Nino, A.Frattolillo, F.Scaramuzzi."Neutron Emission from a Titanium-Deuterium System" In: Proceedings of the Workshop on "Understanding Cold Fusion", Varenna, Italy, September 15-16, 1989, p. 41 (1990).
8. G.V.Fedorovich. "Parametric Resonance in Crystalline Structures as a Possible Cause of High-Energy Emissions." Sov.Phys.: JTP. Vol.63, No.10, p.64 (1993).
9. G.V.Fedorovich. "A Possible Nature of Nuclear Fusion in Crystals" Submitted to APPLIED PHYSICS A (1992).
- 10.S.A.Flerova, N.N.Krainik, S.A.Popov. Ferroelectrics. Vol. 82. p.167 (1988).
- 11.G.I.Rosenman, O.V.Malyshkina, Yu.L.Chepelev."Electron Emission at Switching of Ferroelectrics." Ferroelectrics. Vol.110. p.99 (1990).
- 12.H.Gundel, H.Riege, E.J.N.Wilson et al."Fast Polarization Changes in Ferroelectrics and Their Application in Accelerators."

- Nucl. Instr. Meth. in Phys. Res. Vol.A280, p.1 (1989).
- 13. A.G.Lipson, D.M.Sakov, E.I.Saunin et al. "Cold Nuclear Fusion Induced in KD<sub>2</sub>PO<sub>4</sub> Single Crystals by a Ferroelectric Phase Transition." Sov.Phys.: JETP. Vol.76. p.1070 (1993).
  - 14. B.V.Derjaguin, E.I.Andriankin, A.G.Lipson et al. "On the Possibility of a Nuclear Fusion Stimulation by the Wave of Polarisation Reversal Generated in Deuterated Ferroelectrics at T < T<sub>c</sub>." Sov.Phys.: Dokl. Accepted for publication (1993).
  - 15. A.J.Lichtenberg, M.A.Lieberman. *Regular and stochastic motion.* Springer-Verlag, New York, Heidelberg, Berlin, 1983.
  - 16. R.A.Meyers (Editor). *Encyclopedia of Physical Science and Technology.* Vol.2, Academic Press Inc., New York, 1987, p.241.
  - 17. E.Fermi. Phys.Rev. Vol.57, p.485 (1940).
  - 18. G.M.Zaslavsky. *Stochasticity of dynamic system.* Nauka publ., Moscow, 1984.
  - 19. I.P.Kaminov and T.C.Damen. Phys.Rev.Lett. Vol.20, p.1105 (1968)
  - 20. K.B.Lyons and P.A.Fleury. Phys.Rev.Lett. Vol.37, p.161 (1976).
  - 21. F.Jona and G.Shirane. *Ferroelectric crystals.* Pergamon Press, Oxford, London, New York, Paris, 1962.

# POSSIBLE EVIDENCE OF COLD D(D, p)T FUSION FROM DEE'S 1934 EXPERIMENT

Yeong E. Kim  
Department of Physics  
Purdue University  
West Lafayette, IN 47907

## Abstract

$D(D, p)T$  fusion probabilities for the back-to-back proton-tritium tracks observed in Dee's 1934 experiment are calculated using the conventional theory and found to be many orders of magnitude smaller than those inferred from Dee's data. Our results indicate that Dee's data may be evidence for cold fusion, possibly due to low-energy reaction barrier transparency, as recently proposed. Therefore it is important to repeat Dee's experiment with modern facilities.

## 1. Introduction

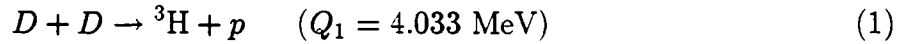
In 1934, Oliphant, Harteck, and Lord Rutherford<sup>1,2</sup> reported the discovery of deuterium-deuterium fusion via the nuclear reactions,  $D(D, p)T$  and  $D(D, n)$   ${}^3\text{He}$ . They bombarded deuterated ammonium chloride ( $ND_4\text{Cl}$ ), ammonium sulphate ( $(ND_4)_2\text{SO}_4$ ) and orthophosphoric acid ( $D_3\text{PO}_4$ ) with a  $20 \sim 200$  keV deuterium (called "diplogen" then) ion ( $D^+$ ) beam generated from a Cockcroft-Walton discharge tube.<sup>3</sup> Later in the same year (1934), Dee<sup>4</sup> studied the nuclear reaction  $D(D, p)T$  more carefully using a 160 keV  $D^+$  beam on a  $(ND_4)_2\text{SO}_4$  target, and photographed ionization tracks of  $p$  and  $T$  in a cloud chamber. Occasionally, proton-tritium ( $p - T$ ) pairs were observed with the angle between the tracks very near to  $180^\circ$ .<sup>5</sup> Dee<sup>5</sup> attributed these tracks to  $D(D, p)T$  reactions involving deuterons which have lost energy by collisions in the target. The expansion chamber detection system used by Dee<sup>4,5</sup> was developed earlier by Dee and Walton.<sup>6</sup> The  $D^+$  beam generation system used by Dee was an improved Cockcroft-Walton<sup>3</sup> discharge tube constructed by Oliphant and Rutherford<sup>7</sup> which generated a higher  $D^+$  beam current ( $\sim 100 \mu\text{A}$ ). Recently, Fleischmann<sup>8</sup> suggested that these results obtained by Dee<sup>5</sup> are the first indication that there are low energy fusion channels in solid lattices as in the case of the cold fusion electrolysis experiments.<sup>9</sup> Fleischmann's suggestion was criticized by Close<sup>10</sup> on two grounds. The first is that Dee's photographs do not show that the tracks are exactly back-to-back and hence one cannot eliminate the possibility that the incident deuteron had even one keV of energy,

which is comparable to the solar core temperature. The second objection by Close (and also by Petrasso<sup>10</sup>) was that no energetic tritium or proton had been observed in the cold fusion electrolysis experiments with deuterated palladium. More recently, Huizenga<sup>11</sup> objected to Fleischmann's statement<sup>8</sup> that *a significant number* of back-to-back tracks were observed by Dee, since what Dee<sup>5</sup> actually stated was that *occasionally* back-to-back  $p - T$  tracks were observed.

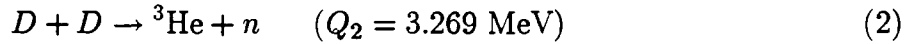
In this paper, Dee's results are analyzed using the conventional theory to establish whether the back-to-back  $p - T$  tracks observed by Dee<sup>5</sup> suggest an anomalous effect, in order to resolve the controversy between Fleischmann's suggestion<sup>8</sup> and its objections by Close,<sup>10</sup> Petrasso,<sup>10</sup> and Huizenga.<sup>11</sup>

## 2. Fusion Kinematics

When  $D^+$  ions (deuterons) are incident on the  $(ND_4)_2SO_4$  target, the dominant fusion reactions are known to be



and



for an incident deuteron laboratory (LAB) kinetic energy  $E_D$  greater than  $\sim 10$  keV,<sup>12</sup> with the  $Q$  values of 4.033 MeV and 3.269 MeV, respectively. For  $D(D, p)T$ , eq. (1), the velocities  $\vec{v}_p$  and  $\vec{v}_T$  of the emitted proton ( $p$ ) and tritium ( ${}^3H$  or  $T$ ) are co-planar with the velocity  $\vec{v}_D$  of the incident deuteron. The scattering angles,  $\theta_L^p$  and  $\theta_L^T$ , of the emitted  $p$  and  $T$ , in the LAB frame, are measured from the direction of the incident deuteron velocity  $\vec{v}_D$  (which is the same as the direction of  $D + D$  center-of-mass (CM) velocity,  $\vec{v}_C$ ) i.e.,  $\cos \theta_L^p = \vec{v}_D \cdot \vec{v}_p = \vec{v}_C \cdot \vec{v}_p$  and  $\cos \theta_L^T = \vec{v}_D \cdot \vec{v}_T = \vec{v}_C \cdot \vec{v}_T$ . In the CM frame, the directions of  $p$  and  $T$  velocities,  $\vec{v}'_p$  and  $\vec{v}'_T$ , are opposite and the  $p$  and  $T$  scattering angles in the CM frame,  $\theta_C^p$  and  $\theta_C^T$ , as measured from  $\vec{v}_C$  add up to  $180^\circ$ ,  $\theta_C^p + \theta_C^T = 180^\circ$ . The proton scattering angles,  $\theta_L^p$  and  $\theta_C^p$ , are related by<sup>13</sup>

$$\tan \theta_L^p = \frac{\sin \theta_C^p}{\gamma_p + \cos \theta_C^p} \quad (3)$$

with

$$\begin{aligned} \gamma_p &= \left[ \frac{m_T(m_p + m_T)}{m_D m_p} \left( \frac{Q_1}{E_D} \right) + \frac{m_T(m_T + m_p - m_D)}{m_D m_p} \right]^{-1/2} \\ &= [5.979(Q_1/E_D) + 2.986]^{-1/2} \end{aligned} \quad (4)$$

while the triton scattering angles,  $\theta_L^T$  and  $\theta_C^T$ , are related by

$$\tan \theta_L^T = \frac{\sin \theta_C^T}{\gamma_T + \cos \theta_C^T} \quad (5)$$

with

$$\begin{aligned}\gamma_T &= \left[ \frac{m_p(m_T + m_p)}{m_D m_T} \left( \frac{Q_1}{E_D} \right) + \frac{\bar{m}_p(m_p + m_T - m_D)}{m_D m_T} \right]^{-1/2} \\ &= [0.6676(Q_1/E_D) + 0.3334]^{-1/2}\end{aligned}\quad (6)$$

where  $m_p$ ,  $m_D$ , and  $m_T$  are the rest masses of proton, deuteron, and tritium, respectively.

For the special case of  $\theta_C^p = \theta_C^T = 90^\circ$ , eqs. (3) and (5) reduce to

$$\tan \theta_L^p = \frac{1}{\gamma_p} = [5.979(Q_1/E_D) + 2.986]^{1/2}. \quad (7)$$

and

$$\tan \theta_L^T = \frac{1}{\gamma_T} = [0.6676(Q_1/E_D) + 0.3334]^{1/2}. \quad (8)$$

The calculated values of  $\theta_L^p$ ,  $\theta_L^T$ , and  $\theta_L^{pT} = \theta_L^p + \theta_L^T$  for the case of  $\theta_C^p = \theta_C^T = 90^\circ$  are listed in Table 1 for several selected values of  $E_D$ . From the description and pictures given in references 5 and 6, Dee's Wilson expansion chamber has acceptance angles of  $\sim 30^\circ$ , i.e.,  $75^\circ \lesssim \theta_L^p \lesssim 105^\circ$  and  $75^\circ \lesssim \theta_L^T \lesssim 105^\circ$ . Within the above acceptance angles, the results of  $\Delta\theta = 180^\circ - \theta_L^{pT}$  listed in Table 1 decrease only by  $\sim 5\%$  for  $E_D \leq 10$  keV. Therefore, if the accuracy of Dee's measurements of  $\theta_L^{pT}$  is  $\sim \pm 1^\circ$ , we expect that  $E_D \leq 2$  keV for the back-to-back  $pT$  tracks with  $\Delta\theta \leq 2^\circ$ , while, for an accuracy of  $\pm 2.0^\circ$  for  $\theta_L^{pT}$ , we expect  $E_D \lesssim 10$  keV, corresponding to  $\Delta\theta \leq 4^\circ$ .

### 3. Conventional Fusion Probability and Rate

The probability  $P(E_i)$  for a deuteron with the initial LAB kinetic energy  $E_i$  to undergo the fusion reaction (1) while slowing down in a deuterated ammonium sulfate  $(ND_4)_2SO_4$  target can be written as

$$P(E_i) = \int dx n_D \sigma(E_{DD}) = \int_0^{E_i} dE_D \frac{n_D \sigma(E_{DD})}{|dE_D/dx|} \quad (9)$$

where  $n_D$  is the target deuteron number density,  $\sigma(E_{DD})$  is the cross-section for reaction (1),  $dE/dx$  is the stopping power for deuteron by the target atoms, and  $E_D$  and  $E_{DD}$  are the deuteron kinetic energies in the LAB and CM frames, respectively ( $E_{DD} = E_D/2$ ).

#### 3.1 Stopping Power

The stopping power for deuteron by the target atom  $j$  with the density  $n_j$ , can be taken from Ref. 14. For a deuteron laboratory kinetic energy  $E_D \leq 20$  keV, it is given by<sup>15</sup>

$$\frac{dE_D}{dx} = n_j A_1 (E_D/2)^{1/2} \times 10^{-18} \text{ keV} - \text{cm}^2 . \quad (10)$$

For  $20 \text{ keV} \leq E_D \leq 1 \text{ MeV}$ , we have

$$\left[ \frac{dE_D}{dx} \right]^{-1} = \left[ \frac{dE_D}{dx} \right]_{\text{slow}}^{-1} + \left[ \frac{dE_D}{dx} \right]_{\text{high}}^{-1} , \quad (11)$$

where

$$\left[ \frac{dE_D}{dx} \right]_{\text{slow}} = n_j A_2 (E_D/2)^{0.45} \times 10^{-18} \text{ keV} - \text{cm}^2 , \quad (12)$$

$$\left[ \frac{dE_D}{dx} \right]_{\text{high}} = (2n_j A_3/E_D) \ell n [(1 + 2A_4/E_D) + (A_5 E_D/2)] \times 10^{-18} \text{ keV} - \text{cm}^2 . \quad (13)$$

with  $E_D$  in units of keV. Since  $[dE_D/dx] \sim [dE_D/dx]_{\text{slow}}$  and  $[dE_D/dx]_{\text{slow}}$  agrees with  $dE_D/dx$  given by eq. (10) within a factor of 2 or less for  $20 \text{ keV} < E_D < 160 \text{ keV}$ , it is fairly accurate to assume that the stopping power is given by eq. (10) for  $E_D < 160 \text{ keV}$ . The atom number densities  $n_j$  for the mixtures of  $\alpha(NH_4)_2SO_4 + \beta(ND_4)_2SO_4$  with  $\alpha + \beta = 1$  are  $n_H = \alpha(6.45 \times 10^{22}/\text{cm}^3)$ ,  $n_D = \beta(6.45 \times 10^{22}/\text{cm}^3)$ ,  $n_N = 1.61 \times 10^{22}/\text{cm}^3$ ,  $n_O = 3.22 \times 10^{22}/\text{cm}^3$ , and  $n_S = 0.806 \times 10^{22}/\text{cm}^3$ , respectively for hydrogen deuterium, nitrogen, oxygen and sulfur, respectively. Using eq. (10), the stopping powers for deuteron by the target atoms,  $H$ ,  $D$ ,  $N$ ,  $O$ , and  $S$  are given by

$$\frac{dE_D}{dx}(H) = \alpha(5.756 \times 10^4) \sqrt{E_D} \text{ keV/cm} \quad (14)$$

$$\frac{dE_D}{dx}(D) = \beta(5.756 \times 10^4) \sqrt{E_D} \text{ keV/cm} \quad (15)$$

$$\frac{dE_D}{dx}(N) = 3.363 \times 10^4 \sqrt{E_D} \text{ keV/cm} \quad (16)$$

$$\frac{dE_D}{dx}(O) = 6.038 \times 10^4 \sqrt{E_D} \text{ keV/cm} \quad (17)$$

and

$$\frac{dE_D}{dx}(S) = 1.965 \times 10^4 \sqrt{E_D} \text{ keV/cm} , \quad (18)$$

respectively. Therefore, the stopping power for  $D$  in the target consisting of  $\alpha(NH_4)_2SO_4$  and  $\beta(ND_4)_2SO_4$  ( $\alpha + \beta = 1$ ) is given by the sum of eqs. (14) through (18),

$$\frac{dE_D}{dx} = 1.712 \times 10^5 \sqrt{E_D} \text{ keV/cm} \quad (19)$$

where  $E_D$  is in units of keV.

### 3.2 Parameterized Cross-Section

The cross-section  $\sigma(E_{DD})$  for the  $D(D, p)T$  reaction has not been measured for  $E_{DD} \lesssim 5$  keV. For  $E_{DD} \lesssim 5$  keV,  $\sigma(E_{DD})$  is calculated by extrapolating the experimental values of  $\sigma(E_{DD})$  at higher energies using the parameterization ( $E = E_{DD}$ )

$$\sigma(E) = \frac{S(E)}{E} T_G(E) \quad (20)$$

where  $T_G(E) = \exp[-(E_G/E)^{1/2}]$ ,  $E_G = (2\pi\alpha Z_D Z_D)^2 \mu c^2 / 2$  or  $E_G^{1/2} \approx 31.39$  (keV) $^{1/2}$  with the reduced mass  $\mu = m_D m_D / (m_D + m_D) = \frac{1}{2} m_D$ . The transmission coefficient (“Gamow” factor)  $T_G(E)$  results from the approximation  $E \ll B$  (Coulomb barrier height). Note that  $\sigma(E)$  described by eq. (20) is valid only for non-resonance fusion reactions. The  $S$ -factor,  $S(E)$ , is extracted from the experimentally measured values<sup>12</sup> of the cross-section,  $\sigma(E)$ , for  $E \gtrsim 4$  keV and is nearly constant,<sup>12</sup>  $S(E) \approx S(0) = 52.9$  keV – barn, for both reactions (1) and (2).

### 3.3 Conventional Estimates of Fusion Probability

Using the results of eqs. (19) and (20) with  $n_D = \beta$  ( $6.45 \times 10^{22}/\text{cm}^3$ ),  $P(E_i)$  given by eq. (9) can be written as

$$\begin{aligned} P(E_i) &= \int_0^{E_i} dE_D \frac{n_D S(E_{DD})}{|dE_D/dx| E_{DD}} e^{-\sqrt{E_G}/\sqrt{E_{DD}}} \\ &\approx \frac{2n_D S(0)}{1.712 \times 10^4 (\text{keV/cm})} \int_0^{E_i} dE_D \frac{e^{-\sqrt{E'_G}/\sqrt{E_D}}}{(E_D)^{3/2}} \\ &= \frac{2n_D S(0)}{1.712 \times 10^4 (\text{keV/cm})} \frac{1}{\sqrt{E'_G}} e^{-\sqrt{E'_G}/\sqrt{E_i}} \end{aligned} \quad (21)$$

where  $\sqrt{E'_G} = \sqrt{2}\sqrt{E_G} = 44.39\sqrt{\text{keV}}$  and  $E_i$  is in units of keV. Using  $S(0) = 52.9 \times 10^{-24} \text{ cm}^2 - \text{keV}$  and  $n_D = \beta(6.45 \times 10^{22}/\text{cm}^3)$ ,  $P(E_i)$  can be written as

$$P(E_i) = \beta(0.90 \times 10^{-6}) e^{-\sqrt{E'_G}/\sqrt{E_i}} \quad (22)$$

The calculated values of  $P(E_i)$  using eq. (22) with  $\beta = 1$  are listed in Table 2 for several selected values of  $E_i$ .

### 3.4 Conventional Estimates of Fusion Rates

As described by Dee and Walton,<sup>6</sup> Dee<sup>5</sup> used a discharge tube similar to that of Oliphant and Rutherford<sup>7</sup> which gave a proton beam current of  $100 \mu\text{A}$  using an accelerating voltage not greater than 250 kV. Assuming that the same system generated the deuteron beam current of  $I = 100 \mu\text{A}$  with a deuteron LAB energy of  $E_i = 160 \text{ keV}$ , we can obtain conventional estimates of the expected fusion rates  $R(E_i)$  from

$$R(E_i) = \Phi P(E_i) \quad (23)$$

where  $\Phi$  is the incident deuteron flux given by

$$\Phi = (0.625 \times 10^{19} D^+/\text{sec}) I \quad (24)$$

with  $I$  in units of amperes. For  $I = 100 \mu\text{A}$ , the conventional estimate of  $R(E_i)$  is

$$R(E_i) = 0.562 \times 10^9 \beta e^{-\sqrt{E'_G}/\sqrt{E_i}} / \text{sec} \quad (25)$$

with  $E_i$  in units of keV. The calculated values of  $R(E_i)$  from eq. (25) with  $\beta = 1$  are listed in Table 2 for several selected values of  $E_i$ . It is likely that Dee used a much lower current than  $100 \mu\text{A}$  by controlling it with a beam shutter in order to have a manageable counting rate for the pT tracks produced in his Wilson expansion chamber.

## 4. Analysis of Dee's Data

From the conventional estimates of  $P_R(E_i)$  given in Table 2, we see that out of a total of  $10^{12}$  pT tracks ( $162^\circ < \theta_L^{pT} < 180^\circ$ ) produced, only one is expected to be a back-to-back ( $178^\circ < \theta_L^{pT} < 180^\circ$ ) pT track, which is impossible to be observed occasionally with Dee's experimental set up. If we interpret Dee's "occasional observations" to mean 1 out of 100 (a reasonable interpretation) which corresponds to a degraded deuteron kinetic energy of  $E_D = 30 \text{ keV}$  (see Table 2), we expect  $\theta_L^{pT} \gtrsim 172^\circ$  (see Table 1), which cannot be the back-to-back pT track with the accuracy of  $\pm 2^\circ$  for measuring  $\theta_L^{pT}$ .

### 4.1 Scattered Deuteron Mechanism

We now investigate a mechanism in which the incident deuteron could be scattered by a target atom into the Wilson expansion chamber acceptance angles,  $\theta_D = 90^\circ \pm 15^\circ$ , prior to fusing with a target deuteron to produce a back-to-back pT track (which is possible if  $\theta_c^P$  or  $\theta_c^T$  is nearly parallel to  $\theta_D$ ).

For a screened Coulomb potential

$$V_c(r) = \frac{Z_D Z_j e^2}{r} e^{-r/a} \quad (26)$$

with a screening radius  $a$ , and atomic numbers  $Z_D (= 1)$  and  $Z_j$  for the deuteron and target atom  $j$ , respectively, the scattering amplitude  $f(\theta_c)$  in the Born approximation is

given by<sup>16</sup>

$$f(\theta_c) = \frac{2 \mu Z_j e^2 a^2}{\hbar^2 (4k^2 a^2 \sin^2 \frac{\theta_c}{2} + 1)} \quad (27)$$

where  $\hbar^2 k^2 / 2 \mu = E_{CM}$  with the reduced mass  $\mu$  and the CM kinetic energy  $E_{CM}$ . The probability of the incident deuteron being scattered by a target atom  $j$  into the CM angle  $\theta_c$  is then

$$\begin{aligned} P_j(\theta_c) &= \left| \frac{f(\theta_c)}{f(0)} \right|^2 = \left[ 8 \left( \frac{m_D}{\hbar^2} \right) \left( \frac{m_D}{m_D + m_j} \right)^2 E_D a^2 \left( \sin \frac{\theta_c}{2} \right)^2 + 1 \right]^{-2} \\ &= \left[ 0.385 \times 10^7 \left( \frac{m_D}{m_D + M_j} \right)^2 E_D a^2 \left( \sin \frac{\theta_c}{2} \right)^2 + 1 \right]^{-2} \end{aligned} \quad (28)$$

where  $E_D$  and  $a$  are in units of keV and Å, respectively. The CM angle  $\theta_c$  is related to the deuteron LAB scattering angle  $\theta_L$  by

$$\tan \theta_L = \frac{\sin \theta_c}{(m_D/m_j) + \cos \theta_c}. \quad (29)$$

Using  $a = \hbar^2/m_e e^2 Z_j^{1/3} = 0.529 \text{Å}/Z_j^{1/3}$  and eq.(29),  $P_S(\theta)$  for deuteron-sulfur atom Coulomb scattering for  $\theta_c = 30^\circ$  or  $\theta_L = 28.3^\circ$  is calculated and found to be  $P_S(30^\circ) = 2.32 \times 10^{-8}$ . Since  $P_D(30^\circ)$ ,  $P_N(30^\circ)$ , and  $P_O(30^\circ)$  are smaller than  $P_S(30^\circ)$ , we can conclude that only a few out of  $10^8$  incident 160 keV deuterons move out beyond  $\theta_L \approx 28^\circ$  of the incident direction after the first encounter with the target atom. Therefore, the scattered deuteron mechanism cannot explain Dee's back-to-back pT tracks.

#### 4.2 Suggested Experimental Tests

Since the conventional estimates of fusion probability and rate for the events observed by Dee<sup>5</sup> with the  $p - T$  opening angle  $180^\circ > \theta_L^{pT} > 178^\circ$  corresponding to the deuteron LAB kinetic energy  $E_D \lesssim 2$  keV are smaller by many orders of magnitude than the inferred values from Dee's experiment, it suggests strongly that the conventional estimates are not reliable at low energies,  $E_D < 2$  keV. It is therefore important to repeat Dee's experiment with improved Wilson expansion chambers. In addition to using the Wilson expansion chamber, one should also use other modern visual detecting systems<sup>17</sup> such as a diffusion cloud chamber, with high current (continuous or pulsed) low-energy deuteron beams.

#### 5. Conclusions

Contrary to the objections raised by Close<sup>10</sup>, Petrasso<sup>10</sup>, and Huizenga<sup>11</sup>, the suggestion made by Fleischmann that Dee's back-to-back pT tracks are the first indication of cold fusion may have validity since it is shown that the conventional theoretical estimates cannot explain the back-to-back pT tracks observed by Dee.<sup>5</sup>

One plausible explanation<sup>18</sup> of Dee's data for the back-to-back pT tracks, based on a general and more realistic solution of the transmission coefficient  $T_{KZ}(E)$  by Kim and Zubarev<sup>18</sup>, is that reaction barrier transparency exists for the transmission coefficient near the fusion threshold energy.<sup>19</sup> The conventional Gamow transmission coefficient,  $T_G(E)$ , is restricted to non-resonant reactions, and hence cannot describe such resonant behavior of the transmission coefficient. In other conventional theoretical models, Breit-Wigner (BW) resonances are included in the S-factor,  $S(E)$ , in eq.(20), but any enhancement of  $\sigma(E)$  due to the BW resonance is limited to at most a few orders of magnitude increase and hence cannot explain Dee's data. Therefore, it is important to repeat Dee's experiment with modern facilities and techniques.

### Acknowledgements

This work has been supported in part by the Electric Power Research Institute.

### References

1. M. L. Oliphant, P. Harteck, and Lord Rutherford, "Transmutation Effects Observed by Heavy Hydrogen," *Nature* **133**, 413 (1934).
2. M. L. E. Oliphant, P. Harteck, and Lord Rutherford, "Transmutation Effects Observed by Heavy Hydrogen," *Proc. Roy. Soc. A* **144**, 692 (1934).
3. J. D. Cockcroft and E. T. S. Walton, "Experiments with High Velocity Positive Ions.—(I) Further Developments in the Method of Obtaining High Velocity Ions," *Proc. Roy. Soc. A* **136**, 619 (1932).
4. P. I. Dee, "Disintegration of the Diplon," *Nature*, **133**, 564 (1934).
5. P. I. Dee, "Some Experiments upon Artificial Transmutation using the Cloud-track Method," *Proc. Roy. Soc. A* **148**, 623 (1935).
6. P. I. Dee and E. T. S. Walton, "A Photographic Investigation of the Transmutation of Lithium and Boron by Proton and of Lithium by Ions of the Heavy Isotope of Hydrogen," *Proc. Roy. Soc. A* **141**, 733 (1933).
7. M. L. E. Oliphant and Lord Rutherford, "Experiments on the Transmutation of Elements by Protons," *Proc. Roy. Soc. A* **141**, 259 (1933).
8. M. Fleischmann, "An Overview of Cold Fusion Phenomena," in the Proceedings of the First Annual Conference on Cold Fusion, Salt Lake City, March 28–31, 1990, pp. 344–349.
9. M. Fleischmann, S. Pons, and M. Hawkins, "Electrochemically Induced Nuclear Fusion of Deuterium," *J. Electroanal. Chem.* **261**, 301 (1989).
10. F. Close, *Too Hot to Handle*, W. H. Allen Publishing (1990), pp. 318–323.

11. J. R. Huizenga, *Cold Fusion: the Scientific Fiasco of the Century*, University of Rochester Press (1992), p. 100.
12. A. Krauss, H. W. Becker, H. P. Trautvetter, and C. Rolfs, "Low-Energy Fusion Cross Sections of  $D + D$  and  $D + {}^3\text{He}$  Reactions," *Nucl. Phys. A* **465**, 150 (1987).
13. A. P. Arya, *Nuclear Physics*, Allyn & Bacon, Inc., Boston (1966), pp. 79–89.
14. H. H. Anderson and J. F. Ziegler, *Hydrogen Stopping Powers and Ranges in All Elements*, Pergamon Press, New York (1977).
15. Y. E. Kim, M. Rabinowitz, Y. K. Bae, G. S. Chulick, and R. A. Rice, "Cluster-Impact Nuclear Fusion: Shock-Wave Analysis," *Mod. Phys. Lett. B* **5**, 941 (1991).
16. L.I. Schiff, *Quantum Mechanics*, McGraw-Hill (1966), p. 325.
17. W. E. Burcham, *Nuclear Physics*, McGraw-Hill (1966), Chapter 6.
18. Y. E. Kim and A. L. Zubarev, "Coulomb Barrier Transmission Resonance for Astrophysical Problems," to be published in *Mod. Phys. Lett. B*.
19. Y. E. Kim, J.-H. Yoon, A. L. Zubarev, and M. Rabinowitz, "Reaction Barrier Transparency for Cold Fusion with Deuterium and Hydrogen," to be published in the Proceedings of the 4th International Conference on Cold Fusion, Maui, Hawaii, December 6–9, 1993.

Table 1

Proton and tritium scattering angles for selected incident deuteron kinetic energies in the LAB frame assuming the CM scattering angles  $\theta_C^p = \theta_C^T = 90^\circ$ .

$E_k$ (keV)	$\theta_L^p$	$\theta_L^T$	$\theta_L^{pT} = \theta_L^p + \theta_L^T$	$\Delta\theta = 180^\circ - \theta_L^{pT}$
1	89.63	88.90	178.53	1.43
2	89.48	88.44	177.92	2.08
3	89.36	88.09	177.45	2.55
5	89.18	87.53	176.71	3.29
10	88.83	86.52	175.35	4.65
20	88.35	85.08	173.43	6.57
30	87.98	83.99	171.97	8.03
160	85.39	76.43	161.82	18.18

Table 2

Fusion probabilities  $P(E_i)$ , relative probabilities  $P_R(E_i)$  (normalized with  $P(160 \text{ keV}) = 1$ ), and fusion rates  $R(E_i)$ , with the incident deuteron current of  $100 \mu\text{A}$ , for incident deuteron LAB kinetic energies,  $E_i$ .  $\beta = 1$  is assumed.

$E_i$ (keV)	$P(E_i)$	$P_R(E_i)$	$R(E_i)$ (sec $^{-1}$ )
1	$0.47 \times 10^{-25}$	$1.76 \times 10^{-18}$	$2.96 \times 10^{-11}$
2	$2.10 \times 10^{-20}$	$0.78 \times 10^{-12}$	$1.31 \times 10^{-5}$
3	$0.66 \times 10^{-17}$	$2.47 \times 10^{-10}$	$0.42 \times 10^{-2}$
5	$2.15 \times 10^{-15}$	$0.80 \times 10^{-7}$	1.34
10	$0.72 \times 10^{-12}$	$2.68 \times 10^{-5}$	$0.45 \times 10^3$
20	$0.44 \times 10^{-10}$	$1.63 \times 10^{-3}$	$2.74 \times 10^4$
30	$2.72 \times 10^{-10}$	$1.01 \times 10^{-2}$	$1.70 \times 10^5$
160	$2.69 \times 10^{-8}$	1.0	$1.68 \times 10^7$

## SEARCHING FOR TRUTH WITH HIGH EXPECTATIONS

—5 Year Studies on Cold Fusion in China —

Li, Xing Zhong  
Department of Physics, Tsinghua University  
Beijing 100084, CHINA

### **Abstract**

The "cold fusion" research in China is reviewed for the past five years. Emphasis is focused on the attempt to set up the Chinese based reproducible experiments and the study on the key parameter which is supposed to control the reproducibility. Theoretical effort in understanding these phenomena is described as well.

### **Introduction**

The situation of "cold fusion" in China is similar to that in Russia. Since communication was somehow delayed, we started the "cold fusion" research based on our own understanding and the resources available to us<sup>1-14</sup>.

After 5 years of studies on "Cold Fusion", more people in China think that there must be some thing behind, and it is worthwhile to seek the truth for the fundamental physics, and for the possible future energy.

Research in China has been conducted in both theory and experiments with more emphasis on experiments. The experiments are in two categories: (1) Attempt to set up a Chinese based experiment; (2) Study the key parameters which might control the reproducibility of the experiments.

We have three efforts to set up the Chinese based experiments: (1) The electrical discharge in deuterium gas with palladium electrode; (2) Gas loading experiments with detectors to search the precursor and the energy carrier for the anomalous phenomena in D/Pd systems; (3) Excess heat measurements in D/Pd and D/Ti systems.

Based on international academic exchange, the loading ratio of deuterium in palladium was selected as a key parameter to study. We designed several systems to study the various treatments which might affect the terminal loading ratio and the loading speed. Some factors have been identified which may enhance the loading ratio to pass the resistance peak, and over the threshold (i.e. D/Pd~0.84).

Theory is important, although it is still in a immature stage. Wherever the experiments continued in the 5 hard years, there must be a plausible "theory" to stimulate the investigators. The penetration of Coulomb barrier is a persistent subject in 5 years. Bohm's theory has been developed in three aspects: (1) The direction of WKB connection formula, which has been a controversy for more than twenty years; (2) The simplified formalism for WKB method which is particularly useful for a chain of potential barriers and wells; (3) The new explanation of the penetration of potential

barrier in quantum mechanics. The recent calculation shows that the split of the Coulomb barrier may be necessary, and some experiments has been suggested to test this idea.

We have started three new sets of experiments:

- (1) The electrolysis of pressurized heavy water to study the "excess heat" in high temperature condition, based on our experience with pressurized light water fission reactors.
- (2) The enhancement of spontaneous fission in uranium due to the hydrogen loading.
- (3) The positron annihilation studies of the surface layer of the palladium sheet during the hydrogen loading.

### Electrical Discharge in Deuterium Gas

Five years ago, when the Fax copies from the US were disseminated in China, a lot of experiments were tried to reproduce the electrolysis or the gas-loading results. Some of the Chinese scientists decided to do something else.<sup>1-4</sup> The electrical discharge in a deuterium gas tube was one of these pioneer works. Xiong<sup>1</sup> et al. at the Southwestern Institute of Nuclear Physics and Chemistry reported the first observation of neutron bursts in an electrical discharge tube with a palladium cathode and a tungsten anode. The neutron yield was  $\sim 10^6$  per burst. It was too high to convince enough people to continue this experiment in that Lab. However, an elder scientist (Long, H.Q.<sup>3,4</sup>) at the Sichuan Institute of Material Technology continued this electrical discharge experiment under a difficult condition. After three years of silent research, it was found that the "anomalous neutron emission" was reproducible as long as three prerequisites were satisfied i.e. (1) a thin film of palladium was formed on the surface of discharge bulb; (2) the deuterium gas was flowing through the discharge bulb at a low pressure(5~17 Pa.); (3) the A.C. voltage between two electrodes was in certain range (6000~17000 V.). The neutron emission was reproducible and verified by an activation method which was free of electromagnetic disturbance, and there was no neutron emission in the control run with hydrogen or helium gas. The neutron emission was considered "anomalous" because an unexpected peak was observed in the neutron energy spectrum. The ordinary D-D neutrons were supposed to peak at 2.45 MeV; however, a high energy component appeared with energy greater than 5 MeV. A careful study on this anomalous neutron emission revealed that this "neutron peak" was indeed caused by the overlap of intensive X-ray radiation.<sup>5,6</sup> However, it is still a puzzle why the low energy radiation is so intensive at this discharge condition? Scientists at the Institute of High Energy Physics<sup>7</sup> were stimulated by this puzzle to redo their early experiment. In 1989, they detected an anomalous low energy radiation with no neutron emission. They stopped their experiment, because four years ago the overwhelming point of view was that neutron emission was the necessary feature of anomalous phenomena. Now more people believe that the neutron is not necessary, but the energy carrier must exist somehow to explain the excess heat. So they returned to their early data again. They have found that in fact there were several peaks in the low energy radiation ( $< 900$  keV). These peaks corresponded to the characteristic lines of spectrum for electrodes: a peak at  $425 \pm 40$  keV which corresponds to the nuclear de-excitation process:  $^{108}\text{Pd}^* \rightarrow ^{108}\text{Pd} +$

$\gamma$  ( $E_\gamma=425$  keV), and a peak at  $870\pm50$  keV which corresponds to  $^{56}\text{Fe}^* \rightarrow ^{56}\text{Fe} + \gamma$  ( $E_\gamma=854$  keV). The electrical voltage between the electrodes of the discharge tube was 10 kV, which was too low to excite the nuclides for  $\gamma$ -ray emission. There should be some energetic charged particles with several MeV. So this was an indication of nuclear reaction products. The A.C. voltage was in a pulse shape, and the instruments for detection of neutron and  $\gamma$ -ray were set to work only in the intermission period when the pulse was over; hence, it was supposed that there was no electromagnetic disturbance. One might suspect that some induced high voltage could accelerate the deuterons to produce the ordinary D-D fusion reactions, but the neutron detector did not register any neutrons above the background level. Hence it is suggested that there were two stages of reactions: the first stage was the anomalous D+D reaction which produced only proton (3MeV) and tritium without the neutron branches; the second stage was the Coulomb excitation induced by 3 MeV protons. Then the de-excitation gave the characteristic gamma ray. Calculations shows that the gamma yields is about  $10^{-6}$  per 3 MeV proton absorbed in palladium, and this result can be probably explained by the decay of excited Pd\* and Fe\*. Since tungsten electrode was used also, there should be a de-excitation process:  $^{184}\text{W}^* \rightarrow ^{184}\text{W} + \gamma$  ( $E_\gamma=110$  keV). If the low energy spectrum could get rid of the noise, one should have seen the 110 keV gamma-ray as well. Recently an unexpected peak has been seen around 130 keV, which could not be attributed to any Coulomb excitation process. Fortunately, Professor Hagelstein is just looking for a peak around 129.5 keV to explain his neutron transfer reaction.

### Gas Loading Experiment

Another early experiment in China was to identify the precursor and the energy carrier for the anomalous nuclear phenomena<sup>8,9</sup>. We proposed that the necessary product of any nuclear process is the energetic charged particle; the neutron is not a necessary product for any nuclear process. The CR-39 plastic track detector was used in a "freeze and thaw cycle" of D/Pd system to detect the energetic charged particles. The CR-39 detector is particularly suitable for this process, because it can be sealed in a high pressure container with direct contact to the palladium surface and is free of any electronic noise. It has the highest sensitivity among all the detectors available to us. It is possible to avoid any cosmic interference by the pre-etching method, and the air-born radiation background can be deduced by control run with hydrogen. We saw the energetic charged particle in the early experiments with the Russian palladium imported in early 60's. However the signal was greatly reduced in the later experiments using other palladium samples or the titanium samples.

In order to reproduce the early experiments, a systematic study<sup>10,11</sup> on the loading ratio (D/Pd) in gas loading experiments was started in 1991 after the visit to Stanford Research Institute. It is clear that the reproducibility depends on the loading process. The annealing in the vacuum, and the multiple-step loading have been identified as two important factors which may affect the terminal loading ratio. Table 1 and Table 2 in Ref. 11 summarize the gas-loading experiments with palladium in hydrogen and in

deuterium. It is possible to reach the loading ratio of D/Pd >0.84 by annealing in the vacuum, and multiple-step loading under 30 atm.

### Excess Heat Experiments

Calorimetric experimentation is difficult and requires more funds and time, so it is done in only a few laboratories in China. The Institute of Chemistry, Academy of Science, keeps a small group using microcalorimetry<sup>12</sup>; and the Institute of Atomic and Molecular Science at High Temperature and High Pressure, Chengdu University of Science and Technology keeps doing electrolysis of heavy water with titanium cathode and platinum anode<sup>13</sup>. They measured the temperature inside the Ti-rod, and observed the extraordinary ascent of temperature five times among seven experiments. Although the explanation of extraordinary ascent of temperature is unclear yet, they found that if a mixture of H<sub>2</sub>O and D<sub>2</sub>O was used as the electrolyte, then no extraordinary ascent of temperature was observed. The extraordinary ascent of temperature was about 1.5~24 °C dependent on the size of the Ti-rod. The SIMS (secondary ion mass spectrum) analysis showed strangely that the Ti-rod sample above the water level absorbed much more hydrogen than deuterium if there was some H<sub>2</sub>O in the electrolyte. However, the Ti-rod sample beneath the water level absorbed both deuterium and hydrogen. The hardness and the metallurgical structure of the Ti-rod were monitored before and after electrolysis.

### Theory — Precursor and Energy Carrier

It is too early to extract any definite theoretical model from these experiments. However, it is essential to have some kind of "plausible" theory to stimulate the effort in experiments. Five years ago when the neutron was taken as the characteristic symbol of the anomaly in D/Pd systems, we proposed that the energetic charged particles might be the necessary signal for any anomalous nuclear reaction. This idea led to a series of studies using CR-39 (plastic track detector). When the sporadic bursts made the experiment unpredictable, we suggested that there had to be some precursors before the anomaly appeared. This idea led to careful studies about the electromagnetic radiation using thermal luminescence detectors.<sup>8,9</sup> When international academic exchange revealed that the excess heat might not be accompanied with nuclear signals, or the amount of excess heat might not be compatible with the weak nuclear signal, we considered that a two-step model<sup>14</sup> might be necessary to reconcile the two facts: (1) More experiments confirmed that there was some excess heat in the closed system<sup>15</sup>, and in the open system<sup>16</sup>; (2) The nuclear signals (helium-4<sup>17</sup> or tritium<sup>18</sup>) seemed always very weak, and were compatible only with low level energy release. The two-step model requires a strong electron screening effect to reduce the Coulomb barrier and release enough energy to explain the experiments. Although it is still premature to imagine some theoretical model for this kind of screening, it is possible to deduce some corollaries from this two-step model, which can be tested by experiment. For example, the screening means a region of high electron density which may be detected by positron annihilation technique; the penetration of the Coulomb barrier by resonance tunneling must help both the fusion and fission, which might affect the spontaneous fission of the fissile elements. Both of these experiments are currently under way in

China. We have to identify what are the precursors, and what are the energy carriers in this D/Pd system.

The another aspect of theoretical work is just to develop the theory itself to make it compatible with the needs in explaining the experiments. For example, the WKB method is commonly used in quantum mechanics for calculating barrier penetration. However, the resonance tunneling needs special attention to the direction of the arrow of the WKB connection formula. Even in Bohm's discussion of resonance tunneling, the problem of the direction of the arrow is barely mentioned. The famous Russian theoretical physicist L.D.Landau said quite differently in the 1960's and 1980's<sup>19</sup>. This is still controversial in the textbooks on quantum mechanics today. We investigate this problem, and find that the existing WKB connection formula can be used only in one direction. In order to use the WKB connection formula in resonance tunneling, it should be modified to include some additional parameters. However, the conclusion is that the resonance tunneling is still possible with a little correction. On the other hand, the physical explanation of resonance tunneling is still an open question. Usually, it is explained by a steady state calculation; however, it is essentially a non-steady state phenomenon. A careful study is necessary through both theory and experiments<sup>20</sup>.

Another example is the uncertainty principle. If the electron cloud shrinks to form a strong screening effect, an energy level lower than usual ground level is always assumed. The Mills model<sup>21</sup> or the solutions of the relativistic Schrodinger equation and Dirac equation<sup>22</sup> are invoked to find this energy level, but the uncertainty principle is not compatible with it. A multiple body problem in the crystal lattice should be investigated.

### Concluding Remarks

After five years of searching with high expectations, we are still working very hard. As long as the experiments are getting stronger in confirmation, we will keep searching for the truth.

### Acknowledgments

This work is supported by the State Commission of Science and Technology and the Natural Science Foundation in China. The author would like to thank the Hawaii Natural Energy Institute at the University of Hawaii - Manoa for partial support of his sabbatical.

### References

1. R. H. Xiong, et al. "Anomalous Neutron Emission from the Discharge Tube with Palladium Electrode and Deuterium Gas," presented at the Symposium on Cold Fusion in China, Beijing, CHINA, (May, 1990).
2. S. Y. Duan, et al. "Fusion Neutron Emission Induced by Injection of Deuterium into Titanium Target in a Mirror Plasma." in *The Science of Cold Fusion*, Edited by T. Bressani, et al., Italian Physical Society, Bologna, pp. 139-143 (1991).

3. H. Q. Long, et al. "The Anomalous Nuclear Effects Induced by the Dynamic Pressure Gas Discharge in a Deuterium/Palladium System." in *Frontiers of Cold Fusion*, Edited by H. Ikegami, Universal Academy Press, Tokyo ,1993, pp.455-459.
4. H. Q. Long, et al. "Anomalous Effects in Deuterium/Metal Systems." in *Frontiers of Cold Fusion*, Edited by H. Ikegami, Universal Academy Press, Tokyo ,1993, pp.447-454.
5. H. Q. Long, et al. "New Experiment Results of Anomalous Nuclear Effects in Deuterium/Metal Systems." presented on ICCF4 at Maui, Dec.6-9, 1993.
6. Z.Q.Ma, X.Z.Li, et al. "The Analysis of the Neutron Emission from the Glow Discharge in Deuterium Gas Tube," presented on ICCF4 at Maui, Dec.6-9, 1993.
7. J.T.He, et al., "A Study on Anomalous Nuclear Fusion Reaction by Using HV Pulse Discharge," presented on ICCF4 at Maui, Dec.6-9, 1993.
8. X. Z. Li, et al. "The Precursor of 'Cold Fusion' Phenomenon in Deuterium/Solid Systems." in *Anomalous Nuclear Effects in Deuterium/Solid Systems*. AIP Conference Proceedings 228, Edited by S. E. Jones, 1991, pp. 419-429.
9. S.Y.Dong, X.Z.Li, et al., "Precursors to 'Cold Fusion' Phenomenon and the Detection of Energetic Charged Particles in Deuterium/Solid System," *Fusion Technology*, 20,330 (1991).
10. D. W. Mo, X.Z.Li, et al. "Real Time Measurements of the Energetic Charged Particles and the Loading Ratio (D/Pd)" in *Frontiers of Cold Fusion*, Edited by H. Ikegami, Universal Academy Press, Tokyo, 1993, pp. 535-538.
11. G.S.Huang, X.Z.Li, et al., "The Measurements and the Control of the Loading Ratio of Deuterium in Palladium," presented on ICCF4 at Maui, Dec.6-9, 1993..
12. Z.L.Zhang, et al., "Calorimetric Measurements of the Electrolysis of Heavy Water at Palladium Cathode," presented on ICCF4 at Maui, Dec.6-9, 1993.
13. Q.F.Zhang, et al., "The Excess Heat Experiments on Cold Fusion in Titanium Lattice," presented on ICCF4 at Maui, Dec.6-9, 1993.
14. X.Z.Li, et al., "The 3-Dimensional Resonance Tunneling in Chemically Assisted Nuclear Fission and Fusion Reactions," presented on ICCF4 at Maui, Dec.6-9, 1993.
15. M.C.H. McKubre, et al. "Excess Power Observations in Electrochemical Studies of the D/Pd System; the Influence of Loading." in *Frontiers of Cold Fusion*, Edited by H. Ikegami, Universal Academy Press, Tokyo ,1993, pp.5-19.
16. M. Fleischmann and S. Pons. "Calorimetry of the Pd-D<sub>2</sub>O System: from Simplicity via Complications to Simplicity." *Physics Letters*, A, Vol. 176, p.118 (1993).
17. M.H.Miles and B.F.Bush, "Heat and Helium Measurements in Deuterated Palladium," presented on ICCF4 at Maui, Dec.6-9, 1993.
18. F.G.Will, K.Cedzynska, et al., "Tritium Generation in Palladium Cathodes with High Deuterium Loading during Heavy Water Electrolysis," presented on ICCF4 at Maui, Dec.6-9, 1993.
19. L. D. Landau, and E. M. Lifshitz. *Quantum Mechanics*. 2-nd editions, Pergamon, Oxford, Addison-Wesley, 1965, pp.15-17.
20. D. K. Roy, *Quantum Mechanical Tunnelling and Its Applications*. Singapore, World Scientific, 1986, pp.1-79.
21. R.L.Mills, et al., "DiHydrino Molecule Identification," private communication (1993).
22. J.A.Maly, et al., "Electron Transitions on Deep Dirac Levels I," *Fusion Technology*, 24, 307 (1993).

# **COLD NUCLEAR FUSION & ENHANCED ENERGY DEVICES: A PROGRESS REPORT**

Hal Fox,  
Editor-in-Chief, *Fusion Facts*; Editor, *New Energy News*  
President, Fusion Information Center, Inc.  
P.O. Box 58639  
Salt Lake City, UT 84158

## **ABSTRACT**

After four and one-half years of reporting on cold fusion and other enhanced energy devices, a bibliography of over 1500 entries has been compiled from papers gathered and reviewed from over 30 countries. This paper presents a summary progress report with an emphasis on demonstrated devices having commercial potential. An enhanced energy device that has the potential to produce 300% excess energy is defined as having commercial potential. Classes of cold fusion devices that qualify include (1) the Pons-Fleischmann palladium/lithium/heavy water system; (2) the Mills-Bush-Eagleton nickel/alkali-metal carbonate systems; (3) the Karabut-Kucherov-Savvatimova palladium/deuterium gas plasma system; (4) the Liaw-Liebert molten-salt system; and probably (5) Kaliev/Baraboshkin/Samgin bronze-crystal deuterium device; and (6) capillary fusion devices. Since March, 1989, the time of the Pons-Fleischmann first public announcement of cold fusion, there has been discovered a rich and diverse number of phenomena that produce nuclear reactions. Although these phenomena had been considered impossible but have been experimentally demonstrated and replicated by serious scientists, the result has been an increase in the study of other enhanced energy devices. Examples are DePalma-type N-machines such as (1) the Tewari Motor-generator and (2) the Inomata N-machine. There are claims, as yet not accepted in peer-reviewed literature, of substantial excess power produced by other magnetic and solid-state devices, for example (1) the J.J.Searl "Searl Effect Generator"; (2) the Methernitha TESTATIKA machine; (3) the Orlowski-Johnson Magnatron Motor; and (4) The QRM machine. Other excess energy devices include the Shoulders patented high-density charge cluster device which has been shown to produce more than 30 times excess power. There is evidence that some of these enhanced-energy phenomena have been a part of some of the experimental findings in cold fusion experiments. Some such evidence is presented and sources cited.

## **A. INTRODUCTION**

The task of collecting, reading, reviewing, and publishing information about the new science of cold nuclear fusion has been a rewarding multi-disciplinary educational

experience. The greatest reward has been the privilege of becoming friends with a large number of dedicated scientists and engineers who have risked their reputations to continue their investigation of the new science of cold nuclear fusion. Chief among these scientists are Dr. Martin Fleischmann and Dr. Stanley Pons whose once-in-a-lifetime discovery of cold nuclear fusion has been replicated in over 30 countries and, under their scientific direction, is approaching commercialization.

This paper evaluates the commercial potential of the heavy water-palladium-lithium system of Pons and Fleischmann. In addition, several other devices are evaluated; all of which have their innovative experimental roots in the March 23, 1989, announcement by Pons and Fleischmann. The orchestrated perennial attackers of cold fusion have vented their criticism on the heavy-water cold fusion cells and have neglected the innovative products engendered by the initial Pons-Fleischmann discovery. Several researchers who accepted the validity of the announcement of cold fusion in the D<sub>2</sub>O-Pd-Li electrochemical cells have invented or visualized additional experimental efforts. Among those who have been the most successful in not only predicting but proving that anomalous reactions can take place in or on the surface of condensed matter (especially palladium, titanium, and nickel) are Randell Mills, Robert Bush, and Robert Eagleton (light water); Bor Yann Liaw and Bruce Liebert (molten salts); Kucherov, Karabut, and Savvatimova (gas plasma); Kaliev, Baraboshkin, and Samgin (tungsten-bronze crystals); Peter and Neal Graneau, J-P Vigier, and M. Rambaut (capillary cold fusion); and Yamaguchi (gold-plated Pd sandwich). Several of these devices appear to have future commercial potential.

In addition to the new technology of heavy-water cold fusion (**controversial**) and light-water cold nuclear fusion (**more controversial**), there are other new science applications such as tapping the energy of space (**much more controversial**) which are described and evaluated in this paper. Some of these devices have been proposed, experimentally verified, and remain unaccepted by the **standard science community**. The biggest problem is that papers describing these devices have failed to pass the peer review procedures. **This peer review problem engenders the following question: If new science has been discovered, who are the peers?** Here is an example: Kenneth Shoulders has an impeccable reputation as one of this country's foremost inventors. He invents but he does not spend time writing technical articles. His most recent achievements have been a series of five patents totaling some 40 embodiments and over 200 claims that have laid the groundwork for an entire new high-speed electronic industry. One of his patents states that over 30 times as much energy has been produced from a high-density charge cluster than required to generate the charge cluster. The patent states, "In any event, energy is provided to the traveling wave output conductor, and the ultimate source of this energy appears to be the zero-point radiation of the vacuum continuum." Ken Shoulders has only few peers, such as Dr. Hal Puthoff, who have the direct experience to evaluate this phenomena. What journal is going to publish articles on "tapping the energy of the vacuum continuum"? If an article is written, where will the journal find peers to review the article? **As amply evidenced by the actions of the Department of Energy in its treatment of cold fusion, the peer-review system fails where new science is involved!**

Today's engineered products would be considered impossible by the science of even one decade ago. Not a month passes without a peer-reviewed article in a scientific journal that provides new facts that contradict the currently acceptable models and theories. Two of the most cherished scientific beliefs of the past decade are (1) the concept that nuclear fusion can only occur with sun-like temperatures and (2) the concept of the emptiness of space. The first concept has been refuted by over 1,000 scientific papers that report on cold nuclear reactions in a rich variety of experimental devices. The second concept is being seriously questioned as there have been over 300 peer-reviewed scientific papers supporting an energetic space<sup>1</sup>. Considerable experimental evidence has been generally ignored or denied.

The Department of Energy could use the following introductory information about space energy: In 1930 Albert Einstein wrote, "The strange conclusion to which we have come is this, that now it appears that space will have to be regarded as a primary thing and that matter is derived from it, so to speak, as a secondary result<sup>2</sup>." Some scientists, who are convinced that Einstein forever took away the ether, discount the energetic nature of space. Designated in the literature variously as zero-point energy, space energy, vacuum energy, ZP fields, etc., the latest peer-reviewed scientific findings demonstrate that space indeed has enormous energy<sup>3</sup> and that space energy can be tapped. The reason that most of us are unaware of the existence and magnitude of space energy is because this energy can only be sensed or measured from an accelerating frame of reference. All of the devices that have been demonstrated to tap the energy of space are characterized by rotating machines or by some highly-accelerated entity (such as Ken Shoulders high-density charge clusters.) Many anomalous discoveries have been dismissed and invention of new devices has been subverted because of the peer-reviewed acceptance that Einstein dismissed the ether and with it any possibility of obtaining energy from space. It is predicted that many scientists will abruptly dismiss the concept that space has energy and that this space energy can be commercially exploited. This paper describes some of the proven and yet-to-be-proven devices that use space energy.

## B. COLD NUCLEAR FUSION DEVICES AND COMMERCIAL POTENTIAL

A variety of anomalous phenomena have been rediscovered, remembered, or newly discovered since the announcement by Pons and Fleischmann of apparent nuclear reactions from the Pons-Fleischmann Effect (PFE). This section briefly describes some of those experimental findings, cites the literature, and speculates on the commercial potential of such devices.

### 1. Heavy-Water Electrochemical Cells

The original Pons-Fleischmann discovery involves electrochemical cells using heavy water, a palladium cathode, usually a platinum anode, and lithium in the electrolyte<sup>4</sup>. Many research groups were unable to replicate the Pons-Fleischmann effect and some became instant critics, even to the extent of accusing Pons and Fleischmann of fraud. However, positive results have been obtained by research groups in more than 25 countries in

replicating the P-F effect<sup>5</sup>. Because of the geographic location of the most active critics (mainly in Eastern U.S. and in the CERN countries of Europe) there has been little cold fusion research among the Ivy-League colleges in eastern U.S. and, except for Italy, only a few cold fusion papers from Western Europe. Several groups in Eastern Europe and Russia have helped to develop a better understanding of the cold fusion technology<sup>6</sup>. However, no group has **fully resolved** the problems associated with the preparation of the palladium metal, the loading of the palladium cathodes, and the "turning on" of the excess heat reactions. See Fig. 1.

A heavy-water cell operated at atmospheric pressure can be expected to produce low-level excess heat, whenever the palladium cathode is loaded with deuterium such that the D/Pd atomic ratio is greater than 0.85 and provided other now well-known protocols are followed. Pressurized heavy-water cells are now being designed and tested and can be expected to produce higher levels of heat. The maximum temperature at which pressurized electrochemical cells can operate is in the range of 700°F. At higher temperatures there is no definite demarkation between liquid and gas regardless of the pressure and it is believed that standard electrochemistry would not function above this critical temperature. Dr. Pons has recently announced the expected completion ("within a year") of a commercial prototype of a cold fusion cell that is expected to produce 10,000 watts or more of thermal power<sup>7</sup>. That achievement is expected to accomplish two major tasks: first to silence the critics and second to demonstrate commercial feasibility.

## 2. Light-Water Electrochemical Cells and Nuclear Transmutations

Although the Pons-Fleischmann patent applications anticipated the use of light-water (as an addition to heavy water) in cold-fusion electrochemical cells, and Matsumoto (Japan) measured nuclear byproducts using light water<sup>8</sup>, it was Randell Mills (Lancaster, Penn.) who first showed that light-water electrochemical cells using some alkali-metal carbonates could produce excess heat<sup>9</sup>. The Mills theory of the functioning of light-water electrochemical cells has not been widely accepted. A recent paper, based on solutions to Schrodinger's and Dirac's equations for hydrogen-like atoms, provides a possible solution (energy-released transitions at deep Dirac levels)<sup>10</sup>. Drs. Bush and Eagleton (Cal-Poly, Pomona, California) have extended the light-water cold-fusion experimental work and Dr. Bush has modified his Transmission Resonance Model (TRM) to explain both the heavy-water and the light-water results as being alkali-metal-hydrogen fusion<sup>11</sup>. See Fig. 2. More recently Bush and Eagleton have demonstrated that there are definite transmutations of alkali elements by fusion with hydrogen (in the light-water electrochemical experiments)<sup>12</sup> to produce elements with an added proton in the nucleus.

Experimental results from Bush and Eagleton and later several groups at BARC, Trombay, India<sup>13</sup>, Dr. Reiko Notoya at Hokkaido University<sup>14</sup>, and Ohmori and Enyo at Hokkaido University<sup>15</sup> have shown that the light-water electrochemical cells are highly reproducible; usually produce 20 to 70% and occasionally up to 300% excess heat; and function with all of the alkali metals (usually as carbonates). The cathodes used are nickel, gold, silver, and tin and range from wire and plate to porous materials (such as the porous nickel used in Nickel-Cadmium batteries.)

There has been some evidence, especially in small-scale light-water electrochemical cells, that excess heat considerably higher than 300% has already been achieved. Therefore, by definition, this technology qualifies for potential commercialization. It is expected that the newer experimental discoveries in light-water electrochemical cells will certainly lead to a better understanding of the **overcoming of the Coulomb barrier, of the basic structure of matter, and the control of nuclear reactions in/on a metal lattice**. Although many scientists lament the end of funding for the Texas superconducting super-collider (SSC), it is increasingly apparent that there are enormous opportunities of learning about the structure and interaction of matter by further study of nuclear reactions in or near metal lattices in cold fusion reactors and at a small fraction of the cost of an SSC. This is an important reason for accelerating funding for further experimental investigations into both heavy- and light-water cold fusion reactors.

### 3. Molten Salts Electrochemistry

Drs. Liaw and Liebert of the University of Hawaii invented and demonstrated the use of molten salts to provide relatively high temperatures in an electrochemical cold-fusion cell<sup>16</sup>. Their work showed that as much as 1500% excess heat could be achieved using palladium as the anode and using an eutectic mixture of salts in an aluminum container. See Fig. 3. It has been found that there are some serious materials problems to be resolved in working at these higher temperatures. The replication of this work has been difficult. Only a few other groups have replicated the Liaw-Liebert molten salt work<sup>17</sup>. However these problems are expected to be resolved and the molten salts "cold fusion" devices become an important part of future enhanced energy systems. The high level of heat achieved does mark this technology as eligible for commercialization after the materials problems are solved. The applications for molten-salts cold-fusion devices are obviously destined for systems where higher temperatures are desired or required, such as in the manufacturing and/or processing of many glasses and metals.

### 4. Gas Plasma Devices

At least one U.S. inventor has filed a patent for a gas-plasma device which is expected to produce excess heat. Some excellent work using gas-plasma devices has also been performed in Russia by Drs. Kucherov, Karabut, and Savvatimova<sup>18</sup>. Other gas plasma replication has been accomplished by Romodanov in Russia<sup>19</sup> and by scientists in the People's Republic of China<sup>20</sup>. This Kucherov et al. device uses deuterium gas at relatively low pressures and in the presence of moderately-high voltages (500 volts). See Fig. 4. It is projected that the development of this gas-plasma device will produce enhanced-energy systems that operate at high temperatures and in aerospace environments. (Neither heavy-water nor light-water electrochemical cells are deemed suitable for either high-temperature or aerospace use.) The best results that have been achieved with gas-plasma devices (over 500% excess heat) appears to make this type of cold fusion device a candidate for future commercialization.

## 5. Capillary Fusion

Some types of metal crystals can be made in which small diameter, long tubes or capillaries are created. Under appropriate conditions it has been experimentally shown that fusion of hydrogen can be achieved in this type of device. Dr. Vigier<sup>21</sup> has described the observation of capillary cold fusion in metal wires using high amperage. After initial successes, work is being continued by Baraboshkin and Samgin in Russia to investigate this approach to the development of excess heat<sup>22</sup>. The Vigier article and other articles about the role of Ampère forces in nuclear fusion<sup>23</sup> suggest that devices using the right combination of capillaries, hydrogen (or deuterium) gas and appropriate treatment with high-amperage electrical current may develop sufficient excess heat to be subject to commercialization. See Fig. 5. Recently, Peter Graneau<sup>24</sup> presented a concept for a capillary fusion reactor. Graneau believes that it will take some expert materials engineering to produce this type of reactor because of the relatively large internal forces that are expected to be produced. However, Graneau's approach is a serious proposal for a device that would lead to commercialization of capillary fusion.

## 6. The Yamaguchi Pd sandwich.

Eiichi Yamaguchi and Takahashi Nishioka<sup>25</sup> have shown that palladium plates that are gold-plated on one side (to prevent migration of deuterium) and plated with MnO on the opposite side (to slow down rate of deuterium diffusion) can produce nuclear reactions. The plates, see Fig. 6, are exposed first to a vacuum then to deuterium gas. Being again exposed to vacuum and triggered with an electrical pulse, both tritium and alpha particles ( ${}^4\text{He}$  nuclei) are produced together with considerable heat. As Yamaguchi & Nishioka reported in the third annual cold fusion conference, "We have for the first time succeeded in detecting  ${}^4\text{He}$  production *in situ* and with high reproducibility. Our *in vacuo* method gives the first definite evidence for the reality of **cold nuclear fusion** in solids.

This work has been of great importance to demonstrate the rich phenomena involved in the production of nuclear reactions in or on the surface of a metal lattice. It is not easy to predict the degree of commercialization that can be achieved by use of the Pd sandwiches, however, the reproducibility is important for studying the parameters that are involved with the production of nuclear by products.

Note: The January issues of *Fusion Facts* for the years 1990 through 1993 have honored the "Fusion Scientists of the Year" who have been Pons and Fleischmann; Liaw and Liebert; Mills, Bush, and Eagleton. and most recently, Kucherov, Karabut, and Savvatimova. Except for the Pons-Fleischmann patents-pending, which are owned by the University of Utah, and Mills, the technologies developed by these other "Fusion Scientists of the Year" have been assigned to ENECO, Inc. (formerly Fusion Energy Applied Technology, Inc.), a Utah corporation, for future development and marketing. This privately-funded corporation, after thorough investigation of the commercial potential of cold fusion, has invested in the future commercialization of this new science. It is suggested that ENECO will likely become one of the world leaders in the commercialization of cold fusion.

## C. OTHER ENHANCED ENERGY DEVICES AND COMMERCIAL POTENTIAL

### 1. The N-Machines

The author has not, as yet, mastered the three-decade history of the development of rotating machines that produce excess power (also known as over-unity machines). The basic device is the homo-polar electrical generator discovered by Michael Faraday in December, 1831. Bruce DePalma is one of the proponents and successful experimenters with machines that appear to obtain excess power by using magnets and coils rotating generator (usually driven by an electric motor.) These electrical generating machines are characterized by the following: (1) the demonstrated ability to produce more electrical power than used to rotate the machines; (2) an electrical output of low voltage but high current; (3) the dynamic characteristic that requires relatively high rotational speeds to produce over-unity power; (4) the apparent lack of increasing counter-torque on the generator shaft as high output is achieved, and (5) the requirement for relatively high magnetic field strengths<sup>26, 27, 28</sup>.

The latest articles by Bruce DePalma<sup>26</sup> have been published recently in *New Energy News*. During the past decade (or more) P. Tewari has developed N-machines with the latest experimental work being documented in both printed<sup>27</sup> and video media. His latest report and video presentations depict a machine driven by an electrical motor that is capable of rotating the generator at more than 4,000 rpm while consuming up to about one-kilowatt of input electrical power from the standard electrical mains in India. See Fig. 7. As shown in the videos and as described in his latest article<sup>27</sup>, the generator has produced more than three times as much output power as being consumed by the driving motor. The output voltage is less than three volts but with high amperage. As shown in his latest paper and confirmed with video recordings, the over-unity condition is achieved at rotational speeds of about 3,000 to 4,000 rpm.

Shiiji Inomata of the Electrotechnical Laboratory in Ibaraki, Japan has developed and tested a smaller motor/generator which has been shown to produce over-unity power output<sup>28</sup>. Recently, Inomata provided *New Energy News* with his latest design which will use superconducting magnets to increase the magnetic field strength<sup>29</sup>. Inomata has derived an equation for the voltage output of the machine showing that the output voltage is directly proportional to rpm and to magnetic strength and proportional to the square of the radius of the rotating copper disks used in his machine. His calculations, based on experimental evidence with the current model (see drawing, Fig. 8) indicates by using superconducting coils to increase the magnetic force, that the output can be increased to provide 10 kW and more from a machine with 25 cm diameter copper disk.

The biggest disadvantage of the N-machines is their low-voltage output (in the range of 1 to 40 volts). The output current can be in thousands of ampères. This combination, together with the requirement that the d.c. output must be taken off a rotating disk, places substantial demands on the development of the electrically-conducting brushes. The second problem is to transform the low-voltage, high-current output into more acceptable electrical

power. Both problems have been potentially resolved by modern engineering developments. The use of hundreds of hair-like conducting-metal fibers for the brushes and the use of modern solid-state devices for transforming low-voltage d.c. into high-voltage a.c. are the proposed solutions.

Tewari's goal is to produce a motor-generator plus transforming circuitry so that the generated power can be used to drive the electrical motor and still have excess power delivered to the output load. This demonstration will be, of course, the final proof that such a machine is transferring power from a heretofore unused energy source. That source is "space energy" or ZPE (zero-point energy). We await such demonstration with keen interest.

## 2. The Searl-Effect Generator

There have been several reports of excess power devices by experimenters who are now deceased. However, J.J. Searl is still alive and pursuing funds to get back into production with his Searl-Effect Generator. Searl is not an academically-qualified scientist, he is, however, a successful experimenter. Although Searl has built about 40 of his power-generating devices and used them in his experimental work with levitating disks (See Fig. 9), there is, at present, no known working model of his generator. His writings are not easy to understand because they are more descriptive than explanatory<sup>30</sup>. The lengthy video tape of his lectures and the pictures of the earlier construction of levitating disks is of poor quality but with some interesting historical pictures that cause the viewer to seriously consider that Searl's work may be real and promotes a desire for further engineering and scientific data on his power generator and levitating disks. One of the interesting video clips shows Searl demonstrating that his early magnets utilizing a spinning magnetic field (the video shows how a paper clip string combination would indicate magnetic spots that cause the paper clip to spin.) It is interesting to learn that Searl revealed (or demonstrated?) his work to the U.S. Air Force at Edwards Air Force base in California in about 1970. A current Air Force project is reportedly test-flying craft that appear to have similarities to Searl's work. Is this development just an historic coincidence?

## 3. The Swiss Methernitha Machine

According to Stefan Marinov<sup>31</sup>, Paul Baumann built the first working prototype of the Methernitha machine while in jail. In his book Divine Electro-Magnetism, Marinov has the following comments: "Paul Baumann is the spiritual head of the Christian religious community **METHERNITHA** in Switzerland... God has given him an amazing intellect, or something more, as according to me, the machine TESTATIKA is constructed rather by inspiration than by brain." Marinov, who has seen and tested various models of the Testatika machines reports that the small single-disk machines produce some 200 Watts of free energy. See Fig. 10. The machines with two counter-rotating disks of about 50 cm in diameter produce about 3 kW and the latest, uncompleted [as of summer 1993], larger machine (disk diameter of 2 meters) is expected to produce 30 kW. All models can be started by hand and, thereafter, produce useable power, according to the many visitors who have been allowed to observe the machines in operation. Photographs of the machine are

shown in Marinov's book<sup>31</sup>. A video of the machine in operation is in existence and was shown at the recent International Conference on New Energy (April 1993, Denver). Under Marinov's urging, the members of the Christian community Methernitha, voted on a proposal to reveal the secret of this machine to the world. The vote was 23-to-1 against doing so at this time. Obviously, no peer-reviewed technical papers about this machine are available. However, it is possible that Marinov's continuing research and development work will produce a similar "free energy" machine. Marinov's latest experimental work is described in "Important Information Added in Proof", pp 287-289 of reference<sup>31</sup>. The Siberian Coliu machine or S-machine, is designed to tap space energy. See Fig. 11. Marinov, who has been exploring the many experimental contradictions to currently taught electricity and magnetism, is one of the world's few scientists who are intellectually prepared to produce machines that tap space energy. This "intellectual preparation" includes acceptance of an energetic space. *New Energy News* will continue to report on Marinov's latest developments and intellectual reports.

#### **4. The Orlowski-Johnson Magnatron Motor**

Prior to his death, Rory Johnson invented, built, and operated various "Magnatron motors", one of which was installed in his 1974 Buick Electra. Reportedly, Johnson operated his automobile for over a year without buying any gasoline. Gerald Orlowski, as an expert in electro-magnetic motors and generators, and as an employee of Greyhound Corporation was sent to investigate the Magnatron motor. As Orlowski relates in his historical review<sup>32</sup> Johnson died after moving to California and finding that promised development funds were not available. One of the more interesting features of this machine was a "fuel cell" which reportedly used a mixture of deuterium and gallium and produced the increased magnetic power that was instrumental in making the engine a success. The use of deuterium and gallium is an interesting selection of chemicals in this cold fusion age, however, this combination was being used by Johnson before 1978. To my knowledge, no one has replicated Johnson's work although hundreds of people witnessed a working demonstration of his motor.

#### **5. Can Magnetic Machines Tap Space Energy?**

The Adams magnetic motor (See Fig. 12) and the magnetic motor development by Troy Reed have had considerable publicity but no peer-reviewed articles have been published. Both Adams and Reed are inventors without the standard Ph.D. qualifications to be called "scientists". Both have made claims for significant over-unity power production. Replication and/or further reports with suitable engineering data so that others can build and test these machines are required before serious comments on commercial potential can be projected. However, the DePalma, Tewari, and Inomata machines have been demonstrated, technical papers have been written and presented, and these machines appear to have significant commercial potential.

## D. THE SHOULDERS INVENTION AND COMMERCIAL POTENTIAL

Dr. Harold Puthoff is one of the scientists who have written extensively about space energy<sup>33</sup>. He and Kenneth Shoulders have been working in this new field of science for several years. The discovery by Kenneth Shoulders that high-density electron clusters can be produced, maintained, and controlled<sup>34</sup> has laid the groundwork for a new revolution in electronic devices. Of most importance for this paper is Shoulders' demonstration (as reported in the patent discussion, prior to the claims) that under certain conditions an EV (Shoulders' name for high-density electron clusters) can produce more than 30 times the amount of energy required to produce the EV. The drawing in Fig. 13 is taken from the patent abstract and illustrates how the EVs are created and how power is obtained. Basically, the EV is produced and launched through a tube or channel which is surrounded by a wire coil. The EV is a traveling bundle of electrons, moves at about 0.1 the speed of light, and induces a surge of electrical power in the coil. The EV is captured by the anode and provides about the same amount of energy that was required to produce the EV. The power from the coil has been measured to be more than 30 times the power required to produce the EV. (In discussions with Shoulders, he reported great difficulties in producing continuous excess power due to induced electrostatic charges caused by the energetic EVs.) Shoulders' latest innovation is expected to overcome the problems and provide for a commercial product.

In the discussion given in the patent, the statement is made (and accepted by the patent examiner) that the source of power "appears to be the zero-point radiation of the vacuum continuum." **It is believed that this is the first U.S. patent that has been granted which claims to tap the energy of space.** The important aspect of the production and use of EVs is that the charge density (in terms of charge per cubic centimeter) is extraordinarily high, perhaps similar to ball lightning or within lightning strokes. It appears that the highly-dynamic nature of the EV actually does tap the energy of space and that a traveling EV is continually giving off energy and having its internal energy restored. There will obviously be an increasing interest in creating, launching, and studying the ways by which the energy of the EV can be coupled to provide useful work in a variety of ways.

## D. PHENOMENA RELATED TO COLD FUSION

Matsumoto reported experimental results in cold fusion<sup>35</sup> that Fox suggested were the results of the production of high-density charge clusters. Fox's letter and Matsumoto's kindly rejection of Fox's suggestions have been published.<sup>36</sup>

EVs or high-density charge clusters can be produced within a variety of dielectrics including low-pressure gases and liquids if the bulk resistance is moderately high. The production of EVs within a palladium deuteride has not been confirmed. However, there have been several photographs shown at various cold fusion meetings (Los Alamos in May 1989 by Sandia, and at Como, Italy in July 1991 by Oak Ridge) where holes about the size of EVs (about 20 microns in diameter) have been photographed and displayed.

Any environment that produces sparks may also produce EVs. The dissolution of an EV (usually when it impacts a metal surface) produces a burst of electromagnetic energy that can be picked up on a transistor radio. Of course one should tune the radio off of any station so that the automatic volume control feature provides maximum amplification. By placing the radio near a reactor, one can easily learn something about the nature of the cell. Please note that most cells are not operated at voltage levels at which sparks may be produced. However, the fracturing of a Pd solid may produce sufficient voltage to cause EVs to be generated.

The production of heat in a cold fusion cell can be influenced by a change in the magnetic field strength in the vicinity of the cell as shown by Cravens.<sup>37</sup> Others have shown that the nuclear reactions (or excess heat) in cold fusion reactors can be influenced by certain electromagnetic frequencies, and even by sonoluminescence.

The discovery of a variety of phenomena associated with the discovery and enhancement of cold fusion is now well publicized. It is to be expected that such diverse phenomena will be found to be influenced by a wide-range of environmental conditions. As these various phenomena are studied and measured, it is suggested that they be included in brief reports (such as could be published in *Fusion Facts* so that theorists can have more data on which to evaluate their work.)

#### **E. PREDICTED TIME AND COST TO COMMERCIAL USE**

The following table lists selected devices that, in my opinion, can be expected to provide commercial devices. My previous forecasts for the commercialization of cold fusion have been overly optimistic. The following table is based on tempered optimism, and to the extent possible, includes inputs from some of the leading researchers for the device listed. Note that an attempt has been made to list the devices in order of their expected appearance on the commercial market. Some new technologies have been identified (but not necessarily from peer-reviewed literature) and some estimates of commercial timing have been included. This list includes some speculations on the development of both room-temperature superconductivity and super batteries. Both of these developments have been demonstrated, one in Russia and the other in Ukraine. In all cases, the forecasts for commercialization are based on the concept that funding will be made available in the near future in the amounts indicated.

TABLE I. ENHANCED ENERGY DEVICES HAVING COMMERCIAL POTENTIAL

System or Device	Energy Output	Percent-Exc. Power	Year to be Commercial	Fund Needs in Millions of \$
PFE Cell	10 - 20 kW	500	1994	\$ 5
Charge Clusters	1 kW	1,000	1994	\$ 1
Lt.Water CF	1 - 10 kW	300	1995	\$ 2
N-Machine	10 - 80 kW	300	1994	\$ 1
Glow-Discharge	1 - 10 kW	500	1997	\$ 5
Molten Salts	1 - 50 kW	1,000	1997	\$ 7
Capillary	1 - 10 kW	300	1998	\$ 3
<b>Associated New Technologies</b>				
Hi-Efficiency Motors/Generators			1994	\$ 1
Room Temp. Superconductivity			1995	\$ 2
Hi-Efficiency Thermal/Electric Conversion			1995	\$ 2
Super Battery Technology			1996	\$ 3 to \$ 5
Commercial Elemental Transmutation and Reduction of Radioactivity.			1997	\$ 5 to \$ 10

Note: All estimates based on discussions with R&D personnel working on various devices shown. All devices listed are based on laboratory experiments. No inventions are scheduled. Costs and times are estimated by Hal Fox from data available up to November 1993.

#### Suggestions to Cold Fusion Skeptics

The cold fusion skeptics have persistently attacked the reality of excess heat in the Pd/D<sub>2</sub>O/Li reactors. This author strongly suggests that the skeptics expand their attacks to include a much wider range of so-called cold fusion phenomena. The experimental evidence now is so pervasive (both geographically and among various research disciplines) that it is now up to the skeptic to explain the nature of the phenomena being reported. There is not now (and probably never was) any substantial evidence for "pathological science", "spiking the experiments", or other attempts to discredit researchers in cold fusion. A confirmed skeptic needs to marshall sufficient scientific evidence that explains the observed, oft repeated, phenomena in the literature of over 1500 articles and papers. **Derision, personal opinions, or appeal to old science is no longer sufficient to convince the cold fusion scientific community that no new science has been discovered.**

The intransigence and fierce denial of new discoveries by many so-called scientists is neither new nor honorable nor is the hasty and unqualified denial of new experimental evidence. New science should create skepticism, and should be followed by intelligent questioning and scholarly replication among interested peers. Emotion-laden arguments in defense of truth are expected, however, scientists should welcome new discoveries and new anomalies and should not attack the personal integrity of the discoverer. Pons and Fleischmann are not the first scientists to be driven from seats of learning to continue their research in other lands. If such as they could be induced to abandon their factual discoveries, regardless of the difficulties with replication, they would not merit the title of scientists. Those who deny new discoveries, such as cold fusion, for reasons of professional territory, fear of loss of grants, or loss of prestige, retard the progress of science and inhibit the spread of new knowledge. **The surest way to lose scientific prestige is to deny new science and then be proven wrong.** Puthoff<sup>33</sup> quotes Podny as saying: "It would be just as presumptuous to deny the feasibility of useful application [of space energy] as it would be irresponsible to guarantee such application."

## REFERENCES

1. Moray B. King, Tapping the Zero-Point Energy, c1989, Paraclete Publishing, P.O. Box 859, Provo, UT 84603.
2. Rolf Schaffranke, "Ether Research: Frontier Perspective in an Age of Revelation," *New Energy News*, Vol 1, No 7, November 1993, pg 9.
3. Daniel C. Cole & Harold E. Puthoff, "Extracting energy and heat from the vacuum," *Physical Review E*, Vol 48, No 2, Aug 1993, pp 1562-1565, 2 figs, 9 refs.
4. Martin Fleischmann, Stanley Pons, and M. Hawkins, "Electrochemically Induced Nuclear Fusion of Deuterium," *J. Electroanal. Chem.* 1989, 261, pp 301-308, and erratum, 263, p187.
5. Hal Fox, Cold Fusion Impact in the Enhanced Energy Age, published by Fusion Information Center: Salt Lake City, UT, 1993, see enclosed bibliography diskette, also available in Russian.
6. Vladimir Tsarev (Lebedev Physical Inst.), "Cold Fusion Researches in Russia," in Frontiers of Cold Fusion. Proceedings of the Third International Conference on Cold Fusion, H. Ikegami, Ed., pp 341-351, 30 refs, c1993, Universal Academy Press, Tokyo.
7. Robin Christmas & Jerry Thompson, The Secret Life of Cold Fusion, a 27-minute video published by Canadian Broadcasting Corporation. aired on CBC Prime Time News, June 24, 1993.

8. T. Matsumoto, "Cold Fusion Observed with Ordinary Water," *Fusion Technology*, May 1990, vol 17, no 3, pp 490-492, 3 figs, 4 refs.
9. Randell L. Mills and Steven P. Kneizys, "Excess Heat Production by the Electrolysis of an Aqueous Potassium Carbonate Electrolyte and the Implications for Cold Fusion", *Fusion Technology*, vol. 20, Aug 1991, pp 65-81, 10 refs, 9 figs, 2 tables.
10. Jaromir A. Maly & Jaroslav Vavra, "Electron Transitions on Deep Dirac Levels 1," *Fusion Technology*, Vol 24, No 3, Nov 1993, 3 tables, 17 refs.
11. Robert T. Bush, "Cold Fusion with Light Water," *Fusion Facts*, December 1991, p 1-2. See also Robert T. Bush, "A Light Water Excess Heat Reaction Suggests that 'Cold Fusion' may be 'Alkali-Hydrogen Fusion,'" *Fusion Technology*, vol 22, Sept 1992, pp 301-322, 61 refs, 2 figs.
12. Robert T. Bush (Cal Poly, Pomona, California), "Towards a Solid State Nuclear Physics: The LANT Model (Lattice-Assisted Nuclear Transmutation) for Cold Nucleosynthesis," *Fusion Technology*, 1993, accepted for publication. See also Peter Glück, "Nuclear Catalysis & Cold Fusion - The SURFDYN Model," *Fusion Facts*, June 1992, pp 1-3, also *Fusion Technology*, vol. 24, no. 2, pp 122-126, 44 refs.
13. M. Srinivasan, A. Shyam, T.K. Shankarnarayanan, M.B. Bajpai, H. Ramamurthy, U.K. Mukherjee, M.S. Krishnan, M.G. Nayar and Y. Naik (Bhabha Atomic Research Centre, Bombay, India), "Tritium and Excess Heat Generation During Electrolysis of Aqueous Solutions of Alkali Salts with Nickel Cathode," Presented at the Third International Conference on Cold Fusion, October 21-25, 1992, Nagoya, Japan.
14. Reiko Notoya (Hokkaido Univ.), "Cold Fusion by Electrolysis in a Light Water - Potassium Carbonate Solution with a Nickel Electrode," *Fusion Technology*, vol 24, no 2, Sept 93, 4 figs, 5 refs.
15. Tadayoshi Ohmori & Michio Enyo (Hokkaido University, Catalysis Research Ctr., Kitaku, Sapporo), "Excess Heat Evolution During Electrolysis of H<sub>2</sub>O with Nickel, Gold, Silver, and Tin Cathodes," *Fusion Technology*, vol 24, no 3, pp 293-295, 9 refs, 2 figs, 4 tables.
16. Bor Yann Liaw, Peng-Long Tao, and Bruce E. Liebert\* (Hawaii Natural Energy Institute, and \*Department of Mechanical Engineering, University of Hawaii), "Recent Progress on Cold Fusion Research Using Molten Salt Techniques," Presented at Second Annual Conference on Cold Fusion, June 29-July 4, 1991, Como, Italy.
17. L.J. Yuan, C.W. Wan, C.Y. Liang and K.S. Chen (National Tsing Hua Univ.), "Neutron Monitoring on Cold Fusion Experiments." in Frontiers of Cold Fusion. Proceedings of the Third International Conference on Cold Fusion. H. Ikegami, Ed., pp 461-464, 5 figs, 2 refs, c1993, Universal Academy Press, Tokyo.

18. A.B. Karabut, Ya. R. Kucherov and I.B. Savvatimova, "Nuclear Product Ratio for Glow Discharge in Deuterium," *Phys. Lett. A*, 1992, 170, pp 265-272.
19. Romodanov, Savin, Skuratnik, & Elksnin, "Reproducibility of Tritium Generation from Nuclear Reactions in Condensed Media," paper presented at the Fourth International Conference on Cold Fusion, Hawaii, Dec. 9, 1993.
20. Xing Zhong Li (Tsinghua Univ. Beijing, China), Personal communication.
21. Jean-Pierre Vigier (Univ. P. and M. Curie, Paris), "New Hydrogen Energies in Specially Structured Dense Media: Capillary Chemistry and Capillary Fusion," Preprint courtesy of the author, to be published in *Phys. Lett. A*.
22. K.A. Kaliev, A.N. Baraboshkin, A.L. Samgin, "Reproducible Nuclear Reactions During Interaction of Deuterium with Oxide Tungsten Bronze," *Phys. Lett. A*, 1993, vol 172, p 199.
23. Peter Graneau (Centre for Electromagnetic Research, Northeastern Univ. Boston, MA), "The Role of Ampère Forces in Nuclear Fusion," *Physics Letters A*, vol 165, 1992, pp 1-13, 10 figs, 29 refs.
24. Peter Graneau, "Concept of a Capillary Fusion Reactor," in *Proceedings of the International Symposium on New Energy*, April 16-18, 1993, Denver, Colorado, pp 153-168, 2 figs, 11 refs.
25. Eiichi Yamaguchi & Takahashi Nishioka, "Direct Evidence for Nuclear Fusion Reactions in Deuterated Palladium," in Frontiers of Cold Fusion, Proceedings of the Third International Conference on Cold Fusion, pp 179-188, 5 figs, 12 refs.
26. Bruce DePalma, "Where Electrical Science Went Wrong," *New Energy News*, vol. 1, no. 5, Sept. 1993, pp 1-4, 5 figs, 3 refs. Also, "On the Nature of Electrical Induction", *New Energy News*, vol 1, no 6, pp 2-8, 5 figs, 14 refs.
27. Paramahansa Tewari, "Generation of Cosmic Energy and Matter from Absolute Space (Vacuum)," *Proceedings of International Symposium on New Energy*, Maury Albertson, Ed., Denver, Colorado, April 16-18, 1993, pp 291-303, 6 figs, 8 refs.
28. Shuji Inomata & Yoshiyuki Mita, "Small Neodymium Magnet Twin N-Machine," *Proceedings of 28th Intersociety Energy Conversion Engineering Conference*, August 8-13, 1993, Atlanta, Georgia, pp 2.347-2.352, 11 figs, 2 refs.
29. Shuji Inomata, "Letter from Shuji Inomata with Conceptual Design of JPI-II Test Machine," *New Energy News*. vol 1, no 7, pp 7-8. 2 tables, 3 figs.

30. John A. Thomas, Jr., Antigravity: The Dream Made Reality, the Story of John R.R. Searl, compiled and published by John A. Thomas, Jr., 373 Rockwell Rd., Rochester, NY 14617-1316, 100 pages of text plus 36 pages of figures and illustrations. [Video also available.]
31. Stefan Marinov, Divine Electro-Magnetism, *East-West Publishers*, Morellengasse 16, 8010 Graz, Austria, c1993, 289 pages, 102 figs, 75 refs, \$70.
32. Gerald Orlowski, "An Historical Review of the Rory Johnson Cold Fusion Motor," *Fusion Facts*, vol 5, no. 2, pp 14-17.
33. Harold E. Puthoff, "The Energetic Vacuum: Implications for Energy Research," *Speculations in Science & Technology*, 1990, vol 13, no 4, pp 247-257, 33 refs.
34. Kenneth R. Shoulders, "Energy Conversion Using High Charge Density," U.S. Patent 5,018,180, May 21, 1991, 80 pages, 97 figs, 42 claims.
35. T. Matsumoto, "Experiments of One-point Cold Fusion", *Fusion Technology*, vol 24, pp 332 (1993).
36. Hal Fox & T. Matsumoto, "Comments and Response on 'Experiments of One-point Cold Fusion'", *Fusion Technology*, vol 24, no 3, Nov 1993, pp 346-347.
37. Dennis Cravens (Vernon College), "Factors Effecting the Success Rate of Heat Generation in CF Cells", paper presented at the Fourth Annual Cold Fusion Conference, Hawaii, Dec. 6-9, 1993.

The first issue of *New Energy News* was mailed in early May, 1993. For subscription information write to P.O. Box 58639, Salt Lake City, UT 84158. The *New Energy Journal* is scheduled for publication in the near future. The author is the editor of *New Energy News* and of *Fusion Facts*, the leading newsletter (now in its fifth year of publishing) reporting on cold fusion and other enhanced energy devices. Information about *Fusion Facts* or *New Energy News* and free sample copies can be obtained from the same address or by phone: Voice (801) 583-6232; Fax (801) 583-6245. The book, Cold Fusion Impact in the Enhanced Energy Age, by Hal Fox is available in English, Russian, and Spanish.

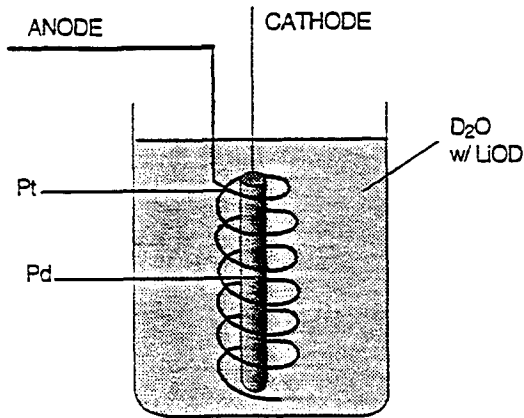


**Fig. 1. FLEISCHMANN AND PONS  
Heavy Water - Palladium - Lithium Cell**

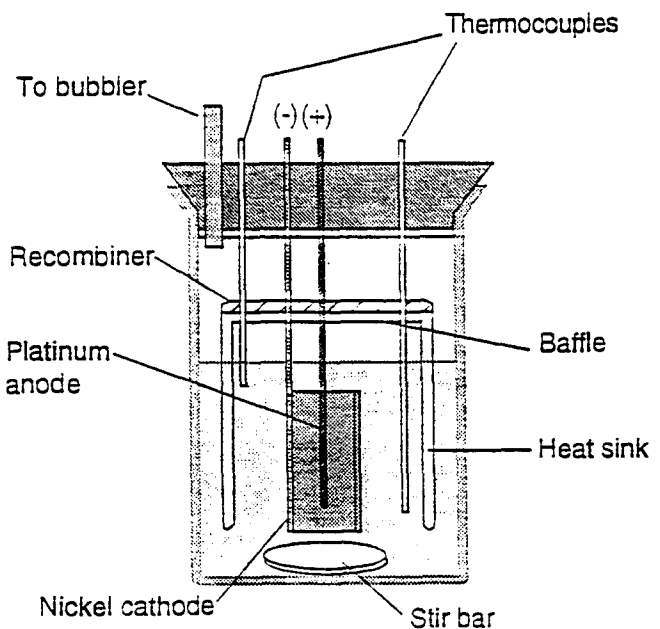


**Fig. 2 CAL POLY LIGHT WATER CELL**

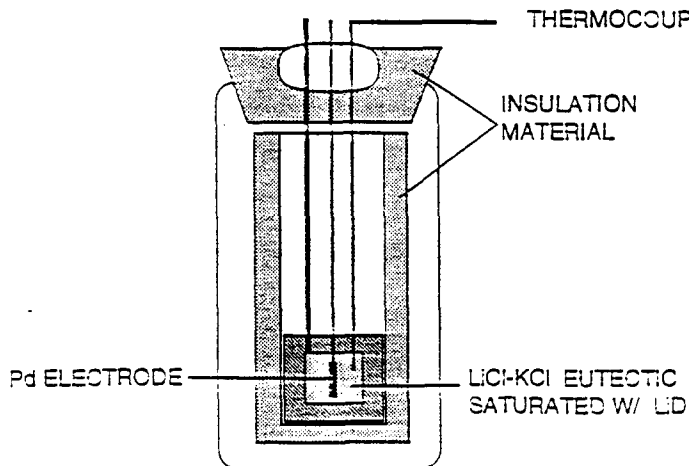


**Fig. 3. MOLTEN SALT ELECTROCHEMICAL CELL**

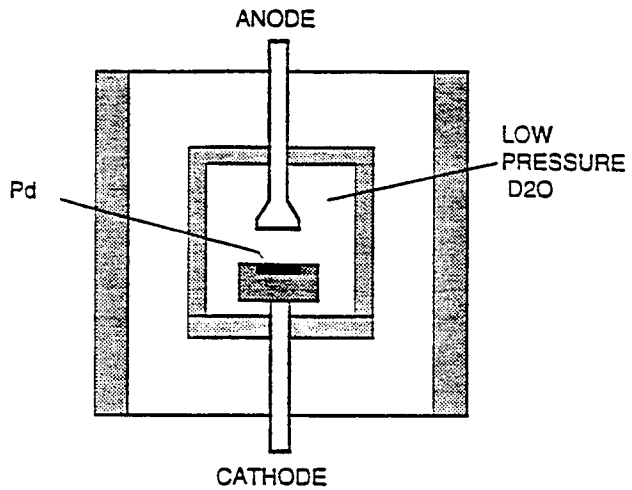


**Fig. 4. GAS PLASMA DEVICE**

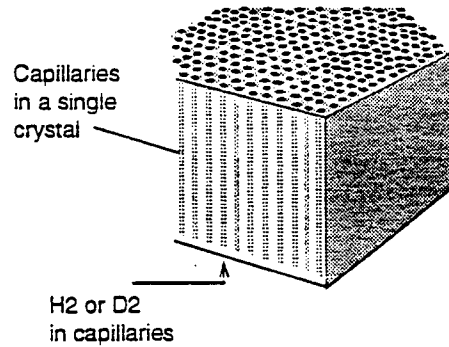


**Fig. 5. CAPILLARY FUSION IN BRONZE CRYSTAL**

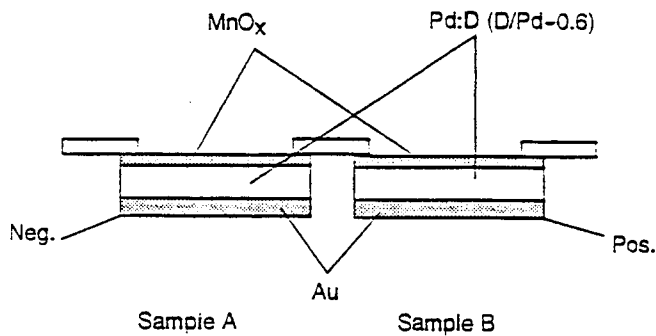


**Fig. 6. YAMAGUCHI PALLADIUM SANDWICH**

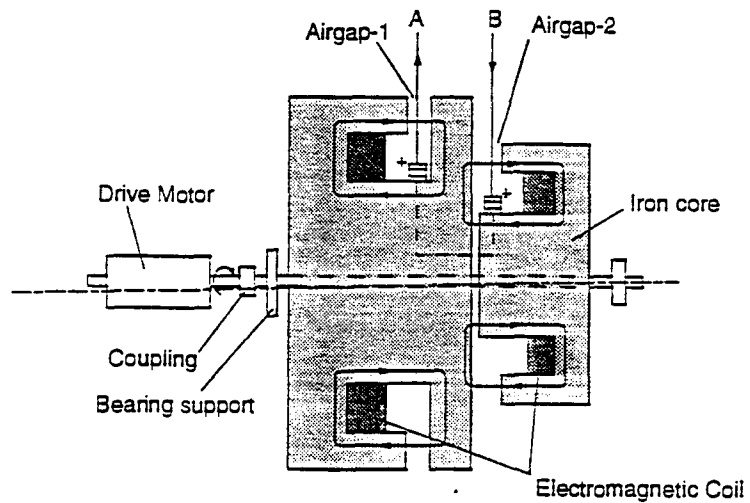


**Fig. 7. TEWARI'S SPACE-POWER GENERATOR**

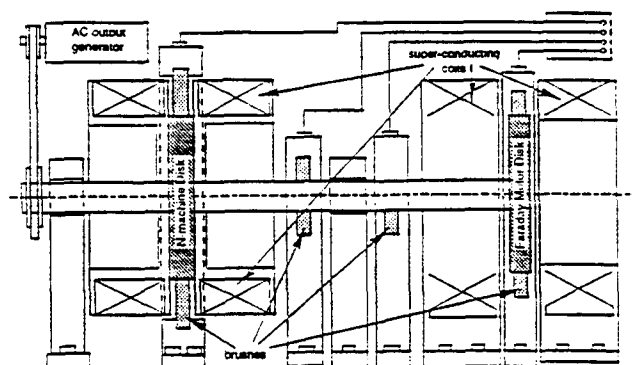


**Fig 8. CONCEPTUAL FIGURE OF JPI-II TEST MACHINE**

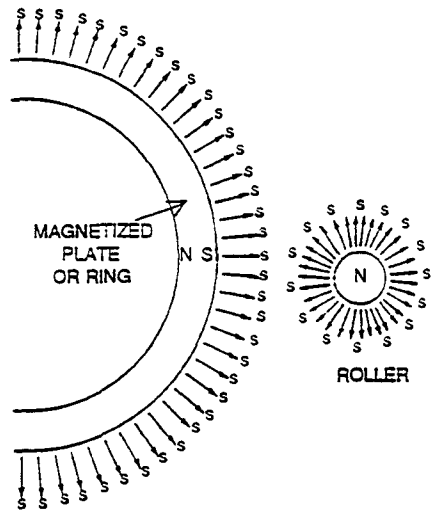
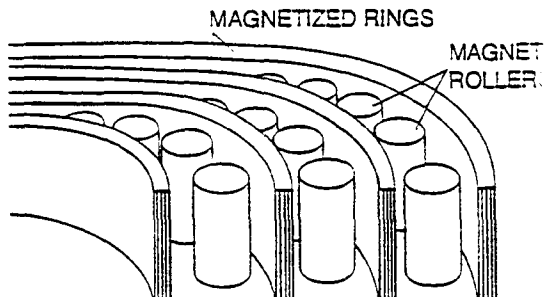


**FIG 9. THE SEARL-EFFECT GENERATOR**



**SECTION SHOWING PLATES AND ROLLERS**

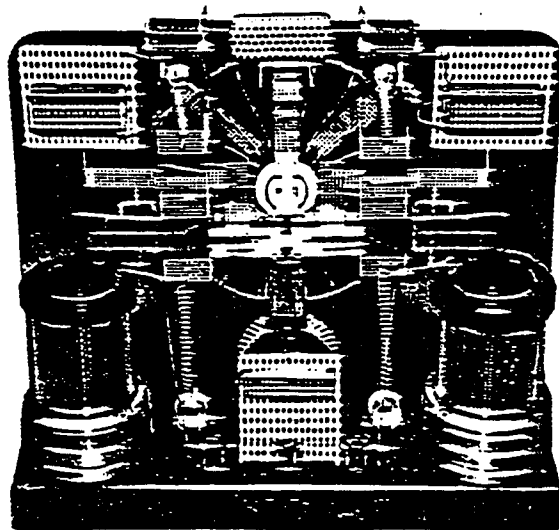


Fig. 10. METHERNITHA MACHINE "TESTATIKA"

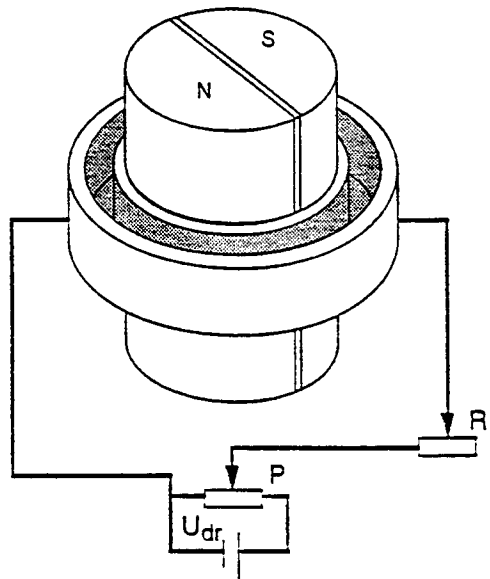


Fig 11. The S-MACHINE SIBERIAN COLIU  
with liquid rotating ring.

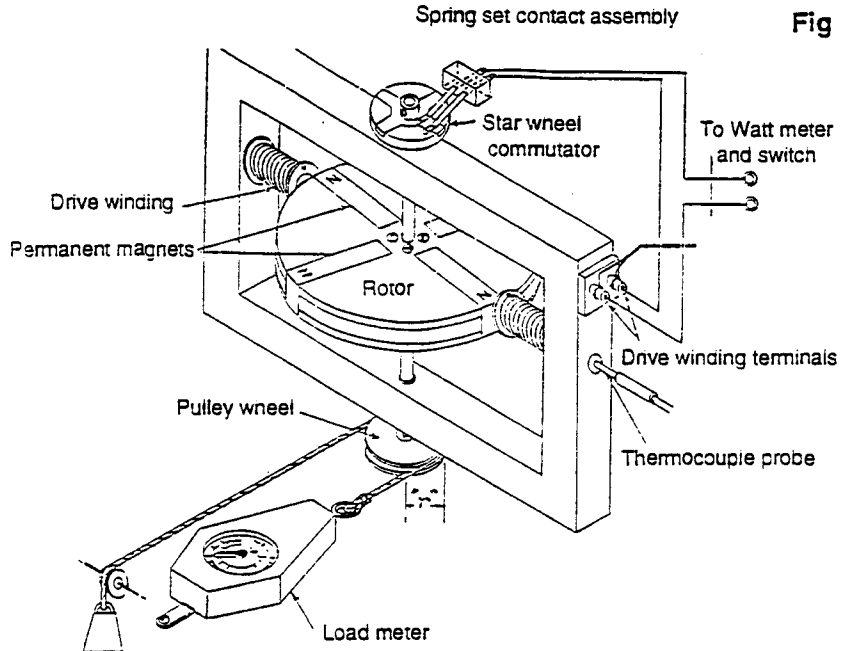


Fig. 12. ADAMS' PERMANENT MAGNET  
ELECTRIC D.C. MOTOR GENERATOR

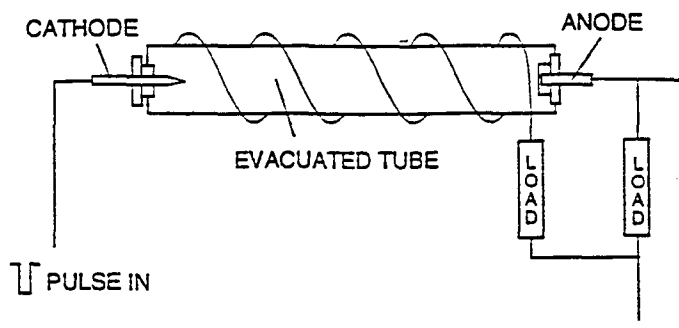


Fig. 13. Energy Conversion Using High Charge Density



## REVIEW OF PROGRESS IN COLD FUSION

Douglas R.O. Morrison  
CERN, Geneva 23, Switzerland.

### ABSTRACT

Experimental papers published over a 12 month period are summarized and the theoretical papers are abstracted. What one would have expected to see is listed and compared with what was published. The conditions for good experiments are listed, in particular "try to prove yourself wrong". The list of four miracles required for Cold Fusion to be fusion are explained. The contradiction is noted between experiments which observe Cold Fusion effects with deuterium and as a control find no such effects with hydrogen, and those experiments which find Cold Fusion with hydrogen. Information is requested on the boundary layer between the inside of the lattice where Cold Fusion is claimed to occur, and the rest of the Universe where the normal laws of Science apply and Cold Fusion is not claimed. Since a claim in 1989 that a working Cold Fusion device existed, the time delay to such a practical device has steadily increased.

### SUBJECTS

1. Introduction
2. Data Base for Review
3. Classification of Published Papers
4. What do we Expect to See?
5. Do Good Experiments
  - 5.1. Do Not use Poor Detectors
  - 5.2. Do Use Detectors that Discriminate
  - 5.3. Do Look for Correlations
  - 5.4. Do Use Adequate Data Recording Instrumentation
  - 5.5. Design Experiments to Avoid Problems
  - 5.6. Try to Prove Yourself Wrong
  - 5.7. Do Experiments to Test Theories
  - 5.8 Do Reproducible Experiments
6. List of Miracles if Cold Fusion is Fusion
  - 6.1. D-D Separation
  - 6.2. Excess Heat with Hydrogen
  - 6.3. Lack of Nuclear Ash with respect to Excess Heat
  - 6.4. Ratios of Nuclear Ash Components
7. Theory - General. Boundary Layer between Cold Fusion and Rest of the Universe
8. List of Theories published in last 12 Months
9. When a Cold Fusion Working Device?
10. Conclusions.

Presented at the Fourth International Conference on Cold Fusion,  
6th to 9th December 1993, Maui, Hawaii.

## 1. INTRODUCTION

At the Third Cold Fusion Conference in Nagoya, October 1993, gave a Review on Cold Fusion[1]. For this Fourth conference, the papers published in the following 12 months are reviewed and a comparison is made between what we expected to see performed in these 12 months and what actually happened. With 5 groups reporting at Nagoya that they had observed excess heat and other effects using not deuterium but normal light hydrogen, new results were expected. The question of when a working device giving useful power, would be produced (or may already have been made) is discussed.

## 2. DATA BASE FOR REVIEW

A review should look at ALL the data, both positive and null experiments. ICCF meetings are unsuitable as very few of the experiments which find no effect (null experiments) are presented even though as shown in ref. 1, most published experimental results find nothing. Hence have taken all the published papers which are said to have been refereed, from the bibliography of Dieter Britz covering his period;

October 1992 to September 1993.

This is a continuation to the compilation presented at Nagoya [1] which covered his period of April 1989 to September 1992.

It is agreed by all that statistics of published papers alone are not decisive in any controversy and hence NO CONCLUSIONS WILL BE DRAWN FROM STATISTICS ALONE. However it is interesting to see trends.

## 3. CLASSIFICATION OF PUBLISHED PAPERS

During the Dieter Britz's period Oct. 1992 to Sept. 1993, 76 papers concerning Cold Fusion were published in refereed journals. 27 were experimental, 26 theory, and 22 were "Others". Of the experimental papers, 13 were null (i.e. no effect found), 10 positive (some effect found) and 4 with no decision. The theory papers had 3 predicting no effect, 20 predicting an effect, and three discussing a possible explanation of claimed effects.

Comparing with previous years, the rate of publishing is slightly higher than the first 9 months of 1992 (43 papers) but appreciable lower than 1989 (237 papers in 9 months), 1990 (305 papers) and 1991 (154 papers). Thus the rate is now about 6 papers per month (of which 2 are experimental) compared with a 1990 peak of 25 papers per month (of which 11 were experimental).

The experimental papers were then classified according to the claim (neutrons tritium etc.) so that a paper could give several entries. It was found that new classifications were needed. After each class two numbers are given, the first is the number of null experimental results and the second is the number of positives. They are;

### 3.1. New Classifications

Fracto-fusion 2 null ; 2 positive. Laser-induced 1 ; 0. Transmutation 0 ; 1

Light Hydrogen (i.e. not deuterium) ? ; 1. Mossbauer 1 ; 0.

Black Holes ? ; 1 Gammas 2 ; 0

Excess heat but no input ("Life after Death") 0 ; 2

### 3.2. Previous Classifications

3He 3;1    4He 1;3    X-Rays 0;0    Protons 1;0    Tritium 6;2  
Neutrons 12;9    Excess Heat 3;10.

It may be recalled that for 1989 to Sept. 1992, all the classes gave more null experiments than positive ones. Adding the new statistics does not change this - for all major classifications there are more null results, than positive ones, e.g. for Excess Heat the totals are 50 null results and 37 positive claims.

## 4. WHAT DO WE EXPECT TO SEE?

Previous meetings held in 1989 to 1992, gave guides for future experiments - these recommendations are hard to find as the meetings tended not to have summary speakers and the concluding Round Table discussions were not written up; so had to rely on notes taken. The advice for future work was;

- 4.1. Do Good Experiments
- 4.2. Make Experimental Results Reproducible
- 4.3. Theory that Fits All Data
- 4.4. Make a Working Model

We will now consider how far these requirements have been met.

## 5. DO GOOD EXPERIMENTS

The field might be expected to be mature now since it is more than four and a half years since the Fleischmann and Pons Press Conference of 23 March 1989, and over 10 years since Fleischmann and Pons started working hard experimentally on Cold Fusion (they claim that they began to work intensively five and a half years before their Press Conference). Also many groups have been well-funded for some period. The main points are;

### 5.1. Do not use Poor Detectors

Certain detectors are notorious for giving artifacts, e.g. BF<sub>3</sub> counters which easily give false signals due to vibration, humidity etc., or X-ray plates which can be stained by many effects.

### 5.2. Do Use Detectors that Discriminate

Instead of using an X-ray plate that records a vague darkening, it much better to use an X-ray detector which can measure the energy of the individual X-rays - for example the observation of the 21 keV line from Palladium would be an important result. Steve Jones has made such a detector which is so small that it can easily be inserted into anyone's experiment. He himself has not observed the 21 keV line in his experiments. For over a year he has offered his detector free to anyone who seriously wants to measure X-rays, but no one took up his offer, though now at Maui, Prof. Oriani has accepted one. Similarly instead of simply counting neutrons, it would be more convincing to measure the energy spectrum and see if there is a peak at 2.45 MeV as expected - the original 1989 Nature paper of Steve Jones et al. [2] reported such a peak and even though its statistical significance was rather small, the fact that it was at 2.45 MeV was impressive; similarly the Turin group has recently reported [3] a peak at the desired value of 2.5 MeV.

### 5.3 Do Look for Correlations

It is unsatisfactory to measure only one effect, e.g. only neutrons, when many effects are predicted to occur simultaneously, e.g. excess heat is expected to occur with  $^4\text{He}$  on some theories and with  $^3\text{He}$  on others and with neutrons, tritons, protons, gammas, X-rays, 14 MeV neutrons on conventional models. By making measurements of these effects simultaneously, the value of the results is greatly increased. It may be commented that up to now when the better experiments have looked for several effects simultaneously, they have observed no effects at all [1]. In this connection it is interesting to recall the statement by Dr. Fleischmann "1992 must be the year of mass spectroscopy" so it is clear that he is in favour of seeking correlations but it is surprising that we are still waiting for such results.

### 5.4 Do Use Adequate Data Recording Instrumentation

Using a single thermister to record temperature changes in a fast changing environment as in the latest Fleischmann and Pons paper [4] is not satisfactory or convincing - it does not allow an adequate check on the detailed heat flow calculations such as the assumption that the heat loss is 100% by radiation whereas the original Fleischmann and Pons paper [5] emphasized that Newton's Law of Cooling was used and the heat flow was 100% conduction - it is the difference between assuming that the heat loss was proportional to the temperature difference to the fourth power of the temperature or to the first power - vastly different assumptions.

Similarly in ref. 4, Fleischmann and Pons describe how the cell boils vigorously and about half-empties in 600 seconds - but this work only has a single temperature recording device and the current and voltage data are only recorded every 300 seconds which means that only about two (or three) readings were recorded during the crucial 600 seconds. This is highly inadequate and casts serious doubts on the claims of huge excess heat. Similarly with the claim that the cell stayed hot for some three hours after the electrolyte had boiled off so that it was believed that there was no input - now called "Life after Death" - it is hard to believe when there is only one local isolated measuring device. It is to be hoped that these experiments will be repeated with adequate convincing measuring instruments.

### 5.5 Design Experiments to Avoid Problems

The design of some experiments is such that a large number of assumptions are needed to analyze the data and many calibrations are required - an example is the open cell calorimetry with no measurements of the out-going gases, of Drs. Fleischmann and Pons where the make assumptions such as (1) that there is no recombination of the deuterium and the oxygen although the anode and cathode are very close, (2) that the heat outflow is 100% radiative or alternatively is 100% conductive, (3) that no lithium is carried out of the cell, (4) that the gas escaping does not carry any liquid with it or is blown out near boiling temperature, etc. Many of these doubtful assumptions (and which are doubted [6]) are treated by calculations. However it would be better if they could be largely avoided by using standard electrochemical technique e.g. employing a closed cell with a catalyser inside and the anode and cathode well-separated. Best technique is to use a null measurement method as in the Wheatstone bridge. Here one could use three baths at temperatures kept by heaters at temperatures of say 30, 40 and 45 degrees C. If there is excess heat produced by a cell in the inner bath, then its heater is turned down and this excess heat measured - this system is easy to calibrate. All is with

no change in the temperatures of the three baths so that complicated calculations and doubtful assumptions are not needed.

Since Fleischmann and Pons often use small specks of palladium (e.g. 0.04 cm<sup>3</sup> of Pd in ref. 4), they then only observe a small effect at lower temperatures and have to multiply by a large factor - it would be better technique to use a larger piece of palladium so that it could be seen if the effect is larger than the background and error assumptions. Note in Polywater, all the experiments produced very small quantities of the controversial water, less than one cc, and the authors did not try to use large samples, thus they did not try to prove themselves wrong.

#### 5.6. Try to Prove Yourself Wrong

"The easiest person in the World to deceive, is yourself" is a well-known warning in Science and one is taught by good professors such as Phillip I. Dee in my case, to go out and actively try and find ways to prove yourself wrong.

If one wishes to assume there is no recombination of the hydrogen and oxygen, then one should not do it by calculation, but do clear active experiments to try and prove yourself wrong, e.g. by varying the distance between the anode and cathode. This has in fact been done by Prof. Lee Hansen at BYU [7] who varied the separation of the anode and cathode. He found that assuming no recombination, there was an calculated excess heat but this disappeared when the electrodes were separated suggesting that the origin of the calculated excess heat was recombination. To check this further, he blew in nitrogen gas from the bottom when the electrodes were close together, and again the calculated excess heat vanished. It is surprising that after ten years intensive work, that Fleischmann and Pons have never published any such experiments to test their assumption that there is no recombination.

The actual excess heats claimed by Fleischmann and Pons in their 1989 and 1990 papers [5, 8] are small, but they are then multiplied up by dubious assumptions e.g normally one uses the well-known fact that the power used to separate the deuterium and oxygen is (1.54 Volts times the current), but in their 1989 paper, Fleischmann and Pons use (0.5 Volts times the current). It is this and other assumptions that allow Fleischmann and Pons to use the of-repeated claim of "one watt in and four watts out". This number of 0.5 Volts seems to be unknown apart from this paper and it is surprising that experiments to justify such a crucial number have not been done. This story of Fleischmann and Pons's unusual excess heat calculations is clearly explained on pages 351 to 353 of Frank Close's book "Too Hot to Handle" [9].

The contradiction between Fleischmann and Pons' 1989 and 1990 papers as to whether the heat loss is 100% by conduction [3] or 100% by radiation [8] could be resolved by experiment, but seems not to have been done (they silvered the top part of the cell later but as it was claimed this changed the heat loss from 100% radiative to 100% radiative, this can hardly be considered a decisive experiment). The estimate of the heat losses is critical to calculations of the excess heat.

The message is do more experiments, vary parameters and seriously try to prove yourself wrong.

#### 5.7. Do Experiments to Test Theory

There are many theories and it is surprising that people do not seriously design experiments to make critical tests of the theories. For example the crucial point about Nobel Prize winner Julian Schwinger's theory[10] is that pd fusion is much more likely

than dd fusion. And pd fusion would give  $^3\text{He}$  rather than  $^4\text{He}$  in the electroweak mode. Hence one would have expected that someone would have varied the hydrogen to deuterium content and looked for the excess heat and for  $^3\text{He}$  and  $^4\text{He}$  as a function of the H to D ratio. For example one could try the following mixtures in the electrolyte;

H2O	1%	25%	50%	75%	99%
D2O	99%	75%	50%	25%	1%.

### 5.8 Do Reproducible Experiments

So far the only reproducible experiments have been achieved by those who find no Cold Fusion effect. Those who find positive Cold Fusion effects do not claim 100% reproducibility.

## 6. LIST OF MIRACLES IF COLD FUSION IS FUSION

### 6.1. D-D Separation

The great problem of D-D fusion is the difficulty of overcoming the Coulomb potential barrier. This can be overcome by using fast deuterium nuclei as in the Sun (keV energies), or in tokamaks, or ion implantation, energetic arc or glow discharges, etc. but these are called Hot Fusion and well appreciated. For Cold Fusion the thermal energies are too small and the probability is very, very small, e.g. Koonin and Nauenberg [1] have calculated that for a separation of 0.74 Angstroms, it is only  $10^{-64}$  fusions per dd pair per second - that is negligible as can be seen that if the mass of deuterium was as large as the solar system mass, there would be only one fusion per second which would give a power of a million millionth of one watt.

Under normal conditions, in D2 gas or deuterium liquid, the separation of the deuterium nuclei is 0.74 Å. as explained the probability is negligible except when a thermal muon (effectively almost zero velocity) with a mass some 200 times greater than the electron mass, approaches the dd pair and displaces one of bound electrons and this causes the dd pair to be pulled closer together giving a separation of about 0.035 Å when fusion can occur - this is called muon-catalyzed fusion. However with the very short lifetime of the muon it can easily be shown that this is not an economic process but it does indicate how the fusion probability varies very steeply with the d-d separation.

There is an enormous literature on hydrogen and deuterium in palladium and other metals - see for example, Fukai at the Third Cold Fusion Conference [12]. The basic fact is that palladium is normally a face-centred crystal with a side of about 3.9 Å - if hydrogen is forced into it, the crystal expands slightly e.g to 4.03 Å for a D to Pd ratio of 0.8. The normal separation of d-d particles is 2.85 Å - this is when they are in the orthohedral sites. When the deuterons are forced into the palladium e.g by ion implantation, then tetrahedral sites can be occupied and the separation is reduced to 1.74 Å, but this value is still much greater than the normal 0.74 Å.

Thus the deuterium nuclei are further apart in the Pd lattice than normal - it goes the wrong way for Cold Fusion, to put deuterium into metal lattices.

There are thousands of experiments, papers and many books on hydrogen and deuterium in metals and there is a unifying theory which fits the data - except Cold Fusion data. To claim excess heat from Cold Fusion is Miracle Number 1.

### 6.2 Excess heat with Hydrogen

If one observes fusion with D-D then one does not expect to observe it with H-H as the rate is many orders of magnitude lower. Thus one would then observe it with D<sub>2</sub>O but not with H<sub>2</sub>O. In the period April 1989 to 1991, Fleischmann and Pons and others claimed to have observed D-D fusion but not H-H fusion so they used H<sub>2</sub>O as a control and stated that the excess heat claimed was from D-D fusion and was a nuclear process. However at the Third Cold Fusion conference in October 1992, five groups claimed to have obtained excess heat using hydrogen. Further some produced theories stating that the excess heat was not from a nuclear reaction, e.g. Vigier [13] who said it was quantum chemistry. At this fourth conference seven groups have reported experimental data supporting the claims of excess heat with hydrogen - (and still living under the banner of Cold Fusion).

There is an enormous contradiction here - most of the Cold Fusion community claim that Cold Fusion is deuterium fusion and the excess heat has a nuclear origin and this is confirmed because it is NOT observed with light hydrogen, but there is a strong minority which claim excess heat with light hydrogen and sometimes say it is not nuclear. Surprisingly this contradiction was not discussed at the Third meeting and seems to be being ignored here at the Fourth.

This is the second miracle.

#### 6.3 Lack of Nuclear Ash with respect to Excess heat

If Cold Fusion has its origin in nuclear reactions as Fleischmann and Pons and others have claimed, then there must be some nuclear particles produced - called the Nuclear Ash by Frank Close [9].

Thousands of experiments have established what this nuclear ash is, both at high energies (hot fusion) and at thermal energies (cold fusion - in muon-catalyzed fusion). The conclusion is that for one watt of power, the products are;

$10^{12}$  particles per second of tritons, neutrons, protons, and  $^3\text{He}$

$10^7$  particles per second of  $^4\text{He}$  and gammas of 24 MeV.

Such numbers of particles are not observed. For watts of power, the above numbers would give fatal doses of radiation but no such casualties have been reported and it appears that most scientists and laboratory assistants or cleaners do not take radiation precautions or do radiation monitoring by wearing film badges.

This is miracle number three.

#### 6.4. Ratios of Nuclear Ash Components

The ratios of the nuclear products given in 6.3 above are very well established, e.g. see Cecil et al. [14] in the proceedings of the Second Cold Fusion conference where he shows that the (neutron plus  $^3\text{He}$ ) channel is equal to the (tritium plus proton) channel as would be expected from charge symmetry, while the ( $^4\text{He}$  plus gamma) is indeed a factor of ten million lower. This is not observed in experiments making Cold Fusion claims, even the tritium to neutron ratio is said to be between  $10^4$  to  $10^9$ .

This Cold Fusion miracle number four.

For many four miracles is a bit too much, especially before breakfast as Alice would say.

## 7 THEORY- GENERAL. BOUNDARY LAYER BETWEEN COLD FUSION AND REST OF THE UNIVERSE

There are many experiments on fusion and there is a well-established theory [12] which fits fusion data and many other aspects of Science. However it is remarkable (a miracle) that this theory is claimed not to apply to Cold Fusion experiments when performed by Fleischmann, Pons and some others but does apply to the larger number of experimenters on Cold Fusion who find no effects. There are a large number of theories which have been proposed to account for the Cold Fusion claims. They concern the behaviour of deuterium (and sometimes hydrogen) in a lattice.

In such theories it is remarkable that this lattice in which Cold Fusion is claimed to occur, is not defined. Questions such as can Cold Fusion occur in ice, do not give clear answers. Some such as Dr. Preparata use their theory that justifies Cold Fusion, to support the claims of Dr. Benveniste et al. [15] that water has a memory and that after diluting it many times (up to  $10^{120}$ ), this memory is retained. One would then expect their theory of Cold Fusion would also apply to water - do they then predict that Cold Fusion should occur in water? It may be noted that Hirst et al. [16] have tried to reproduce the findings of Benveniste et al. using dilutions from  $10^2$  to  $10^{60}$ , but could not reproduce the results of Benveniste et al.

In general it is good that theorists try to prove themselves wrong by applying their theories to other applications as Preparata has done for the memory of water, and this scientific approach is to be encouraged.

A further important question that does not seem to have been considered, is what happens at the boundary of the lattice? Outside the lattice the normal laws of Science seem to apply but on entering the lattice the four miracles listed in section 6, come into operation. It would be important to study and understand this transition layer - it may be a way to distinguish between the very different theories of Cold Fusion.

## 8. LIST OF THEORIES PUBLISHED IN THE LAST 12 MONTHS

In the period of 12 months of Dieter Britz, given in section 2, a variety of theories that might explain Cold Fusion have been published in refereed journals (references and author list are in Dr. Britz's bibliography). These are summarized;

- a). Gerlovin; New unified field theory. The Earth's movements with respect to the vacuum of space are important and best results should be obtained at 10.00 hours, 11.00 hours, and noon.
- b). Hagelstein; coherent and semi-coherent neutron transfer with increased phonon coupling. Under some conditions, gammas should be observed.
- c). Matsumoto; new elementary particle, the Iton which gives di-neutrons and higher neutron assemblies. The theory explains the gravity decays and transmutations observed.
- d). Mendes; ergodic motion. Three-body collisions dominate, especially dde.
- e). Bockris; high fugacity (as Fleischmann and Pons [5]) giving  $10^{26}$  atmospheres. Electron capture by deuterium.
- f). Matsumoto; Nattoh theory. Collapse of neutron clusters giving Black Holes.
- g). Swartz; Quasi-one-dimensional model of loading. Crystal structures are important (defects, dislocations, shape, small surface features - spikes).

- h). Yasui; Fracto-fusion, cracks.
- i). Fisher; polyneutrons.
- j). Yang; D captures electron giving D plus a di-neutron. Theory explains neutron bursts (this claim now withdrawn by Steve Jones).
- k). Cerofolini; Binuclear atoms (dd)ee, capture thermal neutrons giving D, T,  ${}^4\text{He}$ , tritium enrichment, neutron bursts.
- l). Matsumoto; double iton explains warming for three hours afterwards. Could this be the theoretical explanation of the "Life after Death" claimed by Fleischmann and Pons who about a year later also said they had observed a similar three-hour effect?
- m). Takahashi; high loadings give 3-body and 4-body fusions.
- n). Bracci; Collective effects ruled out (contrary to Hagelstein and to Preparata, Bressani and Del Guidice). Explains by high effective electron masses, 5 to 10 times greater.
- o). Lo; Densely coupled plasmas.
- p). Stoppini; Superconductivity,  $< 11^\circ\text{K}$ .
- q). Hora; Dense plasma. Transmutation by neutron swapping, e.g  $\text{Pd} + \text{D} \rightarrow \text{Rh} + {}^4\text{He}$ .
- r). Filimonov; Deuteron soliton coherent with palladium anti-soliton - should coat electrode with palladium black.
- s). Lipson; Super-condensates - fracto-fusion mechanism is improbable.
- t). Chatterjee; stochastic electron accumulation.
- u). Gammon; Negative Joule-Thompson effect.
- v). Granneau; Ampere force.
- w). Hagelstein; n-transfer, 3-phonon.
- x). Ichimark; coherent plasmas. One to two fusions per year per  $\text{cm}^3$ .

Note - in reply to a question as to whether Cold Fusion could be observed in water, Dr. Preparata declared that he had never written a paper applying his theory of Cold Fusion to Benveniste's work. Dieter Britz has written "We have an article from an Italian Magazine, where Preparata and Del Guidice describe their theory of long-range effects in water, and relate this to both cold Fusion and homeopathy (i.e. Benveniste claims)".

It is interesting that there is a rather wide spread of journals - not just Fusion Technology (10 times here) and Physics Letters A where J-P Vigier is an Editor (quoted twice here).

## 9. WHEN A COLD FUSION WORKING DEVICE?

8 December 1993; the previous speaker, Dr. H. Fox, giving he said, a business man's point of view, declared he expected a working Cold Fusion device in 20 years.

November 1993. Dr. S. Pons said that by the year 2000 there should be a household power plant - 6 years.

1992. Dr. M. Fleischmann said a 10 to 20 Kilowatt power plant should be operational in one year.

July 1989. The Deseret News published an article by Jo-Ann Jacobsen-Wells who interviewed Dr. S. Pons. There is a photograph in colour, of Dr. Pons beside an simple apparatus with two tubes, one for cold water in and one for hot water out. This working unit based on Cold Fusion was described as; " It couldn't take care of the family's

electrical needs, but it certainly could provide them with hot water year-round' said Pons".

Later in the article it was written "Simply put, in its current state, it could provide boiling water for a cup of tea".

Time delay to this working model - **Zero years.**

Thus it appears that as time passes, the delay to realisation of a working model increases.

## 10. CONCLUSIONS

No conclusions are presented - everyone can judge for themselves. However some questions can be asked;

Are Cold Fusion results consistent in claiming Cold Fusion effects in Deuterium but not in normal Hydrogen, while other groups claim Cold Fusion effects with hydrogen?

Is the ratio of tritium to neutron production about unity as Fleischmann and Pons originally claimed [5] or is the ratio in the wide range  $10^4$  to  $10^9$  as most other workers claim?

Are transmutations, Black Holes, Biology [17] part of the normal world of Cold Fusion

To explain the null experiments there is one theory - the conventional theory of Quantum Mechanics. but there are a wide variety of theories to explain positive Cold Fusion results - can they all be valid simultaneously - if not which should be rejected?

When can we have a cup of tea?

## Acknowledgements

It is a pleasure to thank Dieter Britz for the use of his Bibliographic compilation.

## REFERENCES

1. D.R.O. Morrison, Cold Fusion Update No. 7, Email.
2. S.E. Jones et al., Nature 338(1989)737.
3. T. Bressani et al. 3rd Intl. Conf. on Cold Fusion, "Frontiers of Cold Fusion", Ed. H. Ikegami, Univ. Acad. Press, Tokyo, (1993), p 433.
4. M. Fleischmann and S. Pons, Phys. Lett. A 176(1993)1.
5. M. Fleischmann and S. Pons, J. Electroanal. Chem. 261(1989)301.
6. J. Wilson et al., J. Electroanal. Chem. 332(1992)1.
7. L. Hansen, priv. comm.
8. M. Fleischmann et al., J. Electroanal. Chem. 287(1990)293.
9. F. Close, "Too Hot To Handle", W.H Allen Publ., London, (1990).
10. J. Schwinger, 1st Annual Conf. on Cold Fusion, National Cold Fusion Institute, Salt Lake City, (1989), p 130.
11. S.E. Koonin and M. Nauenberg, Nature 339(1989)690.
12. Y. Fukai, 3rd Intl. Conf. on Cold Fusion, "Frontiers of Cold Fusion", Ed. H. Ikegami, Univ. Acad. Press, Tokyo, (1993), p 265.

13. J-P. Vigier, 3rd Intl. Conf. on Cold Fusion, "Frontiers of Cold Fusion", Ed. H. Ikegami, Univ. Acad. Press, Tokyo, (1993), p325.
14. F.E. Cecil and G.M. Hale, 2nd Annual Conf. on Cold Fusion, "The Science of Cold Fusion", Ed. T. Bressani, E. Del Guidice, and G. Preparata, Soc. It. di Fisica, Bologna, (1991), p. 271.
15. Davenas et al. Nature 333(1988)816-818.
16. S. J. Hirst et al, Nature 366(1993) 525-527.
17. The IgNobel Prize for Physics was awarded to L. Kervran for his book "Biological Transmutations" in which he argues that a cold fusion process produces the calcium in eggshells, -,Science, 262(1993)509.



## COLD FUSION: THE HIGH FRONTIER -- IMPLICATIONS FOR SPACE TECHNOLOGY

Eugene F. Mallove  
Starbound Engineering  
171 Woodhill-Hooksett Rd.  
Bow, New Hampshire 03304

### Abstract

The confirmation of excess power production and nuclear product evolution in various hydrided metal systems has led many to speculate about technological applications. Here we present a preliminary assessment of how "cold fusion" reactions may affect the technologies that are critical to space exploration. In particular, the implications for space propulsion systems and for non-terrestrial electric power production are considered and found to be potentially very significant. We find that ion-engine thrusters, which are already a well-developed technology, are likely to be the primary beneficiaries of compact cold fusion electric power systems in space. These are highly efficient engines that are characterized by low thrust/weight (T/W), and which are suitable for many deep space missions. It is also possible that high thrust/weight engines that rely on higher-temperature cold fusion reactors could be developed, enabling escape from the surface of celestial bodies, especially Earth. The specific technical parameters of the various engines systems, power modules, and space mission characteristics are compared to define the limits of applicability of cold fusion to space exploration. Though the physical mechanism for "cold fusion" reactions is still being explored by theorists, we refer to this energy source throughout as cold fusion. This is fully justified by common practice -- also because at least some physical systems in which these reactions occur appear to be the cold fusion of deuterons.

### Space Exploration: The Turning Point

Who can guess what strange roads there may yet be on which we  
may travel to the stars?

Arthur C. Clarke, *The Promise of Space*, 1968

The great pioneers of space exploration, Robert H. Goddard, Hermann Oberth, and Konstantin E. Tsiolkovskii, believed -- long before it was done -- that humankind would use rockets to loosen the bonds of gravity, ascend to orbit, and travel to the Moon, Mars, and beyond. From its accelerated growth in the 1950s, space exploration has struggled with the severe limits that chemical energy imposes on rocket propulsion, yet even within those constraints much has been accomplished. Now

space exploration is poised at a great turning point. There is a thirst for progress on the high frontier of space, but progress is limited. Economic and political conditions within the great spacefaring nations have seemed to make the more ambitious goals for expansion into space recede. There is little doubt that the future of space exploration turns on the ability to develop less costly and more effective propulsion systems for lofting massive payloads into low Earth orbit (LEO) and for boosting spacecraft onto fast interplanetary trajectories. It now costs about \$15,000 to \$25,000 per kilogram to place payload into LEO. Furthermore, the fastest chemically-propelled trips to Mars require astronauts to be enroute for a large fraction of a year, with all the attendant risks of cosmic radiation and physiological effects of weightlessness and with high mass life-support requirements.

So within the aerospace community there is a great hunger for new ways into space: single-stage to orbit craft, such as supersonic combustion ramjet (scramjet) hypersonic air-breathing vehicles or more sophisticated rockets typified by the recent DC-X ("Delta Clipper-Experimental") prototype. Virtually all space exploration plans, however, are currently predicated on using cryogenic chemical propellants -- H<sub>2</sub> and O<sub>2</sub> -- for launch from Earth's surface. These propellants were favored in the writings of the early space pioneers, so one might say that space technology has really not yet left the cradle. Many other advanced propulsion concepts have been put forth in the past half-century, but none of these -- including nuclear-powered rockets -- have gone beyond the theoretical or experimental stage and come into common use. Now at the turning point in space exploration in the post-1989 "Cold Fusion Age," it should be possible to find ways to apply the spectacular energies in cold fusion phenomena to spaceflight. These cold fusion space technologies will be developed in parallel with the terrestrial energy and transportation sectors. As cold fusion begins to be applied vigorously to terrestrial needs during the next several years, aerospace applications will become irresistible.

### The Birth of Nuclear Spaceflight

Chemical reactions are typically millions of times less energetic per unit reaction than nuclear reactions, so it is not surprising that there have been efforts during the last four decades to apply nuclear energy to space propulsion in both studies and experimental development -- conventional fission and fusion reactions. Even the early space pioneers recognized that nuclear energy might be extremely useful for space propulsion. The discovery of radioactivity in 1896 and the new understanding of the atom had a profound impact on the thinking of Goddard and Tsiolkovskii, among others. William Reupke has compiled a wonderful historical insight into thinking of the rocket pioneers about atomic energy for spaceflight (1). Reupke points out that by 1903, the year of the Wright brothers' first powered flight, it was already established that the heating effect of radium was a million times greater than chemical reactions.

Even without a detailed understanding of radioactivity, the rocket pioneers were led to speculate about the role of this new energy for the future of space travel. Goddard

(1882-1945) first held the opinion that "atomic energy" would be "impractical." Later, around 1907, Goddard became more optimistic about atomic energy for spaceflight. Goddard had not yet examined the full potential of chemical rocket propulsion -- specifically the importance of rocket *staging* -- so in this era he was pessimistic about space travel *unless* atomic energy could be applied! Hence his 1907 statement, "In conclusion, then, the navigation of interplanetary space depends for its solution on the problem of atomic disintegration....Thus something impossible will probably be accomplished through something else which has always been held equally impossible, but which remains so no longer."

Konstantin Tsiolkovskii (1857-1935) did not incorporate atomic energy into his space travel speculation apparently until 1911-12, but when he did he was a great visionary. He conceived that atomic energy could be used to accomplish *interstellar* space flight, noting that first the radioactive disintegration rate would have to be increased! Tsiolkovskii soon became pessimistic about atomic energy, even as another rocket pioneer, the French aeronautical pioneer Robert Esnault-Pelterie (1881-1957) was becoming a proponent of the new nuclear energy in the 1920s. Goddard, of course, became completely immersed in his development of practical liquid-propellant rockets. The other great astronautical pioneer, Hermann Oberth (1884-1989), considered nuclear energy in some of his correspondence in the 1920s, but was late (1954) in publishing anything about it.

### **Nuclear Powered Flight**

The discovery of fission in 1938 and the advent of fission nuclear power in the 1940s led to a burst of enthusiasm to apply nuclear power to rocket propulsion as well as to aircraft! In an era of aerospace optimism, a vast technical literature emerged, which speculated how nuclear energy -- fission, fusion, antimatter-matter annihilation, etc. -- might eventually be applied to interstellar travel (2). In 1989, the present author and colleague Gregory Matloff reviewed the entire field of nuclear propulsion and interstellar flight concepts in a book that is accessible to the wider public (3).

Nuclear rocket propulsion of the conventional variety came of age with the static testing of prototype engines in the 1960s. Billions of dollars were spent in the U.S. on the Rover and NERVA (Nuclear Energy for Rocket Vehicle Application) programs. The aim was to permit a manned mission to Mars with a much smaller initial mass for the spacecraft than is possible with chemical propellants. The nuclear propelled Mars mission would also have a substantially reduced interplanetary transit time. Conceptually, nuclear rocket engines are very simple. A compact fission reactor provides the thermal energy to heat hydrogen propellant and expel the partially dissociated gas in a high temperature exhaust stream through a conventional converging and diverging nozzle. The hydrogen propellant, initially a cryogenic liquid in a tank, is forced through the reactor so that there is intimate thermal contact between the reactor parts and the gas.

The NERVA-class prototype nuclear engines, which were ground-tested in the U.S. southwest, had *solid* nuclear cores. That is, the uranium-carbide fuel elements were not allowed to get hot enough to melt. The range of performance of these solid core engines is in the range, Specific Impulse (Isp) = 800 - 1100 sec, whereas H<sub>2</sub>-O<sub>2</sub> chemical propulsion has an Isp of about 460 sec. [For those not familiar with rocket propulsion, specific impulse is a measure of the gross efficiency of a rocket engine -- the impulse (force X time) imparted to the rocket per unit weight (mass X gravitational acceleration) of propellant expelled.] The units of Isp are therefore *seconds*. It turns out that Isp (seconds) multiplied by g (9.8 m/sec<sup>2</sup>) gives the exhaust velocity for that engine system. The higher the exhaust velocity, V<sub>e</sub>, the higher the final velocity ("burn out" velocity) that a single stage rocket can reach with a fixed amount of propellant mass. The fundamental rocket equation is:

$$M_0/M_f = \exp(\Delta V/V_e) ,$$

where M<sub>0</sub> is the initial mass of the rocket loaded with propellant; M<sub>f</sub> is the "burn out" mass when all propellant has been expended; V<sub>e</sub> is the exhaust velocity, and ΔV is the total velocity change of the rocket (known as "Delta Vee" in the field of astronautics). The higher V<sub>e</sub>, the smaller the mass ratio, M<sub>0</sub>/M<sub>f</sub>, needs to be. High mass ratio means, of course, that most of the initial mass of the rocket is propellant. This equation is for free space, ignoring the effect of gravity losses during the boosting phase, but it is a good approximation to overall system performance.

Now it is also possible to allow the nuclear core of the rocket to melt, leading to higher temperatures in the rocket pressure chamber, and a higher exhaust velocity. Of course, in such a liquid core rocket, a continuously fissioning (critical) geometry of the fuel-moderator combination must be maintained to allow the fission chain reaction to sustain. The general scheme proposed to do this, which has never been implemented in practice, is to spin up a vortex of uranium fuel-moderator droplets using streams of incoming hydrogen propellant. The hydrogen would come in intimate thermal contact with the extremely hot fuel droplets and thus ultimately achieve a higher exhaust velocity. The vortex also helps to keep most of the nuclear material from being lost out the exhaust nozzle. An intermediate system between the solid core and the liquid core nuclear rocket is the colloidal core concept, in which solid particles of fissionable fuel several hundred microns in diameter are suspended in a rotating (or vortex-driven) fluidized bed.

In general, for thermal rockets -- nuclear and chemical -- the exhaust velocity is proportional to the square root of: (rocket chamber temperature)/(average molecular weight of the exhaust species). There is a great premium for elevated temperatures. Liquid core rockets that have been designed are in the Isp range, 1,300 - 1,600 seconds. It is possible to get even greater Isp in a fission rocket by running at such elevated temperatures that the fission core becomes a vortex of gaseous fuel. Projected Isp is in the range 2,000-7,000 seconds for the gas core nuclear rocket.

None of these fission nuclear rockets are without considerable problems -- including engineering difficulties at elevated temperatures. Each system would release significant radioactivity into the atmosphere were they to be launched from Earth's surface. Even though these systems have high thrust/weight (T/W) ratios and are thus able to lift-off from planetary bodies, their adverse environmental impact would restrict them to operation in space. So these nuclear rockets would have to be boosted into orbit first by chemical rockets. There is another serious disadvantage of fission nuclear rockets: massive shielding of the mission payload and crew against neutron and gamma radiation from the rocket reactor. The reactor itself also has a large mass. Both shielding and reactor add a large weight penalty to the space vehicle, thus detracting to a degree from the advantage of the high Isp.

### **Cold Fusion for Space**

The problems of fission nuclear power for spaceflight would be significantly reduced if there were no radioactive exhaust problem or radiation shielding problem. Therein lies the basic appeal of cold fusion: nearly radiationless nuclear rocketry. A central feature of the scientific controversy surrounding cold fusion --"If it's nuclear, where's the radiation?" -- turns out to be the prime asset for space. Even if cold fusion reactions could not be engineered to make high thrust/weight rockets, cold fusion would still have enormous potential applications in space. Low thrust/weight ion engines, which have high specific impulse, need a low-mass source of electric power. Cold fusion-generated electricity would be ideal for this, reducing the mass and eliminating the shielding of a fission space power reactor. There are many other applications for cold fusion power in space infrastructure: power plants for lunar and Martian surface operations, power for satellite and space station operation in Earth orbit, and power for deep space probes, which now use solar cells and RTG's (radioisotope thermoelectric generators).

For those who examine the technical literature with a reasonably open mind, the existence of what are now called generically "cold fusion" phenomena -- excess energy production and nuclear reactions near room temperature -- is now beyond dispute. By the spring of 1991 the evidence was, in my view, overwhelmingly compelling (4), now it is 100% certain. The body of scientific evidence for these unexpected, astonishing, and allegedly "impossible" phenomena is now broad, deep, and expanding (5-8). Research has revealed what seems to be an entirely new realm of phenomena that has legitimately been called by some researchers *solid state nuclear physics*. There exists at the moment no *generally accepted* theoretical framework to understand these phenomena. It is now clear that even without complete scientific comprehension of cold fusion phenomena, the levels of energy release (and their sustainability and repeatability in many experiments) are technologically useful.

The most exciting potential of cold fusion reactions are the high thermal power densities that have already been observed by several researchers. Drs. Pons and Fleischmann (9) have demonstrated that a thermal power density of 3-4 kW/cm<sup>3</sup> of

cathode material can be created in heavy water electrochemical cells. Kucherov et al (10) have observed similar power densities in metals in low voltage discharge experiments with deuterium gas. Bush and Eagleton (11), using thin films of palladium to coat silver cathodes, have also observed spectacular power densities in the  $\text{kW}/\text{cm}^3$  range. Moreover, several theorists and experimenters (e.g. Professor Peter Hagelstein of MIT and Martin Fleischmann) have suggested that cold fusion power densities may rise with increasing temperature.

### **Cold Fusion - High Thrust/Weight Rockets**

Conventional solid core fission nuclear rockets have already reached an advanced state of development in both the United States and in the former Soviet Union (12-16). These rockets are high engine thrust/weight (T/W) -- on the order of 3 -- at Isp of 800 seconds and above. In the period 1955-1973 the U.S. spent some \$1.4 billion on solid core nuclear rockets -- equivalent to a 1993 level of effort of about \$10 billion. Some 20 ground tests were conducted before the program was terminated in the U.S. -- not for technical reasons, but due to changed Federal budget priorities. The highest power output of one of these solid core reactors reached 4,100 MW (megawatts) at a core temperature in the metal-clad fuel assemblies that reached 2,550 K. The test achieved a high thrust of 200,000 lbs at an Isp of 845 seconds. Demonstrations of multiple start-ups and shut-downs occurred, with thrusting duration exceeding one hour --more than adequate for missions contemplated.

It turns out that the average power density in these solid core fission reactors approached  $3.0 \text{ kW}/\text{cm}^3$ . (There are now reports that Russian nuclear rocket tests have achieved power densities as high as  $40 \text{ kW}/\text{cm}^3$ .) Since there was much zirconium carbide metal cladding and other structure, the uranium fuel itself did not reach such a high power density. It is remarkable, however, that  $3.0 \text{ kW}/\text{cm}^3$  is roughly the power density that some cold fusion experiments have already achieved -- *in metal*. The feasibility of a high performance cold fusion rocket may turn on whether a gas-metal electrical discharge system employing cold fusion surface reactions could operate at this high overall power density. By the suitable use of large surface area channels coated with thin films of Pd alloy material -- a highly "fractalized" electrode system -- such an average power density might be achieved. Whether the surface cold fusion reactions would sustain at the high pressures (gas densities) needed for high thrust/weight systems is an open question.

Perhaps the particle bed reactor or colloidal core geometry would be useful in high T/W cold fusion engines. Colloids suspended in a gas flow offer the highest surface area per unit volume of active material and thus facilitate better heat transfer to the propellant. Perhaps colloid cold fusion reactors would not require electrical gas discharge phenomena to trigger surface reactions. Some researchers in the cold fusion field have speculated that deuterium-loaded metal structures (perhaps clad with ceramics), once triggered, could be made to remain at high temperatures for prolonged periods without electric stimulation. Evidence for this has been provided

at this Fourth International Conference on Cold Fusion by Drs. Pons and Fleischmann and by Professor T. Mizuno of Hokkaido University.

### Cold Fusion - Ion Engines

Ion engines, which are high Isp and low thrust to weight ( $T/W < 10^{-4}$ ), have always been appealing to space mission planners. Their specific impulse range is 5,000 to 100,000 seconds. Ion engines have already been built in the Isp = 5,000 second range and tested in space vacuum simulators for many thousand hours. Several engine tests have been done in Earth orbit. Basically these engines employ atoms such as mercury, cesium, argon, or xenon, which are first ionized and then accelerated in high voltage electrical fields to form a collimated thrust beam. The beam is kept electrically neutral by recombining the atoms downstream with the stripped electrons. Due to low  $T/W$ , ion engines are only suited for operation in orbit, never for launch from the surface of high gravity celestial bodies. The thrust of ion engines that have already been built are rated in the 10 - 200 milli-Newton range -- minute compared to chemical rockets, but at much higher Isp -- 3,000 - 5,000 seconds. There is another disadvantage, which is somewhat compensated for by the high Isp. It may take months for an ion engine-powered vehicle to spiral out of the "gravity well" of a planet on an escape trajectory. When a high  $T/W$  rocket fires, it accomplishes the required velocity change within minutes, not months.

Ion engines require a source of electrical power, and it is here that cold fusion comes in. Cold fusion would not be aimed at improving the ion engine itself, though some might well consider trying to develop charged particle-emitting cold fusion reactions for this purpose! Rather, cold fusion would better the characteristics of the ion engine's electrical power supply. Present power supplies contemplated for deep space ion-engine missions are fission nuclear reactors. This form of propulsion has thus become known as Nuclear Electric Propulsion (NEP). In the U.S. the planned space reactor, "SP-100," is a molten lithium metal-cooled uranium reactor. Thermal energy of 2.5 megawatts (MW) would be converted thermoelectrically to 100 kW of electricity. Much more power than this (several to tens of MW) would be required to boost tens of metric tons to Mars. A 5-10 MW power unit is considered ideal to be clustered for Mars and lunar missions.

The key parameter defining the performance of the electrical system is its specific mass,  $\alpha$ , the "kilograms per kilowatt" of the system. The SP-100 has a design goal of about  $\alpha = 10 \text{ kg/kWe}$  (kWe refers to kilowatts of electricity produced, to distinguish from kW of raw thermal power). Present capability is about  $\alpha = 50 \text{ kg/kWe}$ . Palladium cold fusion cathodes have already demonstrated  $3 \text{ kW/cm}^3$  thermal output, or  $250 \text{ kW/kg}$ . Using this basic thermal output, we can postulate various factors by which the mass of the remaining components of a thermal-to-electric conversion system might exceed the mass of palladium. Then find the specific mass of the power system for two reasonable thermal-to-electric conversion efficiencies,  $\epsilon$ , 10% and 30%:

### Possible Specific Mass of CF Space Electric Power Generation

(Mass of total power system =  $K * \bar{M}$ ass of Pd Electrodes)

(Assumption: 3.0 kW/cm<sup>3</sup> Pd power density)

$\varepsilon = 0.10$

$\varepsilon = 0.30$

<u>K</u>	<u><math>\alpha</math> (kg/kWe)</u>	<u><math>\alpha</math> (kg/kWe)</u>
10	0.4	0.13
100	4.0	1.3
1000	40.0	13

These numbers bracket a range of possible CF electrical power system designs, perhaps using either thermoelectric power conversion or a closed-loop heat engine cycle, both with a required space radiator. Since there will be no nuclear shielding requirement and a CF reactor is expected to be of generally lighter construction than a fission reactor, an  $\alpha$  in the range 1.0 to 4.0 ( $K = 100$ ) seems realistic -- a factor of 10 or more better than current technology.

### **Space Missions and Performance Parameters**

Despite slumping fortunes of the global space effort, the Moon and Mars still beckon powerfully. Do not assume, however, that these are the only worthy destinations for science and commerce. Dana Rotegard (17) and others in the space industrialization movement have pointed to the utility and accessibility of asteroids and the moons of Mars, Phobos and Deimos. In the *energy* required to perform missions to them, they are more accessible than our own Moon! Space missions are characterized by the  $\Delta V$  and payload mass required to carry them out. The enormous payload ratios for a single-stage configuration show how incompatible chemical rocketry is for missions to the outer solar system. The mass ratios become absurdly high. (Those outer planet missions that have been carried out to date have relied heavily on staging and gravity-assist planet swing-by trajectories.) That is why high Isp ion engines are favored for these deep space missions.

Comparing the mission performance of propulsion systems with different Isp's and T/W's was put on a firm footing by W.E. Moeckel in a classic NASA technical report in 1972 (18). It is worth reproducing several figures from the Moeckel study. By using free-space equations (ignoring lift-off from planets) and several simplifying equations, Moeckel put comparative propulsion system performance on a sound footing. In Figure 1., reproduced from the Moeckel report, we see the relation of Isp, specific mass, and thrust/ weight. Specific mass in Figure 1. is the propulsion system mass ratioed to the exhaust beam power, which for the case of ion engines (NEP) is roughly the specific mass of the electrical power system -- so both high and low T/W systems are placed on the same basis of comparison. "Type II" systems, as defined by

Moeckel, are *not* Isp-limited. Their Isp's are high enough to keep mass ratios down, which is their main advantage. Type-II systems are low T/W -- NEP, solar electric, and controlled *hot* fusion rockets . They become better performing -- have higher T/W -- with better (lower) specific mass. "Type I" propulsion systems are limited by attainable Isp, but they have high T/W. This allows them to depart the surfaces of high-gravity celestial bodies like Earth. Chemical propulsion systems have engine T/W's in the 30-60 range, while fission nuclear rockets have engine T/W's around 3 for solid core and 0.3 for gas core. Type-I engines are not limited by specific mass. We expect that cold fusion Type-I engines could be developed with a higher engine T/W than fission nuclear rockets.

Cold fusion propulsion systems will either be: (A) Like the solid core fission Type-I system, equalling or exceeding the solid core fission rocket in Isp and perhaps T/W or (B) Like the NEP (fission nuclear electric ) Type-II system, perhaps being better in specific mass by a factor of ten or more. Figure 2. , also from the Moeckel report, illustrates how Type-I and Type-II systems compare in interplanetary trip times for round trip, rendezvous, and flyby missions to planets from Mars to Pluto [Note: In Figure 2. NI is Isp X number of rocket stages, N.] . Figure 3. from Moeckel portrays the same information as Figure 2., but allows more direct comparison of Type-I and Type-II systems for the round trip and rendezvous missions.

The conclusion for cold fusion rocketry is not different than for the Type-I and Type-II "conventional" systems. Acceptable trip times define the Isp (for Type-I) or specific mass (for Type-II) required to perform the various missions. Simply construct a horizontal line at the acceptable trip time to define the system performance required for the mission. Figure 3. presents the data more conveniently for determining the "cross-over"points where Type-I systems begin to perform more poorly *mission time-wise* than Type-II systems. The cross over point for round trip missions is at about the distance of Jupiter. The cross-over point for planet rendezvous missions lies beyond Saturn.

### **Cold Fusion - Space Power Generation**

Space stations and other spacecraft require electric power and heating . Compact electric generators based on cold fusion should become standard power equipment for spacecraft. Lunar and Martian surface operations will also require cold fusion electrical power and heating. Also, industrial in-situ processing of extraterrestrial materials will require electrical power and heat.

Space mission planners have typically discussed using arrays of solar energy collectors to power operations on planetary surfaces. Solar power is a very weak proposition for Mars, given that solar illumination at the Mars distance from the Sun is about one-half that at Earth. One study projects the required collecting area for a ten person base on Mars (19). The designers concluded that the base would require about  $10^{12}$  joules/Mars year for an average continuous power of 20 kilowatts. For high Martian latitude, this would be provided by an array of Sun-

tracking solar cells 8,760 m<sup>2</sup> in area, with a mass of 113,900 kg. Small cold fusion generators in this power range for terrestrial home use, which are now being developed, could provide the Mars base power for a minute fraction of that mass.

J.R. French (20) has discussed the great benefits for Mars missions of extracting rocket propellants from the thin (mostly CO<sub>2</sub>) Martian atmosphere. Mars air is taken in, compressed, and the CO<sub>2</sub> separated. A thermal decomposition unit then manufactures bi-propellant rocket fuel, liquid CO and liquid O<sub>2</sub>. (Others suggest carrying some liquid hydrogen to Mars and using it to create methane and oxygen rocket bi-propellant from the Martian atmospheric CO<sub>2</sub>). This permits launching a much smaller mass toward Mars on early missions. Using small cold fusion power sources to produce this propellant will make its use even more attractive for surface operations and for the return to Earth. One can readily imagine roving vehicles and Mars aircraft powered by cold fusion motors or the cold fusion-manufactured propellant. Cold fusion energy will also reduce the launch mass of on-board chemical consumables needed for Mars exploration. It will eliminate the hazards and the radiation shielding requirements of proposed Mars mission fission reactors. There is no question that cold fusion will make Mars exploration much more attractive. Since the time frame for Mars missions is early 21st Century, it is likely that the very first human explorers of the planet will rely on cold fusion power generation. When historians look back at the strange 40-year gap that will separate the lunar exploration of 1968-1972 from the Mars missions and Moon trips of the early 21st Century, they may conclude that these had to await cold fusion.

## References:

1. William A. Reupke, "The Rocket Pioneers and Atomic Energy," *Journal of the British Interplanetary Society*, Vol.45, No.7, July 1992, pp. 297-304.
2. E. F. Mallove, Forward, R.L., Paprotny, Z., and Lehmann, J., "Interstellar Travel and Communication: A Bibliography," a special issue of *The Journal of the British Interplanetary Society*, Vol.33, No.6, June 1980, 201-248, the complete issue (and subsequent updates in *JBIS*).
3. E. F. Mallove and Gregory Matloff, *The Starflight Handbook: A Pioneer's Guide to Interstellar Flight*, John Wiley and Sons, New York, August, 1989.
4. E. F. Mallove, *Fire from Ice: Searching for the Truth Behind the Cold Fusion Furor*, John Wiley & Sons, 1991.
5. Edmund Storms (Los Alamos National Laboratory), "Review of Experimental Observations About the Cold Fusion Effect," *Fusion Technology*, 1991, Vol.20, December, 1991, pp.433-477.
6. T. Bressani, E. Del Giudice, and G. Preparata (editors), *The Science of Cold Fusion: Proceedings of the II Annual Conference on Cold Fusion*, June 29 - July 4, 1991, Como, Italy, published by the Italian Physical Society, Bologna, Italy, 1991, (528 pages).
7. Hideo Ikegami (editor), *Frontiers of Cold Fusion, Proceedings of the Third*

- International Conference on Cold Fusion (Nagoya, Japan 21-25 October, 1992),* National Institute for Fusion Science, Nagoya 464-01, Japan (698 pages).
8. Peter L. Hagelstein, "Summary of the Third International Conference on Cold Fusion in Nagoya," MIT Research Laboratory for Electronics report, January, 1993 .
  9. Martin Fleischmann and Stanley Pons, "Calorimetry of the Pd-D<sub>2</sub>O system: from simplicity via complications to simplicity," *Physics Letters A*, Vol.176, May 3, 1993, pp.118-129.
  10. A.B. Karabut, Ya.R. Kucherov, and I.B. Savvatimova, "Nuclear product ratio for glow discharge in deuterium," *Physics Letters A.*, Vol.170, November 9, 1992, pp.265-272.
  11. Robert T. Bush, "Cold 'Fusion': The Transmission Resonance Model Fits Data on Excess Heat, Predicts Optimal Trigger Points, and Suggests Nuclear Reaction Scenarios," *Fusion Technology*, Vol.19, March 1991, pp.313-356.
  12. S.K. Borowski, E.A. Gabris, J. Martinell, , R.J. Bohl, W.L. Kirk, R.R. Holman, D. Budden, A.E. Mensing, T.S. Latham, G.A. Beale, and T.J. Lawrence, "Nuclear thermal rockets: next step to space," a collection of articles by groups of the authors, *Aerospace America*, June, 1989, pp.16-29.
  13. S.K. Borowski, J.S. Clark, M.C. McIlwain, and D.G. Pellaccio, "Nuclear Thermal Rockets: Key to Moon-Mars Exploration," *Aerospace America*, July, 1992, pp.34-37, 48-49.
  14. Milton Klein, "Nuclear Rocket Propulsion - The Past Is Prelude," *Fusion Technology*, Vol.20, Dec., 1991, pp.693-697.
  15. R.J. Bohl, F.P. Durham, and W.L. Kirk, "Nuclear Rocketry Review," *Fusion Technology*, Vol.20, Dec.1991, pp.698-709.
  16. O.C. Jones, "Rotating Fluidized Bed Reactor for Space Power and Propulsion: A Status Report," *Fusion Technology*, Vol.20, Dec. 1991, pp.741-746.
  17. Dana R. Rotegard, "The Development of Space: The Economic Case for Mars," *The Case for Mars III: Strategies for Exploration - Technical*, Vol.75, Technology Series, Ed. by Carol Stoker, American Astronautical Society, 1989.
  18. W.E. Moeckel, "Comparison of Advanced Propulsion Concepts for Deep Space Exploration," NASA Technical Note TN D-6969, Lewis Research Center, September, 1972.
  19. David H. Atkinson and Owen Gwynne, "Design Considerations for a Mars Solar Energy System," *Journal of the British Interplanetary Society*, Vol.45, No.5,, May, 1992, pp.183 -194.
  20. J.R. French, "Some Unconventional Approaches to the Exploration of Mars," *Spaceflight*, Vol.33, February, 1991, pp.62-66.

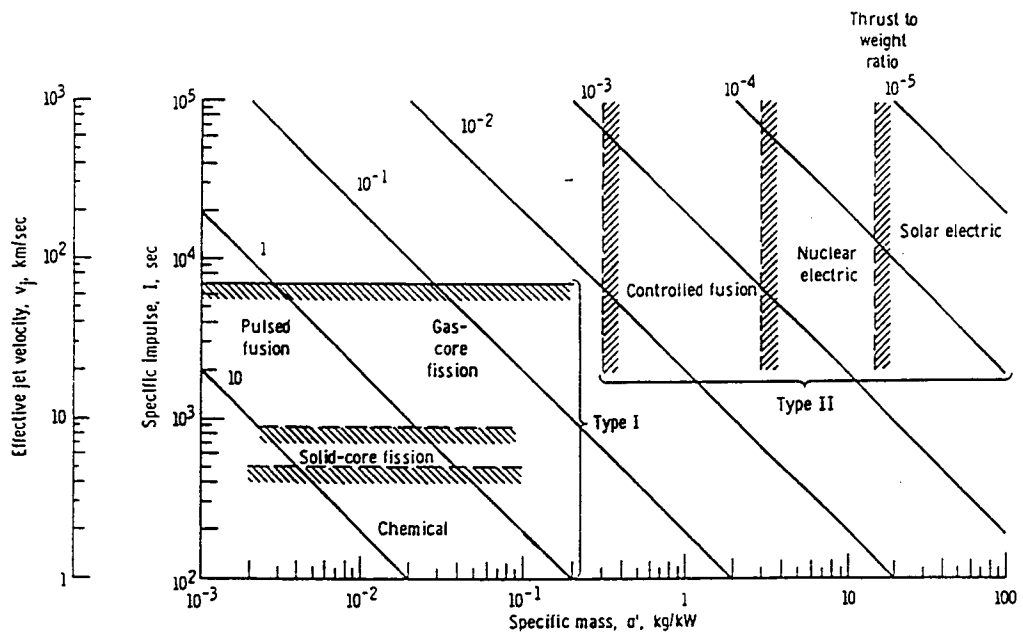


Figure 1. Rocket Propulsion Performance Parameters

From: W.E. Moeckel, "Comparison of Advanced Propulsion Concepts for Deep Space Exploration," NASA TN D-6968, September, 1972.

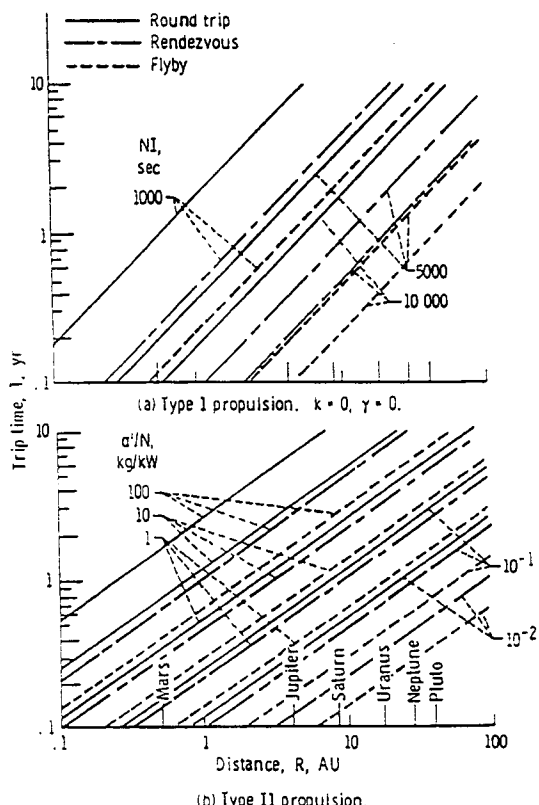


Figure 2. Interplanetary Distance Versus Trip Time

From: W.E. Moeckel, "Comparison of Advanced Propulsion Concepts for Deep Space Exploration," NASA TN D-6968, September, 1972.

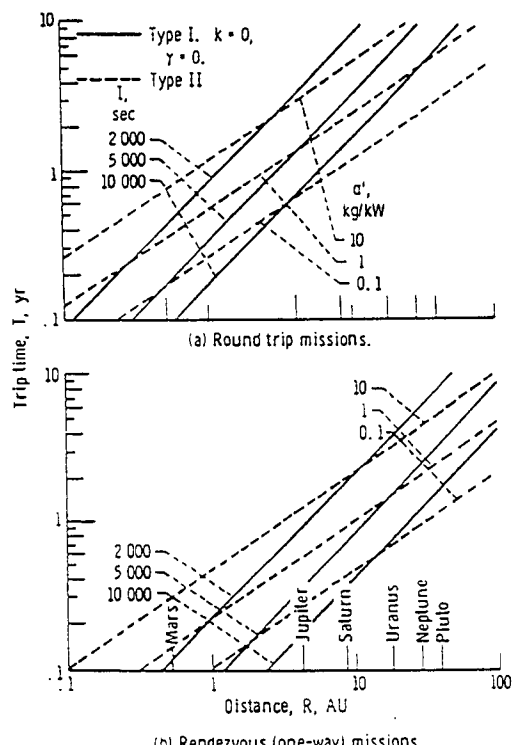


Figure 3. Comparison of Type I and Type II Propulsion for Planetary Distances.  $N = 1$ .

From: W.E. Moeckel, "Comparison of Advanced Propulsion Concepts for Deep Space Exploration," NASA TN D-6968, September, 1972.

## NEW PULSE GAS LOADING COLD FUSION TECHNOLOGY

K. B. Chukanov  
3520 West Old Bingham HWY  
Suite B, West Jordan, Utah 84088  
U.S.A.

### ABSTRACT

In the last few years the shadow of a new limitless and nonpolluting source of energy has begun to trouble the mind of scientists in the world - energy torn out from hypothetical "BLACK HOLES" and "PHYSICAL VACUUM", energy produced by so-called "Cold Fusion" and energy from "Ball Lighting". In the early 1980's my theoretical investigations begun to show me that some exotic objects exist in nature which do not obey the familiar laws of physics<sup>1</sup>. These exotic objects are liquid helium II, Cosmic rays, superconductivity, super rarified solutions, "dark" matter in the universe, quasars, ball lightning, Pons-Fleischmann effect and etc.

In this paper I am going to report on Space Energy ("Cold Fusion" would not be the right name for this phenomenon) theory, measurements and some practical applications.

Experiments were carried out on one Space Energy active material: magnet alloy SmCo<sub>5</sub>. My preliminary investigations have shown me that this alloy is best (point of view energy production) among other rare earth magnetic alloys.

Many scientists have investigated hydrogen absorption and thermal effects in rare earth metals and metal alloys<sup>2,3</sup>. However no one has ever carried out circumstantial thermal investigations on this field. But precisely these thermal measurements (change in the temperature of the metal alloys, calorimetry) are crucial in discovery of a new phenomenon "Space Energy".

### THEORETICAL MODELS

#### 1. Conventional (Type S. Pons - M. Fleishmann) "Cold Fusion".

The unusual property of some metals (Pd, Ti, Ni etc.) to absorb hydrogen from the environment is the basis of the "Cold Fusion" production. Palladium ions have fixed places within the palladium's metal lattice - they vibrate around a fixed position in

the lattice. On the other hand hydrogen nucleus (S. Pons and M. Fleischmann have used the heavy isotope of the hydrogen - deuterium) are relatively free. Palladium's metal lattice forces the hydrogen to behave like a metal too - hydrogen atoms give up its only one electron to the combined electron cloud.

"Cold Fusion" can be explained with the help of the Quantum Boundaries of the World"<sup>1</sup>, Fig. 1.

Let us see Fig. 1. In the initial phase of saturation, when density of hydrogen plasma in palladium's lattice is still low ( $R_{H-H} > R_{k,p,1}$ ), the assembly of hydrogen nucleus is far from the critical quanta point 1. Higher density, however, makes this critical quanta point come closer and closer. There are two options:

- the assembly of hydrogen nucleus may remain in the form of discrete matter.
  - transit to the form of material continuum (material continuum is a new form of matter<sup>1)</sup>)

A universal principle of nature is the tendency of the matter to preserve its initial state. The stronger is the external influence the fiercer is the resistance of the matter. Very important here, however, is the time limit which this external influences is exercised. If it is instantaneous, the material system upon which this influence is exercised has no time to react - the system jumps into another state (material continuum).

This is the mechanism according to which the plasma passes into the state of material continuum - ball lightning, described in some my works<sup>1</sup>.

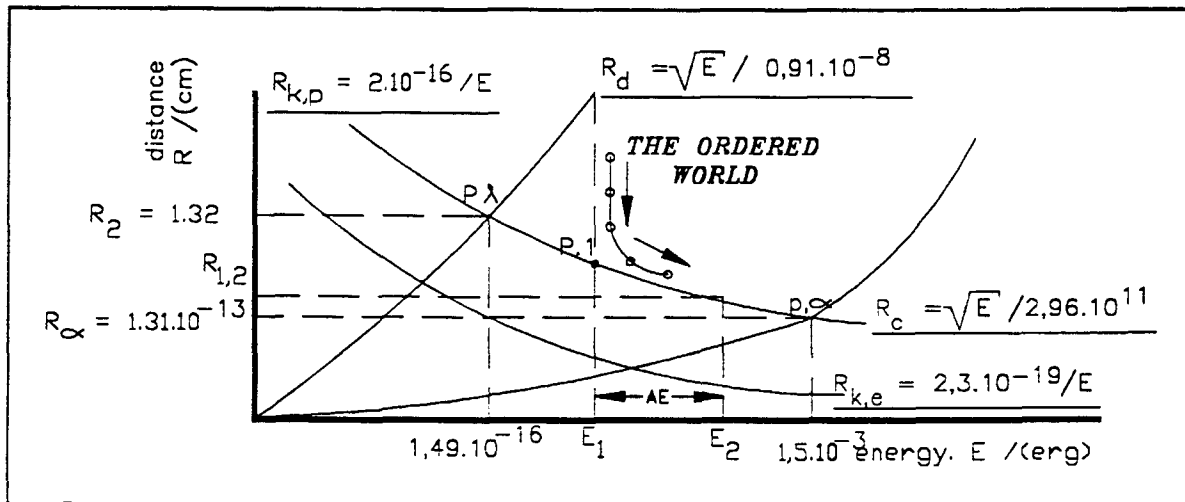


**Figure 1** Quantum Boundaries of the world

The mechanism of cold fusion is different from the mechanism of "Ball lightning". Hydrogen saturates the palladium lattice very slowly - the process continues for hundreds of hours. Hydrogen

nucleus in this case easily resist conversion into a material continuum at p.l in a manner very uncommon to the traditionally thinking scientist. To resist transition into material continuum hydrogen nucleus starts to oscillate and increase their energy in order to stay away from Quantum boundaries  $R_{k,p}$  and thus violate the law of conservation of energy. This increase of energy results into the mysterious excess heat in "Cold Fusion". This phenomenon however, has nothing to do with nuclear fusion. When the palladium electrode is fully saturated with hydrogen, then the kinetic energy of some hydrogen nucleus can reach few KeV.

This high kinetic energy of the hydrogen nucleus can lead to normal "hot fusion" in the case of using of heavy hydrogen (deuterium or tritium). If hot fusion happens it is only secondary process in "Cold Fusion" process. Hydrogen nucleus transfer their excess free energy to the palladium ions - i.e. the temperature of the lattice increases.

Let us analyse several possible nuclear reactions.



The basic principle of the nature to preserve its initial state is true for the unity of hydrogen nucleus. This principle is true for the unity of hydrogen nucleus. Reactions (1), (4) and (5) from above in fact don't lead to "devouring" of parts of hydrogen nucleus, and these reactions are most probable to occur. If we introduce the so-called "hydrogen charge" for every hydrogen ion "1", and for a nonhydrogen ion "0", reactions (2), (3) are unprobable to occur. "Cold Fusion" is accompanied by a very unusual phenomenon - chemical properties of the crystal metal lattice dominate the nuclear characteristics of atomic nucleus.

## 2. Space Energy

The space (volume) which can occupy gas or plasma particles is limited by the quantum boundaries of the world, Fig.1. Properties and behavior of the space-material continuum are described in detail in my book "Quantum boundaries of the world".<sup>1</sup> In this paper I am going to explain very shortly the problem of the space energy generation from the space-material continuum.

Until now contemporary science knows only about the first form of the matter - its discrete form (matter composed by individual particles). Individual particles (elementary particles, nucleus, atoms, molecules,...) interact with each other by means of some material forces - material fields (strong, weak, electromagnetic and gravity) or material particles-mediators of substance, energy and information.

Let us consider the case of the assembly of hydrogen molecules contained in a chamber. Fig.2

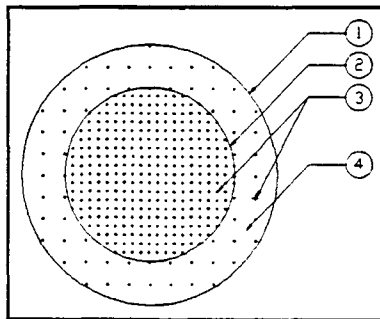


**Figure 2 Space-material continuum of hydrogen gas**

- 1 - Chamber with hydrogen gas volume -  $V_1$ ; pressure -  $p_1$ ; temperature -  $T_1$ ; density -  $n_1$ .
- 2 - Compressed hydrogen gas volume  $V_2 << V_1$ ; pressure -  $p_2$ ; temperature -  $T_2$ ; density -  $n_2$ ;  $n_2 >> n_1$ .
- 3 - Hydrogen molecule (atom).
- 4 - Second face of the hydrogen atom assembly: material continuum - space.

The assembly of hydrogen molecules (or atoms) occupies some volume of the space- $V$ . This space is not empty space (nothingness), but it is a special form of matter-material continuum. The material continuum is strongly personal for the assembly of hydrogen molecules (atoms). This material continuum has nothing to do with any other material continuum which may occupy the same geometrical space. Within this space (material continuum) the individual particles lose their individuality, as if they are dissolved and form an nonstructural liquid.

From thermodynamics we know that if some gas collapses, its temperature will raise and vice versa - if this gas expands, its temperature will drop. This phenomenon is used in refrigerators to create a cold. Material continuum is not simply "nothing", but it is matter. In order to create this matter we need to spend some energy, simultaneous with the collapsing of the space-material continuum produces some energy. Normally energy for creation (or annihilation) of the space-material continuum is taken (or given) from the surrounding media (from the walls of the container, for example). However if there is some drastic and very fast change of the parameters of the assembly of the particles, there will not be enough time for exchange of energy with the surrounding media. In this case Law of Energy conservation could be violated. The transfer of energy between the walls of the gas container and the

gas particles takes some time which is limited by the laws of thermodynamics. If the process of collapsing of expanding of the space-material continuum is a very rapid process (very drastic change of the density of the gas particles in short time) then laws of thermodynamics could be violated.

We know so-called "Cazimir effect" - two plates cooled in a vacuum attract each other. Cazimir assumed that no gases were present to push on the plates, that they were cooled enough for thermal radiation to be negligible, that they were both electrically neutral, and that their mutual gravitational attraction was too small to matter. In short, that there was nothing (point of view classical physics) to cause a force of attraction between the plates. According to Cazimir (and other scientists also) the cause of the mutual attraction between the plates are some fluctuations in the physical vacuum-space. These fluctuations that exist outside the plates would be excluded from the gap between them. Fig. 3

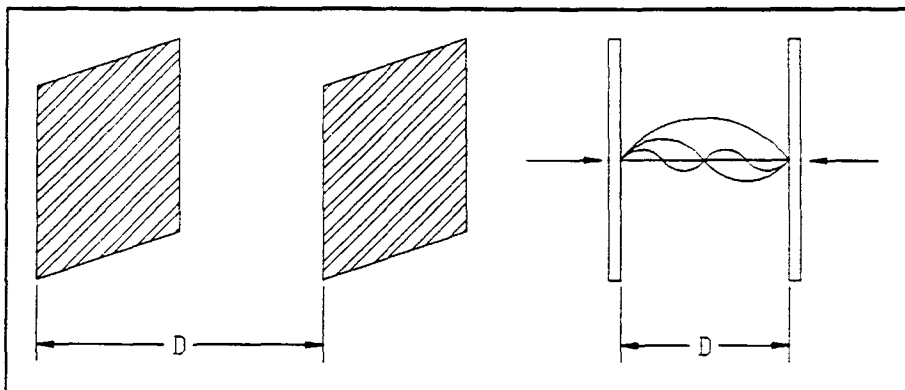


Figure 3. Scheme of Cazimir's experiment

The cause of this mutual attraction however, is not some mystic exchange of impulse between the virtual particles of the vacuum waves as contemporary scientists believe. The main thing is that if the space between the two plates is cooled down then this space collapses i.e. the two plates approach each other. There is no possibility of fast exchange of impulse between the particles of the gas and the plates (or walls of the vacuum chamber). The Law of conservation of energy is violated in this particular case.

#### EXPERIMENTS AND RESULTS

Demagnetized metal alloy SmCo<sub>5</sub> (16-18 % Sm) manufactured by Hitachi was investigated for Space Energy generation. The metal alloy were saturated by light hydrogen gas (not necessarily high purity).

1. Investigation concerning the mechanism of the Space energy generation.

Experimental set-up is shown on Fig. 4.

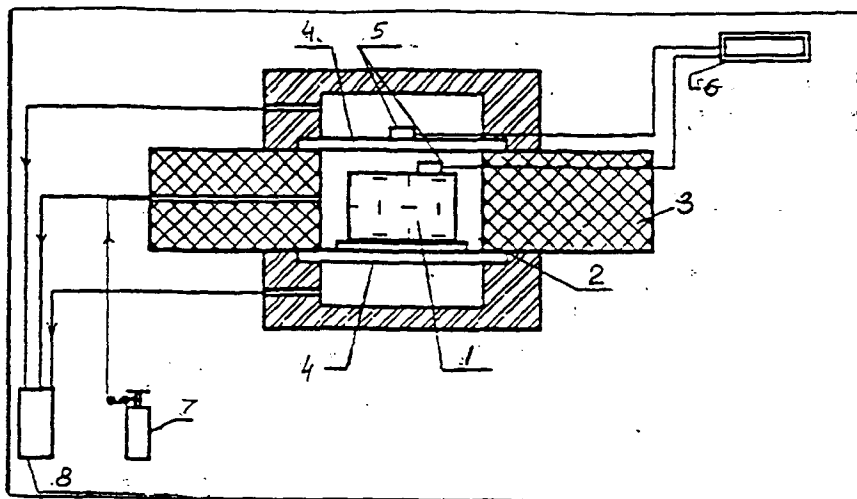


Figure 4. Alloy ( $\text{SmCo}_5$ ) experiment.

- 1 - $\text{SmCo}_5$  sample;
- 2 -hydrogen gas;
- 3 -gas chamber;
- 4 -stainless steel membrane ( $d = 1\text{mm}$ );
- 5 -thermistor prob;
- 6 -thermistor thermometer;
- 7 -gas container;
- 8 -vacuum pump

Experiments were carried out in the following way. In order to evacuate the air from the gas chamber and from the metal lattice of the  $\text{SmCo}_5$  sample the vacuum pump were run for about 2 hrs. The  $\text{SmCo}_5$  initially has an oxide coating which tends to block hydrogen absorption. A high pressure ( $P > 8\text{atm}$ ) during 2-8 hours (this time depends on the degree of oxidation of the  $\text{SmCo}_5$  surface) is needed to destroy this oxide film, making direct contact between the hydrogen gas and the metallic surface. After the stage of activation the  $\text{SmCo}_5$  sample generates small amounts of free space energy - temperature measured by thermometers (5) raise  $3-6^\circ\text{C}$ . Rapidly volumetric saturation of the metallic lattice of the alloy leads to fast achievement of the quantum density (Fig. 1). The assembly of the hydrogen nucleus receives part of its excess energy from the metal lattice and another part from the violation of the Law of conservation of Energy. In fact, we measured the temperature of the system "alloy-hydrogen". Calculations based on Quantum Boundaries of the World show that some of hydrogen nucleus can pick a lot of energy (few KeV) because of the violation of the Law of Energy conservation. These fast hydrogen nucleus break the  $\text{SmCo}_5$  sample down into an assembly of tiny particles. Destruction of the alloy lasts less than 1 sec. During this destruction - explosion we observed the following phenomena - very fast decrease of the temperature of the alloy ( $5-10^\circ\text{C}$ ) and very fast (1 sec)

raise of the temperature in the upper stainless steel membrane. Obviously the source of heat yielded to the upper membrane was the alloy itself. On the other hand, energy transfer was accomplished by a way very different from the energy transfer between two heated bodies. The only possible explanation of this phenomena is the following. During the destruction of the SmCo<sub>5</sub> sample a very powerful flow of fast hydrogen nucleus leaves the metal lattice (i.e. its temperature drops) and bombards the membrane (i.e. their temperature raise). This experiment is good illustration of the mechanism of Space energy generating.

## 2. Energy Measurements

The Thermal effects which occurs during hydrogen loading and unloading of the SmCo<sub>5</sub> alloy were investigated long before my experiments<sup>2,3</sup>. These experiments however, are performed in order to prove a prior accepted as a true chemical origin of these thermal effects. For example, the authors of this work measured the amount of the energy produced and the amount of absorbed hydrogen during the process and calculated the energy range of the "chemical reaction" - about 7.2 Kcal/mole. Authors have no direct proof (spectroscopic or other chemical analysis) about the formation of hydrates. They haven't performed calorimetry (for a long enough period) or another necessary thermodynamical measurements. Our investigations were much deeper. One of our set-up is shown on Fig. 5.

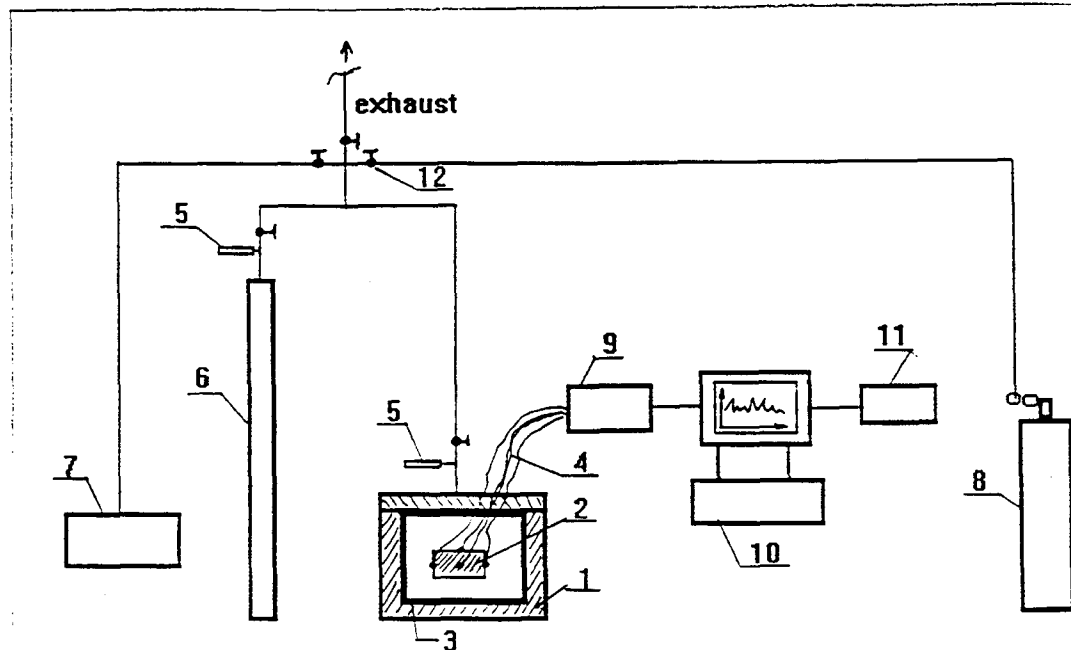
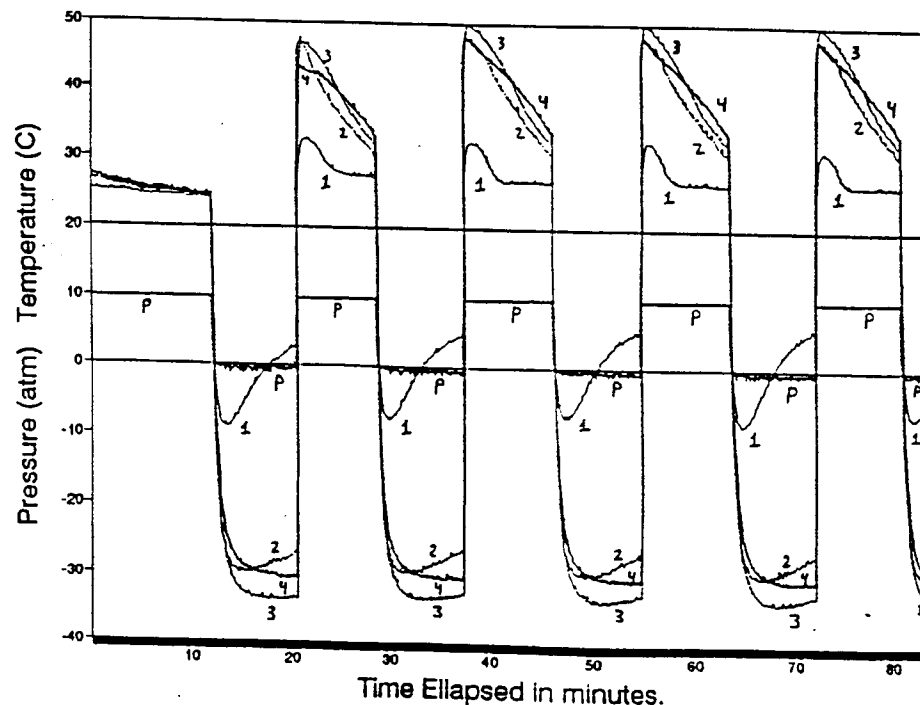


Figure 5. Energy measurements set-up.

- 1 - gas chamber; 2 - SmCo<sub>5</sub> sample; 3 - thermoinsulation;
- 4 - thermocouples;
- 5 - sensitive pressure transducer; 6 - copper tube chamber;
- 7 - vacuum pump;
- 8 - gas hydrogen container; 9 - data acquisition;
- 10 - computer; 11 - printer; 12 - manual valves.

After the stage of activation of the SmCo<sub>5</sub> alloy (destruction of the oxide layer) we realized a pulse regime of loading and unloading of the hydrogen in the metal lattice -few minutes pressure ( $P > 8\text{ atm}$ ) followed by a few minutes of vacuum ( $p \approx 2\text{ atm}$ ). The speed of the change of the pressure (or the speed of loading and unloading) is crucial in this process - greater the speed, higher the change in the temperature of the alloy. If we decrease the speed of change of the pressure we reach some critical speed for which the thermal effect disappears totally. This fact disproves the chemical origin of the thermal effect. On Fig. 6 are shown the plots of temperature of the alloy and the plot of the pressure in the gas chamber 1 (Fig. 5). Within only 1 sec. the temperature of the sample change 80-90 °C. The power realized during this time is several KW! If after long period of vacuum (i.e. there is no hydrogen in the metal lattice of the SmCo<sub>5</sub> alloy) we realize cycles of pressure and vacuum, then the temperature of the alloy becomes -30 to -40°C (during the stage of vacuum). This experimental fact disproves the chemical hypothesis too, because the starting (room temperature) and the final temperature of the alloy have to be equal in the case of chemical origin of the thermal effect.



**Figure 6. Plots of the temperatures of the alloy.**  
**p - pressure of the gas;**  
**1,2,3,4 - temperature of the alloy.**

The kinetics of hydrogen absorption and the energy range of the process were performed in the same experimental set-up (Fig. 5). At the beginning of the experiment the copper tube chamber were filled with hydrogen gas ( $p=30-45\text{ atm}$ ), while the gas chamber was vacuumed ( $p \approx 2\text{ atm}$ ). After that the valves between both chambers

were opened and the pressures were equalized. A free space Energy generating of about 1.2 ev/hydrogen atom was calculated in this experiment. The hydrogen density in the metallic lattice of the alloy SmCo<sub>5</sub> was calculated  $n = 2.5 \times 10^{23}$ , cm<sup>-3</sup>. This density is close to the density of pure liquid or solid hydrogen.

## TECHNICAL APPLICATIONS

The property of the rare earth metals to absorb greedily the hydrogen is used for some technical application: hydrogen storage; hydrogen purification; heat pumps; air conditioning units; etc. In our company "Space Energy L.L.C." we have created several prototypes of Space Energy generators. Our over 20 Kw Space Energy generator incorporates a gas booster that recycles hydrogen during a long period. The generator has a capacity to cycle about 150 L of water in either hot, or cold cycles. The power consumed by the system of recycling of hydrogen gas (this power is input power) is 3.7 KW.

The goal of the company Space Energy L.L.C. is to create a varieties of industrial prototypes of generators: household generators, condominium size generators, individual production plants, or much greater generators feeding energy to whole cities and countries. Air conditioning, refrigeration, heating, electricity production, computer I.C. manufacturing field, cars, airplanes, and beyond.

## CONCLUSIONS

The results obtained from the SmCo<sub>5</sub> and pulse gas loading technology investigated here indicate beyond any doubt that the origin of the observed thermal effects is not either chemical or nuclear. For the first time in the history of science were observed "anti-energy" (like "antimatter"). Theoretically it is proven the existance of a superheavy isotope of the hydrogen <sup>4</sup>H<sub>1</sub> (fortium). Space Energy is a new source of clean, safe and limitless energy.

## ACKNOWLEDGMENTS

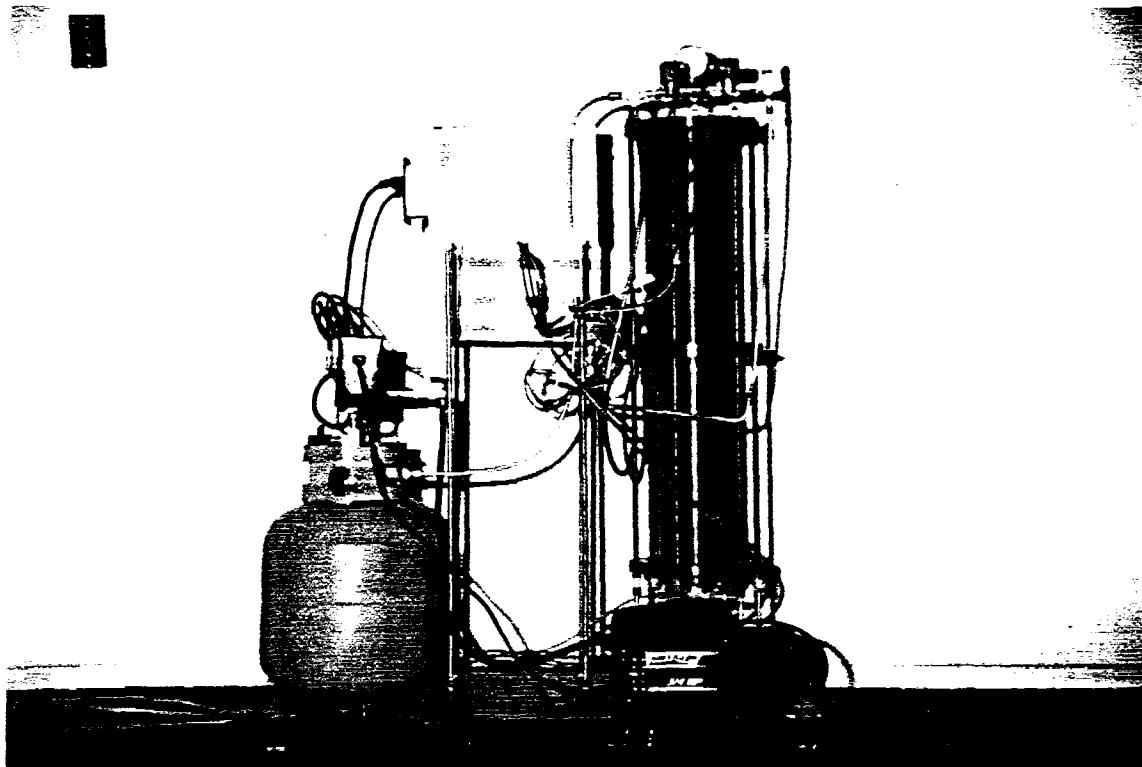
The author would like to thank Joe Johnson, and Dwayne Watson for their financial and technical support. Special Thanks to my wife Angelina who has helped me a lot all these years of hard research, success and failures, doubts and hopes.

## REFERENCES

1. Kiril B. Chukanov, *Quantum Boundries of the World*, Upcoming publication in English, 1993, 1-350 pp [book]

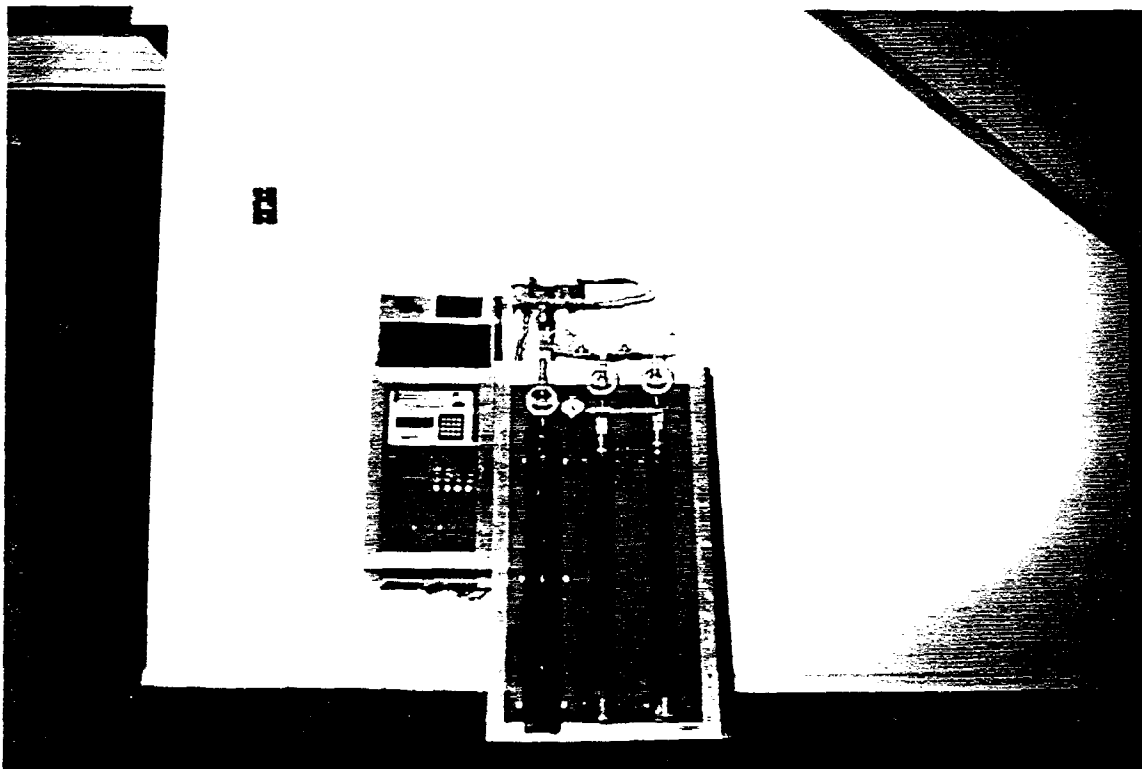
2. Joel S. Raichlen and Robert H. Dovemus. *Kinetics of hydriding and allotropic Transformation in SmCo<sub>5</sub>*, Journal of applied physics, volume 42, number 8, pp 3160-3170. New York, 1971 [magazine article]
3. J.H.N. Van Vucht, F.A. Kuijpeus, and H.C.A.M. Bruning, Phillips Res. Repts. 25, pp. 133 1970 [magazine article]

## DOUBLE CYLINDER TEST CHAMBER



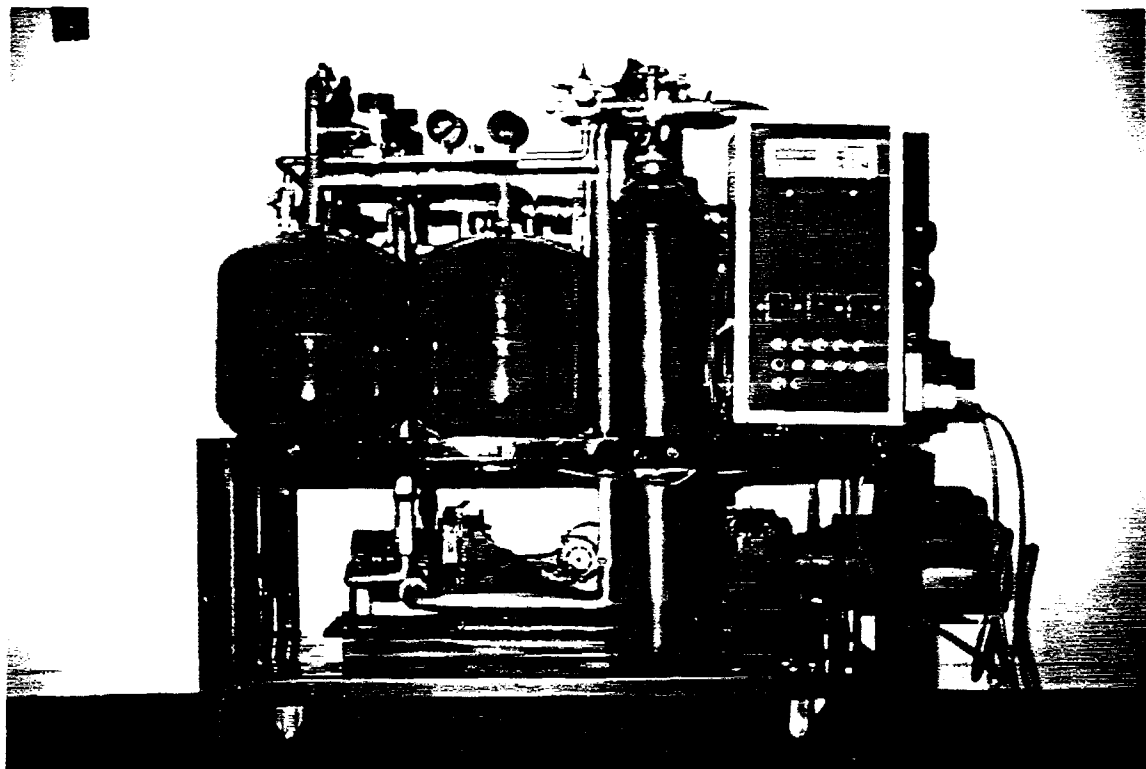
The double cylinder uses the same hydrogen over and over indefinitely by pressurizing and acuuming the test chamber using the motion of the cylinders. The piston is moved by air pressure from a small compressor.

## COMPUTERIZED ENERGY RANGE TEST UNIT

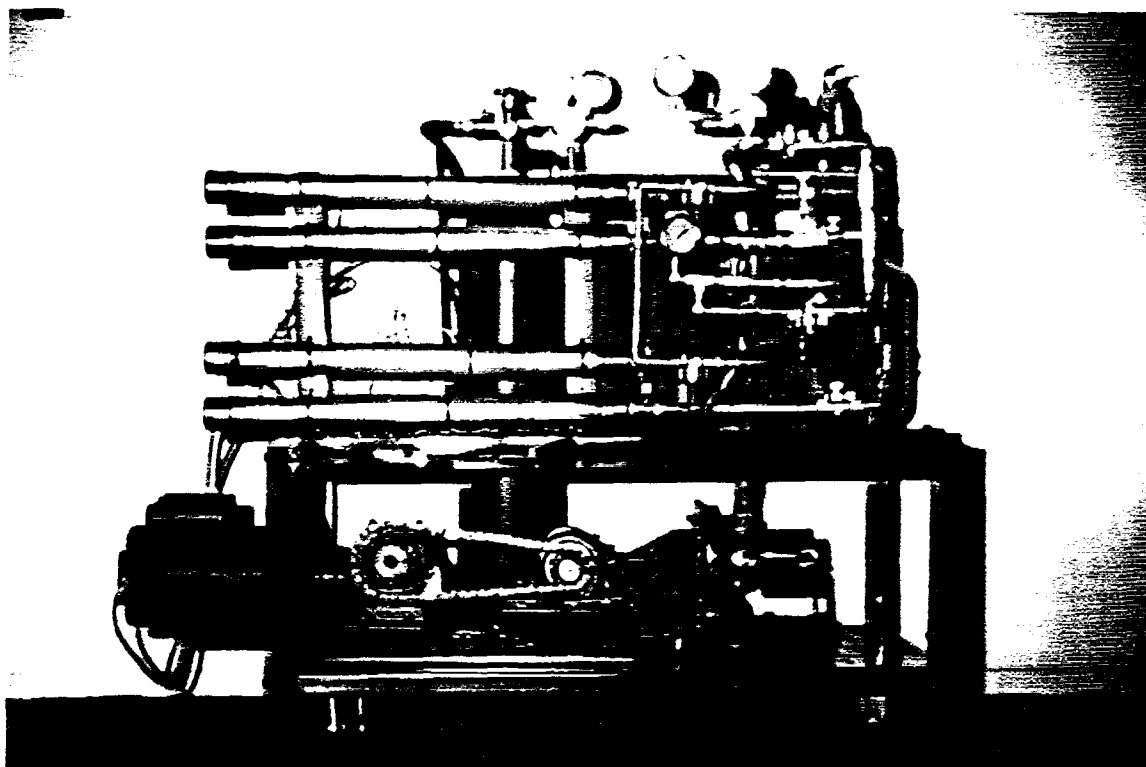


Precise calculation can be made using computerized pressure and temperature readouts.

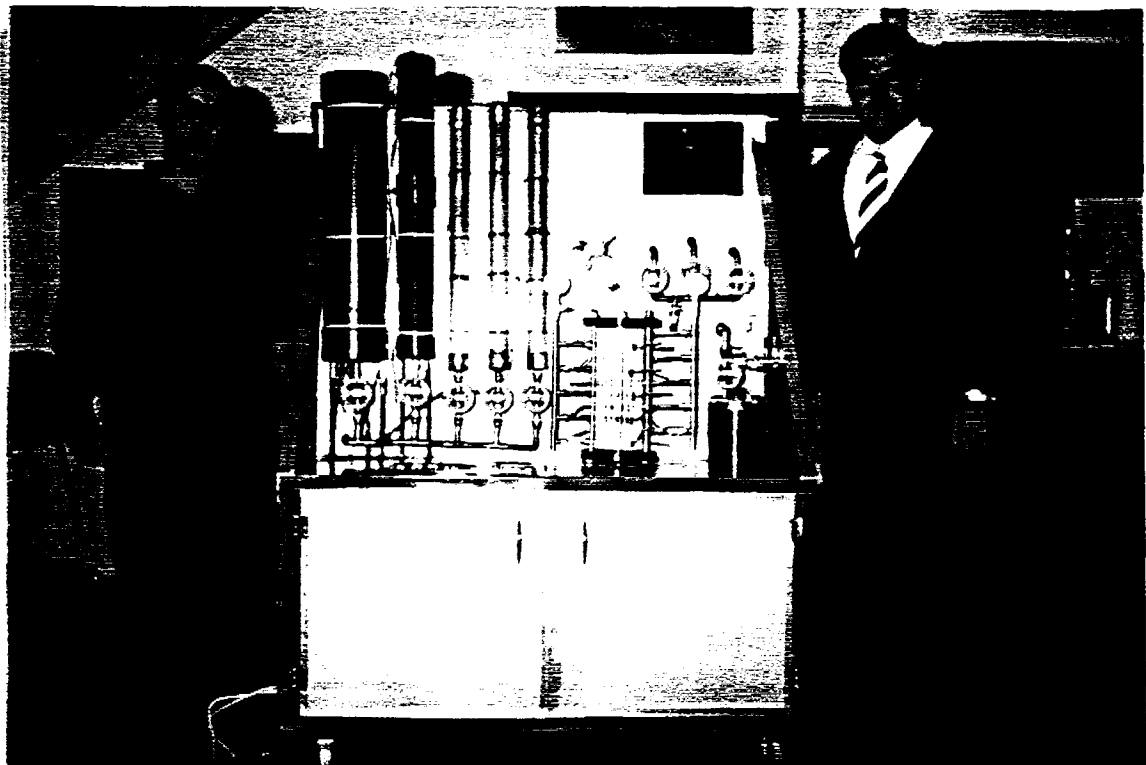
# SPACE ENERGY GENERATOR



*This Space Energy prototype incorporates a modified gas booster hydrogen recycling system. The unit functions automatically using timers and solenoid valves. The recycling system uses less than 1.5 Kw while the 4 Space Energy bars produces about 8 Kw radiant energy.*

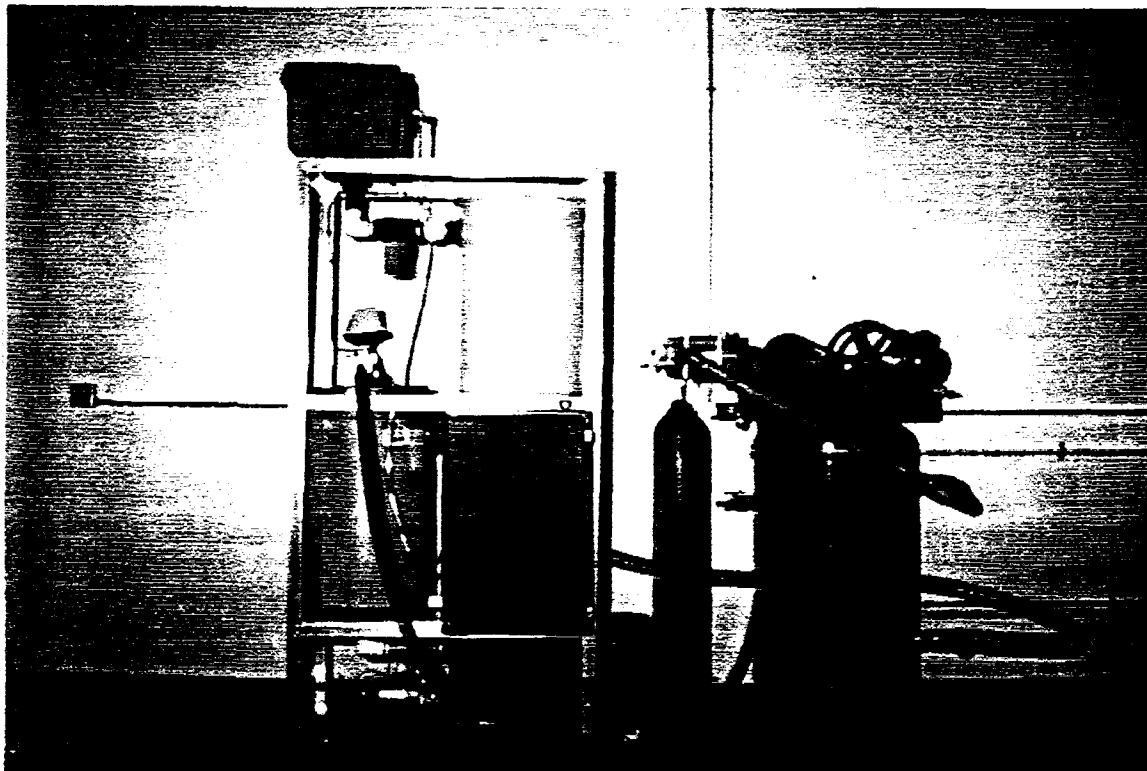


## MULTI-STAGE CALORIMETRIC AND TEST CELL



*With this multi test cell: calorimetric electric and sample test can be independently made with computer precision.*

## LARGE SPACE ENERGY GENERATOR



*The over 20 Kw Space Energy generator incorporates a modified gas booster that recycles hydrogen to up to 78 Space Energy bars. The system has the capacity to cycle 40 gal. of water through the system in either hot, or cold cycles. The system can operate in either full automatic or in manual 36-*



## CHEAP ELECTRIC POWER FROM FUSION?

R. A. Cornog  
Independent Consultant  
2242 20th Street, Suite 4  
Santa Monica, CA 90405

### Abstract

The projected costs of producing electric power in a thermal power plant using fusion as the source of energy are evaluated and compared with the cost of other power sources.

Fuel costs in contemporary fission-fueled nuclear plants are about one-third those in chemically-fueled power plants. Since--with one exception--the same favorable balance is projected for fusion-fueled power plants, the savings in fuel costs can be applied to offset possible increases in other cost components.

In both thermonuclear and cold fusion-powered plants, part of the electric power output must be diverted to run the plant. In both cases, unless the heat output of the fusion device is more than about 10 times the required electric power input, the resultant overall plant efficiency will suffer badly, and the cost of the residual useful portion of the electric power output may become too high to be competitive.

Cost penalties resulting from adverse environmental impact factors are increasing, whether to cope with sulphur dioxide and nitrous oxides found in the exhaust stack gases from fossil fuel plants or with the noxious neutron-induced radioactivity produced during the operation of fission power plants. Similar concerns are projected to accompany thermonuclear fusion power plants. In this area, cold fusion power plants may have a tremendous advantage, for some forms of cold fusion have been reported that are largely unaccompanied by the production of neutrons and induced radioactivity.

### Objective

The generation and sale of electric power is an important industry in the United States. Each year, about three trillion kilowatt hours of electric power are generated and sold in the United States. To survive in this market place, any new source of power must deliver electric power to the grid at a competitive price.

The probable unit costs of delivering electric power to the grid are discussed in this study. Both hot and cold fusion power plants are considered. Then, using the same methods of evaluation, these costs are compared with the costs of electric power produced by fossil-fueled plants and in plants powered by nuclear fission.

## **Methodology**

A commonly used method of projecting the cost of electric power from a D-T fueled Tokamak reactor has been described by Stephen Schulte et al.<sup>1</sup> To apply this method, one needs a detailed knowledge of the costs of all the elements and components of the plant, as well as a lot of information about other relevant cost categories such as tax rates, funding costs, fuel costs, expected plant life, etc.

This method and closely related methods have been widely used in projecting the cost of power from hot fusion power plants. Calculated results for various Tokamak designs range from 4 cents to 11 cents per kilowatt hour.<sup>2</sup> However, at present, this method is not yet applicable for use in computing the cost of electric power from cold fusion power plants. Almost all of the input data needed to calculate the cost of power from such a plant are non-existent at this time. So let's back off and take a fresh look.

A much simplified version of this method has been used in this paper. The costs of producing electric power have been divided into three components. One component is the cost of the fuel consumed, be it fossil or nuclear in origin. A second component is the fixed costs. Here the fixed costs include such items as interest on borrowed capital, depreciation, maintenance and repair, labor, taxes, insurance, profit, etc. It will be found the fixed cost of power plants, both fossil-fueled and nuclear-fueled, works out to be about 2.8 cents per kilowatt hour for each \$1000 of construction cost of each kilowatt of plant capacity. Thus, the fixed costs are assumed to be directly proportional to the construction costs. A third component, of increasing importance for both chemical and nuclear fueled plants, is the added costs caused by the environmental impacts attendant to the plant operation and (especially for nuclear plants) the added safety measures needed to reduce the probability of nuclear accidents.

## **Nuclear Power Plants: Fission Fueled**

A review of the development of fission-fueled power plants may provide insight into how fusion-powered plants could be developed and insight into the economics of their operation.

Uranium-fueled nuclear reactors were developed in the Untied States during World War II. They were used to produce the plutonium used in atomic bombs. In operation these reactors generated enormous amounts of heat; copious water cooling was required.

Could this source of heat be used to replace the burning of fossil fuels in electric power plants? I asked myself this question in 1944 while I was a senior staff member at Los Alamos. Accordingly, I compared the performance of two steam-powered electric power plants, one using a fission-fueled nuclear reactor as a source of heat, the other using a coal-fueled boiler. (See Figures 1 and 2.)

In 1944, roughly half the cost of generating a kilowatt hour of electricity in a coal-fired steam plant was the cost of the fuel consumed. The other half was mostly the fixed costs of

running the plant. I assumed that the fuel costs in a uranium-fueled plant would probably be trivial compared to the fuel costs in a coal-fired plant. On the other hand, I supposed also that a nuclear plant might be more expensive to build and operate than a coal-burning plant. The fixed costs would thereby also be increased. Now, suppose that all the money saved in fuel costs were applied toward paying these increased fixed charges. It would then follow that if these fixed costs of a nuclear plant were less than twice those of a competing coal-burning plant, the total cost of producing power in the nuclear plant would be less than the cost of producing power in the coal-burning plant. Since the construction cost of a coal-burning plant at that time was believed to be about \$150 per kilowatt of capacity, it followed that if uranium-fueled plants could be built for less than \$300 per kilowatt of capacity, they would be cost-competitive and economically viable.

Now let's see what happened. Table 1 tells the story.

It is seen that nuclear plants completed in the early 1970's did indeed cost less than \$300 per kilowatt to build. In addition, the fuel costs of the nuclear plant were less than one-third the fuel costs of the coal-burning plants. Thus, both the two enabling assumptions were largely realized. Power from these newly built nuclear plants was significantly cheaper than power from competing conventional coal-fueled steam plants. In other words, based on these two simple assumptions, it was correctly projected that the cost to produce electric power from uranium-fueled plants would be cheaper than power from contemporary coal-fueled plants.

## Environmental Considerations

So far, so good. For plants completed in the early 1970's, nuclear power was indeed cheaper than coal power. But what happened next? People began to worry about the possible environmental dangers of accidents in nuclear plants and radiation exposure. Also, there were (and are) serious problems attendant to the disposal of radioactive spent fuel elements.

The result? Again, as shown in Table 1, by the middle 1980's, the costs of completed nuclear plants had increased by a factor of 10 or more compared with costs of those completed in the early 1970's. As a result, despite substantial increases in the costs of fossil-fueled power, the cost of nuclear power in this country was no longer cost-competitive. This cost disparity has continued to the present time.

In France it's been a different story. There, today, more than 70% of their electric power is being generated in fission-fueled nuclear plants. At the end of May, 1993, the French Industry Ministry reported that (assuming 5.8 francs per dollar) power was being produced in nuclear reactors at costs ranging from 4.2 - 4.5 cents per kilowatt hour, and about 20% (or more) cheaper than power from fluidized bed coal plants or natural gas combined cycle turbine generators.<sup>3</sup>

The present American bias (1993) against uranium-fueled power plants goes far beyond the mere question of the relative costs of producing electric power. It is probably true that any

power plant that is not perceived as being environmentally benign will carry a crippling political handicap. This factor has come to weigh heavily against the choice of any power source that is seen to impact our environment adversely. For example, more and more coal-burning plants are using fluidized bed combustion of coal to reduce sulfur dioxide emissions. The added cost is about \$300 per kilowatt of plant capacity.

### Nuclear Power Plants: Fusion-Powered

But what about fusion power? Conceptually, controlled nuclear fusion can be used as a source of heat to generate electric power. At present, fusion power seems to be coming in two distinct forms, thermonuclear or hot fusion, and so-called cold fusion. In thermonuclear fusion, a hot plasma is heated to temperatures and a pressure sufficient to overcome Coulomb repulsion and allow the reacting nuclei to get and remain close enough together to fuse. Large amounts of nuclear energy are released in the process. The D-T reaction is usually assumed. (See Figures 3A and 3B.) However, more recently the D-He3 reaction has been considered. (See Figure 4.)

In cold fusion, the other known form of controlled nuclear fusion, the energy-releasing fusion process appears to be catalyzed by conditions obtained within the atomic lattice of certain metals -- as, for example, palladium. (See Figure 5.)

### *Some Numbers*

In the vast majority of reports of excess heat produced in cold fusion cells, the magnitude of the excess is observed to be smaller than the input electric power required to actuate the cell. To date, the same sort of thing is observed in thermonuclear fusion experiments. In fact, only recently has the excess reached zero, i.e., a break-even condition has been obtained.

In order to be of any practical interest for use in the large-scale generation of electric power, the heat energy output of any fusion heat source must be much larger than any electric energy input that may be required. Start with a reference steam cycle as proposed for use in a fusion power plant. In a steam plant of modern design and with a top steam temperature of 664 degrees Fahrenheit and a condenser temperature of 104 degrees Fahrenheit, one might hope for a thermal efficiency of about 31%. (See Figure 6.)

Now suppose that in the same steam plant, and using the same operating temperatures, part of the electric power output is bled off to actuate a fusion-powered heat source, be it either thermonuclear fusion or lattice-assisted cold fusion. The overall efficiency of the plant will thereby be reduced. For example, suppose that the thermal output of the fusion cell is five times its electrical energy input. Then, as shown in Figure 5, the thermal efficiency of the reference plant will be reduced from 31% to a bit over 11%. Under these circumstances, to maintain a given net electrical output, the size of both the fusion heat cell and the matching steam-powered portion of the plant must be increased by the ratio of 0.31/0.11 (i.e., almost 3 times). Put differently, even if the fuel is free, the size--and fixed costs--of the heat engine portion of the

"11%" plant required to produce a given electrical output is likely to be almost three times that of the "31%" plant.

The same increase, a factor three, applies also to the relative fuel costs. Thus, other factors remaining fixed, the amount and cost of the fuel used in the "11%" plant will be three times that of the "31%" plant.

### *Conclusions (Fusion-Fueled Power Plants)*

1. In order to be commercially attractive for use as a heat source in producing electric power, a fusion-powered heat source--be it thermonuclear or cold fusion--must produce an output heat energy that is a substantial multiple (say 10 times or more) of any electric energy input that may be required for its operation.

Conn et al<sup>4</sup> suggest that N lies in the range of between 5 and 10 in most conceptual designs for Tokamak plants. As shown here, values of N as low as 5 can have a disastrous effect on the costs of the electric power output.

2. If acceptable thermal efficiency is to be obtained in a steam plant powered by a fusion device, a working temperature of at least several hundred degrees Celsius will be required.

#### *Notes:*

It has long been suggested that the limits on thermal efficiency imposed by the Rankine Cycle can be avoided. Thus, the fuel cell--even while operating at modest temperatures--can convert chemical energy into electrical energy at efficiencies of 60% and more.

Likewise, from time to time during the last fifty years, several different methods of converting nuclear energy into electrical energy without using a thermal heat engine cycle have been proposed.<sup>5</sup>

## **Economic Viability: Coal-Fired Steam Plant**

### *Background*

In most locations in the United States, coal is the cheapest available fossil fuel to use in a steam power plant.

The practical limit on peak steam temperature is somewhat less than 1200 degrees Fahrenheit (649 degrees Celsius). Because of this temperature limit the maximum practical thermal efficiency obtained in a steam plant is about 38%.

### *Cost of Electricity*

Fixed costs, based on a construction cost of \$1300 per kilowatt for the plant, are about 3.6 cents per kilowatt hour.

Fuel costs are about 1.9 cents per kilowatt hour.

Thus, the total costs of electricity is about 5.5 cents per kilowatt hour.

### *Environment*

Frequently, the stack gases from steam power plants contain, in addition to carbon dioxide, objectionable amounts of nitrous oxides, sulfur dioxide, and fly ash.

These problems can be much reduced by the installation and operation of stack gas scrubbers and fluidized bed combustion. These additions add about 25%, or more, to the cost of the output power.

## **Economic Viability: The Steam-Injected Gas Turbine (The Cheng Cycle)**

### *Costs*

In unit sizes ranging from 100 megawatts to 300 megawatts capacity, steam-injected gas turbine plants can now be built for about \$500 per kilowatt.<sup>6</sup> The fixed charges are then slightly less than 1.5 cents per kilowatt hour. When burning natural gas costing \$2 per million Btu, and at a thermal efficiency of more than 50%, the fuel costs work out to be about 2 cents per kilowatt hour. Thus, the total cost of producing electric power is about 3.5 cents per kilowatt hour -- much cheaper than power from a coal-fired steam plant.

### *Environment*

The sulfur compounds in the natural gas fuel, primarily hydrogen sulfide, are removed by condensation prior to combustion. The formation of nitrous oxides during combustion is reduced to 5 or 6 parts per million by the steam injection.

### *Summary*

At 3.5 cents per kilowatt hour, the steam-injected gas turbine will produce electric power cheaper than almost all other presently available heat-powered devices<sup>7</sup>. It follows that as long as assured supply of natural gas remains available at an acceptable cost, gas turbine plants using the Cheng cycle will continue to be built in preference to both the conventional steam plant and most of the projected fission-fueled nuclear plants.

## **Economic Viability: Plants Powered by Nuclear Fission Reactors**

Cost projections for power from nuclear fission reactors have been extensively studied by Bernard L. Cohen and are reported in his book.<sup>8</sup> In his Table 1, page 169 (see Table 1), he projects future costs of fission power at 4 cents per kilowatt hour. He also describes plants that are designed to be significantly more resistant to accidents and malfunction than any plants existing today. Using the same methodology, he projects:

1. The total cost of power from coal-burning plants to be 4.8 cents per kilowatt hour.
2. Projected fuel costs for the nuclear fission plant to be 0.64 cents per kilowatt hour.
3. Fuel costs for the coal-burning plant to be 2.1 cents per kilowatt hour.

Most recently it has been proposed that substantial reductions in the cost of fission power (to about 3 cents per kilowatt hour) could be obtained by using reactor heat to power a closed cycle gas turbine, rather than the traditional steam plant.<sup>9</sup>

## **Economic Viability: Thermonuclear Fusion**

A number of cost studies have been made to project the cost of thermonuclear power. In most of them, the D-T reaction was assumed. This reaction has a vexing drawback. Most of the energy released is in the form of 14.3 mev neutrons. The resultant fast neutron flux causes severe physical deterioration in structural materials. This problem is especially plaguing in the wall separating the reaction volume space from the surrounding lithium blanket (the "first wall"). According to most current planning for D-T reactors, the entire plant must be shut down periodically while the first wall is replaced -- not a simple task. Note that these enforced shutdowns increase the fixed cost component of the electric power produced.

The neutrons have another vexing property. In addition to structural deterioration, the neutrons induce radioactivity in practically all the structural materials that are used in building the plant. As a result, even with a sophisticated choice of building materials, the plant structure will remain seriously radioactive for some time after the power is turned off. Consequently, even though power costs ranging from 4 cents to more than 10 cents per kilowatt hour have been projected for the D-T reaction, the environmental and political considerations remain a serious drawback.<sup>10</sup>

Environmentally, there may be a more attractive option than using the D-T reaction. As early as 1962, R.F. Post suggested using the D-He3 fusion reaction rather than the D-T reaction. The D-He3 reaction, in itself, does not produce any neutrons, only charged particles. (There are still 2.4 mev neutrons produced in the parasitic D-D reaction. However, by burning deuterium lean, the total neutron output can be reduced up to a hundred-fold compared with the D-T reaction.) There remains only one big question: Where do you get the He3?

A great deal of work has been done trying to find and develop a practical bulk source of He3. As released in the D-He3 reaction, there are 163 million kilowatt hours of energy in each kilogram of He3. Thus, with a conversion efficiency of 0.60 and allowing 2 cents per kilowatt hour for the fuel cost, one can afford to pay almost \$2 million dollars per kilogram for He3.

The present price of He3 is about \$30 million dollars per kilogram. Kulcinski and a group at the University of Wisconsin have suggested that, at these prices, one can profitably establish a human colony on the moon and there extract the He3 that is radiated from the sun and has been impacting the lunar surface for billions of years. There is hope that 30 or 40 years hence, when needed for fusion power plants, the technology of lunar recovery may be developed to the point where lunar He3 can be "harvested" and returned to Earth at a cost of only a few million dollars per kilogram, i.e., cheap enough to be affordable as fuel in a thermonuclear power plant.

If one neglects the cost of the He3 fuel, the projected cost of power from D-He3-burning reactors is usually somewhat lower than the projected cost of power from D-T burners.<sup>11</sup>

### **Economic Viability: Cold Fusion**

Properties of cold fusion power plants are largely speculative at this time. Nonetheless, there are some indications that cold fusion power may, in time, become economically competitive with other forms of producing power.

#### ***Fuel Costs***

First, consider fuel costs. Excepting for fusion plants burning He3, the fuel costs of all forms of nuclear power plants will almost undoubtedly be a minor component of the total costs. At this time there is no apparent reason why this simplifying assumption will not also apply specifically to cold fusion power. That leaves only the fixed costs to be considered in projecting the cost of cold fusion power.

#### ***Fixed Costs***

So consider the fixed costs of a cold fusion power plant. The names, designs, costs, and other relevant properties of the various plant components are almost completely unknown at this time.<sup>12</sup> Hence, it seems senseless to attempt a detailed breakdown of fixed costs. Nonetheless, one can even now put a possible cap on the cost of building cold fusion plants -- when and if they can be built. The reasoning is as follows. Coal-fired steam plants now cost about \$1300 per kilowatt to build. Tomorrow's fission reactor plants are projected to cost about the same. Finally, thermonuclear plants have also sometimes been projected to cost somewhere between \$1500 and \$5000 per kilowatt to build. These thermonuclear plants are quite intricate; they have a large number of complex components. Thus, there is some justification for hoping that the cost of building a cold fusion power plant will be no more than that of a thermonuclear plant of equal power. In other words, the cost of electricity from cold fusion plants may be price

competitive with the cost from thermonuclear plants, or even from future fission plants.

### ***Environmental Considerations***

Speculations about copious construction costs and fuel costs are not the only considerations, however, in deciding whether or not to pursue the development of cold fusion power. Another factor may be cogent, namely the matter of environmental and political acceptability. To date, there is rather strong evidence that the nuclear radiations attendant to energy release in cold fusion are thousands of times less copious than those found in fission power plants of equal power and significantly less than those that accompany the D-T powered thermonuclear fusion reactors. (D-He3 reactors, although relatively benign environmentally, will not be economically competitive until a cheap and reliable supply of He3 is obtained.)

### ***Other Factors***

Because they can probably be built and tested in small sizes, cold fusion plants should prove to be both cheaper and quicker to develop than thermonuclear plants.

Cold fusion plants may be uniquely suited to supply safe and clean electric power at remote locations, especially those where there is no local supply of fossil fuel. Pursuing the same reasoning, cold fusion plants may be placed close to the load. Distribution costs would thereby be reduced.

### **Summation**

Fission power, however cheaply produced, is accompanied by the generation of large amounts of intractable radioactive ash. In consequence, no new fission power plants are being built in the United States.

Thermonuclear fusion, if magnetic confinement and the D-T reaction are used, is plagued by the fact that most of the energy released is in the form of 14.3 mev neutrons. A means of cost-efficient conversion of 14.3 mev neutron energy to electric energy is yet to be demonstrated.

Fusion using the D-He3 reaction gets rid of most of the 14.3 mev neutrons, but requires the burning of He3 fuel in amounts that are presently unavailable.

In both fossil and fission power plants the traditional steam turbine cycle is being replaced by variants of the gas turbine cycle.

Unlike any other form of nuclear power, cold fusion gives promise of producing heat energy with only minor (if any) amounts of ionizing nuclear radiations. In addition, one can hope that the fixed costs of a cold fusion power plant will be low enough so that the cost of the output power will be cost competitive.

But for now? It's too soon to tell.

1. Stephen Schulte, Theodore Wilke, and John Younger. *Fusion Reactor Design Studies -- Standard Accounts for Cost Estimating*. Richland, Washington: Pacific Northwest Laboratory, 1978.
2. G. L. Kulcinski, "Technological Advantages of D-He3 Cycle," Paper No. 3 presented at the First Wisconsin Symposium on D-He3 Fusion, Madison, WI (August 1990).  
G. A. Emmert, "D-He3 Tokamak Power Reactors," Table 2 from Paper No. 7, presented at the First Wisconsin Symposium on D-He3 Fusion, Madison, WI (August 1990).
3. G. L. Kulcinski et al, "The Case for D-He3 Fusion Power Plants," Table 1 from Paper No. 1A1, presented at the Workshop on D-He3 Based Reactor Studies, Moscow, Russia (September 25-October 2, 1991).
4. 3. *Nuclear Issues* 15 p.2 (June 1993)
5. R. W. Conn et al. "Economic, Safety, and Environmental Prospects of Fusion Reactors." *Nuclear Fusion*. Vol. 30, No. 7, p. 1926 (1990).
6. See, for example, Logan, Corvis, and Post, "Novel Direct Conversion Techniques," Paper #8, presented at the First Wisconsin Symposium on D-He3 Fusion, Madison, WI (August 1990).
7. Personal communication with Dr. Dah Yu Cheng.
8. H. Momota, "15 MeV Proton Direct Energy Conversion," Paper No. 2A1, presented at the Workshop on D-He3 Based Reactor Studies, Moscow, Russia (September 25-October 2, 1991).
9. Bernard L. Cohen. *The Nuclear Energy Option -- An Alternative for the 90's*. New York, New York: Plenum Press, 1990.
10. "Interview with Linden Blue." 21st Century Science & Technology. P. 23 (Fall 1993).
11. G. L. Kulcinski et al, "The Case for D-He3 Fusion Power Plants," paper No. 1A1, presented at the Workshop on D-He3 Based Reactor Studies, Moscow, Russia (September 25-October 2, 1991).
12. G. L. Kulcinski, "Technological Advantages of D-He3 Cycle," Paper No. 3 at the First Wisconsin Symposium on D-He3 Fusion, Madison, WI (August 1990).  
See, however, "*Excess Heat, Heat Production Equation*," by Waisman and Kertamus, a paper presented at the Fourth International Conference on Cold Fusion, Maui, HI (1993).

Table 1

# Construction Costs of Nuclear Power Plants (\$/KW)

COMPANY	Year Completed					1982-1984	1985-1987	1986
	1970-1971	1973	1973-1974	1975				
Commonwealth Edison:								
	Dresden	\$146						
	Quad Cities		\$164					
	Zion			\$280				
Byron/Braidwood	La Salle					\$1160		
							\$1880	
Northeast Utilities:								
	Millstone 1	\$153						
	Millstone 2				\$487			
	Millstone 3						\$3326	
Duke Power:								
	Oconee			\$181				
	McGuire					\$848		
	Catauba						\$1703	

13-fold  
Increase  
in  
17 years

22-fold  
Increase  
in  
15 years

Nearly  
22-fold  
Increase  
in  
14 years

Figure 1

# Coal-Fired Steam Plant

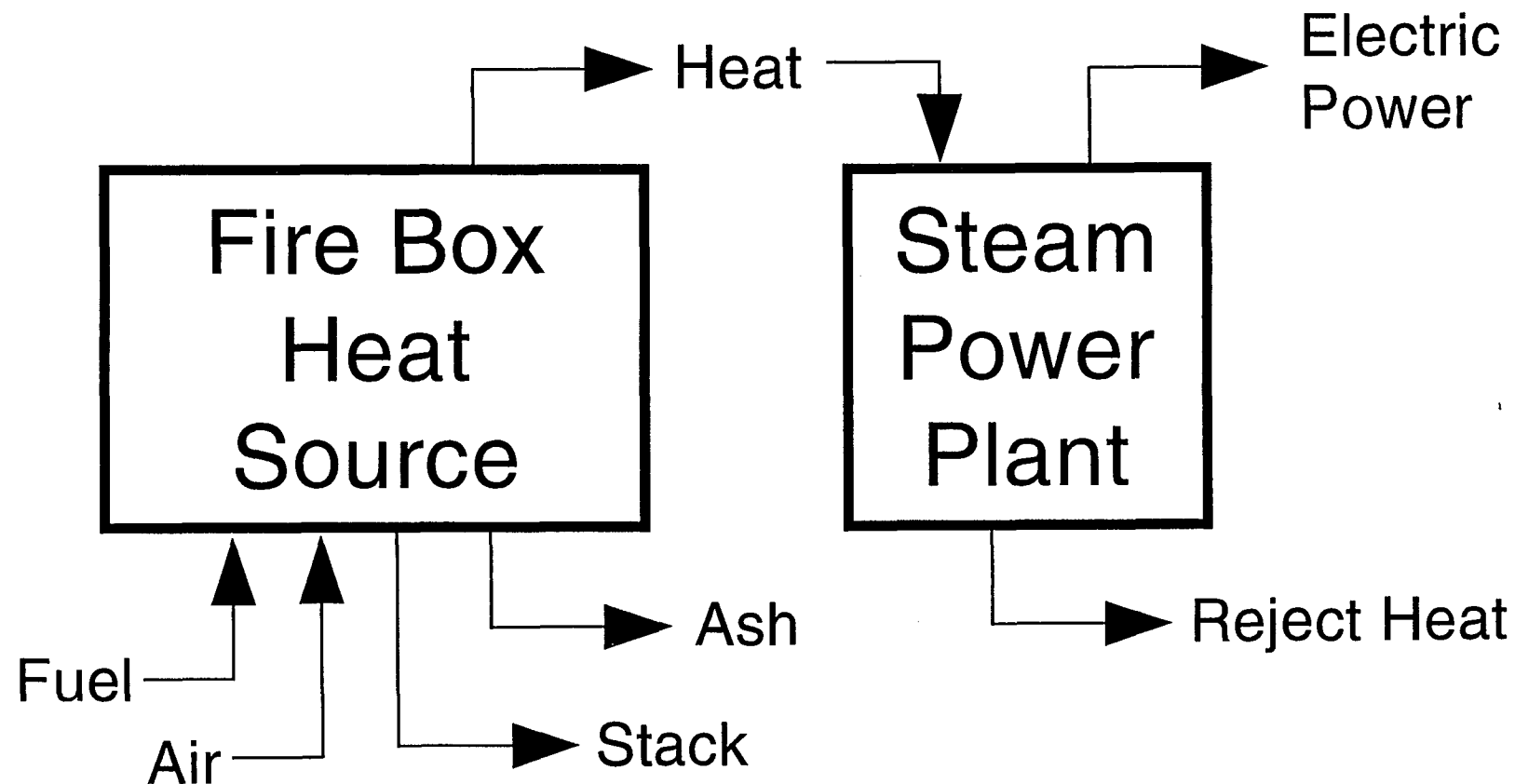


Figure 2

# Fission Power Plant

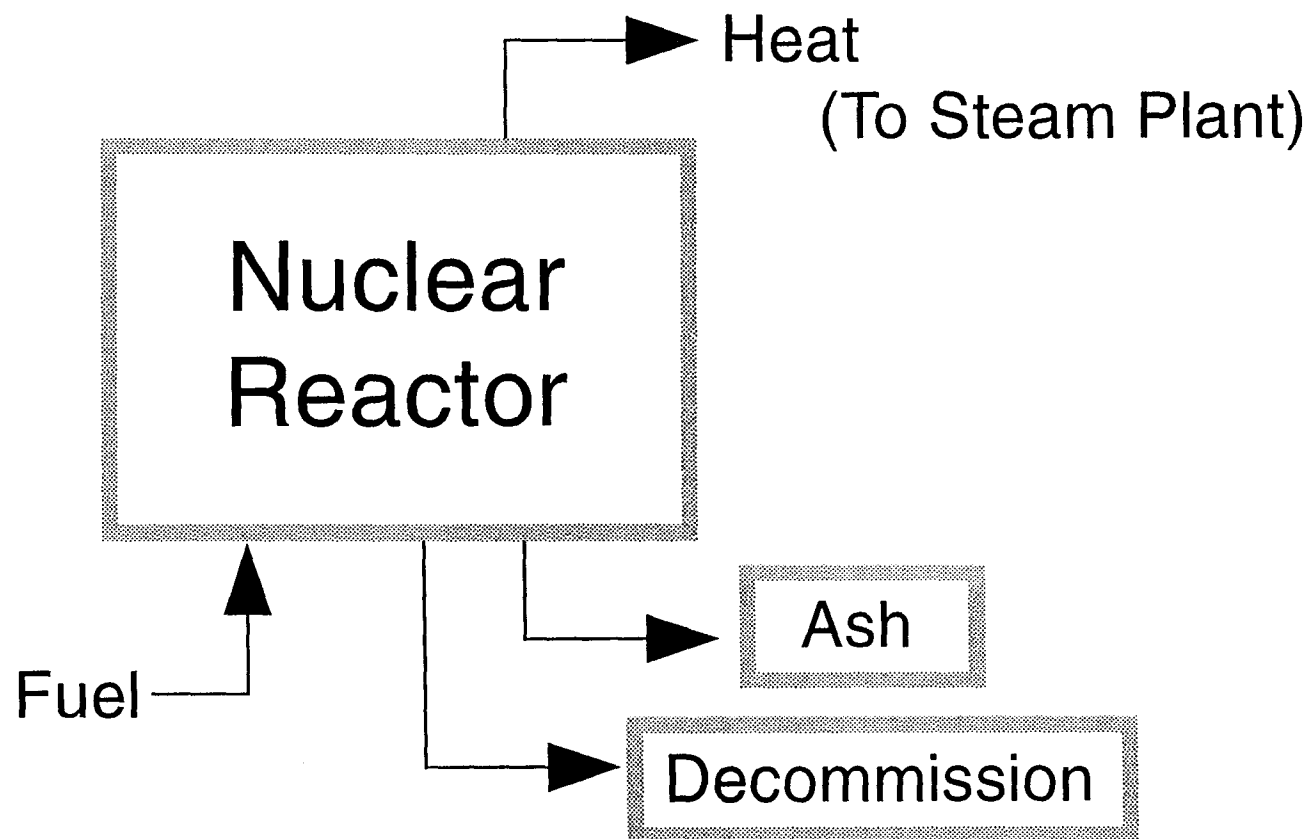


Figure 3A

# Thermonuclear - DT Fueled

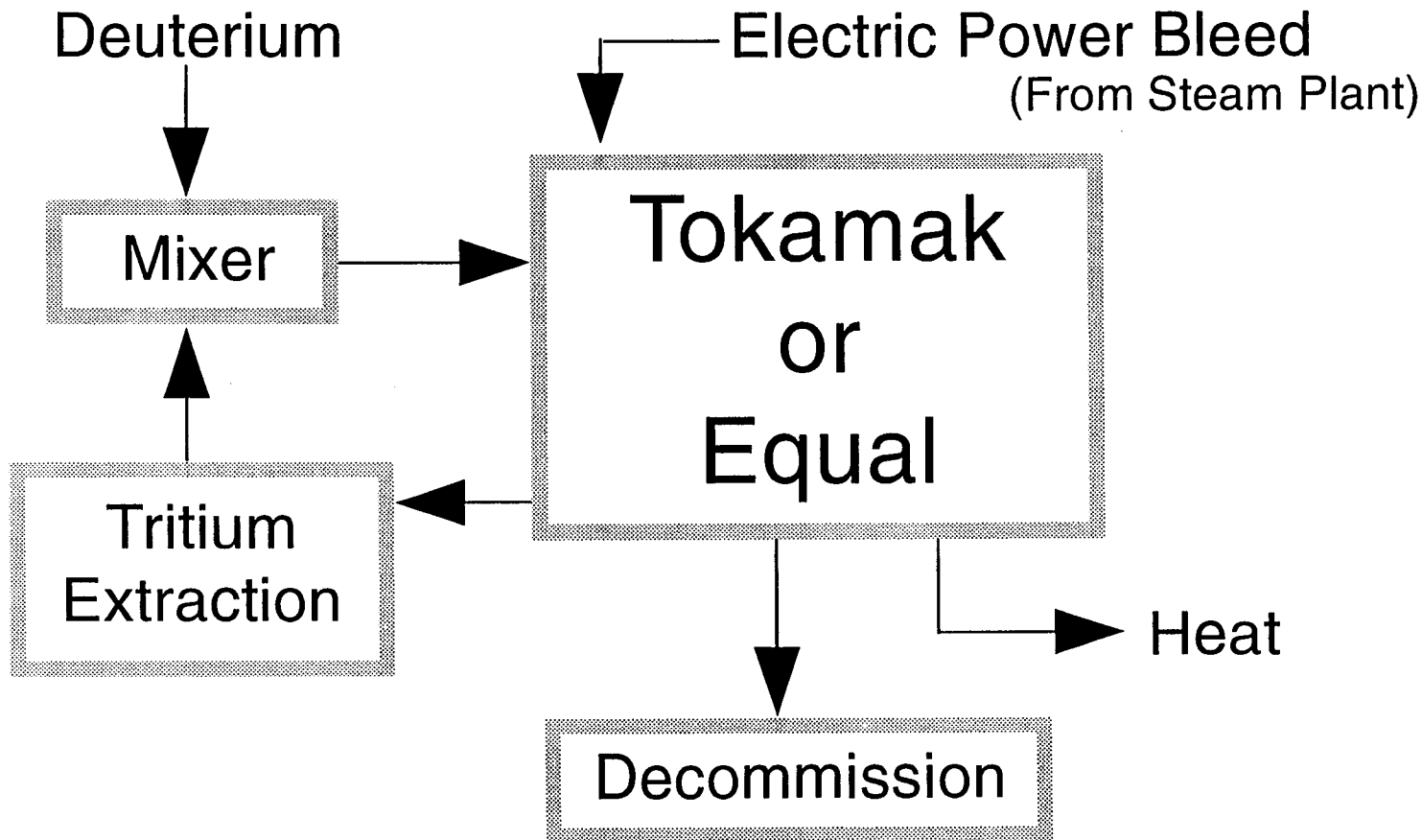


Figure 3B

## Schematic of the Elements of a Magnetic Fusion Energy Power Plant

37-15

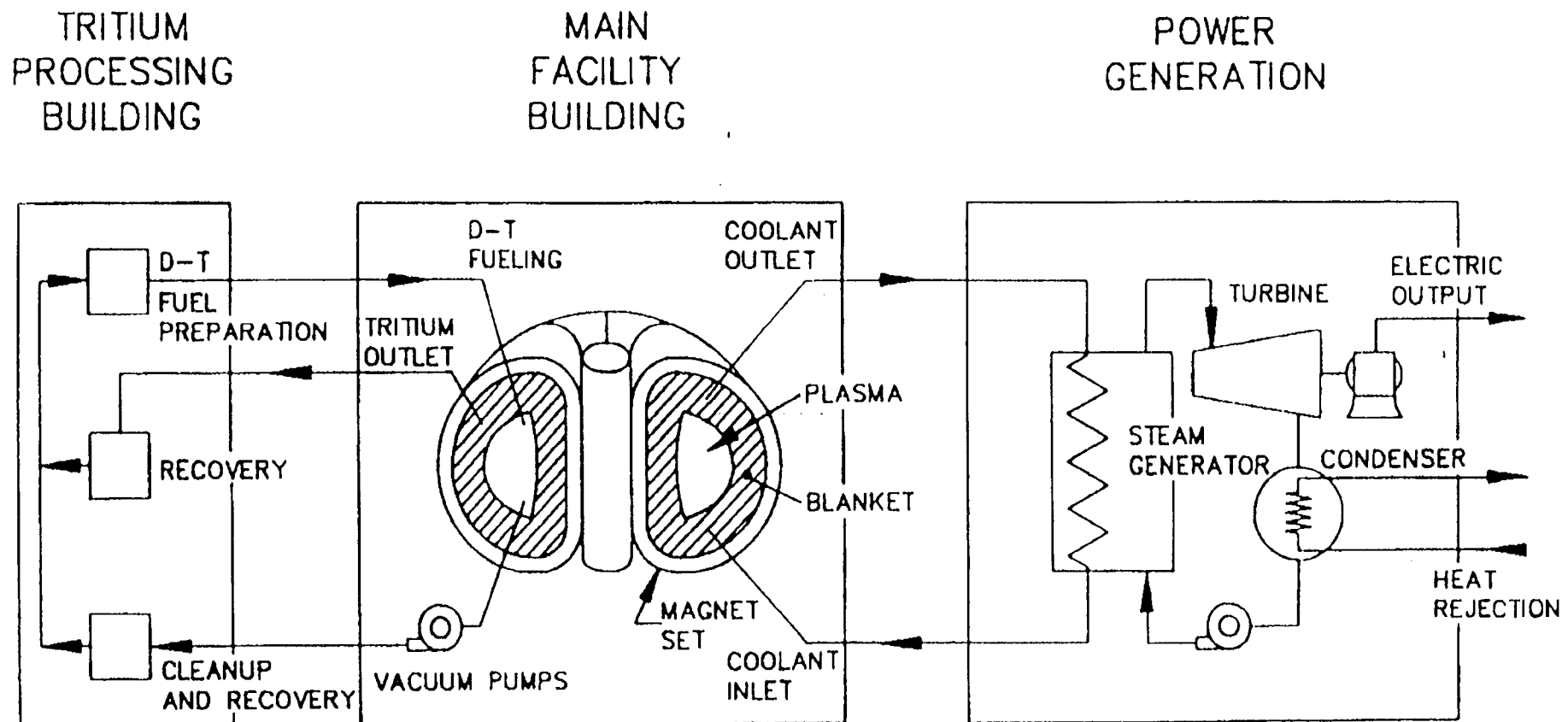


Figure 4

# Thermonuclear - DHe3 Fueled

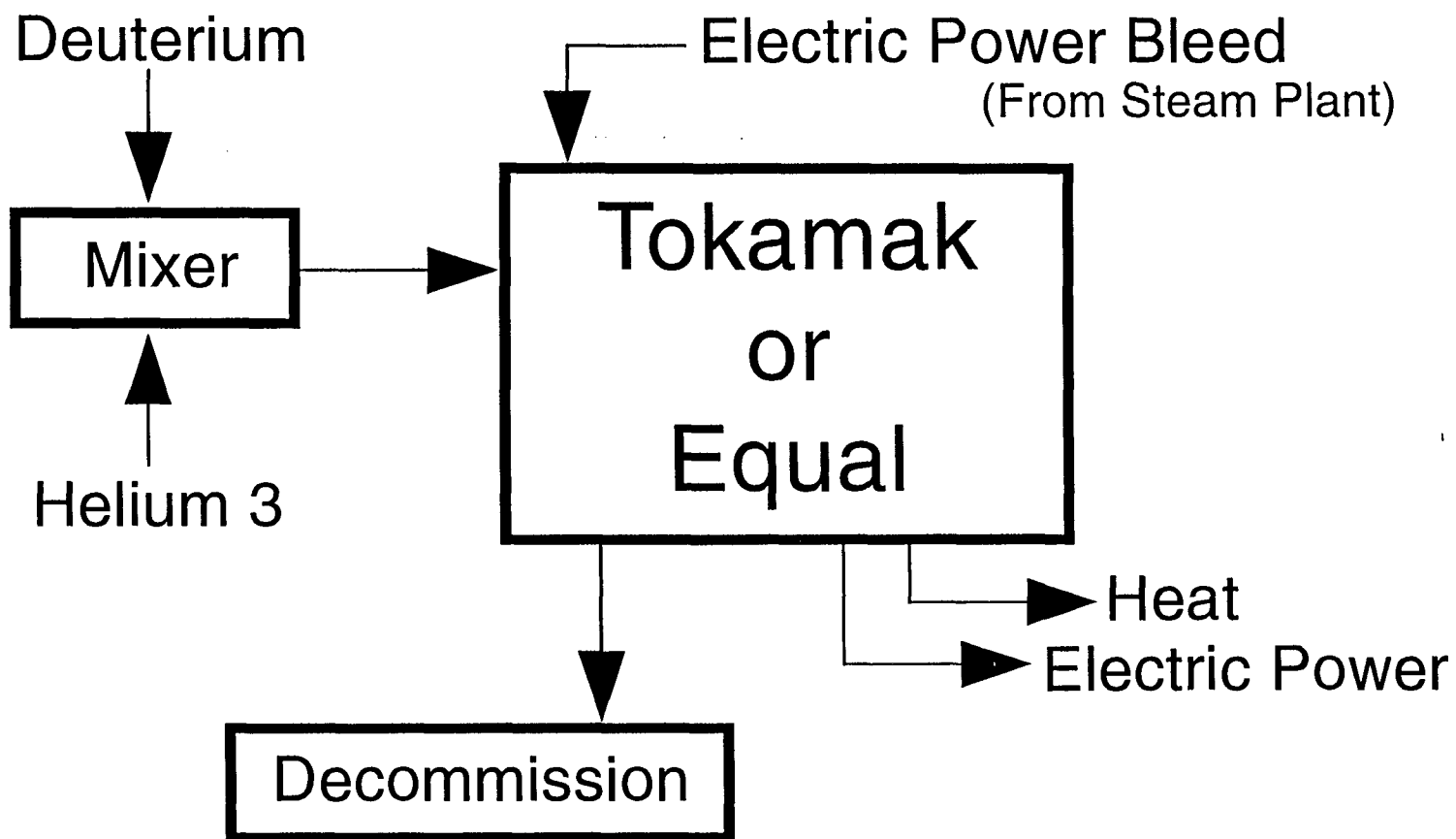


Figure 5

# Cold Fusion

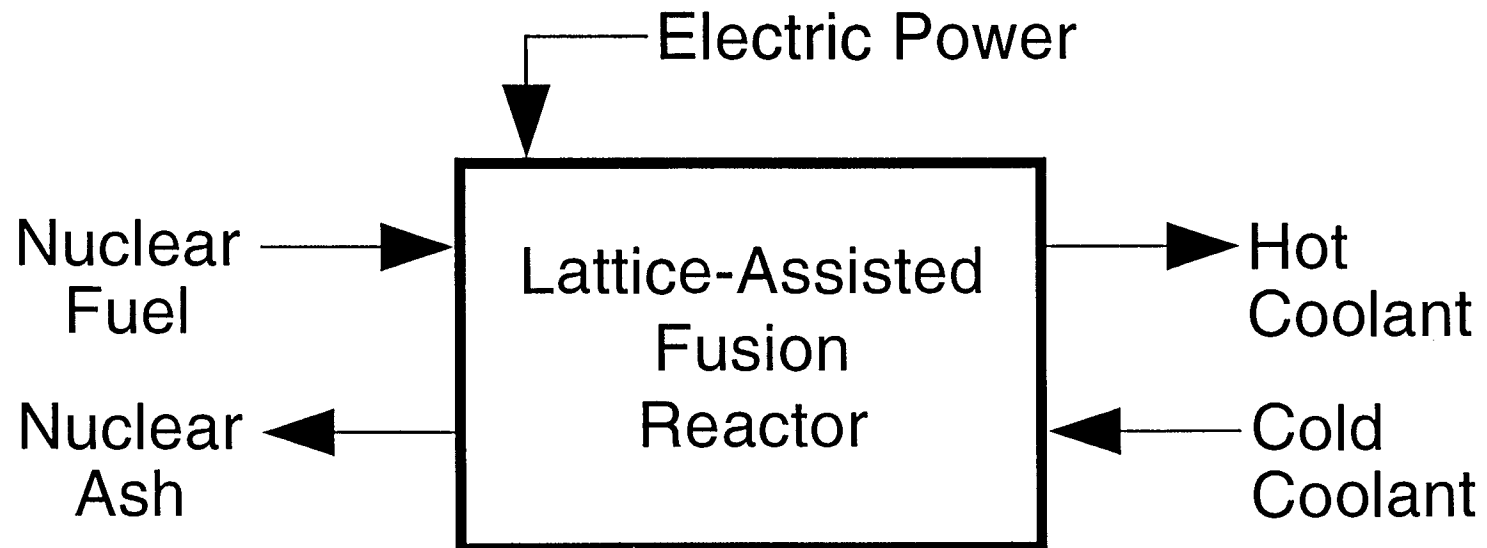
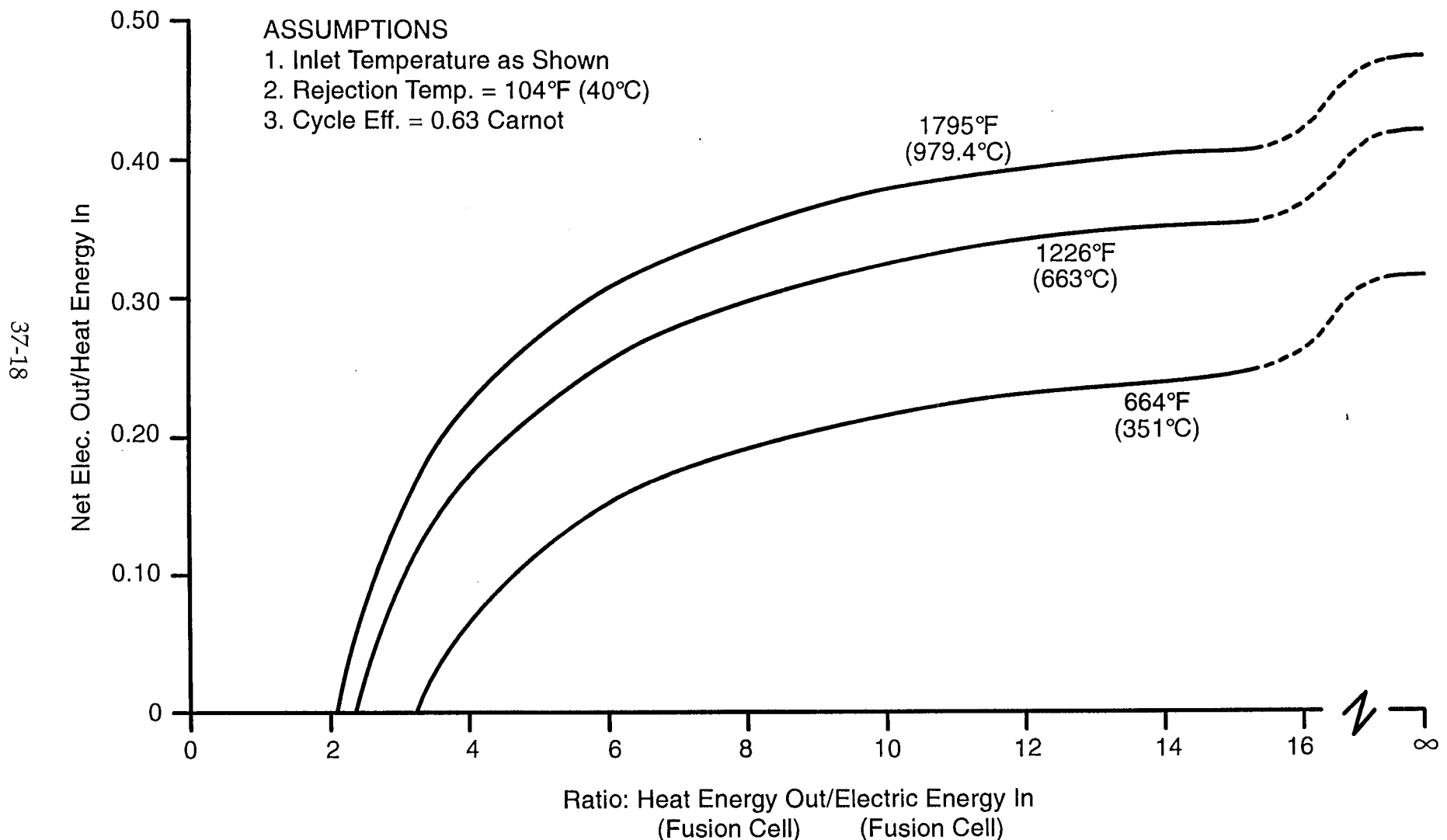


Figure 6

## Efficiency of a Steam Plant Powered by a Fusion Cell



# PROPOSED NUCLEAR PHYSICS EXPERIMENT TO CONCLUSIVELY DEMONSTRATE & EXPLAIN ANEUTRONIC COLD FUSION

Robert W. Bass  
*Scientific Advisory Board, ENECO, Inc.*  
391-B Chipeta Way, Salt Lake City, UT 84108

## Abstract

The protocol of the proposed experiment makes only two plausible assumptions: (1) **CONSERVATION OF BARYON NUMBER**; and (2) that if three identically-prepared **deuteron beams** of mean energy  $E_{\text{crit}}$  eV are injected into three identically-prepared thin frozen samples of fully loaded [beta phase]  $Pd-D_{[1.0]}$  lattices, for times of duration  $T$ ,  $2T$ ,  $3T$ , then the same percentage of deuterons will be wasted in each case (i.e. reflected or not entrant perpendicular to a plane of the embedded  $D$ -lattice): more specifically, if a TOTAL of  $N_T$ ,  $2N_T$ ,  $3N_T$  deuterons are injected in each case, then almost exactly  $N$ ,  $2N$ ,  $3N$  deuterons will enter the lattice perpendicular to a lattice plane, where  $N$  is not predicted (but  $N < N_T$ ). The **DESIDERATUM** is to demonstrate [in comparison to a non-irradiated control sample] the creation of 0,  $N$ ,  $2N$ ,  $3N$  **Alpha Particles** from LOW ENERGY aneutronic fusion of 0,  $2N$ ,  $4N$ ,  $6N$  static-target (near zero-point energy-level) bound deuterons, at a Kinetic Energy Cost of almost exactly 0,  $N \cdot E_{\text{crit}}$  eV,  $2N \cdot E_{\text{crit}}$  eV,  $3N \cdot E_{\text{crit}}$  eV plus unpredicted but proportionate wasted energy (which can be measured). If the experiment is performed and for ANY low-energy (say, less than 20 eV) value of  $E_{\text{crit}}$  eV attains the stipulated desideratum, i.e. the number of Alpha Particles created is **incontrovertibly proportional** to the *beam DOSE*, then the empirical reality of Cold Fusion will have been conclusively **DEMONSTRATED**. However, it will not have been conclusively **EXPLAINED**. The purpose of this paper, besides advocating this novel experiment, is to present the first orthodox quantum-mechanical treatment of *low-energy penetrability* of the 'Coulomb Barrier', by *Resonant Transmission* in a deuterium lattice, which includes quantitative estimates (by the WKB approximation) of the minimum value of  $E_{\text{crit}}$  (below which  $N$  is tangibly reduced), and to prove that to a first approximation this value is about  $E_{\text{crit}} = 6.3$  eV. Alternative versions of the experiment would replace the deuteron beam by a high-intensity flux of coherent monochromatic *ultraviolet* rays providing photons of energy  $E_{\text{crit}}$ , and also Fleischmann-Pons electrochemical-cell calorimetry experiments in which the voltage driving the deuteron current through the palladium cathode is set just below, just at, and just above  $E_{\text{crit}}$  eV.

## Proposed Protocol for Definitive Cold Fusion Demonstration

### • MINIMAL THEORY-DEPENDENCE

It is impossible to design any experiment whose interpretation is totally theory-independent.

However, the ideal Cold Fusion experiment would make use of only one theory:  
CONSERVATION OF BARYON NUMBER.

The here-proposed experiment does make use of a second plausible theory, namely that if 3 identically-prepared beams of  $E_{\text{crit}}$  eV deuterons are directed toward 3 identically-prepared frozen samples of palladium lattices, for times of duration  $T$ ,  $2T$ ,  $3T$ , then the same *percentage* of deuterons will be wasted in each case (i.e. reflected or not entrant perpendicular to a plane of the lattice): specifically, if a TOTAL of

$$0, N_T, 2N_T, 3N_T$$

deuterons are injected in each case, then almost exactly

$$0, N, 2N, 3N$$

deuterons will enter the lattice perpendicular to a plane, where  $N < N_T$ .

#### • DESIDERATUM

To demonstrate the creation of

$$0, N, 2N, 3N$$

**Alpha Particles ( $^4\text{He}$  Nuclei) from LOW-ENERGY aneutronic fusion of**

$$0, 2N, 4N, 6N$$

static-target [near zero-point energy-level] Deuterons, at a Kinetic Energy Cost of exactly

$$0, N \times E_{\text{crit}} \text{ eV}, 2N \times E_{\text{crit}} \text{ eV}, 3N \times E_{\text{crit}} \text{ eV}$$

plus unpredicted but proportionate wasted energy which can be measured.

#### • CONCEPT

Into four identically prepared cryogenic samples of *supersaturated* Deuterated Palladium Lattices (i.e. fully loaded [beta phase: one deuteron per palladium ion] or comprising  $Pd\cdot D_{[1.0]}$ ), inject

$$0, N_T, 2N_T, 3N_T$$

$E_{\text{crit}}$  eV deuterons, perpendicular to a plane of the lattice, and then measure the helium-4 present in each sample.

#### • PROCEDURES

STEP 1. Prepare 4 identical cryogenic samples of fully loaded  $Pd\cdot D_{[1.0]}$  lattices.  
[Cf. COMMENTS below.] Keep one sample apart as a control blank.

STEP 2. Prepare a potential difference of  $E_{\text{crit}}$  eV between each of 3 remaining samples and the final electrode of a deuteron beam injector.

STEP 3. Inject deuterons for times of duration  $T$ ,  $2T$ ,  $3T$ .

STEP 4. Using a Double-Blind test protocol, and independent Testing Laboratories, have *half* of each of the 4 samples chemically assayed for helium-4 content, and the remaining *half* of each sample assayed by a Mass Spectroscopic technique (e.g. SIMS).

#### • COMMENTS

1. There are at least two known methods of testing the electrochemical loading of a

*Pd-D* lattice as to whether or not it has passed from the alpha phase [*Pd-D*<sub>0.67</sub>, or 2 deuterons for each 3 palladium ions] to the beta phase [*Pd-D*<sub>1.0</sub>, or one deuteron for each palladium ion]. It is stated by Dr. Fritz Will, former director of the National Cold Fusion Institute, that the palladium cathode visibly swells in volume up to about 15%, and that this volumetric change can be measured hydraulically or pneumatically. Also, Dr. Michael McKubre of SRI International has published both theory and experiment regarding a definitive electrical current resistivity test: during loading, the resistivity of the palladium cathode increases to a maximum at the onset of the phase change from alpha-phase to beta-phase, and then decreases to a minimum at the completion of the beta-phase loading. At the Second International Cold Fusion Conference, Dr. McKubre stated that in his experiments, *identical preparation ALWAYS* produces identical results, the implication being that in unrepeatable experiments one or more conditions (e.g. metallurgical purity, full loading, critical current density, etc.) had not been repeated properly (i.e. not checked adequately). According to Dr. McKubre, the obvious way to maintain full loading of a *Pd-D* sample would be to maintain it under a large deuterium-gas pressure. However, Dr. John O'M. Bockris and collaborators have published [1] an ingenious way to get around the use of high pressures: they plunged the fully-loaded *Pd-D* lattice into liquid nitrogen in less than one second, and later found massive amounts of helium-4 inside the frozen samples which had produced macroscopically-measured heat. The present experiment proposes to terminate the loading just as, or just before, heat begins to be produced, and instead to use the fully-loaded frozen *Pd-D* lattice as a deuteron-beam target.

2. It will now be necessary to maintain the frozen target samples at the temperature of liquid nitrogen during the deuteron-beam injection.

3. An obvious variation on the proposed experiment would be to maintain the *duration* of beam injection for the *same* time *T*, but to *double* and *triple* the beam *intensity* (in deuterons/sec).

4. Dr. Bockris and his collaborators sawed the frozen samples into multiple sub-samples for independent testing. Here it is proposed to saw each sample into *four* portions, one each for *chemical assay*, and one each for *physical assay*, to *two* independent testing laboratories under a *double-blind* protocol wherein only a neutral third party knows the actual origin of each sample.

### Possible Follow-On or Alternative Experiments

1. Assuming that the basic experiment is successful, it would be desirable to repeat the experiment sufficiently often as to establish an empirical plot of percentage of aneutronic deuteron fusions per injected deuteron, as a function of deuteron beam mean energy. If the theory of Resonant Transparency Energy Levels presented below is correct, there should be found, above  $E_{\text{crit}}$ , an entire spectrum of critical energy levels, spaced extremely closely together: use of the WKB approximation suggests that  $E_{\text{crit}} \approx 6.26$  eV and that between  $E_0 = E_{\text{crit}}$  and  $E_5 \approx 6.59$  eV there are *five* such resonant lines, with line breadths increasing from 1.8% to 7% of the difference between that line and the next higher line. At  $E_{88} \approx 13.7$  eV the line breadth  $\delta E_{88} \approx 0.08$  eV is 74% of the difference  $\Delta E_{88} \approx 0.11$  eV between  $E_{88}$  and  $E_{89}$ . (The line broadening is caused by zero-point fluctuations of the rigidly bound lattice-deuterons, as characterized by the Schwinger Ratio  $\sigma = L/\Lambda = 22.31$ , where  $L = 2.83$  Å is the deuteron-lattice period and  $\Lambda$  is the rms value of the quantum fluctuations in position from the deuteron equilibrium sites.)

2. An alternative to the use of deuteron beams would be the use of high-intensity coherent monochromatic ultraviolet (UV) rays as a source of photons of energy  $E_{\text{crit}}$ .

In this injected-photon case the palladium lattice might have to be thinner than in the preceding injected-deuteron case. Although UV lasers are less ubiquitous and can be more costly than deuteron beams, the use of chemical lasers (such as are based on liquid organic dyes) permits continuous tuning of the wavelength and may be advantageous because of the predicted narrow widths between resonant energy levels and the difficulty of preparation of monochromatic particle beams to differences of 0.1 eV.

3. The stunning Bush-Eagleton experiments [2] with Fleischmann-Pons electrochemical cells, but using closed-cell calorimetry and real-time computerized instrumentation, have resulted in measurements of a dozen ascending local maxima and minima in the curve of *relative* excess enthalpy as a *function* of variation of cell *voltage* (and also of cell temperature), although Bush's Transmission Resonance Model (TRM) theory [3] has been severely criticized by Jändel [4] as fatally defective because of alleged infinitesimal line-breadths, and no independent verification of Bush's seemingly epochal TRM-predicted results has been published. But the Schrödinger-equation based WKB theory presented below appears to surmount Jändel's objection (by zero-point fluctuation line-broadening) and is submitted to be a refinement of Bush's Duane-Rule-based semi-classical theory which adds weight & urgency to the case for independent experimental verification of the Bush TRM-spectrum.

## References

- [1] Chun-Ching Chien, Dalibor Hodko, Zoran Minevski & John O'M. Bockris, "On an Electrode Producing Massive Quantities of Tritium and Helium," *J. Electroanalytical Chemistry*, vol. 338 (1992), pp. 189-212.
- [2] Robert D. Eagleton & Robert T. Bush, "Calorimetric Evidence in Support of the Transmission Resonance Model," *Fusion Technol.*, vol. 20 (1991), p. 239
- [3] Robert T. Bush, "Cold Fusion: the Transmission Resonance Model Fits Data on Excess Heat, Predicts Optimal Trigger Points, and Suggests Nuclear Reaction Scenarios," *Fusion Technology*, vol. 19 (1991), pp. 313-356.
- [4] M. Jändel, "The Fusion Rate in the Transmission Resonance Model," *Fusion Technology*, vol. 21 (1992), p. 176.

---

## Appendix 1

### A CLOSED-FORM EXPRESSION FOR A GENERIC MADELUNG SERIES

#### Abstract

Let  $Z_2$  denote the effective atomic number of a positive ion in an infinite lattice, so that the ion's charge is  $Z_2 \cdot e$  where  $e$  is the charge on an electron. For simplicity, approximate the lattice as one-dimensional and consisting of infinitely many such positive charges, idealized as points, placed *rigidly* at lattice sites  $r = \pm k \cdot L$ , where  $k$  is a positive integer, i.e. at integrally-related distances from the origin  $r = 0$ , where the length  $L$  denotes the lattice *period*. Although the unbound electrons are free to circulate, the lattice outside of the cell  $-L \leq r \leq L$  is taken to be electrically neutral *on average*, which can be approximated by idealizing the averaged electron charges as negative point charges of magnitude  $-Z_1 \cdot e$  also *rigidly* fixed at positions exactly half-way between each of the positive point charges. Into this grossly electrically neutral lattice introduce a test-particle, idealized as a positive point charge of magnitude  $Z_1 \cdot e$ , which is not bound but free to move between

the nearest bound charges, namely those at  $r = -L$  and  $r = L$ ; it is then free to oscillate near the equilibrium position  $r = 0$  of a potential well defined by the convergent series

$$V(r) = Z_1 Z_2 \cdot (e^2/L) \cdot \sum_{k=0}^{+\infty} c_k (r/L)^{2k}, \quad c_m \equiv \sum_{k=0}^{2m} \pi_{k,2m-k} \quad (m = 0, 1, 2, \dots),$$

where, for all non-negative integer pairs  $(i, j)$ , it is proved that

$$\pi_{ij} = \sum_{k=1}^{+\infty} \frac{1}{k^{i+1} \cdot (k + 1/2)^{j+1}} < Z[i+j+1] \leq Z[2] \leq \pi^2/6 = 1.65\dots,$$

where  $Z[m]$  denotes the Riemann Zeta Function. It is shown that  $0 < c_m < 2$  where the coefficients  $c_m$  increase monotonically to the limit 2, attained to 17 decimals for  $m \geq 44$ . Thus the elementary *rational* closed-form approximation

$$V_N(r) = Z_1 Z_2 \cdot (e^2/L) \cdot \left\{ \sum_{k=0}^N c_k (r/L)^{2k} + 2 \cdot (r/L)^{2(N+1)} \cdot [1 - (r/L)^2]^{-1} \right\}$$

can be made arbitrarily accurate by simply increasing  $N \geq 44$ .

### Introduction

According to an encyclopedia of physics [1], the calculation of Madelung constants "requires some care since they are given by slowly and conditionally convergent series. Attempts at direct summation can involve thousands of terms without impressive accuracy."

Here a one-dimensional conditionally convergent generic Madelung series will have its terms rearranged so as to become an absolutely convergent power series whose coefficients are defined by readily computable universal constants derived below.

### Analysis

The electrostatic potential energy  $V_k$  of a free positive point charge  $Z_1 e$  at a distance  $r$  from the origin  $r = 0$ , interacting with bound positive point charges  $Z_2 e$  rigidly fixed at  $r = \pm kL$ , where the distance  $L$  is the lattice *period* length, is given by

$$V_k = \frac{Z_1 Z_2 e^2}{kL - r} + \frac{Z_1 Z_2 e^2}{kL + r} = \frac{Z_1 Z_2 e^2}{L} \left\{ \frac{1}{k - \xi} + \frac{1}{k + \xi} \right\}, \quad (1)$$

where henceforth the distance  $r = \xi \cdot L$  is rendered dimensionless by scaling:

$$\xi \equiv r/L, \quad (|\xi| < 1), \quad (2)$$

and where, by the hypothesis that  $-L < r < L$  it is ensured that  $-1 < \xi < 1$ , and so, *a fortiori*, that  $|\xi| < k$  for every integer  $k \geq 1$ . Hence, upon combining the terms in (1) to get  $\{2k/(k^2 - \xi^2)\}$ , and use of the geometric series  $(1 - \theta)^{-1} \equiv \sum_j \theta^j$  for  $|\theta| < 1$ , one finds that

$$V_k = \frac{2Z_1 Z_2 e^2}{kL} \left\{ \frac{1}{1 - (\xi/k)^2} \right\} = \frac{2Z_1 Z_2 e^2}{L} \sum_{j=0}^{+\infty} \frac{\xi^{2j}}{k^{2j+1}}. \quad (3a)$$

Quite similarly, if negative point charges of charge  $-Z_2 e$  are fixed rigidly at  $r = \pm(k + 1/2)L$  then the electrostatic potential  $W_k$  of their interaction with the free particle of positive charge  $Z_1 e$  located at  $r = \xi \cdot L$  is

$$W_k = -\frac{2Z_1 Z_2 e^2}{L} \sum_{j=0}^{+\infty} \frac{\xi^{2j}}{(k+1/2)^{2j+1}}. \quad (3b)$$

Accordingly, adding (3a) and (3b) and summing over all positive integers, the total potential of interaction of the free positive charge  $Z_1 e$  with all of the infinitely many bound charges in the periodic lattice is given by

$$V(\xi) = Z_1 Z_2 (e^2/L) \cdot \sum_{j=0}^{+\infty} c_j \xi^{2j}, \quad (-1 < \xi < +1), \quad (4)$$

$$c_j = 2 \sum_{k=1}^{+\infty} \left( \frac{1}{k^{2j+1}} - \frac{1}{(k+1/2)^{2j+1}} \right), \quad (j = 0, 1, 2, 3, \dots). \quad (5)$$

Simplification of (5) depends upon the well-known algebraic identity to the effect that  $(1 - \theta) \cdot (1 + \theta + \theta^2 + \dots + \theta^{m-1}) \equiv 1 - \theta^m$  for every positive integer  $m$ . Now let  $\theta = b/a$  and multiply through by  $a^m$  in order to obtain the equivalent identity

$$a^m - b^m \equiv (a - b) \cdot \sum_{p=0}^{m-1} a^{m-p} \cdot b^p. \quad (6)$$

Applying (6) to (5), with  $a = 1/k$ ,  $b = 1/(k + 1/2)$ ,  $m = 2j + 1$  yields

$$\begin{aligned} c_j &= 2 \sum_{k=1}^{+\infty} \left( \frac{1}{k} - \frac{1}{(k+1/2)} \right) \cdot \sum_{p=0}^{2j} \frac{1}{k^{2j-p}} \cdot \frac{1}{(k + 1/2)^p} \equiv \\ &\equiv \sum_{p=0}^{2j} \sum_{k=1}^{+\infty} \frac{1}{k^{2j-p+1} \cdot (k + 1/2)^{p+1}} \equiv \sum_{p=0}^{2j} \pi_{p,2j-p}, \end{aligned} \quad (7)$$

where for convenience the following definition has been introduced: For all pairs of non-negative integers  $(i,j)$  define the absolutely convergent infinite series

$$\pi_{p,q} = \sum_{k=1}^{+\infty} \frac{1}{k^{p+1} \cdot (k + 1/2)^{q+1}} < \zeta[p + q + 1], \quad (8)$$

where

$$\zeta[m] = \sum_{k=1}^{+\infty} \frac{1}{k^m}, \quad (m = 2, 3, 4, \dots), \quad (9)$$

denotes the Riemann Zeta Function, which is well known to satisfy

$$\zeta[m] \leq \zeta[2] \leq \pi^2/6 = 1.645 \dots. \quad (10)$$

Thus, to recapitulate, the generic Madelung series (4) is defined by the sequence of *universal coefficients*

$$c_m = \sum_{k=0}^{2m} \pi_{k,2m-k}, \quad (m = 0, 1, 2, 3, \dots). \quad (11)$$

If these coefficients are uniformly bounded by the real number 2.0, as will be shown, then by the ratio test the series (4) converges absolutely for every  $\xi$  in the open interval  $(-1,1)$ , although it turns out that the convergence is not uniform because  $V(\xi)$

$$\rightarrow +\infty \text{ as } |\xi| \rightarrow 1.$$

Thus the sequence of coefficients  $\{c_m\}$  comprises *universal constants* of some practical scientific interest. Numerically,

$$c_0 = \pi_{0,0} = \sum_{k=1}^{+\infty} \frac{1}{k \cdot (k + 1/2)} = 1.224915957458691\ldots, \quad (12)$$

$$c_1 = \pi_{2,0} + \pi_{1,1} + \pi_{0,2} = 1.575317146547467\ldots, \quad (13)$$

and so on. The values of  $c_m$  for ( $m = 0, 1, 2, 3, \dots, 43, 44$ ) have been computed and are tabulated in the Appendix. Note that to 17-decimal place accuracy the coefficients are monotone increasing toward the apparent limit of 2, namely

$$0 < c_m < c_{m+1} < \dots \leq 2, \quad (m = 0, 1, 2, 3, \dots), \quad (14)$$

$$|c_m - 2| < 10^{-17}, \quad (m \geq 44). \quad (15)$$

The obvious conjecture is that

$$c_m \rightarrow 2, \quad \text{as } m \rightarrow +\infty. \quad (16)$$

While one hopes that this number-theoretic result (16) may be proved rigorously [2], in the sequel it will be assumed to be correct on the basis of the empirical evidence (14)-(15). In this case, the series (4) may be truncated after  $N$  terms, and the coefficients  $c_m$  may be taken to be *exactly*  $c_m = 2$  for all  $m \geq N$ . Then the remainder series, apart from a factor  $2\xi^{2(N+1)}$ , is just the geometric series for  $(1 - \xi^2)^{-1}$ .

### **Conclusion**

If  $N \geq 44$ , the generic Madelung series may be approximated to any desired degree of numerical precision by simply increasing  $N$  in the elementary *rational* potential

$$V_N(\xi) = Z_1 Z_2 \cdot (e^2/L) \cdot \left\{ \sum_{k=0}^N c_k \xi^{2k} + 2 \cdot \xi^{2(N+1)} \cdot [1 - \xi^2]^{-1} \right\}, \quad (17)$$

where the coefficients  $\{c_k\}$  are *universal constants* defined in the Appendix.

## References

- References

  - [1] B. Gale Dick, "Madelung Constant", article in *McGraw-Hill Encyclopedia of Physics*, 2<sup>nd</sup> Ed. 1992, page 723.
  - [2] Robert W. Bass, "An Apparently True Conjecture in Number Theory", to be submitted for publication.

$$RngM := 44 \quad m := 0..RngM$$

$$c_m := \sum_{i=0}^{2-m} \sum_{j=1}^{400} \frac{1}{[i+1 \cdot (j+0.5)^{2-m-i+1}]}$$

## Appendix 2

# PROOF THAT MADELUNG FORCES PREDICT THE SCHWINGER RATIO CORRECTLY & THAT THEY DRASTICALLY ATTENUATE COULOMB SINGULARITIES IN LATTICES

### Abstract

Recently I derived [1] a simple infinite series expression for the Madelung forces on a loosely bound charged particle, assumed oscillating in a stable potential well and surrounded on both sides (in a one-dimensional approximation) by rigidly bound particles of the same sign, whose aggregate electrical charge is rendered effectively neutral by intervening oppositely charged particles. In order to check the validity of my theory, I have used it to compute the Schwinger Ratio  $\sigma$  for a *supersaturated* ("beta phase") deuteron lattice inside a palladium lattice, where the ratio is known accurately from *cold-fusion-relevant* experimental data.

Elsewhere I have defined the Schwinger Ratio  $\sigma = L/\Lambda$  as the ratio of the lattice *periodic length*  $L$  to the *mean-square oscillation amplitude*  $\Lambda$  of a quantized harmonic oscillator, at zero-point energy level, as an approximation to the particle's mean square vibration amplitude in the lattice at a temperature of zero Kelvins.

The theory presented below predicts  $\sigma \approx 22.3$ ; the measured result is  $\sigma \approx 28.2$ , and this *relatively* good agreement (considering the approximation made in replacing a truly anharmonic oscillator by a harmonic oscillator) lends confidence to the theory.

Let  $Z_i$  and  $A_i$  denote, respectively, the atomic number and the atomic weight (baryon number) of two species of nuclei, for  $i = 1, 2$ . Consider a lattice formed of rigidly bound nuclei of the second species located at integrally-related distances from the origin  $r = 0$ , i.e. if  $L$  is the lattice period, located at  $r = \pm kL$ , where  $k$  is a positive integer: ( $k = 1, 2, 3, \dots$ ). Assume that negative charges ( $-Z_2$ ) are located half-way between each of the positive charges. Then consider the vibrations of a particle of the first species placed initially at  $r = 0$ . I claim that the Schwinger Ratio for this particle will be reasonably well approximated by

$$\sigma \equiv L/\Lambda \approx \left\{ [8A_1 Z_1 Z_2 \cdot c_1 \cdot \alpha \cdot (L/\lambda_p)] \right\}^{1/4},$$

where  $c_1$  is a *universal constant* I defined elsewhere, which has the approximate value

$$c_1 = 1.575317146547467;$$

where  $\alpha \approx 7.2973 \times 10^{-3}$  is the *fine-structure constant*; and where  $\lambda_p \approx 2.1 \times 10^{-14}$  cm is the *Compton wavelength* of a proton.  $\square$

### Derivation

Using the definitions posed in the Abstract, and  $q_i \equiv Z_i \cdot e$ , it is immediate that

$$V(r) = \sum_{k=1}^{+\infty} \frac{q_1 q_2}{kL - r} + \sum_{k=1}^{+\infty} \frac{q_1 q_2}{kL + r} - \left\{ \sum_{k=1}^{+\infty} \frac{q_1 q_2}{(k+1/2)L - r} + \sum_{k=1}^{+\infty} \frac{q_1 q_2}{(k+1/2)L + r} \right\}. \quad (1)$$

Elsewhere [1] I have shown how to sum (1) in the form

$$V(r) \equiv Z_1 Z_2 \cdot (e^2/L) \cdot \sum_{k=0}^{+\infty} c_k (r/L)^{2k}, \quad (2)$$

where the coefficients  $c_m$  are defined by simple and readily computable series which converge quite rapidly and so are amenable to tabulation as universal constants, namely

$$c_0 = \pi_{0,0} = \sum_{k=1}^{+\infty} \frac{1}{k \cdot (k + 1/2)} = 1.224915957458691, \quad (3a)$$

$$c_1 = \pi_{2,0} + \pi_{1,1} + \pi_{0,2} = 1.575317146547467, \quad (3b)$$

$$c_m = \sum_{k=0}^{2m} \pi_{k,2m-k}, \quad (m = 0, 1, 2, 3, \dots), \quad (3c)$$

$$\pi_{ij} = \sum_{k=1}^{+\infty} \frac{1}{k^{i+1} (k + 1/2)^{j+1}} < Z[i + j + 2], \quad (3d)$$

and where

$$Z[m] \equiv \sum_{k=1}^{+\infty} \frac{1}{k^m}, \quad (m = 2, 3, 4, \dots), \quad (3e)$$

denotes the Riemann Zeta Function, which is well-known to satisfy  $Z[m] \leq Z[2] = \pi^2/6 = 1.645 \dots$ . The values of  $c_m$  for ( $m = 0, 1, 2, 3, \dots, 43, 44$ ) are tabulated in the Appendix. Note that, to 17 decimal-place accuracy,

$$0 < c_m \leq 2, \quad (m = 0, 1, 2, 3, \dots), \quad (4a)$$

$$c_m = 2, \quad (m \geq 45). \quad (4b)$$

Hence the fact that  $c_m \leq 2$  implies that each term in the series (2) is dominated by the corresponding term in  $2/(1 - [r/L]^2)$ . Hence the  $\nu(r)$  still becomes infinite as  $r \rightarrow \pm L$ , but the slope is much closer to vertical, and on any interval of the form

$$0 < -L + r_n \leq r \leq L - r_n, \quad (4c)$$

where  $r_n$  is the range of the strong nuclear force, the series (2) converges uniformly and absolutely and is well-approximable by a finite number of terms of the series (2), i.e. one can consider the loosely bound deuteron as in a fixed (perhaps zero-point) energy level of a quantized anharmonic oscillator, and bound near  $r = 0$  in the potential well defined by the *closed form RATIONAL* potential (accurate for  $N \geq 44$ )

$$\nu_N(r) + \mathcal{R}_N(r) \equiv Z_1 Z_2 \cdot (e^2/L) \cdot \left\{ \sum_{k=0}^N c_k (r/L)^{2k} + 2 \cdot (r/L)^{2(N+1)} \cdot [1 - (r/L)^2]^{-1} \right\}. \quad (5)$$

Furthermore, one can learn *qualitatively* what occurs in this scenario by truncating (5) at  $N = 2$ , i.e. by omitting the remainder term  $\mathcal{R}_N$  and taking

$$\nu(r) \approx \nu_2(r) \equiv \nu_0 + K \cdot r^2/2, \quad \nu_0 \equiv Z_1 Z_2 \cdot (e^2/L) \cdot c_0, \quad K \equiv 2 Z_1 Z_2 \cdot (e^2/L^3) \cdot c_1, \quad (6)$$

which now produces a *harmonic* oscillator, whose Hamiltonian is

$$\mathcal{H} = (1/2)A_1 m_p (\dot{r})^2 + (1/2)K r^2, \quad (7)$$

where  $m_p$  is the mass of a proton, and therefore whose classical equation of motion is

$$\dot{r} + \omega^2 r = 0, \quad \omega \equiv (K/[A_1 m_p])^{1/2}. \quad (8)$$

According to the Virial Theorem (which applies equally to classical and quantized oscillators), the mean or expected values of the kinetic and potential energies of an oscillator are equal, and each equal to half of the total energy. In the case of a quantized oscillator, this means that

$$2PE = K(\Lambda_n)^2 = 2KE = A_1 m_p (\omega \Lambda_n)^2 = E_n = (n + 1/2)\omega \hbar, \quad (9)$$

where the non-negative integer  $n$  denotes the energy level. At zero Kelvins ( $n = 0$ ), this implies that, for  $\Lambda \equiv \Lambda_0$ , we have (taking  $c$  to denote light-speed)

$$\Lambda^2 = \hbar/(2A_1 m_p \omega), \quad (10a)$$

$$\Lambda^4 = (\hbar)^2/(4A_1 m_p [A_1 m_p \omega^2]) = (\hbar)^2/(4A_1 m_p K) = (\hbar)^2 L^3/(8A_1 m_p Z_1 Z_2 e^2 c_1), \quad (10b)$$

$$\Lambda^4/L^4 = (\hbar)^2/(8A_1 m_p Z_1 Z_2 e^2 L c_1), \quad (10c)$$

$$\sigma^4 \equiv (L/\Lambda)^4 = (8A_1 m_p Z_1 Z_2 e^2 L c_1)/(\hbar)^2 \equiv (8A_1 Z_1 Z_2) c_1 (e^2/[c\hbar])(m_p c/\hbar)L, \quad (10d)$$

which, following Peebles [2], can be rendered dimensionless by recalling that

$$\alpha \equiv (e^2/[c\hbar]) = 7.2973 \times 10^{-3}, \quad (11)$$

denotes the *fine structure constant*, and that

$$\lambda_p \equiv \hbar/(m_p c) \approx 2.1 \times 10^{-14} \text{ cm}, \quad (12)$$

denotes the *Compton wavelength of the proton*. In particular,  $m_p e^2/(\hbar^2) \equiv \alpha/\lambda_p$ . Accordingly, (10d) can be expressed in a dimensionless form as

$$\sigma \equiv L/\Lambda = \{[8A_1 Z_1 Z_2] \cdot [c_1 \alpha (L/\lambda_p)]\}^{1/4}, \quad (13)$$

which proves the result claimed in the *Abstract*.

In the case of a deuteron lattice inside a *supersaturated ("beta phase")* palladium lattice, it is known from crystallography that (allowing for the volumetric swelling in the beta phase)

$$L = 2.83 \text{ \AA}, \quad (14)$$

while from x-ray studies it is known that

$$\Lambda = 0.1002 \text{ \AA}, \quad (15)$$

so that, experimentally,

$$\sigma = 2.83/0.1002 = 28.2. \quad (16)$$

On the other hand, in this case  $Z_1 = Z_2 = 1$ , and  $A_1 = 2$ , so that the only unknown quantity in (13) is  $L$ , whence, using (14), the present theory yields

$$\sigma = 2(c_1 \cdot \alpha \cdot [L/\lambda_p])^{1/4} = 2(1.5492 \times 10^4)^{1/4} = 20(1.1156) = 22.31. \quad (17)$$

The fact that (17) agrees with the experimental value (16) within an error partially explainable by the truncation of the series (2) after only two terms suggests that the

series (2) is actually a fairly good model of physical reality.

Furthermore it appears that  $\Lambda$  is not measured with great accuracy (it is a blur on an x-ray photograph), so that consideration of the experimental error in the measurement of  $\Lambda$  may reduce the apparent discrepancy between the prediction (17) and the measurement (16).

If one considered the loosely bound particle to be in the potential well created by a positive particle rigidly bound at  $r = -L$  and another at  $r = L$ , then one would have only the repulsive Coulomb forces given by the potential

$$\begin{aligned} V_C(r) &\equiv Z_1 Z_2 \cdot (e^2/L) \cdot \left\{ \frac{1}{1 + (r/L)} + \frac{1}{1 - (r/L)} \right\} \equiv \\ &\equiv Z_1 Z_2 \cdot (e^2/L) \cdot \left\{ \frac{2}{1 - (r/L)^2} \right\} \equiv \\ &\equiv Z_1 Z_2 \cdot (e^2/L) \cdot \sum_{k=0}^{+\infty} 2(r/L)^{2k}, \end{aligned} \quad (18)$$

which is a geometric series that, because  $c_m \leq 2$ , majorizes the series (2) term-by-term. This provides a physical interpretation of the Madelung potential, because now we may express (2) as

$$V \equiv V_C - V_A, \quad (19_a)$$

where the repulsive Coulomb energies are modulated by the *attractive energies coming from the remainder of the lattice*, namely

$$V_A(r) \equiv Z_1 Z_2 \cdot (e^2/L) \cdot \sum_{k=0}^{+\infty} (2 - c_m) \cdot (r/L)^{2k} \geq (2 - c_0) > 0. \quad (19_b)$$

Defining the basic Coulomb energy unit

$$E_C \equiv e^2/L = 5.08211 \text{ eV}, \quad (20a)$$

enables one to consider the energy levels as dimensionless, by setting

$$\varepsilon \equiv V/E_C. \quad (20b)$$

These attractive energies make the bottom of the well, namely

$$\varepsilon(0) = c_0 < \varepsilon_C(0) = 2, \quad (21)$$

about 39% *deeper than it would be* if the Madelung forces were not taken into account! It can be shown that, in the case of the Fleischmann-Pons cold fusion experiments, between the energy levels  $\varepsilon = c_0$  and  $\varepsilon = 2$  there are some 88 Transmission Resonance Energy Levels, in which the probability of a particle tunneling through the Coulomb barriers defining the left and right-hand sides of the well are more than  $10^{57}$  times greater than would be calculated if the Coulomb energy alone were considered, i.e. at

$$\varepsilon = 2.1, \quad (22a)$$

if one defines  $r_t$  as the classical *turning point* at which

$$v(r_t) = \epsilon \cdot E_C , \quad (22b)$$

and defines  $r_{Ct}$  similarly by

$$v(r_{Ct}) = \epsilon \cdot E_C , \quad (22c)$$

and if one defines the corresponding *Gamow integrals* by

$$Q = \int_{r_t}^{L-r_n} \sqrt{2m_D(\epsilon \cdot E_c - v(r))} \frac{dr}{\hbar} , \quad (22d)$$

$$Q_C = \int_{r_{Ct}}^{L-r_n} \sqrt{2m_D(\epsilon \cdot E_c - v_C(r))} \frac{dr}{\hbar} , \quad (22e)$$

then the corresponding values of the *Gamow barrier penetration factor*  $\Theta^{-1}$  are

$$\exp(-2Q) = 8.81 \times 10^{-172} > \exp(-2Q_C) = 1.49 \times 10^{-229} , \quad (22f)$$

$$\exp(-2Q)/\exp(-2Q_C) = 5.9 \times 10^{57} . \quad (22g)$$

The result (22g) demonstrates quite explicitly the profound effects of the *long-range* attractive Madelung energies of the entire palladium-deuteride  $Pd \cdot D_{[1.0]}$  crystal and justifies the importance of considering the Madelung potential (2) as more relevant in this context than the Coulomb potential (18).

The skeptical reader may object that the Gamow factor, computed using (2), even though 57 orders of magnitude larger than the Gamow factor using (18), is still so small as to preclude the likelihood of observable cold fusion.

But such a conclusion would rest upon incorrect normalization of the wave function associated with the Gamow factor. Indeed, such a conclusion would be based upon fallacious neglect of the possibility of Resonant Transmission [2], which, since the first draft of this paper was submitted, has been independently studied by Kim *et al* under the highly appropriate name of *Resonance Transparency* [3].

In Bohm's classic book on quantum mechanics [2], it is demonstrated that if the potential well is created by potential barriers which are repeated periodically, then a particle-beam's probability flux intensity transmission coefficient or *transmissivity*  $T$  (i.e the ratio of transmitted to incident probability flux intensities) is given as a function of the energy level  $\epsilon$  of the beam's particles by

$$T = [1 + (1/4) \cdot (4\Theta^2 - \{1/[4\Theta^2]\})^2 \cdot \sin^2 \vartheta]^{-1} , \quad (23)$$

where

$$\Theta = \exp(2Q) , \quad (24)$$

$$\vartheta = (1/2) \cdot (\pi - R) , \quad (25a)$$

$$\mathcal{R} = 4 \int_0^r \sqrt{\frac{2m_D(V(r) - \varepsilon \cdot E_c)}{\hbar}} \frac{dr}{\hbar}. \quad (25b)$$

Whenever the energy  $\varepsilon$  is significantly different from a *resonance transparency* value  $\varepsilon_N$ , then the squared sine term may be replaced by its expected rms *average* value of  $(1/2)$ , and, since  $\Theta^{-2} \ll \Theta^2$ , the value of  $\mathbb{T}$  is then around

$$\mathbb{T} \approx (1/4) \cdot \Theta^4 \equiv (1/4) \cdot \exp(-4Q) = 0.8 \times 10^{-342}. \quad (26)$$

This tiny tunneling transmission coefficient will coincide with the skeptic's expectations and reinforce the tendency to *dismissive neglect* of the subject of cold fusion.

However, the hasty critic will be ignoring the exceedingly well established phenomenon of *resonant transmission through Coulomb barriers*, as proved experimentally in the Ramsauer Effect and in numerous high-energy nuclear physics experiments [2].

In fact, when the energy level  $\varepsilon_N$  of the incident particle has exactly the right value in order to make

$$\mathcal{R} = (2N+1) \cdot \pi, \quad (27)$$

then  $\sin(\vartheta) = 0$ , and  $\mathbb{T} = 1$ , i.e. the probability of tunneling is 100%!!!

The die-hard skeptic will retort, "agreed, if the incident particle's energy is truly resonant to hundreds of decimal places!" (In fact, such a comment has been used by Jändel [4] as the basis for claiming that the Transmission Resonance Model (TRM) of Bush [5] is fatally flawed.)

But this would be to disregard the known phenomenon of *phonon-mediated line broadening* [5] as well as the even stronger line-broadening results (16)-(20) of my paper [6]. In fact, I shall demonstrate elsewhere [6]-[7] that the zero-point energy level fluctuations of the rigidly bound deuterons at  $r = -L$  and at  $r = L$  broadens the resonant energy lines, to the point where any energy within 1.8% of resonance will have a transmission coefficient  $\mathbb{T} \geq 0.5$  and thus lead to *low-energy deuteron tunneling past the Coulomb barriers* on a massive scale, and that the resonant particles which by Resonance Transparency get past the Coulomb barrier at energies of less than 13.7 eV have *vanishing transmission coefficient* from  $r = -(L + r_n)$  to  $r = (L + r_n)$  when the strong nuclear force is *included* in the periodic potential profile as in [6]. In other words, with very high probability certain low-energy deuterons MUST fuse with one of their neighboring deuterons!

## References

- [1] Robert W. Bass, "A Closed-Form Expression for a Generic Madelung Series," to be submitted for publication.
- [2] David Bohm, *Quantum Mechanics*, Dover Publications, 1989.
- [3] Yeong E. Kim, Jin-hee Yoon, Alexander L. Zubarev & Mario Rabinowitz, "Coulomb Barrier Resonance Transparency for Cold Fusion with Deuterium and Hydrogen," *Proceedings*, Fourth International Conference on Cold Fusion (ICCF-4), Dec. 6-9, 1993, Maui, Hawaii (to appear).
- [4] M. Jändel, "The Fusion Rate in the Transmission Resonance Model," *Fusion Technology*, vol. 21 (1992), p. 176.
- [5] Robert T. Bush, "Cold Fusion: The Transmission Resonance Model Fits Data on Excess Heat, Predicts Optimal Trigger Points, and Suggests Nuclear Reaction Scenarios," *Fusion Technology*, vol. 19 (1991), pp. 313-356.
- [6] Robert W. Bass, "Bi-Resonant Transparency of Quadruple Coulomb Barriers in Periodic Potential Wells," submitted for publication.

- [7] Robert W. Bass, "Proof That Zero-Point Fluctuations of Bound Deuterons in a Supersaturated Palladium Lattice Provide Sufficient Line-Broadening to Permit Low-Energy Resonant Penetration of the Coulomb 'Barrier' to Cold Aneutronic Fusion," submitted for publication.

MATHECAD TUNNELING PROBABILITY RATIO DISPLAY

$$c_0 := 1.2249159575 \quad c_1 := 1.57531714655 \quad \epsilon := 2.1$$

$$V_M(x) := c_0 + c_1 x^2 + 2 \frac{x^4}{1-x^2} \quad V_C(x) := \frac{2}{1-x^2}$$

$$F_M(\eta) := \sqrt{\frac{|\eta - c_0|}{2 \left[ c_1 + |\eta - c_0| + \sqrt{(c_1 + |\eta - c_0|)^2 + 4(2 - c_1) \cdot |\eta - c_0|} \right]}} \quad F_C(\eta) := \sqrt{1 - \frac{2}{|\eta|}}$$

$$L := 2.83 \cdot 10^{-8} \quad \lambda_p := 2.1 \cdot 10^{-14} \quad cm1 := 137.036 \quad a := \frac{1}{cm1} \quad \alpha = 0.0072973525$$

$$E_C := 5.082112363 \quad E := \epsilon \cdot E_C \quad E = 10.6724359623 \quad r_n := 2.1 \cdot 10^{-13}$$

$$\zeta_n := \frac{r_n}{L} \quad \zeta_n = 7.4204946996 \cdot 10^{-6} \quad \zeta_{Ln} := 1 - \zeta_n \quad \zeta_{Ln} = 0.9999925795$$

$$\zeta_{M\epsilon} := F_M(\epsilon) \quad \zeta_{M\epsilon} = 0.5808530357 \quad \zeta_{C\epsilon} := F_C(\epsilon) \quad \zeta_{C\epsilon} = 0.2182178902$$

$$\tau(\lambda) := 8 \cdot \sqrt{\left( \frac{\lambda}{\lambda_p} \right)} \quad \tau_L := \tau(L) \quad \tau_L = 793.3342802657$$

$$J_{Mint} := \int_{\zeta_{M\epsilon}}^{\zeta_{Ln}} \sqrt{|\epsilon - V_M(t)|} dt \quad J_{Mint} = 0.9911965944$$

$$Q_M := \tau_L \cdot J_{Mint} \quad Q_M = 786.3502368323$$

$$J_{Cint} := \int_{\zeta_{C\epsilon}}^{\zeta_{Ln}} \sqrt{|\epsilon - V_C(t)|} dt \quad J_{Cint} = 1.3265519393$$

$$Q_C := \tau_L \cdot J_{Cint} \quad Q_C = 1.052399128 \cdot 10^3$$

$$q_M := \frac{Q_M}{2} \quad q_C := \frac{Q_C}{2} \quad \delta q := q_C - q_M \quad \delta q = 133.0244455953$$

$$T_{Msqrt} := \frac{e^{-q_M}}{2} \quad T_{Csqrt} := \frac{e^{-q_C}}{2} \quad e^{2 \cdot \delta q} = 3.4959511907 \cdot 10^{115}$$

$$T_{Msqrtscaled} := T_{Msqrt} \cdot 10^{300} \quad T_{Msqrtscaled}^2 = 7.7691106901 \cdot 10^{257}$$

$$T_{Csqrtscaled} := T_{Csqrt} \cdot 10^{300} \quad T_{Csqrtscaled}^2 = 2.2223166933 \cdot 10^{142}$$

$$RATIO := \left[ \left( \frac{T_{Msqrt}}{T_{Csqrt}} \right)^2 \right] \quad RATIO = 3.4959511907 \cdot 10^{115} \quad \sqrt{RATIO} = 5.9126569245 \cdot 10^{57}$$

$$T_{Msqrtscaled} = 8.8142558904 \cdot 10^{128} \quad T_{Csqrtscaled} = 1.4907436712 \cdot 10^{71}$$

## Appendix 3

# PROOF THAT ZERO-POINT FLUCTUATIONS OF BOUND DEUTERONS IN A SUPERSATURATED PALLADIUM LATTICE PROVIDE SUFFICIENT LINE-BROADENING TO PERMIT LOW-ENERGY RESONANT PENETRATION OF THE COULOMB 'BARRIER' TO COLD ANEUTRONIC FUSION

### Abstract

Between the energy levels of  $E = 6.26$  eV and  $E = 140.96$  eV, there are 600 Resonant Transmission levels  $E_N$ , ( $N = 0, 1, 2, 3, \dots, 600$ ), at which the quantum-mechanical probability flux intensity transmission coefficient, or *transmissivity*,  $\tau = 1$ , i.e. which assure with 100% probability that a loosely bound deuteron of that energy, between two adjacent rigidly bound deuterons, will tunnel through the Coulomb barrier of one of the adjacent deuterons (to within the range of its strong nuclear force) and remain there indefinitely. Use of the standard WKB approximation establishes that between  $E_0 = 6.26$  eV and  $E_5 = 6.59$  eV there are five such resonant lines, which have line breadths increasing from 1.8% to 7% of the difference between that line and the next higher line. At  $N = 88$ , one finds  $E_{88} = 13.7403$  eV, and  $E_{89} = 13.8468$  eV, and the line breadth  $\delta E_{88} = 0.077967$  eV of the 88<sup>th</sup> level is 74% of the difference  $\Delta E_{88} = 0.1065$  eV between the 88<sup>th</sup> and the 89<sup>th</sup> levels. The line broadening is caused by zero-point energy fluctuations of the rigidly bound deuterons, as characterized by the Schwinger Ratio  $\sigma \equiv L/\Lambda = 22.31$ , according to the Madelung potential theory presented in a companion paper [4].

### Detailed Results

The reader is assumed to be familiar with the companion paper [1], in which it was demonstrated that the difference between the repulsive Coulomb potential  $v_C$  of the two nearest rigidly bound deuterons and the Madelung potential  $v_M$  is an attractive potential  $v_A$  which comes from the remainder of the entire lattice.

There we defined

$$E_C \equiv e^2/L = 5.08211 \text{ eV} \quad (1)$$

and rendered other energies  $E$  dimensionless by scaling them with  $E_C$ :

$$\varepsilon = E/E_C \quad (2)$$

Dropping the subscript  $M$  on  $v_M$  for convenience, we defined

$$Q = \int_{r_t}^{L-r_n} \sqrt{2m_D(\varepsilon \cdot E_c - v(r))} \frac{dr}{\hbar}, \quad (3)$$

$$\mathcal{R} = 4 \int_0^{r_t} \sqrt{2m_D(v(r) - \epsilon \cdot E_c)} \frac{dr}{\hbar} . \quad (4)$$

where  $r_t$  is the classical *turning point* at which

$$v(r_t) = \epsilon \cdot E_c . \quad (5)$$

There we also defined the quantum-mechanical probability flux *transmissivity* as

$$\tau = [1 + (1/4) \cdot (4\Theta^2 - \{1/[4\Theta^2]\})^2 \cdot \sin^2 \vartheta]^{-1}, \quad (6)$$

where

$$\Theta = \exp(2Q), \quad (7)$$

$$\vartheta = (1/2) \cdot (\pi - \mathcal{R}), \quad (8)$$

and a *Resonant Energy*  $\epsilon_N$  is an energy level at which

$$\mathcal{R} = (2N+1) \cdot \pi, \quad (N = 0, 1, 2, 3, \dots), \quad (9_a)$$

which provides  $\tau = 1$  (i.e., *perfect transmission*). Subsequent to the submission of a first draft of this paper, I learned that, independently of me, Kim *et al* [2] had introduced the definition of *Resonance Transparency* to define the case

$$\tau = \tau(E) = 1 \quad (9_b)$$

without reference to (6)-(8) or (9<sub>a</sub>), which are approximations derived from the WKB method, whereas the methodology of Kim *et al* [2] is perfectly rigorous mathematically and uses no approximations. Unfortunately, the perfectly rigorous methodology is so difficult to apply that Kim *et al* did not attain any actual results (which would have provided a check on the accuracy of those herein), but simply advocated a rigorous methodology, with which advocacy I concur completely. In fact, I suggest that the following results should be used as a point of departure for use of the more exact methodology, and the discoveries announced below should be refined by being computed with greater precision by the methodology of [2]. Accordingly I shall refer to *Resonant Transparency* even though the limitations of the WKB method (which has led to numerous profoundly important predicted results in both atomic and nuclear physics that were subsequently verified experimentally [3], [4], although its quantitative precision is not as good as its qualitative validity) require that the reader note that I do not mean (9b) in rigorous exactitude, but only that (9b) holds for the WKB approximation (1)-(8) and that, consequently, all that is assured rigorously herein is that  $E = \epsilon_N$  for some value of  $N$  in (9<sub>a</sub>).

Note that in the present model only electrostatic forces are considered, and that the standard theory of resonant transmission through two Coulomb barriers surrounding a single potential well, as presented by Bohm [3], is used. Note also that  $\mathcal{R}$ , and so the values of  $E$  at which  $\tau = 1$ , are completely independent of assumptions about the potential beyond the turning point! Here the unphysical assumption is made that the potential drops to equality with  $E$  inside the nuclear surface, so that the contribution to the integral  $Q$  vanishes beyond  $r = L - r_n$ , where the lattice period  $L = 2.83 \text{ \AA}$ , and, for the range of the strong nuclear force,  $r_n = 2 \times 10^{-13}$  is used. Perhaps a better model would be to assume the electrostatic potential  $v(r)$  has the *constant* value  $v(r_n)$

on the interval  $L - r_n \leq r \leq L$ , in which case the integral  $Q$  would be *increased* slightly, and the resulting *Gamow barrier penetration factor*  $\Theta^4$  would be *increased* somewhat, but this would not have the slightest effect on the results presented herein (because the effects of  $Q$  and  $R$  on  $T$  are *UNCOUPLED* when (9) holds!).

Furthermore, note carefully that, from (6), if we replace  $\sin^2 \vartheta$  by its expected *rms average* value  $(1/2)$ , then, asymptotically,

$$T \cong (1/4) \cdot \Theta^4, \quad (6bis)$$

and it is the enormous value of  $\Theta$  which is responsible for the widespread misconception that the Coulomb barrier "forbids" the possibility of Aneutronic Cold Fusion. For the most part, those proclaiming that "the laws of physics" forbid the possible reality of the phenomenon are thinking about the elementary result (6bis) and have forgotten the more sophisticated result (6) which allows for the possibility of Resonant Transparency (9bis), and even the sophisticated critics of Bush's semi-empirical and semi-classical *Transmission Resonance Model (TRM)* [3], such as Jändel [4] (who claims that, because of the infinitesimal widths of the resonance lines when computed by the standard Breit-Wigner theory, the resonant transmission times in this context would be greater than the accepted age of the universe) have overlooked the possibility of line broadening by the mechanism to which Schwinger [5] brought attention in his theory of *Nuclear Energy in an Atomic Lattice (NEAL)*, which focuses attention on a single ratio, that I have called the Schwinger Ratio in his honor [1], and which is demonstrated below to be the key to rebuttal of Jändel's doubts.

It is convenient to render the preceding formulae dimensionless, which is done as follows. Define

$$\xi = r/L, \quad v(\xi) = V(\xi L)/E_C = \sum_{k=0}^{+\infty} c_k \xi^{2k}, \quad (10)$$

where a general formula for the coefficients  $c_k$ , and numerical values sufficient to permit computation of  $V(\xi L)$  to 17-decimal-place accuracy over the entire domain of definition, namely  $-1 < \xi < 1$  (even though the convergence is not uniform for  $|\xi| < 1$ , and in fact  $v \rightarrow +\infty$  as  $|\xi| \rightarrow 1$ ) was presented in [1]; and let  $\xi = F(\epsilon)$  denote the inverse function to  $\epsilon = v(\xi)$ , i.e.

$$v(F(\epsilon)) \equiv \epsilon. \quad (11)$$

Then by the same sort of manipulations as used in deriving  $\sigma$  in [1], or (22b) below,

$$R = R(L, \epsilon) = \gamma(L) \cdot I(\epsilon), \quad (12)$$

where

$$\gamma = \gamma(\lambda) \equiv 8 \sqrt{\alpha \cdot (\lambda/\lambda_p)}, \quad (13)$$

$$I = I(\epsilon) = \int_0^{F(\epsilon)} \sqrt{v(\xi) - \epsilon} d\xi. \quad (14)$$

The resonant energies are found numerically by solving

$$f(N, \epsilon) \equiv (2N + 1) \cdot \pi - R(L, \epsilon) = 0. \quad (15)$$

I found the 600 values  $\{\epsilon_N\}$  announced in the Abstract above quite rapidly using a modification [to prevent iterates from going outside  $|\xi| \leq 1$ ] of a *BASIC* program for

finding solutions of (15) in Koonin's book on *Computational Physics*; then I used these values as initial iterates for obtaining more accurate values (at the expense of more computational time) using the Levenberg-Marquardt Algorithm implementation of *MATHCAD*. A summary of the results is in an Appendix.

Let

$$\Delta_L \gamma = (d\gamma/dL)/\gamma, \quad \Delta_\varepsilon I = (dI/d\varepsilon)/I, \quad (16)$$

so that, since

$$\Delta_L \gamma = 1/(2L), \quad (17)$$

$$\delta R = R(L, \varepsilon) \cdot \{ (1/2) \cdot (\delta L/L) + [\Delta_\varepsilon I] \cdot \delta \varepsilon \}. \quad (18)$$

Now Schwinger's theory of the zero-point fluctuations of the locations of the bound deuterons, as summarized in [1], provides that  $\delta L$  is a Gaussian random variable of zero mean and standard deviation  $\Lambda$ , where  $\sigma = L/\Lambda$ . Hence in the domain of validity of the local linearization (16),  $\Delta_\varepsilon I$  is also a Gaussian random variable of zero mean and standard deviation computable by the assumption of linearity. Now with 67% probability,

$$|\delta L|/L \leq 1/\sigma. \quad (19)$$

Therefore as  $\delta L$  fluctuates in the range (19), the first term in  $\{\cdot\}$  in (18) will fluctuate between  $-1/(2\sigma)$  and  $1/(2\sigma)$ . If any value in that range corresponds to the negative of  $[\Delta_\varepsilon I] \cdot \delta \varepsilon$ , where  $(\varepsilon_N + \delta \varepsilon)$  is the *actual* energy level, then

$$\delta R = 0, \quad (20)$$

and the actual energy level will truly coincide with a resonant energy level. Therefore to find the allowable bounds on  $\delta \varepsilon$  such that (20) holds, we may use

$$|\delta \varepsilon| \leq 1/(2\sigma \cdot [\Delta_\varepsilon I]), \quad (21)$$

where the variation in  $I$  is evaluated at  $\varepsilon = \varepsilon_N$ . If the actual energy level is sufficiently near to a resonant level that (21) holds, then, returning to a particle picture in the semi-classical interpretation, during each period of vibration, the harmonic oscillator's position sweeps through *every* value in its range; consequently, within the very short period of the zero-point vibrations, the actual energy will sweep through *all* values in the range (21) and so at some time coincide *precisely* with a resonant energy. Note that the *key* to the prediction of the *line breadths*  $\delta \varepsilon$  by (21) is the value of the Schwinger Ratio  $\sigma$ . In [1] we used the first two terms of the Madelung series (10) to predict approximately the value  $\sigma = 22$ , and then quoted experimental measurements of  $\Lambda$  in fully loaded (i.e. supersaturated or beta-phase)  $PdD_{[1.0]}$  lattices which imply that  $\sigma = 28$ . For convenience in the *MATHCAD* programs used in this paper and its companion [1], the theoretical rather than experimental value of  $\sigma$  was used.

Using (2), and  $\sigma = 22.31285$ , the final results are:

$N$	$\varepsilon_N$	$E_N$ [eV]	$\delta E$ [eV]
0	1.2312	6.2574	0.001170
1	1.2440	6.3221	0.001756
2	1.2568	6.3874	0.002918
3	1.2697	6.4530	0.004071

4	1.2828	6.5191	0.005216
5	1.2959	6.5857	0.006354
10	1.3627	6.9252	0.011927
88	2.7037	13.7403	0.077967
89	2.7246	13.8468	

Note that the breadth of the 88<sup>th</sup> line is an amazing 74% of the distance to the next line!

### Comparison with Bush TRM Spectrum

Robert T. Bush has published [3]-[3bis] both theoretical and experimental evidence in favor of a Transmission Resonance Spectrum which not surprisingly does not coincide with the preceding, because the model of a lattice used in [3] is relatively crude in comparison to that used here. Bush's *semi-classical* [and, as applied in electrochemistry to predict *relative* rather than absolute Excess Enthalpy, is admittedly also "*semi-empirical*"] model considers a point-particle of linear momentum  $p_N$  moving freely through a one-dimensional lattice of periodic length  $L$ , and applies the 1923 *DUANE'S RULE* (which preceded quantum mechanics, and, according to Landé, is one of three axioms from which Schrödinger's Equation can be *derived*), according to which the condition for an *inelastic* collision of the particle with the lattice is that any exchange of linear momentum between the particle and the lattice must be such that  $\Delta p$  is an integral multiple of  $h/L$ , from which it is reasonable to postulate that

$$p_N = \sqrt{2m_D E_N} = \sqrt{2m_D \epsilon_N (e^2/L)} = (2N + 1)\pi\hbar/L, \quad (22a)$$

which can be rendered dimensionless by following Peebles [5] in setting  $e^2 m_p / (\hbar)^2 = \alpha / (\lambda_p)$ , where  $\alpha = e^2 / (\hbar c) = 1/137.036$  is the *fine structure constant* and where  $\lambda_p = \hbar / (m_p c) = 2.1 \times 10^{-14}$  cm is the *proton Compton wavelength*; thus

$$E_N = (2N + 1)^2 \cdot E_0, \quad E_0 = \epsilon_0 \cdot E_C, \quad \epsilon_0 = (1/4)(\lambda_p / L) \cdot (\pi^2 / \alpha) = 2.52 \times 10^{-4}, \quad (22b)$$

where  $E_C = 5.082$  eV and so  $E_0 = 0.001275$  eV. Under this scheme, if we define the Bush index  $\tilde{N} \equiv N - 34$ , we get for the above  $N = 1$  and  $E_1 = 6.26$  eV the bracketing  $\tilde{N}$  values of 0 and 1, at which the Bush spectrum would be 6.07 eV and 6.43 eV; similarly, for the present  $N = 88$  and  $E_{88} = 13.74$  eV we get bracketing values of  $\tilde{N}$  of 17 and 18 at which Bush predicts 13.52 eV and 14.06 eV, respectively; finally, for the present  $N = 600$  and  $E_{600} = 140.96$  eV we get bracketing values of  $\tilde{N}$  of 131 and 132 at which Bush

predicts 139.69 eV and 141.38 eV, respectively. Thus, it can be seen that the present Resonant Transparency spectrum, derived from Schrödinger's Equation via the accepted WKB approximation, predicts a spectrum which is between 4.5 and 4.8 times "more dense" than that predicted by Bush. This is a puzzlement, because Bush has published experimental evidence in favor of the "coarser" spectrum of his TRM Model. A possible explanation is suggest by the present author elsewhere [6], in which it is suggested that a freely moving deuteron may collide with a bound deuteron and knock it into a higher energy level, from which the present theory would be applicable. Because of the difficulty of the scattering calculation (the present simplified scenario was difficult enough!), in [6] I used a semi-classical approach, intermediate in rigor between Duane's Rule and Schrödinger's Equation (namely I used Conservation of Momentum and Conservation of Energy but assumed that the energy of a bound deuteron was quantized as in a harmonic oscillator [which agrees with the lower-order energy levels found here, because, as pointed out by Bohm [7], the condition for a deuteron to be bound in a potential well, namely (9) above, is EXACTLY the same as the condition for a particle

to have Resonant Transmissivity if the well is repeated periodically] and that the linear momentum of the colliding particle is quantized as in Duane's Rule); the result is that I have suggested that Bush's empirical data would better fit his TRM Model if, instead of the quantum numbers  $N = 1, 2, 3, \dots, 16, 17$  which he used, the "almost integral, but strictly speaking, fractional quantum numbers"  $N = (31 + 27K)/31$ , or  $N = 1 + (27/31)K$ , corresponding to  $\bar{N} = 31 + 27K$  for  $K = 0, 1, 2, 3, \dots, 15, 16$ . Since I submitted the result [6] suggesting that the Bush spectrum "really" begins at above  $\bar{N} = 31$  BEFORE I had derived the above more-rigorous result that  $\bar{N}$  should begin at  $\bar{N} = 34$  or 35, and stated plainly that the methodology used in [6] was expected to be no better than Bohr's "old quantum theory", I continue to suggest that Bush should re-examine his data to see whether or not it fits the predictions of [6] or the present theory even better than it fits the simpler Duane's Rule QRT theory.

### Conclusion

Despite expert opinion to the contrary, "standard quantum mechanics" most assuredly does *PREDICT* the existence of the phenomenon of cold fusion in a *PERIODIC* lattice when the ratio of deuterons to palladium ions is nearly one-to-one, and when some externally applied force (e.g. a current, or a shock) is driving newly entering deuterons through the adjacent cells of the deuterium lattice.

The lowest resonant energy level at which the line broadening is more than 70% of the distance to the next line is at  $E_{88} = 13.74$  eV.

Applying a deuteron current with a driving voltage of 13.74 volts between the palladium cathode and the platinum anode should produce cold fusion. (Also, any other voltage between 6.26 eV and 6.59 eV should work almost as well.)

### Concluding Postscript

The inherent limitations of the widely used but inexact WKB approximation *preclude over-reliance* upon the *precise* numerical values announced herein, but nevertheless suggest the *qualitative validity* of the *Resonant Transparency Spectrum* presented above. The present spectrum seems to be a refinement of the relatively crudely-derived but experimentally confirmed Bush TRM spectrum [3], because the present quantum-mechanical results predicts 600 resonances in an energy range wherein the Bush spectrum predicts only 132 resonances; also an apparently fatal objection [4] to the concept of Resonant Transparency as used either by Bush [3] or above is asserted by me [8] to have been decisively rebutted. Obviously it would be highly desirable to have the present research repeated with the more exact methodology of Kim, Yoon, Zubarev & Rabinowitz [2] in order to predict *experimentally testable results* about this spectrum with greater numerical precision. But the past successes of the WKB method suggest that the present results have, for the first time, starting with Schrödinger's equation, established the **EXISTENCE** of a Resonant Transparency Spectrum of energy levels of slightly excited deuterons in a frozen deuterium lattice, even at absolute zero temperature, and otherwise composed of rigidly bound deuterons which would be motionless except for zero-point fluctuations, yet according to **standard quantum mechanics** will find the Coulomb 'barrier' to Cold Fusion to be transparent rather than opaque!

### References

- [1] Robert W. Bass, "Proof That Madelung Forces Predict the Schwinger Ratio Correctly, and that they drastically attenuate Coulomb singularities in lattices," submitted for publication on 12/04/93.
- [2] Yeong E. Kim & Jin-Hee Yoon & Alexander L. Zubarev & Mario Rabinowitz, "Coulomb Barrier Resonance Transparency for Cold Fusion with Deuterium and Hydrogen," presented to ICCF-4, Dec. 6-9, 1993, paper T 2.2.
- [3] Robert T. Bush, "Cold Fusion: the Transmission Resonance Model Fits Data on

- Excess Heat, Predicts Optimal Trigger Points, and Suggests Nuclear Reaction Scenarios," *Fusion Technology*, vol. 19 (1991), pp. 313-356.
- [3bis] Robert T. Bush & Robert D. Eagleton, "Experimental Studies Supporting the Transmission Resonance Model for Cold Fusion in Light Water: II Correlation of X-Ray Emission With Excess Power," presented to ICCF-3, Nagoya (1992); printed in *Frontiers of Cold Fusion*, Universal Academy Press Inc., 1992, pp. 409-4-16.
- [4] M. Jändel, "The Fusion Rate in the Transmission Resonance Model," *Fusion Technology*, vol. 21 (1992), p. 176.
- [5] P.J.E. Peebles, *Quantum Mechanics*, Princeton University Press, 1992
- [6] Robert W. Bass, "QRT: Quantum Resonance Triggering Principle," submitted to *Fusion Technology*, on July 4, 1993.
- [7] David Bohm, *Quantum Theory*, Dover Publications, 1989.
- [8] Robert W. Bass, "Bi-Resonant Transparency of Quadruple Coulomb Barriers in Periodic Potential Wells," to be submitted for publication.
- 

#### Appendix 4

### BI-RESONANT TRANSPARENCY OF QUADRUPLE COULOMB BARRIERS IN PERIODIC TRIPLE POTENTIAL WELLS

#### ABSTRACT

Using the phase-integral method of Jeffries (1923), commonly called the WKB method for [qualitatively correct but only quantitatively approximate] solution of the wave equation, expressions are derived which would be, if exact, necessary and sufficient conditions for energy levels of a particle moving toward a triple potential well to encounter Resonant Transparency of all four Coulomb Barriers, i.e. to penetrate all four barriers with 100% probability. As a special case, a 6.3 eV deuteron trapped in a deuteron lattice [inside a  $Pd\cdot D_{1.0}$  lattice] can readily penetrate the nearest two

Coulomb barriers, to reach the vicinity of the strong nuclear force of either adjacent bound deuteron, even if it lacks the full 4.3 MeV energy proved here to be required for Resonant Transmission completely through the nuclear potential wells: so standard quantum mechanics actually PREDICTS "aneutronic cold fusion" in a [supersaturated,

"beta" phase]  $Pd\cdot D_{1.0}$  periodic palladium-deuterium lattice.

#### Derivation of Transmissivity

If one looks up all of the references to "resonant transmission" in a standard text on Quantum Mechanics by Bohm [1], or nuclear physics by Blatt & Weisskopf [2], one finds a plethora of qualitative predictions in both atomic and nuclear physics, derived by the WKB method (herein called the JWKB method because of priority by mathematical physicist H. Jeffries [3]), which have been subsequently confirmed by experiment. (For more mathematical details about the JWKB method, see [4] and [5]; note that if one uses the approach of Mathews & Walker [5], quantitative error bounds on the JWKB approximation are available.)

Here the methodology of the double-well result exposited by Bohm [4] will be followed slavishly; the triple-well result is then a straightforward exercise in application of the "*asymptotic connection formulae*" for joining solutions of the wave equation in exponentially-decaying regions with solutions in undamped-sinusoid regions. The exercise requires an inordinate amount of brute-force algebra & trigonometry: unless the reader is more infallible about sign errors and the like than the present author, it may take hundreds of hours of tedious manual labor to derive the present result and to verify its validity.

Although the present result is applicable to an arbitrary potential  $V(r)$ , the

present author has demonstrated [6], [7], [8] that inclusion of the "attractive Madelung forces" from the remainder of the periodic lattice, in the manner of Schwinger's NEAL [Nuclear Energy in an Atomic Lattice] theory [9], makes the Coulomb well defined by two adjacent deuterons in a deuterium lattice (inside a supersaturated [or "beta" phase]  $Pd-D_{1.0}$  palladium-deuterium lattice) some 50% deeper, and in this deepened well there are between  $E = 6.3$  eV and  $E = 13.7$  eV some 88 resonant transparency lines with line widths increasing from 1.8% to 74% of the difference between the resonant line and the next higher adjacent line. (Exploiting an idea of Schwinger [9], validated by the present author [10], the line-widths depend upon the zero-point motion of the lattice's bound deuterons; therefore it is rigorously correct to assert that **"cold fusion would not occur were it not for the quantum-mechanical background vacuum energy providing a lattice's zero-point energy!"**

Consider now the Coulomb-Madelung potential  $v_M(r)$  defined [6-8,10] between adjacent deuterons of mass  $m_D$  bound rigidly at locations  $r = -L$  and  $r = L$ , where in the particular application in mind,  $L = 2.83 \text{ \AA}$ . Actually, the Coulomb force is modified by the strong nuclear force between  $r = -(L + r_n)$  and  $r = -L + r_n$ , and between  $r = L - r_n$  and  $r = L + r_n$ , where the approximate value  $r_n \cong 2 \times 10^{-13} \text{ cm}$  is used for the range of the strong nuclear force, and so the Coulomb-Madelung potential  $v_M$  is truncated outside of the potential well interval  $-L + r_n < r < L - r_n$  and the potential  $v = -|v_n|$  is used in the two disjoint bordering barrier intervals just defined, with  $|v_n| = 21.1 \text{ MeV}$  used in the presently pursued application. Finally, the potential may be extended to a periodic function in an entire lattice by taking  $v(r) \equiv v(r + 2L)$  for  $r$  less than  $-(L + r_n)$  and  $v(r) \equiv v(r - 2L)$  for  $r$  greater than  $(L + r_n)$ , which extends  $v$  to the interval  $-4L < r < 4L$ , and then inductively repeating this extension *mutatis mutandis*.

The *quadruple* Coulomb-Madelung barrier, *triple* potential well just defined is qualitatively depicted in Fig. 1 (not to scale). Thus the potential's domain is divided into 9 regions,  $\mathcal{R}_i$ , labelled in Roman Numerals,  $\mathcal{R}_I, \mathcal{R}_{II}, \dots, \mathcal{R}_{IX}$ ; and by  $v_i$  is denoted the potential in region  $i$ , where  $i = I, II, III, IV, V, VI, VII, VIII, IX$ . Then, following the notation of Bohm [1], one defines

$$p_{[i]} \equiv \sqrt{2m_D |E - v_i|}, \quad (1)$$

where  $[i]$  denotes the Arabic numeral corresponding to the Latin numeral  $i$ . For convenience, taking  $m = (1, 2, 3, 4)$ , the obvious notations

$p_w = p_1$  or  $p_5$  or  $p_9$ ,  $p_n = p_3$  or  $p_7$ ,  $p_b = p_{2m}$ ,  $p_i$  pertaining to the *well*, *nuclear*, and *barrier* regions, are used, where the particular  $p_i$  designated can be discerned from the context.

Next, define the *Gamow barrier penetration factor* as  $\Theta^4$  where

$$\mu_b = \int_{\mathcal{R}_b} p_b \frac{dr}{\hbar}, \quad \Theta = \exp(\mu_b) \gg 1, \quad (3)$$

where  $\mathcal{R}_b$  denotes any of the even-numbered barrier regions, and where the enormously large value of  $\Theta$  is responsible for the unwarranted prejudice against the possibility of cold fusion. Thus, for example,

## QUADRUPLE COULOMB BARRIERS

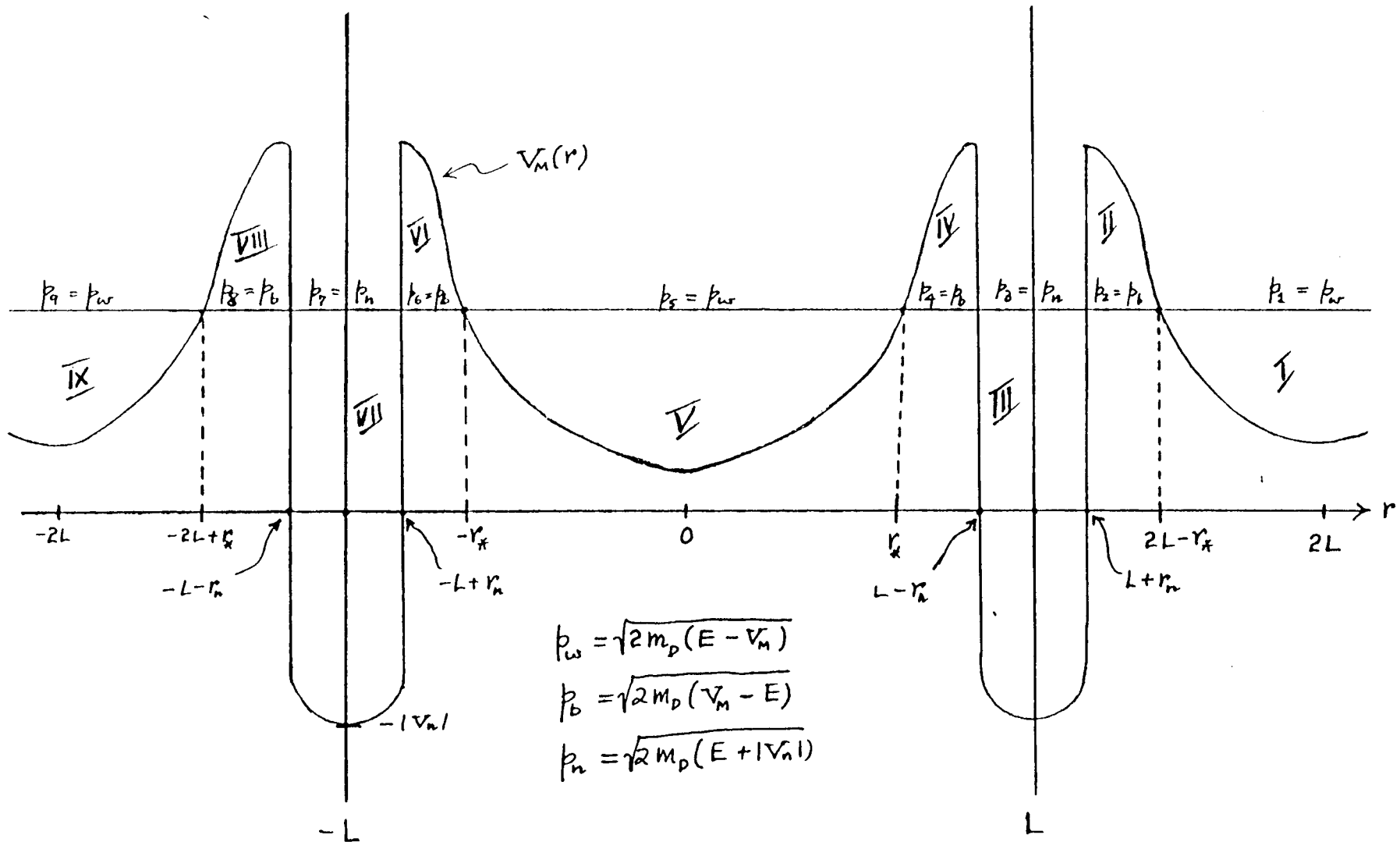


Fig. 1

$$\Theta = \exp \left( \int_{L+r_n}^{2L-r_*} p_2 \frac{dr}{\hbar} \right), \quad V_M(r_*) = E. \quad (4a,b)$$

Finally, for the conciseness required in enormously long trigonometric manipulations, define

$$c_j = \cos(\beta_j), \quad s_j = \sin(\beta_j), \quad (5)$$

$$\beta_j = (1/2)(\pi - [(J_j)/\hbar]), \quad J_j = 2 \int_{R_j}^{\infty} p_j dr, \quad j = w \text{ or } n. \quad (6)$$

The idea behind the following quantum-mechanical scattering-theory calculation is the following.

Consider a particle of mass  $m_D$  and energy  $E$ , inside  $\mathcal{R}_{IX}$ , impinging from the left on the quadruple barrier beginning at  $R_{VIII}$ , at  $r = -2L + r_*$  where (4b) holds. What is the wave-mechanical probability that such a particle will be found in  $\mathcal{R}_I$ ?

Convert to the *wave picture* and note that by the JWKB approximation a real solution of Schrödinger's equation in  $\mathcal{R}_{IX}$  has the form

$$\Psi_{IX} = \Psi_{inc} + \Psi_{refl}, \quad \Psi_{refl} = \overline{\Psi_{inc}}, \quad (7a)$$

$$\Psi_{inc} = (A/[2\sqrt{p_w}]) \cdot \exp(i\theta) \cdot (R_1 - iR_2), \quad (7b)$$

where, in the *complex probability amplitude*  $\Psi_{inc}$  for the *incident wave*, the numbers  $(A, \theta, R_1, R_2)$  are all *real* and (7b) represents a wave moving to the right *toward* the barrier, and where its complex conjugate  $\Psi_{refl}$  represents the probability amplitude of the corresponding *reflected wave*. Now use the *asymptotic connection formulae* to connect the solution  $\Psi_{IX}$  to the solution  $\Psi_{VIII}$  in  $R_{VIII}$ , and then proceed inductively, alternating between the exponential and sinusoidal JWKB approximations as representations of  $\Psi$  in a piecewise manner, until the *transmitted solution*

$$\Psi_{tm} = \Psi_I = (A/[2\sqrt{p_w}]) \cdot \exp(i[\theta + \Delta\theta]), \quad (7c)$$

is obtained, where as usual it is assumed that  $A$  is arbitrary and that  $R_1$  and  $R_2$  have been so adjusted that  $\Delta\theta$  is a real number and that

$$(R_1)^2 + (R_2)^2 \geq 4. \quad (7d)$$

Then the *Transmissivity*  $T$  is defined as usual as the ratio of the *intensities* of the transmitted and incident *probability fluences*, namely

$$T = |\Psi_{tm}|^2 / |\Psi_{inc}|^2 = 4 / |R_1 - iR_2|^2 \equiv 4 / [(R_1)^2 + (R_2)^2] \leq 1. \quad (7e)$$

Except at extraordinarily particular values of  $E$ , it will be proved that  $T \ll 1$ . But in the special case wherein the nuclear wells are neglected and the

electrostatic potential truncated as a constant at the value of this potential at the nuclear surface [Example 2 below, upon replacing  $s_w^2$  by its expected rms average  $1/2$ ]

$$\tau = \tau(E) \cong 4^{-1} \cdot \Theta^{-4} \ll 1, \quad (7f)$$

which has led to the widespread but erroneous misconception about the "difficulty of penetration of the Coulomb barrier", according to which the majority of contemporary physicists have expressed *a priori* radical skepticism that cold fusion is compatible with "the known laws of physics."

However such a conclusion ignores the possibility of *resonant transmission* when the transmissivity  $\tau = 1$  at particular levels of energy  $E$  at which  $s_w = 0$  (in the case of Example 2 below). To emphasize the intuitively understandable optical analogy, Kim *et al* [11] have recently DEFINED "Resonance Transparency" at a particular energy level  $E_{\#}$  as the condition for *perfect transmissivity*, i.e.

$$\tau(E_{\#}) = 1. \quad (7g)$$

In the present **general case** (7e) it will be proved that (7g) holds whenever  $s_n^2 = 1/3$  and  $s_w \cong 1/(4 \cdot 2^{1/2} \cdot \Theta^2) \cong 0$ .

For brevity in derivation of the *transmissivity* function  $\tau(E)$ , it is convenient to introduce the following new definitions:

$$\Phi = \Theta + \Theta^{-1}, \quad \Phi \geq 2, \quad (\Rightarrow \Phi^2 \geq 4), \quad (7h,i)$$

$$\delta = 1/(2\Theta), \quad \Delta = \delta^{-1} \equiv 2\Theta, \quad \Gamma = (\delta^2 + \Delta^2)/2, \quad (7j,k,l)$$

$$\Psi = 2^{-1}\delta^3 + 2\Delta^3, \quad \Lambda = \Psi/\Phi, \quad (7m,n)$$

where, asymptotically, for large  $\Theta$ ,

$$\Phi \cong \Theta, \quad \Psi \cong 16\Theta^3, \quad \Gamma \cong 2\Theta^2, \quad \Lambda \cong 16\Theta^2. \quad (7o,p,q,r)$$

Now introduce a quadratic form  $Q$  in  $(s_w, c_w)$  defined in vector-matrix notation by

$$Q = x \cdot P x, \quad P = P^T > 0, \quad x = (s_w, c_w)^T, \quad (8a,b,c)$$

where the superscript  $T$  denotes vector-matrix transposition and where  $P$  is a *positive-definite* matrix [for  $c_n \neq 1$ ] defined as

$$P = M^T \cdot M, \quad M = \begin{pmatrix} -2\Gamma c_n s_n & c_n^2 - s_n^2 \\ c_n^2 - \Lambda s_n^2 & 2c_n s_n \end{pmatrix}, \quad (8d,e)$$

$$\det(P) \equiv [\det(M)]^2, \quad \det(M) = -\Lambda + (4\Gamma + 3\Lambda + 1)c_n^2 - 2(2\Gamma + \Lambda + 1)c_n^4, \quad (8d,ebis)$$

where  $\det(M) < 0$  if  $c_n^2 \neq 1$ ;  $\det(M) = 0$  if  $c_n^2 = 1$ . Because  $x$  is a unit vector,

$$0 \leq \lambda_{\min} \equiv \|P^{-1}\|^{-1} \leq Q \leq \|P\| \equiv \lambda_{\max}, \quad (8f)$$

where  $0 < \lambda_{\min}$  if  $c_n \neq 1$ , and because  $P$  is of dimension  $n = 2$ ,

$$0 < \lambda_{\min} + \lambda_{\max} \equiv \text{trace}(P), \quad 0 \leq \lambda_{\min} \cdot \lambda_{\max} \equiv [\det(M)]^2, \quad (8g,h)$$

where, again, it is important to note that *strict inequality* holds in (8h) if  $c_n \neq 1$ . By elementary trigonometric identities

$$\text{trace}(P) = 1 + 4\Gamma^2 c_n^2 s_n^2 + (\Lambda s_n^2 - c_n^2)^2. \quad (8g,hbis)$$

Because both  $\text{trace}(P)$  and  $\det(M)$  are, using  $s_n^2 \equiv 1 - c_n^2$ , quadratic forms in  $\zeta$  defined as  $\zeta \equiv c_n^2$ , it is not difficult to use elementary-calculus curve-sketching methods to prove that, on  $0 \leq \zeta \leq 1$ ,  $\text{trace}(P)$  is monotone decreasing from  $(\Lambda^2 + 1)$  to 2, and  $\det(M)$  is *strictly* monotone increasing from  $-\Lambda$  to 0 [so that  $\det(P)$  is *strictly* monotone decreasing from  $\Lambda^2$  to 0], which enables appraisals of upper and lower bounds for each by simple evaluation at  $\zeta = 0$  and  $\zeta = 1$ , with the rigorous result that

$$0 \leq c_n^2 \leq 1, \quad \Lambda^2 + 1 \geq \text{trace}(P) \geq 2, \quad \Lambda^2 \geq \det(P) \geq 0, \quad (8i,j,k)$$

where, again, it is important to note that  $\det(P) > 0$  if  $c_n \neq 1$ , i.e. that  $\det(P) = 0$  is possible only if  $c_n = 1$ , in which case  $P$  is merely non-negative definite instead of positive-definite. Combining the two preceding results one finds that

$$\lambda_{\text{MAX}} < \text{trace}(P) \leq \Lambda^2 + 1, \quad \lambda_{\text{MIN}} \equiv \det(P)/\lambda_{\text{MAX}} \geq 0, \quad (8l,m)$$

from which we know about  $Q$ , *a priori*, that

$$0 \leq Q \leq \Lambda^2 + 1, \quad (\Lambda^2 + 1)^{-1} \leq Q^{-1} \leq +\infty. \quad (8n,o)$$

**REMARK.** For purposes of comparison, recall from Bohm [1, p. 286, eqn. (64)] that in the case of *double* barriers and a *single* well, the transmissivity is given by

$$0 < \tau = 4/[4c_w^2 + \Xi^2 s_w^2], \quad \Xi = 4\Theta^2 + 4^{-1}\cdot\Theta^{-2}, \quad (9a)$$

consistent with (7f) above, so that the condition for *Resonant Transparency* in that case was

$$s_w = 0, \quad \iff \quad J_w = (N_w + 1/2)\cdot h, \quad (N_w = 1, 2, 3, \dots). \quad (9b)$$

Note that if one replaces  $s_w^2$  and  $c_w^2$  by their expected rms *average* values of  $1/2$  then  $\tau$  is asymptotically equal to  $(4/16)\cdot\Theta^4 \equiv (1/4)\Theta^4$  as claimed in (7f), which confirms the widespread misconception about the "impossibility" of "low energy penetration of the Coulomb barrier". [Another misconception, that even granting the transparency according to the "accepted laws of physics", the tunneling time for any particle whose energy does not agree with that specified to hundreds of decimal places by (7g) would be longer than the accepted age of the universe, is dispelled in [10].]

**THEOREM.** Under the preceding assumptions, the quadruple-barrier transmissivity  $\tau = \tau(E)$  is given for every  $E \geq \nu_{\text{MIN}}$  by

$$0 < \tau = \frac{4}{\Phi^2 \cdot Q} \leq 1, \quad (10)$$

where the upper bound on  $\tau$  represents a sharpening of (8n).

**COROLLARY.** In the present case of quadruple barriers and a triple well, sufficient conditions for Bi-Resonant Transparency are that the energy level  $E$  should simultaneously satisfy both of the following conditions:

$$s_n = 1/(3^{1/2}), \quad \Leftrightarrow \quad J_n = [(N_n)/3] \cdot h, \quad (N_n = 1, 2, 3, \dots), \quad (11a)$$

$$s_w = [1/(4 \cdot 2^{1/2} \cdot \Theta^2)] + \dots, \quad (11b)$$

where the neglected terms in (11b) are of order  $\Theta^3$ , and where, because of the enormously large value of  $\Theta$ , (11b) for all practical purposes is identical with (9b). (Thus the practical effect of the inclusion of the nuclear potential wells in the model of the Coulomb-Madelung wells is to add an additional constraint upon the Resonant Transparency energy levels, making complete transparency less likely to occur, even if already predicted by the single-well model (9b).)

Proof of Corollary. If one uses the asymptotic expressions (7o,p,q,r), then, neglecting lower order terms in (8a,bis) and (8g,hbis),

$$\text{trace}(P) = 1 + 16s_n^2(15s_n^2 + 1)\Theta^4 + \dots, \quad (12a)$$

$$\det(P) = 64\Theta^4 s_n^6(3s_n^2 - 1)^2 + \dots, \quad (12b)$$

which suggests minimizing  $\det(P)$  by assuming (11a) on a trial basis. Then, assuming that  $s_w$  is sufficiently small that its cubes and higher powers can be neglected in comparison to its first and second powers, and simplifying  $P$  by use of (11a), one finds after a little algebra that

$$Q = 32\Theta^4 s_w^2 - 8 \cdot 2^{1/2} \cdot \Theta^2 s_w + 1 + \dots. \quad (13a)$$

Now by (10) one may choose  $s_w$  to satisfy the Resonant Transparency condition (7g) by solving the quadratic equation

$$32\Theta^4 s_w^2 - 8 \cdot 2^{1/2} \cdot \Theta^2 s_w + 1 + \dots = 4\Phi^{-2} \approx 4\Theta^{-2}, \quad (13b)$$

which immediately yields (11b) as claimed.  $\square$

Proof of Theorem. The strategy behind the derivation of (10) is to assume the desired final form (7c) in  $R_1$ , with

$$\theta + \Delta\theta \equiv \left[ \int_{2L - r_*}^r p_w \frac{dr}{\hbar} \right] - \frac{\pi}{4}, \quad (14)$$

and then to work *backwards*, from right to left, through the successive regions using the WKB connection formulae [1]. For example, defining

$$\alpha_3 \equiv \left[ \int_r^{L + r_n} p_n \frac{dr}{\hbar} \right] - \frac{\pi}{4}, \quad (15a)$$

$$\theta_3 \equiv \left[ \int_{L - r_n}^L p_n \frac{dr}{\hbar} \right] - \frac{\pi}{4}, \quad (15b)$$

one finds that

$$\begin{aligned}\Psi_{\text{III}} &= (A/\sqrt{p_w}) \cdot \{ \sin(\alpha_3) \cdot H_1 + \cos(\alpha_3) \cdot H_2 \} \equiv \\ &\equiv (A/\sqrt{p_w}) \cdot \{ \cos(\theta_3) \cdot H_3 + \sin(\theta_3) \cdot H_4 \},\end{aligned}\quad (16a)$$

$$H_1 = \delta, \quad H_2 = i\Delta, \quad H_3 = \delta s_n - i\Delta c_n, \quad H_4 = -\delta c_n - i\Delta s_n, \quad (17b)$$

where the second version of (16a) is mandated by the need to use the connection formulae (41)-(42) of Ch. 12 of Bohm [1]. Next, defining

$$\alpha_4 \equiv \int_r^L p_4 \frac{dr}{\hbar}, \quad (17a)$$

$$\theta_4 \equiv \int_{r_*}^R p_4 \frac{dr}{\hbar}, \quad (17b)$$

one finds that

$$\begin{aligned}\Psi_{\text{IV}} &= (A/\sqrt{p_b}) \cdot \{ \exp(-\alpha_4) \cdot H_5 + \exp(\alpha_4) \cdot H_6 \} \equiv \\ &\equiv (A/\sqrt{p_b}) \cdot \{ \exp(\theta_4) \cdot H_7 + \exp(-\theta_4) \cdot H_8 \},\end{aligned}\quad (18a)$$

$$H_5 = (1/2)H_3, \quad H_6 = H_4, \quad H_7 = \delta \cdot H_3, \quad H_8 = 2^{-1}\Delta \cdot H_4. \quad (18b)$$

Continuing in this manner, one must repeat the preceding 4 steps 5 more times. Finally, after an exercise of almost intolerable tediousness, including the chore of keeping track of the real and imaginary parts of the astronomically-escalating, gargantuan formulae for the coefficients  $H_j$ , one arrives at

$$\Psi_{\text{IX}} = (A/\sqrt{p_w}) \cdot \{ \cos(\theta) \cdot R_1 + \sin(\theta) \cdot R_2 \}, \quad (19a)$$

$$\theta \equiv \left( \int_{-L-r_n}^R p_w \frac{dr}{\hbar} \right) - \frac{\pi}{4}, \quad (19b)$$

which, upon comparing (14) and (19b), can readily be put into the required form (7a,b).  $\square$

NOTE. For brevity, a score of straightforward but lengthy intermediate steps have been omitted; readers desiring a copy of the omitted details will be sent a complete derivation upon written request.

**EXAMPLE 1.** The main new result (11a) can be reformulated in a dimensionless form (as in Peebles [12]) by noting that

$$J_n = 4p_n r_n = [(N_n)/3] \cdot h, \quad (N_n = 1, 2, 3, \dots), \quad (20a)$$

$$p_n \equiv \sqrt{2M_D |E - V_n|} = \sqrt{\frac{4m_p(\epsilon + \mu)}{e^2} E_C}, \quad (20b)$$

$$E = \epsilon E_C, \quad |V_n| = \mu E_C, \quad E_C = e^2/L = 5.06 \text{ eV}, \quad (20c,d,e)$$

$$\mu = 4.17 \times 10^6, \quad (20f)$$

and by use of the *proton Compton wavelength*

$$\lambda_p = \hbar/(m_p c) = 2.1 \times 10^{-14} \text{ cm}, \quad (21a)$$

and the *fine structure constant*

$$\alpha = e^2/(\hbar c) = 1/137.036, \quad (21b)$$

to form the combination

$$m_p e^2/(\hbar)^2 = \alpha/\lambda_p, \quad (21c)$$

according to which (20a) becomes, after simplification by (20b-f) and (21a,b),

$$0 < \epsilon = \mu \cdot \{ (N_n/N_0)^2 - 1 \}, \quad (22a)$$

$$N_0 \equiv (12/\pi) \cdot \sqrt{\mu\alpha(r_n/\lambda_p)(r_n/L)} = 5.5 < 6. \quad (22b)$$

Therefore (22a) is impossible, i.e. *resonant transparency is impossible*, unless one considers *only* indices  $N_n \geq 6$ . Taking  $N_n = 6$  in (22a), one finds that the *minimum* viable value of  $\epsilon$ , and so of  $E$ , is given by

$$\epsilon_6 = 0.85 \times 10^6, \quad E_6 = 4.31 \text{ MeV}. \quad (22c)$$

Accordingly, a deuteron having the energy range of interest in cold fusion, namely from  $E = 6.3 \text{ eV}$  to  $E = 13.7 \text{ eV}$ , cannot pass through either adjacent bound deuteron; once it reaches the vicinity of the strong nuclear force of either adjacent bound deuteron, it must remain there indefinitely (unless some other reaction ensues, such as a fusion into a  ${}^4\text{He}$  nucleus, with release of the excess 23.8 MeV into the ambient palladium lattice in the form of phonon excitations [as in Schwinger's NEAL theory [8]]).

That having been established, it is of interest to use the present theory to prove that a deuteron having any one of the 88 Resonant Transmission energy levels in the just-specified energy range [10] actually can penetrate the Coulomb barrier and reach the vicinity of the strong nuclear force.

**EXAMPLE 2.** Ignore the strong nuclear force, and consider *only* the electrostatic forces. This can be done by replacing the nuclear potential well by a continuous but truncated Coulomb-Madelung potential, i.e. by taking the potential to be *constant* inside the regions  $R_{\text{III}}$  and  $R_{\text{VII}}$  and there of the *large positive* value

$$V = e^2/r_n \equiv (L/r_n) \cdot E_C, \quad (23)$$

in which case the problem is only of the well-known double-barrier, single-well type recalled in the Remark preceding (9b), which remains valid and unaltered; the only part

of (9<sub>a</sub>) which is modified is an increase in the size of  $\Theta$  from the value in (4<sub>a</sub>) to

$$\Theta = \exp \left( \int_{L}^{2L - r_*} p_2 \frac{dr}{\hbar} \right), \quad v_M(r_*) = E, \quad (24)$$

but this adjustment to the value of  $\Theta$  has no effect whatsoever on the condition for Resonant Transparency (9<sub>b</sub>), so that the 88 LOW Energy Levels for Resonant Transparency of the Coulomb-Madelung barrier [absent the strong force] remain as previously computed in [10].

### References

- [1] David Bohm, *Quantum Theory*, Dover Publications, 1989.
- [2] John M. Blatt & Victor F. Weisskopf, *Theoretical Nuclear Physics*, Dover Publications, 1991.
- [3] H. Jeffries, *Proc. London Math. Soc.*, vol. 23 (1923), p. 428.
- [4] Roscoe B. White, *Theory of Tokamak Plasmas*, Elsevier Science Publishers, 1989, Ch. 9., pp. 331-356.
- [5] Jon Mathews & R.L. Walker, *Mathematical Methods of Physics*, Benjamin/Cummings, 2<sup>nd</sup> Ed., 1970.
- [6] Robert W. Bass, "An Apparently True Conjecture in Number Theory," to be submitted for publication.
- [7] Robert W. Bass, "A Closed Form Expression for a Generic Madelung Potential in Periodic Crystal Lattices," to be submitted for publication.
- [8] Robert W. Bass, "Proof That Madelung Forces Predict the Schwinger Ratio Correctly," to be submitted for publication.
- [9] Julian Schwinger, "Nuclear Energy in an Atomic Lattice. 1," *Zeitschrift für Physik D*, vol. 15 (1990), pp. 221-225; cf. additional references in [9bis], p. 320.
- [9bis] Eugene F. Mallove, *Fire From Ice*, Wiley, 1991.
- [10] Robert W. Bass, "Proof That Zero-Point Fluctuations of Bound Deuterons in a Supersaturated Palladium Lattice Provide Sufficient Line-Broadening to Permit Low-Energy Resonant Penetration of the Coulomb 'Barrier' to Cold Aneutronic Fusion," to be submitted for publication.
- [11] Yeong E. Kim, Jin-Hee Yoon, Alexander L. Zubarev & Mario Rabinowitz, "Coulomb Barrier Transmission Resonance Transparency for Cold Fusion with Deuterium and Hydrogen," *Proceedings*, Fourth International Conference on Cold Fusion (ICCF-4), to appear. Cf. also [11bis].
- [11bis] Yeong E. Kim & Alexander L. Zubarev, "Coulomb Barrier Transmission Resonance for Astrophysical Problems," *Mod. Phys. Lett. B*, to appear.
- [12] P.J.E. Peebles, *Quantum Mechanics*, Princeton University Press, 1992.

## Appendix 5

### 4 INDEPENDENT EXPERIMENTAL EVIDENCES THAT $D + D \rightarrow {}^4He$ DOMINATES COLD FUSION

[POSTSCRIPT: Apologies for inexact literature citations.] Some experts in cold fusion research for whom I have the greatest respect have doubted that the *OBVIOUS* reaction in Fleischmann-Pons cells and similar deuterium-based work is that stated. But this is not only the most elementary explanation for the observed Excess Enthalpy, it seems to me almost incontrovertibly established by the published evidence:

(1) In their paper, "Two Innocent Chemists Look at Cold Fusion," Cheves Walling & Jack Simons, two University of Utah colleagues of Fleischmann & Pons, mentioned in a footnote that F & P had told them how much Excess Enthalpy they were getting in certain experiments in which the effluent gases were searched for reaction by-products. They assumed that the excited Alpha Particle dropped into its stable ground state NOT by emission of a gamma ray but by transfer of energy to the electron cloud, which they called *Internal Conversion* (IC), leading by IC ultimately to phonon excitations of the *Pd* lattice observable as macroscopic heat, in a *Radiationless Reaction* (RR). A simple calculation based upon the hypothesis that all excess heat came from the 23.85 MeV shown in high-energy physics experiments upon essentially isolated particles colliding *in vacuo* to be emitted as a  $\gamma$ -ray but here hypothesized as some novel IC, produced the expected number of  ${}^4He$  atoms to look for; these were found, but at the borderline of reliability of the resolution of the instruments available in Utah; consequently F&P did not pursue further publication of this early clue.

(2) The China Lake NWC double-blind experiments by Mel Miles, Ben Bush *et al* provided with great care *perfect* correlation: either NO, or NO, or a SMALL amount, or a LARGE amount of  ${}^4He$  in the effluent gases from a light water control or a heavy-water F&P cell producing either NO or a SMALL amount or a LARGE amount of excess heat.

(3) The Texas A&M experiments by John O'M. Bockris *et al* provided massive amounts of both tritium & helium in a cathode that had been quick-frozen while producing heat.

(4) The ingenious experiment by Nippon Telegraph & Telephone produced Alpha Particles in profusion from a *D*-loaded *Pd*-lattice (NO Li!) by heat-or-electric shocks!



## COLD FUSION AND NUCLEAR PROLIFERATION

Joseph Peter GUOKAS  
J&J Manufacturing  
2820 Honolulu Ave, Suite 325  
Verdugo City, CA 91046-4601

### **Abstract**

"Cold fusion" anomalies are reviewed for their possible impact on nuclear proliferation. Even without a consensus regarding the processes generating the anomalies, some observed properties of "cold fusion" experiments suggest reasons for concern.

Reactions of most concern would generate fissile material from nuclear source material by either: (a) generating free neutrons, or (b) directly transferring neutrons to nuclear source material nuclei. Such reactions will impact nuclear proliferation only if their reaction rates are orders of magnitude above those reported thus far in "cold fusion" experiments.

The "cold fusion" literature is reviewed for indicators of reactions (a) and (b), and indicators of potential for higher reaction rates. Of particular interest are high-Z anomalies, chain reactions, conditions for changing branching ratios, isotopic changes, bursts, and neutron activation.

Also examined are the proliferation implications of recent theories and experiments suggesting "cold fusion" may generate neutron traps of high cross section.

## **Introduction**

The following is a compilation of the slides and the approximate text of talk number D1.7 at ICCF-4.

[slide 1]

Because of improvements in rates and understanding of cold fusion, we may soon have to look closer at possible nuclear proliferation aspects of cold fusion.

[slide 2]

Two major concerns about cold fusion and nuclear proliferation we will examine today are:

\* Can cold fusion breed fissile material from available materials?

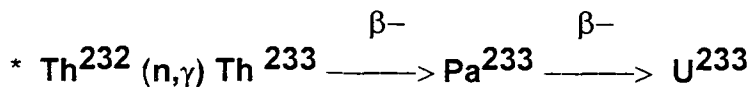
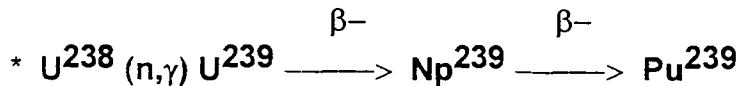
\* Can cold fusion make a breeder reactor out of natural - unenriched - uranium?

We will go through the first part faster than planned because it is straightforward and probably not imminent, while the second topic (in light of information revealed at this conference) may merit a closer look.

### **First Concern: Can Cold Fusion Breed Fissile Material?**

[slide 3:]

#### **REACTIONS BREEDING FISSILE MATERIAL**



Either of these two reactions could be used to breed fissile material.

In each case, easily available material is activated by neutrons, leading to a chain of reactions resulting in fissile material. These fissile elements can be easily extracted chemically from the original material, avoiding the difficulties of isotopic separation.

All that is needed is a source of high neutron flux.

## COLD FUSION NEUTRON SOURCES

- \* Free n
- \* Free p, then (p,n)
- \* Free energetic t, then  $t + d \longrightarrow \text{He}^4 + n$
- \* Direct transfer of n
- \* Other

Aside from the free neutrons observed emitted by cold fusion cells, there are several indirect mechanisms that can result in neutrons. At present, their branching ratios are less than free neutrons', but as we learn more about cold fusion they may be of interest.

Under "transfer of neutrons": You are all familiar with the theories and experiments regarding isotopic change in cold fusion. If this process works with fertile isotopes, it would be a concern. This was suggested by Ragheb and Miley<sup>1</sup> as a way of breeding fissile isotopes in subcritical reactors.

Alternatively, if these neutron transfers trigger fissions, they could produce free neutrons.

Under "other": High-Z reactions, reactions with elements other than hydrogen, have generated much interest recently. This includes the experiments of Notoya<sup>2</sup> and the theories and experiments of R.T. Bush.<sup>3,4,5</sup> Also the Karabut/Kucherov<sup>6,7</sup> experiments indicate cold high-Z reactions in their gamma lines. If cold nuclear reactants can include high-Z elements, then there are many more combinations of reactants available than previously thought. Some of these might generate free neutrons and, nuclear reactions being as influenced by resonances as they are, may do so at higher cross sections than yet seen.

How high must the neutron flux be to be a nuclear proliferation hazard? A simple, direct way to answer that is to compare fluxes with existing sources.

Below  $10^{10}$  neutrons/cm<sup>2</sup>-s, the source would be less effective than accelerator-based neutron generators, which are easily available. So such a source would not add to nuclear proliferation dangers. At  $10^{15}$  neutrons/cm<sup>2</sup>-s the source would clearly be a nuclear proliferation hazard, as this is about the level seen in reactors. So somewhere between  $10^{10}$  and  $10^{15}$  neutrons/cm<sup>2</sup>-s this becomes a problem.

## SIGNS THAT CF RATES CAN BE INCREASED

- \* High rates in some conditions
- \* Conditions change branching ratios
- \* Bursts
- \* Signs, theories of chaining
- \* Signs of precursor
- \* Present level unexplained

The strongest fluxes seen in cold fusion - even the neutron bursts - are several orders of magnitude below this. But there are signs that the neutron flux in cold fusion could be increased.

You are all familiar with the many experiments in the first three categories.

Regarding chaining: there have been many theories that invoke multiplicative chaining to explain the unexpectedly high rates of reaction in cold fusion. These include theories by J.C. Jackson<sup>8</sup>, Takahashi<sup>9</sup>, Case<sup>10</sup>, and Becker.<sup>11</sup> Experiments indicating chaining include those showing bursts, Takahashi's experiments showing high energy deuterons, and the Gad Shani<sup>12</sup> experiment, which showed high energy neutrons released when thermal neutrons were beamed into a cold fusion cell.

If cold fusion involves a precursor, as suggested by the exotic chemistry theories of Gryzinski<sup>13</sup>, Vigier<sup>14</sup>, Barut<sup>15</sup>, or R.L. Mills<sup>16</sup>, then several means of optimization become available. In particular, exotic chemistry would permit separation of the heat-yielding reactions from the neutron-yielding reactions, making large increases of neutron flux practical. The experiments by S.Y. Dong [et al.] and reported at Nagoya by Xing Zhong Li and the experiments of R.K. Rout [et al.] indicate exotic chemistry precursor behavior in both light hydrogen and deuterium.

The strongest argument that cold fusion rate limits are not known, is that the cause of the present rate is unknown. Jones reports reactions 40 orders of magnitude above those expected. Fleischmann and Pons report reactions more than 50 orders of magnitude above those expected. So it is reasonable to anticipate a few orders of magnitude increase, when we do understand the

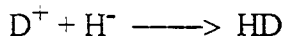
chains, the bursts, the branching ratios, and the optimizing conditions. What we don't know can hurt us - and there is much we still don't know about cold fusion.

### **Second Concern: Can Cold Fusion Make a Breeder From Natural Uranium?**

To explain the basis of the second concern - that cold fusion might make a natural uranium breeder possible - we will look at a recent experiment by G. F. Cerofolini [et al.].<sup>17</sup>

In his experiment Cerofolini observed gas from a cold fusion cell trap neutrons, then later release them.

The cold fusion cell created a redox reaction of



in a special anhydrous solvent. The reaction goes to completion in about 200 to 400 seconds. The evolved gases are sent to a paraffin tank. The paraffin thermalizes any background neutrons. Inside the tank, neutrons are counted by He(3) detectors. In each trial the neutron count was much below background while the redox reaction was occurring. When the redox reaction reached completion, the neutron count rose beyond background level until the approximate number of counts missing during the reaction were caught up.

This is a very distinct effect. Cerofolini reports a 4 sigma confidence level of neutron depletion during the reaction and neutron catchup after the reaction. The flux reduction by this gas (about 40% to 50%) is greater than that of cadmium foil (about 15%) in the same chamber.

Cerofolini presents a possible explanation of his neutron trapping. He suggests that the redox reaction (like other cold fusion stimuli) forms metastable molecular states of unusually small internuclear separation. This internuclear separation being near the wavelength of thermal neutrons, he feels a neutron could be trapped in the molecule by Anderson localization.

A slightly different explanation could be that the whole gas region, if it contains many randomly placed states of unusually small internuclear separation which can scatter neutrons, could hold neutrons by Anderson localization. And yet another possible explanation appeared at this conference: Dr. Hideo Kozima<sup>18</sup> showed how the interface between regions of differing internuclear separation may trap neutrons. Whatever the explanation, the experiment itself is very interesting.

Imagine the effect of this neutron trapping in the following configuration. A region of fissile material could be surrounded by a moderator, which is then surrounded by this neutron trapping gas. The gas could flow continuously from here into the region of fissile material. In this arrangement, no neutrons would be lost at the surface; the neutrons would be recycled to the fissile core.

This could be so efficient in maintaining criticality, that:

(a) A mass much less than what is normally required for criticality could go critical. (Though it is a delayed criticality - not prompt criticality.)

(b) Natural uranium - unenriched uranium - could efficiently breed fissile materials. (Ordinarily, natural uranium can only marginally maintain criticality, leaving few neutrons available for breeding.)

So, these hazards are possible if neutrons can really be trapped and later released. (provided this can happen at high flux density. If the neutron trapping is due to Anderson localization, the trapping will fail above a threshold level.)

We're running out of time, so I will leave up this last slide during the question-and-answer period. It shows some of the experimental findings to watch for, findings that would signal an increased likelihood that cold fusion may lead to a nuclear proliferation hazard.

Thank you.

[slide 7:]

**WATCH FOR:**

- \* **High-Z reactions**
- \* **High rate of nuclear reactions**
- \* **Large increase of CF rate**
- \* **Increase of nuclear/heat ratio**
- \* **Confirmation of n trap**
- \* **Trap remains even in high flux**
- \* **Understanding of CF mechanisms**

## References

1. M. Ragheb and G. H. Miley, "Deuteron Disintegration in Condensed Media," *Journal of Fusion Energy*. Vol. 9, No. 4, p. 429 (1990). (This was from a special issue on the U.S. Department of Energy Workshop on Cold Fusion Phenomena.)
2. R. Notoya and M. Enyo, "Excess Heat Production in Electrolysis of Potassium Carbonate Solution with Nickel Electrodes," *Frontiers of Cold Fusion: Proceedings of the Third International Conference on Cold Fusion*. Tokyo: Universal Academy Press, 1993, pp. 421-426 (1993).
3. R. T. Bush, "A Light Water Excess Heat Reaction Suggests That 'Cold Fusion' May Be 'Alkali-Hydrogen Fusion,'" *Fusion Technology*. Vol. 22, September, p. 301 (1992).
4. R. T. Bush and R. D. Eagleton, "Experiments Supporting the Transmission Resonance Model for Cold Fusion in Light Water: I. Correlation of Isotopic and Elemental Evidence with Excess Heat," *Frontiers of Cold Fusion: Proceedings of the Third International Conference on Cold Fusion*. Tokyo: Universal Academy Press, 1993, pp. 405-408 (1993).
5. R. T. Bush and R. D. Eagleton, "Experimental Studies Supporting the Transmission Resonance Model for Cold Fusion in Light Water: II Correlation of X-Ray Emission with Excess Power," *Frontiers of Cold Fusion: Proceedings of the Third International Conference on Cold Fusion*. Tokyo: Universal Academy Press, 1993, pp. 409-416 (1993).
6. A. B. Karabut, Y. R. Kucherov, I. B. Savvatimova, " Possible Nuclear Reaction Mechanisms at Glow Discharge in Deuterium," *Frontiers of Cold Fusion: Proceedings of the Third International Conference on Cold Fusion*. Tokyo: Universal Academy Press, 1993, pp. 165-168 (1993).
7. A. B. Karabut, Y. R. Kucherov, I. B. Savvatimova, " Nuclear Product Ratio for Glow Discharge in Deuterium." *Physics Letters A*. Vol. 170, pp. 265-272 (1992).
8. J. C. Jackson, letter in *Nature*. Vol. 339, 1 June, p. 345 (1989).
9. A. Takahashi, "Opening Possibility of Deuteron-Catalyzed Cascade Fusion Channel in PdD under D<sub>2</sub>O Electrolysis," *Journal of Nuclear Science and Technology*. Vol. 26, No. 5, pp. 558-560 (1989).
10. L. C. Case, "The Reality of 'Cold Fusion'," *Fusion Technology*. Vol. 20, December, pp. 478-480 (1991).
11. E. W. Becker, "Triple Collision reaction of deuterons as a Possible Explanation of Cold Nuclear Fusion," *Naturwissenschaften*. Vol. 76, p. 214 (1989).

12. G. Shani, C. Cohen, A. Grayevsky, and A. Brokman, "Evidence for a Background Neutron Enhanced Fusion in Deuterium Absorbed Palladium," *Solid State Communications*. Vol. 72, No. 1, pp.53-57 (1989).
13. M. Gryzinski, "Theory of Electron Catalyzed Fusion in Pd Lattice," *Anomalous Nuclear Effects in Deuterium/Solid Systems*. pp. 717-733 (1991).
14. J.-P. Vigier, "New Hydrogen Energies in Specially Structured Dense Media: Capillary Chemistry and Capillary Fusion," *Frontiers of Cold Fusion: Proceedings of the Third International Conference on Cold Fusion*. Tokyo: Universal Academy Press, pp. 325-334 (1993).
15. A. O. Barut, "Prediction of New Tightly-/bound States of H<sub>2</sub> and D<sub>2</sub> and Cold Fusion Experiments," *International Journal of Hydrogen Energy*. Vol. 15, No. 12, pp.907-909 (1990).
16. R. L. Mills and S. P. Kneizys, "Excess Heat Production of an Aqueous Potassium Carbonate Electolyte and the Implications for Cold Fusion," *Fusion Technology*. Vol.20, August, p. 65 (1991).
17. G. F. Cerofolini, G. Boara, S. Agosteo, and A. F. Para, "Giant Neutron Trapping by a Molecular Species Produceced During the Reaction of D<sup>+</sup> with H<sup>-</sup> in a Condensed Phase," *Fusion Technology*. Vol. 23, July, p.465 (1993).
18. Hideo Kozima, "Trapped Neutron Catalyzed Fusion of Deuterons and Protons in Inhomogeneous Solids," Paper No. T 2.5, presented at the Fourth International Conference on Cold Fusion, Lahaina, Hawaii (December 6-9, 1993).

# ECOLOGICAL ASPECTS OF THERMAL SYSTEMS USING HYDROGEN ISOTOPES

V.A.Romodanov, V.I.Savin, S.G. Korneev, A.E.Glagolev

142100 Podolsk, Moscow Region, Zheleznodorozhnaya 24,  
SRI of SPA LUTCH

Tel.: 095-137-9258

Fax; 095-137-9384

Ya.B.Skuratnik  
SRPCI named after Karpov, Obukha 10, Moscow

## ABSTRACT

Having used the obtained data extrapolation is developed a conceptual design of the air heater having an output thermal power of 1-10 kW and mains supply for living space heating. The main advantage of the developed air heater is the fact that the generated heat 2-10 times exceeds the electric power consumption. Such devices filled with deuterium every 1-3 years will be necessary in regions with sudden temperature differences and at the shortage of traditional power carriers and electric power.

We have been developing a power device with a modified Sterling engine ( $P \sim 10$  kW), which can be used in vehicles.

Some nuclear safety and ecological problems of the proposed nuclear devices have been considered and discussed.

## 1. INTRODUCTION

The active investigation on nuclear reactions in condensed media (NRCM) began after M.Eleischmann and S.Pons, who have been working in this field, declared that by means of so-called "cold" fusion devices it was possible to release the thermal energy amount which considerably exceeded the expenses,

e.g. in electrolytic cell with heavy water and a palladium cathode /1/. The subsequent active search can be summed up by the following results: the stable heat excess obtained when electrolyzing both heavy and light water is within the range 20-70% /2, 3/. The values of the heat excess from 100 up to 1500%, which were mentioned before, can be referred to the bursts having a poor reproducibility /4, 5/. At the same time one has developed the experimental procedures where a great heat amount is generated, e.g. in the process of fast desorption of hydrogen from palladium or tungsten bronze /6, 7/. At present one can consider proven the fact that when hydrogen interacts with metals, one can observe the heat release excess, however, its nature hasn't been detected in a unique manner. In spite of the fact that one has proposed some models according to which the NRCM energy can convert mainly into the heat with the accompanying  $^4\text{He}$  and  $\gamma$ -radiation release or the alkali elements transmutation /8-10/, the problem can't be considered to be settled because the experimental results are either close to the background noise or unlikely high and the connection with the process parameters hasn't been detected well /11-13/. We think that one will be also to understand the nature of the observed phenomena after, besides the experiment repetition, the plots of the results as functions of different condition effect have been constructed. These plots will help to detect cause-and-consequence connections and to understand the mechanism of the abnormalities under study.

In spite of the fact that the thermal effect nature isn't clear yet, about one hundred patents, in which the generated heat is supposed to serve some commercial purposes, have been taken out all over the world /14/. One should note that in over 20% of all the patents electric discharges both in gas and in liquid are already considered to be effective means of stimulating the NRCMs. The detected heat excess is possible not to have nuclear nature, but if as a result of the search one can detect its source, the performed work will be considered successful and correct.

Having used the glow discharge of a higher density in our systematic investigation for the first time, we have managed to achieve the tritium generation rate  $\sim 10^9$  atom.s $^{-1}$  at the neutron-to-tritium yield ratio within the range of  $10^{-9}$ - $10^{-7}$ , to show the possibility of yttrium transmutation and to obtain the heat yield excess up to 100% as compared with the applied power /15/. This work seeks to use the results obtained before for developing some energy-generating devices.

## 2. SPECIFICATIONS

The tritium generation results obtained before are the base of thermal device development /15/. Firstly, it is for reasons of the fact that the nature of such a great amount of the generated tritium is detected beyond any doubt. Secondly, and it is the main point, we have detected the reproducible connection between the tritium generation rate and different parameters of the ion bombardment of the target out of the plasma of the dense glow discharge /16, 17/.

At present we have a stable tritium generation rate  $\sim 10^9$  atom.s $^{-1}$  at the nuclear interaction coefficient  $\sim 10^{-10}$  atom.ion $^{-1}$ . For using the NRCMs in thermal devices we require the tritium generation rate at the level of  $10^{16}$  atom.s $^{-1}$  (at the output power  $\sim 10$  kW) and the nuclear interaction coefficient  $\sim 10^{-4}$  atom.ion $^{-1}$ , i.e. for using the proposed method in thermal devices both the tritium generation rate and the NRCM efficiency (that is the most important) should be higher by 6-7 orders of magnitude. Proceed from the conclusions of works /16, 17/ and by extrapolating the obtained results we intend to increase the efficiency of our NRCM method in the following way:

1. According to our estimations one can increase the NRCM efficiency by an order of magnitude by using more promising materials which are heavier and have a higher hydrogen capacity.

2. We suppose to increase the NRCM efficiency by another order of magnitude by optimizing the energy level of the bombarding ions.
3. We can increase the NRCM efficiency by about an order of magnitude by revising the temperature conditions. This revision seeks to increase the deuterium concentration in the target material when keeping its mobility unchanged.
4. One can increase the NRCM efficiency by about an order of magnitude by means of further optimization of the plasma-generating gas pressure.
5. We suppose to increase the NRCM efficiency by the rest of 2-3 orders of magnitude by increasing the density of the deuterium ion flux bombarding the target.

According to our methods the proposals on increasing the NRCM efficiency are well-defined and in spite of the fact that their realization will entail great difficulties and rather arbitrary estimations, it will help to advance in solving the NRCM problem.

According to our design the thermal device has the output power of 10 kW at an electric power consumption of 1-5 kW, the tritium generation rate being equal to  $\sim 10^{16}$  atom $\cdot$ s $^{-1}$ . At this very high tritium generation rate, even if the neutron-to-tritium generation rate ratio is at the level of  $10^{-9}$ , the neutron generation rate will be equal to  $10^7$  neutron $\cdot$ s $^{-1}$ . At the same time the excitation of the heavy target nuclei by the protons having the energy of  $\sim 3$  MeV should result in  $\gamma$ -radiation with the intensity of  $\sim 10^{12}$   $\gamma$ -quantum $\cdot$ s $^{-1}$  from the NRCM area.

However, one can't observe any strong radiation of  $\gamma$ -quanta during the NRCM experiments, so we took the results obtained in the work by the scientists from China as a basis /18/. The

results of the neutron flux and  $\gamma$ -radiation measurements made for different target materials under glow discharge conditions at the energies of  $\sim 20$  keV are given in this work. The results can be considered rather reliable because they have been obtained at rather high energies. In this work the neutron yield-to- $\gamma$ -quanta generation ratio is  $\sim 10^2$ . We decrease this ratio by an order of magnitude (down to  $10^1$ ). Therefore, under our conditions the  $\gamma$ -quanta generation rate is equal to  $10^7 \times 10^{-1} = 10^6$  quantum.s $^{-1}$ . The neutron and  $\gamma$ -radiation spectra used for our calculations are also taken from work /18/ and shown in fig. 1-3. One should pay attention to the fact that the neutron spectra obtained for the target made of palladium are very close to the spectrum obtained by A.Takahashi /8/ during the electrolysis. For the biological neutron activity calculations we use the spectrum of the target made of niobium because it has shown the most considerable results.

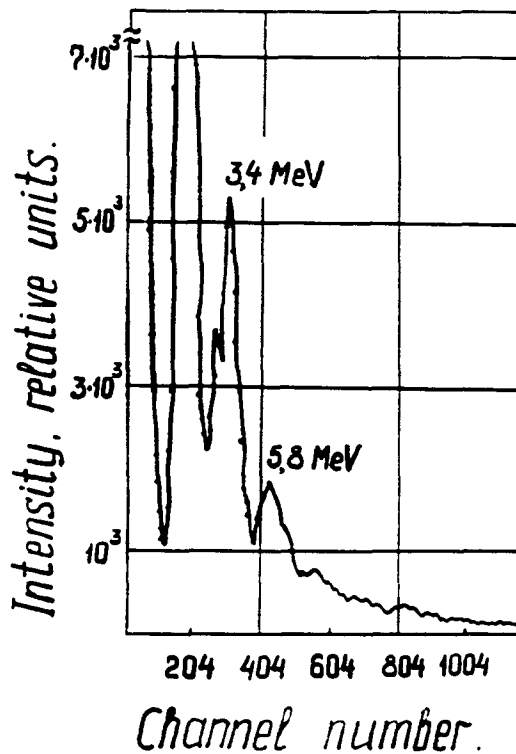


Fig. 1. The  $\gamma$ -quanta spectrum when the deuterium ions bombard the target made of niobium in the glow discharge plasma ( $U = 17-21$  kV) /18/

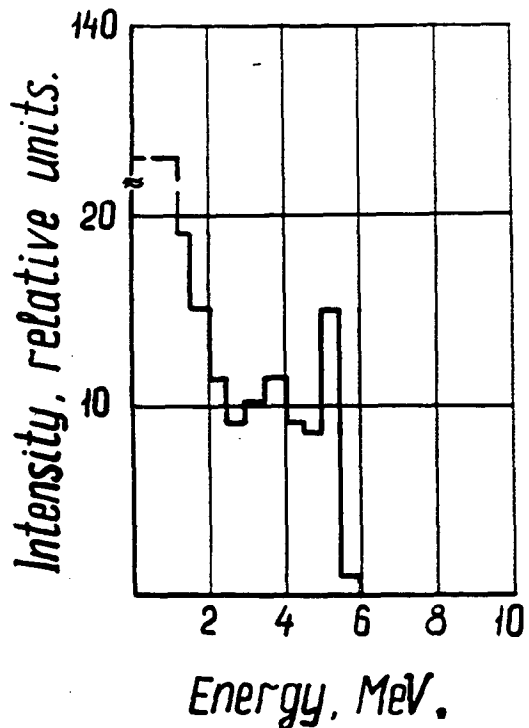


Fig. 2. The neutron spectrum when the deuterium ions bombard the target made of palladium in the glow discharge plasma ( $U = 17-21$  kV) /18/

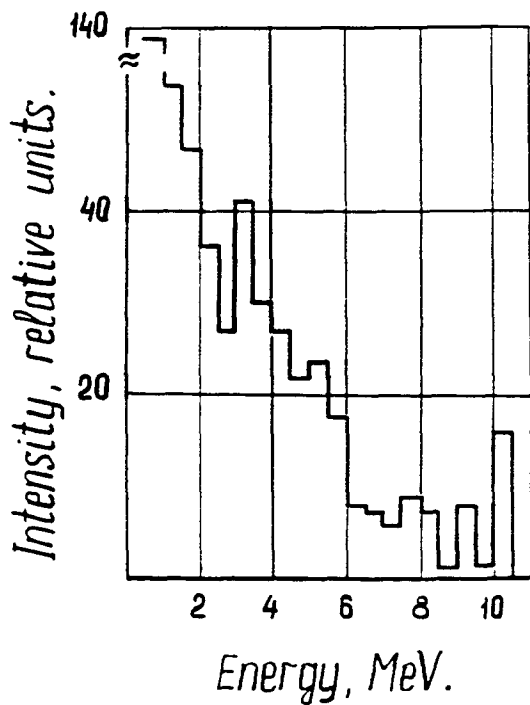


Fig. 3. The neutron spectrum when the deuterium ions bombard the target made of niobium in the glow discharge plasma ( $U = 17-21$  kV) /18/

### 3. TECHNICAL DATA

One of the main principles of a household air heater design is its maximum simplicity. Therefore, it is supposed to operate at higher plasma-generating gas pressures giving an opportunity to keep out the pressure control systems and to replace the plasma-generating gas (deuterium) every 1-3 years. In case of electric power-line supply the thermal output power should be within the range of 1-10 kW, the thermal power exceeding the consumed electric one by 100-1000%. Lower values of the power excess are acceptable for simple air heater modifications. These values will increase with the design and technology modernization.

The air heater (fig. 4) consists of a discharge chamber 1 having a plasma unit 2. At the same time the discharge chamber doubles as a heat exchanger and a reservoir for the plasma-generating gas. The technological spacer 3 is used for supporting the accessories for gas leak-in and pumping-out, pressure control, voltage supply to the chamber. The electric power supply unit 4 is used for supplying the controlled voltage of a given level and mode, converted from the supply-line voltage, to the plasma unit. The biological shielding 5 decreases the neutron and  $\gamma$ -radiation level down to the acceptable one. These devices will be necessary in regions with sudden temperature variations and at a shortage of the traditional energy carriers and electric power.

The power plant having a thermal power of  $\sim 10$  kW and an output shaft power of the modified Steerling engine or electric generator of  $\sim 5$  kW is shown in fig. 5. The above-mentioned output parameters of this power plant can be obtained if the thermal power of the plasma heater on NRCMs base exceeds the consumed electric one by  $\sim 1000\%$ .

The plant in fig. 5 consists of some large units. The plasma heater 1 on NRCM base, operating as an air heater, is surro-

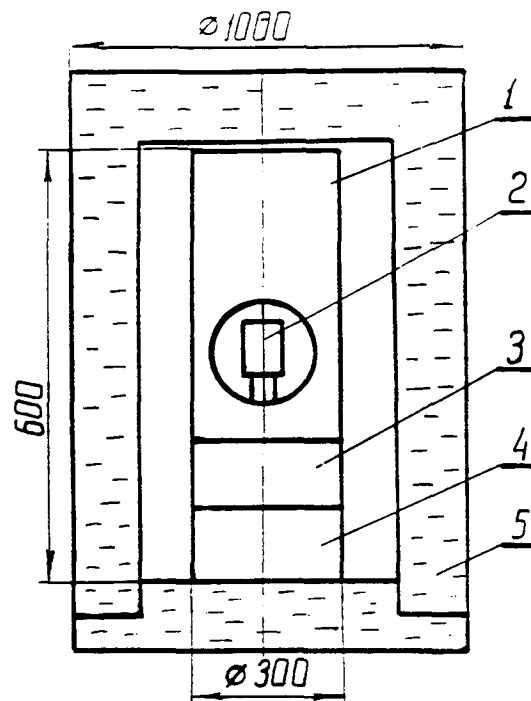


Fig. 4. The diagram of the air heater on NRCM base for flat heating ( $P = 1-10 \text{ kW}$ )

1 - discharge chamber; 2 - plasma unit; 3 - technological spacer; 4 - electric power supply unit; 5 - biological shielding

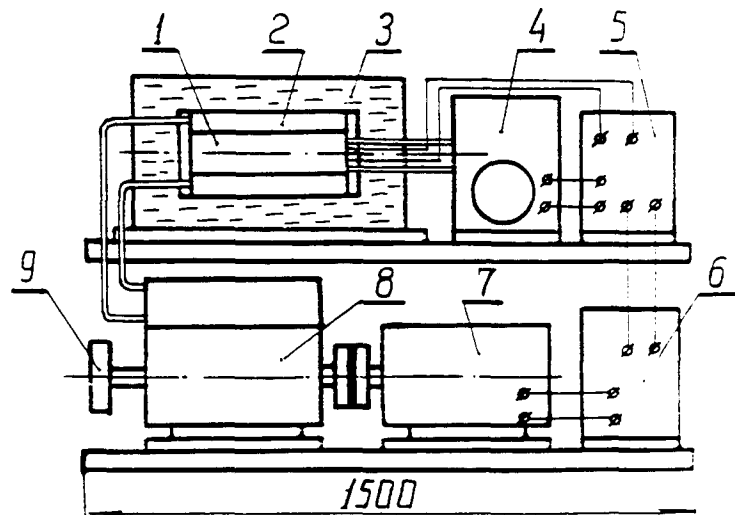


Fig. 5. The diagram of the power plant on NRCM base and the modified Steerling engine ( $P_{th}=10 \text{ kW}$ ,  $P_{out}=5-6 \text{ kW}$ )

1 - plasma heater; 2 - heat exchanger; 3 - biological shielding; 4 - pressure stabilizer; 5 - converter; 6 - accumulator; 7 - generator; 8 - Steerling engine; 9 - output shaft

The plant in fig. 5 consists of some large units. The plasma heater 1 on NRCM base, operating as an air heater, is surrounded by the heat exchanger 2 giving up some heat to the modified Steerling engine 8. The plasma heater has a device 4 for controlling and maintaining the given pressure in the plasma heater chamber and it is surrounded by the biological shielding 3. The electric power is supplied to the plasma heater from the converter 5 generating the given voltage. The electric power is supplied to the converter from the generator 7 through the stabilization and accumulation system 6. The electric generator is driven to rotate by the modified Steerling engine through the intermediary of a suitable. For moving devices the power can be picked off directly from the shaft 9 of the modified Steerling engine. The generator can have a power of  $\sim 6$  kW under power plant conditions and  $\sim 2$  kW when the power is transferred through the shaft. The overall dimensions of the power plant depend to a large extent on those of the plasma heater and biological shielding. The calculated technical data on the air heater and the power plant are given in Table 1. The biological shielding has a great effect both on the overall dimensions and the mass characteristics of the devices under design (see Table 1).

#### 4. SAFETY PROBLEMS

##### - Nuclear safety

According to the result of work /16/ the NRCM efficiency achieves its maximum at a certain optimal temperature. Therefore, if due to any reason the power of the ion beam bombarding the target of thermal devices on NRCM base starts increasing, the NRCM efficiency will decrease and the heat amount generated in the process of the NRCMs will start decreasing too when the target temperature approaches the melting point. It will result in a temperature decrease at the constant heat pick-up level.

Table 1  
Technical data on air heater and power plant on NRCM base

Parameter	Unit of measurement	Air heater	Power plant
Thermal power	kW	1-10	10
Thermal power excess over consumed one	%	100-1000	1000
Electric output power	kW	-	5
Mechanical output power	kW	-	6
Mass with biological shielding	kg	50	200
Mass without biological shielding	kg	25	100
Continuous operation when being filled once	year	0.3-3	0.3-3
Overall dimensions with biological shielding	mm	1000x1000x1000	1500x1000x1000
Overall dimensions without biological shielding	mm	D=300, H=600	1000x500x500

This process will be self-regulated to some extent and one should check mainly the supplied electric power (its level, regulation, limitation). The particular reliability requirements are specified to the cooling systems of the devices under design because their failure though won't result in a spontaneous reactor runaway and explosion, but it will result in the target penetration and failure because of the high power density required for the normal operation of such devices.

#### - Biological safety

We used the neutron flux up to  $10^7 \text{ neutron} \cdot \text{s}^{-1}$  having a spectrum up to 10 MeV (see fig. 3) and the  $\gamma$ -quanta flux up to

$10^6$  quantum $\cdot$ s $^{-1}$  having a spectrum up to 6 MeV (see fig. 1) as factors of the proposed power plant effect on the environment.

To estimate the dose rate dependence on the neutron radiation we used the spectra shown in fig. 3 and the neutron flux-to-dose rate ratio taken from /19/. We also determined the corresponding dose rate using the coefficients of the  $\gamma$ -quanta flux density conversion into the dose rate /20/ and the spectrum shown in fig. 1. The dose rate dependence on the neutron flux and  $\gamma$ -radiation at different distances from the radiator is given in Table 2.

Table 2  
Dose rate for neutron and  $\gamma$ -radiation at different distances from radiator ( $P = 10$  kW)

Distance from radiator, m	0.5		1		2	
Radiation type	n	$\gamma$	n	$\gamma$	n	$\gamma$
Dose rate, $\text{rad} \cdot \text{s}^{-1}$	1.6	$5 \cdot 10^{-2}$	0.4	$1.2 \cdot 10^{-2}$	0.07	$3 \cdot 10^{-3}$

When the ultimate dose rate for population is equal to  $0.08 \text{ rad} \cdot \text{s}^{-1}$  /21/, the safe distance from the thermal device having the output power of 10 kW is  $\sim 2$  m. The neutron radiation is a limiting factor under given conditions. No doubt, such a long distance isn't acceptable for indoor devices. Therefore, the shielding in a form of water layer (Table 3) decreasing the ultimate dose rate down to the level of  $0.08 \text{ rad} \cdot \text{s}^{-1}$  at different distances has been provided.

Therefore, when the thickness of the shielding water layer is 0.2 m, the diameter of the proposed thermal device can be 1 m (see Table 3).

Table 3

Thickness of water layer decreasing neutron radiation dose rate down to  $0.08 \text{ rad} \cdot \text{s}^{-1}$  at different distances from radiator (neutron flux -  $10^7 \text{ neutrons} \cdot \text{s}^{-1}$ )

Distance from radiator, m	0.5	1	2
Water layer thickness, m	0.2	0.1	0

Tritium generation is a considerable problem for the devices like that. Tritium is one of the least radioactive materials from D-group. When it is in a tight reservoir, it isn't dangerous. However, one should solve the problem of waste deuterium replacement and tritium waste recovery. With time tritium converts to safe  ${}^3\text{He}$  which can have a wide application. Tritium itself still has a limited application and the waste recovery of its great amount is a serious problem because of its considerable mobility and explosion hazard. It is convenient to keep a small tritium amount, e.g. for thermal device chambers, by dissolving it in some metals (titanium, zirconium).

- Other safety problems

The explosion hazard of the hydrogen isotopes and air mixtures is a problem too. During the seal failure of the plasma device chamber the hydrogen amount enough to form some explosive mixtures with air can be available in it. To reduce the consequences of these events to the utmost it is necessary to decrease the hydrogen amount in the reaction chamber and to provide some safety valves and monitoring devices.

## 5. CONCLUSIONS

5.1. We have proposed conceptual designs of the indoor air heater and the power plant with a modified Steerling engine having the thermal power of 10 kW. They operate on the dense

glow discharge base and use tritium generation as a dominant NRGM type.

5.2. We have shown that the biological shielding of the proposed nuclear plants has a considerable effect on their weight parameters, overall dimensions and economic characteristics.

5.3. We have noted that in spite of the fact that the proposed devices are rather simple in design and operation, one should thoroughly study the problems of nuclear, biological and explosion hazard at the early design stage because of the nuclear nature of these devices.

#### REFERENCES

1. M.Fleischmann, S.Pons. Electrochemically Induced Nuclear Fusion of Deuterium. - Journal of Electrochemical Chemistry, 1989, 261, p. 301-308.
2. M.C.H.McKubre, S.Crouch-Baker, A.M.Riley et al. Excess Power Observations in Electrochemical Studies of the D/Pd System. - Frontiers of Cold Fusion. Proceedings of the Third International Conference on Cold Fusion. October 21-25, 1992, Nagoya, Japan. Ed. by H.Ikegami. Universal Academy Press Inc., Tokyo, p. 5-20.
3. M.Srinivasan, A.Shyam, T.S.Sankaranarayanan et al. Tritium and Excess Heat Generation during Electrolysis of Aqueous Solutions of Alkali Salts with Nickel Cathode. - Ibidem // p. 123-138.
4. M.Fleischmann and S.Pons. Calorimetry of the Pd. D<sub>2</sub>O System: from Simplicity via Complications to Simplicity. - Ibidem // p. 47-66.
5. B.Y.Liau and B.E.Liebert. A Potential Shuttle Mechanism for Charging Hydrogen Species into Metals in Hydride-Containing Molten Salt System. - Ibidem //. p. 401-404.

6. E.Yamaguchi and T.Nishioka. Direct Evidence for Nuclear Fusion Reactions in Deuterated Palladium. - *Ibidem //.* p. 179-188.
7. K.Kaliev, A.Baraboshkin, A.Samgin et al. Reproducible Nuclear Reactions during Interaction of Deuterium with Oxide Tungsten Bronze. - *Ibidem //.* p. 241-244.
8. A.Takahashi, A.Mega, T.Takeuchi et al. Anomalous Excess Heat by D2O/Pd Cell under L-H Mode Electrolysis. - *Ibidem //.* p. 79-91.
9. P.L.Hagelstein. Coherent and Semi-Coherent Neutron Transfer Reactions. - *Ibidem //.* p. 297-306.
10. R.T.Bush and R.D.Eagleton. Experiments Supporting the Transmission Resonance Model for Cold Fusion in Light Water:  
I. Correlation of Isotopic and Elemental Evidence with Excess Heat. - *Ibidem //.* p. 405-408.
11. R.T.Bush and R.D.Eagleton. Experiments Supporting the Transmission Resonance Model for Cold Fusion in Light Water:  
II. Correlation of X-Ray emission with Excess Power. - *Ibidem //.* p. 409-416.
12. M.N.Miles and B.F.Bush. Search for Anomalous Effects Involving Excess Power and Helium during D2O Electrolysis Using Palladium Cathodes. - *Ibidem //.* p. 189-199.
13. H.Sakaguchi, G.Adachi and K.Nagao. Helium Isotopes from Deuterium Absorber in LaNi5. - *Ibidem //.* p. 189-199.
14. Hal Fox. Cold Fusion Impact in the Enhanced Energy Age. - Fusion Information Center; Salt Lake City, UT, USA, 1992.
15. V.Romodanov, V.Savin, Ya. Skuratnik and Yu. Timofeev. Nuclear Fusion in Condensed Matter. - Frontiers of Cold Fusion. Proceedings of the Third International Conference on Cold Fusion. October 21-25, 1992, Nagoya, Japan. Ed. by H.Ikegami. Universal Academy Press Ins., Tokyo, Japan, 1993, p. 307-319.

16. V.Romodanov, V.Savin, Ya.Skuratnik, V.Elksnin.  
Reproducibility of Tritium Generation from Nuclear Reactions  
in Condensed Media. - Submitted to ICCF4, 1993.
17. V.Romodanov, V.Savin, Ya.Skuratnik, S.Korneev. Concept of  
Target Material Choice for Nuclear Reactions in Condensed  
Media. - Submitted to ICCF4, 1993.
18. H.Q.Long, S.H.Sun, H.Q.Liu et al. Anomalous Effects in  
Deuterium/Metal Systems. - Frontiers of Cold Fusion. Pro-  
ceedings of the Third International Conference on Cold  
Fusion. October 21-25, 1992, Nagoya, Japan. Ed. by H.Ike-  
gami. Universal Academy Press Inc., Tokyo, Japan, 1993,  
p. 447-454.
19. B.R.Bergl'son, G.A.Zorikoev. The Handbook on Protection  
from ionizing of extent Sources. - M.: Atomizdat, 1965,  
176 p. (in Russian).
20. A.A.Moiseev, V.I.Ivanov. The Handbook on dosemeasurement  
and a hygiene of radiations. - M.: Atomizdat, 1974, 236 p.  
(in Russian).
21. The Standarts of Radiations Safety NRB-76/87. - M.: Energo-  
atomizdat, 1988, 160 p. (in Russian).



## **Investigation of Deuterium Glow Discharges of the Kucherov Type**

Elliot B. Kennel  
Arnold G. Kalandarachvili  
Space Exploration Associates  
PO Box 579  
Cedarville, OH 45314

### **ABSTRACT**

Recent experiments with deuterium glow discharges by Y. Kucherov et al. have yielded extremely intriguing results, including the production of anomalous nuclear radiation and excess heat.<sup>1,2</sup> Among the experimental observations are:

- a. Gamma radiation, neutrons and charged particles are produced in a simple deuterium glow discharge.
- b. The nuclear radiation is often accompanied by excess heat.
- c. The cathode surface is contaminated with elements as  ${}^6\text{Li}$ ,  ${}^{11}\text{B}$ , C, Na, Mg, Al, Si, S, Ca, Ti, Cr, Fe, Ni, Zn, Ge, Ga, Br, Sr; and Mo, possibly suggesting that the palladium cathode is transmuted during the course of this experiment.
- d. The observed signatures of the anomalous reactions can be reproducibly achieved provided that the system is extremely clean and free from contaminants such as oxygen.

Our group set out to duplicate these results. Initial experiments focused on confirming the nuclear character of the results. Later efforts will attempt to verify the presence of excess heat, and to determine possible means to extend the temperature regime and lifetime.

The experiment has been run with apparent gamma emission under the following conditions:

1. The palladium cathode is known to be of very high purity; i.e., Johnson Matthey Lot #01334 or equivalent.
2. The electrode geometry is well defined--metal leads to the cathode and anode are insulated, allowing the current density to be precisely regulated.
3. The glow discharge is not able to contact materials other than alumina, palladium (cathode), or niobium (anode), thus reducing the likelihood that surface sputtering from contamination sources such as stainless steel can occur.
4. Gasses are of high purity 99.999% (DeLille).

## DISCUSSION

This experiment is still in progress. Initial efforts appear to show that gamma radiation is indeed produced by the experimental apparatus when deuterium is introduced to the system. However, due to the possibility that electromagnetic interference could generate false signals which could be inductively coupled to the counting system, final confirmation will await production of a gamma spectrum with a multichannel analyzer. These experiments are planned for the near future.

There are many conditions under which signals are rarely (or never) obtained, for example:

- a. Exposed stainless steel leads to the cathode cause uncertainty concerning the actual current density in the system (that is, they cause the effective cathode area to be variable), and may act as sputtering sources to contaminate the palladium.
- b. The presence of copper near the cathode may present similar problems; in addition, the low vapor pressure of copper at high temperatures results in mass transfer to the cathode via sublimation.
- c. The cathode can be "damaged" by subjecting it to high currents ( $>100 \text{ mA/cm}^2$ ) of hydrogen or deuterium.

## IMPLICATIONS

The Kucherov method as reported from tests at Scientific Industrial Association, Luch, provide interesting clues to the presence of excess heat. If transmutation reactions occur in significant quantities as indicated in Ref. 2, then excess heat can be generated by the reaction products. If these product nuclei are often stable, then very little radiation signature will be present. Secondary reactions due to collisions between reaction products and deuterium can produce fusions and other activation reactions, but at very low levels.

It is perhaps worthy to note that Fermi won the Nobel prize for mistakenly believing that he had transmuted uranium by bombarding it with neutrons. So strong was the prevailing belief in the integrity of all atoms that the splitting of uranium was inconceivable. Hence Fermi's experiment was not interpreted correctly at first. Thus, the finding that palladium may be transmuted under the influence of electromagnetic fields in the presence of deuterium may likewise be inconceivable, but ought to be considered nevertheless.

The research we have done to date suggests that the Kucherov method may warrant further investigation. However, at present, our preliminary data needs to be augmented before we can positively verify the character of the reactions which have been observed.

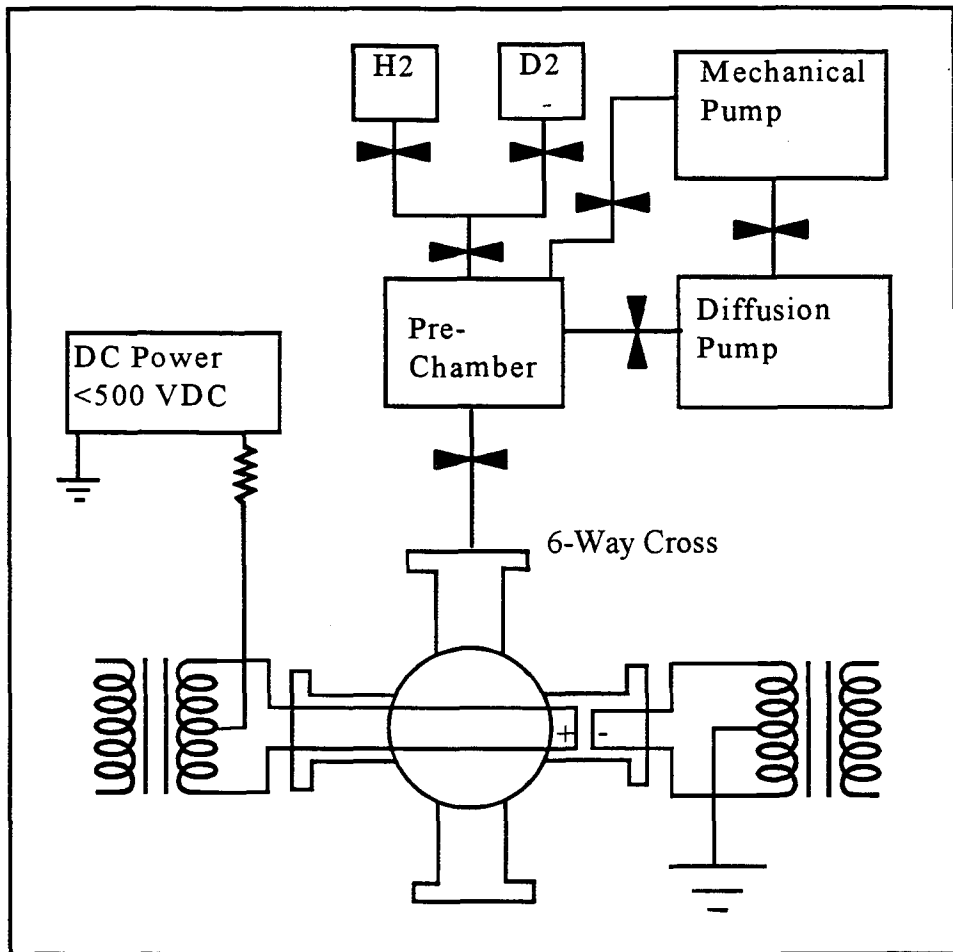


Figure 2. Block Diagram of Glow Discharge Apparatus.

#### Acknowledgement

The authors wish to thank Drs. Yan Kucherov, Peter Hagelstein, Louis Smullin and Gus Bambakidis; and Messrs. Fred Jaeger, Robert Svensson, Erik Van Kemenade, and Alexander Lagounov for their technical advice and help in carrying out the experiment.

#### References.

1. Ya. R. Kucherov et al., "Nuclear Product Ratio for Glow Discharge in Deuterium," Physics Letters A 170 (1992) 265-272.
2. Ya. R. Kucherov et al., "Impurities in Cathode Material and Possible Nuclear Reaction Mechanisms in a Glow Discharge" to be published in Physics Letters A.



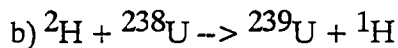
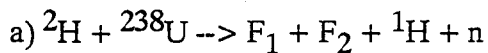
# Oklo isotope anomalies and Cold Fusion.

W. J. M. F. Collis

Strada Sottopiazzo 18, 14056 Boglietto (AT), ITALY

---

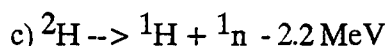
A small site in the extensive Oklo uranium mine in Gabon, Africa is believed to have been a natural reactor where uranium fission took place about 1,800,000,000 years ago during pre-Cambrian times. This is confirmed by the presence of fission products and a depletion  $^{235}\text{U}$ . There is no evidence of any excess of  $^{235}\text{U}$  relative to  $^{238}\text{U}$ , however the missing  $^{235}\text{U}$  is insufficient to explain all the fission products. Shaheen et al. point out the depletion of deuterium in water derived from Oklo rocks[1]. Normal D/H ratio is 150 ppm but at Oklo it is reduced to about 127 ppm. Shaheen et al. suggest that both uranium and hydrogen isotope anomalies might be due to neutron swapping reactions:-



The uranium isotope anomalies can be explained by the principles of fission reactors. The natural reactor was almost certainly moderated by normal light water and fission took place because in pre-cambrian times  $^{235}\text{U}$  was more abundant. Extrapolating back 1800 million years there would have been about 3%  $^{235}\text{U}$  in natural uranium (half life  $7 \times 10^8$  years). The heat generated by the fission reaction would tend to drive off the water resulting, on average, in a just critical but under moderated reactor. Under moderation means that neutron energies will be greater than thermal in dryer zones where we would expect relatively more neutron absorption by  $^{238}\text{U}$ . The  $^{239}\text{Pu}$  so formed eventually decays to  $^{235}\text{U}$  resulting in a partial regeneration of this isotope.

Let us now turn to the proposed induction of fission by neutron swapping. A nucleus with atomic weight of around 240 requires to be excited by 5-6 MeV to overcome the coulomb barrier to fission[6]. This energy is not available if the neutron must be split off from the deuteron in reaction a). Reactions a) and b) require no critical mass of uranium as there is no chain reaction. We would expect uranium isotope anomalies in sub-critical ore bodies, but this has not been observed. Indeed Oklo is the only known site where important uranium isotope anomalies have been detected. If neutron swapping reactions exist, they might occur with other elements besides uranium. However the D / H ratio is particularly uniform on this planet.

If deuterium depletion required merely the presence of uranium in contact with water, then any disintegration could have taken place over geological time, (billions of years) not just the estimated duration of the neutron fluence (a mere million years). In fact there is evidence that the deuterium anomaly may not be correlated with fission at all. The isotopic composition of Oklo samples were extensively analysed for fission products. Conspicuous by their absence at the reactor zones are those water soluble isotopes such as cesium, barium etc. This suggests that water has been cycling through the natural reactor site. It is probable that the deuterium anomaly also exists in the water of neighbouring rocks which did not host any significant fission. What then could be the cause of deuterium disintegration? What special effect could uranium have? The uranium decay chain can supply energetic alpha particles (> 6.6 MeV) or gamma rays to fission deuterium directly.



This reaction has been considered (and excluded) [3,4,5] as an alternative source of neutrons in cold fusion experiments. However the alpha particle and gamma ray flux in a uranium ore deposit may be sufficient. It would be interesting to measure D / H ratios in thorium and uranium ores. Alessandrello et al. [4] have observed deuteron photo-disintegration by placing a 300 kBq  ${}^{232}\text{Th}$  (natural thorium) 30 cm from an electrolytic cell containing heavy water. Karamdoust[5] and co-workers have reported neutron emission caused by alpha particle bombardment from a 1.08 uCi (4000 Bq) radium ( ${}^{226}\text{Ra}$ ) source dissolved in 2ml of 50% heavy water. Fascinating though these results are, it appears that any deuterium disintegration may be too slow to account for the measured isotope depletion even if it occurred over the entire age of the ore deposits ( $2 \times 10^9$  years). The difficulty arises because any deuterium disintegration comparable to the uranium decay rate (half life  $4.5 \times 10^9$  years) requires an exceptionally high efficiency for reaction c).

Vlasov[2] suggests a speculative alternative to the conventional natural fission reactor explanation whereby the explosion of say a  $10^6$ g anti-matter meteorite could supply the  $10^{21}$  neutrons  $\text{cm}^{-2}$  (over 100m radius) required to explain fission products. Such an explosion would produce intense gamma rays capable of causing deuterium disintegration. However the energy concentrated on such a small area would also vapourize and disperse any nuclear products. Ion probe studies show rare earth fission products and uranium present in the same grains. So we can exclude any hypothesis based on massive explosions as the fission products have remained in place. In contrast, no significant explosions would be expected from a low power fission reactor generating the same neutron flux over a period of say a million years. Further, the fission reactor theory, unlike the anti-matter explosion does not require the uranium to be exposed on or near the surface at the time of the neutron flux. In fact, as the uranium oxide is somewhat soluble in water it is likely to have been buried underground for much of its geological life.

In conclusion, the evidence available suggests that the hydrogen isotope anomaly, in contrast to uranium isotope anomalies, may have occurred substantially independently of natural fission at Oklo. However more measurements need to be made to clarify the issue. In particular, is there a correlation between the uranium isotope ratios and the hydrogen isotope ratios at various sites? What is the rate of decay of deuterium when yellow cake is immersed in heavy water? How does this decay rate change with scale?

### **Acknowledgements**

The author is grateful to Prof. Felice Iazzi for useful discussions.

### **References.**

- [1] Shaheen M., Ragheb M., Miley G. M., Hora H., Kelly J., "Anomalous deuteron to hydrogen ratio in Oklo samples and the possibility of deuteron disintegration." in Proc. ACCF2, 1991.
- [2] Vlasov N. A., "On the possibility that certain isotopic anomalies on the Earth may be due to an annihilation explosion", Soviet Atomic Energy Vol 34, No. 5, p395, May 1973.
- [3] Cribier M. , Spiro M. Favier J., "Conventional sources of fast neutrons in 'Cold Fusion' experiments". Phys. Lett. B 228 (1989) 163.
- [4] Alessandrello A. et al. "An Experimental Search for Conventional Sources of 'Cold Fusion'", in "Understanding Cold Nuclear Fusion Phenomena". Conference Proceedings SIF Vol 24, edited by R. A. Ricci, E. Sindoni and F. De Marco. (Editrice Compositori, Bologna, 1989).
- [5] Karamdoust N.A., Majeed A., Durrani S.A.; Nucl. Tracks Radiat. Meas. Vol 19 (1991) pp 627-628. "Cold fusion: Radon contribution to neutron production ?".
- [6] Cottingham W. N., Greenwood D. A., "An Introduction to Nuclear Physics", p 99, Cambridge University Press 1986.
- [7] Cowan G. A., "A Natural Fission Reactor", in Scientific American, Vol 235, July 1976, pp 36-47.
- [8] Ragheb M., O'Connor C., Shaheen M., "On the Anomalous deuterium to hydrogen and the U235 to U238 ratios in Oklo phenomenon samples." Abstract submitted to ICCF3 1992.



A BRIEF INTRODUCTION TO THE HYDROSONIC PUMP  
AND  
THE ASSOCIATED "EXCESS ENERGY" PHENOMENON

James L. Griggs, Hydro Dynamics Inc.,  
611 Grassdale Road, Cartersville, Georgia 30120

## HISTORY OF THE PUMP

The Hydrosonic Pump was invented by Jim Griggs, an electrical engineer, who has specialized in the field of energy conservation. Jim is a member of the Association of Energy Engineers and a member of the National Society of Professional Engineers. He has received numerous awards in the field of energy conservation and has been a consultant to several national companies.

The first production model of the Hydrosonic Pump was completed in 1989. Hydro Dynamics was incorporated in 1990, and the first patent was issued in February of 1993.

## OPERATIONAL PRINCIPLES

Although called a "pump", the Hydrosonic pump is not a pump in the conventional sense of the word. While fluid will move through the Hydrosonic Pump unassisted to a minor extent, it requires a conventional circulation pump to achieve satisfactory results in most applications. It is called a pump for marketing reasons. Company management preferred not to associate the Hydrosonic Pump with the negative connotations arising from the term "steam boiler"

The Hydrosonic Pump uses shock waves to generate sufficient energy to produce hot water (fluids) or steam. When water or other liquids flowing in a restriction are suddenly stopped, pressure of approximately 63.4 PSI is created for each foot of extinguished velocity. This pressure wave then travels back up the conduit to the reservoir or other source of the liquid, and cycles are established and repeated. Normally, the waves dissipate in a short period of time. The term used to describe this wave and cycle effect is commonly called "water hammer". It is also stated in textbooks that as the shock waves pass through the liquid that a portion of the energy is converted into heat energy and is dissipated into the mass. The thermodynamic aspects of this effect were considered small and of no significant harm or value. However, this is where the Hydrosonic Pump achieves its objective.

The pump was designed to accomplish a more energy efficient and environmentally safe way of producing hot water and steam. The basic premise of operation are as follow: Water (basically any aqueous solution or fluid) is injected through an opening and is moved across a spinning rotor which is powered by an external source. The rotor is designed as a sphere with numerous cavities drilled in a specific pattern around the surface. This patented

design ( patent number 5,188,090 ) causes several things to occur. There is a shearing stress created as the water first enters the chamber and a small amount of heat energy is created and released into the water. Because the water enters the chamber under a specified amount of pressure, additional heat is generated and absorbed into the water. The shearing stress (dynamic viscosity) increases as the water continues its movement across the rotor to the outlet port. As the water moves across the rotor surface it is being drawn into the numerous dead end openings. Millions of shock waves are generated thereby producing heat.

As the shock waves are produced a standing wave effect is established and a resonance is set up within the water. As the rotor continues to spin these waves are intensified and resonances of 25 kilo hertz and higher ( frequencies vary with rotor size and design) are produced continuously.

It also appears that tiny air bubbles are formed at some point in the process and the formation and eventual collapse of those bubbles may aid the heat transfer process.

As the heated water leaves the outlet side of the Hydrosonic Pump, it will leave as a combination of steam and condensate, or 100% hot water (liquid). The temperature at which it exits and the state (liquid or gas) in which it exits depends on rotor speeds, hole designs, tolerances between the rotor and housing, water flow rate into the Hydrosonic Pump, and several other design items. An exhaust pressure is also created at this point which can be varied to satisfy the end user's process requirements.

#### **"ENERGY PHENOMENON"**

Testing completed to date by both the Company and independent agencies indicates that the Hydrosonic Pump has a significant energy efficiency advantage over conventional boiler(s) or heat transfer processes. Numerous tests conducted by the Company as well as independent third parties continue to reveal an as yet unexplained phenomenon occurring within the patented process relating to energy input and output. Shortly after the Hydrosonic Pump is operational, the "measurable energy" required to operate the Hydrosonic Pump is less than the measured energy output of the Pump. Present during such tests have been representatives from large utility companies as well as independent engineers and consultants.

The initial reaction from the "experts" when reviewing these results is almost always the same "this is impossible"! On the surface, these results would seem to violate the first law of thermodynamics; however, the Company believes that because of ultrasonic fields and other unknown forces possibly affecting fluids flowing through the Hydrosonic Pump, it is possible that an energy source is being tapped that has to date not been identified. We at Hydro Dynamics believe that further testing will prove that such an additional source does exist and, most importantly, will identify the source.

#### TESTING

When the idea for using shock waves to produce heat was conceived it was thought that such a process might be highly efficient and environmentally clean. The possibility that Coefficient of Performance ( COP ) greater than 1.0 could be achieved became apparent immediately, but because this contradicted the laws of thermodynamics the results were viewed with skepticism; ( COP = energy out / energy in ). However, the phenomenon has continued to persist throughout the years and is still evident in the tests that will be discussed.

It should be noted that these test results on the Hydrosonic System show power out / power in ratios greater than 1:1. The tests being presented follow a procedure we have recently been requested to use. We perform other tests with different procedures, routinely, in a continuing effort to find the best combination of energy efficiency, reduced capital cost, ease of maintenance, etc. for our market. We believe that these tests, along with all the others performed for the past three years, may not be representative of the best possible results that can be obtained from the Pump from purely an energy efficiency standpoint.

When Hydro Dynamic Inc. was formed, the working prototypes at that time were bulky and could possibly require considerable maintenance and repairs. It was not unusual to get COP's of the order of 2:1. It was believed at that time the Pump should be basically simple to operate and "maintenance free". The housing and bearing configuration were completely redesigned with that concept in mind, and in so doing this reduced the Pump efficiency.

It was thought at this time that the reduced efficiency would not affect the company's specialty marketing effort, which emphasized other features of the Pump. However, because there has been

extreme interest in the "energy phenomenon" and the manner in which the Hydrosonic Pump achieves it, the company is in the process of building a new "old" Pump.

Specifications and data on that system should be available in January 1994.

At this point, with or without the "excess energy" phenomenon, there are numerous applications for the Pump. The Company is continuing its intensified research and development efforts and welcome any suggestions by phone, mail, or personal visits to our operations in Cartersville, Georgia.

#### **FORCED STEAM BARREL TEST**

On November 30, 1993 a test was conducted at the offices of Hydro Dynamics Inc. to determine the efficiency of a Hydrosonic Pump system producing steam. The coefficient of performance ( COP ) is the basic parameter used to compare the performance of heating systems, and is defined in the Handbook of Energy Engineers, The Fairmont Press, 1989, page 249, as follows:

$$\text{COP} = \frac{\text{RATE OF NET HEAT REMOVAL}}{\frac{\text{energy out}}{\text{energy in}}}$$

The test was conducted by Jim Griggs, Kelly Hudson, Phillip Griggs and Marvin Dawkins according to the following procedures: Two 55 gallon barrels were weighed empty and the weights recorded. The barrels were then placed on scales and filled with 200 pounds of water from the county water system. (A. & C. data sheet) When the barrels were filled, one was placed under the steam supply area of the Hydrosonic system and the other barrel was placed under the condensate return line from the system.

Additional valves were added to the steam supply line ( see exhibit 1 ) and the condensate return line ( see exhibit 1 ) so that the system could be operated until it reached equilibrium without heat or energy being added to the water in the barrels.

Also thermocouples and dial type thermometers were added to the steam ( see 1-A ) and condensate ( see 1-B ) lines so the temperature of the lines could be monitored during the test.

A thermocouple and a hand held thermometer were used to continually check the temperature in the two barrels before, during, and after the test.

A separate steam supply line was placed into one of the barrels with the exhaust of the line well below the water level ( see exhibit 2 page 1 ). Another supply line leading directly from the condensate trap located at the bottom of the steam reservoir was placed in the second barrel, again with the exhaust well below the water level ( see exhibit 2 page 2 ).

The condensate supply tank was drained and refilled with tap water, then weighed to determine the total mass of supply water available to the system. When the supply tank volume had been determined a water hose was placed in the top of the supply tank. The tank was filled and allowed to overflow until the test began. The hose was then removed and an fixed amount of water was available to the Hydrosonic Pump ( see exhibit 3-A ).

A dial thermometer and hand held unit were used to verify the temperature of the supply water.

A standard condensate pump ( Burks 1/2 hp ) supplies water to the Hydrosonic Pump with a constant flow and pressure ( see exhibit 3-B ). The flow and pressure was monitored with in line flow control and pressure gauges ( see exhibit 3-C ).

A Lincoln 40 horsepower electric motor was coupled to the drive shaft of the Hydrosonic Pump and provided a power source to the system ( see exhibit 3-D ).

A Dranetz 808 demand analyzer was connected to the electrical panel to monitor all electrical energy being supplied to the system ( see exhibit 3-E ).

When the test began water was supplied to the Hydrosonic Pump though a water feed line under constant pressure and flow ( see exhibit 4-A ).

The Hydrosonic Pump heats the water converting it to a combination of hot water and steam ( see exhibit 4-B ). This mixture of hot water and steam travels from the Hydrosonic Pump through a supply line ( see exhibit 4-C ) and through a valve ( see exhibit 4-D ) to a separation tank ( see exhibit 4-E ) where the steam and condensate will separate.

The steam flowed from the system through a steam line located at the top of the separation tank ( see exhibit 4-F ). The steam was exhausted to the atmosphere until the test began. It was then routed to the barrel of water to capture the steam heat ( see exhibit 2 page 1 ).

The hot condensate was removed through a trap located at the bottom of the separation tank ( see exhibit 4-G ). This condensate was then diverted to a drain until the test began, at which time it was routed to a barrel to capture the heat energy available in the condensate ( see exhibit 2, page 2 ).

When the system was powered it was allowed to reach a state of equilibrium. The pressure and temperature of the system remains constant and was monitored by gauges in the separation tank ( see exhibit 4-H ). The test was now ready to begin.

#### TEST PROCEDURE

Simultaneously the following occurred:

The supply water hose was removed from the system, the steam was diverted to barrel 1 ( see exhibit 2 page 1 ), as valve 5-A was closed and 5-B was opened. The condensate was diverted to barrel 2 ( see exhibit 2 page 2 ), as valve 6-A was closed and valve 6-B was opened. The Dranetz 808 was activated and the time was recorded by a stop watch.

At the end of the 15 minutes, the above procedure was reversed. The power to the system was disconnected. The steam was removed from barrel 1, as valve 5-A was opened and 5-B was closed. The condensate was diverted from barrel 2, as valve 6-A was opened and 6-B was closed. The Dranetz has recorded all incoming electrical power ( S. data sheet ).

The temperature rise in barrels 1 & 2 were recorded by a thermocouple and hand held unit and the data was logged ( F. & H. data sheet ). Barrels 1 & 2 were weighed to determine the additional mass that was added during the test, and the data was logged ( E. & G. data sheet ).

The total electrical power input in kilowatt hours as recorded by the Dranetz was recorded and logged.

With the recorded data, as listed in appendix A , calculations indicate that the efficiency of the system (COP) was 1.03 or 103% ( V. data sheet ).

When a comparison is made between the amount of water supplied to the Pump during the test (P. data sheet) and the amount of water added to the barrels at the end of the test (O. data sheet), there is a 2 pound difference (Q. data sheet). This loss was due to evaporation. When this is taken into consideration the resulting COP was 1.10.

When radiant and convection losses that occur naturally during testing are considered (U. data sheet), the COP of the Pump becomes 1.14.

The electric motor efficiency is factory rated at 82.5% maximum efficient (appendix C.). When the additional losses of the electric motor are taken into consideration, the COP of the Hydrosonic Pump becomes 1.39 (Y. data sheet).

All the recorded data and calculations have been listed and attached as appendix A.

Specific data sheets for the Dranetz 808 demand analyzer, Omron sensors and thermocouple and the Lincoln electric motor are available from Hydro Dynamics Inc., or form the manufacturer.

#### DIRECT LINE STEAM TEST

On December 1, 1993, a direct line steam test of the Hydrosonic Pump system was performed at the offices of Hydro Dynamics Inc. The purpose of the test was to test the efficiency of a Hydrosonic Pump steam system.

Present and conducting the test were Jim Griggs, Kelly Hudson, Phillip Griggs and Marvin Dawkins.

The basic set up of the Hydrosonic system was similar to the previous test except for two changes. There was only one barrel used and it collected the hot condensate as it is expelled from the trap (see exhibit 5).

The collection barrel was located near the trap area, and is empty. The weight of the barrel has been recorded so that the total mass of hot condensate collected at the end of the test can be weighed.

In this test the steam system was at equilibrium, and the steam was exhausted to the atmosphere continuously.

The water supply system was filled with tap water and weighed to determine the mass of supply water available to the system. A water hose was placed in the supply tank. The tank was allowed to overflow until the test began (see exhibit 3-A).

A thermocouple and a handheld unit verified the temperature of the supply system.

Thermocouples and dial thermometers were placed in the steam lines and the separation tank to monitor the temperature of the steam (see exhibit 1-A).

A thermocouple and dial thermometers was placed in the hot condensate line to monitor the temperature of the condensate before and after it crosses the trap (see exhibit 1-B).

#### TEST PROCEDURE

Simultaneously the following occurred: The supply water hose was removed from the system. The condensate was diverted to the barrel for collection as valve 6-A was closed and 6-B was opened. The steam was exhausting to atmosphere. The steam pressure on the separation tank was maintained at a constant 60 psi gauge and 310 degrees F. The Dranetz 808 was activated and the time was recorded by a stop watch.

At the end of 25 minutes, the above procedure was reversed. Power to the system was disconnected, and the flow of hot condensate to the barrel was stopped as valve 6-A was opened and valve 6-B was closed. The mass of the hot condensate that had been collected was weighed and recorded. The temperature of the condensate was recorded. The remaining water in the supply tank was drained, weighed, and recorded. The kilowatt hours, as recorded by the Dranetz, was logged.

The total water supply availabl less total water remaining in supply tank at end of test less total pounds of condensate collected equals total mass in pounds to steam.

Results of this test indicated a COP of 1.18.

Results of this test considering radiant and convection losses (T. data sheet) indicated a COP of 1.21.

The motor used in this test was a Lincoln 75 hp with a factory rated maximum efficiency of 87.5%. Results of this test considering the efficiency of the motor indicate an overall COP of 1.38.

The calculations and recorded data have been listed as appendix AA.

## **DIRECT HOT WATER**

COP calculations for direct hot water tests have ranged from .86 to 1.15 depending on the test. However, we have not determined whether it is best to produce hot water on a direct basis for instantaneous demand or by using a simple heat exchanger, to remove energy from the steam and producing steam with the pump.

Research is continuing in this regard and additional data should be available in the near future.

## **CONCLUSION**

It appears that the label "COLD FUSION" is being applied to all research that involves the "excess energy" phenomenon. Previous Hydro Dynamics' tests, including these results, strongly suggest the presence of excess energy. At this stage of our research we are not theorizing as to the source of the "excess".

We are open minded to the possibility that " COLD FUSION" might be occurring, however there are many other possible explanations that we are exploring with the same vigor.

As stated earlier we, at Hydro Dynamics Inc., do feel that this phenomenon is real and that at some point in the future it, will be fully explained. I personally have empathy for those of you who have continued to search for an answer to this phenomenon. It seems as though when you try to discuss this phenomenon with intelligent people their response remains the same, "IMPOSSIBLE".

To quote from the great physicist, Albert Einstein,  
" All the laws of physics are absolute, not in the sense of being unalterable by the progress of research but in the sense I have already noted-they are consistent throughout the universe."

The two tests that have been examined in this paper were conducted under the strictest control conditions available to the researchers. Manufacturers specifications as to the accuracy of all test equipment has been supplied in appendix B, and based on the company's interpretation of these specifications, instrumentation error cannot possibly explain away the large amounts of excess heat energy produced by the Hydrosonic Pump.

During the past three years the tests performed at Hydrodynamics continue to indicate COP's greater than one. We believe additional research in this area must continue.

#### AUTHOR'S NOTE

Hydro Dynamics Inc. as a company and I myself personally invite any input in the form of recommendation, possible explanations, and criticism as to our process or testing techniques. We realize that we do not have the final answer, but the question remains open, what is the source of the "excess"? We invite anyone to our facility at anytime for a demonstration, or an attempt to prove us wrong.

#### UPDATED TEST SINCE ICCF-4

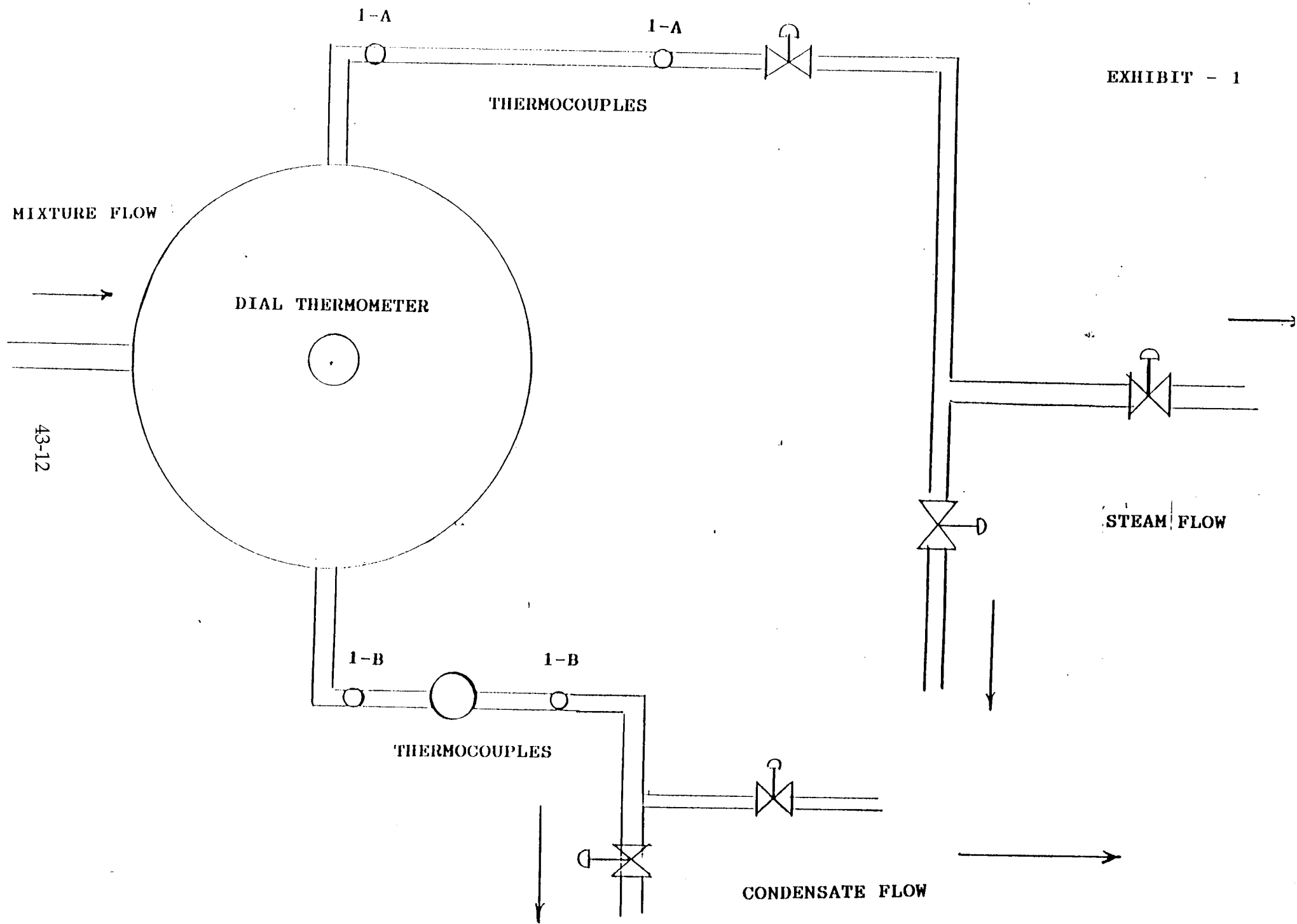
On January 5 and 6 1994 Mr. Jed Rothwell and Dr. Eugene F. Mallove took us up on our above invitation and visted our plant in Cartersville, Georgia.

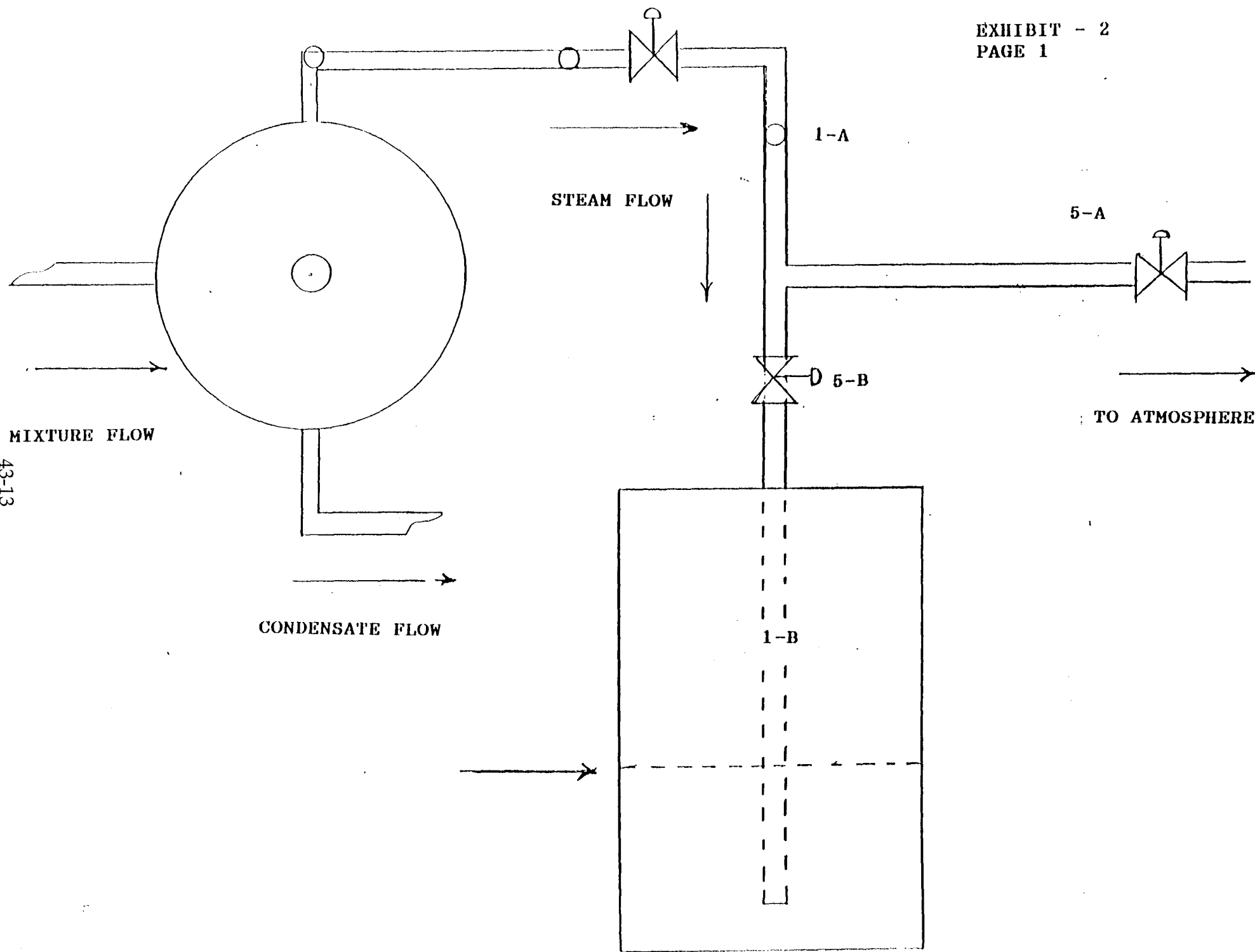
During the visit we conducted a series of test with their assistance on an updated design change in the pump. During these test the pump was producing 100% steam with no condensate to be captured. The steam line was placed in a barrel of water as in the previous described test and all the energy captured in the water mass.

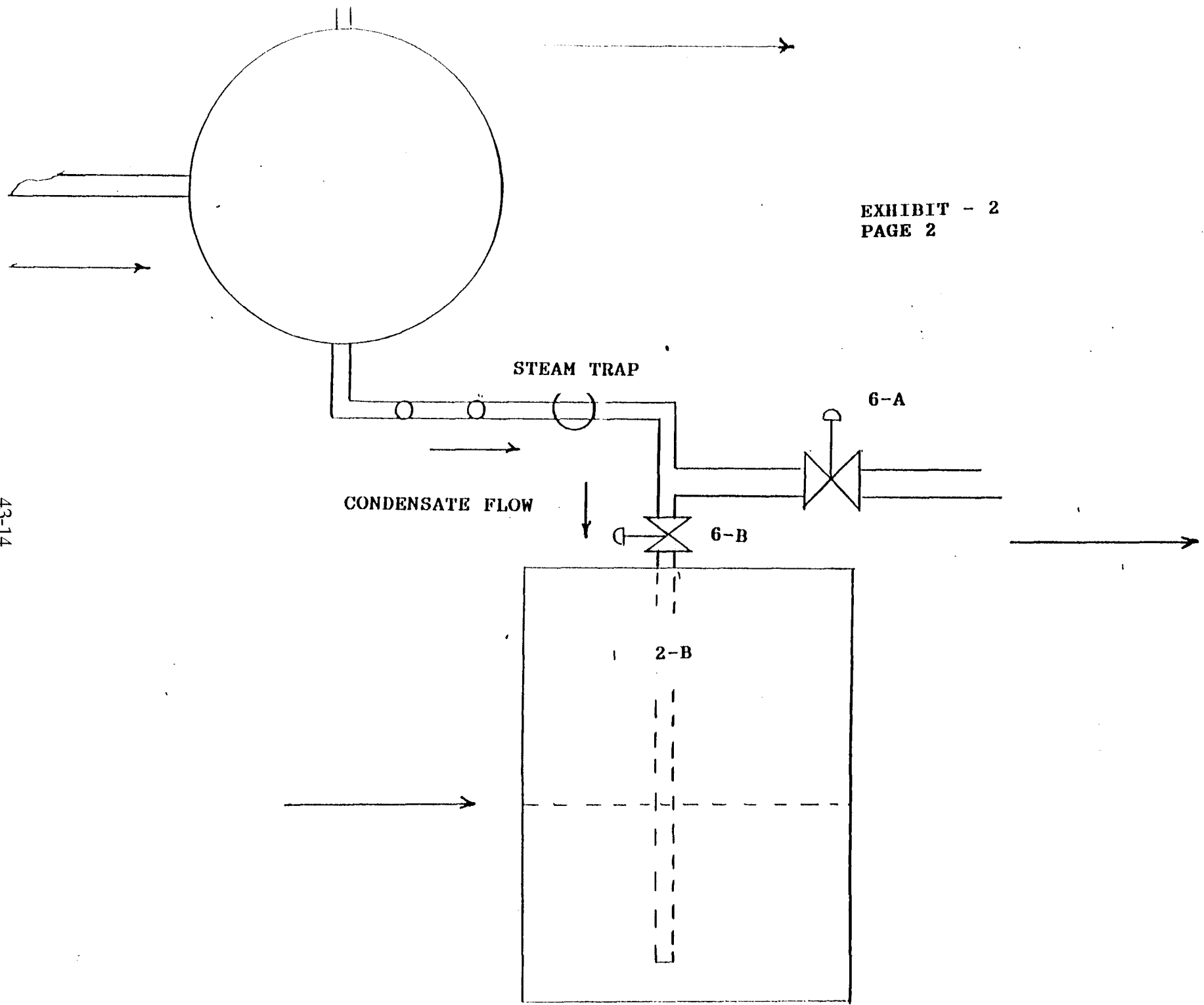
COP's for these test were in the 1.7 to 1.8 range.

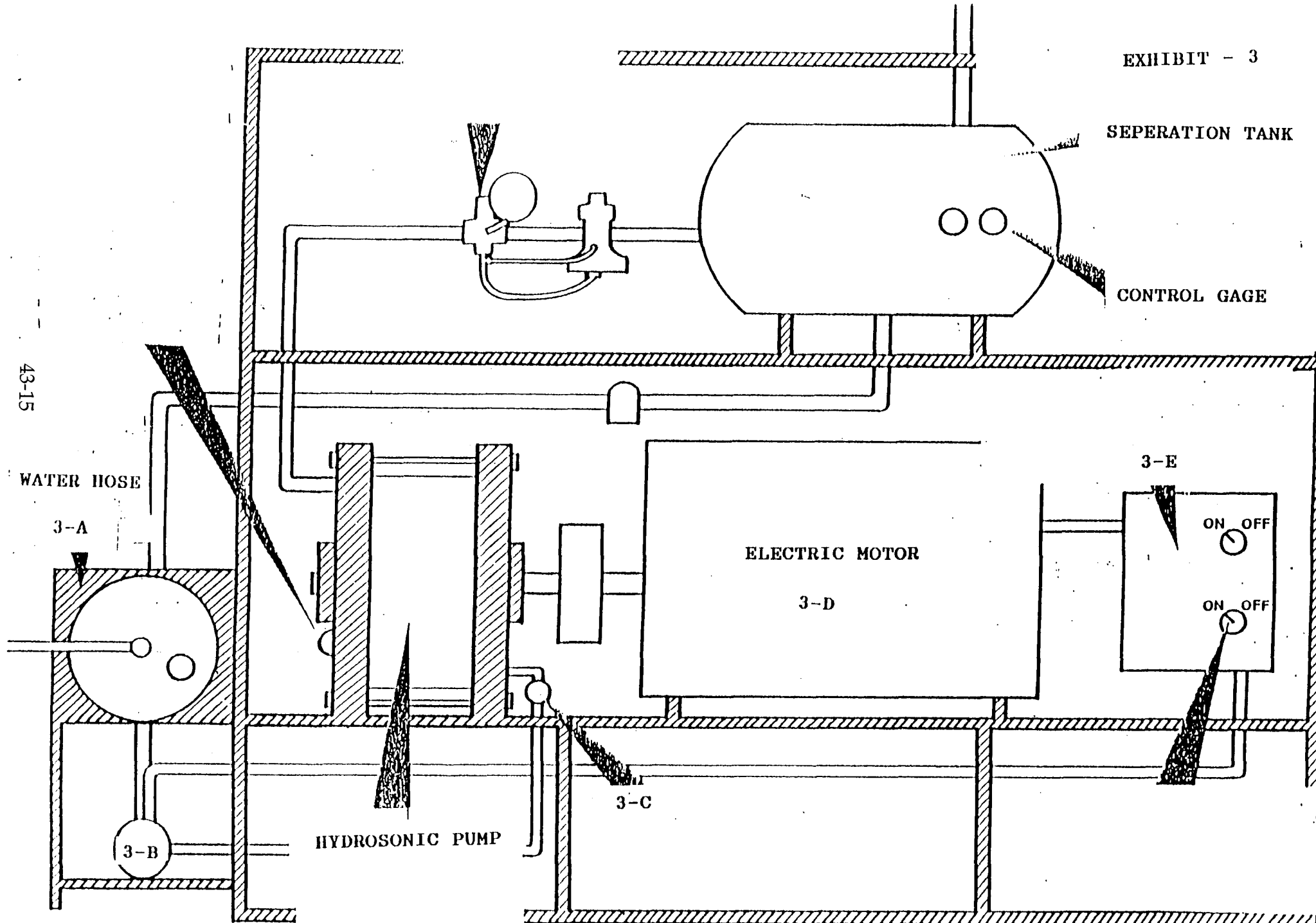
A complete report on these test is available from Hydro Dynamics Inc. upon request.

EXHIBIT - 1



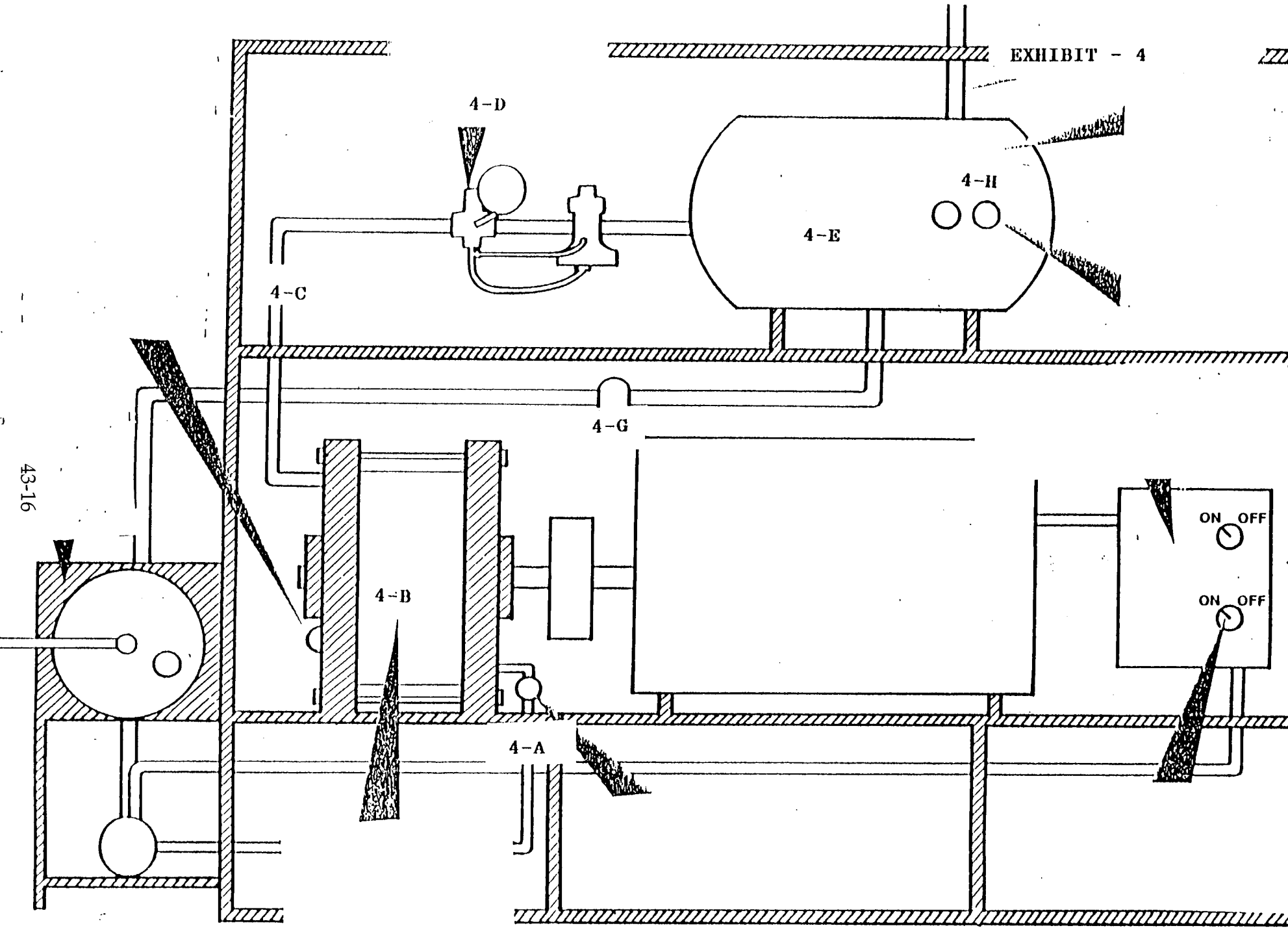


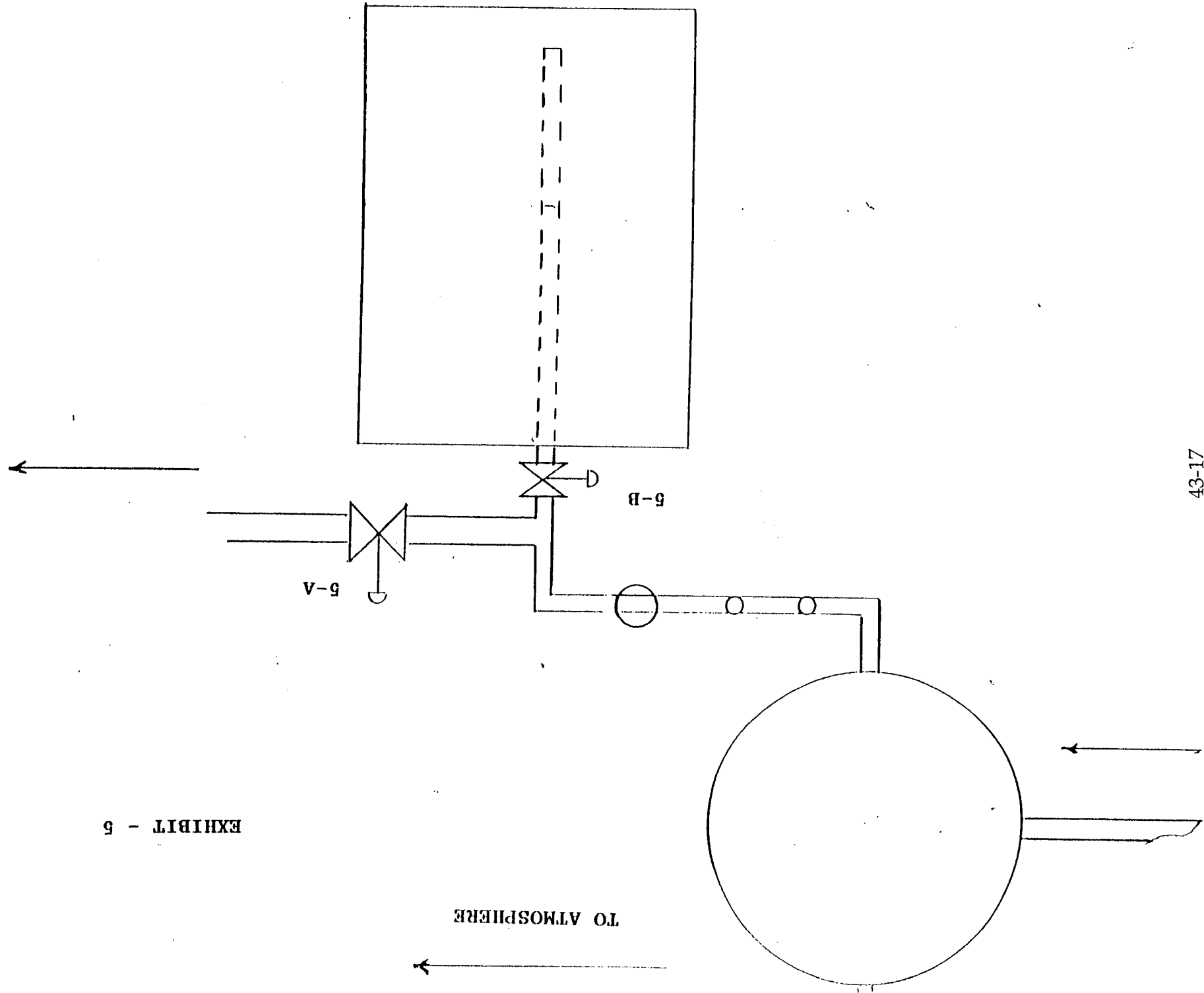




**the Hydrosonic Pump svstem**

EXHIBIT - 4





43-17

**APPENDIX A**

DATE	NOV 30, 1993
PUMP SIZE	HYD 12 X 6
MOTOR SIZE	HP 40
MOTOR EFFICIENCY	0.825
TEST TIME IN MINUTES	15
A. STARTING MASS IN POUNDS ( BARREL 2 )	200
B. STARTING TEMP DEGREES F (BARREL 2)	58
C. STARTING MASS IN POUNDS ( BARREL 1 )	200
D. STARTING TEMP DEGREES F (BARREL 1)	58
E. ENDING MASS WEIGHT (BARREL 2)	283
F. ENDING MASS TEMP DEGREES F (BARREL 2)	136
G. ENDING MASS WEIGHT (BARREL 1)	205
H. ENDING TEMP DEGREES F (BARREL 1)	89
I. DELTA T (BARREL 2)	78
J. DELTA T (BARREL 1)	31
K. BTU'S ADDED (BARREL 2)	22074
L. BTU'S ADDED (BARREL 1)	6355
M. TOTAL BTU'S ADDED DURING TEST	28429
N. WATER AVAILABLE IN POUNDS (SUPPLY TANK)	153
O. TOTAL MASS ADDED ( BARREL 1 & 2 )	88
P. WATER USED FROM SUPPLY TANK	90
Q. MASS LOST TO EVAPORATION	2
R. BTU'S LOST TO EVAPORATION	1940
S. ELECTRICAL INPUT RECORDED IN KWH	8.07
T. ELECTRICAL INPUT IN BTU'S	27542.91
U. ESTIMATED RADIANT & CONVECTION LOSS	1184.892291
V. COP HEAT ADDED TO BARRELS 1 & 2	1.0321712557
W. COP INCLUDING EVAPORATIVE LOSSES ( Q. )	1.1026068052
X. C.O.P. AFTER ESTIMATED LOSSES	1.1456266709
Y. C.O.P. ASSUMING MOTOR LOSSES	1.388638389

ALL BTU RATING COME FROM STEAM TABLES OBTAINED FROM, The American Society of Mechanical Engineers, United Engineering Center, 345 East 47th Street, New York, New York 10017.

1 BTU RAISES 1 POUND OF WATER 1 DEGREE F

1000 WATTS = 1 KILOWATT

1000 WATTS FOR 1 HOUR = 1 KILOWATT HOUR

1 KILOWATT HOUR = 3413 BTU'S

1 KILOWATT (KW) = 1.341 HORSEPOWER (HP)

1 GALLON (US) WATER = 8.34 POUNDS

1 HORSEPOWER (HP) = .746 KILOWATT (KW)

1 HORSEPOWER HOUR = .746 KILOWATT HOUR (KWH)

1 HORSEPOWER HOUR = 2545 BTU

**APPENDIX AA**

DATE	DECEMBER 1 1993
PUMP NUMBER	DEMO
PUMP SIZE	HYD D. 15.3 X 4
A. TOTAL SUPPLY WATER MASS AVAILABLE	307.5
B. MEASURED REMAINING MASS (TEST COMPLETE)	79
STEAM MEASUREMENTS	
C. TOTAL MASS IN POUNDS TO STEAM	39
D. SUPPLY WATER TEMP IN DEGREES F.	123
E. OPERATIONAL STEAM PRESSURE	60
F. TEMPERATURE RECORDED IN DEGREES F.	310
G. BTU'S PER POUNG OF STEAM ( STEAM TABLES )	1091.4
H. DURATION OF TREST IN MINUTES	25
I. BTU PRODUCTION DURING TEST PERIOD	42564.6
J. ESTIMATED HOURLY OUTPUT OF STEAM (BTU'S)	102155.04
CONDENSTAE MEASUREMENTS	
K. TOTAL MASS IN POUNDS TO CONDENSATE	189.5
L. TEMPERATURE RECORDED AT TRAP IN DEGREES F.	305
M. BTU'S PER POUND OF CONDENSATE ( TABLES )	187.04
N. BTU PRODUCTION DURING TEST PERIOD	35444.08
O. ESTIMATED HOURLY OUTPUT FROM CONDENSATE	85065.792
P. TOTAL BTU OUTPUT DURING TEST	78008.68
Q. ELECTRICAL INPUT AS MEASURED BY DRANETZ	19.35
R. ELECTRICAL INPUT CONVERTED TO BTU'S	66041.55
S. ESTIMATED HOURLY INPUT IN BTU'S	158499.72
T. RADIANT & CONVECTION LOSSES	1926.6583786
V. DRIVE SYSTEM SIZE ( ELECTRIC MOTOR )	HP-75
W. EFFICIENCY OF DRIVE SYSTEM	0.875
U. COP ( INPUT TO OUTPUT )	1.1812060741
W. COP INCLUDING RADIANT & CONVECTION LOSS	1.2103795017
X. COP INCLUDING MOTOR LOSSES	1.3832908591

ALL BTU RATING COME FROM STEAM TABLES OBTAINED FROM, The American Society of Mechanical Engineers, United Engineering Center, 345 East 47th Street, New York, New York 10017.

1 BTU RAISES 1 POUND OF WATER 1 DEGREE F

1000 WATTS = 1 KILOWATT

1000 WATTS FOR 1 HOUR = 1 KILOWATT HOUR

1 KILOWATT HOUR = 3413 BTU'S

1 KILOWATT (KW) = 1.341 HORSEPOWER (HP)

1 GALLON (US) WATER = 8.34 POUNDS

1 HORSEPOWER (HP) = .746 KILOWATT (KW)

1 HORSEPOWER HOUR = .746 KILOWATT HOUR (KWH)

1 HORSEPOWER HOUR = 2545 BTU



[Presented for 4th International Conference on Cold Fusion, ICCF-4, Hyatt Regency Maui, Hawaii, U.S.A., December 6th to 10th 1993]

## AN APPROACH TO THE PROBABLE MECHANISM OF THE NON-RADIOACTIVE BIOLOGICAL COLD FUSION OR SO-CALLED KERVRAN EFFECT (Part 2)

Prof. Dr. Hisatoki KOMAKI

The Biological and Agricultural Research Institute.  
2-6-18 SAKAMOTO, OTSU, SHIGA-KEN, JAPAN

### Introduction

Our observations on the non-radioactive biological cold fusion or the biological transmutation of elements has been presented at the 3rd International Conference on Cold Fusion (Oct. 21 to 25, 1992, Nagoya, Japan).<sup>1)</sup> In previous several papers<sup>2)~8)</sup>, with Prof. Dr. C. Louis Kervran, we suggested the probable occurrence of non-radioactive biological cold fusion or the biological transmutation of elements. In this paper, in order to confirm the phenomena, under the more controlled condition, potassium, magnesium, iron and calcium were determined in the cells of *Aspergillus niger* IFO 4066, *Penicillium chrysogenum* IFO 4689, *Saccharomyces cerevisiae* IFO 0308, *Torulopsis utilis* IFO 0396, cultured in normal medium and media deficient in one of potassium, magnesium, iron or calcium. The probable mechanism of the biological cold fusion (non-radioactive) in these microorganisms will be discussed.

### Method and Results

The method of culture, and the composition of the normal media (for mold and for yeast), and that of the media deficient in one of potassium, magnesium, iron or calcium, are quite equal to that in our previous paper.<sup>1)</sup> The experimental results, under more controlled condition, are shown in Table I and II.

### Conclusion

Our observations on the non-radioactive cold fusion or the biological transmutations of elements (so-called Kervran effect), in previous papers, have been reconfirmed under more controlled conditions. With Prof. Dr. C. Louis Kervran, the probable mechanism of the biological transmutations of elements, or non-radioactive biological cold fusion, may be summarized as follows:—



References

- (1) Hisatoki KOMAKI: Observations on the biological cold fusion or the biological transmutation of elements. Proceedings of ICCF-3 (Nagoya, Japan, 1992)
- (2) Hisatoki KOMAKI: Production de proteines par 29 souches de microorganismes et augmentation du potassium en milieu de culture sodique, sans potassium (Revue de Pathologie Comparee 67, 213-216, 1967)
- (3) Hisatoki KOMAKI: Formation de proteines et variations minerales par des microorganismes en milieu de culture, sort avec ou sans potassium, sort avec ou sans phosphore (Revue de Pathologie Comparee, 69, 83-88, 1969)
- (4) Hisatoki KOMAKI: C.L.Kervran: Experiences de Komaki, Premiere Serie de Recherches (PREUVES EN BIOLOGIE DE TRANSMUTATIONS A FAIBLE ENERGIE, MALOINE, S.A., PARIS, 1975. p. 116-120)
- (5) Hisatoki KOMAKI: C. Louis Kervran: Deuxieme Serie D'Experiences de KOMAKI (Ibid., p. 120-121)
- (6) Hisatoki KOMAKI: C. Louis Kervran: Troisieme Serie D'Experiences de H. KOMAKI (Ibid., p. 122-130)
- (7) Hisatoki KOMAKI et al.: Proceedings of 13th International Congress of Biochemistry, Amsterdam, 1986
- (8) Hisatoki KOMAKI et al.: An approach to the probable mechanism of the non-radioactive biological cold fusion or so-called Kervran effect, Proceedings of 4th International Conference on Biophysics and Synchrotron Radiation, (Tsukuba, Japan, 1992)

In previous papers<sup>(1)-(6)</sup>, with Prof. Dr. C. Louis Kervran, I suggested the probable occurrence of the biological cold fusion or the biological transmutation of elements.

May I have Slide No. 1 [References <sup>(1)-(6)</sup>]

Of course I do not insist that our observations, with Prof. Dr. C. Louis Kervran, are the completely reliable evidences of the biological cold fusion.

In previous papers, with Prof. Dr. C. Louis Kervran, I merely suggested the probable occurrence of the biological transmutations of elements.

In 1799, Vauguelin, a French chemist, reported that, according to his observations, the hen was found to have excreted five times more lime than it had taken in the food. He concluded that lime had been produced but he could not determine the cause.

In 1831, the French chemist Choubard reported that the young plants (watercress, etc.) contained minerals which had not existed in the seeds.

In 1875, von Herzele went a step further by verifying a weight increase in the ashes of young plants stemmed from germinating seeds. He concluded that there was a transmutations of elements.

In 1959, Prof. Dr. C. Louis Kervran began to publish his discoveries, but I did not yet know them.

It was in 1962 that Prof. Dr. Kervran's academic book "Biological Transmutations" was published by Librairie Maloine, Paris, France. In 1963, we began to verify the formation of several minerals from another minerals (atoms), using some microorganisms.

These observations — Reference (1) to (6) — were presented for Revue de Pathologie Comparee, etc, since 1965.

In order to confirm the phenomena, under the more controlled condition, potassium, magnesium, iron and calcium were determined in cells of *Aspergillus niger* IFO 4066, *Penicillium chrysogenum* IFO 4689, *Rhizopus nigricans* IFO 5781, *Mucor rouxii* IFO 0396, *Saccharomyces cerevisiae* IFO 0308, *Torulopsis utilis* IFO 0396, *Saccharomyces ellipsoideus* IFO 0213 and *Hansenula anomala* IFO 0118 cultured in normal medium and media deficient in one of potassium, magnesium, iron or calcium.

The experimental results were presented for 4th International Conference on Biophysics and Synchrotron Radiation, August 30th to September 4th 1992 at Tsukuba, Japan.<sup>(7)</sup>

May I have a next slide (Slide No.2) (Table 1)

Table I shows the components of normal media, K-deficient, Mg-deficient, Ca-deficient and Fe-deficient media for mold. Of course, all components used are pure chemicals.

May I have a next slide. (Slide No.3) (Table 2)

Table 2 shows the components of normal media, and K-deficient, Mg-deficient, Ca-deficient and Fe-deficient media for yeast.

All components used are, of course, pure chemicals.

May I have a next slide. (Slide No.4) (Table 3)

Table 3 shows the outline of the experimental results, which I presented for 4th International Conference on Biophysics at Tsukuba, last year, for your reference.

Table 3 shows the comparison of the yield, as the weight of dried cells(mg) of mold and yeast obtained by normal media and potassium-deficient, magnesium-deficient, iron-deficient, and calcium-deficient culture. (Cultured with each 200ml of culture media; shaking culture at 30°C for 72 hours)

Then, may I have a next slide (Slide No.5) (Table 4)

Table 4 shows the comparison of the contents of potassium, magnesium, iron, and calcium( $\mu$ g) of the whole amount of, and 1g of the dried cells of mold and yeast obtained by normal culture, and potassium-deficient, magnesium-deficient, iron-deficient and calcium-deficient culture. (Each 200ml: 30°C: 72 hours).

The each upper figure shows the content of potassium, magnesium, iron and calcium per whole amount of the obtained dried cells.

The each lower figure shows the content of potassium, magnesium, iron and calcium per 1g of the obtained dried cells.

These are our experimental data that I presented for 4th International Conference of Biophysics at Tsukuba, last year.

For your reference I would like to show the growth curve of several sorts of microorganisms in normal media and potassium-deficient media.

May I have a next slide. (Slide No.6) (Fig.1)

The left curve shows the growth curve of Aspergillus niger in normal and potassium-deficient media.

The middle curve shows the growth curve of Urococcaus in normal and potassium-deficient media.

The right curve shows the growth curve of Saccharomyces rouxii in normal and potassium-deficient media.

May I have a next slide (Slide No.7) (Fig.2)

The curve No.1 shows the growth curve of Aspergillus niger in normal and phosphorus-deficient media.

The curve No.2 shows the growth curve of Penicillium chrysogenum in normal and phosphorus-deficient media.

The curve No.3 shows the growth curve of Urobacillus in normal and phosphorus-deficient media.

The curve No.4 shows the growth curve of *Saccharomyces cerevisiae* in normal and phosphorus-deficient media.

The curve No.5 shows the growth curve of *Candida lypolitica* in normal and phosphorus-deficient media.

The curve No.6 shows the growth curve of *Torulopsis lactis condensi* in normal and phosphorus-deficient media.

To avoid the data, concerning our experimental results which I<sup>(8)</sup> presented for the 3rd International Conference on Cold Fusion (ICCF-3), Nagoya, 1992, please refer to the Abstract of ICCF-3.

Then, in order to confirm these observations, which I presented for ICCF-3. last year, I determined the content of potassium, magnesium iron and calcium in the dried cells of *Aspergillus niger* IFO 4066, *Penicillium chrysogenum* IFO 4689, *Saccharomyces cerevisiae* IFO 0308, *Torulopsis utilis* IFO 0396, cultured in normal medium and media deficient in one of potassium, magnesium, iron or calcium, under more controlled conditions.

May I have a next slide (Slide No.8) (Table 5)

This is our main data.

Table 5 shows the comparison of the yield, as the weight of the dried cells(mg) of mold and yeast, obtained by normal media and potassium-deficient, magnesium-deficient, iron-deficient and calcium-deficient culture. (Cultured with each 200ml of culture media; shaking culture at 30°C for 72 hours.)

May I have a next slide. (Slide No.9) (Table 6)

This is our most chief and most important data.

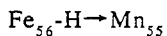
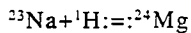
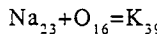
Table 6 shows the comparison of the content of potassium, magnesium, iron, and calcium ( $\mu\text{g}$ ) of the whole amount of. and 1g of, the dried cells of mold and yeast obtained by normal media, and potassium deficient, magnesium-deficient, iron-deficient and calcium-deficient culture (Each 200ml; 30°C; 72 hours)

The each upper figure shows the content of potassium, magnesium, iron and calcium per whole amount of the obtained dried cells.

The each lower figure shows the content of potassium, magnesium, iron and calcium per 1g of the obtained dried cells.

Our conclusions would be summarized as follows.

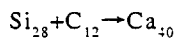
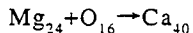
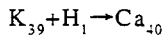
May I have a next slide. (Slide No.10)



Our observations on the non-radioactive cold fusion or the biological transmutations of elements (so-called Kervran effect), in previous papers, have been reconfirmed under more controlled conditions.

With Prof. Dr. C. Louis Kervran, the probable mechanism of the biological transmutations of elements, or non-radioactive biological cold fusion, may be summarized as the Slide No.10 and Slide No.11 shows.

Then, may I have a next slide. (Slide No.11)



My coworkers and I would like to conclude that the non-radioactive biological transmutations of elements, whether we call the phenomena as the biological cold fusion or not, are the real fact.

The non-radioactive biological transmutations of elements, or the biological cold fusion, would be the key of obtaining the endless and very clean energy, which my coworkers and I sincerely hope to promote my "Four Steps to Absolute Peace" Programme<sup>(9)(10)</sup> into the real practice in the nearest future.

The problems to be solved in future, by us, may be summarized as follows: —

Dr. Goldfein<sup>(12)</sup>, of the U.S. Army Laboratory, kindly suggested that the biological transmutations of elements (biological cold fusion, my coworkers and I would like to say) must be catalyzed by Mg-ATP as biological particle accelerator. In this connection, we have much concern with Prof. Dr. Katsuzo Wakabayashi (Osaka University) and Prof. Dr. Takeyuki Wakabayashi (Tokyo University)'s small-angle X-ray scattering analysis of conformational changes of the myosin head (SI) during hydrolysis of ATP (Mg-ATP)<sup>(13)</sup>.

We sincerely hope that the late Prof. Dr. C. Louis Kervran's working hypothesis on the probable mechanism of the non-radioactive biological transmutations of elements (or the non-radioactive biological cold fusion) would be confirmed by the specialists in the field of biophysics, especially in the field of synchrotron radiation or in the related fields

(14)(15)(16)(17)(18) (National Laboratory of High Energy Physics, Tsukuba, must be one of the best laboratories in these fields), and by the specialists in the field of nuclear physics, especially in the field of cold nuclear fusion: National Institute for Fusion Science, Nagoya, must be one of the best laboratories in these fields. Thank you.

#### REFERENCES

- (1) Hisatoki KOMAKI: Production de protéines par 29 souches de microorganismes et augmentation du potassium en milieu de culture sodique, sans potassium (Revue de Pathologie Comparee 67, 213-216, 1967)
- (2) Hisatoki KOMAKI: Formation de protéines et variations minérales par des microorganismes en milieu de culture, soit avec ou sans potassium, soit avec ou sans phosphore (Revue de Pathologie Comparee, 69, 83-88, 1969)
- (3) Hisatoki KOMAKI: C.L. Kervran: Experiences de Komaki, Premiere Serie de Recherches (PREUVES EN BIOLOGIE DE TRANSMUTATIONS A FAIBLE ENERGIE. MALOINE, S.A., PARIS, 1975, p.116-120)
- (4) Hisatoki KOMAKI: C. Louis Kervran: Deuxieme Serie D'Experiences de KOMAKI (Ibid., p.120-121)
- (5) Hisatoki KOMAKI: C. Louis Kervran: Troisieme Serie D'Experiences de H. KOMAKI (Ibid., P.122-130)
- (6) Hisatoki KOMAKI et al.: Proceedings of 13th International Congress of Biochemistry, Amsterdam, 1986.
- (7) Hisatoki KOMAKI et al: An Approach to the Probable Mechanism of the Non-radioactive Biological Cold Fusion or So-called Kervran Effect, Abstract of 4th International Conference on Biophysics and Synchrotron Radiation (BSR 92), p.272, Tsukuba, August 30th~September 5th 1992.
- (8) Hisatoki KOMAKI: Observations on the Biological Cold Fusion or the Biological Transmutations of Elements. presented for 3rd International Conference on Cold Fusion, Nagoya, October 21st to 25th 1992: Frontiers of Cold Fusion. Universal Academy Press, 1993. p.555-558.
- (9) Hisatoki KOMAKI: "Selected Works of Prof. Dr. HISATOKI KOMAKI— FOUR STEPS TO ABSOLUTE PEACE Programme", Vol. I~Vol. IX. in English, French, German, Italian, Spanish and Russian version. The Earth Environment University Press. New York and Otsu, 1993.
- (10) Hisatoki KOMAKI: Outline of Selected Works of Prof. Dr. HISATOKI KOMAKI, Vol. I ~Vol. IX. New York Times. Book Review. 1993, p.16-17
- (11) Hisatoki KOMAKI: Outline of the Earth Environment University Roundtable (EEUR) and the Earth Environment Science Academy Foundation (EESAF), The Earth Environment University Press. New York and Otsu, 1993.
- (12) Goldfein: United States Army Research Laboratories Report, No. (19 )
- (13) K. Wakabayashi et al.: Small -angle X-ray Scattering Analysis of Conformational Changes of the Myosin Head (S1) during Hydrolysis of ATP Ibid., F107. 1992.
- (14) J. Deisenhofer: Developments in Studies of Macromolecular Structure by X-ray Crystallography. Abstract of BSR 92. Tsukuba. 1992.
- (15) D.T. Goodhead: Soft X-ray Radiobiography and Synchrotron Radiation. Ibid., 1992.

- (16) G. Schmahl: Natural Imaging of Biological Specimens with X-ray microscopes, *Ibid.*, 1992.
- (17) H.B. Stuhrmann: Solution Scattering, *Ibid.*, 1992.
- (18) J.R. Helliwell: Time-resolved macromolecular crystallography, *Ibid.*, 1992.

About the Author:—

Five Hundred Leaders of Influence

## Hisatoki Komaki

Since 1990, Prof. Dr. Hisatoki Komaki has held the position of President of the Earth Environment University of Japan and U.S.A. (Hon. President is Prof. Dr. Linus Pauling, Nobel Prize Winner). He began his career as a professor at Nara Women's University in 1960, after receiving his Ph.D. in the field of biological science in 1959 from Kyoto University, and he later served as a professor at Mukogawa University (1963) and at L'Universite Transnational in Paris (1973). He is a fellow member of the Japan Society for Bioscience and the Japan Society for Nutrition and Food Sciences. In 1989 he was named a Paul Harris Fellow of Rotary International, U.S.A.

Throughout his career, Prof. Komaki has written a number of scientific works, including *Selected Works of Prof. Dr. Hisatoki Komaki*, Volumes 1-9 (in English, French, German, Italian, Spanish and Russian, 1992), *Discovery of Biological Cold Fusion*. For his work, he has received the Medal of Honor with Dark Blue Ribbon of the Japanese Government, the Highest Gold Medal of the Red Cross of Japan, and an Academic Grand Prize of the Japanese Academy. He was also a nominee for the Nobel Prize, as the discoverer of Biological Cold Fusion.

Prof. Dr. Komaki was born in Kyoto, Japan, on 29 August 1926. He is married to Yoriko Komaki and is the son of the late Prof. Dr. Saneshige and Mrs. Kiyoko Komaki.

(Reprinted from FIVE HUNDRED LEADERS OF INFLUENCE) American Biographical Institute, Inc., 1993, p.203)

**Table 1.** Composition of the Normal, K-deficient, Mg-deficient, Ca-deficient and Fe-deficient Media for Mold

Components	Normal	K-deficient	Mg-deficient	Ca-deficient	Fe-deficient
Sucrose	3%	3%	3%	3%	3%
NaNO <sub>3</sub>	0.3%	0.3%	0.3%	0.3%	0.3%
K <sub>2</sub> HPO <sub>4</sub>	0.1%	—	0.1%	0.108%	0.1%
KCl	0.05%	—	0.05%	0.05%	0.05%
MgSO <sub>4</sub> ·7H <sub>2</sub> O	0.05%	0.05%	—	0.05%	0.05%
FeSO <sub>4</sub> ·7H <sub>2</sub> O	0.001%	0.001%	0.001%	0.001%	—
CaHPO <sub>4</sub>	0.008%	0.008%	0.008%	—	0.008%
Na <sub>2</sub> HPO <sub>4</sub>	—	0.1%	—	—	—
NaCl	—	0.05%	—	—	—
Na <sub>2</sub> SO <sub>4</sub>	—	—	0.05%	—	—
MnSO <sub>4</sub> ·7H <sub>2</sub> O	—	—	—	—	0.001%
Pure Water	to 100%	to 100%	to 100%	to 100%	to 100%

All components used are pure chemicals

**Tabel 2.** Composition of the Normal, K-deficient, Mg-deficient, Ca-deficient and Fe-deficient media for Yeast

Components	Normal	K-deficient	Mg-deficient	Ca-deficient	Fe-deficient
Sucrose	10%	10%	10%	10%	10%
Ammonium Tartarate	1%	1%	1%	1%	1%
MgSO <sub>4</sub> ·7H <sub>2</sub> O	0.25%	0.25%	—	0.25%	0.25%
FeSO <sub>4</sub> ·7H <sub>2</sub> O	0.001%	0.001%	0.001%	0.001%	—
CaHPO <sub>4</sub> ·2H <sub>2</sub> O	0.008%	0.008%	0.008%	—	0.008%
K <sub>3</sub> PO <sub>4</sub>	0.5%	—	0.5%	0.5%	0.5%
Na <sub>3</sub> PO <sub>4</sub>	—	0.5%	—	—	—
Na <sub>2</sub> SO <sub>4</sub>	—	—	—	—	—
K <sub>2</sub> HPO <sub>4</sub>	—	—	—	0.08%	—
MnSO <sub>4</sub> ·7H <sub>2</sub> O	—	—	—	—	0.001%
Pure Water	To 100%	To 100%	To 100%	To 100%	To 100%

**Table 3.** Comparison of the yield, as the weight of dried cells (mg) of mold and yeast obtained by normal media and K-deficient, Mg-deficient, Fe-deficient, and Ca-deficient culture. (Cultured with each 200ml of culture media ; shaking cultur at 30°C for 72 hours.)

Species	Culture media				
	Normal	K-deficient	Mg-deficient	Fe-deficient	Ca-deficient
<i>Aspergillus niger</i> (IFO No.4066)	574	54	72	56	125
<i>Penicillium chrysogenum</i> (IFO No.4689)	907	83	99	90	196
<i>Rhizopus nigricans</i> (IFO No.5781)	496	42	56	45	121
<i>Mucor rouxii</i> (IFO No.5773)	388	35	40	38	98
<i>Saccharomyces cerevisiae</i> (IFO No.0308)	1480	141	146	138	281
<i>Torulopsis utilis</i> (IFO No.0396)	2710	253	263	220	365
<i>Saccharomyces ellipsoideus</i> (IFO No.0213)	1540	155	163	159	294
<i>Hansenula anomala</i> (IFO No.0118)	1060	98	105	103	215

**Table 4.** Comparison of the contents of K, Mg, Fe, Ca ( $\mu\text{g}$ ) of the whole amount of, and 1g of, the dried cells of mold and yeast obtained by normal culture, and K-deficient, Mg-deficient, Fe-deficient and Ca-deficient culture (Each 200ml : 30°C ; 72 hours). (Upper : Per whole amount of the obtained dried cells ; Lower : Per 1g of the obtained dried cells)

Species	Normal culture				K-deficient	Mg-deficient	Fe-deficient	Ca-deficient
	K	Mg	Fe	Ca	K	Mg	Fe	Ca
<i>Aspergillus niger</i> (IFO No.4066)	5280	1110	390	260	130 (90)	32	7	12
	9198	1934	679	453	2407(1667)	472	125	96
<i>Penicillium chrysogenum</i> (IFO No.4689)	10100	1910	570	390	150 (110)	50	9	14
	11136	2106	628	429	1807(1325)	505	100	71
<i>Rhizopus nigricans</i> (IFO No.5781)	4240	960	250	190	110 (70)	21	5	10
	8548	1935	504	383	2619(1667)	375	111	83
<i>Mucor rouxii</i> (IFO No.5773)	3940	780	210	160	69 (29)	18	4	6
	10155	2010	389	412	1971 (829)	450	105	61
<i>Saccharomyces cerevisiae</i> (IFO No.0308)	16300	2820	1180	720	310 (270)	68	15	22
	11014	1905	797	486	2199(1916)	466	109	176
<i>Torulopsis utilis</i> (IFO No.0396)	23900	1750	2050	1380	490 (450)	130	22	29
	8819	645	756	493	1937(1779)	494	100	148
<i>Saccharomyces ellipsoideus</i> (IFO No.0213)	18400	2990	1220	790	340 (300)	62	16	28
	11948	1942	792	513	2194(1935)	380	101	231
<i>Hansenula anomala</i> (IFO No.0118)	12500	2060	840	520	170 (130)	42	12	15
	11792	1943	792	491	1735(1327)	117	400	153

**Table 5.** Comparison of the yield, as the weight of dried cells (mg) of mold and yeast obtained by normal media and K-deficient, Mg-deficient, Fe-deficient, and Ca-deficient culture. (Cultured with each 200 ml of culture media ; shaking culture at 30°C for 72 hours.)

Species	Culture media				
	Normal	K-deficient	Mg-deficient	Fe-deficient	Ca-deficient
<i>Aspergillus niger</i> (IFO No. 4066)	560	45	62	48	120
<i>Penicillium chrysogenum</i> (IFO No. 4689)	855	73	85	81	183
<i>Saccharomyces cerevisiae</i> (IFO No. 0308)	1350	135	139	126	263
<i>Torulopsis utilis</i> (IFO No. 0396)	1810	214	223	204	318

**Table 6.** Comparison of the contents of K, Mg, Fe, Ca ( $\mu\text{g}$ ) of the whole amount of, and 1g of, the dried cells of mold and yeast obtained by normal culture, and K-deficient, Mg-deficient, Fe-deficient and Ca-deficient culture (each 200 ml; 30°C; 72 hours).  
 (Upper: Per whole amount of the obtained dried cells; Lower: Per 1g of the obtained dried cells)

Species	Normal Culture				K-deficient	Mg-deficient	Fe-deficient	Ca-deficient
	K	Mg	Fe	Ca	K	Mg	Fe	Ca
<i>Aspergillus niger</i> (IFO No. 4066)	5070 9055	109 1940	366 654	259 463	105 ( 65) 2350 (1440)	29 461	6 121	10 86
<i>Penicillium chrysogenum</i> ( No. 4689)	8840 10340	175 2050	593 694	369 431	174 ( 134) 2380 (1830)	41 483	66 81	12 66
<i>Saccharomyces cervisiae</i> (IFO No. 0308)	13700 10150	255 1890	1057 783	641 475	290 ( 250) 2148 (1851)	58 415	12 94	38 144
<i>Torulopsis utilis</i> (IFO No. 0396)	15440 8534	1381 763	1341 741	871 481	141 ( 101) 658 ( 471)	94 423	22 91	36 114

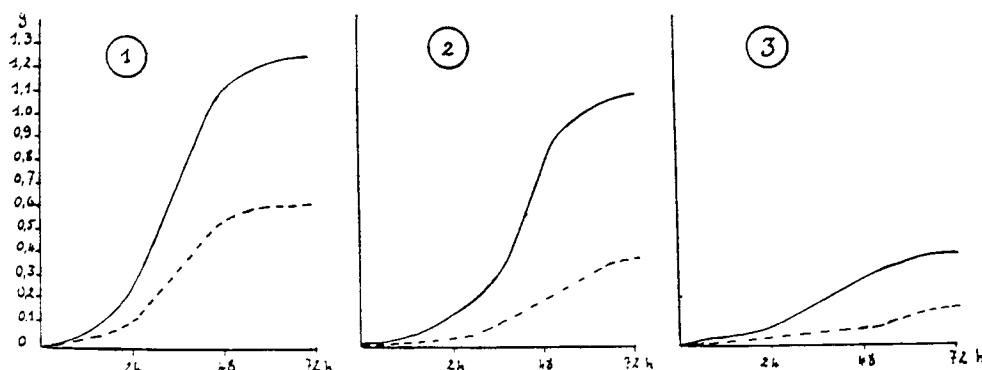


**Fig. 1.** — Quelques exemples de variation en 72 heures des poids de matière sèche.

— en traits pleins : dans un milieu avec K

- - - en tirets : dans un milieu sans K

Chiffres cercrés : 1. *Aspergillus niger* ; 2. *Urococcus* ; 3. *Saccharomyces rouxii*

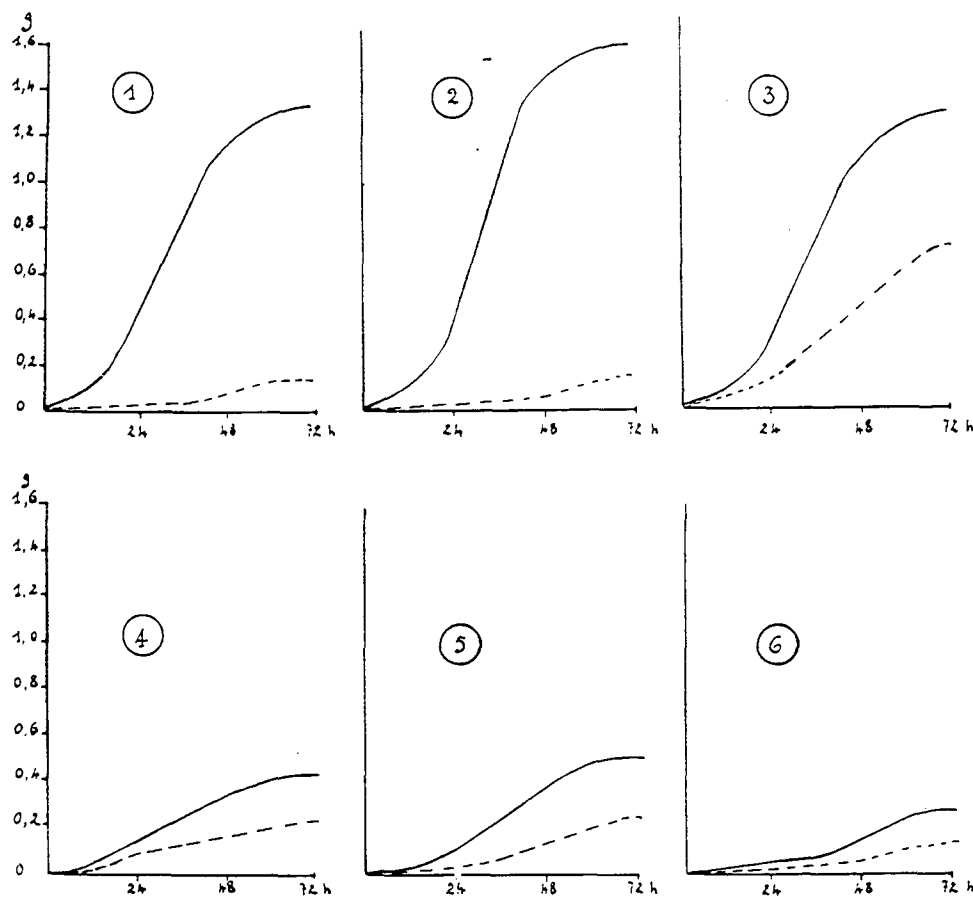


**Fig. 2.** — Quelques exemples de variation en 72 heures des poids de matière sèche.  
 — en traits pleins : dans un milieu avec P  
 - - - - en tirets : dans un milieu sans P, ou avec  $P = 1/100$  de P normal  
 Chiffres cercrés : 1. *Aspergillus niger* ; 2. *Penicillium chrysogenum* ; 3. *Urobacillus* ;  
 4. *Saccharomyces cerevisiae* ; 5. *Candida lypolitica* ; 6. *Torulopsis lactis condensi*.  
 (On remarquera que, de loin, c'est un urobacille qui est le plus actif en milieu carencé en P)

## **ABOUT EPRI**

*The mission of the Electric Power Research Institute is to discover, develop, and deliver high value technological advances through networking and partnership with the electricity industry.*

Funded through annual membership dues from some 700 member utilities, EPRI's work covers a wide range of technologies related to the generation, delivery, and use of electricity, with special attention paid to cost-effectiveness and environmental concerns.

At EPRI's headquarters in Palo Alto, California, more than 350 scientists and engineers manage some 1600 ongoing projects throughout the world. Benefits accrue in the form of products, services, and information for direct application by the electric utility industry and its customers.

*EPRI—Leadership in Electrification through Global Collaboration*



*Printed on recycled paper (50% recycled fiber, including 10% postconsumer waste) in the United States of America.*